APPENDIX K:
UNCERTAINTY AND SENSITIVITY ANALYSIS RESULTS

K1 INTRODUCTION

This appendix (Appendix K) presents uncertainty and sensitivity analysis results obtained in support of the Total System Performance Assessment for the License Application (TSPA-LA) based on the analysis structure described in Appendix J and the technical basis described in Section 6. Uncertainty analyses determine the uncertainty in analysis results that derives from uncertainty in analysis inputs. Sensitivity analyses determine the contribution to the uncertainty in analysis results that derives from individual analysis inputs.

The appendix begins with two background sections that briefly describe the uncertainty and sensitivity procedures in use (Section K2) and the independent and dependent variables under consideration (Section K3). These sections also provide references to additional sources of information about sensitivity analysis methods. Then, uncertainty and sensitivity analysis results are presented for the following scenario classes: nominal scenario class (Section K4), early failure scenario classes (Section K5), igneous scenario classes (Section K6), and seismic scenario classes (Section K7). In addition, results are presented for expected dose to the reasonably maximally exposed individual (RMEI) from all sources (Section K8). The appendix concludes with a summary of the analysis results (Section K9).

K2 UNCERTAINTY AND SENSITIVITY ANALYSIS PROCEDURES

Conceptually, the TSPA-LA analysis can be represented by

$$\mathbf{y} = \mathbf{f}(\mathbf{e}), \tag{Eq. K2-1}$$

where

$$\mathbf{e} = [\mathbf{e}_A, \mathbf{e}_M] = [e_1, e_2, \ldots, e_{nE}] \tag{Eq. K2-2}$$

is a vector of epistemically uncertain inputs to the TSPA-LA (see Section J4.9),

$$\mathbf{y} = [y_1, y_2, \ldots, y_{nY}] \tag{Eq. K2-3}$$

is a vector of epistemically uncertain TSPA-LA results, and the function $\mathbf{f}$ denotes the integrated suite of models that constitute the TSPA-LA modeling system. Major categories of epistemic uncertainties represented in $\mathbf{e}$ are summarized in Table 6.1.3-2. The elements of $\mathbf{e}$ are listed in Table K3-1 by the abbreviated name given the element in the sensitivity analyses, and in Table K3-2 by the name given the element in the TSPA-LA Model. Each element is presented in more detail in Table K3-3. Selected elements of $\mathbf{y}$ are summarized in Table K3-, and $\mathbf{f}$ is the function resulting from the integration of the models described in Section 6 of this AMR and in more detail in the cited background references to this section.

The TSPA-LA employs uncertainty and sensitivity analysis procedures based on a mapping between analysis inputs and analysis results generated with use of Latin hypercube sampling. As discussed in Section J4.9, a Latin hypercube sample (LHS)

$$\mathbf{e}_i = [\mathbf{e}_{Ai}, \mathbf{e}_{Mi}], i = 1, 2, \ldots, nLHS, \quad \text{(Eq. K2-4)}$$

is generated from the epistemically uncertain analysis inputs in consistency with the probability space ($\mathcal{E}$, E, p_E) used to characterize epistemic uncertainty (see Equation (J4.1-3) and associated discussion). In the computational implementation of the TSPA-LA, the probability space ($\mathcal{E}$, E, p_E) is, in effect, defined by assigning a probability distribution D_j to each element e_j of **e**. A high-level summary of the elements of **e** and their associated distributions is given in Table K3-1, and a more detailed summary is given in Table K3-3. Additional information on Latin hypercube sampling is available in Helton and Davis (2003) [DIRS 170518].

The TSPA-LA analysis uses an LHS sample of size *nLHS* = 300 from the elements **e** of $\mathcal{E}$. Further, as discussed in Section J4.10, this sample is replicated *nRL* = 3 times to test for the stability of analysis results.

Evaluation of TSPA-LA results for each element $\mathbf{e}_i = [\mathbf{e}_{Ai}, \mathbf{e}_{Mi}]$ of the LHS in Equation K2-4 generates a mapping

$$\mathbf{y}_i = \mathbf{f}(\mathbf{e}_i), \; i = 1, 2, \ldots, nLHS, \quad \text{(Eq. K2-5)}$$

from epistemically uncertain TSPA-LA inputs contained in $\mathbf{e}_i$ to epistemically uncertain TSPA-LA results contained in $\mathbf{y}_i$. Once generated, this mapping forms the basis for both uncertainty analysis and sensitivity analysis. Specifically, the weights associated with the individual LHS elements (i.e., 1/*nLHS*) permit the construction of distributions for elements of **y** that characterize epistemic uncertainty, and the mapping itself can be explored with a variety of sensitivity analysis procedures to determine the effects of individual elements of **e** on elements of **y**. The structure and implementation of analyses of this type are extensively discussed in the review by Helton et al. (2006) [DIRS 183873].

The primary sensitivity analysis procedures in use involve the determination and presentation of partial rank correlation coefficients (PRCCs), stepwise rank regression analyses, and scatterplots.

PRCCs provide a measure of the strength of the monotonic relationships between an independent variable *e* (i.e., an element of **e**) and a dependent variable *y* (i.e., an element of **y**) after a correction has been made to remove the monotonic effects of the other independent variables in the analysis (i.e., the elements of **e** other than *e*). Most of the elements of **y** under consideration are functions of time. For such variables, the presentation of PRCCs as functions of time provides an informative display of sensitivity analysis results (Figure K2-1).

As indicated by the name, PRCCs involve the analysis of rank-transformed data. With this approach, the values for variables are replaced with their ranks and then the PRCCs are calculated with these ranks rather than with the original values for the variables. Specifically, the smallest value of a variable is given a rank of 1; the next largest value is given a rank of 2; equal observations are assigned the average of what their ranks would have been if they had not been equal; and so on up to the largest value, which is given a rank equal to the number of sample elements in use (i.e., *nLHS* = 300 in Appendix K). The effect of the rank transformation

is to transform monotonic relationships into linear relationships. Further, the rank transform tends to reduce the skewing effects of outliers, which permits the regression analyses to represent the general relationships between the inputs and the output of interest. Although no variable transformation is universally successful in improving the resolution of a sensitivity analysis in the presence of nonlinear relationships, the rank transformation has been found to be a broadly effective and useful means of enhancing the insights in sensitivity analyses based on partial correlation and also in sensitivity analyses based on stepwise regression.

In the example in Figure K2-1, the time-dependent results for the variable under consideration (i.e., *NCSFL*, number of failed commercial spent nuclear fuel (CSNF) waste packages (WPs) in percolation bin 3 under nominal conditions) are presented in the top left frame (i.e., Figure K2-1a) and the corresponding PRCCs are presented in the top right frame (i.e., Figure K2-1b). Figure K2-1a contains 300 time-dependent values for *NCSFL*. Thus, at each time there are 300 values for *NCSFL* for which a PRCC is calculated for each element *e* of **e** (Note: In the calculation of PRCCs for a particular dependent variable *y* that is not influenced by all elements of **e**, such as release of a particular radionuclide from the engineered barrier system (EBS), the elements of **e** that are known to be unrelated to the determination of the dependent variable *y* are excluded from this calculation. The exclusion of these elements reduces the occurrence of spurious correlations in the PRCC calculation results). Then, the PRCCs are plotted above the time at which they were calculated and connected for each independent variable *e* to show the effect of *e* on the dependent variable (i.e., *NCSFL* in this example) as a function of time. To limit the number of time-dependent PRCC curves in a given plot frame, the PRCC plots in Appendix K only show PRCC curves for the six variables with the largest PRCCs in absolute value over the time interval under consideration. Further, plots are only shown for variables whose PRCCs exceed 0.3 in absolute value at some point in time. Variables with PRCCs less than 0.3 in absolute value have only a limited monotonic effect on the output variable under consideration. In the legend of a figure showing PRCCs, the variables are listed in decreasing order of PRCC, i.e., the variable having the largest PRCC in absolute value over the time interval under consideration is listed first.

Values of PRCCs fall in the interval [−1, 1], with (i) positive PRCCs indicating that two variables tend to increase and decrease together (i.e., the independent variable has a positive effect on the dependent variable), (ii) negative PRCCs indicating that two variables tend to move in opposite directions (i.e., the independent variable has a negative effect on the dependent variable), and (iii) the absolute value of a PRCC indicating the strength of the relationship between two variables (i.e., a PRCC close to 1 in absolute value indicates a strong monotonic relationship between two variables after the removal of the monotonic effects associated with the other independent variables under consideration; a PRCC close to 0 in absolute value indicates no monotonic relationship after the removal of the monotonic effects associated with the other variables under consideration; and the strength of the effect increases as the absolute value of a PRCC increases from 0 to 1). Thus, in the example in Figure K2-1b, *WDGCA22* has a negative effect on *NCSFL* with this effect increasing with time; *WDZOLID* has a positive effect on *NCSFL* with this effect increasing with time; and *INFIL*, *WDNSCC*, *THERMCON* and *SCCTHR* have small negative effects on *NCSFL* with these effects also increasing with time.

An alternative to the use of PRCCs is to carry out stepwise rank regressions to determine the effects of uncertain inputs on analysis results of interest. In analyses of this type, the regressions

are carried out with rank transformed variable values as previously discussed rather than with the original variables.

In a stepwise rank regression, the single independent variable that makes the largest contribution to the uncertainty in the dependent variable is selected in the first step. Then, at the second step, the single independent variable that, in conjunction with the first variable, makes the largest contribution to the uncertainty in the dependent variable is selected. This process then continues until no additional variables are found that make identifiable (i.e., significant) contributions to the uncertainty in the dependent variable; at this point, the stepwise selection process terminates. In Appendix K, a significance level of $\alpha = 0.01$ is used as the criterion for both dropping a previously selected variable from a stepwise regression and for terminating a stepwise regression analysis. Selection of this significance level was based on preliminary sensitivity analyses, in which it was observed that a greater value tended to introduce obviously spurious variables into the regression models. The significance levels were intended to be set at 0.01 for entering variables and 0.02 for departing variables. However, through an oversight, a value of 0.01 was used for both entering and departing variables. Under very unlikely conditions, this inconsistency could cause unintended looping in the stepwise variable selection process if the same variable was repeatedly added and then dropped from the regression model. An examination of the regression analyses showed that such looping did not occur. Thus, the specification of 0.01 rather than 0.02 for the dropping of a previously selected variable has no effect on the presented regression results. In the context of stepwise regression analysis, variable importance is indicated by (i) order of selection in the stepwise selection process, (ii) incremental changes in R^2 values with the successive entry of individual variables into the regression model, and (iii) the sign and size of the standardized regression coefficients, (i.e., standardized rank regression coefficients (SRRCs), when rank regression is being used) in the final regression model.

As an example, stepwise rank regressions for NCSFL at 600,000, 800,000 and 1,000,000 yr are shown in Figure K2-1c. For the analysis at each time, the first column lists the independent variables in the order of selection in the stepwise process; the second column lists the cumulative R^2 value with the entry of each variable into the regression model; and the third column lists the SRRCs for the variables in the final regression model.

The R^2 value corresponds to the fraction of the uncertainty in the dependent variable that is accounted for by a regression model. Thus, R^2 values monotonically increase as additional variables are added to the regression model and, for a very successful regression analysis, approach 1 as additional variables are added to the model. The SRRCs provide a measure of the fractional contribution of individual independent variables to the uncertainty in the dependent variable under consideration. Further, like PRCCs, a positive SRRC indicates that the independent variable and dependent variable tend to increase and decrease together, and a negative SRRC indicates that the independent variable and dependent variable tend to move in opposite directions.

In the analysis that follows, PRCCs are presented as plots of PRCC values over time for the six parameters with the highest absolute PRCC values over the time interval under consideration. The PRCCs are computed at each time at which TSPA-LA Model output is provided. In contrast, SRRCs are computed at 3 fixed times (usually at 2,000, 5,000 and 10,000 years for a

model result calculated out to 20,000 years, and at 50,000 years, 200,000 years and 500,000 years for a model result calculated out to 1,000,000 years). These typical times for SRRC computation were chosen to illustrate the changes in importance of uncertain parameters over time. The same analysis times are generally used for analysis of all TSPA-LA Model output variables to facilitate comparisons between the sensitivity analysis results across output variables. For a few output variables that do not have meaningful values at these typical times, SRRC computations are done at times at which the output variable is meaningful.

Related, but not identical, information is provided by PRCCs and SRRCs. Specifically, PRCCs measure the strength of the monotonic relationship between an independent variable and a dependent variable after correcting for the effects of other independent variables, and SRRCs provide a measure of the fractional contribution of an individual independent variable to the uncertainty in the dependent variable under consideration. Except in rare situations involving SRRCs from a regression model involving multiple correlated variables, PRCCs and SRRCs have the same sign, which indicates either a positive or negative correlation between an input variable and an output variable. Because PRCCs are selected for display based on the maximum absolute value over time, and SRRCs are computed at specific times, the selection and order of important variables indicated by PRCCs and SRRCs may be different between the two analyses. However, when there are no correlations between the independent variables (i.e., the variables in the LHS), then, at a fixed time, an ordering of variable importance based on the absolute value of PRCCs is the same as an ordering of variable importance based on the absolute value of SRRCs.

In addition to PRCCs and stepwise rank regression analyses, Appendix K makes use of scatterplots to present and explain the relationships between independent and dependent variables. A scatterplot is simply a plot of the points (e_i, y_i), $i = 1, 2, \ldots, nLHS$, where e_i are the sampled values for an independent variable and the y_i are the corresponding values for a dependent variable. If e has a significant effect on y, then this will be apparent in the scatterplot; if e does not have a significant effect on y, then the points in the scatterplot will have a random distribution conditional on the marginal distributions for e and y. As an example, scatterplots involving the pair

$$(e_i, y_i) = (WDGA22_i, NCSFL_i),\ i = 1, 2, \ldots, nLHS = 300, \qquad \text{(Eq. K2-6)}$$

for results obtained at 600,000 and 800,000 yr are presented in Figure K2-1d, e. As can be seen, a strong and complex relationship exists between *WDGA22* and *NCSFL*. In some instances, scatterplots can reveal relationships that may be too complex to be adequately captured by the numeric effect summaries provided by PRCCs and stepwise rank regression analyses. An example of such a relationship may be found in Figure K4.5-3, with an explanation provided in the accompanying text.

More detailed information on the sensitivity analysis techniques in use is available in several reviews (Helton et al. 2006 [DIRS 183873]; Helton and Davis 2000 [DIRS 156572]). Further, these reviews describe a number of additional sensitivity analysis techniques that can be used in the exploration of the mapping between analysis inputs and analysis results indicated in Equation (K2-5).

The examples contained in Figure K2-1 are taken from Figures K4.2-2 and K4.2-3. The discussions associated with Figures K4.2-2 and K4.2-3 describe the physical processes underlying the presented results and the roles that the variables identified in the sensitivity analyses have in these processes.

K3 INDEPENDENT AND DEPENDENT VARIABLES

As indicated in conjunction with Equation (J4.1-3), the TSPA-LA involves a large number of epistemically uncertain variables. These variables and their associated distributions collectively define the probability space ($\mathcal{E}$, E, p_E) for epistemic uncertainty. Notationally, the elements of $\mathcal{E}$ can be represented by a vector

$$\begin{aligned}\mathbf{e} &= [\mathbf{e}_A, \mathbf{e}_M] \\ &= \left[e_{A1}, e_{A2}, \ldots, \cdots e_{A,nAE}, e_{M1}, e_{M2}, \ldots, e_{M,nME}\right] \\ &= [e_1, e_2, \ldots, e_{nE}], nE = nAE + nME,\end{aligned} \qquad \text{(Eq. K3-1)}$$

where

$$\mathbf{e}_A = \left[e_{A1}, e_{A2}, \ldots, e_{A,nAE}\right]$$

is a vector of epistemically uncertain quantities used in the characterization of aleatory uncertainty (e.g., a rate term that defines a Poisson process) and

$$\mathbf{e}_M = \left[e_{M1}, e_{M2}, \ldots, e_{M,nME}\right]$$

is a vector of epistemically uncertain quantities used in the determination of dose (e.g., a distribution coefficient).

The vector **e** contains a total of $nE = 387$ elements. Thus, $\mathcal{E}$ is a subset of $R^{nE} = R^{387}$. However, not every element of **e** is used in uncertainty and sensitivity analysis for every scenario class. For example, **e** contains 44 elements corresponding to the dose conversion factors for inhalation pathways used to calculate the dose following an igneous eruptive event. These elements are only used in the igneous eruptive scenario class. In addition, certain of elements of **e** are correlated to other elements of **e**. Each subset of correlated variables is represented in the sensitivity analyses by one member of the set of correlated variables. By excluding variables that are not used in a scenario class and by choosing representatives for correlated sets of variables, the total number of uncertain input variables considered for the sensitivity analysis of a scenario class is less than 387, with the exact number depending on the scenario class.

Table K3-1 provides a high-level summary of the elements of **e**. Of the variables listed in Table K3-1, only *IGRATE*, *PROBDSEF* and *PROBWPEF* are elements of $\mathbf{e}_A$. Thus, $nAE = 3$ and

$$\mathbf{e}_A = [IGRATE, PROBDSEF, PROBWPEF]. \quad \text{(Eq. K3-2)}$$

The remaining variables contained in Table K3-1 constitute the elements of $\mathbf{e}_M$. Thus $nME = nE - 3 = 384$ and

$$\mathbf{e}_M = [ALPHAL, ALPHANL, \ldots, WPFLUX] \quad \text{(Eq. K3-3)}$$

contains all variables in Table K3-1 except for the three elements of $\mathbf{e}_A$. Not all variables listed in Table K3-1 are included in the sensitivity analysis because of correlations between elements of $\mathbf{e}$. Table K3-1 and Table K3-2 show an asterisk (*) at the end of a variable name to indicate that the variable is excluded from the sensitivity analysis because of correlations. Table K3-3 provides references to descriptions of the correlations between input variables.

The problems that can result from correlated variables are discussed and illustrated in Section 8.7 of Helton and Davis 2000 [DIRS 156572]. Where correlations exist, only one of the correlated variables is retained as an input variable in the sensitivity analyses. The sensitivity analyses were conducted iteratively to ensure that correlations between input variables were identified and that no significantly correlated pairs of input variables were used in the analyses. Examination of the final regression model produced from a stepwise regression analysis allows the identification of the presence of correlations that affect the assessment of variable importance. In particular, unless there are correlations between the selected variables, the SRRCs for the variables selected in a stepwise regression analysis will monotonically decrease in order of selection in the stepwise process. A significant deviation from a monotonic decrease in the absolute values of the SRRCs indicates that there are correlations between variables that are affecting the structure of the constructed regression models.

Table K3-1 is intended primarily as a quick reference to variable definitions for use in conjunction with the sensitivity analyses presented in the remainder of this appendix. However, Table K3-1 does not provide enough information to actually track an individual variable back through the TSPA-LA analysis and ultimately to its original sources of documentation. To assist with this traceability, Table K3-2 lists the variables by the name given in the TSPA-LA Model, and Table K3-3 provides more information on the individual variables contained in $\mathbf{e}$, including references to supporting documentation.

Appendix J concentrated on TSPA-LA results for two analysis outcomes: dose to the RMEI as a function of time and expected dose to the RMEI as a function of time. However, these are only two of a very large number of TSPA-LA results. As indicated in Equation (K2-3), the TSPA-LA actually produces a vector $\mathbf{y}$ of results, with most of these results functions of time. A subset of the potential elements of $\mathbf{y}$ is considered in the sensitivity analyses presented in this appendix. The elements of $\mathbf{y}$ specifically considered in this appendix are listed in Table K3-4. Thus, in the context of this appendix,

$$\mathbf{y} = [BACSFLAD, BACSFLND, \ldots, UZTC99C], \quad \text{(Eq. K3-4)}$$

where *BACSFLAD*, *BACSFLND*, …, *UZTC99C* are defined in Table K3-4. However, even this representation for **y** is a simplification for **y** in two ways. First, most of the elements of **y** are functions of individual scenario classes or specific modeling assumptions and also possibly functions of location within the repository system (e.g., percolation bin). Second, **y** contains only a subset of the TSPA-LA results that could be considered for uncertainty and sensitivity analysis.

The TSPA-LA Model calculations are performed for the two time periods: from 0 years to 20,000 years, and from 0 years to 1,000,000 years after repository closure. Separate calculations are performed for these time periods because of a necessarily coarser temporal discretization in the GoldSim component of the TSPA-LA Model for 1,000,000 years calculations (Section 7.3.3). The calculations for the 20,000-year simulations are extended to 20,000 years to assess whether or not the trends present at the end of 10,000 years continue.

The dependent variables included in the analysis, summarized in Table K3-4, were selected to provide insight into the behavior of the repository system, rather than solely on the basis of the importance of individual variables to repository performance. For scenario class, expected dose to the RMEI is analyzed, and for most scenario classes, results for a select set of radionuclides are also analyzed. The selection of radionuclides considered for analysis was made in part to cover a wide range of radionuclide behavior. As a result, (i) the colloidal forms of ^{239}Pu were selected to allow the examination of the behavior of glass and ferrous colloids in the EBS and the behavior of fast and slow colloids downstream of the EBS, (ii) dissolved ^{239}Pu was selected to allow the consideration of a highly retarded radionuclide with an intermediate half life that is important to dose, (iii) dissolved ^{237}Np was selected to allow the consideration of a retarded radionuclide with a long half life that is important to dose, and (iv) dissolved ^{99}Tc was selected to allow the consideration of an unretarded radionuclide with a long half life that is important to dose. In addition to analyses of expected dose and of individual radionuclides, the discussion of some scenario classes includes analyses of variables related to the state of EBS components (e.g. number of failed WPs) and conditions within the EBS (e.g. temperature, relative humidity).

For scenario classes defined by an event (i.e. igneous intrusive, igneous eruptive, seismic ground motion, and seismic fault displacement scenario classes), analyses of dependent variables other than expected dose are conducted on model results calculated conditional on the occurrence of a specific event. Fixing the aleatory parameters that describe the event allows the sensitivity analyses to determine the effects on model results of the uncertainty in epistemic parameters. In general, events are chosen at the earliest time available in the Goldsim calculations. Because the Goldsim timesteps are necessarily different in 20,000 yr and 1,000,000 yr calculations, and because event times must align with a Goldsim timestep, sensitivity analyses are generally conducted for different event times for the two different calculations.

K4 NOMINAL SCENARIO CLASS

K4.1 Nominal Scenario Class: Summary

The nominal scenario class consists of the future in which no disruptions of any kind (i.e., early drip shield (DS) failures, early WP failures, igneous events, and seismic events) occur

(Section J5). This section (Section K4) presents uncertainty and sensitivity analysis results for selected analysis outcomes associated with the nominal scenario class (Table K4.1-1).

The results of most direct interest to repository performance are DS failure time (*DSFLTM*, yr), numbers of failed CSNF (*NCSFL*) and co-disposed (CDSP) (*NCDFL*) WPs, and dose to the RMEI (*DOSTOT*, mrem/yr). In addition to these analysis results, other results related to environmental conditions in the EBS are presented.

The value for *DSFLTM* is the same for all DSs and falls between 2.65×10^5 and 3.32×10^5 yr (Figure K4.2-1). The uncertainty in *DSFLTM* is completely dominated by *WDDSAGGC* (rate of aggressive general corrosion on top of the DS, nm/yr) and *WDDSBEGC* (rate of benign general corrosion on bottom of the DS, nm/yr).

The values for *NCSFL* and *NCDFL* range from very limited WP failure to failure of all WPs (Figures K4.2-2 to K4.2-5). The uncertainty in *NCSFL* and *NCDFL* is dominated by *WDGCA22* (temperature dependence coefficient associated with general corrosion rate for alloy 22, K). Specifically, the general corrosion rate for alloy 22, and hence the values for *NCSFL* and *NCDFL*, decreases as *WDGCA22* increases.

The values for *DOSTOT* range up to 7 mrem/yr but are much smaller for most sample elements (Figure K4.5-1). The uncertainty in *DOSTOT* is dominated by *WDGCA22* because of its effects on the number of failed WPs.

K4.2 Nominal Scenario Class: Drip Shield and Waste Package Failure

This section presents analysis results for DS failure time, number of failed WPs and the average breached area on failed WPs.

Drip Shield Failure Time: *DSFLTM*. The uncertainty and sensitivity analyses for DS failure time (*DSFLTM*, yr) are summarized in Figure K4.2-1. The possible values for *DSFLTM* fall between 265,000 and 332,000 yr (Figure K4.2-1a). The value for *DSFLTM* is determined by *WDDSAGGC* (rate of aggressive general corrosion on the top of the DS, nm/yr) and *WDDSBEGC* (rate of benign general corrosion on the bottom of the DS, nm/yr) (Figure K4.2-1b,c,d). The uncertainty in the value for *DSFLTM* is dominated by *WDDSAGGC*, which accounts for approximately 64 percent of the uncertainty in *DSFLTM* (i.e., the R^2 value associated with *WDDSAGGC* in the regression in Figure K4.2-1b is 0.64). The addition of *WDDSBEGC* results in a regression model with an R^2 value of 0.93. The regression model does not achieve an R^2 value of 1.00 because of the use of discrete timesteps in GoldSim. The effects of *WDDSAGGC* and *WDDSBEGC* on *DSFLTM* are independent and additive (Figure K4.2-1e).

Number of Failed Waste Packages: *NCSFL*, *NCSFLAD*, *NCSFLND*, *NCDFL*, *NCDFLAD*, *NCDFLND*. The uncertainty and sensitivity analyses for numbers of failed CSNF WPs (*NCSFL*) and failed CDSP WPs (*NCDFL*) in percolation bin 3 are summarized in Figures K4.2-2 and K4.2-3. Percolation bin 3 contains 3285 CSNF WPs and 1366 CDSP WPs (approximately 40 percent of the WPs in the repository), more than any one of the other four percolation bins, and is selected for analysis for this reason. Comparisons of dose results between percolation bins

for early failed WP and DS cases (Figure J6.2-13 and Figure J6.3-13, respectively) indicate little variation in dose among percolation bins for either diffusive dominated (early failed WP) or advective dominated (early failed DS) conditions. The earliest WP failures occur for some, but not all, sample elements approximately 200,000 yr after repository closure (Figure K4.2-2a,b,c,d). However, there is significant uncertainty with respect to when initial WP failure will occur, with initial WP failure occurring after 500,000 yr for many sample elements. Many sample elements result in the failure of all WPs before 1,000,000 yr (Figure K4.2-2a,b,c,d). The jumps in failures evident at 300,000 years, 500,000 years and 700,000 years are due to the timesteps used by the WAPDEG code.

The PRCCs in Figure K4.2-2e,f indicate that the uncertainty in *NCSFL* and *NCDFL* is dominated by *WDGCA22* (temperature dependence coefficient associated with the general corrosion rate for alloy 22, K). Specifically, *WDGCA22* corresponds to a coefficient used to alter the general corrosion rate for alloy 22 as function of temperature, with the alloy 22 general corrosion rate decreasing as *WDGCA22* increases when temperature is below 60 ºC. The strong negative effect of *WDGCA22* on *NCSFL* and *NCDFL* is indicated by the associated PRCCs having values very close to −1.0 (Figure K4.2-2e,f). In addition, a lesser positive effect is indicated for *WDZOLID* (scale factor used to incorporate uncertainty into the stress intensity factor for closure-lid weld), with this positive effect resulting because increasing *WDZOLID* increases the stress at the closure lid. Small negative effects are also indicated for *INFIL* (infiltration level), *THERMCON* (host rock thermal conductivity level), *WDNSCC* (stress corrosion cracking growth rate exponent), and *SCCTHR* (stress corrosion cracking threshold, MPa). These negative effects result because (i) increasing *INFIL* and *THERMCON* tends to lower WP temperatures and thus reduce the rate of corrosion, (ii) increasing *WDNSCC* increases the threshold stress intensity factor, which determines the threshold stress at which stress corrosion cracks propagate, and thus reduces failures at the closure-lid weld, and (iii) increasing *SCCTHR* increases the stress level at which stress corrosion cracking initiates and thus reduces failures at the closure-lid weld.

More detailed sensitivity analysis results for *NCSFL* based on stepwise rank regression are presented in Figure K4.2-3a. The results are the same for *NCDFL* and thus are not presented; further, the pattern of results is the same for all five percolation bins as the processes leading to nominal WP failures are not very affected by environmental conditions. As the regressions show, the uncertainty in *NCSFL* is dominated by *WDGCA22*, with *WDGCA22* having R^2 values of 0.86, 0.90 and 0.91 in the three presented regressions. The dominant effect of *WDGCA22* on the uncertainty in *NCSFL* can also been seen in the three presented scatterplots (Figure K4.2-3b,c,d); the horizontal lines of points in the scatterplots result from sample elements in which all CSNF WPs in percolation bin 3 have failed by the time under consideration. The remaining variables selected in the regressions are generally the same as those identified in the analyses with PRCCs in Figure K4.2-2e,f. The changes in the R^2 values associated with entry of these variables into the regression analyses are small (e.g., 0.01 – 0.02) and provide an indication of the extent to which the uncertainty in these variables impacts the uncertainty in *NCSFL*.

The pointer variable *WDGCUA22* used to select the distribution of base corrosion rates of alloy 22 at 60 ºC over the patches on the WPs is also identified in all three regressions in

Figure K4.2-3a as having a small positive effect on the uncertainty in *NCSFL*. Specifically, *WDGCUA22* is a pointer variable used to select from three uncertain distributions that derive from both the uncertainty in a base corrosion rate for alloy 22 at 60 ºC and the uncertainty that exists in the prediction of small scale variability in chemical and physical conditions across patches used in the modeling of WP degradation. In turn, *WDGCA22* is used in the correction of the corrosion rates defined by the distributions indexed by *WDGCUA22* for temperature effects. It should be noted that the impact of the uncertainty associated with *WDGCA22* is much greater than the impact of the uncertainty associated with *WDGCUA22*.

Uncertainty and sensitivity analyses for numbers of failed CSNF WPs under dripping conditions (*NCSFLAD*) and nondripping conditions (*NCSFLND*) in percolation bin 3 are summarized in Figures K4.2-4 and K4.2-5. The terminal designators *AD* and *ND* in *NCSFLAD* and *NCSFLND* derive from the alternative use of "always dripping" and "never dripping" as designators for dripping and nondripping conditions. Time-dependent values for *NCSFLAD* and *NCSFLND* appear in Figure K4.2-4a,b,c,d. As already indicated, the processes leading to nominal WP failures are not affected by seepage conditions. Because of this, WPs experiencing nondripping conditions have the same likelihood of failure as WPs experiencing dripping conditions. As a result, the division of *NCSFL* into *NCSFLAD* and *NCSFLND* (reminder: *NCSFL* = *NCSFLAD* + *NCSFLND*) is determined by the fractions of WPs that experience dripping and nondripping conditions.

As indicated by the PRCCs in Figure K4.2-4e,f, the uncertainty in *NCSFLAD* and *NCSFLND* is dominated by *WDGCA22*, with the number of failed WPs decreasing as *WDGCA22* increases. In consistency with the analyses for *NCSFL* and *NCDFL*, a small positive effect is indicated for *WDZOLID* and a small negative effect is indicated for *WDNSCC* for both *NCSFLAD* and *NCSFLND*. A small negative effect is also indicated for *THERMCON* for *NCSFLAD*, with this small effect probably resulting from the slower corrosion rate for alloy 22 at reduced temperatures. The effects of *WDGCA22*, *WDZOLID*, *WDNSCC* and *THERMCON* on *NCSFLAD* and *NCSFLND* result from their influence on WP failure.

In contrast, other variables appear in the sensitivity analysis as a result of their effects on the numbers of WPs experiencing dripping or nondripping conditions. For example, *INFIL* has a negative effect on *NCSFLND* because increasing its value decreases the number of WPs experiencing nondripping conditions (Figure K4.2-4f). Two variables identified in the analysis that affect both *NCSFLAD* and *NCSFLND* are *SEEPUNC* (pointer variable used to determine local seepage rates) and *SEEPPRM* (mean fracture permeability in lithophysal rock units, m^2; as sampled, *SEEPPRM* is actually the logarithm of the indicated permeability) (Figure K4.2-4e,f). Increasing *SEEPUNC* tends to increase seepage into the EBS through an upscaling of base seepage rates while increasing *SEEPPRM* tends to decrease seepage into the repository by increasing the diversion of water around the drifts. As a result, increasing *SEEPUNC* has a positive effect on *NCSFLAD* and a negative effect on *NCSFLND*, and in a reverse pattern, increasing *SEEPPRM* has a negative effect on *NCSFLAD* and a positive effect on *NCSFLND*.

More detailed sensitivity analysis results for *NCSFLAD* and *NCSFLND* based on stepwise rank regression are presented in Figure K4.2-5a,b. Although more detailed, these results are consistent with the PRCC results in Figure K4.2-4e,f. In particular, the uncertainty in *NCSFLAD* and *NCSFLND* is dominated by *WDGCA22,* with small incremental contributions to this

uncertainty from a number of additional variables. The dominant effect of *WDGCA22* can be seen in the scatterplots in Figure K4.2-5c,e.

The numbers of WPs experiencing dripping and nondripping conditions varies widely from sample element to sample element (Figure K4.2-5g,h). In particular, the straight lines of points in Figure K4.2-5g,h correspond to sample elements in which all WPs in percolation bin 3 have failed. As examination of the points associated with these lines shows, the possibilities range from almost all failed WPs experiencing dripping conditions to almost all failed WPs experiencing nondripping conditions.

The results presented in Figures K4.2-4 and K4.2-5 are for CSNF WPs in percolation bin 3. Essentially identical results hold for numbers of failed CDSP WPs under dripping conditions (*NCDFLAD*) and nondripping conditions (*NCDFLND*) in percolation bin 3 and are not presented. Similar results also hold for the other percolation bins.

Averaged Breached Area on Failed Waste Packages: *BACSFLAD*, *BACSFLND*, *BACDFLAD, BACSFLND*. The uncertainty and sensitivity analyses for average breached area (m^2) on failed CSNF WPs under dripping conditions (*BACSFLAD*) and nondripping conditions (*BACSFLND*) in percolation bin 3 are summarized in Figures K4.2-6 and K4.2-7. As indicated in Figure K4.2-6d, there is no meaningful difference in *BACSFLAD* and *BACSFLND*. For this reason, analyses are presented only for *BACSFLAD*. Further, the uncertainty and sensitivity analyses for average breached area on failed CDSP WPs under dripping conditions (*BACDFLAD*) and nondripping conditions (*BACDFLND*) in percolation bin 3 are the same as those shown in Figures K4.2-6 and K4.2-7 for CSNF WPs and are also not shown.

As shown in Figure K4.2-6a,b, *BACSFLAD* increases monotonically with time and ranges at 1×10^6 yr from less than 10^{-4} m^2 to almost 10 m^2. The uncertainty in *BACSFLAD* is dominated by *WDGCA22* (temperature dependence coefficient associated with the general corrosion rate for alloy 22, K), with *BACSFLAD* tending to increase as *WDGCA22* as decreases (Figures K4.2-6c and K4.2-7a). Specifically, the dominant effect of *WDGCA22* on the uncertainty in *BACSFLAD* is indicated by PRCCs close to -1 in Figure K4.2-6c and R^2 values ranging from 0.81 to 0.91 in Figure K4.2-7a. The dominant effect of *WDGCA22* can also be seen in the scatterplot in Figure K4.2-7b. Smaller effects are also indicated for the following variables: *WDZOLID* (stress intensity factor for closure-lid weld), *INFIL* (infiltration level), *THERMCON* (host rock thermal conductivity level), *WDNSCC* (stress corrosion cracking growth rate exponent), *SCCTHR* (stress corrosion cracking threshold, MPa), and *WDGCUA22* (pointer variable used to select the distribution of base corrosion rates of alloy 22 at 60 ºC over the patches on the WPs). The effects of these variables are the same as previously discussed for number of failed WPs (see discussion for *NCSFL* and *NCDFL*).

The results for the other percolation bins are the same as those shown in Figures K4.2-6 and K4.2-7 for percolation bin 3 and, for this reason, are not presented.

K4.3 Nominal Scenario Class: Engineered Barrier System Conditions

This section presents analysis results describing seepage rates, temperature and relative humidity in the drifts, as well as partial pressure of CO_2, ionic strength and pH in the invert.

Seepage Rate into Drifts: *SPRATECS*, *SPRATECD*. The uncertainty and sensitivity analyses for seepage rate (m^3/yr/WP) into the repository above CSNF WPs (*SPRATECS*) and CDSP WPs (*SPRATECD*) in percolation bin 3 are summarized in Figures K4.3-1 and K4.3-2. The jumps evident at 2,000 years and at 10,000 years are due to modeling the changes in climate as instantaneous changes in UZ flow fields. As examination of Figure K4.3-1 shows, there is effectively no difference in the values for *SPRATECS* and *SPRATECD*. The uncertainty in *SPRATECS* and *SPRATECD* is dominated by *INFIL* (infiltration level). Specifically, the PRCCs for *SPRATECS* and *SPRATECD* are close to 1.0, which indicates that *SPRATECS* and *SPRATECD* tend to increase as *INFIL* increases (Figure K4.3-1e,f). The regression analyses for *SPRATECS* in Figure K4.3-2a also indicate the dominate effect of *INFIL*, with the individual regression analyses having R^2 values of 0.67, 0.73 and 0.68 when only *INFIL* is included in the regression model. Similar regression results exist for *SPRATECD* and are not presented.

In addition to *INFIL*, the following variables have lesser effects on the uncertainty in *SPRATECS* and *SPRATECD*: *THERMCON* (host rock thermal conductivity level), *ALPHAL* (capillary strength parameter in lithophysal rock units), *SEEPPRMN* (mean fracture permeability in nonlithophysal rock units, m^2; as sampled, *SEEPPRMN* is actually the logarithm of the indicated permeability), *SEEPPRM* (mean fracture permeability in lithophysal rock units, m^2; as sampled, *SEEPPRM* is actually the logarithm of the indicated permeability), and *SEEPUNC* (pointer variable used to determine local seepage rates). The variable *THERMCON* has a positive effect at early times (i.e., before 1,000 yr as indicated in Figure K4.3-1e,f), with this effect resulting because increasing *THERMCON* increases the rate at which the repository cools to a temperature level (i.e., less than 100 ºC) at which seepage can occur. The negative effect for *ALPHAL* (Figure K4.3-2a) results from increasing the capillary "hold" on water in the drift walls. The negative effects for *SEEPPRMN* and *SEEPPRM* (Figures K4.3-1e,f and K4.3-2a) result from their role in increasing water flow around the drifts. Finally, increasing *SEEPUNC* tends to increase seepage into the EBS through an upscaling of base seepage rates (Figures K4.3-1e,f and K4.3-2a); however, *SEEPUNC* has no effect after 10,000 yr as shown by its PRCC dropping to 0 after this time (Figure K4.3-1e,f). Several spurious variables with no significant effect on the final R^2 values are also selected at the end of the regressions in Figure K4.3-2a.

The dominant effect of *INFIL* can also be seen in the 1,000 yr scatterplots in Figure K4.3-2b,c,d,e; similar patterns of behavior also exist at later times as indicated by the variables selected in the regression analyses for 50,000 and 100,000 yr (Figure K4.3-2a).

Results for the other percolation bins are similar to those shown in Figures K4.3-1 and K4.3-2 for percolation bin 3. However, given the interest in and potential importance of seepage into the repository, seepage rates (i.e., *SPRATECS* and *SPRATECD*) for the other percolation bins are presented without discussion in Figures K4.3-3 and K4.3-4.

Temperature in Drifts: *TMPCSWL*, *TMPCSWP*, *TMPCSINV*, *TMPCDWL*, *TMPCDWP*, *TMPCDINV*. The uncertainty and sensitivity analyses for drift temperatures (ºC) in percolation bin 3 are summarized in Figure K4.3-5. Specifically, the following results are presented: temperatures for CSNF WPs at the drift wall (*TMPCSWL*), on the WP (*TMPCSWP*) and in the invert beneath the WP (*TMPCSINV*) and similarly temperatures for CDSP WPs at the drift wall (*TMPCDWL*), on the WP (*TMPCDWP*) and in the invert beneath the WP (*TMPCDINV*).

Because of the use of a representative WP to determine the drift-wall temperature in each percolation bin (see Section 6.3.2.2.2), the uncertainty in drift temperature is determined entirely by the variables *INFIL* (infiltration level) and *THERMCON* (host rock thermal conductivity level). The variables *INFIL* and *THERMCON* have 4 and 3 levels, respectively. Specifically, *INFIL* takes on values of 1, 2, 3 and 4, with these values serving as pointers to different time-dependent flow fields, and *THERMCON* takes on values of 1, 2 and 3, with these values serving as pointers to different levels of thermal conductivity in the region surrounding the drifts. In turn, seven heat flow fields were calculated and mapped to the 12 (i.e., 4×3) combinations of *INFIL* and *THERMCON*; the mapping is summarized in Section 6.3.2.2, and is described in detail in *Multiscale Thermohydrologic Model* (SNL 2007 [DIRS 181383], Section 6.3.15[a]). For the sensitivity analysis, these seven heat flow fields are indexed by the variable *TH_INFIL*, which has the possible values of 1, 2, …, 7, corresponding to the seven uncertainty cases computed by the Multiscale Thermohydrology Model. Each possible value for *TH_INFIL* indicates the heat flow field to be used for a specific sample element. In turn, *TH_INFIL* is a function of *INFIL* and *THERMCON* defined by

TH_INFIL = 1 if [*INFIL*, *THERMCON*] = [2, 3], [3, 3] or [4, 2] (uncertainty case P90)

TH_INFIL = 2 if [*INFIL*, *THERMCON*] = [4,3] (uncertainty case P90H)

TH_INFIL = 3 if [*INFIL*, *THERMCON*] = [3,2] (uncertainty case P50)

TH_INFIL = 4 if [*INFIL*, *THERMCON*] = [2,2], [4,1] (uncertainty case P30)

TH_INFIL = 5 if [*INFIL*, *THERMCON*] = [1,1], [2,1] (uncertainty case P10L)

TH_INFIL = 6 if [*INFIL*, *THERMCON*] = [1,3] (uncertainty case P10H)

TH_INFIL = 7 if [*INFIL*, *THERMCON*] = [1,2], [3,1] (uncertainty case P10),

where the uncertainty case descriptions are provided in *Multiscale Thermohydrologic Model* (SNL 2007 [DIRS 181383], Section 6.3.15[a]). As inspection of Figure K4.3-5 shows, the values for *TMPCSWL*, *TMPCSWP*, *TMPCSINV*, *TMPCDWL*, *TMPCDWP* and *TMPCDINV* are completely determined by *TH_INFIL*, with the same temperature values used for both dripping and nondripping conditions. The results for all 300 sample elements are shown in Figure K4.3-5, but only 7 curves appear in each plot frame as a result of the mapping associated with *TH_INFIL*. Overall, higher values for *INFIL* and *THERMCON* tend to be associated with lower temperatures. The temperatures associated with CSNF WPs are slightly higher than those associated with CDSP WPs, but the difference is not large. Similar temperature behavior occurs in all 5 percolation bins; also, dripping and nondripping conditions have the same temperature values for a given value for *TH_INFIL*.

Relative Humidity in Drifts: *RHCSWP*, *RHCSINV*, *RHCDWP*, *RHCDINV*. The uncertainty and sensitivity analyses for relative humidity in percolation bin 3 are summarized in Figure K4.3-6. Specifically, the following relative humidity results are presented: on the WP (*RHCSWP*) and in the invert beneath the WP (*RHCSINV*) for CSNF WPs and, similarly, on the

WP (*RHCDWP*) and in the invert beneath the WP (*RHCDINV*) for CDSP WPs. As for the temperature results in Figure K4.3-5, the uncertainty in *RHCSWP*, *RHCSINV*, *RHCDWP* and *RHCDINV* is completely determined by the heat flow fields indexed by *TH_INFIL*. The results for all 300 sample elements are shown in Figure K4.3-6, but only 7 curves appear in each plot frame as a result of the mapping associated with *TH_INFIL*. Because of assumed thermal effects, relative humidities associated with CDSP WPs tend to be higher at early times than those associated with CSNF WPs. Similar temperature behavior occurs in all 5 percolation bins; also, dripping and nondripping conditions have the same relative humidity values for a given value for *TH_INFIL*.

Partial Pressure of CO_2 in Invert: *PCO2CSIA*, *PCO2CSIN*, *PCO2CDIA*, *PCO2CDIN*. The uncertainty and sensitivity analyses for the partial pressure of CO_2 (bars) in the invert in percolation bin 3 are summarized in Figures K4.3-7 and K4.3-8. Specifically, time-dependent partial pressure results for CSNF WPs under dripping conditions (*PCO2CSIA*) are presented in Figure K4.3-7a,c and corresponding results for CDSP WPs (*PCO2CDIA*) are presented in Figure K4.3-7b,d. As examination of preceding results shows, there is little difference in the partial pressure results for CSNF and CDSP WPs. Similar results were also obtained for nondripping conditions (i.e., for *PCO2CSIN* and *PCO2CDIN* for CSNF and CDSP WPs, respectively, under nondripping conditions); the results are also similar for all 5 percolation bins. The partial pressures initially divide into two groups, which then monotonically converge through time to a partial pressure of 0.001 bar. The grouping of partial pressures results from the use of two bounding models that determine the minimum and maximum values for the partial pressure of CO_2 (bars) in the invert (SNL 2007 [DIRS 177412], Section 6.3.2.8). At each time, partial pressure in the invert is calculated by linearly interpolating between the ambient value of 10^{-3} bar and one of the bounding models, which is selected by the sign of the sampled value of the variable *DELPPCO2* (scale factor used to incorporate uncertainty into the value for the partial pressure of CO_2); the linear interpolation is based on the absolute value of *DELPPCO2*.

The PRCCs in Figure K4.3-7e,f indicate that the uncertainty in *PCO2CSIA* and *PCO2CDIA* is dominated by *DELPPCO2*, with *PCO2CSIA* and *PCO2CDIA* increasing as *DELPPCO2* increases. The dominance of *DELPPCO2* with respect to the uncertainty in *PCO2CSIA* and *PCO2CDIA* is also apparent in the regressions for *PCO2CSIA* in Figure K4.3-8a (i.e., models containing only *DELPPCO2* have R^2 values of 0.99, 0.94 and 0.92) and in the associated scatterplots in Figure K4.3-8b,c. The scatterplots in Figure K4.3-8b,c demonstrate the effect of the linear interpolation between ambient and minimum or maximum partial pressure of CO_2 (bars) using the sampled values of *DELPPCO2*. The banding evident in Figure K4.3-8c for positive values of *DELPPCO2* arises because of differences in temperature among CSNF WPs, which in turn is due to the value for *TH_INFIL* for each sample element. For *TH_INFIL*=1 and *TH_INFIL*=2 (see Figure K4.3-5e), the lower temperatures at 10,000 yr result in the lower band of values for *PCO2CSIA* for positive values of *DELPPCO2*. The scatterplots in Figure K4.3-8b,c also indicate the effects of variables that collectively determine the equilibrium of the gas and aqueous phases of CO_2 at the evaporation front, which include starting water (*SEEPWAT*) and variables which determine temperature, i.e., infiltration level (*INFIL*) and thermal conductivity (*THERMCON*) (SNL 2007 [DIRS 177412], Section 6.15.1).

Ionic Strength in Invert: *ISCSINAD*, *ISCSINND*, *ISCDINAD*, *ISCDINND*. The uncertainty and sensitivity analyses for ionic strength in percolation bin 3 are summarized in Figures K4.3-9, K4.3-10 and K4.3-11. Specifically, the following ionic strength results are presented: in the invert beneath the WP for CSNF WPs under dripping (*ISCSINAD*) and nondripping (*ISCSINND*) conditions (Figure K4.3-9a,b,c,d) and, similarly, in the invert beneath the WP for CDSP WPs under dripping (*ISCDINAD*) and nondripping (*ISCDINND*) conditions (Figure K4.3-10 a,b,c,d). Further, sensitivity analysis results are presented in Figures K4.3-9 e,f (PRCCs for *ISCSINAD* and *ISCSINND*), K4.3-10 (PRCCs for *ISCDINAD* and *ISCDINND*), and K4.3-11 (stepwise rank regression analyses and scatterplots for *ISCSINAD*).

The analyses for *ISCSINAD*, *ISCSINND*, *ISCDINAD* and *ISCDINND* are similar up to the time of DS failure between approximately 260,000 and 300,000 yr (Figures K4.3-9 a,b,c,d and K4.3-10 a,b,c,d; see Figure 4.2-1a for DS failure times). Over the time period prior to approximately 3,000 yr, the values for *ISCSINAD*, *ISCSINND*, *ISCDINAD* and *ISCDINND* are determined primarily by temperatures in the repository, which are indexed by the variable *TH_INFIL* (Figures K4.3-9 a,b,c,d and K4.3-10 a,b,c,d). In turn, *TH_INFIL* is a function of the variables *INFIL* (infiltration level) and *THERMCON* (host rock thermal conductivity level), which is why *INFIL* and *THERMCON* appear in the PRCC analyses prior to approximately 3,000 yr. After 3,000 yr and until the time of DS failure, the values for *ISCSINAD*, *ISCSINND*, *ISCDINAD* and *ISCDINND* for the individual sample elements are almost constant and vary within approximately an order of magnitude (i.e., 5×10^{-3} to 5×10^{-2} mol/kg) across sample elements (Figures K4.3-9 a,b,c,d and K4.3-10 a,b,c,d). During this time, *SEEPWAT* (indicator variable for seepage water type) and *RHI85* (scale factor for ionic strength at humidities above 85 percent; as sampled, *RHI85* is the logarithm of the indicated scale factor) are indicated as having positive effects on *ISCSINND* and *ISCDINND* (Figures K4.3-9e and K4.3-10e). The variables *INFIL* and *THERMCON* also continue to have negative effects on *ISCSINAD* and *ISCSINND* (Figure K4.3-9e,f) and similar but lesser effects on *ISCDINAD* and *ISCDINND* (Figure K4.3-10e,f).

The behavior of *ISCSINAD* and *ISCDINAD* undergoes substantial change at the time of DS failure (Figures K4.3-9 b,d and K4.3-10 b,d), typically around 300,000 years. Specifically, *ISCSINAD* and *ISCDINAD* show sudden increases in value after DS failure. This jump is due to changing the model for determining chemistry in the invert from the EBS Chemical Environment Submodel (Section 6.3.4.2.2) to the In-Package Chemistry Submodel (Section 6.3.7.2.2). This change should have been made only for realizations in which general corrosion patches in the WP outer barrier allow advection through the waste, but due to an error in the GoldSim component of the TSPA-LA Model, all realizations experience the change in models (see Appendix P, Section P5, for a discussion of the error and its effects on the TSPA-LA Model results). An additional step change is evident at later times, after about 500,000 years. This step change is due to switching from vapor influx conditions in the In-Package Chemistry Submodel to liquid influx conditions, which has the effect of lowering the calculated ionic strength.

Although it is hard to read in Figures K4.3-9f and K4.3-10f, *WDDSAGGC* (rate of aggressive general corrosion on the top of the DS, nm/yr) and *WDDSBEGC* (rate of benign general corrosion on the bottom of the DS, nm/yr) (Figure K4.2-1b,c,d) show a brief period of positive effect over the period of DS failure as a result of the jump in the values for *ISCSINAD* and *ISCDINAD* at the time of DS failure. After DS failure, the uncertainty in *ISCSINAD* is

dominated by *ISCSNS* (pointer variable used to determine ionic strength in CSNF WP Cell 1 under vapor influx conditions), and the uncertainty in *ISCDINAD* is dominated by *IS2MCONS* (pointer variable used to determine ionic strength in CDSP WP Cell 2MCO, i.e., Cell 1b, under vapor influx conditions). The vapor influx model is significant even after DS failure because early corrosion failures of WPs generally occur as stress corrosion cracking rather than as a result of general corrosion. As WPs fail by general corrosion, patches open on the WP outer barrier that allow seepage water to flow into the WPs. This effect is evident by the increasing importance of *WDGCA22* (temperature dependence coefficient associated with the general corrosion rate for alloy 22, K) after 500,000 yr. As patches open, the ionic strength is determined by liquid influx conditions with the result that *ISCSNS* becomes less significant.

More detailed sensitivity analyses for *ISCSINAD* based on stepwise rank regression and the examination of scatterplots are presented in Figure K4.3-11.

pH in Invert: *PHCSINAD*, *PHCSINND*, *PHCDINAD*, *PHCDINND*. The uncertainty and sensitivity analyses for pH in the invert for CSNF WPs experiencing nondripping conditions (*PHCSINND*) and dripping conditions (*PHCSINAD*) in percolation bin 3 under nominal conditions are summarized in Figures K4.3-12 and K4.3-13. Further, Figure K4.3-14 provides a summary analogous to the summary in Figure K4.3-12 for pH in the invert for CDSP WPs experiencing nondripping conditions (*PHCDINND*) and dripping conditions (*PHCDINAD*) in percolation bin 3 under nominal conditions.

The time dependent behavior of pH in the invert is similar for both CSNF and CDSP WPs (Figures K4.3-12a,b,c,d and K4.3-14a,b,c,d), with pH showing a bifurcated behavior into a high and a low range of values until the occurrence of DS failures between 260,000 and 300,000 yr. This bifurcation is most obvious prior to 1,000 yr but continues to be visually apparent out to the time of DS failure (Figures K4.3-12a,b,c,d and K4.3-14a,b,c,d).

Neither the PRCCs in Figures K4.3-12e,f and K4.3-14e,f nor the regression analyses in Figure K4.3-13a,b provide a clear indication of the reason for this bifurcated behavior. However, these analyses do indicate that *SEEPWAT* (indicator variable for seepage water type), *RHPH0* (uncertainty factor for pH of in-drift waters at relative humidities less than 65 percent), and *RHPH75* (uncertainty factor for pH of in-drift waters at relative humidities greater than 75 percent) are affecting *PHCSINND*, *PHCSINAD*, *PHCDINND* and *PHCDINAD* prior to DS failure. Fortunately, the needed insights as to what is causing the bifurcated behavior can be obtained by examining the scatterplots involving *SEEPWAT* and *RHPH75* in Figure K4.3-13c,d,e,f,g,h. These scatterplots show that pH divides into high and low values on the basis of seepage water type as specified by *SEEPWAT*. Specifically, high pH values are associated with seepage water type 1, and low pH values are associated with seepage water types 2, 3 and 4 (Figure K4.3-13c,e,g). For a given seepage water type, the uncertainty factors *RHPH0* and *RHPH75* define linear scalings of a base pH value (Figure K4.3-13d,f,h). This scaling is particularly obvious in Figure K4.3-13d,h but is less obvious in Figure K4.3-13f as a result of the presence of different relative humidity conditions at 1,000 yr for different LHS elements. The grouping of pH values associated with each seepage water type into a few distinct, parallel lines, as evident in the scatterplot in Figure K4.3-13d, results from the interpolation technique implemented in the TSPA-LA Model. In particular, pH is determined by interpolation using

tables of values provided in *Engineered Barrier System: Physical and Chemical Environment* (SNL 2007 [DIRS 177412]), with the independent variables being relative humidity, temperature, partial pressure of CO_2, and water-rock interaction parameter. The interpolation is not simultaneous in all four variables. Rather, the relative humidity is determined first, and is then used as a constant in the interpolation involving the other three variables. Because pH is quite sensitive to small changes in relative humidity when relative humidity is very close to unity, this calculation scheme results in the data grouping observed in Figure K4.3-13d.

The PRCC and stepwise analyses correctly identify that *PHCSINND*, *PHCSINAD*, *PHCDINND* and *PHCDINAD* prior to DS failure as being affected by *SEEPWAT*, *RHPH0* and *RHPH75*. However, the effects are indicated as being smaller than they really are as shown by the scatterplots in Figure K4.3-13c,d,e,f,g,h. The reason for this performance is the introduction of complex patterns through the effects of discrete variables that the effectively linear analyses with PRCCs and stepwise rank regressions cannot capture. However, the underlying patterns are revealed by the associated scatterplots. Fortunately, this is often the case when stepwise regression fails to produce a model with a high R^2 value.

There is no change in the behavior of *PHCSINND* and *PHCDINND* after DS failure (Figures K4.3-12a,c and K4.3-14a,c). However, the behavior of *PHCSINAD* and *PHCDINAD* changes significantly after DS failure (Figures K4.3-12b,d and K4.3-14b,d). After DS failure in a dripping location, the chemistry of water in the invert should be determined by the in-package chemistry model if advection occurs through the waste. Otherwise, the invert chemistry model is applied. However, the version of the TSPA-LA model that produced the results displayed in this appendix contains an error discovered after calculations were completed in that, after DS failure in a dripping location, the chemistry of water in the invert is always determined by the in-package chemistry model (see Appendix P Section P5 for a discussion of the error and its effects on the TSPA-LA Model results). The in-package chemistry model computes pH using one of two submodels for estimating water inside the package: a vapor influx model and a liquid influx model. Once the in-package chemistry model is in use (after DS failure), pH is computed using the vapor influx model until general corrosion results in a patch opening in the WP outer barrier, after which time the liquid influx model is used. Hence, the uncertainty in *PHCSINAD* and *PHCDINAD* after DS failure is determined primarily *WDGCA22* (temperature dependence coefficient associated with the general corrosion rate for alloy 22, K) and *PH2RGER* (error term in regression equation used to determine pH of corrosion products domain), with the effects of *WDGCA22* acting as a switch to divide *PHCSINAD* and *PHCDINAD* into two sets of results (vapor influx model for in-package pH and liquid influx model for in-package pH) and *PH2RGER* defining a linear scaling of pH within each set (Figure K4.3-13i,j).

K4.4 Nominal Scenario Class: Release Results for Engineered Barrier System, Unsaturated Zone and Saturated Zone

Release results are available for individual radioactive species for the EBS, the UZ and the SZ. For the nominal scenario class, these results are completely dominated by the time and extent of WP failure, which in turn is determined by *WDGCA22* (temperature dependence coefficient associated with the general corrosion rate for alloy 22, K). As a result, the effects of the physical processes associated with radionuclide transport through the EBS, the UZ and the SZ tend to be obscured by the dominant effects of *WDGCA22*. Because of this, the nominal scenario class

results for the EBS, the UZ and the SZ provide less informative uncertainty and sensitivity analysis results than can be obtained from release results calculated for other scenario classes. For this reason, extensive presentation and discussion of uncertainty and sensitivity analysis results for radionuclide transport in the EBS, the UZ and the SZ will be deferred to later sections.

For perspective on the dominant role played by *WDGCA22* for the nominal scenario class, uncertainty and sensitivity analysis results for the release rate (*ESNP237*, g/yr) and cumulative (i.e., integrated) release (*ESNP237C*, g) of ^{237}Np from the EBS are presented and briefly discussed (Figures K4.4-1 and K4.4-2).

Prior to 400,000 yr, *ESNP237* and *ESNP237C* are very small (Figure K4.4-1a,b,c,d). For example, almost all values for *ESNP237* are less than 10^{-3} g/yr at 400,000 yr (Figure K4.4-1a). The limited release of ^{237}Np from the EBS prior to 400,000 yr results from the absence of DS failures prior to approximately 260,000 yr and the limited number of WP failures prior to 200,000 yr (see Figures K4.2-1a and K4.2-2a). By 300,000 yr, all DSs have failed and the number of failed WPs steadily increases (see Figures K4.2-1a and K4.2-2a). As a result, *ESNP237* tends to show a monotonic increase with time, although there is some nonmonotonicity, especially prior to approximately 500,000 yr, when the release of highly mobile species from the failure of individual WPs still has the potential to dominate the value for *ESNP237*. With increasing time and hence increasing numbers of failed WPs, the value for *ESNP237* tends to be dominated by the slower releases from a large number of previously failed WPs rather than by the quicker releases of highly mobile species from recently failed WPs. As a result, *ESNP237* tends to become increasing monotonic with increasing time.

The sensitivity analysis results for *ESNP237* and *ESNP237C* are very similar. For example, the analysis based on PRCCs in Figure K4.4-1e,f identifies *WDGCA22* as the most important variable with respect to both *ESNP237* and *ESNP237C*, with *ESNP237* and *ESNP237C* decreasing as *WDGCA22* increases. This effect results because increasing *WDGCA22* decreases both the number of failed WPs and the total failed area on failed WPs (see Figures K4.2-2 to K4.2-7). The next most important variable indicated in the analyses with PRCCs is *EP1NPO2* (scale factor used to incorporate uncertainty into NpO_2 solubility below 1 molal ionic strength; as sampled, *EP1NPO2* is actually the logarithm of the indicated scale factor), with *ESNP237* and *ESNP237C* increasing as *EP1NPO2* increases. This effect results because increasing *EP1NPO2* increases the concentration of dissolved ^{237}Np in the EBS, which in turn results in larger values for *ESNP237* and *ESNP237C*.

In addition, the analyses with PRCCs also identify smaller effects for the following four variables: *PHCSNS* (pointer variable used to determine pH in CSNF cell 1 under nondripping conditions), *GOESITED* (density of sorption sites on goethite, sites/nm^2), *WDZOLID* (scale factor used to incorporate uncertainty into the stress intensity factor for closure-lid weld), and *CORRATSS* (stainless steel corrosion rate, μm/yr). The negative effects associated with *PHCSS*, *GOESITED* and *CORRATSS* result because (i) increasing *PHCSNS* reduces the solubility of neptunium in CSNF WPs and thus reduces the dissolved concentration ^{237}Np, (ii) increasing *GOESITED* increases the sorption of neptunium onto goethite and thus reduces the dissolved concentration ^{237}Np, and (iii) increasing *CORRATSS* increases the generation of corrosion products, which turn results in more sorption sites in the WP. The positive effect associated with

WDZOLID results because increasing *WDZOLID* increases the stress at the closure lid, which in turn increases the number of WP failures.

More detailed sensitivity analysis results for *ESNP237* and *ESNP237C* are provided by the regression results in Figure K4.4-2a,b. Specifically, *WDGCA22* is the dominant variable in all six regression analyses in Figure K4.4-2a,b with R^2 values between 0.71 and 0.74. Overall, the results in the regression analyses are very similar to the results obtained with PRCCs. With some minor variations, the regressions initially pick the same six variables as the analyses with PRCCs. After the selection of six variables, the individual regression analyses have R^2 values between 0.80 and 0.86. The incremental R^2 values with the addition of each variable to a regression model provide an indication of variable importance. As examination of the individual regressions shows, the effects of the individual variables selected after *WDGCA22* on the uncertainty in *ESNP237* and *ESNP237C* is relatively small (i.e., incremental R^2 values between 0.05 and 0.01). However, a number of variables with small effects are identified, with the result that the final regression models contain from 10 to 16 variables and have R^2 values from 0.83 to 0.92. The regressions at 400,000 yr have the smaller R^2 values because of the presence of many zero values for *ESNP237* and *ESNP237C* that result from the absence of WP failures for many sample elements, which in turn creates patterns that are difficult for the regression techniques in use to capture.

The dominant effect of *WDGCA22* on *ESNP237* and *ESNP237C* and the lesser effects of *EP1NPO2* and *PHCSNS* on *ESNP237* and *ESNP237C* can be seen in the scatterplots in Figure K4.4-2c,d,e,f,g,h.

K4.5 Nominal Scenario Class: Dose to Reasonably Maximally Exposed Individual

The uncertainty and sensitivity analyses for total dose to the RMEI (*DOSTOT*, mrem/yr) are summarized in Figures K4.5-1 and K4.5-2. Nonzero values for *DOSTOT* begin at about 200,000 yr as a result of WP failure and then show a general tendency to increase (Figure K4.5-1a,b). However, some dose curves and especially some of the curves with the largest values for *DOSTOT*, change from increasing to decreasing at some point in time. This change results from inventory depletion, and hence decreasing or terminating releases, for highly mobile species such as ^{99}Tc and ^{129}I. All curves remain below 10 mrem/yr.

The PRCCs in Figure K4.5-1c indicate that the uncertainty in *DOSTOT* is dominated by *WDGCA22* (temperature dependence coefficient associated with the general corrosion rate for alloy 22, K), with *DOSTOT* tending to decrease as *WDGCA22* increases. This effect results because the general corrosion rate for alloy 22 decreases as *WDGCA22* increases. Smaller effects are indicated for *SCCTHR* (stress corrosion cracking threshold, MPa), *WDZOLID* (scale factor used to incorporate uncertainty into the stress intensity factor for closure-lid weld), *THERMCON* (host rock thermal conductivity level), *WDNSCC* (stress corrosion cracking growth rate exponent), and *INRFRCTC* (initial release fraction for ^{99}Tc in a CSNF WP). The variables *SCCTHR*, *WDZOLID*, *THERMCON* and *WDNSCC* affect *DOSTOT* through their effects on WP failure. Specifically, increasing *SCCTHR* increases the stress level at which stress corrosion cracking initiates and thus reduces failures at the closure-lid weld; increasing *WDZOLID* increases the stress at the closure lid and thus increases failures at the closure-lid weld;

increasing *THERMCON* tends to lower WP temperatures and thus reduce the rate of corrosion; and increasing *WDNSCC* tends to increase the threshold stress intensity factor, which determines the threshold stress at which stress corrosion cracks propagate, and thus to reduce failures at the closure-lid weld. The variable *INRFRCTC* has small effects that are initially positive and then negative on *DOSTOT*. This pattern results because increasing *INRFRCTC* increases the releases of ^{99}Tc at the time of initial WP failure, which causes *INRFRCTC* to have a positive effect on *DOSTOT* at early times. However, early releases of ^{99}Tc reduce the amount of ^{99}Tc that can be released at later points in time, with the result that increasing *INRFRCTC* has a negative effect on *DOSTOT* at later times.

More detailed sensitivity analysis results for *DOSTOT* are provided by the regression results in Figure K4.5-2a. Specifically, *WDGCA22* is the dominant variable with R^2 values of 0.77, 0.84 and 0.60. Actually, the indicated R^2 values tend to under represent the effect of *WDGCA22* because of the nonlinear relationship between *WDGCA22* and *DOSTOT* that can be seen in Figure K4.5-2b and is more apparent in Figure K4.5-3. Specifically, large values of *WDGCA22* result in small values for *DOSTOT* at late times because of limited WP failure and hence limited radionuclide releases, and small values of *WDGCA22* result in small values for *DOSTOT* at late times because of extensive, early WP failure and the resultant reduction in radionuclide inventory by late times.

In addition to *WDGCA22*, the regressions in Figure K4.5-2a indicate small effects for the following variables that affect WP failure: *WDZOLID*, *THERMCON*, *INFIL* (infiltration level), *SCCTHR*, *WDNSCC*, and *WDGCUA22* (pointer variable used to select the distribution of base corrosion rates of alloy 22 at 60 ºC over the patches on the WPs). The effects of *WDZOLID*, *THERMCON*, *SCCTHR* and *WDNSCC* have already been discussed in conjunction with Figure K4.5-1c. Like *THERMCON*, the negative effect associated with *INFIL* probably results because increased values for *INFIL* result in lower WP temperatures and thus lower rates of corrosion. The variable *WDGCUA22* has a small positive effect on the uncertainty in *DOSTOT*. Specifically, *WDGCUA22* is a pointer variable used to select from three uncertain distributions that derive from both the uncertainty in a base corrosion rate for alloy 22 at 60 ºC and the uncertainty that exists in the prediction of small scale variability in chemical and physical conditions across patches used in the modeling of WP degradation. Increasing *WDGCUA22* results in higher overall corrosion rates and thus higher values for *DOSTOT*. The dominance of *WDGCA22* with respect to the uncertainty associated with *DOSTOT* can be seen in the scatterplots in Figure K4.5-2b,c,d.

The regressions in Figure K4.5-2a also indicate very small effects of several variables related physical processes. However, the effects of these variables are minor given the much larger effects of variables related to WP failure and, in particular, the dominant effect of *WDGCA22* on WP failure.

K5 EARLY FAILURE SCENARIO CLASSES

K5.1 Early Failure Scenario Classes: Summary

The early failure scenario classes are defined on the basis of futures that involve one or more early failure events (Section J6). This section (Section K5) presents uncertainty and sensitivity

analysis results for selected analysis outcomes associated with the early failure scenario classes (Table K5.1-1).

The primary results considered for the early failure scenario classes are radionuclide movement from the EBS to the UZ (Table K5.1-2), radionuclide movement from the UZ to the SZ (Table K5.1-3), radionuclide movement in the SZ at the location of the RMEI (Table K5.1-4), dose to the RMEI from selected radionuclides (Table K5.1-5), and expected dose to the RMEI from all radionuclides (Table K5.1-6). High-level summaries of the uncertainty and sensitivity analysis results presented in this section are provided in Tables K5.1-2 to K5.1-6. Particular emphasis is given to releases from the EBS to the UZ (Table K5.1-2). Additional uncertainty analysis results are also available in Section J6.

From a regulatory perspective, expected dose to the RMEI (*EXPDOS*, mrem/yr) is the analysis outcome of greatest interest associated with the early failure classes (Table K5.1-6).

For the early DS failure scenario class, *EXPDOS* tends to show a sharp early peak prior to 1,000 yr and then monotonically decrease over the time (Figures K5.7.1-1, K5.7.1-3). The observed range of possible values for *EXPDOS* over the time interval [0, 10^6 yr] is approximately [10^{-8}, 0.02 mrem/yr] (Figure K5.7.1-1, K5.7.1-3). For the [0, 20,000 yr] time interval, the dominant variable contributing to the uncertainty in *EXPDOS* for the early DS failure scenario class is *PROBDSEF* (probability that a randomly selected DS will experience an early failure) (Figures K5.7.1-1, K5.7.1-2). For the [0, 10^6 yr] time interval, *INFIL* (infiltration level) is also an important contributor to the uncertainty in *EXPDOS* (Figures K5.7.1-3, K5.7.1-4). A number of additional variables also have small effects on *EXPDOS*.

For the early WP failure scenario class, *EXPDOS* shows two distinct patterns of behavior (Figure K5.7.2-1). Prior to 10^4 yr, *EXPDOS* is dominated by the failure of CDSP WPs and generally falls in the range [10^{-5}, 0.1 mrem/yr]; after 10^4 yr, *EXPDOS* is dominated by the failure of CSNF WPs and generally falls in the range [10^{-4}, 1 mrem/yr] as the failures of the CSNF WPs result in dose to the RMEI. This effect can be seen in the sharp jump in the values for *EXPDOS* that takes place shortly after 10^4 yr (Figure K5.7.2-1). This effect results from the delayed releases from the hotter CSNF WPs. However, the uncertainty in *EXPDOS* over the time interval [0, 20,000 yr] is dominated by *PROBWPEF* (probability that a randomly selected WP will experience an early failure) (Figures K5.7.2-1, K5.7.2-2). After initial peaks, *EXPDOS* tends to decrease with time, although there is a jump in values at beginning at about 2.6×10^5 yr as the DSs start to fail. At 5×10^5 yr, values for *EXPDOS* fall in the range [10^{-6}, 0.1 mrem/yr] (Figure K5.7.2-3). At later times, *PROBWPEF* remains the most important variable with respect to the uncertainty in *EXPDOS*; however, a number of additional variables also have effects (Figures K5.7.2-3, K5.7.2-4).

Expected dose to the RMEI from both early DS failure and early WP failure is also determined (Figures K5.7.3-1, K5.7.3-2, K5.7.3-3, K5.7.3-4). However, as a result of the expected doses from early WP failures being substantially larger than the expected doses from early DS failures, the combined results for expected dose from early WP and early DS failures are similar to the results for early WP failure alone (Figures K5.7.2-1, K5.7.2-2, K5.7.2-3, K5.7.2-4).

An additional analysis considers expected dose to the RMEI from early DS failure, early WP failure and nominal process WP failure (Figures K5.7.4-1, K5.7.4-2). In this case, the results prior to about 2×10^5 yr are essentially the same as the early WP failure analyses and the results after 2×10^5 yr are essentially the same as the analyses for nominal conditions.

K5.2 Early Failure Scenario Classes: Engineered Barrier System Conditions

The environmental conditions in the EBS after early WP failures are the same as discussed and illustrated in Section K4 for nominal conditions.

For early DS failures under dripping conditions, the seepage rates, EBS temperatures, relative humidities and partial pressures for CO_2 are the same as for nominal conditions. However, the ionic strength and pH in the invert associated with a failed DS under dripping conditions are different from the values present in the absence of a failed DS under dripping conditions (i.e., compare results in Figures K5.2-1 and K5.2-2 with the corresponding 0 to 20,000 yr results in Figures K4.3-9, K4.3-10 and K4.3-12).

The uncertainty results for time-dependent ionic strength (mol/kg) in the invert for CSNF WPs (*ISCSINAD*) and CDSP WPs (*ISCDINAD*) experiencing an early DS failure under dripping conditions in percolation bin 3 are similar (Figure K5.2-1a,b). The transient behavior before about 600 yr results from the thermal evolution of the WPs. While the WPs are above 100 ºC ionic strength is not computed because no liquid water is present in the waste. During this time period the ionic strength variable is assigned an artificial value of 1.0 to indicate in Goldsim that ionic strength is not computed. The uncertainty in the ionic strength results is dominated by *ISCSS* (pointer variable used to determine ionic strength in CSNF WP Cell 1 under dripping conditions) for CSNF WPs (Figure K5.2-1e) and by *IS2MCOS* (pointer variable used to determine ionic strength in CDSP WP Cell 2MCO, i.e., Cell 1b, under dripping conditions) for CDSP WPs (Figure K5.2-1f), with ionic strength increasing as each of these variables increases.

The uncertainty results for time-dependent pH in the invert for CSNF WPs (*PHCSINAD*) and CDSP WPs (*PHCDINAD*) experiencing an early DS failure under dripping conditions in percolation bin 3 are similar (Figure K5.2-2a,b). The uncertainty in both *PHCSINAD* and *PHCDINAD* is dominated by *PH2RGER* (error term in regression equation for pH of corrosion product domain) and *DELPPCO2* (scale factor used to incorporate uncertainty into the value for the partial pressure of CO_2), with increasing *PH2RGER* having a strong positive effect on *PHCSINAD* and *PHCDINAD* and increasing *DELPPCO2* having a strong negative effect on *PHCSINAD* and *PHCDINAD*.

K5.3 Early Failure Scenario Classes: Release from Engineered Barrier System

This section contains analysis results for EBS releases over the time interval [0, 20,000 yr] resulting from:

- Early DS failure over a CDSP WP in percolation bin 3 under dripping conditions (Section 5.3.1);

- Early DS failure over a CSNF WP in percolation bin 3 under dripping conditions (Section 5.3.2);
- Early failure of a CDSP WP in percolation bin 3 under dripping conditions (Section 5.3.3);
- Early failure of a CSNF WP in percolation bin 3 under dripping conditions (Section 5.3.5).
- For the time interval [0, 1,000,000 yr] results are presented for:
- Early DS failure over a CDSP WP in percolation bin 3 under dripping conditions (Section 5.3.7);
- Early DS failure over a CSNF WP in percolation bin 3 under dripping conditions (Section 5.3.8);
- Early failure of a CDSP WP in percolation bin 3 under dripping conditions (Section 5.3.9);
- Early failure of a CDSP WP in percolation bin 3 under non-dripping conditions (Section 5.3.10);
- Early failure of a CSNF WP in percolation bin 3 under dripping conditions (Section 5.3.11);
- Early failure of a CSNF WP in percolation bin 3 under non-dripping conditions (Section 5.3.12).

K5.3.1 Early Failure Scenario Classes: Release from Engineered Barrier System over the Time Interval [0, 20,000 yr] for Early Drip Shield Failure above a CDSP WP

Movement of ^{239}Pu Irreversibly Attached to Glass (i.e., Ic) Colloids: *ESIC239* and *ESIC239C*. The uncertainty and sensitivity analyses for the time-dependent release rates (*ESIC239*, g/yr) and cumulative releases (*ESIC239C*, g) over the time interval [0, 20,000 yr] for the movement of ^{239}Pu irreversibly attached to glass (i.e., Ic) colloids from the EBS to the UZ resulting from the early failure of one DS above a CDSP WP in percolation bin 3 under dripping conditions are summarized in Figures K5.3.1-1 and K5.3.1-2.

The values for *ESIC239* are small (i.e., $< 10^{-3}$ g/yr) and tend to be constant for each period of constant infiltration (Figure K5.3.1-1a,c). As a result, the values for *ESIC239C* are also small and less than 10 g over 20,000 yr for most sample elements (Figure K5.3.1-1b,d). For some sample elements, drift-wall condensation occurring before 1,000 yr increases water flow through the affected WPs for a short period, which causes the higher releases of ^{239}Pu irreversibly attached to glass colloids during this period. More discussion is provided below in the analysis for the movement of dissolved ^{237}Np.

As indicated by the PRCCs in Figure K5.3.1-1e,f, the uncertainty in *ESIC239* and *ESIC239C* is dominated by *INFIL* (infiltration level) and *CPUCOLWF* (maximum concentration of plutonium irreversibly attached to glass colloids, mol/L), with *ESIC239* and *ESIC239C* increasing as each of these variables increases. These effects result because increasing *INFIL* increases water flow in the EBS and the UZ and increasing *CPUCOLWF* increases the amount of ^{239}Pu that can potentially be irreversibly attached to glass colloids. In addition to *INFIL* and *CPUCOLWF*, negative effects are indicated for *SEEPPRM* (mean fracture permeability in lithophysal rock units, m^2; as sampled, *SEEPPRM* is actually the logarithm of the indicated permeability) and *SEEPPRMN* (mean fracture permeability in nonlithophysal rock units, m^2; as sampled, *SEEPPRMN* is actually the logarithm of the indicated permeability). The negative effects associated with *SEEPPRM* and *SEEPPRMN* result from increasing water flow around the EBS and thus decreasing water flow through the EBS.

The variables *THERMCON* (host rock thermal conductivity level) and *DIAMCOL* (colloid particle diameter, nm) have indicated effects prior to 1,000 yr that may or may not be real. After 1,000 yr, no identifiable effects are indicated for these variables. Prior to 1,000 yr, *ESIC239* and *ESIC239C* have values of zero for many of the sample elements. Performing rank correlations where many output variables have the value zero can cause input variables to appear to have effects when they actually do not. It is also possible that the early positive effect associated with *THERMCON* results from an enhanced cooling of the repository and a resultant earlier initiation of water flow into and out of the EBS, or from a relationship between *THERMCON* and the occurrence of condensation.

More detailed sensitivity analysis results for *ESIC239* and *ESIC239C* are provided by the regression analyses in Figure K5.3.1-2a,b. Specifically, all six regressions contained in Figure K5.3.1-2a,b initially select the following five variables in the same order: *INFIL*, *CPUCOLWF*, *SEEPPRM*, *SEEPPRMN* and *ALPHAL* (capillary strength parameter in lithophysal rock units, Pa). The effects of *INFIL*, *CPUCOLWF*, *SEEPPRM* and *SEEPPRMN* on *ESIC239* and *ESIC239C* have already been discussed in conjunction with Figure K5.3.1-1e,f. Similarly to *SEEPPRM* and *SEEPPRMN*, the negative effect associated with *ALPHAL* results from increasing water diversion around the EBS. The individual regressions containing only *INFIL* and *CPUCOLWF* have R^2 values between 0.83 and 0.86; thus, these two variables account for most of the uncertainty associated with *ESIC239* and *ESIC239C*. The variables *SEEPPRM*, *SEEPPRMN* and *ALPHAL* have smaller effects, and their inclusion in the regression models produces cumulative R^2 values between 0.87 and 0.90. After the first five variables, five of the six regression analyses in Figure K5.3.1-2a,b select additional variables that have very small effects on *ESIC239* and *ESIC239C*. The selection of the pointer variable used to determine pH in cell 1 of CSNF WPs under dripping conditions (*PHCSS*) as the final variable selected in all three regressions for *ESIC239* is probably spurious.

The dominant effects of *INFIL* and *CPUCOLWF* on *ESIC239* and *ESIC239C* and the lesser effect of *SEEPPRM* can be seen in the scatterplots in Figure K5.3.1-2c,d,e,f,g,h.

Movement of ^{239}Pu Irreversibly Attached to Ferrous (i.e., If) Colloids: *ESIF239* and *ESIF239C*. Uncertainty and sensitivity analyses for the movement of ^{239}Pu irreversibly attached to ferrous colloids are not presented due to an error in the GoldSim component of the

TSPA-LA Model that affects the calculation of the stability of ferrous colloids. Consequently, Figure K5.3.1-3 and Figure K5.3.1-4 have been removed from this document. See Appendix P, Section P18, for a discussion of the error and the effect of the error on TSPA-LA Model results.

Movement of Dissolved ^{237}Np: *ESNP237* and *ESNP237C*. The uncertainty and sensitivity analyses for the time-dependent release rates (*ESNP237*, g/yr) and cumulative releases (*ESNP237C*, g) over the time interval [0, 20,000 yr] for the movement of dissolved ^{237}Np from the EBS to the UZ resulting from the early failure of one DS above a CDSP WP in percolation bin 3 under dripping conditions are summarized in Figures K5.3.1-5 and K5.3.1-6.

The values for *ESNP237* exhibit an initial pulse release prior to 1,000 yr, a subsequent increase in rates at 2,000 yr, and then a monotonic decrease with time until 10,000 yr (Figure K5.3.1-5a,c). The initial pulse occurs because of condensation on the drift wall, which adds to the seepage flux falling onto the failed WP. The Drift Wall Condensation Abstraction divides time into three stages: Stage 1 is the initial stage when all WPs in the drift are above 96°C; Stage 2 is the middle stage after the first WP in the drift cools to below 96 ºC, but before the last WP in the drift cools to below 96 ºC; and Stage 3 is the final stage after all WPs in the drift are below 96 ºC (see Section 6.3.3.2.2 for details). Condensation can begin as soon the drift wall temperature falls below 96 ºC for at least one WP in a drift, and continues until 2,000 yr. However, the condensation rate varies, with Stage 2 rates applied until the drift wall temperatures for all WPs fall below 96 ºC, and Stage 3 ratesapplied from that time until 2,000 yr. Condensation during Stage 2 is generally much larger than during Stage 3, and can be much larger than seepage during the Stage 2 period. The effect of the Stage 2 condensation is to increase water flow into a failed WP, which in turn increases the rate of mass release from the WP during Stage 2. After Stage 3, condensation greatly decreases, resulting in the drop in release rates observed at about 1,000 yr. At 10,000 yr, the climate changes from monsoon to glacial transition, and percolation rates generally increase, which in turn increases seepage and the release rate of ^{237}Np. The initial release of ^{237}Np is primarily from DSNF waste forms, which are conservatively assumed to immediately degrade when the WP is breached. The later releases of ^{237}Np are primarily from high-level radioactive waste (HLW), which degrades slowly over time, and thus allows for other processes to affect the release of ^{237}Np from the WP.

The release rates of ^{237}Np after about 1,000 years generally evolve toward a steady state value, as environmental conditions inside the WP evolve toward steady state. These environmental variables determine the solubility of ^{237}Np as a function of time. This evolution is apparent in the changing values of the PRCCs for *DELPPCO2* (scale factor used to incorporate uncertainty into the value for the partial pressure of CO_2) and *PH2MCOS* (pointer variable used to incorporate uncertainty into pH in cell 1b of CDSP WPs under dripping conditions). The steady state release rate is determined by the balance between waste form degradation and reversible sorption onto ferrous corrosion products as indicated by the PRCCs for *GOESITED* (density of sorption sites on goethite, sites/nm^2) and *HFOSA* (hydrous ferrous oxide surface area, m^2/g).

Movement of Dissolved ^{239}Pu: *ESPU239* and *ESPU239C*. The uncertainty and sensitivity analyses for the time-dependent release rates (*ESPU239*, g/yr) and cumulative releases (*ESPU239C*, g) over the time interval [0, 20,000 yr] for the movement of dissolved ^{239}Pu from

the EBS to the UZ resulting from the early failure of one DS above a CDSP WP in percolation bin 3 under dripping conditions are summarized in Figures K5.3.1-7 and K5.3.1-8.

The values for *ESPU239* display an initial pulse release prior to 1,000 yr and then a monotonic increase with time thereafter toward a steady state value (Figure K5.3.1-7a,c). The pulse occurs because of condensation on the drift wall, and the steady state release rate is due to reversible sorption on corrosion products, as explained in the discussion of ^{237}Np. The initial release of ^{239}Pu is primarily from DSNF waste forms, which are conservatively assumed to immediately degrade when the WP is breached. The later releases of ^{239}Pu are primarily from HLW, which degrades slowly over time. Much of the mobilized plutonium sorbs onto ferrous corrosion products and its subsequent release depends on the rates of desorption. However, because other radionuclides (i.e. uranium) also sorb onto the ferrous corrosion products, there is a complex interplay between the rates of waste degradation, concentrations of radionuclides in solution, and rates of sorption and desorption, which result in the slow but steady increase in the release rates of ^{239}Pu from the WP. At 20,000 yr, *ESPU239* and *ESPU239C* fall below 0.1 g/yr and 1,000 g, respectively, for all sample elements (Figure K5.3.1-7a,b,c,d).

The most important variable with respect to the uncertainty in *ESPU239* and *ESPU239C* is *EP1LOWPU* (scale factor used to incorporate uncertainty into plutonium solubility under low ionic strength conditions; as sampled, *EP1LOWPU* is actually the logarithm of the indicated scale factor), with *ESPU239* and *ESPU239C* tending to increase as *EP1LOWPU* increases (Figures K5.3.1-7e,f and K5.3.1-8a,b) This effect results because increasing *EP1LOWPU* increases the solubility limit for plutonium and hence increases the amount of dissolved ^{239}Pu that is available for movement from the EBS to the UZ. In various orders, all six regressions in Figure K5.3.1-8a,b select *EP1LOWPU*, *DELPPCO2* (scale factor used to incorporate uncertainty into the value for the partial pressure of CO_2), and *INFIL* (infiltration level) as the first three variables in the stepwise process. Both *DELPPCO2* and *INFIL* have positive effects on *ESPU239* and *ESPU239C*. Specifically, increasing *DELPPCO2* increases the solubility limit for plutonium, and increasing *INFIL* increases water flow in the EBS and UZ. The regression models containing *EP1LOWPU*, *DELPPCO2* and *INFIL* have cumulative R^2 values between 0.67 and 0.78.

After *EP1LOWPU*, *DELPPCO2* and *INFIL*, the regression analyses select a number of additional variables that have small effects on *ESPU239* and *ESPU239C* (Figure K5.3.1-8a,b). For example, the analysis for *ESPU239* at 10,000 yr selects the following 10 additional variables: *SEEPPRM* (mean fracture permeability in lithophysal rock units, m^2; as sampled, *SEEPPRM* is actually the logarithm of the indicated permeability), *SEEPPRMN* (mean fracture permeability in nonlithophysal rock units, m^2; as sampled, *SEEPPRMN* is actually the logarithm of the indicated permeability), *GOESITED* (density of sorption sites on goethite, sites/nm^2), *ALPHAL* (capillary strength parameter in lithophysal rock units, Pa), *PH2MCOS* (pointer variable used to incorporate uncertainty into pH in cell 1b of CDSP WPs under dripping conditions), *EBSDIFCF* (scale factor used to incorporate uncertainty into invert diffusion coefficient; as sampled, *EBSDIFCF* is actually the logarithm of the indicated scale factor), *PH2MCOS* (pointer variable used to incorporate uncertainty into pH in cell 1b of CDSP WPs under dripping conditions), *GP2NO3* (ratio of Cl to NO_3 in Group 2 pore waters, dimensionless), *RHPH75* (scale factor used to incorporate uncertainty into pH of in-drift waters at relative

humidities above 75 percent), *GOESA* (specific surface area for goethite, m^2/g), and *DIFPATHL* (diffusive path length from WP outer corrosion barrier to midpoint of invert, m) (Figure K5.3.1-8a). The variables *SEEPPRM*, *SEEPPRMN* and *ALPHAL* have negative effects on *ESPU239* as a result of increasing water flow around the EBS and thus reducing water flow through the EBS. The variables *GOESITED* and *GOESA* have negative effects on *ESPU239* as a result of increasing the sorption of ^{239}Pu on goethite. The variables *EBSDIFCF* and *DIFPATHL* have opposite effects on diffusion in the invert. Specifically, *EBSDIFCF* has a positive effect on *ESPU239* because diffusion in the invert increases as *EBSDIFCF* increases, and *DIFPATHL* has a negative effect on *ESPU239* because diffusion in the invert decreases as *DIFPATHL* increases. The variables *PH2MCOS* and *RHPH75* are involved in the definition of pH in the WP and the invert, respectively. The negative effects associated with *PH2MCOS* and *RHPH75* result because increasing either variable increases pH, which in most realizations decreases Pu solubility, thus decreasing *ESPU239*. Finally, the negative effect associated with *GP2NO3* is spurious as there is no functional relationship in the TSPA-LA Model between transport of ^{239}Pu and the ratio of Cl to NO_3 concentrations. The final regression model for *ESPU239* at 10,000 yr contains 13 variables and has an R^2 value of 0.85; thus most of the uncertainty in *ESPU239* is being accounted for.

The remaining five regressions in Figure K5.3.1-8a,b are similar to the just discussed regression for *ESPU239* at 10,000 yr and will not be discussed. The effects of the three dominant variables *EP1LOWPU*, *DELPPCO2* and *INFIL* on the uncertainty in *ESIC239* and *ESIC239C* at 10,000 yr can be seen in the scatterplots in Figure K5.3.1-8c,d,e,f,g,h.

Movement of Dissolved ^{99}Tc: *ESTC99* and *ESTC99C*. The uncertainty and sensitivity analyses for the time-dependent release rates (*ESTC99*, g/yr) and cumulative releases (*ESTC99C*, g) over the time interval [0, 20,000 yr] for the movement of dissolved ^{99}Tc from the EBS to the UZ resulting from the early failure of one DS above a CDSP WP in percolation bin 3 under dripping conditions are summarized in Figures K5.3.1-9 and K5.3.1-10.

Because technetium is assumed to have no solubility limit and to undergo no retardation in the invert (or anywhere else in the disposal system), released technetium moves very rapidly from the EBS to the UZ. This behavior can be seen in the rapidly decreasing values for *ESTC99* in Figure K5.3.1-9a,c and the rapid approach of *ESTC99C* to an asymptote in Figure K5.3.1-9b,d.

Because of the rapid decrease in *ESTC99*, the sensitivity analysis results for *ESTC99* and *ESTC99C* are very different (e.g., compare the PRCCs for *ESTC99* and *ESTC99C* in Figure K5.3.1-9e,f). For example, *HLWDRALK* (dissolution rate of HLW glass under alkaline conditions, $g/m^2/d$) has a negative effect on *ESTC99* and a positive effect on *ESTC99C*. These contrasting effects result because increasing *HLWDRALK* increases dissolution rate of HLW glass and hence increases the rate of release of ^{99}Tc. This results in a negative effect on *ESTC99* because increasing the amount of ^{99}Tc released at early times reduces the amount of ^{99}Tc that can be released at later times and, as a result, reduces *ESTC99* as time increases. In contrast, increasing *HLWDRALK* increases the total amount of ^{99}Tc released from HLW glass by a given time and thus increases *ESTC99C*.

As an example, the analysis for *ESTC99* at 10,000 yr is discussed in more detail (Figure K5.3.1-10a). The two dominant variables are *HLWDRALK* and *WFDEGEXF* (surface area exposure factor for amount of HLW glass contacted by water). As already discussed, *HLWDRALK* has a negative effect on *ESTC99* at 10,000 yr as a result of increasing the release of ^{99}Tc at earlier times. Similarly, *WFDEGEXF* has a negative effect on *ESTC99* at 10,000 yr as a result of increasing HLW glass degradation and thus increasing the release of ^{99}Tc at earlier times. Together, *HLWDRALK* and *WFDEGEXF* result in a regression model with an R^2 value of 0.47. After *HLWDRALK* and *WFDEGEXF*, the regression analysis indicates small positive effects for *THERMCON* (host rock thermal conductivity level), *PH2DHLS* (pointer variable used to determine pH in Cell 1a, i.e. Cell 2DHLW, of CDSP WPs under dripping conditions), and *SEEPPRMN* (mean fracture permeability in nonlithophysal rock units, m^2; as sampled, *SEEPPRMN* is actually the logarithm of the indicated permeability), and small negative effects for *HLWDRACD* (dissolution rate of HLW glass under acidic conditions, $g/m^2/d$) and *GP4NO3* (ratio of Cl to NO_3 in Group 4 pore waters, dimensionless). The positive effects result because (i) increasing *THERMCON* reduces EBS temperatures, which in turn reduces the degradation rate of HLW glass and thus reduces early releases of ^{99}Tc, (ii) increasing *PH2DHLS* increases pH in the vicinity of HLW glass and thus reduces its rate of degradation and associated early releases of ^{99}Tc, and (iii) increasing *SEEPPRMN* reduces water flow through the EBS and thus reduces early releases of ^{99}Tc. The negative effects result because (i) increasing *HLWDRACD* increases the dissolution of HLW glass and at early times and thus reduces the release of ^{99}Tc at later times. The correlation of *ESTC99* to *GP4NO3* is spurious, as there is no functional relationship in the TSPA-LA Model between transport of ^{99}Tc and the ratio of Cl to NO_3 concentration. The final regression model has a rather low R^2 value of 0.56. This low R^2 value probably results from a lack of resolution in calculating the very small values that exist for *ESTC99* at 10,000 yr as a result of inventory depletion (Figure K5.3.1-9a,c).

The analysis for *ESTC99C* at 10,000 yr is now considered. Overall, the dominant variables are *HLWMASS* (scale factor used to characterize uncertainty in amount of HLW in CDSP WPs), *HLWDRACD*, *DSNFMASS* (scale factor used to characterize uncertainty in amount of DSNF in CDSP WPs), *HLWDRALK*, *WFDEGEXF* and *PH2DHLS*. The variables *HLWMASS* and *DSNFMASS* have positive effects on *ESTC99C* because increasing their values increases the amount of ^{99}Tc in CDSP WPs. The variables *HLWDRACD*, *HLWDRALK*, and *WFDEGEXF* have positive effects on *ESTC99C* because increasing their values increases the amount of ^{99}Tc released from the degradation of HLW glass, which is the opposite of the effect that these variables have on *ESTC99* at 10,000 yr. In contrast, *PH2DHLS* has a negative effect on *ESTC99C* because increasing its value reduces the rate of HLW glass degradation. Collectively, *HLWMASS*, *HLWDRACD*, *DSNFMASS*, *HLWDRALK*, *WFDEGEXF* and *PH2DHLS* result in a model with an R^2 value of 0.79. After these variables, the analysis selects several additional variables with small effects and produces model with an R^2 value of 0.81; thus, most of the uncertainty associated with *ESTC99C* at 10,000 yr is being accounted for.

The remaining four regressions in Figure K5.3.1-10a,b are similar to the just discussed regressions for *ESTC99* and *ESTC99C* at 10,000 yr and will not be discussed. The effects of the first three variables selected in the regression analyses for *ESTC99* and *ESTC99C* at 10,000 yr can be seen in the scatterplots in Figure K5.3.1-10c,d,e,f,g,h.

K5.3.2 Early Failure Scenario Classes: Release from Engineered Barrier System over the Time Interval [0, 20,000 yr] for Early Drip Shield Failure above a CSNF WP

For completeness, this section presents summaries of the uncertainty and sensitivity analyses for release from the EBS over the time interval [0, 20,000 yr] for early DS failure above a CSNF WP without discussion.

Movement of ^{239}Pu Irreversibly Attached to Glass (i.e., Ic) Colloids: *ESIC239* and *ESIC239C*. The uncertainty and sensitivity analyses for the time-dependent release rates (*ESIC239*, g/yr) and cumulative releases (*ESIC239C*, g) over the time interval [0, 20,000 yr] for the movement of ^{239}Pu irreversibly attached to glass (i.e., Ic) colloids from the EBS to the UZ resulting from the early failure of one DS above a CSNF WP in percolation bin 3 under dripping conditions are summarized in Figure K5.3.2-1.

Movement of ^{239}Pu Irreversibly Attached to Ferrous (i.e., If) Colloids: *ESIF239* and *ESIF239C*. Uncertainty and sensitivity analyses for the movement of ^{239}Pu irreversibly attached to ferrous colloids are not presented due to an error in the GoldSim component of the TSPA-LA Model that affects the calculation of stability of ferrous colloids. Consequently, Figure K5.3.2-2 has been removed from this document. See Appendix P, Section P18, for a discussion of the error and the effect of the error on TSPA-LA Model results.

Movement of Dissolved ^{237}Np: *ESNP237* and *ESNP237C*. The uncertainty and sensitivity analyses for the time-dependent release rates (*ESNP237*, g/yr) and cumulative releases (*ESNP237C*, g) over the time interval [0, 20,000 yr] for the movement of dissolved ^{237}Np from the EBS to the UZ resulting from the early failure of one DS above a CSNF WP in percolation bin 3 under dripping conditions are summarized in Figure K5.3.2-3.

Movement of Dissolved ^{239}Pu: *ESPU239* and *ESPU239C*. The uncertainty and sensitivity analyses for the time-dependent release rates (*ESPU239*, g/yr) and cumulative releases (*ESPU239C*, g) over the time interval [0, 20,000 yr] for the movement of dissolved ^{239}Pu from the EBS to the UZ resulting from the early failure of one DS above a CSNF WP in percolation bin 3 under dripping conditions are summarized in Figures K5.3.2-4.

Movement of Dissolved ^{99}Tc: *ESTC99* and *ESTC99C*. The uncertainty and sensitivity analyses for the time-dependent release rates (ESTC99, g/yr) and cumulative releases (ESTC99C, g) over the time interval [0, 20,000 yr] for the movement of dissolved ^{99}Tc from the EBS to the UZ resulting from the early failure of one DS above a CSNF WP in percolation bin 3 under dripping conditions are summarized in Figure K5.3.2-5.

K5.3.3 Early Failure Scenario Classes: Release from Engineered Barrier System over the Time Interval [0, 20,000 yr] for Early Failure of a CDSP Waste Package under Dripping Conditions

For completeness, this section presents summaries of the uncertainty and sensitivity analyses for release from the EBS over the time interval [0, 20,000 yr] for early failure of a CDSP WP under dripping conditions without discussion.

Movement of ^{239}Pu Irreversibly Attached to Glass (i.e., Ic) Colloids: *ESIC239* and *ESIC239C*. Uncertainty and sensitivity analyses for the movement of ^{239}Pu irreversibly attached to glass colloids are not presented when transport is predominantly by diffusion (i.e., for early failed WP and seismic ground motion scenario classes), due to an error in the GoldSim component of the TSPA-LA Model that affects the calculation of concentration of glass colloids when glass colloids are unstable. Consequently, Figure K5.3.3-1 has been removed from this document. See Appendix P, Table P-6, for a discussion of the error and the effect of the error on TSPA-LA Model results.

Movement of ^{239}Pu Irreversibly Attached to Ferrous (i.e., If) Colloids: *ESIF239* and *ESIF239C*. Uncertainty and sensitivity analysis for the movement of ^{239}Pu irreversibly attached to ferrous colloids are not presented due to an error in the GoldSim component of the TSPA-LA Model that affects the calculation of stability of ferrous colloids. Consequently, Figure K5.3.3-2 has been removed from this document. See Appendix P, Section P18, for a discussion of the error and the effect of the error on TSPA-LA Model results.

Movement of Dissolved ^{237}Np: *ESNP237* and *ESNP237C*. The uncertainty and sensitivity analyses for the time-dependent release rates (*ESNP237*, g/yr) and cumulative releases (*ESNP237C*, g) over the time interval [0, 20,000 yr] for the movement of dissolved ^{237}Np from the EBS to the UZ resulting from the early failure of a CDSP WP in percolation bin 3 under dripping conditions are summarized in Figure K5.3.3-3.

Movement of Dissolved ^{239}Pu: *ESPU239* and *ESPU239C*. The uncertainty and sensitivity analyses for the time-dependent release rates (*ESPU239*, g/yr) and cumulative releases (*ESPU239C*, g) over the time interval [0, 20,000 yr] for the movement of dissolved ^{239}Pu from the EBS to the UZ resulting from the early failure of a CDSP WP in percolation bin 3 under dripping conditions are summarized in Figure K5.3.3-4.

Movement of Dissolved ^{99}Tc: *ESTC99* and *ESTC99C*. The uncertainty and sensitivity analyses for the time-dependent release rates (*ESTC99*, g/yr) and cumulative releases (*ESTC99C*, g) over the time interval [0, 20,000 yr] for the movement of dissolved ^{99}Tc from the EBS to the UZ resulting from the early failure of a CDSP WP in percolation bin 3 under dripping conditions are summarized in Figure K5.3.3-5.

K5.3.4 Early Failure Scenario Classes: Release from Engineered Barrier System over the Time Interval [0, 20,000 yr] for Early Failure of a CDSP Waste Package under Nondripping Conditions

Releases from the EBS over the time interval [0, 20,000 yr] for early failure of a CDSP WP under nondripping conditions are small. Therefore, no uncertainty and sensitivity analyses are presented for this case.

K5.3.5 Early Failure Scenario Classes: Release from Engineered Barrier System over the Time Interval [0, 20,000 yr] for Early Failure of a CSNF Waste Package under Dripping Conditions

For completeness, this section presents summaries of the uncertainty and sensitivity analyses for release from the EBS over the time interval [0, 20,000 yr] for early failure of a CSNF WP under dripping conditions without discussion.

Movement of ^{239}Pu Irreversibly Attached to Glass (i.e., Ic) Colloids: *ESIC239* and *ESIC239C*. Uncertainty and sensitivity analysis of movement of ^{239}Pu irreversibly attached to glass colloids are not presented when transport is predominantly by diffusion (i.e. for early failed WP and seismic ground motion scenario classes), due to an error in the GoldSim component of the TSPA-LA Model that affects the calculation of concentration of glass colloids when glass colloids are unstable. Consequently, Figure K5.3.5-1 has been removed from this document. See Appendix P, Table P-6, for a discussion of the error and the effect of the error on TSPA-LA Model results.

Movement of ^{239}Pu Irreversibly Attached to Ferrous (i.e., If) Colloids: *ESIF239* and *ESIF239C*. Uncertainty and sensitivity analyses for the movement of ^{239}Pu irreversibly attached to ferrous colloids are not presented due to an error in the GoldSim component of the TSPA-LA Model that affects the calculation of stability of ferrous colloids. Consequently, Figure K5.3.5-2 has been removed from this document. See Appendix P, Section P18, for a discussion of the error and the effect of the error on TSPA-LA Model results.

Movement of Dissolved ^{237}Np: *ESNP237* and *ESNP237C*. The uncertainty and sensitivity analyses for the time-dependent release rates (*ESNP237*, g/yr) and cumulative releases (*ESNP237C*, g) over the time interval [0, 20,000 yr] for the movement of dissolved ^{237}Np from the EBS to the UZ resulting from the early failure of a CSNF WP in percolation bin 3 under dripping conditions are summarized in Figure K5.3.5-3.

Movement of Dissolved ^{239}Pu: *ESPU239* and *ESPU239C*. The uncertainty and sensitivity analyses for the time-dependent release rates (*ESPU239*, g/yr) and cumulative releases (*ESPU239C*, g) over the time interval [0, 20,000 yr] for the movement of dissolved ^{239}Pu from the EBS to the UZ resulting from the early failure of a CSNF WP in percolation bin 3 under dripping conditions are summarized in Figure K5.3.5-4.

Movement of Dissolved ^{99}Tc: *ESTC99* and *ESTC99C*. The uncertainty and sensitivity analyses for the time-dependent release rates (*ESTC99*, g/yr) and cumulative releases (*ESTC99C*, g) over the time interval [0, 20,000 yr] for the movement of dissolved ^{99}Tc from the EBS to the UZ resulting from the early failure of a CSNF WP in percolation bin 3 under dripping conditions are summarized in Figure K5.3.5-5.

K5.3.6 Early Failure Scenario Classes: Release from Engineered Barrier System over the Time Interval [0, 20,000 yr] for Early Failure of a CSNF Waste Package under Nondripping Conditions

Releases from the EBS over the time interval [0, 20,000 yr] for early failure of a CSNF WP under nondripping conditions are small. Therefore, no uncertainty and sensitivity analyses are presented for this case.

K5.3.7 Early Failure Scenario Classes: Release from Engineered Barrier System over the Time Interval [0, 1,000,000 yr] for Early Drip Shield Failure above a CDSP WP

This section presents summaries of the uncertainty and sensitivity analyses for the releases of dissolved ^{237}Np and dissolved ^{239}Pu from the EBS over the time interval [0, 1,000,000 yr] for early DS failure above a CSNF WP without discussion. Dissolved ^{237}Np is used as an example because of its long half life (2.14×10^6 yr). Dissolved ^{239}Pu is used as an example because of its significant but shorter half life (2.41×10^5 yr). The plutonium colloids are omitted because they involve smaller releases from the EBS than dissolved ^{239}Pu and also, like dissolved ^{239}Pu, their long term releases are dominated by the effects of radioactive decay. Owing to its rapid release from the EBS, there is no reason to show results for ^{99}Tc for the 1,000,000 yr case (see Figures K5.3.1-9a and K5.3.2-5a for results for the time interval [0, 20,000 yr]).

Movement of Dissolved ^{237}Np: *ESNP237* and *ESNP237C*. The uncertainty and sensitivity analyses for the time-dependent release rates (*ESNP237*, g/yr) and cumulative releases (*ESNP237C*, g) over the time interval [0, 1,000,000 yr] for the movement of dissolved 237Np from the EBS to the UZ resulting from the early failure of one DS above a CDSP WP in percolation bin 3 under dripping conditions are summarized in Figure K5.3.7-1.

Movement of Dissolved ^{239}Pu: *ESPU239* and *ESPU239C*. The uncertainty and sensitivity analyses for the time-dependent release rates (*ESPU239*, g/yr) and cumulative releases (*ESPU239C*, g) over the time interval [0, 200,000 yr] for the movement of dissolved 239Pu from the EBS to the UZ resulting from the early failure of one DS above a CDSP WP in percolation bin 3 under dripping conditions are summarized in Figures K5.3.7-2.

K5.3.8 Early Failure Scenario Classes: Release from Engineered Barrier System over the Time Interval [0, 1,000,000 yr] for Early Drip Shield Failure above a CSNF WP

See discussion at start of Section K5.3.7.

Movement of Dissolved ^{237}Np: *ESNP237* and *ESNP237C*. The uncertainty and sensitivity analyses for the time-dependent release rates (*ESNP237*, g/yr) and cumulative releases (*ESNP237C*, g) over the time interval [0, 1,000,000 yr] for the movement of dissolved ^{237}Np from the EBS to the UZ resulting from the early failure of one DS above a CSNF WP in percolation bin 3 under dripping conditions are summarized in Figure K5.3.8-1.

Movement of Dissolved ^{239}Pu: *ESPU239* and *ESPU239C*. The uncertainty and sensitivity analyses for the time-dependent release rates (*ESPU239*, g/yr) and cumulative releases (*ESPU239C*, g) over the time interval [0, 1,000,000 yr] for the movement of dissolved ^{239}Pu from the EBS to the UZ resulting from the early failure of one DS above a CSNF WP in percolation bin 3 under dripping conditions are summarized in Figures K5.3.8-2.

K5.3.9 Early Failure Scenario Classes: Release from Engineered Barrier System over the Time Interval [0, 1,000,000 yr] for Early Failure of a CDSP Waste Package under Dripping Conditions

See discussion at start of Section K5.3.7.

Movement of Dissolved ^{237}Np: *ESNP237* and *ESNP237C*. The uncertainty and sensitivity analyses for the time-dependent release rates (*ESNP237*, g/yr) and cumulative releases (*ESNP237C*, g) over the time interval [0, 1,000,000 yr] for the movement of dissolved ^{237}Np from the EBS to the UZ resulting from the early failure of a CDSP WP in percolation bin 3 under dripping conditions are summarized in Figure K5.3.9-1. The significant increase in release rates around 300,000 yr is due to failure of the DS from general corrosion. Prior to DS failure, dissolved ^{237}Np moves from the EBS primarily by diffusion; after DS failure, advection becomes the dominant mechanism for dissolved ^{237}Np movement. The change in release mechanisms is reflected in the change in PRCCs for *EBSDIFCF* (exponential term representing uncertainty in the invert diffusion coefficient (dimensionless)) and *INFIL* (infiltration level).

Movement of Dissolved ^{239}Pu: *ESPU239* and *ESPU239C*. The uncertainty and sensitivity analyses for the time-dependent release rates (*ESPU239*, g/yr) and cumulative releases (*ESPU239C*, g) over the time interval [0, 200,000 yr] for the movement of dissolved ^{239}Pu from the EBS to the UZ resulting from the early failure of a CDSP WP in percolation bin 3 under dripping conditions are summarized in Figures K5.3.9-2. Results are plotted only to 200,000 yr because most of the ^{239}Pu decays within this time interval.

K5.3.10 Early Failure Scenario Classes: Release from Engineered Barrier System over the Time Interval [0, 1,000,000 yr] for Early Failure of a CDSP Waste Package under Nondripping Conditions

See discussion at start of Section K5.3.7.

Movement of Dissolved ^{237}Np: *ESNP237* and *ESNP237C*. The uncertainty and sensitivity analyses for the time-dependent release rates (*ESNP237*, g/yr) and cumulative releases (*ESNP237C*, g) over the time interval [0, 1,000,000 yr] for the movement of dissolved ^{237}Np

from the EBS to the UZ resulting from the early failure of a CDSP WP in percolation bin 3 under nondripping conditions are summarized in Figure K5.3.10-1. Because these results involve a WP in nondripping conditions, DS failure does not affect the movement of dissolved ^{237}Np.

Movement of Dissolved ^{239}Pu: *ESPU239* and *ESPU239C*. The uncertainty and sensitivity analyses for the time-dependent release rates (*ESPU239*, g/yr) and cumulative releases (*ESPU239C*, g) over the time interval [0, 200,000 yr] for the movement of dissolved ^{239}Pu from the EBS to the UZ resulting from the early failure of a CDSP WP in percolation bin 3 under nondripping conditions are summarized in Figures K5.3.10-2.

K5.3.11 Early Failure Scenario Classes: Release from Engineered Barrier System over the Time Interval [0, 1,000,000 yr] for Early Failure of a CSNF Waste Package under Dripping Conditions

See discussion at start of Section K5.3.7.

Movement of Dissolved ^{237}Np: *ESNP237* and *ESNP237C*. The uncertainty and sensitivity analyses for the time-dependent release rates (*ESNP237*, g/yr) and cumulative releases (*ESNP237C*, g) over the time interval [0, 1,000,000 yr] for the movement of dissolved ^{237}Np from the EBS to the UZ resulting from the early failure of a CSNF WP in percolation bin 3 under dripping conditions are summarized in Figure K5.3.11-1.

Movement of Dissolved ^{239}Pu: *ESPU239* and *ESPU239C*. The uncertainty and sensitivity analyses for the time-dependent release rates (*ESPU239*, g/yr) and cumulative releases (*ESPU239C*, g) over the time interval [0, 200,000 yr] for the movement of dissolved ^{239}Pu from the EBS to the UZ resulting from the early failure of a CSNF WP in percolation bin 3 under dripping conditions are summarized in Figures K5.3.11-2.

K5.3.12 Early Failure Scenario Classes: Release from Engineered Barrier System over the Time Interval [0, 1,000,000 yr] for Early Failure of a CSNF Waste Package under Nondripping Conditions

See discussion at start of Section K5.3.7.

Movement of Dissolved ^{237}Np: *ESNP237* and *ESNP237C*. The uncertainty and sensitivity analyses for the time-dependent release rates (*ESNP237*, g/yr) and cumulative releases (*ESNP237C*, g) over the time interval [0, 1,000,000 yr] for the movement of dissolved ^{237}Np from the EBS to the UZ resulting from the early failure of a CSNF WP in percolation bin 3 under nondripping conditions are summarized in Figure K5.3.12-1.

Movement of Dissolved ^{239}Pu: *ESPU239* and *ESPU239C*. The uncertainty and sensitivity analyses for the time-dependent release rates (*ESPU239*, g/yr) and cumulative releases (*ESPU239C*, g) over the time interval [0, 200,000 yr] for the movement of dissolved ^{239}Pu from the EBS to the UZ resulting from the early failure of a CSNF WP in percolation bin 3 under nondripping conditions are summarized in Figures K5.3.12-2.

K5.4 Early Failure Scenario Classes: Release from Unsaturated Zone

This section contains analysis results for releases from the UZ over the time interval [0, 20,000 yr] resulting from early failure of one DS over a CDSP WP in percolation bin 3 under dripping conditions (Section 5.4.1). Analysis results for other early failures are discussed in Section K5.4.2.

K5.4.1 Early Failure Scenario Classes: Release from Unsaturated Zone over the Time Interval [0, 20,000 yr] for Early Drip Shield Failure above a CDSP WP

Movement of ^{239}Pu Irreversibly Attached to Slow (i.e., Ic) Colloids: *UZIC239* and *UZIC239C*. To understand the presented analyses for colloids in the UZ and SZ, it is important to bear in mind that the ^{239}Pu irreversibly attached to glass (i.e., Ic) and ferrous (i.e., If) colloids in the EBS is reapportioned upon entry into the UZ. Specifically, (i) Ic now designates slow moving colloids, (ii) If now designates fast moving colloids, and (iii) the total amount of ^{239}Pu attached to Ic and If colloids in the EBS is reapportioned so that 99.832 percent of the total ^{239}Pu is attached to slow colloids (i.e., the new Ic colloids) upon entry into the UZ and the remaining 0.168 percent is attached to fast colloids (i.e., the new If colloids) upon entry into the UZ. Because the mass of ^{239}Pu attached to glass colloids in the EBS is much greater than the mass of ^{239}Pu attached to ferrous colloids in the EBS, the mass of ^{239}Pu attached to slow colloids entering the UZ is effectively the same as the mass of ^{239}Pu attached to glass colloids leaving the EBS. However, because the mass of ^{239}Pu attached to glass colloids in the EBS is much greater than the mass of ^{239}Pu attached to ferrous colloids in the EBS, the indicated reapportioning results in the release of ^{239}Pu attached to fast colloids into the UZ having very different properties from the release of ^{239}Pu attached to ferrous colloids out of the EBS.

The uncertainty and sensitivity analyses for the time-dependent release rates (*UZIC239*, g/yr) and cumulative releases (*UZIC239C*, g) over the time interval [0, 20,000 yr] for the movement of ^{239}Pu irreversibly attached to slow (i.e., Ic) colloids from the UZ to the SZ resulting from the early failure of one DS above a CDSP WP in percolation bin 3 under dripping conditions are summarized in Figures K5.4.1-1 and K5.4.1-2.

Retardation of slow colloids in the UZ is illustrated by Figure K5.4.1-3. By 10,000 yr after the breach in the WP, most of the ^{239}Pu that entered the UZ attached to slow colloids has exited the UZ. Consequently, retardation in the UZ is not sufficient to permit significant reduction in ^{239}Pu due to radioactive decay. As a result, the behavior of *UZIC239* and *UZIC239C* shown in Figures K5.4.1-1 and K5.4.1-2 is essentially the same as the behavior of *ESIC239* and *ESIC239C* shown in Figures K5.3.1-1 and K5.3.1-2. Because of this similarity, the discussions for Figures K5.3.1-1 and K5.3.1-2 are also applicable to Figures K5.4.1-1 and K5.4.1-2.

The results for *UZIC239* in Figure K5.4.1-1a,c,e are choppier than the corresponding results for *ESIC239* in Figure K5.3.1-1a,c,e. This choppiness results from the use of a particle tracking algorithm to numerically solve the radionuclide transport equations for the UZ. Despite the choppiness of the results, in Section 7.3.5 the UZ transport model is shown to be stable in the sense that increasing the number of particles does not change the model results. The use of a different numerical solution algorithm may result in less choppy results for *UZIC239*. One

potential way to reduce the choppiness in *UZIC239* and other similar results is to incorporate a smoothing procedure into the particle tracking algorithm that produces a locally weighted average (e.g., with a Gaussian kernel function) of time-dependent releases into the SZ. The results for *UZIC239C* in Figure K5.4.1-1b,d,f are much smoother than the results for *UZIC239* because of the smoothing effect of the integration that defines *UZIC239C*.

Movement of ^{239}Pu Irreversibly Attached to Fast (i.e., If) Colloids: *UZIF239* and *UZIF239C*. The uncertainty and sensitivity analyses for the time-dependent release rates (*UZIF239*, g/yr) and cumulative releases (*UZIF239C*, g) over the time interval [0, 20,000 yr] for the movement of ^{239}Pu irreversibly attached to fast (i.e., If) colloids from the UZ to the SZ resulting from the early failure of one DS above a CDSP WP in percolation bin 3 under dripping conditions are summarized in Figures K5.4.1-4 and K5.4.1-5.

Very little retardation of fast colloids takes place in the UZ (Figure K5.4.1-6). As a result, the behavior of *UZIF239* and *UZIF239C* shown in Figures K5.4.1-4 and K5.4.1-5 has essentially the same structure as the behavior of *ESIC239* and *ESIC239C* shown in Figures K5.3.1-1 and K5.3.1-2 for ^{239}Pu irreversibly attached to glass (i.e., Ic) colloids in the EBS. The behavior of *ESIC239* and *ESIC239C* rather than the behavior of *ESIF239* and *ESIF239C* is relevant to the behavior of *UZIF239* and *UZIF239C* because the previously described reapportioning of ^{239}Pu onto slow and fast colloids upon entry into the UZ results in ^{239}Pu irreversibly attached to glass colloids in the EBS being the primary source of ^{239}Pu irreversibly attached to fast colloids in the EBS. Because of this similarity, the discussions for Figures K5.3.1-1 and K5.3.1-2 are also applicable to Figures K5.4.1-1 and K5.4.1-2.

As previously discussed for *UZIC239* in conjunction with Figure K5.4.1-1a,c,f, the choppiness of the values for *UZIF239* in Figure K5.4.1-4a,c,e results from the use of a particle tracking algorithm to solve the radionuclide transport equations for the UZ.

Movement of Dissolved ^{237}Np: *UZNP237* and *UZNP237C*. The uncertainty and sensitivity analyses for the time-dependent release rates (*UZNP237*, g/yr) and cumulative releases (*UZNP237C*, g) over the time interval [0, 20,000 yr] for the movement of dissolved ^{237}Np from the UZ to the SZ resulting from the early failure of one DS above a CDSP WP in percolation bin 3 under dripping conditions are summarized in Figures K5.4.1-7 and K5.4.1-8.

Dissolved ^{237}Np is somewhat retarded in the UZ (Figure K5.4.1-9). As demonstrated by these scatterplots, by 10,000 years, roughly half or more of the dissolved ^{237}Np that has entered the UZ from the EBS has also moved from the UZ to the SZ. As a result, the mass of dissolved ^{237}Np that leaves the UZ is primarily determined by the mass of dissolved ^{237}Np entering the UZ. Consequently the behavior of *UZNP237* and *UZNP237C* shown in Figures K5.4.1-7 is essentially the same as the behavior of *ESNP237* and *ESNP237C* shown in Figures K5.3.1-5, and the dominant variables in the regression models for *UZNP237* and *UZNP237C* (Figure K5.4.1-8) are generally the same as those in the regression model for *ESNP237* and *ESNP237C* (Figure K5.3.1-6). Because of this similarity, the discussions for Figures K5.3.1-5 and K5.3.1-6 are also applicable to Figures K5.4.1-7 and K5.4.1-8.

As previously discussed for *UZIC239* in conjunction with Figure K5.4.1-1a,c,f, the choppiness of the values for *UZNP237* in Figure K5.4.1-7a,c,e results from the use of a particle tracking algorithm to solve the radionuclide transport equations for the UZ.

Movement of Dissolved ^{239}Pu: *UZPU239* and *UZPU239C*. The uncertainty and sensitivity analyses for the time-dependent release rates (*UZPU239*, g/yr) and cumulative releases (*UZPU239C*, g) over the time interval [0, 20,000 yr] for the movement of dissolved ^{239}Pu from the UZ to the SZ resulting from the early failure of one DS above a CDSP WP in Bin 3 under dripping conditions are summarized in Figures K5.4.1-10 and K5.4.1-11.

Some retardation of dissolved ^{239}Pu takes place in the UZ (Figure K5.4.1-12). For example, *UZKDPUDT* (sorption coefficient for plutonium in devitrified tuff units of UZ, mL/g) appears in the analyses for *UZPU239* and *UZPU239C* with a negative PRCC (Figure K5.4.1-10e,f), and *UZTORRG3* (tortuosity in rock group 3 of the UZ, dimensionless ; as sampled, *UZTORRG3* is actually the logarithm of the indicated tortuosity) also appears in the analysis for *UZPU239C* with a negative PRCC (Figure K5.4.1-10f). These effects result because increasing *UZKDPUDT* results in more retardation of ^{239}Pu in the UZ and increasing *UZTORRG3* results in slower water flow in the UZ. However, the effects associated with *UZKDPUDT* and *UZTORRG3* are small. For example, the inclusion of *UZKDPUDT* in the regression model for *UZPU239* at 10,000 years raises the R^2 value from 0.78 to 0.83 (Figure K5.4.1-11a), and the inclusion of *UZKDPUDT* in the regression model for *UZPU239C* at 10,000 yr raises the R^2 value from 0.73 to 0.80 (Figure K5.4.1-11b). Further, *UZTORRG3* is not selected in any of the regression analyses in Figure K5.4.1-11a,b.

Overall, the behavior of *UZPU239* and *UZPU239C* shown in Figures K5.4.1-10 and K5.4.1-11 is very similar to the behavior of *ESPU239* and *ESPU239C* shown in Figures K5.3.1-7 and K5.3.1-8. Because of this similarity, the discussions for Figures K5.3.1-7 and K5.3.1-8 are also applicable to Figures K5.4.1-10 and K5.4.1-11.

Movement of Dissolved ^{99}Tc: *UZTC99* and *UZTC99C*. The uncertainty and sensitivity analyses for the time-dependent release rates (*UZTC99*, g/yr) and cumulative releases (*UZTC99C*, g) over the time interval [0, 20,000 yr] for the movement of dissolved ^{99}Tc from the UZ to the SZ resulting from the early failure of one DS above a CDSP WP in percolation bin 3 under dripping conditions are summarized in Figures K5.4.1-13 and K5.4.1-14.

The release of ^{99}Tc from the EBS takes place very rapidly (Figure K5.3.1-9a,c). The movement of ^{99}Tc through the UZ takes place at a slower rate. For example, the very small values for *ESTC99* that result at later times for some sample elements (Figure K5.3.1-9a,c) are not present in the values for *UZTC99* (Figure K5.4.1-13a,c) because of the slowing and spreading effect of transport in the UZ. However, almost all ^{99}Tc released to the UZ ultimately is released to the SZ (Figure K5.4.1-15).

The dominant variable with respect to the uncertainty associated with *UZTC99* is *INFIL* (infiltration level). As shown by the PRCCs in Figure K5.4.1-13e, increasing *INFIL* initially has a positive effect on *UZTC99* and then at later times increasing *INFIL* has a negative effect on *UZTC99*. This pattern of effects results because large values for *INFIL* increase water flow in the

EBS and UZ, which speeds ^{99}Tc transport through the EBS and UZ and results in the positive effect for *INFIL* at early times. However, the effect of speeding ^{99}Tc transport through the EBS and UZ at early times is to reduce the amount of ^{99}Tc available to be released to the SZ at later times, which is why *INFIL* has a negative effect on *UZTC99* at later times. The regressions in Figure K5.4.1-14a were performed during the later time period (i.e., after 2000 years) in which *INFIL* has a negative effect on *UZTC99*. In particular, the regression models for *UZTC99* containing only *INFIL* have R^2 values of 0.59, 0.58 and 0.46, respectively, at 3,000, 5,000 and 10,000 yr. After *INFIL*, the regressions select a number of additional variables, with most of these variables having been previously discussed in conjunction with the analyses for *ESTC99* in Figures K5.3.1-9 and K5.3.1-9. The final regression models for *ESTC99* have R^2 values of 0.81, 0.68 and 0.62, respectively, at 3,000, 5,000 and 10,000 yr. The decreasing R^2 values with time probably results for a lack of resolution in the calculation of the small values for *ESTC99* that are present at later times.

With the exception of the positive effect of *INFIL* on *UZTC99C*, the sensitivity analyses for *UZTC99C* in Figures K5.4.1-13 and K5.4.1-14 are generally the same as the sensitivity analyses for *ESTC99C* in Figures K5.3.1-9 and K5.3.1-10. This similarity results because most ^{99}Tc releases to the UZ are transported rapidly and with little reduction to the SZ (Figure K5.4.1-15). The increased importance for *INFIL* with respect to *UZTC99C* over its importance with respect to *ESTC99C* results from the greater transport distances associated with the UZ relative to the transport distances associated with the SZ.

As previously discussed for *UZIC239* in conjunction with Figure K5.4.1-1a,c,f, the choppiness of the values for *ESTC99* in Figure K5.4.1-13a,c,f results from the use of a particle tracking algorithm to solve the radionuclide transport equations for the UZ.

K5.4.2 Early Failure Scenario Classes: Release from Unsaturated Zone (UZ) for Early Failures Considered in Sections K5.3.2- K5.3.12

Results specific to movement through the UZ for the early failures considered in Sections K5.3.2 – K5.3.12 are similar to the results presented in Section K5.3.1 for the early failure of one DS above a CDSP WP in percolation bin 3 under dripping conditions and also to the results presented in Section K6.4.1 for an igneous intrusive event at 10 yr. For this reason, uncertainty and sensitivity analysis results for radionuclide movement in the UZ are not presented for the early failures considered in Sections K5.3.2 – K5.3.12.

K5.5 Early Failure Scenario Classes: Release from Saturated Zone (SZ)

This section contains analysis results for releases from the SZ over the time interval [0, 20,000 yr] resulting from early failure of one DS over a CDSP WP in percolation bin 3 under dripping conditions (Section 5.5.1). Analysis results for other early failures are discussed in Section K5.5.2.

K5.5.1 Early Failure Scenario Classes: Release from Saturated Zone (SZ) over the Time Interval [0, 20,000 yr] for Early Drip Shield Failure above a CDSP WP

This section presents summaries of the uncertainty and sensitivity analyses for radionuclide movement in the SZ without discussion. The same processes operate in the SZ for all scenario classes. Thus, the sensitivity analysis results for the SZ are similar for all scenario classes. However, somewhat sharper results are obtained for the scenario classes that involve large releases from the EBS. In particular, the numerical noise associated with the solution of the transport equations in the UZ for very low radionuclide concentrations is reduced when larger releases from the EBS are under consideration. For this reason, the presentation and discussion of detailed sensitivity results for radionuclide transport in the SZ is delayed to Section K6.5.1, where results associated with the igneous intrusive scenario class are presented and discussed.

Movement of ^{239}Pu Irreversibly Attached to Slow (i.e., Ic) Colloids: *SZIC239* and *SZIC239C*. The uncertainty and sensitivity analyses for the time-dependent release rates (*SZIC239*, g/yr) and cumulative releases (*SZIC239C*, g) over the time interval [0, 20,000 yr] for the movement of ^{239}Pu irreversibly attached to slow (i.e., Ic) colloids across a subsurface plane at the location of the RMEI resulting from the early failure of one DS above a CDSP WP in percolation bin 3 under dripping conditions are summarized in Figure K5.5.1-1. Discussion is provided in conjunction with Figures K6.5.1-1, K6.5.1-2 and K6.5.1-3.

Movement of ^{239}Pu Irreversibly Attached to Fast (i.e., If) Colloids: *SZIF239* and *SZIF239C*. The uncertainty and sensitivity analyses for the time-dependent release rates (*SZIF239*, g/yr) and cumulative releases (*SZIF239C*, g) over the time interval [0, 20,000 years] for the movement of ^{239}Pu irreversibly attached to fast (i.e., If) colloids across a subsurface plane at the location of the RMEI resulting from the early failure of one DS above a CDSP WP in percolation bin 3 under dripping conditions are summarized in Figure K5.5.1-2. Discussion is provided in conjunction with Figures K6.5.1-4, K6.5.1-5 and K6.5.1-6.

Movement of Dissolved ^{237}Np: *SZNP237* and *SZNP237C*. The uncertainty and sensitivity analyses for the time-dependent release rates (*SZNP237*, g/yr) and cumulative releases (*SZNP237C*, g) over the time interval [0, 20,000 yr] for the movement of dissolved ^{237}Np across a subsurface plane at the location of the RMEI resulting from the early failure of one DS above a CDSP WP in percolation bin 3 under dripping conditions are summarized in Figure K5.5.1-3. Discussion is provided in conjunction with Figures K6.5.1-7, K6.5.1-8 and K6.5.1-9.

Movement of Dissolved ^{239}Pu: *SZPU239* and *SZPU239C*. The uncertainty and sensitivity analyses for the time-dependent release rates (*SZPU239*, g/yr) and cumulative releases (*SZPU239C*, g) over the time interval [0, 20,000 yr] for the movement of dissolved ^{239}Pu across a subsurface plane at the location of the RMEI resulting from the early failure of one DS above a CDSP WP in percolation bin 3 under dripping conditions are summarized in Figure K5.5.1-4. Discussion is provided in conjunction with Figures K6.5.1-10, K6.5.1-11 and K6.5.1-12.

Movement of Dissolved ^{99}Tc: *SZTC99* and *SZTC99C*. The uncertainty and sensitivity analyses for the time-dependent release rates (*SZTC99*, g/yr) and cumulative releases (*SZTC99C*, g) over

the time interval [0, 20,000 yr] for the movement of dissolved ^{99}Tc across a subsurface plane at the location of the RMEI resulting from the early failure of one DS above a CDSP WP in percolation bin 3 under dripping conditions are summarized in Figure K5.5.1-5. Discussion is provided in conjunction with Figures K6.5.1-13, K6.5.1-14 and K6.5.1-5.

K5.5.2 Early Failure Scenario Classes: Release from Saturated Zone (SZ) for Early Failures Considered in Sections K5.3.2- K5.3.12

Results specific to movement through the SZ for the early failures considered in Sections K5.3.2 – K5.3.12 are similar to the results presented in Section K5.5.1 for the early failure of one DS above a CDSP WP in percolation bin 3 under dripping conditions, and also to the results presented in Section K6.5.1 for an igneous intrusive event at 10 yr. For this reason, uncertainty and sensitivity analysis results for radionuclide movement in the SZ are not presented here for the early failures considered in Sections K5.3.2 – K5.3.12.

K5.6 Early Failure Scenario Classes: Dose to Reasonably Maximally Exposed Individual

This section contains analysis results for the dose to a RMEI (RMEI) over the time interval [0, 20,000 yr] resulting from an early DS failure over a CDSP WP in percolation bin 3 under dripping conditions (Section K5.6.1). Analysis results for other early failures are discussed in Section K5.6.2.

K5.6.1 Early Failure Scenario Classes: Dose to Reasonably Maximally Exposed Individual over the Time Interval [0, 20,000 yr] for Early Drip Shield Failure above a CDSP WP

This section presents summaries of the uncertainty and sensitivity analyses for dose to the RMEI without discussion. The same processes affect the conversion of radionuclide concentration in groundwater to dose to the RMEI for all scenario classes. Thus, the sensitivity analysis results for dose to the RMEI are similar for all scenario classes. However, somewhat sharper results are obtained for the scenario classes that involve large releases from the EBS. In particular, the numerical noise associated with the solution of the transport equations in the UZ and SZ for very low radionuclide concentrations is reduced when larger releases from the EBS are under consideration. For this reason, the presentation and discussion of detailed sensitivity results for dose to the RMEI is delayed to Section K6.6.1, where results associated with the igneous intrusive scenario class are presented and discussed.

Dose to RMEI from ^{239}Pu Irreversibly Attached to Slow (i.e., Ic) Colloids: *DOIC239*. The uncertainty and sensitivity analyses for dose to the RMEI (*DOIC239*, mrem/yr) over the time interval [0, 20,000 yr] for the movement of ^{239}Pu irreversibly attached to slow (i.e., Ic) colloids across a subsurface plane at the location of the RMEI resulting from the early failure of one DS above a CDSP WP in percolation bin 3 under dripping conditions are summarized in Figure K5.6.1-1. Discussion is provided in conjunction with Figures K6.6.1-1 and K6.6.1-2.

Dose to RMEI from ^{239}Pu Irreversibly Attached to Fast (i.e., Ic) Colloids: *DOIF239*. The uncertainty and sensitivity analyses for dose to the RMEI (*DOIF239*, mrem/yr) over the time

interval [0, 20,000 yr] for the movement of ^{239}Pu irreversibly attached to fast (i.e., Ic) colloids across a subsurface plane at the location of the RMEI resulting from the early failure of one DS above a CDSP WP in percolation bin 3 under dripping conditions are summarized in Figure K5.6.1-2. Discussion is provided in conjunction with Figures K6.6.1-3 and K6.6.1-4.

Dose to RMEI from Dissolved ^{237}Np: *DONP237*. The uncertainty and sensitivity analyses for dose to the RMEI (*DONP237*, mrem/yr) over the time interval [0, 20,000 yr] for the movement of dissolved ^{237}Np across a subsurface plane at the location of the RMEI resulting from the early failure of one DS above a CDSP WP in percolation bin 3 under dripping conditions are summarized in Figure K5.6.1-3. Discussion is provided in conjunction with Figures K6.6.1-5 and K6.6.1-6.

Dose to RMEI from Dissolved ^{239}Pu: *DOPU239*. The uncertainty and sensitivity analyses for dose to the RMEI (*DOPU239*, mrem/yr) over the time interval [0, 20,000 yr] for the movement of dissolved ^{239}Pu across a subsurface plane at the location of the RMEI resulting from the early failure of one DS above a CDSP WP in percolation bin 3 under dripping conditions are summarized in Figure K5.6.1-4. Discussion is provided in conjunction with Figures K6.6.1-7 and K6.6.1-8.

Dose to RMEI from Dissolved ^{99}Tc: *DOTC99*. The uncertainty and sensitivity analyses for dose to the RMEI (*DOTC99*, mrem/yr) over the time interval [0, 20,000 yr] for the movement of dissolved ^{99}Tc across a subsurface plane at the location of the RMEI resulting from the early failure of one DS above a CDSP WP in percolation bin 3 under dripping conditions are summarized in Figure K5.6.1-5. Discussion is provided in conjunction with Figures K6.6.1-9 and K6.6.1-10.

K5.6.2 Early Failure Scenario Classes: Dose to Reasonably Maximally Exposed Individual for Early Failures Considered in Sections K5.3.2- K5.3.12

Results specific to dose to the RMEI for the early failures considered in Sections K5.3.2 - K5.3.12 are similar to the results presented in Section K5.6.1 for the early failure of one DS above a CDSP WP in percolation bin 3 under dripping conditions, and also to results presented in Section K6.6.1 for an igneous intrusive event at 10 yr. For this reason, uncertainty and sensitivity analysis results for radionuclide movement in the UZ are not presented for the early failures considered in Sections K5.3.2 – K5.3.12.

K5.7 Early Failure Scenario Classes: Expected Dose to Reasonably Maximally Exposed Individual

This section contains analysis results for expected dose to a RMEI (RMEI) resulting from early failures. Expected dose is computed as discussed in Section J6.3. The following cases are presented:

- Expected dose to the RMEI for the time intervals [0, 20,000 yr] and [0, 1,000,000 yr] resulting from early DS failure (Section 5.7.1);

- Expected dose to the RMEI for the time intervals [0, 20,000 yr] and [0, 1,000,000yr] resulting from early WP failure (Section 5.7.2);

- Expected dose to the RMEI for the time intervals [0, 20,000 yr] and [0, 1,000,000 yr] resulting from early failures (considering both DSs and WPs) (Section 5.7.3);

- Expected dose to the RMEI for the time intervals [0, 20,000 yr] and [0, 1,000,000 yr] resulting from early failures (considering both DSs and WPs) and nominal processes (Section 5.7.4).

K5.7.1 Early Failure Scenario Classes: Expected Dose to Reasonably Maximally Exposed Individual from Early Drip Shield Failure

Expected Dose to RMEI over [0, 20,000 yr]: *EXPDOSE*. The uncertainty and sensitivity analyses for expected dose to the RMEI (*EXPDOSE*, mrem/yr) over the time interval [0, 20,000 years] resulting from early DS failure are summarized in Figures K5.7.1-1 and K5.7.1-2. There is sharp peak in *EXPDOSE* prior to 1000 yr resulting from the release of ^{99}Tc. At the time of this peak, maximum values for *EXPDOSE* are in the vicinity of 0.01 mrem/yr, although the values for most sample elements are considerably smaller (Figure K5.7.1-1a,b). After the early peak, *EXPDOSE* has values in a range from 10^{-7} to 10^{-3} mrem/yr.

The PRCCs in Figure K5.7.1-1c indicate that the uncertainty in *EXPDOSE* is dominated by *PROBDSEF* (probability that a randomly selected DS will experience an early failure), with the value for *EXPDOSE* increasing as *PROBDSEF* increases. This effect results because increasing *PROBDSEF* increases the expected number of DSs that experience early failure and hence increases *EXPDOSE.*

In addition to *PROBDSEF*, smaller effects are indicated for *SZFIPOVO* (flowing interval porosity in the volcanic unit of the SZ), *SZGWSPDM* (groundwater specific discharge multiplier*;* as sampled, *SZGWSPDM* is actually the logarithm of the indicated multiplier), *SEEPUNC* (pointer variable used to determine local seepage rates), *THERMCON* (host rock thermal conductivity level), and *INFIL* (infiltration level) (Figure K5.7.1-1c). A negative effect is indicated for *SZFIPOVO* at early times (i.e., prior to 3,000 yr), with this effect then going to zero. This effect results because increasing *SZFIPOVO* increases the time required for the initial releases of mobile species such as ^{99}Tc to reach the location of the RMEI. The positive effect associated with *SZGWSPDM* results from increasing the flow velocity in the SZ, which in turn moves radioactive species more rapidly to the location of the RMEI. This effect is especially pronounced at early times (i.e., prior to 2000 yr) because increasing *SZGWSPDM* decreases the time of first arrival of radioactive species at the location of the RMEI. Both *THERMCON* and *INFIL* have small positive effects on *EXPDOSE* at early times (i.e., prior to 3,000 yr). These effects are possibly related to the influence of these variables on repository temperature and hence the time at which release from the EBS can begin. Specifically, increasing *THERMCON* and *INFIL* tends to reduce EBS temperatures and thus reduce the time at which releases from the EBS can begin. After 3,000 yr, *THERMCON* has no effect on *EXPDOSE*; however, *INFIL* continues to have a small effect, with effect probably resulting from increased water flow through the EBS and UZ that results as *INFIL* increases in value.

More detailed sensitivity analyses for *EXPDOSE* are provided by the regression analyses in Figure K5.7.1-2a. The dominant effect of *PROBDSEF* on the uncertainty in *EXPDOSE* is indicated by R^2 values of 0.74, 0.76 and 0.69 for the regressions containing only *PROBDSEF* at 3,000, 5,000 and 10,000 yr. After *PROBDSEF*, the most important variable is *SEEPUNC*. However the incremental effect associated with *SEEPUNC* is small as the R^2 values for the regression models containing both *PROBDSEF* and *SEEPUNC* are 0.79, 0.82 and 0.75.

After *PROBDSEF* and *SEEPUNC*, smaller effects are indicated for a number of variables (Figure K5.7.1-2a). For example, the following additional variables are indicated as affecting *EXPDOSE* at 10,000 yr: *INFIL*, *SEEPPRM* (mean fracture permeability in lithophysal rock units, m^2; as sampled, *SEEPPRM* is actually the logarithm of the indicated permeability), *ALPHAL* (capillary strength parameter in lithophysal rock units), *MICTC99* (dose conversion factor for ^{99}Tc for modern interglacial climate, (rem/yr)/(pCi/L)), *MICPU239* (dose conversion factor for ^{239}Pu for modern interglacial climate, (rem/yr)/(pCi/L)), *PHCSS* (pointer variable used to determine pH in Cell 1 of CSNF WP under liquid influx conditions), *CPUCOLWF* (concentration of irreversibly attached plutonium on stable glass colloids, mol/L), *SZCOLRAL* (colloid retardation factor in alluvial unit of SZ, dimensionless; as sampled, *SZCOLRAL* is actually the logarithm of the indicated retardation factor), *RHMU0* (scale factor used to represent uncertainty in chloride concentration in drift waters for relative humidities in the range [0, 0.2]; as sampled, *RHMU0* is actually the logarithm of the indicated scale factor), and *DSFLUX* (flux splitting factor for DS). Specifically, the positive effect associated with *INFIL* results from increasing water flux through the EBS; the negative effects associated with *SEEPPRM* and *ALPHAL* result from increasing water diversion around the EBS; the positive effects associated with *MICTC99* and *MICPU239* result from increasing the received dose for a given exposure level; and the remaining variables have very small effects that may be real or may be spurious.

The dominant effect of *PROBDSEF* is readily apparent in the scatterplot in Figure K5.7.1-2b. Further, the smaller effects of *SEEPUNC* and *INFIL* can be seen in the scatterplots in Figure K5.7.1-2b,c.

It may seen strange that several of the variables identified in the analysis with PRCCs (i.e., *SZFIPOVO*, *SZGWSPDM*, *THERMCON*) in Figure K5.7.1-1c do not appear in the regressions in Figure K5.7.1-2a. However, the times at which these variables have identifiable effects on *EXPDOSE* in Figure K5.7.1-1c are not the times at which the regressions in Figure K5.7.1-2a are performed.

Expected Dose to RMEI over [0, 1,000,000 yr]: *EXPDOSE*. The uncertainty and sensitivity analyses for expected dose to the RMEI (*EXPDOSE*, mrem/yr) over the time interval [0, 1,000,000 years] resulting from early DS failure are summarized in Figures K5.7.1-3 and K5.7.1-4. The time dependent results for *EXPDOSE* tend to decrease until about 200,000 yr and then level off (Figure K5.7.1-a,b). This decrease is probably due to the decay of ^{239}Pu, which has a half life of 24,100 yr. The values for *EXPDOSE* are bounded above by 0.01 mrem/yr and, after 200,000 yr, by 0.001 mrem/yr.

The sensitivity analyses for the time interval [0, 1,000,000 yr] are similar to those for the time interval [0, 20,000 yr]. Specifically, the sensitivity analysis with PRCCs for [0, 1,000,000 yr] in Figure K5.7.1-3c identifies the following variables as influencing the uncertainty in *EXPDOSE*:

PROBDSEF (probability that a randomly selected DS will experience an early failure), *INFIL* (infiltration level), *SEEPPRM* (mean fracture permeability in lithophysal rock units, m^2; as sampled, *SEEPPRM* is actually the logarithm of the indicated permeability), *SZFIPOVO* (flowing interval porosity in the volcanic unit of the SZ), *SEEPUNC* (pointer variable used to determine local seepage rates), and *SZGWSPDM* (groundwater specific discharge multiplier; as sampled, *SZGWSPDM* is actually the logarithm of the indicated multiplier). Similarly, the sensitivity analysis with PRCCs for [0, 20,000 yr] in Figure K5.7.1-1c identifies the following variables as influencing the uncertainty in *EXPDOSE*: *PROBDSEF*, *SZFIPOVO*, *SZGWSPDM*, *SEEPUNC*, *THERMCON* (host rock thermal conductivity level), and *INFIL*. For both time periods, *PROBDSEF* is the dominant contributor to the uncertainty in *EXPDOSE*, with the other variables making much smaller contributions to the uncertainty in *EXPDOSE*. The PRCC plots are constrained to contain a maximum of 6 variables. As a result, the slight differences in the variables shown in Figures K5.7.1-1c and K5.7.1-3c results from slight variations in the importance of individual variables over the time intervals under consideration.

More detailed sensitivity analyses for the time interval [0, 1,000,000 yr] are provided by the regressions in Figure K5.7.1-4a. As for the regressions in Figure K5.7.1-2a, the dominant variable is *PROBDSEF*. Specifically, the dominant effect of *PROBDSEF* on the uncertainty in *EXPDOSE* is indicated by R^2 values of 0.44, 0.51 and 0.48 for the regressions containing only *PROBDSEF* at 50,000, 200,000 and 500,000 yr. These values are lower than the corresponding R^2 values of 0.74, 0.76 and 0.69 obtained in the analyses in K5.7.1-2a at 3,000, 5,000 and 10,000 yr , which suggests that more variables are having small effects on the uncertainty in *EXPDOSE* at later times than is the case for the first 20,000 yr. This is borne out by the large number of variables indicated as having small effects on *EXPDOSE* in the regression analyses in Figure K5.7.1-4a. After *PROBDSEF*, the next most important variable in all three regressions is *INFIL*, with *EXPDOSE* tending to increase as *INFIL* increases as a result of increased water flow through the EBS and UZ. Together, *PROBDSEF* and *INFIL* result in regressions with R^2 values of 0.55, 0.60 and 0.61 at 50,000, 200,000 and 500,000 yr.

After *PROBDSEF* and *INFIL*, all three regressions select *SZGWSPDM*, *SEEPUNC* and *SEEPPRM* as the next three variables to add to the regression models, although not necessarily in the same order (Figure K5.7.1-4a). Addition of these three variables brings the R^2 values up to 0.74, 0.75 and 0.73 at 50,000, 200,000 and 500,000 yr. As previously discussed, *SZGWSPDM* has a positive effect on *EXPDOSE* as a result of speeding up flow in the SZ; *SEEPUNC* has a positive effect on *EXPDOSE* as a result of increasing water flow through the EBS; and *SEEPPRM* has a negative effect on *EXPDOSE* as a result of increasing water flow around the EBS and thus reducing water flow through the EBS.

After *PROBDSEF*, *INFIL*, *SZGWSPDM*, *SEEPUNC* and *SEEPPRM*, the regressions at 50,000, 200,000 and 500,000 yr add 9, 9 and 10 additional variables, respectively, and produce models with R^2 values of 0.84, 0.85 and 0.86 (Figure K5.7.1-4a). Thus, as noted earlier, a large number of variables are having small effects on the uncertainty in *EXPDOSE* at later times.

The dominant effect of *PROBDSEF* on the uncertainty in *EXPDOSE* can also been seen in the scatterplot in Figure K5.7.1-4b. In contrast, the much smaller effects of *INFIL* and *SZGWSPDM* on the uncertainty in *EXPDOSE* can been in the scatterplots in Figure K5.7.1-4c,d.

K5.7.2 Early Failure Scenario Classes: Expected Dose to Reasonably Maximally Exposed Individual from Early Waste Package Failure

Expected Dose to RMEI over [0, 20,000 yr]: *EXPDOSE*. The uncertainty and sensitivity analyses for expected dose to the RMEI (*EXPDOSE*, mrem/yr) over the time interval [0, 20,000 yr] resulting from early WP failure are summarized in Figures K5.7.2-1 and K5.7.2-2. There is a sharp peak in *EXPDOSE* between 1,000 and 2000 yr resulting from the release of ^{99}Tc from the failure of CDSP WPs (Figure K5.7.1-2a,b). At the time of this peak, maximum values for *EXPDOSE* are in the vicinity of 0.1 mrem/yr, although the values for most sample elements are considerably smaller. After this initial early peak, *EXPDOSE* has values in a range from approximately 10^{-5} to 10^{-3} mrem/yr until a time of about 10, 000 yr.

At 10,000 yr, there is a sharp jump in the values for *EXPDOSE* (Figure K5.7.1-2a,b). This jump results from the arrival of radionuclide releases at the location of the RMEI that result from the failure of CSNF WPs. The CSNF WPs are hotter than the CDSP WPs, with the result that releases from CSNF WPs are delayed until both the WP temperature falls below 100ºC and the relative humidity interior to these packages reaches 95 percent, at which time diffusive transport begins. The jump in *EXPDOSE* between approximately 9000 and 14,000 yr results from the arrival of ^{99}Tc at the location of the RMEI. After this jump, the values for *EXPDOSE* again decrease as the pulse of ^{99}Tc passes.

This bimodal behavior of *EXPDOSE* with different peaks for the two waste types does not occur for early DS failure (compare Figures K5.7.1-1a,b and K5.7.2-2a,b). Early DS failure is assumed to result in WP failure only if the failed DS is experiencing dripping conditions; otherwise, there is no WP failure and hence no radionuclide release. Because all failed WPs are in dripping conditions, water flows into every failed WP as soon as WP temperature falls below 100ºC and advective transport occurs immediately, with the result that there is little temporal variability in the start of radionuclide releases from the EBS for different WP types.

The PRCCs in Figure K5.7.2-1c indicate that the uncertainty in *EXPDOSE* is dominated by *PROBWPEF* (probability that a randomly selected WP will experience an early failure), with the value for *EXPDOSE* increasing as *PROBWPEF* increases. This effect results because increasing *PROBWPEF* increases the expected number of WPs that experience early failure and hence increases *EXPDOSE*. The PRCCs for *PROBWPEF* decrease in value over the period from approximately 9000 to 14,000 yr as a result of the noise introduced into the analysis as a result of the pulse releases arriving from the failed CSNF WPs.

In addition to *PROBWPEF*, smaller effects are indicated for *INFIL* (infiltration level), *THERMCON* (host rock thermal conductivity level), *SZFIPOVO* (flowing interval porosity in the volcanic unit of the SZ), *SZGWSPDM* (groundwater specific discharge multiplier*;* as sampled, *SZGWSPDM* is actually the logarithm of the indicated multiplier), and *DSNFMASS* (scale factor used to characterize uncertainty in the amount of DSNF contained in CDSP WPs) (Figure K5.7.2-1c). The effects of *INFIL*, *SZFIPOVO* and *SZGWSPDM* are the same as previously discussed in conjunction with Figure K5.7.1-1c. The effect of *THERMCON* is similar, although more pronounced. Increasing *THERMCON* leads to lower drift temperatures and earlier arrival of seepage waters, and thus to earlier beginning of diffusive transport. This effect is evident in the positive correlation between *THERMCON* and *EXPDOSE* between 0 yr and

1,500 yr. However, between 2,500 yr and 9,500 yr, the correlation becomes negative. This change in correlation results from the effect of temperature on waste form degradation. Increasing temperature increases the dissolution rate of the HLW in CDSP WPs (BSC 2004 ANL-EBS-MD-000016 REV 02, [DIRS 169988], Section 6.5.2.1). Consequently, as *THERMCON* increases, temperatures decrease and HLW degradation slows, resulting in less radionuclides available for mobilization and transport, and in turn reducing *EXPDOSE*. This pattern repeats for the CSNF waste, which starts diffusive transport at about 9,500 yr. The positive effect associated with *DSNFMASS* results from increasing the amount of ^{99}Tc in CDSP WPs and hence the dose from ^{99}Tc that results from the failure of these WPs.

More detailed sensitivity analyses for *EXPDOSE* are provided by the regression analyses in Figure K5.7.2-2a. The dominant effect of *PROBWPEF* on the uncertainty in *EXPDOSE* is indicated by R^2 values of 0.62, 0.79 and 0.47 for the regressions containing only *PROBWPEF* at 3,000, 5,000 and 10,000 yr.

As for the PRCCs for *PROBWPEF* in Figure K5.7.2-1c, the R^2 value for the regression at 10,000 years decreases in value as a result of the noise introduced into the analysis by the pulse releases arriving from the failed CSNF WPs over the period from approximately 9000 to 14,000 yr. Because of this noise, the final regression model at 10,000 contains only 5 variables and has an R^2 value of 0.67. However, a clearer view of what is driving the uncertainty in *EXPDOSE* at 10,000 yr is provided by the scatterplots in Figure K5.7.2-2b,c,d. Specifically, the uncertainty in *EXPDOSE* is still clearly dominated by *PROBWPEF* (Figure K5.7.2-2b), with smaller contributions to this uncertainty from *INFIL* (Figure K5.7.2-2c) and *THERMCON* (Figure K5.7.2-2d). The scatterplot for *PROBWPEF* (Figure K5.7-2b) shows an interesting pattern in that it contains two separate populations of points that each increase monotonically with *PROBWPEF*. The upper population of points consists of realizations in which the CSNF WPs in one or more percolation bins have begun diffusive transport (relative humidity interior to the WP exceeds 95 percent) by 10,000 yr. Because infiltration rates and temperatures vary between percolation bins, the time at which diffusive transport begins also varies, with most CSNF WPs beginning diffusive transport between 9,000 yr and 14,000 yr, whereas CDSP WPs begin diffusive transport between 500 yr and 3,000 yr. The differences are also apparent in Figure K5.7.2-1a as two jumps in expected dose corresponding to the occurrence of dose from each of the two WP types.

Figure K5.7.2-2c indicates that the expected dose at 10,000 yr decreases as *INFIL* increases. As *INFIL* increases, percolation rates tend to increase in most percolation bins, leading to earlier arrival of seepage into a drift. Because increased infiltration also leads to lower temperatures, and at lower drift temperatures, the difference in relative humidity on WPs of different temperatures becomes more pronounced, increasing infiltration results in the counter-intuitive effect that the warmer WPs (CSNF WPs) have lower relative humidity at higher values of infiltration. These lower values of relative humidity are less likely to permit diffusive transport, which in turn yields a negative relationship between *INFIL* and expected dose at 10,000 years. The relationship between infiltration, temperature and relative humidity is described and documented in (SNL 2007, DIRS [181383]).

Figure K5.7.2-2c indicates that expected dose at 10,000 yr increases as *THERMCON* (thermal conductivity) increases. This correlation is valid at 10,000 yr because at this time CSNF WPs are

just beginning diffusive transport, so the correlation indicates the positive relationship between *THERMCON* and *EXPDOSE* described above. If the correlation were to be performed at later times, after transport has begun, the relationship between *THERMCON* and *EXPDOSE* would be reversed, because at these times *THERMCON* is affecting waste degradation rates, as described above. .

In contrast, more informative results are given by the regression analyses at 3,000 and 5,000 years without the added need to examine scatterplots (Figure K5.7.2-2a). Specifically, both the indicated regressions select the following four variables after *PROBWPEF*: *MICTC99* (dose conversion factor for ^{99}Tc for modern interglacial climate, (rem/yr)/(pCi/L)), *MICC14* (dose conversion factor for ^{14}C for modern interglacial climate, (rem/yr)/(pCi/L)), *DSNFMASS*, and *UZFAG8* (fracture aperture for Group 8 rock units in UZ). Increasing *MICTC99* and *MICC14* has a positive effect on *EXPDOSE* that results from increasing the received dose for a given exposure level; increasing *DSNFMASS* has a positive effect on *EXPDOSE* that results from increasing the amount of ^{99}Tc in CDSP WPs and hence the dose from ^{99}Tc that results from the failure of these WPs; and increasing *UZFAG8* has a negative effect on *EXPDOSE* that results from decreasing the proportion of radionuclides moving through fractures in the UZ. Specifically, increasing *UZFAG8* increases the proportion of the interface area between the EBS and the UZ that consists of fractures, which increases the mass of radionuclides that diffuse into fractures in the UZ, where radionuclide movement is relatively rapid, and decreases the mass of radionuclides that diffuse into the surrounding rock matrix, where radionuclide movement is slower. Collectively, the inclusion of *MICTC99*, *MICC14*, *DSNFMASS* and *UZFAG8* increases the R^2 values for the two regressions to 0.75 and 0.87. After *MICTC99*, *MICC14*, *DSNFMASS* and *UZFAG8*, the regressions add an additional six variables that have small effects and result in final models that have R^2 values of 0.80 and 0.90. The regression models at 3,000 yr tend to have smaller R^2 values than the regression models at 5,000 yr because of the noise introduced by the arrival of the ^{99}Tc releases (i.e., compare the smoothness of the time-dependent releases at 3,000 and 5,000 yr in Figure K5.7.2-2a,b).

Expected Dose to RMEI over [0, 1,000,000 yr]: *EXPDOSE*. The uncertainty and sensitivity analyses for expected dose to the RMEI (*EXPDOSE*, mrem/yr) over the time interval [0, 1,000,000 yr] resulting from early WP failure are summarized in Figures K5.7.2-3 and K5.7.2-4.

Except for very early times, the values for *EXPDOSE* fall between 10^{-6} and 0.1 mrem/yr for the 0 to 1,000,000 yr time interval (Figure K5.7.2-3a). For most sample elements, the values for *EXPDOSE* monotonically decrease until about 300,000 yr, at which time they show a sharp increase in value as the result of the failure of the DSs from general corrosion. This failure allows seeping water to directly contact the failed WPs, and as a consequence, produces larger radionuclide releases from the failed WPs.

The single most important variable with respect to the uncertainty in *EXPDOSE* is *PROBWPEF* (probability that a randomly selected WP will experience an early failure), with the value for *EXPDOSE* increasing as *PROBWPEF* increases. This effect results because increasing *PROBWPEF* increases the expected number of WPs that experience early failure and hence

increases *EXPDOSE* (Figures K5.7.2-3c, K5.7.2-4a). The positive effect of *PROBWPEF* can be seen in the scatterplot in Figure K5.7.2-4b.

Prior to 300,000 yr, *ISCSNS* (pointer variable used to determine ionic strength in CSNF cell under vapor influx conditions) and *SZGWSPDM* (groundwater specific discharge multiplier*;* as sampled, *SZGWSPDM* is actually the logarithm of the indicated multiplier) also have significant positive effects on the uncertainty in *EXPDOSE* (Figures K5.7.2-3c, K5.7.2-4a). These effects result because increasing *ISCSNS* increases plutonium solubility, and increasing *SZGWSPDM* increases water flow in the SZ. After 300,000 yr, *INFIL* (infiltration level) and again *SZGWSPDM* are indicated as having positive effects on *EXPDOSE* (Figures K5.7.2-3c, K5.7.2-4a). These effects result because increasing *INFIL* increases water flow in the EBS and UZ, and increasing *SZGWSPDM* increases water flow in the SZ. After *PROBWPEF*, *ISCSNS*, *SZGWSPDM* and *INFIL*, the analyses identify a number of additional variables that have small effects on *EXPDOSE*.

K5.7.3 Early Failure Scenario Classes: Expected Dose to Reasonably Maximally Exposed Individual from Both Early Drip Shield Failure and Early Waste Package Failure

Expected Dose to RMEI over [0, 20,000 yr]: *EXPDOSE*. The uncertainty and sensitivity analyses for expected dose to the RMEI (*EXPDOSE*, mrem/yr) over the time interval [0, 20,000 yr] resulting from both early DS failure and early WP failure are summarized in Figures K5.7.3-1 and K5.7.3-2. Because the expected doses from early WP failure tend to be one or more orders of magnitude greater than the expected doses from early DS failure (i.e., compare the results in Figures K5.7.1-1a,b and K5.7.2-1a,b), the results in Figures K5.7.3-1 and K5.7.3-2 from both early DS failure and early WP failure are very similar to the results in Figures K5.7.2-1 and K5.7.2-2 for early WP failure alone. For this reason, the discussion associated with Figures K5.7.2-1 and K5.7.2-2 for early WP failure is also applicable to the results in Figures K5.7.3-1 and K5.7.3-2 for both early DS failure and early WP failure and will not be repeated.

Expected Dose to RMEI over [0, 1,000,000 yr]: *EXPDOSE*. The uncertainty and sensitivity analyses for expected dose to the RMEI (*EXPDOSE*, mrem/yr) over the time interval [0, 1,000,000 yr] resulting from both early DS failure and early WP failure are summarized in Figures K5.7.3-3 and K5.7.3-4. As for the 20,000 yr time period, the behavior of *EXPDOSE* for the combined releases from early DS failure and early WP failure is essentially the same as obtained for early WP failure alone (i.e., compare the results in Figures K5.7.1-3a,b and K5.7.2-3a,b). For this reason, the discussion associated with Figures K5.7.2-3 and K5.7.2-4 for early WP failure is also applicable to the results in Figures K5.7.3-3 and K5.7.3-4 for both early DS failure and early WP failure and will not be repeated.

K5.7.4 Early Failure Scenario Classes: Expected Dose to Reasonably Maximally Exposed Individual from Early Drip Shield Failure, Early Waste Package Failure, and Nominal Processes

Expected Dose to RMEI over [0, 20,000 yr]: *EXPDOSE*. Nominal processes cause no WP failures within the 0 to 20,000 yr time interval. As a result, the combined early DS failure and early WP failure results summarized in Figures K5.7.3-1 and K5.7.3-2 are the same as what would be obtained if (the nonexistent) releases from nominal processes were included in the analysis.

Expected Dose to RMEI over [0, 1,000,000 yr]: *EXPDOSE*. The uncertainty and sensitivity analyses for expected dose to the RMEI (*EXPDOSE*, mrem/yr) over the time interval [0, 1,000,000 yr] resulting from early DS failure, early WP failure and nominal process WP failure are summarized in Figures K5.7.4-1 and K5.7.4-2.

Prior to 200,000 yr, the value of *EXPDOSE* is determined by processes related to early DS failure and early WP failure. As a result, the regression at 50,000 yr in Figure K5.7.3-4a conditional on early DS failure and early WP failure is the same as the corresponding regression in Figure K5.7.4-2a conditional on early DS failure, early WP failure, and nominal process WP failure. By 200,000 yr, failures resulting from nominal processes are starting to occur. As a result, the regression at 200,000 yr in Figure K5.7.4-2a is slightly different from the corresponding regression in Figure K5.7.3-4a. For example, *WDGCA22* (temperature dependence associated with the general corrosion rate for alloy 22, K) now appears in the regression model. However, the regression model at 200,000 yr has a relatively low R^2 value of 0.51 as a result of the noisy behavior of the time-dependent values for *EXPDOSE* in the vicinity of 200,000 yr (Figure K5.7.4-1a,b). This noisy behavior creates patterns that the regression model cannot capture and results from *EXPDOSE* changing for individual sample elements from being dominated by effects associated with early DS and WP failures to effects associated with WP failures from nominal processes.

After 200,000 yr, the value of *EXPDOSE* is determined primarily by processes related to the failure of WPs from nominal processes (i.e., compare the post 200,000 yr results in Figure K5.7.3-3a,b for early DS and WP failure with the corresponding results in Figure K5.7.4-1a,b for all three failure processes). As a result, the regression at 500,000 yr in Figure K5.7.4-2a is very different from the regression at 500,000 yr in Figure K5.7.3-4a when only early DS and WP failures are considered in the definition of *EXPDOSE*. In particular, the dominant variable in the regression in Figure K5.7.3-4a when only early DS and WP failures are considered is *PROBWPEF* (probability that a randomly selected WP will experience an early failure). In contrast, the dominant variable in the regression in Figure K5.7.4-2a when all three failure processes are considered is *WDGCA22*, with a relatively small effect indicated for *PROBWPEF*. Specifically, the regression model containing only *WDGCA22* has an R^2 value of 0.78; in contrast, *PROBWPEF* is the fourth variable selected in the stepwise process and only increases the R^2 value from 0.83 to 0.84.

The dominant effect of *WDGCA22* can be seen in the scatterplot in Figure K5.7.4-2b, with *EXPDOSE* decreasing as *WDGCA22* increases. After *WDGCA22*, the regression at 500,000 yr in

Figure K5.7.4-2a selects *THERMCON* (host rock thermal conductivity level) and *WDNSCC* (stress corrosion cracking growth rate exponent) to add to the model. However, as can be seen in the scatterplots in Figure K5.7.4-2c,d, *THERMCON* and *WDNSCC* have relatively small effects on *EXPDOSE* and only increase the R^2 value from 0.78 for a model containing only *WDGCA22* to (i) 0.83 for a model containing *WDGCA22*, *THERMCON* and *WDNSCC* and (ii) 0.84 for a model containing *WDGCA22*, *THERMCON*, *WDNSCC* and *PROBWPEF*. After *WDGCA22*, *THERMCON*, *WDNSCC* and *PROBWPEF*, the regression analysis selects 9 additional variables that have small effects on *EXPDOSE* and produces a final model with an R^2 value of 0.88.

K6 IGNEOUS SCENARIO CLASSES

K6.1 Igneous Scenario Classes: Summary

The igneous scenario classes are defined on the basis of futures that involve one or more igneous events (Section J7). This section (Section K6) presents uncertainty and sensitivity analysis results for selected analysis outcomes associated with the igneous scenario classes (Table K6.1-1). The primary emphasis is on the igneous intrusive scenario class but expected dose results for igneous eruptive scenario class are also presented.

The primary results considered for the igneous intrusive scenario class are radionuclide movement from the EBS to the UZ (Table K6.1-2), radionuclide movement from the UZ to the SZ (Table K6.1-3), radionuclide movement in the SZ at the location of the RMEI (Table K6.1-4), dose to the RMEI from selected radionuclides (Table K6.1-5), and expected dose to the RMEI from all radionuclides (Table K6.1-6). High-level summaries of the uncertainty and sensitivity analysis results presented in this section are provided in Tables K6.1-2 to K6.1-6. Additional uncertainty analysis results are also available in Section J7.

From a regulatory perspective, expected dose to the RMEI (*EXPDOS*, mrem/yr) is the analysis outcome of greatest interest associated with the igneous scenario classes (Table K6.1-6). For the igneous intrusive scenario class, *EXPDOS* tends to monotonically increase over the time interval [0, 2×10^4 yr], and the range of possible values for *EXPDOS* at 10^4 yr is approximately [10^{-4}, 3 mrem/yr] (Figure K6.7.1-1). For the [0, 10^6 yr] time interval, *EXPDOS* tends to monotonically increase over the time interval [0, 10^5 yr], monotonically decrease over the time interval [10^5, 2×10^5 yr], and then monotonically increase over the time interval [2×10^5, 10^6 yr] (Figure K6.7.2-1). Over the time interval [0, 10^6 yr], the range of possible values for *EXPDOS* is approximately [10^{-4}, 100 mrem/yr]. The dominant variable with respect to the uncertainty associated with *EXPDOS* is *IGRATE* (rate of occurrence of igneous intrusive events, yr^{-1}) (Figures K6.7.1-1, K6.7.1-2, K6.7.2-1, K6.7.2-2). A smaller contribution to the uncertainty in *EXPDOS* are made by *SZGWSPDM* (groundwater specific discharge multiplier; as sampled, *SZGWSPDM* is actually the logarithm of the indicated multiplier) and a number of additional variables.

For the igneous eruptive scenario class, the possible values for *EXPDOS* fall in the interval [2×10^{-7}, 2×10^{-3} mrem/yr] for both the [0, 2×10^4 yr] and [0, 10^6 yr] time intervals (Figures K6.8.1-1, K6.8.2-1). The dominant variable with respect to the uncertainty in *EXPDOS* for the igneous eruptive scenario class is *IGERATE* (rate of occurrence of igneous eruptive

events, yr^{-1}; *IGERATE* = (0.29) (0.27) *IGRATE*, where 0.29 is the probability that an igneous intrusive event will have an eruptive component and 0.27 is the probability that the eruptive component of an igneous intrusive event will intercept waste) (Figures K6.8.1-1, K6.8.1-2, K6.8.2-1, K6.8.2-2).

K6.2 Igneous Intrusive Scenario Classes: Engineered Barrier System Conditions over the Time Interval [0, 1,000,000 yr] for an Event at 250 yr

This section discusses conditions in the EBS after an igneous intrusive event at 250 yr that damages all WPs in the repository. Similar conditions exist after igneous intrusive events at other times.

The EBS is assumed to rapidly cool after an igneous intrusive event. Specifically, the EBS is assumed to revert to temperature conditions consistent with heating from radioactive decay 250 yr after an igneous intrusive event (Figure K6.2-1). Consistent with this, the post 500 year results in Figure K6.2-1 are the same as the post 500 yr results in Figure K4.3-5. Similarly, the relative humidity conditions and the partial pressures for CO_2 in the EBS are assumed to revert to conditions consistent with heating from radioactive decay 250 yr after an igneous event. As a result, the post 500 yr relative humidity conditions and the partial pressures for CO_2 in the EBS are the same as the post 500 yr results in Figures K4.3-6 and K4.3-7.

After an igneous intrusion, the drift is assumed to be filled with basalt. In consistency with the assumption that the resultant basalt has properties similar to the host rock that surrounds the drift, seepage into the EBS (m^3/yr/WP) is determined by multiplying the percolation rate (m^3/m^2/yr) at the base on the PTn (an overlying rock formation) by the footprint area (m^2/WP) of the drift segment containing a WP (Section 6.5.1.1) (Figure K6.2-2). The seepage levels for CSNF and CDSP WPs in a given percolation bin are assumed to be the same. Further, all WPs are assumed to experience seepage (i.e., dripping conditions).

An igneous intrusion causes a change in chemical conditions in the EBS. As a result, the ionic strengths of EBS waters after an igneous intrusion (Figure K6.2-3) are different from the ionic strengths of EBS waters under nominal conditions (Figures K4.3-9 and K4.3-11). As indicated by the PRCCs in Figure K6.2-3e, the uncertainty in ionic strength (mol/kg) under dripping conditions in the invert for CSNF WPs (*ISCSINAD*) is completely dominated by *ISCSS* (pointer variable used to determine ionic strength in CSNF cell 1 under dripping conditions), with *ISCSINAD* increasing as *ISCSS* increases. Similarly, the PRCCs in Figure K6.2-3f indicate that the uncertainty in ionic strength (mol/kg) under dripping conditions in the invert for CDSP WPs (*ISCDINAD*) is completely dominated by *IS2MCOS* (pointer variable used to determine ionic strength in CDSP WP cell 1b under liquid influx conditions), with *ISCDINAD* increasing as *IS2MCOS* increases. As a reminder, all WPs are assumed to experience dripping conditions after an igneous event.

Because of the changed chemical conditions, the pH conditions of EBS waters after an igneous intrusion (Figure K6.2-4) are different from the pH conditions of EBS waters under nominal conditions (Figures K4.3-12 and K4.3-14). As indicated by the PRCCs in Figure K6.2-4e, the uncertainty in pH in the invert for CSNF WPs experiencing dripping conditions (*PHCSINAD*) is dominated by *PH2RGER* (error term in regression equation used to determine pH of corrosion

products domain), with *PHCSINAD* increasing as *PH2RGER* increases. Prior to 10,000 yr, a negative effect is indicated for *DELPPCO2* (scale factor used to incorporate uncertainty into the value for the partial pressure of CO_2). Smaller effects are indicated for several other variables, but it is *PH2RGER* that dominates the uncertainty in *PHCSINAD*. The PRCC analysis in Figure K6.2-4f for pH in the invert for CDSP WPs experiencing dripping conditions (*PHCDINAD*) is similar to the corresponding analysis for *PHCSINAD* in Figure K6.2-4e.

K6.3 Igneous Intrusive Scenario Classes: Release from Engineered Barrier System

K6.3.1 Igneous Intrusive Scenario Classes: Release from Engineered Barrier System over the Time Interval [0, 20,000 yr] for an Event at 10 yr

Movement of ^{239}Pu Irreversibly Attached to Glass/Waste Form (i.e., Ic) Colloids: *ESIC239* and *ESIC239C*. The uncertainty and sensitivity analyses for the time-dependent release rates (*ESIC239*, g/yr) and cumulative releases (*ESIC239C*, g) over the time interval [0, 20,000 yr] for the movement of ^{239}Pu irreversibly attached to glass/waste form (i.e., Ic) colloids from the EBS to the UZ resulting from an igneous intrusive event at 10 yr that destroys all WPs in the repository are summarized in Figures K6.3.1-1 and K6.3.1-2. Except for transient spikes in release rates before 1,000 yr, the release rates maintain steady values for each climate period.

As indicated by the PRCCs in Figure K6.3.1-1e,f and the regression analyses in Figure K6.3.1-2a,b, the dominant variables contributing to the uncertainty in *ESIC239* and *ESIC239C* are *CPUCOLWF* (maximum concentration of plutonium irreversibly attached to glass colloids, mol/L) and *INFIL* (infiltration level), with *ESIC239* and *ESIC239C* increasing as each of these variables increases. These effects result because increasing *CPUCOLWF* increases the amount of ^{239}Pu that can potentially be irreversibly attached to glass colloids and increasing *INFIL* increases water flow in the EBS and the UZ. The regression models for *ESIC239* and *ESIC239C* containing only *CPUCOLWF* have R^2 values of 0.63 or 0.64, and the models containing both *CPUCOLWF* and *INFIL* have R^2 values between 0.91 and 0.93 (Figure K6.3.1-2a,b). Thus, the uncertainty in *CPUCOLWF* and *INFIL* dominates the uncertainty in *ESIC239* and *ESIC239C*. In addition to *CPUCOLWF* and *INFIL*, the regression analyses indicate small effects for several additional variables. The dominant effects of *CPUCOLWF* and *INFIL* can be seen in the scatterplots in Figure K6.3.1-2c,d,e,f,g,h.

The PRCCs indicate effects for *THERMCON* (host rock thermal conductivity level) prior to 1,000 yr (Figure K6.3.1-1e,f). The effects associated with *THERMCON* result from an implementation error in the Goldsim component of the TSPA-LA Model that incorrectly allowed drift-wall condensation to occur after an igneous intrusion (Appendix P, Table P-6). When condensation occurs, water flow through the waste is increased by the condensation, resulting in the transient spikes in release rates evident in Figure K6.3.1-1a,c and also in the correlation of release rates and cumulative releases with *THERMCON*.

Movement of ^{239}Pu Irreversibly Attached to Ferrous (i.e., If) Colloids: *ESIF239* and *ESIF239C*. Uncertainty and sensitivity analyses for the movement of ^{239}Pu irreversibly attached to ferrous colloids are not presented due to an error in the GoldSim component of the TSPA-LA Model that affects the calculation of stability of ferrous colloids. Consequently,

Figure K6.3.1-3 and Figure K6.3.1-4 have been removed from this document. See Appendix P, Section P18, for a discussion of the error and the effect of the error on TSPA-LA Model results.

Movement of Dissolved ^{237}Np: *ESNP237* and *ESNP237C*. The uncertainty and sensitivity analyses for the time-dependent release rates (*ESNP237*, g/yr) and cumulative releases (*ESNP237C*, g) over the time interval [0, 20,000 yr] for the movement of dissolved ^{237}Np from the EBS to the UZ resulting from an igneous intrusive event at 10 yr that destroys all WPs in the repository are summarized in Figures K6.3.1-5 and K6.3.1-6.

As indicated by the PRCCs in Figure K6.3.1-5e,f and the regression analyses in Figure K6.3.1-6a,b, the most important variable with respect to the uncertainty in *ESNP237* and *ESNP237C* is *PHCSS* (pointer variable used to determine pH in CSNF cell 1 under liquid influx conditions), with *ESNP237* and *ESNP237C* tending to decrease as *PHCSS* increases. This effect results because increasing *PHCSS* reduces the solubility of neptunium in CSNF WPs. The five individual regressions containing only *PHCSS* have R^2 values between 0.27 or 0.3; thus, the uncertainty in *ESNP237* and *ESNP237C* is not dominated by *PHCSS*.

In addition to the effects associated with *PHCSS*, significant effects on the uncertainty in *ESNP237* and *ESNP237C* are indicated for *EP1NPO2* (scale factor used to incorporate uncertainty into NpO_2 solubility below 1 molal ionic strength; as sampled, *EP1NPO2* is actually the logarithm of the indicated scale factor), *EP1LOWAM* (scale factor used to incorporate uncertainty into americium solubility under low ionic strength conditions; as sampled, *EP1LOWAM* is actually the logarithm of the indicated scale factor), *CORRATSS* (corrosion rate for stainless steel, μm/yr), *INFIL* (infiltration level), and *DELPPCO2* (scale factor used to incorporate uncertainty into the value for the partial pressure of CO_2), and *EP1LOWNU* (scale factor used to incorporate uncertainty into uranium solubility under low ionic strength conditions for nominal and seismic conditions; as sampled, *EP1LOWNU* is actually the logarithm of the indicated scale factor; in the present analysis, *EP1LOWNU* was used instead of the corresponding and intended variable *EP1LOWOU* for igneous conditions; however, this has no effect on analysis outcomes as *EP1LOWNU* and *EP1LOWOU* are assigned the same distribution) (Figures K6.3.1-5e,f and K6.3.1-6a,b).

The indicated effects associated with *EP1NPO2*, *CORRATSS*, *INFIL* and *DELPPCO2* result because (i) increasing *EP1NPO2* increases the solubility of neptunium and hence the dissolved concentration ^{237}Np, (ii) increasing *CORRATSS* increases the corrosion rate of stainless steel and thus decreases the dissolved concentration ^{237}Np as a result of sorption on corrosion products, (iii) increasing *INFIL* increases water flow through the EBS and thus increases the rate at which ^{237}Np is transported out of the EBS, and (iv) increasing *DELPPCO2* increases the partial pressure of CO_2, which tends to increase the solubility of Np.

The positive effects for *EP1LOWAM* and *EP1LOWNU* result from increasing the amounts of uranium and americium that go into solution. In turn, this increases the amount sorbed uranium and americium and thus reduces the sorption sites available for the sorption of neptunium. This reduction in the number of sorption sites tends to increase the concentration of dissolved ^{237}Np and hence increase *ESNP237* and *ESNP237C*. It is also possible that the decay of ^{241}Am to

^{237}Np may have a positive effect on the amount of dissolved ^{237}Np and hence on *ESNP237* and *ESNP237C*.

The effects of *EP1NPO2*, *INFIL* and *PHCSS* on *ESNP237* and *ESNP237C* can be seen in the scatterplots in Figure K6.3.1-6c,d,e,f,g.

After *PHCSS*, *EP1NPO2*, *CORRATSS*, *EP1LOWAM*, *INFIL*, *DELPPCO2* and *EP1LOWNU*, the regression analyses select a number of additional variables that have small effects on *ESNP237* and *ESNP237C*. The final regression models for *ESNP237* and *ESNP237C* have R^2 values between 0.77 and 0.82 (Figure K6.3.1-6a,b). Thus, most of the uncertainty associated with *ESNP237* and *ESNP237C* is accounted for.

It is possible that some of the variables selected near the ends of the regression analyses for *ESNP237* and *ESNP237C* may be spurious (Figure K6.3.1-6a,b). For example, *WDCRCDEN* (scale factor to convert area on a WP experiencing stress corrosion cracking to a resultant diffusive area) should have no effect on *ESNP237* and *ESNP237C* for igneous intrusive events and thus its selection is most likely spurious as a result of a slight nonrandom pattern in the mapping between the sampled values for *WDCRCDEN* and the calculated values for *ESNP237* and *ESNP237C*. However, variables such as *WDCRCDEN* added near the end of a stepwise regression analysis have little effect on the final R^2 values. An occasional spurious variable near the end of a stepwise regression analysis will often occur when a large number of analyses with large numbers of sampled variables are being performed.

Movement of Dissolved ^{239}Pu: *ESPU239* and *ESPU239C*. The uncertainty and sensitivity analyses for the time-dependent release rates (*ESPU239*, g/yr) and cumulative releases (*ESPU239C*, g) over the time interval [0, 20,000 yr] for the movement of dissolved ^{239}Pu from the EBS to the UZ resulting from an igneous intrusive event at 10 yr that destroys all WPs in the repository are summarized in Figures K6.3.1-7 and K6.3.1-8.

The dominant contributors to the uncertainty in *ESPU239* and *ESPU239C* are *EP1LOWPU* (scale factor used to incorporate uncertainty into plutonium solubility under low ionic strength conditions; as sampled, *EP1LOWPU* is actually the logarithm of the indicated scale factor), *DELPPCO2* (scale factor used to incorporate uncertainty into the value for the partial pressure of CO_2), *INFIL* (infiltration level), and *PHCSS* (pointer variable used to determine pH in CSNF cell 1 under liquid influx conditions) (Figures K6.3.1-7e,f and K6.3.1-8a,b). The variables *EP1LOWPU*, *DELPPCO2* and *INFIL* have positive effects on *ESPU239* and *ESPU239C* because increasing *EP1LOWPU* increases plutonium solubility, increasing *DELPPCO2* increases the partial pressure of CO_2, which, although decreasing pH, also increases the solubility of Pu and thus has a net effect of increasing the amount of dissolved ^{239}Pu, and increasing *INFIL* increases water flow through the EBS. In contrast, increasing *PHCSS* has a negative effect on *ESPU239* and *ESPU239C* because increasing *PHCSS* increases pH, which (as long as pH is below about 9) tends to decrease Pu solubility. The regression models containing *EP1LOWPU*, *DELPPCO2*, *INFIL* and *PHCSS* have R^2 values between 0.75 and 0.90 (Figure K6.3.1-8a,b).

The effects of *EP1LOWPU*, *DELPPCO2* and *INFIL* on *ESPU239* and *ESPU239C* can be seen in the scatterplots in Figure K6.3.1-8c,d,e,f,g.

After *EP1LOWPU*, *DELPPCO2*, *INFIL* and *PHCSS*, the regression analyses select a number of additional variables that have small effects on *ESPU239* and *ESPU239C* and produce final models with R^2 values between 0.82 and 0.92 (Figure K6.3.1-8a,b). Thus, most of the uncertainty associated with *ESPU239* and *ESPU239C* is accounted for

Movement of Dissolved ^{99}Tc: *ESTC99* and *ESTC99C*. The uncertainty and sensitivity analyses for the time-dependent release rates (*ESTC99*, g/yr) and cumulative releases (*ESTC99C*, g) over the time interval [0, 20,000 yr] for the movement of dissolved ^{99}Tc from the EBS to the UZ resulting from an igneous intrusive event at 10 yr that destroys all WPs in the repository are summarized in Figures K6.3.1-9 and K6.3.1-10.

The release of ^{99}Tc from the EBS is very rapid (Figure K6.3.1-9a,b,c,d). As time progresses, the uncertainty in *ESTC99* is dominated by *HLWDRALK* (dissolution rate of HLW glass under alkaline conditions, g/m^2/d) (Figures K6.3.1-9e and K6.3.1-10a,c). The negative effect associated with *HLWDRALK* at later times results because increasing *HLWDRALK* increases dissolution rate of HLW glass and hence increases the rate of release of ^{99}Tc. This results in a negative effect on *ESTC99* at later times because increasing the amount of ^{99}Tc released at early times reduces the amount of ^{99}Tc that can be released at later times and, as a result, reduces *ESTC99* as time increases. However, further investigation of model results determined that the HLW degradation after an igneous intrusion was not implemented correctly (see Appendix P, Section P16). Consistent with TSPA-LA Model assumptions, the HLW should degrade completely and instantaneously at the time of the igneous intrusion. Thus, the sensitivity of *ESTC99* to uncertainty in *HLWDRALK*, while phenomenologically correct, appears in the model results due to an error in the TSPA-LA Model.

The uncertainty in *ESTC99C* is completely dominated by *CSNFMASS* (scale factor used to characterize uncertainty in amount of CSNF in CSNF WPs) (Figures K6.3.1-9f and K6.3.1-10b,f). The positive effect of *CSNFMASS* on *ESTC99C* results because increasing *CSNFMASS* increases the mass of ^{99}Tc present in the repository. The dominant effect of *CSNFMASS* results from the rapid and unimpeded transport of ^{99}Tc out of the EBS. Specifically, the only thing that determines how much ^{99}Tc is transported out of the EBS is how much ^{99}Tc is present in the repository. Because the uncertainty in this amount is dominated by *CSNFMASS*, the uncertainty in *ESTC99C* is also dominated by *CSNFMASS*. In contrast, *CSNFMASS* is not significant in the regression analyses for *ESTC99* (rate of ^{99}Tc transport) due to the numerical resolution of this highly transient quantity. Because the solubility of ^{99}Tc is not limited, all of the ^{99}Tc available from degraded waste is mobilized and transported from the EBS over a few timesteps after the intrusion. During this interval, the rate of transport should depend on the mass of ^{99}Tc present, because the solubility of ^{99}Tc is high enough that any ^{99}Tc released from the waste is dissolved and transported immediately. Although the transport of ^{99}Tc during this interval is sufficiently resolved numerically to estimate dose (see Section 7.3.3), it is not sufficiently resolved numerically that the sensitivity analysis reported in Figures K6.3.1-9 and K6.3.1-10 can determine the effect of *CSNFMASS* on *ESTC99* during the time of initial transport.

K6.3.2 Igneous Intrusive Scenario Classes: Release from Engineered Barrier System over the Time Interval [0, 1,000,000 yr] for an Event at 250 yr

For completeness, this section presents summaries of the uncertainty and sensitivity analyses for release from the EBS over the time interval [0, 1,000,000 yr] for an igneous intrusive event at 250 yr that destroys all WPs in the repository without discussion.

Movement of ^{239}Pu Irreversibly Attached to Glass/ Waste Form (i.e., Ic) Colloids: *ESIC239* and *ESIC239C*. The uncertainty and sensitivity analyses for the time-dependent release rates (*ESIC239*, g/yr) and cumulative releases (*ESIC239C*, g) over the time interval [0, 1,000,000 yr] for the movement of ^{239}Pu irreversibly attached to glass/ waste form (i.e., Ic) colloids from the EBS to the UZ resulting from an igneous intrusive event at 250 yr that destroys all WPs in the repository are summarized in Figure K6.3.2-1.

Movement of ^{239}Pu Irreversibly Attached to Ferrous (i.e., If) Colloids: *ESIF239* and *ESIF239C*. Uncertainty and sensitivity analyses for the movement of ^{239}Pu irreversibly attached to ferrous colloids are not presented due to an error in the GoldSim component of the TSPA-LA Model that affects the calculation of stability of ferrous colloids. Consequently, Figure K6.3.2-2 has been removed from this document. See Appendix P, Section P18, for a discussion of the error and the effect of the error on TSPA-LA Model results.

Movement of Dissolved ^{237}Np: *ESNP237* and *ESNP237C*. The uncertainty and sensitivity analyses for the time-dependent release rates (*ESNP237*, g/yr) and cumulative releases (*ESNP237C*, g) over the time interval [0, 1,000,000 yr] for the movement of dissolved ^{237}Np from the EBS to the UZ resulting from an igneous intrusive event at 250 yr that destroys all WPs in the repository are summarized in Figure K6.3.2-3.

Movement of Dissolved ^{239}Pu: *ESPU239* and *ESPU239C*. The uncertainty and sensitivity analyses for the time-dependent release rates (*ESPU239*, g/yr) and cumulative releases (*ESPU239C*, g) over the time interval [0, 1,000,000 yr] for the movement of dissolved ^{239}Pu from the EBS to the UZ resulting from an igneous intrusive event at 250 yr that destroys all WPs in the repository are summarized in Figure K6.3.2-4.

Movement of Dissolved ^{99}Tc: *ESTC99* and *ESTC99C*. The uncertainty and sensitivity analyses for the time-dependent release rates (*ESTC99*, g/yr) and cumulative releases (*ESTC99C*, g) over the time interval [0, 1,000,000 yr] for the movement of dissolved ^{99}Tc from the EBS to the UZ resulting from an igneous intrusive event at 250 yr that destroys all WPs in the repository are omitted because of the rapid depletion of the 99Tc inventory (see Figure K6.3.1-9a,c).

K6.4 Igneous Intrusive Scenario Classes: Release from Unsaturated Zone (UZ)

K6.4.1 Igneous Intrusive Scenario Classes: Release from Unsaturated Zone (UZ) over the Time Interval [0, 20,000 yr] for an Event at 10 yr

Movement of ^{239}Pu Irreversibly Attached to Slow (i.e., Ic) Colloids: *UZIC239* and *UZIC239C*. To understand the presented analyses for colloids in the UZ and SZ, it is necessary to realize that a reapportioning of colloids takes place upon entry into the UZ (Section 6.3.8.3, EBS Transport Submodel Outputs). The EBS release involves ^{239}Pu attached to Ic colloids (i.e., glass colloids for releases from CDSP WPs and waste form colloids for releases from CSNF WPs). Upon entry into the UZ, the ^{239}Pu irreversibly attached to glass/waste form (i.e., Ic) and ferrous (i.e., If) colloids in the EBS is reapportioned. Specifically, (i) Ic now designates slow moving colloids, (ii) If now designates fast moving colloids, and (iii) the total amount of ^{239}Pu attached to Ic and If colloids in the EBS is reapportioned so that 99.832 percent of the total ^{239}Pu is attached to slow colloids (i.e., the new Ic colloids) upon entry into the UZ and the remaining 0.168 percent is attached to fast colloids (i.e., the new If colloids) upon entry into the UZ. Because the mass of ^{239}Pu attached to glass/waste form colloids in the EBS is much greater than the mass of ^{239}Pu attached to ferrous colloids in the EBS, the mass of ^{239}Pu attached to slow colloids entering the UZ is effectively the same as the mass of ^{239}Pu attached to glass colloids leaving the EBS. However, because the mass of ^{239}Pu attached to glass/waste form colloids in the EBS is much greater than the mass of ^{239}Pu attached to ferrous colloids in the EBS, the indicated reapportioning results in the release of ^{239}Pu attached to fast colloids into the UZ having very different properties from the release of ^{239}Pu attached to ferrous colloids out of the EBS.

The uncertainty and sensitivity analyses for the time-dependent release rates (*UZIC239*, g/yr) and cumulative releases (*UZIC239C*, g) over the time interval [0, 20,000 yr] for the movement of ^{239}Pu irreversibly attached to slow (i.e., Ic) colloids from the UZ to the SZ resulting from an igneous intrusive event at 10 yr that destroys all WPs in the repository are summarized in Figures K6.4.1-1, K6.4.1-2 and K6.4.1-3. Transport through the UZ occurs relatively rapidly, with ^{239}Pu irreversibly attached to slow (i.e., Ic) colloids leaving the UZ within 2,000 yr after the intrusion for all sample elements (Figure K6.4.1-3).

With increasing time, most ^{239}Pu irreversibly attached to slow (i.e., Ic) colloids moves from the UZ to the SZ (Figure K6.4.1-3). As a result, the analyses for *UZIC239* and *UZIC239C* in Figures K6.4.1-1 and K6.4.1-2 are very similar to the analyses for *ESIC239* and *ESIC239C* in Figures K6.3.1-1 and K6.3.1-2. For example, *CPUCOLWF* (maximum concentration of plutonium irreversibly attached to glass colloids, mol/L) and *INFIL* (infiltration level) are the first two variables selected in the regression analyses for *ESIC239* and *ESIC239C* (Figure K6.3.1-2a,b) and also the first two variables selected in the regression analyses for *UZIC239* and *UZIC239C* (Figure K6.3.4-2a,b). The dominant effects of *CPUCOLWF* and *INFIL* on *UZIC239* and *UZIC239C* can be seen in the scatterplots in Figure K6.3.4-2c,d,f,g.

The only UZ parameter that has a noticeable effect on *UZIC239* and *UZIC239C* is *UZRCOL* (retardation coefficient for colloids in UZ), with *UZIC239* and *UZIC239C* tending to decrease as *UZRCOL* increases (Figures K6.4.1-1a,b and K6.4.1-2a,b). However, the effect of *UZRCOL* is

primarily to delay the movement of ^{239}Pu irreversibly attached to slow (i.e., Ic) colloids from the UZ to the SZ (i.e., compare Figure K6.4.1-3a and Figure K6.4.1-3d). This effect can also be seen in the decreasing importance of *UZRCOL* with increasing time in the regression analyses in Figure K6.4.1-2a,b.

Movement of ^{239}Pu Irreversibly Attached to Fast (i.e., If) Colloids: *UZIF239* and *UZIF239C*. The uncertainty and sensitivity analyses for the time-dependent release rates (*UZIF239*, g/yr) and cumulative releases (*UZIF239C*, g) over the time interval [0, 20,000 yr] for the movement of ^{239}Pu irreversibly attached to fast (i.e., If) colloids from the UZ to the SZ resulting from an igneous intrusive event at 10 yr that destroys all WPs in the repository are summarized in Figures K6.4.1-4, K6.4.1-5 and K6.4.1-6. Transport through the UZ happens within about 1,000 yr after the intrusion.

The ^{239}Pu irreversibly attached to fast (i.e., If) colloids moves rapidly from the UZ to the SZ (Figure K6.4.1-6). As discussed in conjunction with *UZIC239* and *UZIC239C*, the release into the UZ of ^{239}Pu irreversibly attached to fast (i.e., If) colloids is, in effect, defined by the release from the EBS of ^{239}Pu irreversibly attached to glass/waste form (i.e., Ic) colloids. As a result, the analyses for *UZIC239* and *UZIC239C* in Figures K6.4.1-4 and K6.4.1-5 are effectively the same as the analyses for *ESIC239* and *ESIC239C* in Figures K6.3.1-1 and K6.3.1-2.

Movement of Dissolved ^{237}Np: *UZNP237* and *UZNP237C*. The uncertainty and sensitivity analyses for the time-dependent release rates (*UZNP237*, g/yr) and cumulative releases (*UZNP237C*, g) over the time interval [0, 20,000 yr] for the movement of dissolved ^{237}Np from the UZ to the SZ resulting from an igneous intrusive event at 10 yr that destroys all WPs in the repository are summarized in Figures K6.4.1-7, K6.4.1-8 and K6.4.1-9. Transport through the UZ occurs relatively rapidly, with dissolved ^{237}Np leaving the UZ within 1,500 yr after the intrusion.

With increasing time, most dissolved ^{237}Np moves from the UZ to the SZ (Figure K6.4.1-9). As a result, the analyses for *UZNP237*and *UZNP237C* in Figures K6.4.1-7 and K6.4.1-8 are similar to the analyses for *ESNP237* and *ESNP237C* in Figures K6.3.1-5 and K6.3.1-6. For example, the first six or seven variables selected in the regression analyses for *ESNP237* and *ESNP237C* (Figure K6.3.1-6a,b) are generally the same as the first six or seven variables selected in the regression analyses for *UZNP237* and *UZNP237C* (Figure K6.4.1-8a,b), although the order of selection may vary slightly. As a result, the discussions for *ESNP237* and *ESNP237C* associated with Figures K6.3.1-5 and K6.3.1-6 also apply to *UZNP237* and *UZNP237C*.

Movement of Dissolved ^{239}Pu: *UZPU239* and *UZPU239C*. The uncertainty and sensitivity analyses for the time-dependent release rates (*UZPU239*, g/yr) and cumulative releases (*UZPU239C*, g) over the time interval [0, 20,000 yr] for the movement of dissolved ^{239}Pu from the UZ to the SZ resulting from an igneous intrusive event at 10 yr that destroys all WPs in the repository are summarized in Figures K6.4.1-10, K6.4.1-11 and K6.4.1-12. Transport through the UZ occurs relatively rapidly, with dissolved ^{239}Pu leaving the UZ within 2,000 yr after the intrusion.

With increasing time, most dissolved ^{239}Pu moves from the UZ to the SZ (Figure K6.4.1-12). As a result, the analyses for *UZPU239* and *UZPU239C* in Figures K6.4.1-10 and K6.4.1-11 are similar to the analyses for *ESPU239* and *ESPU239C* in Figures K6.3.1-7 and K6.3.1-8. For example, all six regression analyses for *ESPU239* and *ESPU239C* in Figure K6.3.1-8a,b and also all six regression analyses for *UZPU239* and *UZPU239C* in Figure K6.4.1-11a,b initially select the following three variables: *EP1LOWPU* (scale factor used to incorporate uncertainty into plutonium solubility under low ionic strength conditions; as sampled, *EP1LOWPU* is actually the logarithm of the indicated scale factor), *DELPPCO2* (scale factor used to incorporate uncertainty into the value for the partial pressure of CO_2), and *INFIL* (infiltration level).

In all the regression analyses for *ESPU239* and *ESPU239C*, the fourth selected variable is *PHCSS* (pointer variable used to determine pH in CSNF cell 1 under liquid influx conditions) (Figure K6.3.1-8a,b). In all the regression analyses for *UZPU239* and *UZPU239C* except the analysis for *UZPU239* at 10,000 yr, the fourth and fifth selected variables are *PHCSS* and *UZKDPUDT* (sorption coefficient for plutonium in devitrified tuff units of UZ, mL/g), although the order of selection varies in the individual analyses (Figure K6.4.1-11a,b). Further, *UZKDPUDT* is the sixth variable selected in the regression analysis for *UZPU239* at 10,000 yr. The presence of *UZKDPUDT* in the regression analyses for *UZPU239* and *UZPU239C* indicates that retardation in the UZ is having a negative effect on the rate of movement of dissolved ^{239}Pu through the UZ to the SZ. However, incremental R^2 values associated with the addition of *UZKDPUDT* to the individual regression models varies between 0.01 and 0.08, with the size of this increment decreasing with increasing time (Figure K6.4.1-11a,b). Thus, *UZKDPUDT* does not have a large effect on the uncertainty associated with *UZPU239* and *UZPU239C*.

Figure 6.4.1-12 compares the cumulative mass of ^{239}Pu released from the EBS to the UZ (*ESPU239C*, g) to the cumulative mass of ^{239}Pu released from the UZ to the SZ (*UZPU239C*, g) after an igneous intrusive event at 10 years. The separation of each point from the isoline indicates the proportion of ^{239}Pu released from the EBS that is still within the UZ, at several times (1,000 years, 3,000 years, 5,000 years and 10,000 years). At 10,000 years, most points lie remain below the isoline, indicating the reduction of ^{239}Pu by decay during transport in the UZ, and also the possibility that some ^{239}Pu is still in transit through the UZ. The few realizations with points above the isoline are those in which a substantial amount of ^{243}Am is released from the EBS into the UZ, and subsequently decays in the UZ to ^{239}Np and then to ^{239}Pu. Thus, in these realizations, because ^{239}Pu is being produced by decay in the UZ, more ^{239}Pu can be released from the UZ than is released into the UZ.

Overall, the sensitivity analyses for *UZPU239* and *UZPU239C* in Figures K6.4.1-10e,f and K6.4.1-11a,b are very similar to the sensitivity analyses for *ESPU239* and *ESPU239C* in Figures K6.3.1-7e,f and K6.3.1-8a,b. As a result, the discussions for *ESPU239* and *ESPU239C* associated with Figures K6.3.1-7 and K6.3.1-8 also apply to *UZPU239* and *UZPU239C*.

Movement of Dissolved ^{99}Tc: *UZTC99* and *UZTC99C*. The uncertainty and sensitivity analyses for the time-dependent release rates (*UZTC99*, g/yr) and cumulative releases (*UZTC99C*, g) over the time interval [0, 20,000 yr] for the movement of dissolved ^{99}Tc from the UZ to the SZ resulting from an igneous intrusive event at 10 yr that destroys all WPs in the

repository are summarized in Figures K6.4.1-13, K6.4.1-14 and K6.4.1-15. Transport through the UZ occurs rapidly, with ^{99}Tc leaving the UZ within 1,000 yr after the intrusion.

With increasing time, effectively all dissolved ^{99}Tc moves from the UZ to the SZ (Figure K6.4.1-15). However, the UZ does delay this movement (i.e., compare Figures K6.4.1-15a and K6.4.1-15d). This delay is more apparent for ^{99}Tc than the other radioactive species under consideration because of the very rapid release of ^{99}Tc from the EBS (i.e., compare Figures K6.4.1-15 with Figures K6.4.1-3, K6.4.1-6, K6.4.1-9 and K6.4.1-12).

As indicated by the PRCCs in Figure K6.4.1-13e,f and the regression analyses in Figure K6.4.1-14a,b, the dominant variables influencing the uncertainty in *UZTC99* and *UZTC99C* are *INFIL* (infiltration level) and *CSNFMASS* (scale factor used to characterize uncertainty in amount of CSNF in CSNF WPs). The variable *INFIL* has a complex pattern of effects on *UZTC99* and *UZTC99C*. For *UZTC99*, the effect of *INFIL* is positive at early times (Figure K6.4.1-13e) and then negative at later times (Figures K6.4.1-13e and K6.4.1-14a). This pattern results because increasing *INFIL* initially increases water flow in the EBS and UZ, which increases the movement of ^{99}Tc in the EBS and UZ. However, by increasing the early movement of ^{99}Tc in the EBS and UZ, increasing *INFIL* also reduces the amount of ^{99}Tc that can be released from the UZ to the SZ at later times. As a result, increasing *INFIL* has a negative effect on *UZTC99* at later times. In contrast, *INFIL* has a positive effect on *UZTC99C* at all times (Figures K6.4.1-13f and K6.4.1-14b) because *UZTC99C* is the cumulative release of ^{99}Tc from the UZ to the SZ. Increasing *CSNFMASS* has positive effect on both *UZTC99* and *UZTC99C*, which results from increasing the amount of ^{99}Tc placed in the repository (Figures K6.4.1-13e,f and K6.4.1-14a,b). Similar but smaller effects are also indicated for *HLWMASS* (scale factor used to characterize uncertainty in amount of HLW in CDSP WPs) and *DSNFMASS* (scale factor used to characterize uncertainty in amount of DSNF in CDSP WPs) for *UZTC99C* at 10,000 yr (Figure K6.4.1-14b).

The opposite effects of *INFIL* on *UZTC99* and *UZTC99C* at 10,000 yr can be seen in the scatterplots in Figure K6.4.1-14c,d,f,g, with *UZTC99* tending to decrease as *INFIL* increases and *UZTC99C* tending to increase as *INFIL* increases.

In addition to *INFIL* and *CSNFMASS*, a number of variables related to flow in the UZ have small effects on *UZTC99* and *UZTC99C*, with the effects of these variables tending to decrease with increasing time (Figures K6.4.1-13e,f and K6.4.1-14a,b). For example, the regression analysis for *UZTC99* at 3,000 yr selects the following four variables after *INFIL* and *CSNFMASS*: *UZTORRG3* (tortuosity in rock group 3 of the UZ; as sampled, *UZTORRG3* is the logarithm of the indicated tortuosity, m), *UZGAM* (parameter gamma in active fracture model, dimensionless), *UZFAG8* (fracture aperture for rock group 8 in UZ, m), and *UZFAG3* (fracture aperture for rock group 3 in UZ, m). As indicated by the PRCCs in Figure K6.4.1-13e, variables such as *UZTORRG3*, *UZGAM*, *UZFAG8* and *UZFAG3* tend to have temporally dependent effects on *UZTC99* that derive from the role that the individual variable plays on speeding up or slowing down the movement of ^{99}Tc in the UZ. However, as previously noted, these effects tend to diminish with time as a result of the essentially complete movement ^{99}Tc through the UZ. For example, adding *UZTORRG3*, *UZGAM*, *UZFAG8* and *UZFAG3* to the regression model for *UZTC99* at 3,000 yr increases the R^2 value from 0.78 for a model containing only *INFIL* and

CSNFMASS to 0.90 for a model containing *INFIL*, *CSNFMASS*, *UZTORRG3*, *UZGAM*, *UZFAG8* and *UZFAG3* (Figure K6.4.1-14a). In contrast, the regression analysis for *UZTC99* at 5000 yr initially selects *INFIL* and *CSNFMASS* and produces a model with an R^2 value of 0.78; then, only *UZTORRG3* and *UZGAM* are selected from the variables that affect ^{99}Tc movement in the UZ for a resultant model containing *INFIL*, *CSNFMASS*, *UZTORRG3* and *UZGAM* with an R^2 value of 0.79 (Figure K6.4.1-14a).

As previously noted, the uncertainty in *UZTC99C* is dominated by *INFIL* and *CSNFMASS*. Specifically, the regression model for *UZTC99C* at 3,000 yr containing only *INFIL* has an R^2 value of 0.59, and the regression models for *UZTC99C* at 5,000 and 10,000 yr containing only *CSNFMASS* have R^2 values of 0.62 and 0.84, and the corresponding models containing both *CSNFMASS* and *INFIL* have R^2 values of 0.90, 0.94 and 0.97 (Figure K6.4.1-14b). Further, there is an interesting pattern in the relationship between *UZTC99C, INFIL* and *CSNFMASS* (Figure K6.4.1-14f). Specifically, there are two linear relationships between *UZTC99C* and *CSNFMASS*, with the possibilities *INFIL* = 1 and *INFIL* = 2, 3 or 4 acting as switches between these two relationships. The role of *INFIL* as a switch occurs because the water flow for *INFIL* = 2, 3 or 4 is rapid enough that almost all the ^{99}Tc from the CSNF waste (comprising between 5.7×10^7 g and 8.8×10^7 g) is transported through the UZ by 10,000 yr, whereas for *INFIL* = 1 the transport of ^{99}Tc through the UZ is still in progress. For *INFIL* = 1 the average seepage rate (over all percolation bins) is about 0.55 m^3/yr/WP, whereas for *INFIL* = 2 the average seepage rate is about 1.24 m^3/yr/WP (Figure K6.2-2). The inventory of ^{99}Tc in CDSP WPs is much less, ranging between 2.5×10^6 g and 5.1×10^6 g.

K6.4.2 Igneous Intrusive Scenario Classes: Release from Unsaturated Zone (UZ) over the Time Interval [0, 1,000,000 yr] for an Event at 250 yr

Uncertainty and sensitivity analysis results for this case are not presented because of the relatively rapid transport of material through UZ (see Figures K6.4.1-3, K6.4.1-6, K6.4.1-9, K6.4.1-12 and K6.4.1-15).

K6.5 Igneous Intrusive Scenario Classes: Release from Saturated Zone (SZ)

K6.5.1 Igneous Intrusive Scenario Classes: Release from Saturated Zone (SZ) over the Time Interval [0, 20,000 yr] for an Event at 10 yr

Movement of ^{239}Pu Irreversibly Attached to Slow (i.e., Ic) Colloids: *SZIC239* and *SZIC239C*. The uncertainty and sensitivity analyses for the time-dependent release rates (*SZIC239*, g/yr) and cumulative releases (*SZIC239C*, g) over the time interval [0, 20,000 yr] for the movement of ^{239}Pu irreversibly attached to slow (i.e., Ic) colloids across a subsurface plane at the location of the RMEI resulting from an igneous intrusive event at 10 yr that destroys all WPs in the repository are summarized in Figures K6.5.1-1, K6.5.1-2 and K6.5.1-3. The delay in arrival of ^{239}Pu irreversibly attached to slow (i.e., Ic) colloids due to transport through the SZ is apparent in Figure K6.6.1-1(a), which shows that ^{239}Pu irreversibly attached to slow (i.e., Ic) colloids arrives at the RMEI location within 5,000 yr for many sample elements, but may be delayed out to and beyond 20,000 yr for some sample elements.

As indicated by the PRCCs in Figure K6.5.1-1e,f and the regression analyses in Figure K6.5.1-2a,b, the uncertainty in *SZIC239* and *SZIC239C* is dominated by *SZCOLRAL* (colloid retardation factor in alluvial unit of SZ; as sampled, *SZCOLRAL* is actually the logarithm of the indicated retardation factor), *SZFIPOVO* (flowing interval porosity in the volcanic unit of the SZ), *SZGWSPDM* (groundwater specific discharge multiplier; as sampled, *SZGWSPDM* is actually the logarithm of the indicated multiplier), and *CPUCOLWF* (concentration of irreversibly attached plutonium on stable glass colloids, mol/L). The negative effects associated with *SZCOLRAL* and *SZFIPOVO* result because increasing *SZCOLRAL* increases colloid retardation in the SZ and increasing *SZFIPOVO* slows water flow in the SZ. The positive effects associated with *SZGWSPDM* and *CPUCOLWF* result because increasing *SZGWSPDM* increases water flow in the SZ and increasing *CPUCOLWF* increases the amount of ^{239}Pu released from the EBS that is irreversibly attached to glass colloids. In addition to *SZCOLRAL*, *SZFIPOVO*, *SZGWSPDM* and *CPUCOLWF*, the analyses indicate a number of additional variables that have small effects on *SZIC239* and *SZIC239C*. Most of these additional variables relate to properties of the SZ. However, the final R^2 values in the regressions in Figure K6.5.1-2a,b are not very high (i.e., the range in R^2 values is 0.52 to 0.72).

The relatively low R^2 values result from the large number of sample elements for which *SZIC239* and *SZIC239C* are effectively zero (Figure K6.5.1-2f,g,h). These small values create a pattern that the regression models cannot effectively capture. As shown by the scatterplot in Figure K6.5.1-2f, the small values for *SZIC239* and *SZIC239C* tend to be associated with large values for *SZCOLRAL*, which indicates that the larger values for colloid retardation can result in no colloid transport through the SZ to the location of the RMEI. However, the extent of colloid retardation varies widely across the sample elements (Figure K6.5.1-3).

Movement of ^{239}Pu Irreversibly Attached to Fast (i.e., If) Colloids: SZ*IF239* and *SZIF239C*. The uncertainty and sensitivity analyses for the time-dependent release rates (*SZIF239*, g/yr) and cumulative releases (*SZIF239C*, g) over the time interval [0, 20,000 yr] for the movement of ^{239}Pu irreversibly attached to ferrous (i.e., If) colloids across a subsurface plane at the location of the RMEI resulting from an igneous intrusive event at 10 yr that destroys all WPs in the repository are summarized in Figures K6.5.1-4, K6.5.1-5 and K6.5.1-6. The relatively rapid transport through the SZ of ^{239}Pu irreversibly attached to fast (i.e., If) colloids is evident in Figure K6.6.1-3(a), which shows that ^{239}Pu irreversibly attached to fast colloids arrive at the RMEI location within 2,000 yr after the intrusion.

The uncertainty in *SZIF239* and *SZIF239C* is dominated by *CPUCOLWF* (concentration of irreversibly attached plutonium on stable glass colloids, mol/L) and *INFIL* (infiltration level) (Figures K6.5.1-4e,f and K6.5.1-5a,b,c,d,f,g). In particular, the interacting effects of *CPUCOLWF* and *INFIL* are particularly evident in the scatterplots in Figure K6.5.1-5c,f. The positive effect associated with *CPUCOLWF* results from increasing the amount of ^{239}Pu released from the EBS that is irreversibly attached to slow colloids, and the positive effect associated with *INFIL* results form increasing water flow in the EBS and UZ. Together, *CPUCOLWF* and *INFIL* result in regression models for *SZIF239* and *SZIF239C* with R^2 values between 0.87 and 0.93. After *CPUCOLWF* and *INFIL*, the analyses select several additional variables with small effects on *SZIF239* and *SZIF239C*. However, as indicated by the

scatterplots in Figure K6.5.1-5c,f, the uncertainty in *SZIF239* and *SZIF239C* is determined primarily by *CPUCOLWF* and *INFIL*.

As shown by the scatterplots in Figure K6.5.1-6, effectively all ^{239}Pu entering the SZ irreversibly attached to fast (i.e., If) colloids transports through the SZ to the location of the RMEI.

Movement of Dissolved ^{237}Np: *SZNP237* and *SZNP237C*. The uncertainty and sensitivity analyses for the time-dependent release rates (*SZNP237*, g/yr) and cumulative releases (*SZNP237C*, g) over the time interval [0, 20,000 yr] for the movement of dissolved ^{237}Np across a subsurface plane at the location of the RMEI resulting from an igneous intrusive event at 10 yr that destroys all WPs in the repository are summarized in Figures K6.5.1-7, K6.5.1-8 and K6.5.1-9. The delay in arrival of dissolved ^{237}Np due to transport through the SZ is apparent in Figure K6.5.1-9a, which shows that dissolved ^{237}Np arrives at the RMEI location within 5,000 yr for many sample elements, but may be delayed out to and beyond 20,000 yr for some sample elements.

As indicated by the PRCCs in Figure K6.5.1-7e,f and the regression analyses in Figure K6.5.1-8a,b, the uncertainty in *SZNP237*and *SZNP237C* is affected by a large number of variables. At 3000 yr, *SZGWSPDM* (groundwater specific discharge multiplier*;* as sampled, *SZGWSPDM* is actually the logarithm of the indicated multiplier) is the dominant variable affecting *SZNP237*and *SZNP237C*. Specifically, the regressions for *SZNP237*and *SZNP237C* at 3000 yr have R^2 values of 0.44 and 0.50 for models including only *SZGWSPDM*. However, the importance of *SZGWSPDM* diminishes with time. At 5000 yr, *SZGWSPDM* is the again the first variable selected in the regressions for *SZNP237*and *SZNP237C*, but the R^2 values are only 0.18 and 0.27. At 10,000 yr, *PHCSS* (pointer variable used to determine pH in CSNF cell 1 under liquid influx conditions) is the first variable selected in the regressions for *SZNP237*and *SZNP237C* but with R^2 values of only 0.21 and 0.22; in contrast, *SZGWSPDM* is now the fourth and third variable selected in the regressions for *SZNP237*and *SZNP237C*, respectively. This declining importance for *SZGWSPDM* results because *SZGWSPDM* affects the early arrival of ^{237}Np at the location of the RMEI but becomes less important with increasing time as additional variables start to affect the amount of ^{237}Np arriving at the location of the RMEI. Overall, the uncertainty in *SZNP237*and *SZNP237C* is determined by small effects associated with a large number of variables.

The analysis for *SZNP237C* at 10,000 yr is used as an example (Figure K6.5.1-8b). The first four variables selected in the regression analysis are *PHCSS*, *INFIL* (infiltration level), *SZGWSPDM*, and *SZFISPVO* (flowing interval spacing in volcanic unit of SZ, m). The negative effect associated with *PHCSS* results because increasing *PHCSS* increases pH, which (as long as pH is below about 9) tends to decrease Np solubility. The positive effects associated with the remaining variables result because (i) increasing *INFIL* increases water flow in the EBS and UZ and hence increases the release of ^{237}Np into the SZ, (ii) increasing *SZGWSPDM* increases water flow in the SZ, and (iii) increasing *SZFISPVO* decreases the diffusion of ^{237}Np from fractures in the volcanic unit of the SZ into the surrounding matrix. Together, these variables result in a model with an R^2 value of 0.56.

The next four variables selected are *EP1NPO2* (scale factor used to incorporate uncertainty into NpO_2 solubility below 1 molal ionic strength; as sampled, *EP1NPO2* is actually the logarithm of the indicated scale factor), *DELPPCO2* (scale factor used to incorporate uncertainty into the value for the partial pressure of CO_2), *EP1LOWAM* (scale factor used to incorporate uncertainty into americium solubility under low ionic strength conditions; as sampled, *EP1LOWAM* is actually the logarithm of the indicated scale factor), and *SZDIFCVO* (diffusion coefficient in fractured volcanic units, m^2/s) (Figure K6.5.1-8b). The positive effects associated with *EP1NPO2*, *DELPPCO2* and *EP1LOWAM* result from their influence on the amount of ^{237}Np that moves from the EBS (Section K6.3.1). The negative effect associated with *SZDIFCVO* results from increasing the amount of ^{237}Np that diffuses from fractures in the volcanic unit of the SZ to the surrounding matrix. The addition of these four variables raises the R^2 value for the model from 0.56 to 0.67.

After the first eight variables, the regression analysis selects the following six additional variables: *CORRATSS* (corrosion rate for stainless steel, μm/yr), *EP1LOWNU* (scale factor used to incorporate uncertainty into uranium solubility under low ionic strength conditions for nominal and seismic conditions; as sampled, *EP1LOWNU* is actually the logarithm of the indicated scale factor; in the present analysis, *EP1LOWNU* was used instead of the corresponding and intended variable *EP1LOWOU* for igneous conditions; however, this has no effect on analysis outcomes as *EP1LOWNU* and *EP1LOWOU* are assigned the same distribution), *COLGW* (concentration of groundwater colloids when colloids are stable, mg/L), *SZKDCSVO* (sorption coefficient for cesium in volcanic unit of SZ, mL/g), *SZKDNPVO* (sorption coefficient for neptunium in volcanic unit of SZ, mL/g), and *THERMCON* (host rock thermal conductivity level). The negative and positive effects of *CORRATSS* and *EP1LOWNU*, respectively, result from their influence on the amount of ^{237}Np that moves from the EBS (Section K6.3.1). The negative effect associated with *SZKDNPVO* results from its role in slowing the movement of ^{237}Np in the SZ. The small indicated effects associated with *COLGW*, *SZKDCSVO* and *THERMCON* are probably spurious. The model containing all 14 variables has an R^2 value of 0.74. Elimination of the three possibly spurious variables reduces the R^2 value to 0.72, which is only slightly higher than the R^2 value of 0.67 obtained with the first eight variables. The relatively low R^2 value for the final model is resulting from the large number of variables that have relatively small effects on *SZNP237C*.

The same general pattern of effects observed for *SZNP237C* at 10,000 yr also holds for *SZNP237*and *SZNP237C* at other times (Figure K6.5.1-8a,b).

As indicated by the scatterplots in Figure K6.5.1-9, substantial hold up of ^{237}Np occurs in the SZ.

Movement of Dissolved ^{239}Pu: *SZPU239* and *SZPU239C*. The uncertainty and sensitivity analyses for the time-dependent release rates (*SZPU239*, g/yr) and cumulative releases (*SZPU239C*, g) over the time interval [0, 20,000 yr] for the movement of dissolved ^{239}Pu across a subsurface plane at the location of the RMEI resulting from an igneous intrusive event at 10 yr that destroys all WPs in the repository are summarized in Figures K6.5.1-10, K6.5.1-11 and K6.5.1-12.

For many sample elements, there is no significant movement of ^{239}Pu through the SZ to the location of the RMEI (Figure K6.5.1-12). In particular, the uncertainty in whether or not significant movement of ^{239}Pu through the SZ to the location of the RMEI occurs is dominated by *SZGWSPDM* (groundwater specific discharge multiplier*;* as sampled, *SZGWSPDM* is actually the logarithm of the indicated multiplier), with no significant movement occurring when *SZGWSPDM* is less than 0 and often no significant movement occurring when *SZGWSPDM* is less than 0.5 (Figure K6.5.1-11f).

The PRCCs in Figure K6.5.1-10e,f and the regression analyses in Figure K6.5.1-11a,b are hindered in their effectiveness by the large number of effectively zero values for *SZPU239* and *SZPU239C*. However, the source of the uncertainty associated with *SZPU239* and *SZPU239C* is clearly revealed by the scatterplot in Figure K6.5.1-11f. Specifically, smaller values for *SZGWSPDM* result in no significant movement of ^{239}Pu through the SZ to the location of the RMEI, and when significant movement does occur, the values for *SZPU239* and *SZPU239C* tend to increase as *SZGWSPDM* increases.

The extensive retardation of ^{239}Pu in the SZ can also be seen in Figure K6.5.1-12.

Movement of Dissolved ^{99}Tc: *SZTC99* and *SZTC99C*. The uncertainty and sensitivity analyses for the time-dependent release rates (*SZTC99*, g/yr) and cumulative releases (*SZTC99C*, g) over the time interval [0, 20,000 yr] for the movement of dissolved ^{99}Tc across a subsurface plane at the location of the RMEI resulting from an igneous intrusive event at 10 yr that destroys all WPs in the repository are summarized in Figures K6.5.1-13, K6.5.1-14 and K6.5.1-15.

The movement of ^{99}Tc through the SZ is rapid (Figure K6.5.1-13a,b,c,d). With the exception of a small jump associated with the climate change at 2,000 yr, *SZTC99* monotonically decreases with time from an initial high value.

The PRCCs for *SZTC99* are very choppy because of the noise introduced into the analysis by the particle tracking algorithm used for solution of the transport equations in the UZ (Figure K6.5.1-13e). However, as indicated by both the PRCCs in Figure K6.5.1-13e and the regression analyses in Figure K6.5.1-14a, the most important variable with respect to the uncertainty in *SZTC99* is *INFIL* (infiltration level), with *SZTC99* tending to increase with increasing values for *INFIL* at early times and to decrease with increasing values for *INFIL* at later times. This pattern of effects results because increasing *INFIL* increases the early release of ^{99}Tc and thus reduces the amount of ^{99}Tc available for release at later times. Similarly, *SZGWSPDM* (groundwater specific discharge multiplier*;* as sampled, *SZGWSPDM* is actually the logarithm of the indicated multiplier) has a positive effect on *SZTC99* at early times and a negative effect on *SZTC99*at later times as a result of increasing the rate of ^{99}Tc movement through the SZ at early times and thus reducing the amount of ^{99}Tc available for release at later times. The PRCCs indicate a positive effect for *THERMCON* (host rock thermal conductivity level) prior to 1,000 yr as result of its influence on repository cooling and the time at which radionuclide movement from the repository begins (Figure K6.5.1-13e); specifically, increasing *THERMCON* results in earlier radionuclide releases from the EBS. Similarly to *INFIL* and *SZGWSPDM*, *SZFISPVO* (flowing interval spacing in volcanic unit of SZ, m). has positive effect on *SZTC99* at early times and a negative effect at later times; again, this pattern results from

increasing the release of ^{99}Tc at early times and thus reducing the amount of ^{99}Tc available for release at later times. In contrast, *SZFIPOVO* (flowing interval porosity in the volcanic unit of the SZ) has the opposite pattern of effects, with increasing values for *SZFIPOVO* tending to decrease *SZTC99* at early times and increase *SZTC99* at later times. This pattern results because increasing *SZFIPOVO* slows water flow in the SZ, which reduces the release of ^{99}Tc at early times and thus results in larger values for *SZTC99* at later times. Further, *CSNFMASS* (scale factor used to characterize uncertainty in amount of CSNF in CSNF WPs) has a positive effect on *SZTC99* because of its role in defining the amount of ^{99}Tc in the repository.

The effects of *INFIL*, *SZGWSPDM* and *SZFISPVO* on *SZTC99* at 10,000 yr can be seen in the scatterplots in Figure K6.5.1-14c,d,e.

The PRCCs in Figure K6.5.1-13f indicate the same early time effects of *THERMCON* and *SZFIPOVO* on *SZTC99C* as previously discussed for *SZTC99*. Then, as time increases, the PRCCs indicate that the dominant variables are *CSNFMASS*, *SZGWSPDM INFIL* and *SZFISPVO*, with *SZTC99C* tending to increase as each of these variables increases. These effects result because (i) increasing *CSNFMASS* increases the amount of ^{99}Tc present in the repository, (ii) increasing *SZGWSPDM* increases water flow in the SZ, (iii) increasing *INFIL* increases the release of ^{99}Tc from the UZ to the SZ, and (iv) increasing *SZFISPVO* reduces the movement of ^{99}Tc from fractures in the volcanic unit of the SZ to the surrounding matrix. Similar effects are indicated in the regression analyses in Figure K6.5.1-14b. Specifically, the analyses for *SZTC99C* at 3000, 5000 and 10,000 yr all pick *CSNFMASS*, *SZGWSPDM*, *INFIL* and *SZFISPVO* as the first four variables, although not in the same order, and produce models with R^2 values of 0.75, 0.77 and 0.81, respectively. Thus, *CSNFMASS*, *SZGWSPDM*, *INFIL* and *SZFISPVO* give rise to most of the uncertainty in *SZTC99C*. The fifth variable selected in each of the regressions in Figure K6.5.1-14b is *SZDIFCVO* (diffusion coefficient in fractured volcanic units, m^2/s), with *SZTC99C* tending to decrease as *SZDIFCVO* increases. The negative effect associated with *SZDIFCVO* results from increasing the amount of ^{99}Tc that diffuses from fractures in the volcanic unit of the SZ to the surrounding matrix. The inclusion of *SZDIFCVO* increases the R^2 values to 0.80, 0.81 and 0.85 for the three regression models.

The dominant effects of *CSNFMASS*, *SZGWSPDM* and *INFIL* on *SZTC99C* at 10,000 yr can be seen in the scatterplots in Figure K6.5.1-14f,g,h.

As shown in Figure K6.5.1-15, there can be a substantial delay in the movement of ^{99}Tc in the SZ from the discharge location of the UZ to the location of the RMEI over time periods of 1,000 and 3000 yr. However, as the time period increases to 10,000 yr, substantial movement of ^{99}Tc to the location of the RMEI takes place.

K6.5.2 Igneous Intrusive Scenario Classes: Release from Saturated Zone (SZ) beyond 20,000 yr for an Event at 250 yr

For completeness, this section presents summaries of the uncertainty and sensitivity analyses for release from the SZ beyond 20,000 yr for an igneous intrusive event at 250 yr that destroys all WPs in the repository without discussion. Section K6.5.1 presents uncertainty and sensitivity analyses for release from the SZ over the time interval [0, 20,000 yr] for an intrusion that occurs

at 10 yr. The uncertainties affecting release from the SZ following an intrusion at 250 yr are similar to the uncertainties affecting release from the SZ following an intrusion at 10 yr.

Movement of ^{239}Pu Irreversibly Attached to Slow (i.e., Ic) Colloids: *SZIC239* and *SZIC239C*. The uncertainty and sensitivity analyses for the time-dependent release rates (*SZIC239*, g/yr) and cumulative releases (*SZIC239C*, g) over the time interval [0, 200,000 yr] for the movement of ^{239}Pu irreversibly attached to slow (i.e., Ic) colloids across a subsurface plane at the location of the RMEI resulting from an igneous intrusive event at 250 yr that destroys all WPs in the repository are summarized in Figure K6.5.2-1.

Movement of ^{239}Pu Irreversibly Attached to Fast (i.e., If) Colloids: S*ZIF239* and *SZIF239C*. The uncertainty and sensitivity analyses for the time-dependent release rates (*SZIF239*, g/yr) and cumulative releases (*SZIF239C*, g) over the time interval [0, 200,000 yr] for the movement of ^{239}Pu irreversibly attached to fast (i.e., If) colloids across a subsurface plane at the location of the RMEI resulting from an igneous intrusive event at 250 yr that destroys all WPs in the repository are summarized in Figure K6.5.2-2.

Movement of Dissolved ^{237}Np: *SZNP237* and *SZNP237C*. The uncertainty and sensitivity analyses for the time-dependent release rates (*SZNP237*, g/yr) and cumulative releases (*SZNP237C*, g) over the time interval [0, 1,000,000 yr] for the movement of dissolved ^{237}Np across a subsurface plane at the location of the RMEI resulting from an igneous intrusive event at 250 yr that destroys all WPs in the repository are summarized in Figure K6.5.2-3.

Movement of Dissolved ^{239}Pu: *SZPU239* and *SZPU239C*. The uncertainty and sensitivity analyses for the time-dependent release rates (*SZPU239*, g/yr) and cumulative releases (*SZPU239C*, g) over the time interval [0, 200,000 yr] for the movement of dissolved ^{239}Pu across a subsurface plane at the location of the RMEI resulting from an igneous intrusive event at 250 yr that destroys all WPs in the repository are summarized in Figure K6.5.2-4.

Movement of Dissolved ^{99}Tc: *SZTC99* and *SZTC99C*. The uncertainty and sensitivity analyses for the time-dependent release rates (*SZTC99*, g/yr) and cumulative releases (*SZTC99C*, g) over the time interval [0, 1,000,000 yr] for the movement of dissolved ^{99}Tc across a subsurface plane at the location of the RMEI resulting from an igneous intrusive event at 250 yr that destroys all WPs in the repository are omitted because of the rapid transport of ^{99}Tc through the repository system (see Figure K6.3.1-9a,c).

K6.6 Igneous Intrusive Scenario Classes: Dose to Reasonably Maximally Exposed Individual

This section presents analysis results for dose to the RMEI from individual radionuclides for the time intervals [0, 20,000 yr] and [0, 1,000,000 yr].

K6.6.1 Igneous Intrusive Scenario Classes: Dose to Reasonably Maximally Exposed Individual over the Time Interval [0, 20,000 yr] for an Event at 10 yr

Dose to RMEI from ^{239}Pu Irreversibly Attached to Slow (i.e., Ic) Colloids: *DOIC239*. The uncertainty and sensitivity analyses for dose to the RMEI (*DOIC239*, mrem/yr) over the time interval [0, 20,000 yr] for the movement of ^{239}Pu irreversibly attached to slow (i.e., Ic) colloids across a subsurface plane at the location of the RMEI resulting from an igneous intrusive event at 10 yr that destroys all WPs in the repository are summarized in Figures K6.6.1-1 and K6.6.1-2.

The uncertainty in *DOIC239* is dominated by the uncertainty in the groundwater concentration of ^{239}Pu irreversibly attached to slow (i.e., Ic) colloids at the location of the RMEI. This concentration is proportional to *SZIC239*. As shown by the scatterplot in Figure K6.6.1-2e, the uncertainty in *DOIC239* is small relative to the uncertainty in *SZIC239*. As a result, the sensitivity analyses for *DOIC239* in Figures K6.6.1-1 and K6.6.1-2 are very similar to the sensitivity analyses for *SZIC239* in Figures K6.5.1-1 and K6.5.1-2. Because of this similarity, the discussion of the sensitivity analyses for *SZIC239* is also applicable to the sensitivity analyses for *DOIC239*. For this reason, the sensitivity analyses for *DOIC239* will not be extensively discussed.

The similarity of the sensitivity analyses for *DOIC239* and *SZIC239* results because the impact of the uncertainty in the dose conversion factor *MICPU239* (dose conversion factor for ^{239}Pu for modern interglacial climate, (rem/yr)/(pCi/L)) is small relative to the impact of the uncertainty in other variables that effect *SZIC239* and hence *DOIC239*. For example, *MICPU239* is the sixth variable selected in the regression analysis for *DOIC239* at 10,000 yr and only raises the R^2 value from 0.50 to 0.52 (Figure K6.5.1-2a).

The regressions for *DOIC239* also indicate small effects for *MICI129* (dose conversion factor for ^{129}I for modern interglacial climate, (rem/yr)/(pCi/L)) and *MICCL36* (dose conversion factor for ^{36}Cl for modern interglacial climate, (rem/yr)/(pCi/L)) (Figure K6.5.1-2a). These selections are spurious and may result from underlying correlations involving *MICPU239*, *MICI129* and *MICCL36* that derive from the presence of common underlying variables in the determination of the uncertainty distributions used for dose conversion factors.

Dose to RMEI from ^{239}Pu Irreversibly Attached to Fast (i.e., If) Colloids: *DOIF239*. The uncertainty and sensitivity analyses for dose to the RMEI (*DOIF239*, mrem/yr) over the time interval [0, 20,000 yr] for the movement of ^{239}Pu irreversibly attached to fast (i.e., If) colloids across a subsurface plane at the location of the RMEI resulting from an igneous intrusive event at 10 yr that destroys all WPs in the repository are summarized in Figures K6.6.1-3 and K6.6.1-4.

Similarly to *DOIC239*, the uncertainty in *DOIF239* is dominated by the uncertainty in the groundwater concentration of ^{239}Pu irreversibly attached to fast (i.e., If) colloids at the location of the RMEI. This concentration is proportional to *SZIF239*. As shown by the scatterplot in Figure K6.6.1-4e, the uncertainty in *DOIF239* is small relative to the uncertainty in *SZIF239*. As a result, the sensitivity analyses for *DOIF239* in Figures K6.6.1-3 and K6.6.1-4 are very similar to the sensitivity analyses for *SZIF239* in Figures K6.5.1-4 and K6.5.1-5. Because of this similarity, the discussion of the sensitivity analyses for *SZIF239* is also applicable to the

sensitivity analyses for *DOIF239*. For this reason, the sensitivity analyses for *DOIF239* will not be extensively discussed.

The similarity of the sensitivity analyses for *DOIF239* and *SZIF239* results because the impact of the uncertainty in the dose conversion factor *MICPU239* (dose conversion factor for ^{239}Pu for modern interglacial climate, (rem/yr)/(pCi/L)) is small relative to the impact of the uncertainty in other variables that effect *SZIF239* and hence *DOIF239*. For example, *MICPU239* is the third variable selected in the regression analysis for *DOIF239* at 10,000 yr and raises the R^2 value from 0.81 to 0.91 (Figure K6.5.1-4a).

Dose to RMEI from Dissolved ^{237}Np: *DONP237*. The uncertainty and sensitivity analyses for dose to the RMEI (*DONP237*, mrem/yr) over the time interval [0, 20,000 yr] for the movement of dissolved ^{237}Np across a subsurface plane at the location of the RMEI resulting from an igneous intrusive event at 10 yr that destroys all WPs in the repository are summarized in Figures K6.6.1-5 and K6.6.1-6.

Similarly to *DOIC239* and *DOIF239*, the uncertainty in *DONP237* is dominated by the uncertainty in the groundwater concentration of dissolved ^{237}Np at the location of the RMEI. This concentration is proportional to *SZNP237*. As shown by the scatterplot in Figure K6.6.1-6e, the uncertainty in *DONP237* is small relative to the uncertainty in *SZNP237*. As a result, the sensitivity analyses for *DONP237* in Figures K6.6.1-5 and K6.6.1-6 are very similar to the sensitivity analyses for *SZNP237* in Figures K6.5.1-7 and K6.5.1-8. Because of this similarity, the discussion of the sensitivity analyses for *SZNP237* is also applicable to the sensitivity analyses for *DONP237*. For this reason, the sensitivity analyses for *DONP237* will not be extensively discussed.

The similarity of the sensitivity analyses for *DONP237* and *SZNP237* results because the impact of the uncertainty in the dose conversion factor *MICNP237* (dose conversion factor for ^{237}Np for modern interglacial climate, (rem/yr)/(pCi/L)) is small relative to the impact of the uncertainty in other variables that effect *SZNP237* and hence *DONP237*. For example, *MICNP237* is the seventh variable selected in the regression analysis for *DONP237*at 10,000 yr and only raises the R^2 value from 0.61 to 0.64 (Figure K6.5.1-6a).

The regressions for *DONP237* also indicate small effects for *MICTH229* (dose conversion factor for ^{229}Th for modern interglacial climate, (rem/yr)/(pCi/L)) at 3000 and 5000 yr (Figure K6.5.1-6a). These effects are spurious and result from underlying correlations involving *MICNP237* and *MICTH229* that derive from the presence of common underlying variables in the determination of the uncertainty distributions used for dose conversion factors.

Dose to RMEI from Dissolved ^{239}Pu: *DOPU239*. The uncertainty and sensitivity analyses for dose to the RMEI (*DOPU239*, mrem/yr) over the time interval [0, 20,000 yr] for the movement of dissolved ^{239}Pu across a subsurface plane at the location of the RMEI resulting from an igneous intrusive event at 10 yr that destroys all WPs in the repository are summarized in Figures K6.6.1-7 and K6.6.1-8.

The uncertainty in *DOPU239* is totally dominated by the uncertainty in *SZPU239* (Figure K6.6.1-8e). Therefore, the discussion associated with the sensitivity analyses for

SZPU239 presented in Figures K6.5.1-10 and K6.5.1-11 also applies to the sensitivity analyses for *DOPU239*. The appearance of *MICC14* (dose conversion factor for ^{14}C for modern interglacial climate, (rem/yr)/(pCi/L)) in the regression for *DOPU239* at 10,000 yr is spurious and results from the previously discussed correlations involving the dose conversion factors.

Dose to RMEI from Dissolved ^{99}Tc: *DOTC99*. The uncertainty and sensitivity analyses for dose to the RMEI (*DOTC99*, mrem/yr) over the time interval [0, 20,000 yr] for the movement of dissolved ^{99}Tc across a subsurface plane at the location of the RMEI resulting from an igneous intrusive event at 10 yr that destroys all WPs in the repository are summarized in Figures K6.6.1-9 and K6.6.1-10.

Unlike the other doses considered in this section, the uncertainty in *DOTC99* is not dominated by the corresponding radionuclide flux (i.e., *SZTC99*) at the location of the RMEI (Figure K6.6.1-10e). Because of this, *MICTC99* (dose conversion factor for ^{99}Tc for modern interglacial climate, (rem/yr)/(pCi/L)) is an important contributor to the uncertainty in *DOTC99* (Figures K6.6.1-9c and K6.6.1-10a). The important effect of *MICTC99* on the uncertainty in *DOTC99* is shown by *MICTC99* having the largest PRCC in Figure K6.6.1-9c and being the first variable selected in each of the regressions in Figure K6.6.1-10a.

K6.6.2 Igneous Intrusive Scenario Classes: Dose to Reasonably Maximally Exposed Individual over the Time Interval [0, 1,000,000 yr] for an Event at 250 yr

For completeness, this section presents summaries of the uncertainty and sensitivity analyses for dose to the RMEI over the time interval [0, 1,000,000 yr] for an igneous intrusive event at 250 yr that destroys all WPs in the repository without discussion.

Dose to RMEI from ^{239}Pu Irreversibly Attached to Slow (i.e., Ic) Colloids: *DOIC239*. The uncertainty and sensitivity analyses for dose to the RMEI (*DOIC239*, mrem/yr) over the time interval [0, 200,000 yr] for the movement of ^{239}Pu irreversibly attached to slow (i.e., Ic) colloids across a subsurface plane at the location of the RMEI resulting from an igneous intrusive event at 250 yr that destroys all WPs in the repository are summarized in Figure K6.6.2-1.

Dose to RMEI from ^{239}Pu Irreversibly Attached to Fast (i.e., If) Colloids: *DOIF239*. The uncertainty and sensitivity analyses for dose to the RMEI (*DOIF239*, mrem/yr) over the time interval [0, 200,000 yr] for the movement of ^{239}Pu irreversibly attached to fast (i.e., If) colloids across a subsurface plane at the location of the RMEI resulting from an igneous intrusive event at 250 yr that destroys all WPs in the repository are summarized in Figure K6.6.2-2.

Dose to RMEI from Dissolved ^{237}Np: *DONP237*. The uncertainty and sensitivity analyses for dose to the RMEI (*DONP237*, mrem/yr) over the time interval [0, 1,000,000 yr] for the movement of dissolved ^{237}Np across a subsurface plane at the location of the RMEI resulting from an igneous intrusive event at 250 yr that destroys all WPs in the repository are summarized in Figure K6.6.2-3.

Dose to RMEI from Dissolved ^{239}Pu: *DOPU239*. The uncertainty and sensitivity analyses for dose to the RMEI (*DOPU239*, mrem/yr) over the time interval [0, 200,000 yr] for the movement

of dissolved ^{239}Pu across a subsurface plane at the location of the RMEI resulting from an igneous intrusive event at 250 yr that destroys all WPs in the repository are summarized in Figure K6.6.2-4.

Dose to RMEI from Dissolved ^{99}Tc: *DOTC99*. The uncertainty and sensitivity analyses for dose to the RMEI (*DOTC99*, mrem/yr) over the time interval [0, 1,000,000 yr] for the movement of dissolved ^{99}Tc across a subsurface plane at the location of the RMEI resulting from an igneous intrusive event at 250 yr that destroys all WPs in the repository are omitted because of the rapid depletion of the ^{99}Tc inventory (see Figure K6.3.1-9a,c).

K6.7 Igneous Intrusive Scenario Classes: Expected Dose (*EXPDOSE*) to Reasonably Maximally Exposed Individual

This section presents analysis results for expected dose to the RMEI resulting from igneous intrusions over the time intervals [0, 20,000 yr] and [0, 1,000,000 yr].

K6.7.1 Igneous Intrusive Scenario Classes: Expected Dose (*EXPDOSE*) to Reasonably Maximally Exposed Individual over [0, 20,000 yr]

The uncertainty and sensitivity analyses for expected dose to the RMEI (*EXPDOSE*, mrem/yr) over the time interval [0, 20,000 yr] resulting from igneous intrusion are summarized in Figures K6.7.1-1 and K6.7.1-2. Initial transport to the location of the RMEI takes up to 2000 yr; after the earliest possible arrival time for released radionuclides at the location of the RMEI, *EXPDOSE* increases monotonically with time (Figure K6.7.1-1a,b). At 10,000 yr, the value for *EXPDOSE* falls between 10^{-4} and 1 mrem/yr for most sample elements, with a few sample elements having values for *EXPDOSE* between 1 and 10 mrem/yr.

The PRCCs in Figure K6.7.1-1c indicate that the uncertainty in *EXPDOSE* is dominated by *IGRATE* (rate of occurrence of igneous intrusive events, yr^{-1}), with the value for *EXPDOSE* increasing as *IGRATE* increases. This effect results because increasing *IGRATE* increases the probability that an igneous intrusive event will occur and hence increases *EXPDOSE.*

In addition to *IGRATE*, smaller effects are indicated for *SZGWSPDM* (groundwater specific discharge multiplier*;* as sampled, *SZGWSPDM* is actually the logarithm of the indicated multiplier), *SZFIPOVO* (flowing interval porosity in the volcanic unit of the SZ), *SZCOLRAL* (colloid retardation factor in alluvial unit of SZ, dimensionless*;* as sampled, *SZCOLRAL* is actually the logarithm of the indicated retardation factor), *INFIL* (infiltration level), and *SZDENAL* (density of alluvial unit of the SZ, kg/m^3) (Figure K6.7.1-1c). The variables *SZGWSPDM* and *INFIL* have positive effects on *EXPDOSE*, with these effects resulting because increasing *SZGWSPDM* increases water flow in the SZ and increasing *INFIL* increases water flow through the EBS and UZ. The variables *SZFIPOVO*, *SZCOLRAL* and *SZDENAL* have negative effects on *EXPDOSE*, with these effects resulting because increasing *SZFIPOVO* slows flow in the SZ and increasing *SZCOLRAL* and *SZDENAL* increases retardation in the alluvial unit of the SZ.

More detailed sensitivity analyses for *EXPDOSE* are provided by the regression analyses in Figure K6.7.1-2a. The dominant effect of *IGRATE* on the uncertainty in *EXPDOSE* is indicated

by R^2 values of 0.74, 0.80 and 0.78 for the regressions containing only *IGRATE* at 3000, 5000 and 10,000 yr. After *IGRATE*, the most important variable is *SZGWSPDM*. However the incremental effect associated with *SZGWSPDM* is small as the R^2 values for the regression models containing both *IGRATE* and *SZGWSPDM* are 0.79, 0.84 and 0.83.

After *IGRATE* and *SZGWSPDM*, all three regressions select *MICTC99* (dose conversion factor for ^{99}Tc for modern interglacial climate, (rem/yr)/(pCi/L)) and *INFIL* as the next two variables to include in the model, with *EXPDOSE* tending to increase as each of these variables increases (Figure K6.7.1-2a). These effects result because increasing *MICTC99* increases the received dose for a given exposure to ^{99}Tc and increasing *INFIL* increases water flow in the EBS and UZ. Inclusion of *IGRATE*, *SZGWSPDM*, *MICTC99* and *INFIL* in the regression models results in R^2 values of 0.86, 0.89 and 0.86. Thus, *IGRATE*, *SZGWSPDM*, *MICTC99* and *INFIL* account for most of the uncertainty in *EXPDOSE*, with the dominant contribution coming from *IGRATE*. After these four variables, the individual regressions pick an additional 10, 11 and 9 variables, respectively, that have small effects on *EXPDOSE* (Figure K6.7.1-2a). The final regressions have R^2 values of 0.91, 0.93 and 0.92, which indicates that most of the uncertainty in *EXPDOSE* is being accounted for.

The dominant effect of *IGRATE* on the uncertainty in *EXPDOSE* can be seen in the scatterplot in Figure K6.7.1-2b. The much smaller effects associated with *SZGWSPDM* and *MICTC99* can be seen in the scatterplots in Figure K6.7.1-2c,d.

K6.7.2 Igneous Intrusive Scenario Classes: Expected Dose (*EXPDOSE*) to Reasonably Maximally Exposed Individual over [0, 1,000,000 yr]

The uncertainty and sensitivity analyses for expected dose to the RMEI (*EXPDOSE*, mrem/yr) over the time interval [0, 1,000,000 yr] resulting from igneous intrusion are summarized in Figures K6.7.2-1 and K6.7.2-2. The values for *EXPDOSE* tend to increase until about 100,000 yr and then decrease until about 200,000 yr (Figure K6.7.2-1a,b). This behavior results because, with increasing time, more and more potential igneous intrusive events contribute to *EXPDOSE*. As a result, *EXPDOSE* initially increases with time. However, ^{239}Pu is an important contributor to *EXPDOSE* and has a half life of 24,100 yr. As a result, the contribution of ^{239}Pu to *EXPDOSE* declines after 100,000 yr and causes the drop in *EXPDOSE* between 100,000 and 200,000 yr. After 200,000 yr, *EXPDOSE* again increases due to the increasing number of potential igneous intrusions but without a significant contribution from ^{239}Pu.

The PRCCs in Figure K6.7.2-1c indicate that the uncertainty in *EXPDOSE* is dominated by *IGRATE* (rate of occurrence of igneous intrusive events, yr^{-1}), with the value for *EXPDOSE* increasing as *IGRATE* increases. This effect results because increasing *IGRATE* increases the probability that an igneous intrusive event will occur and hence increases *EXPDOSE.*

In addition to *IGRATE*, smaller effects are indicated for *SZGWSPDM* (groundwater specific discharge multiplier*;* as sampled, *SZGWSPDM* is actually the logarithm of the indicated multiplier), *SZFIPOVO* (flowing interval porosity in the volcanic unit of the SZ), *SZCOLRAL* (colloid retardation factor in alluvial unit of SZ*;* as sampled, *SZCOLRAL* is actually the logarithm of the indicated retardation factor), *EP1LOWPU* (scale factor used to represent

uncertainty in plutonium solubility in solutions below 1 molal ionic strength; as sampled, *EP1LOWPU* is actually the logarithm of the indicated scale factor) and *INFIL* (infiltration level) (Figure K6.7.2-1c). With the exception of *EP1LOWPU*, the preceding variables were also identified in the analysis in Figure K6.7.1-1c for the 0 to 20,000 yr time period. The variables *SZGWSPDM, EP1LOWPU* and *INFIL* have positive effects on *EXPDOSE*, with these effects resulting because increasing *SZGWSPDM* increases water flow in the SZ, increasing *EP1LOWPU* increases the solubility of plutonium, and increasing *INFIL* increases water flow through the EBS and UZ. The variables *SZFIPOVO* and *SZCOLRAL* have negative effects on *EXPDOSE*, with these effects resulting because increasing *SZFIPOVO* slows flow in the SZ and increasing *SZCOLRAL* increases retardation in the alluvial unit of the SZ. However, the negative effects associated with *SZFIPOVO* and *SZCOLRAL* occur prior to 200,000 yr, with the PRCCs indicating little effect for these variables on the uncertainty in *EXPDOSE* after this time.

More detailed sensitivity analyses for *EXPDOSE* are provided by the regression analyses in Figure K6.7.2-2a. The dominant effect of *IGRATE* on the uncertainty in *EXPDOSE* is indicated by R^2 values of 0.52, 0.55 and 0.59 for the regressions containing only *IGRATE* at 50,000, 200,000 and 500,000 yr. After *IGRATE*, the most important variable is *SZGWSPDM*. However the incremental effect associated with *SZGWSPDM* is moderate as the R^2 values for the regression models containing both *IGRATE* and *SZGWSPDM* are 0.69, 0.69 and 0.68.

The analyses at 50,000 and 200,000 yr then select *EP1LOWPU* and *INFIL* as the next two variables, and the analysis at 500,000 yr selects *INFIL* and flowing interval spacing in the volcanic unit of the SZ (*SZFISPVO*) as the next two variables (Figure K6.7.2-2a). The effects of *EP1LOWPU* and *INFIL* on *EXPDOSE* have already been discussed. The positive effect associated with *SZFISPVO* results from reducing the surface area associated with fractures in the volcanic unit of the SZ; in turn, this reduces radionuclide movement from fractures into the surrounding matrix and thus reduces radionuclide movement to the location of the RMEI. The regression models with the indicated variables now have R^2 values of 0.77, 0.76 and 0.75. After the first four variables, the individual regressions pick an additional 10, 9 and 10 variables, respectively, that have small effects on *EXPDOSE* (Figure K6.7-4a). The final regressions have R^2 values of 0.85, 0.85 and 0.84, which indicates that most of the uncertainty in *EXPDOSE* is being accounted for.

The dominant effect of *IGRATE* on the uncertainty in *EXPDOSE* can be seen in the scatterplot in Figure K6.7.2-2b. The much smaller effects associated with *SZGWSPDM* and *INFIL* can be seen in the scatterplots in Figure K6.7.2-2c,d.

K6.8 Igneous Eruptive Scenario Classes: Expected Dose (*EXPDOSE*) to Reasonably Maximally Exposed Individual

This section presents analysis results for expected dose to the RMEI resulting from igneous eruptions for the time intervals [0, 20,000 yr] and [0, 1,000,000 yr].

K6.8.1 Igneous Eruptive Scenario Classes: Expected Dose (*EXPDOSE*) to Reasonably Maximally Exposed Individual over [0, 20,000 yr]

The uncertainty and sensitivity analyses for expected dose to the RMEI (*EXPDOSE*, mrem/yr) over the time interval [0, 20,000 yr] resulting from igneous eruptive events are summarized in Figures K6.8.1-1 and K6.8.1-2. The values for *EXPDOSE* range between 10^{-7} and 10^{-3} mrem/yr and show a slight tendency to increase with time (Figure K6.8.1-1a,b). The relative flatness of *EXPDOSE* with time results from the rapid decrease of dose to the RMEI after individual eruptive events. As a result, *EXPDOSE* shows little increase with time as increasing numbers of potential eruptive events are included in its calculation.

The PRCCs in Figure K6.8.1-1c indicate that the uncertainty in *EXPDOSE* is dominated by *IGERATE* (rate of occurrence of igneous eruptive events, yr^{-1}; *IGERATE* = (0.28)(0.2968)*IGRATE*, where 0.28 is the probability that an igneous intrusive event will have an eruptive component, 0.2968 is the probability that the eruptive component of an igneous intrusive event will intercept waste, and *IGRATE* is the rate of occurrence (yr^{-1}) of igneous intrusive events), with the value for *EXPDOSE* increasing as *IGERATE* increases. This effect results because increasing *IGERATE* increases the probability that an igneous eruptive event will occur and hence increases *EXPDOSE.*

Smaller effects on *EXPDOSE* are indicated for *INHLTPV* (pointer variable for long-term inhalation dose), *DDIVIDE* (diffusivity of radionuclides in divides of the Fortymile Wash alluvial fan, cm^2/yr), *CSNFMASS* (scale factor used to characterize uncertainty in radionuclide content of CSNF, dimensionless), and *DASHAVG* (mass median ash particle diameter, cm) (Figure K6.8.1-1c). Increasing *INHLTPV* increases the BDCF for all radionuclides contributing to long-term inhalation dose. Increasing *DDIVIDE* increases the rate at which radionuclides diffuse downward and out of the biosphere and thus reduces *EXPDOSE*. Increasing *CSNFMASS* increases the mass of radionuclides intercepted by eruptive events. Increasing *DASHAVG* increases the fraction of ash mass consisting of larger ash particles, which in turn permits an increased fraction of the waste particles to be incorporated into ash particles and thus results in a larger fraction of the waste affected by the eruption being deposited in contaminated tephra.

More detailed sensitivity analyses for *EXPDOSE* are provided by the regression analyses in Figure K6.8.2-2a at 3000, 5000 and 10,000 yr. The three regression analyses are almost identical and each contains the following four variables in the same order: *IGERATE*, *INHLTPV*, *DDIVIDE*, *CSNFMASS*, and *DASHAVG*. The dominant effect of *IGERATE* on the uncertainty in *EXPDOSE* is indicated by R^2 values of 0.76, 0.76 and 0.76 for the regressions containing only *IGERATE*. After *IGERATE*, the most important variable is *INHLTPV*. However the incremental effect associated with *INHLTPV*is significant as the R^2 value for the regression models containing both *IGERATE* and *DDIVIDE* is 0.91. Inclusion of *DDIVIDE*, *CSNFMASS* and *DASHAVG* in the regression models brings the final R^2 value up to 0.95.

The dominant effect of *IGERATE* on the uncertainty in *EXPDOSE* and the lesser effects of *INHLTPV* and *DDIVIDE* can be seen in the scatterplots in Figure K6.8.1-2b,c.d.

K6.8.2 Igneous Eruptive Scenario Classes: Expected Dose (*EXPDOSE*) to Reasonably Maximally Exposed Individual over [0, 1,000,000 yr]

The uncertainty and sensitivity analyses for expected dose to the RMEI (*EXPDOSE*, mrem/yr) over the time interval [0, 1,000,000 yr] resulting from igneous eruptive events are summarized in Figures K6.8.2-1 and K6.8.2-2. The values for *EXPDOSE* tend to increase up to 50,000 yr, then decrease up to 150,000 yr, and then slowly increase again (Figure K6.8.2-1a,b). This pattern results from an initial build up of the contribution of multiple possible igneous eruptive events over the first 50,000 yr to *EXPDOSE*. Then, *EXPDOSE* decreases up to about 150,000 yr because of the decay of radionuclides such as ^{239}Pu. After 150,000 yr, *EXPDOSE* increases again from the build up of the contributions of multiple possible igneous eruptive events. The relatively slow increase of *EXPDOSE* after 150,000 yr results from the rapid decrease of dose to the RMEI after individual eruptive events. Overall, the values for *EXPDOSE* are small and range between 10^{-7} and 10^{-3} mrem/yr (Figure K6.8.2-1a,b).

The PRCCs in Figure K6.8.2-1c indicate that the uncertainty in *EXPDOSE* is dominated by *IGERATE* (rate of occurrence of igneous eruptive events, yr^{-1}; *IGERATE* = (0.28)(0.2968)*IGRATE*, where 0.28 is the probability that an igneous intrusive event will have an eruptive component, 0.2968 is the probability that the eruptive component of an igneous intrusive event will intercept waste, and *IGRATE* is the rate of occurrence (yr^{-1}) of igneous intrusive events), with the value for *EXPDOSE* increasing as *IGERATE* increases. This effect results because increasing *IGERATE* increases the probability that an igneous eruptive event will occur and hence increases *EXPDOSE.*

Smaller effects on *EXPDOSE* are indicated for *INHLTPV* (pointer variable for long-term inhalation dose), *FRACCHNL* (fraction of Fortymile Wash alluvial fan subject to fluvial deposition), *DDIVIDE* (diffusivity of radionuclides in divides of the Fortymile Wash alluvial fan, cm^2/yr), *BTILLAGE* (depth of soil within which radionuclides contribute to dose from external exposure, m), and *CSNFMASS* (scale factor used to characterize uncertainty in radionuclide content of CSNF). Increasing *INHLTPV* increases the BDCF for all radionuclides contributing to long-term inhalation dose. Increasing *FRACCHNL* increases the area on which redistributed tephra is deposited. Within a relatively short time after an eruption, the radionuclide concentration in redistributed tephra in channels is much higher than in the surface soil layers on divides. As a consequence, increasing *FRACCHNL* has the effect of increasing the spatially-averaged radionuclide concentration at the RMEI location from all eruptions preceding a specific time *t*, and thus effectively increases *EXPDOSE* at time *t*. Increasing *DDIVIDE* increases the rate at which radionuclides diffuse downward past the tillage depth and out of the biosphere. Increasing *BTILLAGE* increases the depth to which radionuclides remain accessible to the biosphere through plant root uptake and other processes. Increasing *CSNFMASS* increases the mass of radionuclides intercepted by eruptive events.

The reduction in importance of *INHLTPV* after 50,000 yr is due to two factors: (i) the decay of ^{239}Pu, which is the primary radionuclide contributing to inhalation dose from igneous eruptive events during the first 100,000 years (Figure 8.2-10), and (ii) the reduction in contribution to annual dose from inhalation pathways. The dose from plutonium occurs primarily though the inhalation pathways (SNL 2007 [DIRS 177399], Table 6.14-2). The radionuclides considered for dose through inhalation pathways are limited to the resuspendable mass very near the surface

(i.e. within a depth defined by *RSUSTHIK*. Diffusion out of this depth is relatively rapid, hence the contribution from inhalation pathways to annual dose is reduced with time. The change in importance of *BTILLAGE* between 0 yr and 200,000 yr is due to the increasing importance of the external exposure pathway with time. The input variable *BTILLAGE* is used to estimate the mass of radionuclides below the near-surface layers of soil that contribute to annual dose from external exposure pathways (SNL 2007 [DIRS 177399], Section 6.4.1.1). Before 100,000 yr, ^{239}Pu and ^{240}Pu are the major contributors to dose from eruptive events. These radionuclides have relatively low rates of plant uptake, with the result that plutonium below the critical depth *RSUSTHIK* but within the tillage depth given by *BTILLAGE* contributes little to dose from external exposure, and thus has little effect on annual dose. After roughly 100,000 yr, the major contributor to annual dose is ^{226}Ra, which has a large contribution to dose from external exposure. The Biosphere Model conservatively assumes that all radionuclides down to the tillage depth (*BTILLAGE*) contribute to dose from external exposure. Thus, as ^{226}Ra becomes the dominant radionuclide, the influence of *BTILLAGE* increases. The change in importance of *FRACCHNL* parallels the change in importance of *BTILLAGE* because increasing the area on which redistributed tephra is deposited increases the mass of radionuclides in the soil down to the depth given by *BTILLAGE*.

More detailed sensitivity analyses for *EXPDOSE* are provided by the regression analyses in Figure K6.8.2-2a. The dominant effect of *IGERATE* on the uncertainty in *EXPDOSE* is indicated by R^2 values of 0.80, 0.86 and 0.86 for the regressions containing only *IGERATE* at 50,000, 200,000 and 500,000 yr.

After *IGERATE*, the regression for *EXPDOSE* at 50,000 yr selects *INHLTPV*, *DDIVIDE*, *CSNFMASS*, *FRACCHNL*, *DASHAVG, BTILLAGE, CRITSLOP* (critical gradient for tehpra mobilization from hillsides) and *DCHANL* (diffusivity of radionuclides in channels of the Fortymile Wash alluvial fan, cm^2/yr) and produces a final model with an R^2 values of 0.96 (Figure K6.8.2-2a). Thus, most of the uncertainty in *EXPDOSE* at 50,000 yr is being accounted for. The effects of *INHLTPV*, *DDIVIDE*, *CSNFMASS*, *FRACCHNL*, *DASHAVG* and *BTILLAGE* on the uncertainty in *EXPDOSE* have already been discussed. The small negative effect associated with *CRITSLOP* results because ash is mobilized from terrain at which the downhill gradient exceeds *CRITSLOP*; thus, increasing *CRITSLOP* decreases the area from which ash is mobilized and thus decreases the mass of radionuclides that are transported with the mobilized ash. The small negative effect associated with *DCHANL* results because increasing this diffusivity reduces the time required for radionuclides to diffuse down out of the biosphere.

The regressions for *EXPDOSE* at 200,000 and 500,000 yr are similar and select the following first five variables in the same order: *IGERATE*, *INHLTPV, BTILLAGE*, *FRACCHNL* and *CSNFMASS* (Figure K6.8.2-2a). With all five variables, the regression models have R^2 values of 0.95 and 0.96. Thus, the regression models at 200,000 and 500,000 yr are very successful in accounting for the uncertainty in *EXPDOSE*. The effects of *IGERATE*, *BTILLAGE*, *FRACCHNL, INHLTPV* and *CSNFMASS* on *EXPDOSE* have already been discussed. After *IGERATE*, *BTILLAGE*, *FRACCHNL, INHLTPV* and *CSNFMASS*, the regressions at 200,000 and 500,000 yr add several additional variables that have very small effects on *EXPDOSE* and end with R^2 values of 0.97 and 0.98.

The dominant effect of *IGERATE* on the uncertainty in *EXPDOSE* at 500,000 yr and the lesser effects of *BTILLAGE* and *FRACCHNL* can be seen in the scatterplots in Figure K6.8.2-2b,c.d.

K7 SEISMIC SCENARIO CLASSES

K7.1 Seismic Scenario Classes: Summary

The seismic scenario classes are defined on the basis of futures that involve one or more seismic events (Section J8). This section (Section K7) presents uncertainty and sensitivity analysis results for selected analysis outcomes associated with the seismic scenario classes (Table K7.1-1). The primary emphasis is on the seismic ground motion scenario class but expected dose results for the seismic fault displacement scenario class are also presented.

The primary results considered for the seismic ground motion scenario class for 20,000 yr are radionuclide movement from the EBS to the UZ (Table K7.1-2), radionuclide movement from the UZ to the SZ (Table K7.1-3), radionuclide movement in the SZ at the location of the RMEI (Table K7.1-4), dose to the RMEI from selected radionuclides (Table K7.1-5), and expected dose to the RMEI from all radionuclides (Table K7.1-6). High-level summaries of the uncertainty and sensitivity analysis results presented in this section are provided in Tables K7.1-2 to K7.1-6. Additional uncertainty analysis results are also available in Section J8.

The analysis of radionuclide movement considers releases following a seismic event at 200 years that causes a fractional damaged area of 10^{-6}(32.6 m^2) at 200 yr to all CDSP WPs in the repository. The variability in dose to the RMEI following seismic GM events at different times is shown in Figure J8.3-1. Because of the similarity in dose following events at different times, it is anticipated that sensitivity analysis results would be similar if different event times were to be considered. Figure J8.3-2 illustrates that dose to the RMEI changes in proportion to damaged area for damaged area within a range between has 10^{-7}(32.6 m^2) and 10^{-5}(32.6 m^2). A damaged area of 10^{-6}(32.6 m^2) was selected within this range. This damaged area is typical of the damaged area that may result from a seismic event that initially damages CDSP WPs (DTN: MO0708CDSPSEIS.000_R0 [DIRS183007], CDSP_Damage_Fraction_CDF.JNB).

From a regulatory perspective, expected dose to the RMEI (*EXPDOS*, mrem/yr) is the analysis outcome of greatest interest associated with the seismic scenario classes (Table K7.1-6). For the seismic ground motion scenario class, *EXPDOS* tends to monotonically increase over the time interval [0, 2×10^4 yr], with the value for *EXPDOSE* between 10^{-4} and 1 mrem/yr for most sample elements, with a few sample elements having values for *EXPDOSE* between 1 and 10 mrem/yr. (Figure K7.7.1-1). The uncertainty in *EXPDOSE* is dominated by the residual stress threshold *SCCTHRP* (as sampled, *SCCTHRP* is a percent of a base value of 351 MPa and is related to the stress corrosion cracking threshold, *SCCTHR*, by *SCCTHRP* = (*SCCTHR* × 100)/(351 MPa)), with the value for *EXPDOSE* decreasing as *SCCTHRP* increases.

For the [0, 10^6 yr] time interval, the sensitivity analysis considers only expected dose to the RMEI (*EXPDOS*, mrem/yr). The individual realizations of *EXPDOS* are noisy (Figure K7.7.2-1) due to the combination of nominal processes and seismic events in this scenario class, and the resultant use of a Monte Carlo method to evaluate expected dose. This noise propagates into the sensitivity analysis results and appears as time-dependent noise in the correlations between

EXPDOS and uncertain parameters. Over the time interval [0, 10^6 yr], the observed range of possible values for *EXPDOS* with the current sample size is approximately [10^{-4}, 70 mrem/yr]. Because the peak values of *EXPDOS* are associated with spikes, these values may not be representative of the peak values of *EXPDOS* that may result from an improved numerical calculation. The use of larger sample sizes in the integration over aleatory uncertainty (i.e., over seismic events and their associated properties) or the use of appropriate numerical smoothing techniques would reduce the noise in each individual realization and would produce smoother time-dependent results for *EXPDOS*. Despite the noise present in the individual realizations of expected dose, Figure 7.3.1-11 demonstrates that the distribution of uncertainty in expected dose is stable at the sample size used in the TSPA-LA analysis. Thus, the noise evident in *EXPDOS* affects the tails of the distribution of *EXPDOS* at each point in time, but does not influence the mean dose.

The dominant variables contributing to the uncertainty in *EXPDOS* for the seismic ground motion scenario class over the time interval [0, 10^6 yr] are *SCCTHRP* and *WDGCA22* (temperature dependence coefficient associated with the general corrosion rate for alloy 22, K) (Figures K7.7.1-1, K7.7.1-2, K7.7.2-1, K7.7.2-2). The effect associated with *SCCTHRP* results from its role in decreasing the stress level at which stress corrosion cracking will initiate after a seismic event. The 10^6 yr seismic analysis also includes WP thinning and failure due to nominal processes. The importance of *WDGCA22* results from its role in affecting general corrosion of alloy 22 and hence WP thinning, which in turn affects both WP failure caused by seismic events and WP failure from nominal processes. Prior to approximately 2×10^5 yr, *SCCTHRP* is the dominant variable affecting the uncertainty associated with *EXPDOS*; after 2×10^5 yr, *SCCTHRP* and *WDGCA22* are both important contributors to the uncertainty in *EXPDOS*. This analysis does not include the uncertainty in the seismic hazard curve; if included, this uncertainty would probably also be an important contributor to the uncertainty in *EXPDOS*.

The sensitivity analysis for the [0, 10^6 yr] time interval did not investigate radionuclide movement within the repository system. As described in Appendix J, Section J8.4, a Monte Carlo method is used to evaluate annual dose from the combined effects of nominal processes and seismic events for each combination of a sampled future and an LHS element. Figure J8.4-1 illustrates a few of the 9,000 annual dose histories calculated by the Monte Carlo technique. In the Monte Carlo analysis, the futures describing each sequence of seismic events are sampled independently for each LHS element in order to obtain a more stable estimate of the mean dose than would result if the same sampled futures were used for all LHS elements. As a consequence, the uncertainty analysis does not produce a set of results that are conditional on a common future. Hence, sensitivity analysis to determine the effects of epistemic uncertainty can be performed only on expected values of model outputs, where the expected values are averages of model output results for each epistemic sample. Sensitivity analyses are performed on expected dose to the RMEI. These analyses show that the uncertainty in expected dose to the RMEI is dominated by the uncertainty in two variables that determine when WPs fail: *SCCTHRP* and *WDGCA22*. As a result, it is anticipated that the uncertainty in the expected value of the rates of radionuclide movement would also be dominated by these same two variables as these variables determine the likelihood of releases from the WP.

For the seismic fault displacement scenario class, the possible values for *EXPDOS* fall in the interval [10^{-4}, 4 mrem/yr] over the [0, 10^6 yr] time interval (Figures K7.8.1-1, K7.8.2-1). Overall, the two most important variables with respect to the uncertainty in *EXPDOS* for the seismic fault displacement scenario class over the time interval [0, 10^6 yr] are *SZGWSPDM* (groundwater specific discharge multiplier*;* as sampled, *SZGWSPDM* is actually the logarithm of the indicated multiplier) and *INFIL* (infiltration level) (Figures K7.8.1-1, K7.8.1-2, K7.8.2-1, K7.8.2-2). At early times (e.g., prior to 2×10^4 yr), *MICTC99* (dose conversion factor for ^{99}Tc for modern interglacial climate, (rem/yr)/(pCi/L)) is also important but has limited effect on the uncertainty in *EXPDOS* at later times. However, no individual variable has a dominant effect on the uncertainty in *EXPDOS* for the seismic fault displacement scenario class. Similarly to the seismic ground motion scenario class, the uncertainty in the occurrence rate for the seismic fault displacement events is not included in the analysis. Movement of radionuclides through the repository system is not investigated for the seismic fault displacement scenario class.

K7.2 Seismic Ground Motion Scenario Classes: Engineered Barrier System Conditions over the Time Interval [0, 20,000 yr]

The environmental conditions in the barrier system for seismic ground motion events in the time interval [0, 20,000 yr] are the same as described in Section K4 for the nominal scenario class.

K7.3 Seismic Ground Motion Scenario Classes: Release from Engineered Barrier System over the Time Interval [0, 20,000 yr]

Movement of ^{239}Pu Irreversibly Attached to Glass (i.e., Ic) Colloids: *ESIC239* and *ESIC239C*. Uncertainty and sensitivity analyses for movement of ^{239}Pu irreversibly attached to glass colloids are not presented when transport is predominantly by diffusion due to an error in the GoldSim component of the TSPA-LA Model that affects the calculation of concentration of glass colloids when glass colloids are unstable. Consequently, Figure K7.3-1 and Figure K7.3-2 have been removed from this document. See Appendix P, Table P-6, for a discussion of the error and the effect of the error on TSPA-LA Model results.

Movement of ^{239}Pu Irreversibly Attached to Ferrous (i.e., If) Colloids: Uncertainty and sensitivity analyses for movement of ^{239}Pu irreversibly attached to ferrous colloids are not presented due to an error in the Goldsim component of the TSPA-LA Model that affects the calculation of stability of ferrous colloids. Consequently, Figure K7.3-3 and Figure K7.3-4 have been removed from this document. See Appendix P, Section P18, for a discussion of the error and the effect of the error on TSPA-LA Model results.

Movement of Dissolved ^{237}Np: *ESNP237* and *ESNP237C*. The uncertainty and sensitivity analyses for the time-dependent release rates (*ESNP237*, g/yr) and cumulative releases (*ESNP237C*, g) over the time interval [0, 20,000 yr] for the movement of dissolved ^{237}Np from the EBS to the UZ resulting from a seismically induced fractional damaged area of 10^{-6} (32.6 m^2) at 200 yr to all CDSP WPs in the repository are summarized in Figures K7.3-5 and K7.3-6.

The values for *ESNP237C* at 20,000 yr fall between 10^{-2} and 10^{1} g (Figure K7.3-5b). Thus, from a risk perspective, the values for *ESNP237* and *ESNP237C* for this analysis case are inconsequential because of their small sizes (i.e., the dose resulting from dissolved ^{237}Np is much less than the dose resulting from other radionuclides such as ^{99}Tc (Section 8.2.4.1)).As indicated by the PRCCs in Figure K7.3-5e,f, the uncertainty in *ESNP237* and *ESNP237C* at early times is affected by *THERMCON* (host rock thermal conductivity level) and *INFIL* (infiltration level). The positive effects associated with these two variables at early times result from their role in decreasing the time at which the EBS cools to the level at which radionuclide movement is possible. A very early effect is also indicated for *DIAMCOLL* (diameter of colloid particles, nm); however, this effect occurs during the early period when the results are very noisy and also include many zero values. As a result, the selection of *DIAMCOLL* is probably spurious. As time increases, *GOESITED* (density of sorption sites on goethite, sites/nm^2) is the only variable with large PRCCs. In particular, the negative PRCCs associated with *GOESITED* indicate that *ESNP237* and *ESNP237C* decrease as *GOESITED* increases. This effect results because increasing *GOESITED* increases the amount of ^{237}Np sorbed onto goethite and thus reduces the amount of dissolved ^{237}Np available for release from the EBS.

As shown in Figure K7.3-5a,c, the release rates of dissolved ^{237}Np after about 1,000 years generally evolve toward a steady state value as environmental conditions inside the WP evolve toward steady state. These environmental variables determine the solubility of ^{237}Np at each time. This evolution is apparent in the changing values of the PRCCs for *DELPPCO2* (scale factor used to incorporate uncertainty into the value for the partial pressure of CO_2) and *PH2MCOS* (pointer variable used to incorporate uncertainty into pH in cell 1b of CDSP WPs under liquid influx conditions). The steady state release rate is determine by the balance between waste form degradation and reversible sorption onto ferrous corrosion products as indicated by the PRCC for *GOESITED* (density of sorption sites on goethite, sites/nm^2). The effect of climate changes at 2,000 yr and 10,000 yr can also be observed in Figure K7.3-5a,c, where the assumption that climate change is instantaneous (Section 5.1.1) results in temporary jumps in release rates.

Overall, the absence of variables with large PRCCs in Figure K7.3-5e,f suggests that the uncertainty in *ESNP237* and *ESNP237C* is determined by small effects associated with a large number of individual variables. This is borne out by the regression analyses in Figure K7.3-6a,b. For example, the first variable selected in the individual regressions in Figure K7.3-6a,b is either *GOESITED* or *DELPPCO2* and the resultant regression model has an R^2 value between 0.13 and 0.24. Further, after the selection of six variables, the resultant regression models have R^2 values between 0.50 and 0.54, and the final regression models contain from 11 to 14 variables and have R^2 values between 0.60 and 0.64. Thus, the uncertainty in *ESNP237* and *ESNP237C* is affected by a large number of variables without being dominated by the uncertainty in a small number of variables.

As an example, the regression analysis for *ESNP237* at 10,000 yr will be discussed. The first six variables selected in the analysis are *GOESITED*, *EP1LOWNU* (scale factor used to incorporate uncertainty into uranium solubility under low ionic strength conditions for nominal and seismic conditions; as sampled, *EP1LOWNU* is actually the logarithm of the indicated scale factor; in the present analysis, *EP1LOWNU* was used instead of the corresponding and intended variable

EP1LOWOU for igneous conditions; however, this has no effect on analysis outcomes as *EP1LOWNU* and *EP1LOWOU* are assigned the same distribution), *DSNFMASS* (scale factor used to characterize uncertainty in amount of DSNF in CDSP WPs), *HFOSA* (hydrous ferrous oxide surface area, m^2/g), *GOESA* (specific surface area of goethite, m^2/g), and *IS2MCONS* (pointer variable used to determine ionic strength in 2MCO Cell i.e., Cell 1b, of CDSP WPs under nondripping conditions) (Figure K7.3-6a). Of the preceding variables, *GOESITED* and *HFOSA* have negative regression coefficients, and the remaining variables have positive regression coefficients. The negative effects associated with *GOESITED* and *HFOSA* result because increasing these variables increases the sorption of ^{237}Np onto stationary surfaces and thus reduces the amount of dissolved ^{237}Np available for release from the EBS. The positive effects associated with *EP1LOWNU*, *DSNFMASS*, *GOESA* and *IS2MCONS* result because (i) increasing *EP1LOWNU* increases the amount of dissolved uranium which in turn competes with ^{237}Np for sorption sites, with the result that the dissolved concentration of ^{237}Np increases because less ^{237}Np is sorbed onto stationary sites, (ii) increasing *DSNFMASS* increases the amount of DSNF in CDSP WPs, which in turn increases the amount of ^{237}Np available for release from the EBS, (iii) increasing *GOESA* increases the surface area of corrosion products, which increases the sorption of water onto the corrosion products, thereby increasing saturation of the corrosion products and facilitating transport, and (iv) increasing *IS2MCONS* increases ionic strength which in turn increases neptunium solubility. Together, *GOESITED*, *EP1LOWNU*, *DSNFMASS*, *HFOSA*, *GOESA* and *IS2MCONS* result in a regression model with an R^2 value of 0.54. For perspective, the scatterplots for *GOESITED*, *EP1LOWNU* and *DSNFMASS* are presented in Figure K7.3-6c,d,e.

The next six variables selected in the regression analysis for *ESNP237* at 10,000 years are *DELPPCO2*, *PH2MCONS* (pointer variable used to incorporate uncertainty into pH in cell 1b of CDSP WPs under vapor influx conditions), *CSRINDSA* (specific surface area of CSNF and DSNF degradation rind, m^2/g), *EP1NPO2* (scale factor used to incorporate uncertainty into NpO_2 solubility below 1 molal ionic strength; as sampled, *EP1NPO2* is actually the logarithm of the indicated scale factor), *GOERELAB* (fraction of total iron oxide that is goethite), and *HFOSITED* (sorption site density for hydrous ferric oxide, sites/nm^2) (Figure K7.3-6a). Of these variables, *DELPPCO2*, *CSRINDA, EP1NPO2* and *GOERELAB* have positive regression coefficients, and *PH2MCONS* and *HFOSITED* have negative regression coefficients. The positive effects associated with *DELPPCO2*, *CSRINDA, EP1NPO2* and *GOERELAB* result because (i) increasing *DELPPCO2* tends to increase the solubility of ^{237}Np**,** (ii) increasing *CSRINDA* increases water saturation in the degraded waste form, thus facilitating diffusive transport of dissolved species, (iii) increasing *EP1NPO2* increases the solubility of neptunium and thus increases the amount of dissolved ^{237}Np available for release from the EBS, and (iv) increasing *GOERELAB* increases the fraction of total iron oxide that is goethite, which generally results in a net decrease in the number of sorption sites on the corrosion products. The negative effects associated with *PH2MCONS* and *HFOSITED* result because (i) increasing *PH2MCONS* increases pH and thus generally decreases the solubility of neptunium in the commonly observed chemical environments, and (ii) increasing *HFOSITED* increases the number of sorption sites on corrosion products, which increases the sorption of ^{237}Np onto stationary surfaces and thus reduces the amount of dissolved ^{237}Np available for release from the EBS. The addition of *DELPPCO2*, *PH2MCONS*, *CSRINDSA*, *EP1NPO2*, *GOERELAB* and *HFOSITED* to the

regression model results in a final model containing twelve variables and having an R^2 value of 0.64 (Figure K7.3-6a).

The remaining five regression analyses in Figure K7.3-6a (i.e., for *ESNP237* at 3000 and 5000 years and *ESNP237C* at 3000, 5000 and 10,000 years) are generally similar to the regression analysis just discussed for *ESNP237* at 10,000 yr.

Movement of Dissolved ^{239}Pu: *ESPU239* and *ESPU239C*. The uncertainty and sensitivity analyses for the time-dependent release rates (*ESPU239*, g/yr) and cumulative releases (*ESPU239C*, g) over the time interval [0, 20,000 yr] for the movement of dissolved ^{239}Pu from the EBS to the UZ resulting from a seismically induced fractional damaged area of 10^{-6}(32.6 m^2) at 200 yr to all CDSP WPs in the repository are summarized in Figures K7.3-7 and K7.3-8.

The values for *ESPU239C* at 20,000 yr fall between 10^{-2} and 10^2 g (Figure K7.7-7b). Thus, from a risk perspective, the values for *ESPU239*and *ESPU239C* for this analysis case are inconsequential, because of their small sizes (i.e., the dose resulting from dissolved ^{239}Pu is much less than the dose resulting from other radionuclides such as ^{99}Tc (Section 8.2.4.1)). Similar to the evolution of the release rates of dissolved ^{237}Np (Figure K7.3.1-5a,c), the release rates of dissolved ^{239}Pu generally evolve toward a steady state value, as environmental conditions inside the WP evolve toward steady state. The effect of climate changes at 2,000 yr and 10,000 yr can also be observed in Figure K7.3-7a,c, where the assumption that climate change is instantaneous (Section 5.1.1) results in temporary jumps in release rates.

As indicated by the PRCCs in Figure K7.3-7e,f, the uncertainty in *ESPU239*and *ESPU239C* is dominated by *EP1LOWPU* (scale factor used to incorporate uncertainty into plutonium solubility under low ionic strength conditions; as sampled, *EP1LOWPU* is actually the logarithm of the indicated scale factor). Further, *EP1LOWPU* is the first variable selected in each of the regressions in Figure K7.3-8a,b, with the individual regressions containing only *EP1LOWPU* having R^2 values between 0.30 and 0.51. For both *ESPU239* and *ESPU239C*, the R^2 values increase with increasing time. Thus, the importance of *EP1LOWPU* with respect to the uncertainty in *ESPU239* and *ESPU239C* increases with time. The positive effects indicated for *EP1LOWPU* on *ESPU239* and *ESPU239C* result because increasing *EP1LOWPU* increases the solubility of plutonium and thus increases the amount of dissolved ^{239}Pu available to be released from the EBS.

After *EP1LOWPU*, the PRCCs in Figure K7.3-7e,f indicate effects for several additional variables. In particular, positive effects are indicated for *THERMCON* (host rock thermal conductivity level) and *INFIL* (infiltration level) at early times because of the influence that these two variables have on the cooling of the EBS and the resultant initiation of radionuclide movement. At later times, positive effects are indicated for *INFIL* and *DELPPCO2* (scale factor used to incorporate uncertainty into the value for the partial pressure of CO_2), and negative effects are indicated for *PH2MCONS* (pointer variable used to incorporate uncertainty into pH in cell 1b of CDSP WPs under vapor influx conditions) and *SEEPPRM* (fracture permeability in lithophysal rock units, m^2; as sampled, *SEEPPRM* is actually the logarithm of the indicated permeability) (Figure K7.3-7e,f). The positive effects associated with *INFIL* and *DELPPCO2* result because (i) increasing *INFIL* increases water movement in the EBS and (ii) increasing

DELPPCO2 increases the solubility of plutonium. The negative effects associated with *PH2MCONS* and *SEEPPRM* result because (i) increasing *PH2MCONS* increases pH and thus reduces the solubility of plutonium for most chemical conditions that are observed and (ii) increasing *SEEPPRM* increases water flow around the EBS and thus reduces water flow into the EBS.

The same pattern of effects is present in the regression analyses in Figure K7.3-8a,b. Specifically, the first three variables selected in all six regression analyses are *EP1LOWPU*, *DELPPCO2* and *INFIL*, with the resultant regression models having R^2 values between 0.57 and 0.65. Thus, these three variables are having a large influence on the uncertainty in *ESPU239* and *ESPU239C*. Further, *PH2MCONS* is the fourth variable selected in five of the six regressions and is the fifth variable selected in the remaining regression. More specifically, the next three variables selected after *EP1LOWPU*, *DELPPCO2* and *INFIL* in all six regressions are *PH2MCONS*, *SEEPPRM* and *GOESITED* (density of sorption sites on goethite, sites/nm^2). The inclusion of *PH2MCONS*, *SEEPPRM* and *GOESITED* in the regression models results in R^2 values between 0.72 and 0.75. Thus, these six variables can account for most of the uncertainty associated with *ESPU239*and *ESPU239C*. The effects of *EP1LOWPU*, *DELPPCO2*, *INFIL*, *PH2MCONS* and *SEEPPRM* on *ESPU239* and *ESPU239C* have already been discussed in conjunction with the PRCCs in Figure K7.3-7e,f. The negative effect associated with *GOESITED* results because increasing *GOESITED* increases the amount of plutonium sorbed to stationary surfaces and thus reduces the amount of dissolved ^{239}Pu available to be released from the EBS. After the first six variables, the individual regression analysis select a number of additional variables having small effects on *ESPU239* and *ESPU239C*. At completion, the individual regression models contain 11 or 12 variables and have R^2 values between 0.77 and 0.81.

For perspective, scatterplots showing the effects of *EP1LOWPU*, *DELPPCO2* and *INFIL* on *ESPU239* and *ESPU239C* at 10,000 yr are given in Figure K7.3-8c,d,e,f,g,h. The positive effects of *EP1LOWPU*, *DELPPCO2* and *INFIL* on *ESPU239* and *ESPU239C* can be seen in these plots.

Movement of Dissolved ^{99}Tc: *ESTC99* and *ESTC99C*. The uncertainty and sensitivity analyses for the time-dependent release rates (*ESTC99*, g/yr) and cumulative releases (*ESTC99C*, g) over the time interval [0, 20,000 yr] for the movement of dissolved ^{99}Tc from the EBS to the UZ resulting from a seismically induced fractional damaged area of 10^{-6} (32.6 m^2) at 200 yr to all CDSP WPs in the repository are summarized in Figures K7.3-9 and K7.3-10.

Unlike the results for the other two radioactive species (i.e., ^{237}Np and ^{239}Pu) used to illustrate the effects of seismic ground motion damage, substantial releases of ^{99}Tc from the EBS are observed. Specifically, the value for *ESTC99C* at 20,000 yr falls between 10^5 and 10^6 g (Figure K7.3-9b). As shown in Figure 8.2-12 and Figure J8.3-8, the release of dissolved ^{99}Tc from the repository results in the largest contribution to expected dose to the RMEI. As shown in Figure K7.3-9a,c, the values for *ESTC99* tend to decrease monotonically with time; however, this decrease is not nearly as rapid as is the case when the WP is destroyed (e.g., see Figures K5.3.3-5, K5.3.5-5). The less rapid release of ^{99}Tc following a seismic event results because the seismic event damages a relatively small area on each WP, which in turn limits the

rate of diffusion of ^{99}Tc from the interior of the WP. The spikes in release rates at 2,000 yr and 10,000 yr are due to climate change at these times.

The sensitivity analyses for *ESTC99* are discussed first. As shown by the PRCCs in Figure K7.3-9e, the uncertainty in *ESTC99* at early times is dominated by *THERMCON* (host rock thermal conductivity level) and *INFIL* (infiltration level). The positive effects associated with these two variables at early times results from their role in decreasing the time at which the EBS cools to the level at which radionuclide movement is possible. At later times, *THERMCON* and *INFIL* have a negative effect on *ESTC99* because the release of ^{99}Tc at early times reduces the amount of ^{99}Tc available to be released at later times. Higher values of *THERMCON* and *INFIL* generally correspond to more rapid cooling of the waste. Lower temperatures result in slower degradation of HLW and in corresponding less total ^{99}Tc released over 10,000 yr. Specifically, HLW contains almost all of the ^{99}Tc in CDSP WPs (between 2.5×10^6 g and 5.1×10^6 g). In contrast, the DSNF component of waste in CDSP WPs contains between 1.0×10^4 g and 6.0×10^4 g of ^{99}Tc. In addition, positive effects are indicated for *GOESA* (specific surface area of goethite**,** m^2/g), *HLWMASS* (scale factor used to characterize uncertainty in radionuclide content of HLW in CDSP WPs), and *HLWDRALK* (dissolution rate of HLW glass under alkaline conditions, $g/m^2/d$); and a negative effect is indicated for *CORRATSS* (stainless steel corrosion rate, μm/yr). The positive effects associated with *GOESA*, *HLWMASS* and *HLWDRALK* result because (i) increasing *GOESA* increases the saturation of the corrosion products, thereby facilitating diffusive transport, (ii) increasing *HLWMASS* increases the amount of ^{99}Tc in CDSP WPs, and (iii) increasing *HLWDRALK* increases the dissolution rate of HLW glass and thus accelerates the release of ^{99}Tc within CDSP WPs. The negative effect associated with *CORRATSS* results because increasing *CORRATSS* increases the amount of corrosion products in WPs, which in turn decreases the saturation of the corrosion products and hence slows the diffusion rate of ^{99}Tc out of damaged WPs.

More detailed sensitivity analysis results for *ESTC99* are provided by the regression analyses in Figure K7.3-10a. The three regressions all select *GOESA* first and then either *HLWDRALK* or *HLWMASS*. The regression models at 3000, 5000 and 10,000 yr with only *GOESA* have R^2 values of 0.18, 0.18 and 0.14, respectively, and the models with two variables have R^2 values of 0.37, 0.32 and 0.29. Thus, although important, the uncertainty in *GOESA, HLWDRALK* and *HLWMASS* does not dominate the uncertainty in *ESTC99*. The variables selected at steps 2 through 6 in the individual regression analyses are subsets of the variables *HLWDRALK*, *HLWMASS*, *CORRATSS*, *THERMCON*, *INFIL* and *DSNFMASS* (scale factor used to characterize uncertainty in amount of DSNF in CDSP WPs). With the exception of *DSNFMASS*, these variables were also identified as having similar effects in the analysis with PRCCs (see Figure K7.3-9e and associated discussion). Similarly to *HLWMASS*, the positive effect associated with *DSNFMASS* results from increasing the amount of ^{99}Tc in CDSP WPs. The regression models at 3000, 5000 and 10,000 yr with the first six variables have R^2 values of 0.65, 0.63 and 0.60, respectively; thus, the first six variables selected in the regression analyses account for over half the uncertainty associated with *ESTC99*. The final regressions for *ESTC99* at 3000, 5000 and 10,000 yr contain 12, 13 and 15 variables, respectively, and have R^2 values of 0.77, 0.78 and 0.78. However, variables selected near the end of the stepwise procedures that have small incremental effects on the cumulative R^2 values may be spurious. For example, the selection of

WDGCUA22 (pointer variable used to select the distribution of base corrosion rates of alloy 22 at 60 ºC over the patches on WPs) in the regression analysis for *ESTC99* at 10,000 yr is spurious as this variable is not involved in the present analysis.

For perspective, scatterplots showing the effects of *GOESA*, *HLWMASS* and *CORRATSS* on *ESTC99* at 10,000 yr are given in Figure K7.3-10c,d,e. The positive effects of *GOESA* and *HLWMASS* and the negative effect of *CORRATSS* on *ESTC99* can be seen in these plots.

The sensitivity analyses for *ESTC99C* are now discussed. As shown by the PRCCs in Figure K7.3-9f, the uncertainty in *ESTC99C* at early times is dominated by *THERMCON* and *INFIL*. The positive effects associated with these two variables at early times results from their role in decreasing the time at which the EBS cools to the level at which radionuclide movement is possible. At later times, *THERMCON* and *INFIL* have a negative effect on *ESTC99C* because higher values of *THERMCON* and *INFIL* generally correspond to lower temperatures at late times. The lower temperatures result in slower degradation of HLW and in corresponding less total ^{99}Tc released over 10,000 yr. As previously noted, HLW contains almost all of the ^{99}Tc in CDSP WPs (between 2.5×10^6 g and 5.1×10^6 g). In contrast, the DSNF component of waste in CDSP WPs contains between 1.0×10^4 g and 6.0×10^4 g of ^{99}Tc. With increasing time, positive effects are indicated for *GOESA, DSNFMASS*, *HLWDRALK* and *HLWMASS*. As discussed in conjunction with *ESTC99*, the indicated positive effects result because (i) increasing *GOESA* increases the saturation of the corrosion products, thereby facilitating diffusive transport, (ii) increasing *DSNFMASS* and *HLWMASS* increases the amount of ^{99}Tc in CDSP WPs, and (iii) increasing *HLWDRALK* increases the dissolution of HLW glass and thus increases the release of ^{99}Tc within CDSP WPs.

More detailed sensitivity analysis results for *ESTC99C* are provided by the regression analyses in Figure K7.3-10b. The three regressions all sequentially select *GOESA*, *HLWDRALK*, *HLWMASS* and *DSNFMASS* as the first four variables for inclusion in the regression models. The resultant models at 3000, 5000 and 10,000 yr with all four variables have R^2 values of 0.60, 0.59 and 0.53, respectively; thus, the first four variables selected in the regression analyses account for slightly over half the uncertainty associated with *ESTC99C*. The positive effects of *GOESA*, *HLWDRALK*, *HLWMASS* and *DSNFMASS* on *ESTC99C* are the same as previously discussed in conjunction with the PRCCs in Figure K7.3-9f.

After *GOESA*, *HLWDRALK*, *HLWMASS* and *DSNFMASS*, the regression analyses for *ESTC99C* select a number of additional variables with small effects (Figure K7.3-10b). The analysis for *ESTC99C* at 10,000 yr will be discussed as an example. The next three variables selected after *GOESA*, *HLWDRALK*, *HLWMASS* and *DSNFMASS* are *CORRATSS*, *THERMCON* and *INFIL*, with all three variables having negative effects on *ESTC99C*. The negative effect associated with *CORRATSS* results because increasing *CORRATSS* increases the amount of corrosion products in WPs, which in turn slows the diffusion rate of ^{99}Tc diffuses out of damaged WPs. The negative effects associated with *THERMCON* and *INFIL* are the same as previously discussed in conjunction with the PRCCs in Figure K7.3-9f. Inclusion of *CORRATSS*, *THERMCON* and *INFIL* results in a regression model with seven variables and raises the R^2 value from 0.53 to 0.66. The remaining five variables selected in the regression analysis are *PH2DHLNS* (pointer variable used to determine pH in 2DHLW Cell, i.e., Cell 1, of CDSP WPs under vapor influx

conditions), *WFDEGEXF* (surface area exposure factor for amount of HLW glass contacted by water), *HLWDRACD* (dissolution rate of HLW glass under acidic conditions, g/m^2/d), *FHHISSCP* (Frenkel-Halsey-Hill water vapor adsorption isotherm parameter *s* for corrosion products), and *DIAMCOLL* (diameter of colloid particles, m). The negative effect associated with *PH2DHLNS* results because increasing pH decreases the degradation rate of DHLW in acidic conditions (BSC 2004 *Defense HLW Glass Degradation Model*, Section 8.1, [DIRS169988]) and thus decreases the mass of ^{99}Tc released within 20,000 yr**;** the positive effects associated with *WFDEGEXF* and *HLWDRACD* result from their role in increasing the degradation of HLW glass and hence the release of ^{99}Tc from HLW glass; and the negative effect associated with *FHHISSCP* results because increasing *FHHISSCP* decreases the number of monolayers of water adsorbed onto the corrosion products, thereby inhibiting transport (EBS Radionuclide Transport Abstraction, Equation 6.3.4.3.2-2, [DIRS177407]). The selection of *DIAMCOLL* as the last variable in the stepwise process is spurious.

For perspective, scatterplots showing the effects of *GOESA*, *HLWDRALK* and *HLWMASS* on *ESTC99C* at 10,000 yr are given in Figure K7.3-10f,g,h. The positive effects of *GOESA*, *HLWDRALK* and *HLWMASS* on *ESTC99C* can be seen in these plots.

K7.4 Seismic Ground Motion Scenario Classes: Release from Unsaturated Zone (UZ) over the Time Interval [0, 20,000 yr]

For completeness, this section presents summaries of the uncertainty and sensitivity analyses for release from the UZ to the SZ over the time interval [0, 20,000 yr] resulting from a seismically induced fractional damaged area of 10^{-6} (32.6 m^2) at 200 yr to all CDSP WPs in the repository without discussion.

Movement of ^{239}Pu Irreversibly Attached to Slow (i.e., Ic) Colloids: *UZIC239* and *UZIC239C*. The uncertainty and sensitivity analyses for the time-dependent release rates (*UZIC239*, g/yr) and cumulative releases (*UZIC239C*, g) over the time interval [0, 20,000 yr] for the movement of ^{239}Pu irreversibly attached to slow (i.e., Ic) colloids from the UZ to the SZ resulting from a seismically induced fractional damaged area of 10^{-6} (32.6 m^2) at 200 yr to all CDSP WPs in the repository are summarized in Figure K7.4-1.

Movement of ^{239}Pu Irreversibly Attached to Fast (i.e., If) Colloids: *UZIF239* and *UZIF239C*. The uncertainty and sensitivity analyses for the time-dependent release rates (*UZIF239*, g/yr) and cumulative releases (*UZIF239C*, g) over the time interval [0, 20,000 yr] for the movement of ^{239}Pu irreversibly attached to fast (i.e., If) colloids from the UZ to the SZ resulting from a seismically induced fractional damaged area of 10^{-6} (32.6 m^2) at 200 yr to all CDSP WPs in the repository are summarized in Figure K7.4-2.

Movement of Dissolved ^{237}Np: *UZNP237* and *UZNP237C*. The uncertainty and sensitivity analyses for the time-dependent release rates (*UZNP237*, g/yr) and cumulative releases (*UZNP237C*, g) over the time interval [0, 20,000 yr] for the movement of dissolved ^{237}Np from the UZ to the SZ resulting from a seismically induced fractional damaged area of 10^{-6} (32.6 m^2) at 200 yr to all CDSP WPs in the repository are summarized in Figure K7.4-3.

Movement of Dissolved ^{239}Pu: *UZPU239* and *UZPU239C*. The uncertainty and sensitivity analyses for the time-dependent release rates (*UZPU239*, g/yr) and cumulative releases (*UZPU239C*, g) over the time interval [0, 20,000 yr] for the movement of dissolved ^{239}Pu from the UZ to the SZ resulting from a seismically induced fractional damaged area of 10^{-6} (32.6 m^2) at 200 yr to all CDSP WPs in the repository are summarized in Figure K7.4-4.

Movement of Dissolved ^{99}Tc: *UZTC99* and *UZTC99C*. The uncertainty and sensitivity analyses for the time-dependent release rates (*UZTC99*, g/yr) and cumulative releases (*UZTC99C*, g) over the time interval [0, 20,000 yr] for the movement of dissolved ^{99}Tc from the UZ to the SZ resulting from a seismically induced fractional damaged area of 10^{-6} (32.6 m^2) at 200 yr to all CDSP WPs in the repository are summarized in Figures K7.4-5.

K7.5 Seismic Ground Motion Scenario Classes: Release from Saturated Zone (SZ) over the Time Interval [0, 20,000 yr]

For completeness, this section presents summaries of the uncertainty and sensitivity analyses for radionuclide movement across a subsurface plane at the location of the RMEI over the time interval [0, 20,000 yr] resulting from a seismically induced fractional damaged area of 10^{-6} (32.6 m^2) at 200 yr to all CDSP WPs in the repository without discussion.

Movement of ^{239}Pu Irreversibly Attached to Slow (i.e., Ic) Colloids: *SZIC239* and *SZIC239C*. The uncertainty and sensitivity analyses for the time-dependent release rates (*SZIC239*, g/yr) and cumulative releases (*SZIC239C*, g) over the time interval [0, 20,000 yr] for the movement of ^{239}Pu irreversibly attached to slow (i.e., Ic) colloids across a subsurface plane at the location of the RMEI resulting from a seismically induced fractional damaged area of 10^{-6} (32.6 m^2) at 200 yr to all CDSP WPs in the repository are summarized in Figure K7.5-1.

Movement of ^{239}Pu Irreversibly Attached to Fast (i.e., If) Colloids: *SZIF239* and *SZIF239C*. The uncertainty and sensitivity analyses for the time-dependent release rates (*SZIF239*, g/yr) and cumulative releases (*SZIF239C*, g) over the time interval [0, 20,000 yr] for the movement of ^{239}Pu irreversibly attached to fast (i.e., If) colloids across a subsurface plane at the location of the RMEI resulting from a seismically induced fractional damaged area of 10^{-6} (32.6 m^2) at 200 yr to all CDSP WPs in the repository are summarized in Figure K7.5-2.

Movement of Dissolved ^{237}Np: *SZNP237* and *SZNP237C*. The uncertainty and sensitivity analyses for the time-dependent release rates (*SZNP237*, g/yr) and cumulative releases (*SZNP237C*, g) over the time interval [0, 20,000 yr] for the movement of dissolved ^{237}Np across a subsurface plane at the location of the RMEI resulting from a seismically induced fractional damaged area of 10^{-6} (32.6 m^2) at 200 yr to all CDSP WPs in the repository are summarized in Figure K7.5-3.

Movement of Dissolved ^{239}Pu: *SZPU239* and *SZPU239C*. The uncertainty and sensitivity analyses for the time-dependent release rates (*SZPU239*, g/yr) and cumulative releases (*SZPU239C*, g) over the time interval [0, 20,000 yr] for the movement of dissolved ^{239}Pu across

a subsurface plane at the location of the RMEI resulting from a seismically induced fractional damaged area of 10^{-6} (32.6 m^2) at 200 yr to all CDSP WPs in the repository are summarized in Figure K7.5-4.

Movement of Dissolved ^{99}Tc: *SZTC99* and *SZTC99C*. The uncertainty and sensitivity analyses for the time-dependent release rates (*SZTC99*, g/yr) and cumulative releases (*SZTC99C*, g) over the time interval [0, 20,000 yr] for the movement of dissolved ^{99}Tc across a subsurface plane at the location of the RMEI resulting from a seismically induced fractional damaged area of 10^{-6} (32.6 m^2) at 200 yr to all CDSP WPs in the repository are summarized in Figure K7.5-5.

K7.6 Seismic Ground Motion Scenario Classes: Dose to Reasonably Maximally Exposed Individual over the Time Interval [0, 20,000 yr]

For completeness, this section presents summaries of the uncertainty and sensitivity analyses for dose to the RMEI over the time interval [0, 20,000 yr] for a seismically induced fractional damaged area of 10^{-6} (32.6 m^2) at 200 yr to all CDSP WPs in the repository without discussion.

Dose to RMEI from ^{239}Pu Irreversibly Attached to Slow (i.e., Ic) Colloids: *DOIC239*. The uncertainty and sensitivity analyses for dose to the RMEI (*DOIC239*, mrem/yr) over the time interval [0, 20,000 yr] for the movement of ^{239}Pu irreversibly attached to slow (i.e., Ic) colloids across a subsurface plane at the location of the RMEI resulting from a seismically induced fractional damaged area of 10^{-6} (32.6 m^2) at 200 yr to all CDSP WPs in the repository are summarized in Figure K7.6-1.

Dose to RMEI from ^{239}Pu Irreversibly Attached to Fast (i.e., Ic) Colloids: *DOIF239*. The uncertainty and sensitivity analyses for dose to the RMEI (*DOIF239*, mrem/yr) over the time interval [0, 20,000 yr] for the movement of ^{239}Pu irreversibly attached to fast (i.e., Ic) colloids across a subsurface plane at the location of the RMEI resulting from a seismically induced fractional damaged area of 10^{-6} (32.6 m^2) at 200 yr to all CDSP WPs in the repository are summarized in Figure K7.6-2.

Dose to RMEI from Dissolved ^{237}Np: *DONP237*. The uncertainty and sensitivity analyses for dose to the RMEI (*DONP237*, mrem/yr) over the time interval [0, 20,000 yr] for the movement of dissolved ^{237}Np across a subsurface plane at the location of the RMEI resulting from a seismically induced fractional damaged area of 10^{-6} (32.6 m^2) at 200 yr to all CDSP WPs in the repository are summarized in Figure K7.6-3.

Dose to RMEI from Dissolved ^{239}Pu: *DOPU239*. The uncertainty and sensitivity analyses for dose to the RMEI (*DOPU239*, mrem/yr) over the time interval [0, 20,000 yr] for the movement of dissolved ^{239}Pu across a subsurface plane at the location of the RMEI resulting from a seismically induced fractional damaged area of 10^{-6} (32.6 m^2) at 200 yr to all CDSP WPs in the repository are summarized in Figure K7.6-4.

Dose to RMEI from Dissolved ^{99}Tc: *DOTC99*. The uncertainty and sensitivity analyses for dose to the RMEI (*DOTC99*, mrem/yr) over the time interval [0, 20,000 yr] for the movement of dissolved ^{99}Tc across a subsurface plane at the location of the RMEI resulting from a seismically induced fractional damaged area of 10^{-6} (32.6 m^2) at 200 yr to all CDSP WPs in the repository are summarized in Figure K7.6-5.

K7.7 Seismic Ground Motion Scenario Classes: Expected Dose to Reasonably Maximally Exposed Individual

This section presents analysis results for expected dose to the RMEI resulting from seismic ground motion over the time intervals [0, 20,000 yr] and [0, 1,000,000 yr].

K7.7.1 Seismic Ground Motion Scenario Classes: Expected Dose (*EXPDOSE*) to Reasonably Maximally Exposed Individual over the Time Interval [0, 20,000 yr]

The uncertainty and sensitivity analyses for expected dose to the RMEI (*EXPDOSE*, mrem/yr) over the time interval [0, 20,000 yr] resulting from seismic ground motion events are summarized in Figures K7.7.1-1 and K7.7.1-2. After the earliest arrival of released radionuclides at the location of the RMEI, *EXPDOSE* increases monotonically with time (Figure K7.7-1a,b). At 10,000 yr, the value for *EXPDOSE* falls between 10^{-4} and 1 mrem/yr for most sample elements, with a few sample elements having values for *EXPDOSE* between 1 and 10 mrem/yr. Due to the use of the quadrature-based methods rather than Monte Carlo methods to evaluate expected dose to the RMEI over the time interval [0, 20,000 yr] (see Equations J8.3-8 and J8.3-13), the expected dose results in Figure 7.7.1-1a,b are relatively smooth.

The PRCCs in Figure K7.7.1-1c indicate that the uncertainty in *EXPDOSE* is dominated by residual stress threshold *SCCTHRP* (as sampled, *SCCTHRP* is a percent of a base value of 351 MPa and is related to the stress corrosion cracking threshold, *SCCTHR*, by *SCCTHRP* = (*SCCTHR* × 100)/(351 MPa)). The value for *EXPDOSE* decreases as *SCCTHRP* increases. This effect results because increasing *SCCTHRP* increases the stress required toinitiate stress corrosion cracking and thus decreases the probability that a given seismic ground motion event will cause WP damage.

In addition to *SCCTHRP*, smaller effects are indicated for *SZGWSPDM* (groundwater specific discharge multiplier*;* as sampled, *SZGWSPDM* is actually the logarithm of the indicated multiplier), *SZFIPOVO* (flowing interval porosity in the volcanic unit of the SZ), *INFIL* (infiltration level), *DSNFMASS* (scale factor used to characterize uncertainty in the radionuclide content of DSNF contained in CDSP WPs), and *WDCRCDEN* (scale factor to convert area on a WP experiencing stress corrosion cracking to a resultant diffusive area) (Figure K7.7.1-1c). The variables *SZGWSPDM*, *DSNFMASS* and *WDCRCDEN* have positive effects on *EXPDOSE*, with these effects resulting because (i) increasing *SZGWSPDM* increases water flow in the SZ, (ii) increasing *DSNFMASS* increases the amount of ^{99}Tc in CDSP WPs and hence the dose from ^{99}Tc that results from the failure of these WPs, and (iii) increasing *WDCRCDEN* increases the diffusive area on damaged WPs for a given seismic ground motion event. The variables *SZFIPOVO* and *INFIL* have effects prior to 5000 and 10,000 yr, respectively, but no indicated effects after these times. The negative effect for *SZFIPOVO* results from slowing water flow in the SZ and thus delaying the initial arrival of radionuclides at the location of the RMEI. In

contrast, the positive effect for *INFIL* results from accelerating the initial arrival of radionuclides at the location of the RMEI; specifically, increased values for *INFIL* result (i) in cooler conditions in the EBS, which contributes to earlier radionuclide releases and also (ii) in more water flux in the EBS and UZ, which contributes to more rapid radionuclide movement. Owing to the nature of the integration process that defines *EXPDOSE*, the indicated effects associated with *SZFIPOVO* and *INFIL* decrease and then disappear with increasing time.

More detailed sensitivity analyses for *EXPDOSE* are provided by the regression analyses in Figure K7.7.1-2a. The dominant effect of *SCCTHRP* on the uncertainty in *EXPDOSE* is indicated by R^2 values of 0.81, 0.86 and 0.87 for the regressions containing only *SCCTHRP* at 3,000, 5,000 and 10,000 yr. After *SCCTHRP*, the regressions select a large number of variables that have small effects on *EXPDOSE*. For example, the regression at 3000 yr then selects *SZGWSPDM*, *INFIL* and *MICTC99* (dose conversion factor for ^{99}Tc for modern interglacial climate, (rem/yr)/(pCi/L)) and produces a model with an R^2 value of 0.87; the regression at 5,000 yr then selects *MICTC99*, *DSNFMASS* and *MICC14* (dose conversion factor for ^{14}C for modern interglacial climate, (rem/yr)/(pCi/L)) and produces a model with an R^2 value of 0.90; and the regression at 10,000 yr then selects *MICTC99*, *DSNFMASS* and *HLWDRACD* (rate term for dissolution of HLW glass in CDSP WPs under low pH conditions, g/m^2/d) and produces a model with an R^2 value of 0.91. After the first four variables, the regressions at 3000, 5000 and 10,000 yr select an additional 12, 12 and 11 variables, respectively, and produce final models with R^2 values of 0.92, 0.94 and 0.95. Thus, the uncertainty in *EXPDOSE* is dominated by *SCCTHRP*, with small contributions to this uncertainty by many additional variables.

The doses that are integrated to obtain *EXPDOSE* arise primarily from ^{99}Tc (Figure 8.2-12(a), Figure J8.3-8). The importance of ^{99}Tc to *EXPDOSE* is also evident in the regression results at 10,000 yr (Figure K7.7.1-2a). Specifically, the three variables selected immediately after *SCCTHRP* (i.e., *MICTC99*, *DSNFMASS* and *HLWDRACD*) are variables that affect the dose received from ^{99}Tc. Specifically, increasing *MICTC99* increases the dose received from a fixed concentration of ^{99}Tc in groundwater; increasing *DSNFMASS* increases the mass of ^{99}Tc present to be released from the CDSP WPs; and increasing *HLWDRACD* increases the rate at which ^{99}Tc is released from the waste form.

The dominant effect of *SCCTHRP* on the uncertainty in *EXPDOSE* can be seen in the scatterplot in Figure K7.7.1-2b. The much smaller effects associated with *MICTC99* and *DSNFMASS* can be seen in the scatterplots in Figure K7.7.1-2c,d.

It is important to recognize that the results in Figures K7.7.1-1 and K7.7.1-2 reflect the sensitivity of *EXPDOSE* to the parameters that are treated as being uncertain in the TSPA-LA Model. Some important parameters and model inputs are not treated as being uncertain, but are instead represented by conservative, fixed values or by assumptions. The sensitivity of *EXPDOSE* to these parameters can be discussed qualitatively but can not be quantified. For example, the results in Figures K7.7.1-1 and K7.7.1-2 were generated with a fixed value for the seismic hazard curve, estimated as the mean of a distribution of possible seismic hazard curves. This mean seismic hazard curve underlies the probabilistic weightings of the seismic events that give rise to *EXPDOSE* through an integration process (Section 6.1.2.4). Significant uncertainty is associated with the definition of the mean seismic hazard curve (SNL 2007 [DIRS 176828],

Section 6.4.1). If the uncertainty associated with the seismic hazard curve was incorporated into the analysis, it is likely that this uncertainty would have a significant effect on the uncertainty associated with *EXPDOSE*. Including this uncertainty in the TSPA-LA Model would likely improve the estimated repository performance, because the mean seismic hazard curve typically lies above the 80th percentile of the distribution of seismic hazard curves. Including the uncertainty in the seismic hazard curve would reduce the frequency of damaging seismic events in most realizations, which would reduce releases from the repository and improve repository performance. Thus, the use of the mean seismic hazard curve results in conservative estimates of repository performance.

K7.7.2 Seismic Ground Motion Scenario Classes: Expected Dose (*EXPDOSE*) to Reasonably Maximally Exposed Individual over the Time Interval [0, 1,000,000 yr]

The uncertainty and sensitivity analyses for expected dose to the RMEI (*EXPDOSE*, mrem/yr) over the time interval [0, 1,000,000 yr] resulting from seismic ground motion are summarized in Figures K7.7.2-1 and K7.7.2-2.

The time-dependent values for *EXPDOSE* for the 1,000,000 yr period in Figure K7.7.2-1a,b are much choppier than the values for the 20,000 yr time period in Figure K7.7.1-1a,b. This difference results from the numerical procedures used over 20,000 yr and 1,000,000 yr, respectively, to evaluate the integrals that define *EXPDOSE*. Because the effects of the seismic ground motion events are relatively well behaved for the 20,000 yr time period, it is possible to use a quadrature procedure to evaluate *EXPDOSE* for this time period. This results in the relatively smooth time-dependent values for *EXPDOSE* in Figure K7.7.1-1a,b. In contrast, the effects of seismic ground motion events are much more complex for the 1,000,000 yr time period. As a result of this complexity, it is not possible to use a quadrature procedure to evaluate the defining integral for *EXPDOSE* over this longer time period. Instead, it was necessary to use a sampling-based (i.e., Monte Carlo) integration procedure to evaluate the defining integral for *EXPDOSE*. Specifically, 30 1,000,000 yr futures involving seismic ground motion events were randomly sampled for each LHS element and then the 30 time-dependent dose results associated with these futures were vertically averaged at each point in time to produce the estimated time-dependent value for *EXPDOSE* for each sample element. Because individual seismic ground motion events are discrete occurrences that initiate radionuclide releases that ultimately lead to doses to the RMEI, the time dependent doses associated with individual futures and their vertical averages to produce expected doses for individual LHS elements tend to be choppy. In addition, the progression of nominal processes and the occurrence of resultant DS and WP failures contribute to the complexity of the 1,000,000 yr dose calculations. The individual curves in Figure K7.7.2-1a,b would eventually converge to smooth curves if a sufficiently large number of futures was sampled for each LHS element, or if an appropriate kernel smoother was used on the time-dependent results for each LHS element. However, despite the lack of smoothness in the results presented in Figure 7.7.2-1a,b, the distribution of expected annual doses (*EXPDOSE*) is shown to be statistically stable (Section 7.3.1) by means of a replicated sampling procedure (Section J4.10). In addition, confidence intervals are computed which show that the mean annual dose is estimated with sufficient accuracy (Section 7.3.1).

Most values for *EXPDOSE* Figure K7.7.2-1a,b are less than 10 mrem/yr, with a few values between 10 and 100 mrem/yr. The largest values for *EXPDOSE* in Figure K7.7.2-1a,b are associated with peaks that derive form single seismic ground motion events. These peaks would go away if the sampling-based approximations to the integrals defining *EXPDOSE* were more fully converged.

Although the results in Figure K7.7.2-1a,b are choppy, insights can be gained from a careful examination. In particular, Figure K7.7.2-1b is more informative that Figure K7.7.2-1a because the time-dependent values for *EXPDOSE* for individual LHS elements are more distinct. Overall, there is a tendency for *EXPDOSE* to decrease up to about 200,000 yr, with this decrease resulting from the decay of ^{239}Pu and possibly other radionuclides. In this time period, the values of *EXPDOSE* derive from the occurrence of seismic ground motion events as the failure of WPs from nominal processes does not begin until about 200,000 yr. The dominance of seismic ground motion events is indicated by the importance of the residual stress threshold *SCCTHRP* (as sampled, *SCCTHRP* is a percent of a base value of 351 MPa and is related to the stress corrosion cracking threshold, *SCCTHR*, by *SCCTHRP* = (*SCCTHR* × 100)/(351 MPa)); specifically, the PRCCs in Figure K7.7.2-1c indicate that *SCCTHRP* dominates the uncertainty in *EXPDOSE* out to approximately 200,000 yr. This result is also indicated by the regression for *EXPDOSE* at 50,000 yr in Figure K7.7.2-2a, where *SCCTHRP* is the first variable selected in the analysis with an R^2 value of 0.71.

Between 200,000 and 300,000 yr, there is a jump in the values for *EXPDOSE* (Figure K7.7.2-1a,b). This increase in *EXPDOSE* (Figure K7.7.2-1a,b) occurs between 200,000 and 300,000 yr because of the conservative manner in which the interaction between corrosion processes and seismic events was implemented. As explained in Appendix P, Section P.3, the increase in *EXPDOSE* occurs when corrosion failures occur before seismic damage to CSNF WPs and before failure of the DS. The implementation results in a dramatic increase in the probability of seismic damage to CSNF WPs between 200,000 and 300,000 years for a minority of realizations, as is evident in Figure 8.1-5(b). Consistent with this, the PRCCs in Figure K7.7.2-1c indicate that the uncertainty in *EXPDOSE* becomes dominated by *WDGCA22* (temperature dependence coefficient associated with the general corrosion rate for alloy 22, K). Specifically, *WDGCA22* corresponds to a coefficient used to alter the general corrosion rate for alloy 22 as function of temperature, with the alloy 22 corrosion rate decreasing as *WDGCA22* increases. As indicated in Figures K4.2-2e,f and K4.5-1c, *WDGCA22* is the dominant variable with respect to the uncertainty associated with the failure of WPs from nominal processes. After 400,000 yr, the values for *EXPDOSE* tend to increase and beyond 700,000 years are somewhat smoother than at earlier times (Figure K7.7.2-1a,b). This smoothness results from an increasing dominance of nominal corrosion processes in the values for *EXPDOSE*.

In addition to *SCCTHRP* and *WDGCA22*, the PRCCs in Figure K7.7.2-1c indicate effects for several additional variables. However, the effects are small and the PRCCs are very choppy as a result of the choppiness in the values for *EXPDOSE*. Smoother results for *EXPDOSE* would result in smoother values for the PRCCs in Figure K7.7.2-1c.

More detailed sensitivity analyses for *EXPDOSE* are provided by the regression analyses in Figure K7.7.2-2a. Specifically, *SCCTHRP* is the dominant contributor to the uncertainty in *EXPDOSE* at 50,000 yr; *SCCTHRP* is the dominant contributor to the uncertainty in *EXPDOSE*

at 200,000 yr with a contribution from *WDGCA22*; and *WDGCA22* is the dominant contributor to the uncertainty in *EXPDOSE* at 500,000 yr with a contribution from *SCCTHRP*. The individual regressions then add several additional variables that have small effects on *EXPDOSE*. The final regression models 50,000, 200,000 and 500,000 yr have R^2 values of 0.79, 0.56 and 0.71, which are not particularly high. These values are probably due in part to the choppiness of the values for *EXPDOSE* (Figure K7.7.2-1a,b) and in part to the large number of processes that affect *EXPDOSE* for the 1,000,000 yr seismic ground motion calculation. .

For perspective, the scatterplots in Figure K7.7.2-2b,c,d show the effects of *WDGCA22*, *SCCTHRP* and *WDNSCC* (stress corrosion cracking growth rate exponent) at 500,000 yr. The negative effects of *WDGCA22* and *SCCTHRP* can be easily seen in the scatterplots in Figure K7.7.2-2b,c. The negative effect for *WDNSCC* is more subtle but still discernable in the scatterplot in Figure K7.7.2-2d.

As previously indicated in conjunction with Figures K7.7.1-1 and K7.7.1-2 for the 20,000 yr time period, it is important to recognize that the results in Figures K7.7.2-1 and K7.7.2-2 reflect the sensitivity of *EXPDOSE* for the 1,000,000 yr time period to those parameters that are treated as being uncertain in the TSPA-LA Model. Some important parameters and model inputs are not treated as being uncertain, but are instead represented by conservative, fixed values or by assumptions. The sensitivity of *EXPDOSE* to these parameters can be discussed qualitatively but can not be quantified. In particular, significant uncertainty is associated with the definition of the seismic hazard curve that underlies the occurrence of seismic events and the effects of seismic events. If the uncertainty associated with the seismic hazard curve was incorporated into the analysis, it is likely that this uncertainty would have a significant effect on the uncertainty associated with *EXPDOSE*.

K7.8 Seismic Fault Displacement Scenario Classes: Expected Dose (*EXPDOSE*) to Reasonably Maximally Exposed Individual

This section presents analysis results for expected dose to the RMEI resulting from seismic fault displacement over the time intervals [0, 20,000 yr] and [0, 1,000,000 yr].

K7.8.1 Seismic Fault Displacement Scenario Classes: Expected Dose (*EXPDOSE*) to Reasonably Maximally Exposed Individual over the Time Interval [0, 20,000 yr]

The uncertainty and sensitivity analyses for expected dose to the RMEI (*EXPDOSE*, mrem/yr) over the time interval [0, 20,000 yr] resulting from seismic fault displacement are summarized in Figures K7.8.1-1 and K7.8.1-2. After the earliest arrival time for released radionuclides at the location of the RMEI, *EXPDOSE* increases monotonically with time (Figure K7.8.1-1a,b). At 10,000 yr, the value for *EXPDOSE* falls between 10^{-4} and 10^{-2} mrem/yr for most sample elements, with two sample elements having values for *EXPDOSE* between 10^{-2} and 10^{-1} mrem/yr.

The PRCCs in Figure K7.8.1-1c indicate that the uncertainty in *EXPDOSE* is affected by the following variables: *SZGWSPDM* (groundwater specific discharge multiplier*;* as sampled, *SZGWSPDM* is actually the logarithm of the indicated multiplier), *SZFIPOVO* (flowing interval porosity in the volcanic unit of the SZ), *INFIL* (infiltration level), *SEEPUNC* (pointer variable

used to determine local seepage rates), *MICTC99* (dose conversion factor for ^{99}Tc for modern interglacial climate, (rem/yr)/(pCi/L)), and *SEEPPRM* (mean fracture permeability in lithophysal rock units, m^2**;** as sampled, *SEEPPRM* is actually the logarithm of the indicated permeability). The variables *SZGWSPDM*, *INFIL*, *SEEPUNC* and *MICTC99* have positive effects on *EXPDOSE*. Specifically, increasing *SZGWSPDM* increase water flow in the SZ; increasing *INFIL* increases water flow in the EBS and UZ; increasing *SEEPUNC* increases water flow in the EBS; and increasing *MICTC99* increases the received dose for a given exposure to ^{99}Tc. The variables *SZFIPOVO* and *SEEPPRM* have negative effects on *EXPDOSE*. The negative effect of *SZFIPOVO* takes place at early times because increasing *SZFIPOVO* tends to delay the time at which released radionuclides first reach the RMEI; the nature of the integration process that produces *EXPDOSE* reduces the importance of *SZFIPOVO* with increasing time. The negative effect of *SEEPPRM* results from increasing water flow around the EBS and hence reducing water flow through the EBS.

More detailed sensitivity analyses for *EXPDOSE* are provided by the regression analyses in Figure K7.8.1-2a at 3000, 5000 and 10,000 yr. The three regression analyses are similar and indicate that a large number of variables have small effects on *EXPDOSE*. However, no single variable dominates the uncertainty in *EXPDOSE*. For example, the first variables selected in the three regressions in Figure K7.8.1-2a have R^2 values of only 0.16, 0.16 and 0.21. The final regression models contain 14, 15 and 15 variables, respectively, and have R^2 values of 0.74, 0.75 and 0.67. The relatively low R^2 values probably results from the complex interaction of a large number of variables in determining the uncertainty in *EXPDOSE*.

For perspective, scatterplots are given in Figure K7.8.1-2b,c,d for the first three variables selected in the regression analysis for *EXPDOSE* at 10,000 yr in Figure K7.8.1-2a. Specifically, these variables are *MICTC99*, *SZGWSPDM* and *DTDRHUNC* (pointer variable for collapsed drift rubble thermal conductivity). The previously discussed positive effects associated with *MICTC99* and *SZGWSPDM* can be seen in the scatterplots in Figure K7.8.1-2b,c. A positive effect for *DTDRHUNC* can be seen in the scatterplot in Figure K7.8.1-2d. A value of 2 for *DTDRHUNC* corresponds to selecting a high thermal conductivity for the rubble surrounding packages affected by fault displacement. Higher values of thermal conductivity lead to more rapid cooling of the affected WPs (SNL 2007 [DIRS 181383], Figure 6.3-87[a]) and consequently to earlier occurrence of seepage, or earlier return of seepage if seepage had occurred prior to the fault displacement event. In Figure K7.8.1-2, results are shown following a seismic fault displacement at 200 years. In this case, the higher values of thermal conductivity lead to earlier occurrence of seepage, which leads to somewhat higher expected dose at 10,000 years, but the effect is relatively minor.

It is important to recognize that the results in Figures K7.8.1-1 and K7.8.1-2 reflect the sensitivity of *EXPDOSE* for the 20,000 yr time period to those parameters that are treated as being uncertain in the TSPA-LA Model. Some important parameters and model inputs are not treated was being uncertain, but are instead represented by conservative, fixed values or by assumptions. The sensitivity of *EXPDOSE* to these parameters can be discussed qualitatively but can not be quantified. In particular, the results in Figures K7.8.1-1 and K7.8.1-2 were generated without consideration of the uncertainty in the rate of occurrence of seismic fault displacement events. The rates of occurrence of seismic fault displacement events represent mean rates of

occurrence of various fault displacements, and these mean rates underlie the probabilistic weightings of the events that give rise to *EXPDOSE* through an integration process (Section 6.1.2.4). Significant uncertainty is associated with the definition of these rates of occurrence (SNL 2007 [DIRS 176828], Section 6.11.5). If the uncertainty associated with the rates of occurrence of seismic fault displacement events was incorporated into the analysis, this uncertainty would likely be a major contributor to the uncertainty associated with *EXPDOSE*. However, because seismic fault displacement events are not a major contributor to total expected dose when all sources of potential dose to the RMEI are considered (Figure 8.1-3), the use the mean rates yields an adequate estimate of *EXPDOSE* without adding unnecessary complexity to the calculation of *EXPDOSE*.

K7.8.2 Seismic Fault Displacement Scenario Classes: Expected Dose (*EXPDOSE*) to Reasonably Maximally Exposed Individual over the Time Interval [0, 1,000,000 yr]

The uncertainty and sensitivity analyses for expected dose to the RMEI (*EXPDOSE*, mrem/yr) over the time interval [0, 1,000,000 yr] resulting from seismic fault displacement are summarized in Figures K7.8.2-1 and K7.8.2-2. Many sample elements show a rise and then a decrease in *EXPDOSE* over the time interval [0, 200,000 yr] followed by a monotonic increase in *EXPDOSE* after 200,000 yr (Figure K7.8.2-1a,b). The rise and fall in *EXPDOSE* over the time interval [0, 200,000 yr] results from the decay of ^{239}Pu, which is an important contributor to dose but has a half-life of 24,100 yr. As a result, the contribution of ^{239}Pu to dose is initially high but decreases with time; by 200,000 yr, the ^{239}Pu inventory has been reduced by a factor of approximately $(1/2)^8$. The monotonic increase in *EXPDOSE* after 200,000 yr results from the inclusion of the effects of the increasing number of possible prior events with increasing time. As a reminder, *EXPDOSE* at a specific time is not the dose from a single prior event but rather is the expected dose from all possible prior events. Overall, the maximum value for *EXPDOSE* falls between 10^{-4} and 10^{-1} mrem/yr for most sample elements and has maximum values between 10^{-1} and 10^{0} mrem/yr for a few sample elements (Figure K7.8.2-1a).

The sensitivity analyses indicate that the two most important variables with respect to the uncertainty in *EXPDOSE* are *SZGWSPDM* (groundwater specific discharge multiplier*;* as sampled, *SZGWSPDM* is actually the logarithm of the indicated multiplier) and *INFIL* (infiltration level) (Figures K7.8.2-1c and K7.8.2-2a). Together, *SZGWSPDM* and *INFIL* result in regression models for *EXPDOSE* with R^2 values of 0.40, 0.31 and 0.31 at 50,000, 200,000 and 500,000 yr, respectively (Figure K7.8.2-2a). Thus, *SZGWSPDM* and *INFIL* are important contributors to the uncertainty in *EXPDOSE* but do not dominate this uncertainty. Rather, the regression analyses indicate that the uncertainty in *EXPDOSE* arises from the cumulative effects of a large number of individual variables. After *SZGWSPDM* and *INFIL*, all three regressions then select *WPFLUX* (WP flux splitting factor) and *EP1LOWPU* (scale factor used to incorporate uncertainty into plutonium solubility under low ionic strength conditions; as sampled, *EP1LOWPU* is actually the logarithm of the indicated scale factor). The positive effects associated with *WPFLUX* and *EP1LOWPU* result because increasing *WPFLUX* increases the fraction of seepage water falling on a WP that actually enters the WP and increasing *EP1LOWPU* increases the solubility of plutonium and thus the amount of dissolved plutonium (e.g., ^{239}Pu or ^{242}Pu) that is available for movement out of the EBS. The inclusion of *WPFLUX*

and *EP1LOWPU* results in regression models with four variables and R^2 values of 0.49, 0.45 and 0.45. The individual regression analyses in Figure K7.8.2-2a then continue, with each selecting a total of 16 variables and producing final models with R^2 values of 0.69, 0.68 and 0.69. The relatively low R^2 values result from the interacting effects of a large number of uncertain analysis inputs.

For perspective, scatterplots showing the effects of *INFIL*, *SZGWSPDM* and *EP1LOWPU* on *EXPDOSE* at 500,000 yr are given in Figure K7.8.2-2b,c,d. The positive effects of *INFIL*, *SZGWSPDM* and *EP1LOWPU* on *EXPDOSE* can be seen in these plots.

It is important to recognize that the results in Figures K7.8.2-1 and K7.8.2-2 reflect the sensitivity of *EXPDOSE* for the 20,000 yr time period to the parameters that are treated as being uncertain in the TSPA-LA Model. Some important parameters and model inputs are not treated as being uncertain, but are instead represented by conservative, fixed values or by assumptions. The sensitivity of *EXPDOSE* to these parameters can be discussed qualitatively but can not be quantified. For example, the results in Figures K7.8.2-1 and K7.8.2-2 were generated without consideration of the uncertainty in the rates of occurrence of seismic fault displacement events. The rates of occurrence of seismic fault displacement events represent mean rates of occurrence of various fault displacements, and these mean rates underlie the probabilistic weightings of the events that give rise to *EXPDOSE* through an integration process (Section 6.1.2.4). Significant uncertainty is associated with the definition of these rates of occurrence (SNL 2007 [DIRS 176828], Section 6.11.5). If the uncertainty associated with the rates of occurrence of seismic fault displacement events was incorporated into the analysis, this uncertainty would likely be a major contributor to the uncertainty associated with *EXPDOSE*. However, because seismic fault displacement events are not a major contributor to total expected dose when all sources of potential dose to the RMEI are considered (Figure 8.1-3), the use the mean rates yields an adequate estimate of *EXPDOSE* without adding unnecessary complexity to the calculation of *EXPDOSE*.

K8 ALL SCENARIO CLASSES: EXPECTED DOSE (*EXPDOSE*) TO REASONABLY MAXIMALLY EXPOSED INDIVIDUAL

This section presents analysis results for expected dose to the RMEI resulting from all scenario classes over the time intervals [0, 20,000 yr] and [0, 1,000,000 yr].

K8.1 All Scenario Classes: Expected Dose (*EXPDOSE*) to Reasonably Maximally Exposed Individual over the Time Interval [0, 20,000 yr]

The uncertainty and sensitivity analyses for expected dose to the RMEI (*EXPDOSE*, mrem/yr) over the time interval [0, 20,000 yr] resulting from all scenario classes are summarized in Figures K8.1-1 and K8.1-2. Initial transport to the location of the RMEI takes up to 2000 yr; after the earliest possible arrival time for released radionuclides at the location of the RMEI, *EXPDOSE* increases monotonically with time (Figure K8.1-1a,b). At 10,000 yr, the value for *EXPDOSE* falls between 10^{-3} and 3 mrem/yr. As indicated by Figure 8.1-3(a), the expected dose to the RMEI from all scenario classes is predominantly determined by the expected dose to the RMEI resulting from seismic ground motion and from igneous intrusion. However, for some sample elements, minor effects from early WP failures can be observed in Figure K8.1-1b, where

the initiation of transport from CNSF WPs after 9,000 yr produces spikes in the expected dose. In turn, these spikes result in minor variability in the PRCCs (Figure K8.1-1c).

The PRCCs in Figure K8.1-1c indicate that the three most important variables with respect to the uncertainty in *EXPDOSE* are *SCCTHRP* (residual stress threshold; as sampled, *SCCTHRP* is a percent of a base value of 351 MPa and is related to the stress corrosion cracking threshold, *SCCTHR*, by *SCCTHRP* = (*SCCTHR* × 100)/(351 MPa)), *IGRATE* (rate of occurrence of igneous intrusive events, yr^{-1}), and *SZGWSPDM* (groundwater specific discharge multiplier*;* as sampled, *SZGWSPDM* is actually the logarithm of the indicated multiplier). The negative effect associated with *SCCTHRP* results because increasing *SCCTHRP* results in WPs being more resistant to seismic ground motion damage; the positive effect associated with *IGRATE* results because increasing *IGRATE* increases the probability of occurrence for igneous events; and the positive effect associated with *SZGWSPDM* results because increasing *SZGWSPDM* increases water flow in the SZ.

After *SCCTHRP*, *IGRATE* and *SZGWSPDM*, smaller effects are indicated for *SZFIPOVO* (flowing interval porosity in the volcanic unit of the SZ), *INFIL* (infiltration level), and *HLWGRNDS* (specific surface area for rind on HLW glass) (Figure K8.1-1c). The negative effect associated with *SZFIPOVO* at early times results from initially slowing the movement of radioactive species in the SZ, and the positive effect associated with *INFIL* results from its role in both speeding the cooling of the repository and increasing water flow in the EBS and UZ. The small negative effect indicated for *HLWGRNDS* results because increasing HLW specific surface area increases the effective saturation of the rind on the HLW glass, which reduces the concentration of those radionuclides without saturation limits (such as ^{99}Tc), which in turn reduces the gradient for diffusion out of the waste form cell and thus reduces the rate of release and the consequent dose.

More detailed sensitivity analyses for *EXPDOSE* are provided by the regression analyses and associated scatterplots in Figure K8.1-2. Overall, the dominant variable with respect to the uncertainty in *EXPDOSE* is *SCCTHRP*. Specifically, the regressions containing only *SCCTHRP* have R^2 values of 0.55, 0.66 and 0.69 at 3000, 5000 and 10,000 yr, respectively (Figure K8.1-2a). After *SCCTHRP*, the next variable selected in all regressions is *IGRATE*, with the inclusion of *IGRATE* raising the cumulative R^2 values to 0.62, 0.73 and 0.73. Thus, the effect of *IGRATE* on *EXPDOSE* is not as great as the effect of *SCCTHRP*. In consistency with the analysis with PRCCs, *SZGWSPDM* is then the third or fourth variable selected in the three regressions analyses. The negative effect associated with *SCCTHRP* and the positive effects associated with *IGRATE* and *SZGWSPDM* can be seen in the scatterplots in Figure K8.1-2a,b,c. After *SCCTHRP*, *IGRATE* and *SZGWSPDM*, The regressions select a number of additional variables that have small effects on *EXPDOSE*. The final regression models have R^2 values of 0.80, 0.84 and 0.83, which indicates that they are reasonably successful in accounting for the uncertainty in *EXPDOSE*. However, as is always the case, some of the variables selected at the ends of individual regression analyses that have very small effects on cumulative R^2 values may be spurious.

It is important to recognize that the results in Figures K8.1-1 and K8.1-2 reflect the sensitivity of *EXPDOSE* for the 20,000 yr time period to those parameters that are treated as being uncertain in

the TSPA-LA Model. Where parameters and model inputs are not treated as being uncertain, but are instead represented by conservative, fixed values or by assumptions, the sensitivity of *EXPDOSE* to these parameters can be discussed qualitatively but can not be quantified. For example, significant uncertainty is associated with the definition of the seismic hazard curve that underlies the occurrence of seismic events and the effects of seismic events. If the uncertainty associated with the seismic hazard curve was incorporated into the analysis, it is likely that this uncertainty would have an effect on the uncertainty associated with *EXPDOSE*.

K8.2 All Scenario Classes: Expected Dose (*EXPDOSE*) to Reasonably Maximally Exposed Individual over the Time Interval [0, 1,000,000 yr]

The uncertainty and sensitivity analyses for expected dose to the RMEI (*EXPDOSE*, mrem/yr) over the time interval [0, 1,000,000 yr] resulting from all scenario classes are summarized in Figures K8.2-1 and K8.2-2. As indicated by Figure 8.1-3(b), the expected dose to the RMEI from all scenario classes is predominantly determined by the expected dose to the RMEI resulting from seismic ground motion and from igneous intrusion.

The time-dependent values for *EXPDOSE* appear somewhat choppy as a result of the sampling-based calculation of the combined doses that result from nominal processes and seismic ground motion events (Figure K7.7.2-1). Smoother results could be obtained by using a larger sample of aleatory futures for seismic ground motion events or possibly a more sophisticated integration procedure for the incorporation of such events. However, because the distribution of *EXPDOSE* has been shown to be statistically stable (Section 7.3.1.3), improved convergence or use of a better integration procedure would produce smoother estimates of expected dose, but would not produce results that differ statistically from those shown in Figure K8.2-1. Overall, most sample elements result in values for *EXPDOSE* in a range from 10^{-2} to 30 mrem/yr, with a few sample elements resulting in values for *EXPDOSE* between 30 and 100 mrem/yr. These sample elements with high values for *EXPDOSE* result from an unbounded range for the longitudinal dispersivity parameter (*LDISP* in Table K3-1) or from conservatism in the extent of seismic damage to WPs that have been breached by general corrosion processes. The sample element in which *EXPDOSE* approaches 100 mrem/yr involves an extreme value for the longitudinal dispersivity parameter (*LDISP*) that consequently produces unrealistically rapid transport of ^{226}Ra as described in Appendix P, Section P15. Other realizations in which *EXPDOSE* spikes above 30 mrem/yr result from the conservative manner in which WPs with corrosion failures are affected by seismic events (see Appendix P, Section P3, for details).

The PRCCs in Figure K8.2-1c indicate that the three most important variables with respect to the uncertainty in *EXPDOSE* are *IGRATE* (rate of occurrence of igneous intrusive events, yr^{-1}), *SZGWSPDM* (groundwater specific discharge multiplier*;* as sampled, *SZGWSPDM* is actually the logarithm of the indicated multiplier), and *WDGCA22* (temperature dependence coefficient associated with the general corrosion rate for alloy 22, K). The positive effect associated with *IGRATE* results because increasing *IGRATE* increases the probability of occurrence for seismic events; the positive effect associated with *SZGWSPDM* results because increasing *SZGWSPDM* increases water flow in the SZ; and the negative effect associated with *WDGCA22* results from its role in slowing the rate of general corrosion of alloy 22, which in turn delays and reduces WP failures due to both seismic ground motion events and general corrosion.

Smaller effects are indicated for *SZFIPOVO* (flowing interval porosity in the volcanic unit of the SZ), *EP1LOWPU* (scale factor used to incorporate uncertainty into plutonium solubility under low ionic strength conditions; as sampled, *EP1LOWPU* is actually the logarithm of the indicated scale factor), and *KDCSCOL* (distribution coefficient for reversible sorption of cesium on uranophane colloids, mL/g). The positive relationship between these variables and *EXPDOSE* at about 100,000 years indicates that the uncertainty in these variables contributes to some degree to uncertainty in *EXPDOSE*. However, in general the PRCCs for these variables do not indicate any meaningful relationship after about 100,000 years.

As previously indicated in conjunction with Figures K8.1-1 and K8.1-2 for the 20,000 yr time period, it is important to recognize that the results in Figures K8.2-1 and K8.2-2 reflect the sensitivity of *EXPDOSE* for the 1,000,000 yr time period to those parameters that are treated as being uncertain in the TSPA-LA Model. Some important parameters and model inputs are not treated as being uncertain, but are instead represented by conservative, fixed values or by assumptions. In particular, if the uncertainty associated with the seismic hazard curve was incorporated into the analysis, it is likely that this uncertainty would have an effect on the uncertainty associated with *EXPDOSE*.

K9 SUMMARY

This appendix documents results of uncertainty and sensitivity analyses for the TSPA-LA. Sensitivity analyses identify the contribution of uncertain model inputs to the uncertainty in model output. The analyses reported in this Appendix identify the dominant sources of uncertainty in total expected dose to the RMEI. For each scenario class, the analyses also investigate the sources of uncertainty in expected dose to the RMEI and in the movement of several key radionuclides (i.e., ^{239}Pu, both dissolved and sorbed to colloids, ^{237}Np, and ^{99}Tc). These radionuclides were chosen to illustrate a range of radionuclide behavior, including colloid-facilitated transport. In addition, for some of the scenario classes, the analyses investigate uncertainty in other process model results, such as the time of DS failure and the chemical environment in the drifts.

Table K9-1 summarizes sensitivity analysis results for total expected dose and expected dose by scenario class by listing the key uncertain inputs identified by the analysis. The key uncertain inputs in Table K9-1 are listed in decreasing order of importance, with the first listed input having the most effect on the output quantity. The key uncertain inputs are identified on the basis of sensitivity analysis results at roughly the time at which the mean of the output variable achieves its maximum value.

Generally, the uncertain inputs that predominantly determine uncertainty in expected dose for each scenario class are those inputs that describe the occurrence and extent of failure of EBS components. For the seismic ground motion scenario class, the key uncertain input is *SCCTHRP* (residual stress threshold; as sampled, *SCCTHRP* is a percent of a base value of 351 MPa and is related to the stress corrosion cracking threshold, *SCCTHR*, by *SCCTHRP* = (*SCCTHR* × 100)/(351 MPa)), which essentially determines the probability of damage to CDSP or CSNF WPs for each seismic event. For the igneous intrusive scenario class, the key uncertain input is *IGRATE* (rate of occurrence of igneous intrusive events, yr^{-1}). For the nominal scenario class the key uncertain input is *WDGCA22* (temperature dependence coefficient associated with

general corrosion rate for alloy 22, K), which essentially determines the uncertainty in the time and extent of general corrosion failures (both by stress-corrosion cracking and by patches). For the early failure scenario classes key uncertain inputs are *PROBWPEF* (probability that a randomly selected WP will experience an early failure) and *PROBDSEF* (probability that a randomly selected DS will experience an early failure). For the igneous eruptive scenario class the key uncertain input is *IGERATE* (rate of occurrence of igneous eruptive events, yr^{-1}). For the seismic fault displacement scenario class, no single input emerged as predominant. Rather, the analysis identified several uncertain inputs with moderately monotonic effect on the expected dose for the scenario class.

The sensitivity analysis confirms that uncertain inputs are propagated through the TSPA-LA Model and that the effects of uncertainty in these inputs are consistent with physical principles. The confirmation is demonstrated through causal explanations of the relationships between input and output variables. For example, where the analysis indicates a positive correlation between the input and output variables, the causal explanation illustrates the reasons why a positive correlation should be observed.

The final sensitivity analysis also identified a relatively small number of implementation errors present in the version of the TSPA-LA Model (v5.000) that was subject to analysis. These errors, along with others identified by check and review activities, are documented in Appendix P along with impact assessments investigating the effect of each error on the TSPA-LA Model v5.000 results. Although the errors do not significantly affect the output from the TSPA-LA Model, the errors influence the selection of uncertain input variables correlated to uncertainty in the transport of plutonium sorbed to certain colloids. As a consequence, the affected results were removed from the final version of Appendix K.

Table K3-1. High-Level Summary of Epistemically Uncertain Variables (i.e., elements of **e**) Considered in the TSPA-LA (Sensitivity Analysis Name)

NOTE: * indicates variable not considered in sensitivity analysis due to correlations.

ALPHAL. van Genuchten capillary strength parameter in lithophysal rock units (Pa). *Distribution:* Triangular. *Range:* -105 to 105. *Mean/Median/Mode:* 0. *TSPA-LA Name:* Alpha_Uncert_Lith_a. *Location in TSPA-LA:* Sections 6.3.3.1.2 and 6.3.3.1.3; Tables 6.3.3-1, 6.3.3-3 and 6.3.5-4.
ALPHANL*. van Genuchten capillary strength parameter in nonlithophysal rock units (Pa). *Distribution:* Triangular. *Range:* -105 to 105. *Mean/Median/Mode:* 0. *TSPA-LA Name:* Alpha_Uncert_NonLith_a*. *Location in TSPA-LA:* Section 6.3.3.1.2; Tables 6.3.3-1, 6.3.3-3 and 6.3.5-4.
ASHDENS. Tephra settled density (kg/m^3). *Distribution:* Truncated normal *Range:* 300 to 1,500. *Mean:* 1,000. *Standard Deviation:* 100. *TSPA-LA Name:* Ash_Density_a. *Location in TSPA-LA:* Table 6.5-5.
BCKALPHA. Natural background levels of alpha emitters in groundwater (pCi/L). *Distribution:* Truncated normal. *Range:* 0 to 0.71. *Mean/Median/Mode:* 0.5. *TSPA-LA Name:* Background_Alpha_a. *Location in TSPA-LA:* Sections 6.3.10.2, 6.3.11.2, and Table 6.3.10-6.
BCKRA226. Natural background levels of combined ^{226}Ra and ^{228}Ra in groundwater (pCi/L). *Distribution:* Truncated normal. *Range:* 0 to 0.71. *Mean/Median/Mode:* 0.5. *TSPA-LA Name:* Background_Ra226_Ra228_a. *Location in TSPA-LA:* Sections 6.3.10.2, 6.3.11.2, and Table 6.3.10-6.
BETA. Column diffusion constant (dimensionless). *Distribution:* Uniform. *Range:* 0.01 to 0.5. *TSPA-LA Name:* Beta_Dist_a. *Location in TSPA-LA:* Table 6.5-4.
BTILLAGE. Depth of soil within which radionuclides contribute to dose from external exposure (m). *Distribution:* Uniform. *Range:* 0.05 to 0.3. *TSPA-LA Name:* b_Tillage_a. *Location in TSPA-LA:* Table 6.5-5.
CFLUXOUT. Ratio of radionuclide mass associated with colloids (reversible and irreversible) to radionuclide mass associated with colloids and dissolved radionuclide mass (dimensionless). *Distribution:* Uniform. *Range:* 0.9 to 0.99. *TSPA-LA Name:* Target_Flux_Out_Ratio_a. *Location in TSPA-LA:* Table 6.3.7-65.
COLFEOCS. FeOx colloid concentration when carbon steel is corroding (mg/L). *Distribution:* Truncated log normal. *Range:* 0.3 to 30. *Mean:* 3.69. *Standard Deviation:* 2.79. *TSPA-LA Name:* Conc_Col_FeOx_CS_Sampled_a. *Location in TSPA-LA:* Table 6.3.7-65.
COLFEOSS. FeOx colloid concentration when degraded stainless steel is present, but no degrading carbon steel is present (mg/L). *Distribution:* Piecewise uniform. *Range:* 1.00E-03 to 3.00E+01. *TSPA-LA Name:* Conc_Col_FeOx_SS_Sampled_a. *Location in TSPA-LA:* Table 6.3.7-65.
COLGW. Concentration of groundwater colloids when colloids are stable (mg/L). *Distribution:* Piecewise uniform. *Range:* 0.001 to 200. *Median:* 0.1. *TSPA-LA Name:* Conc_Col_Gw_Sampled_a. *Location in TSPA-LA:* Table 6.3.7-66.
COLU. Concentration of uranophane colloids when colloids are stable (mg/L). *Distribution:* Piecewise uniform. *Range:* 0.001 to 200. *Median:* 0.1. *TSPA-LA Name:* Conc_Col_U_Sampled_a. *Location in TSPA-LA:* Table 6.3.7-64.
CORRATSS. Stainless steel corrosion rate (μm/yr). *Distribution:* Truncated log normal. *Range:* 0.01 to 0.51. *Mean/Median/Mode:* 0.267. *Standard Deviation:* 0.209. *TSPA-LA Name:* SS_Corrosion_Rate_a. *Location in TSPA-LA:* Tables 6.3.8-1 and 6.3.8-4.
CPUCOLCS. Concentration of irreversibly attached plutonium on CSNF colloids when colloids are stable (mol/L). *Distribution:* Piecewise uniform. *Range:* 1.00E-10 to 5.00E-06. *Median:* 1.00E-07. *TSPA-LA Name:* CPu_Col_CSNF_Sampled_a. *Location in TSPA-LA:* Section 6.3.7.6.2 and Table 6.3.7-63.
CPUCOLWF. Concentration of irreversibly attached plutonium on glass/waste form colloids when colloids are stable (mol/L). *Distribution:* Uniform. *Range:* 1.00E-11 to 1.00E-08. *TSPA-LA Name:* CPu_Col_Wf_Embed_Sampled_a. *Location in TSPA-LA:* Section 6.3.7.6.2 and Table 6.3.7-62.
CPUPERCS. Concentration of irreversibly attached plutonium per concentration of CSNF colloids ((mol/L)/(mg/L)). *Distribution:* Uniform. *Range:* 5.00E-07 to 1.00E-06. *TSPA-LA Name:* CPu_Per_CSNF_Embed_Col_a. *Location in TSPA-LA:* Section 6.3.7.6.2 and Table 6.3.7-63.
CPUPERWF. Concentration of irreversibly attached plutonium per concentration of waste form colloids ((mol/L)/(mg/L)). *Distribution:* Triangular. *Range:* 5.00E-09 to 2.5E-08. *Most Likely:* 2.00E-08. *TSPA-LA Name:* CPu_Per_WF_Embed_Col_a. *Location in TSPA-LA:* Section 6.3.7.6.2 and Table 6.3.7-62.

Table K3-1. High-Level Summary of Epistemically Uncertain Variables (i.e., elements of **e**) Considered in the TSPA-LA (Sensitivity Analysis Name) (Continued)

NOTE: * indicates variable not considered in sensitivity analysis due to correlations.

CR2O3SA. Specific surface area of Cr_2O_3 (m^2/g). *Distribution:* Uniform. *Range:* 1 to 20. *TSPA-LA Name:* Cr2O3_SA_a. *Location in TSPA-LA:* Table 6.3.8-4 and S_{CP} in Equation 6.3.8-19.
CRITSLOP. Critical gradient for tephra mobilization from hillslopes (dimensionless). *Distribution:* Uniform. *Range:* 0.21 to 0.47. *TSPA-LA Name:* Critical_Slope_a. *Location in TSPA-LA:* Table 6.5-5.
CSCORRAT. Carbon steel corrosion rate (μm/yr). *Distribution:* Truncated log normal. *Range:* 25 to 135. *Mean:* 78.5. *Standard Deviation:* 25. *TSPA-LA Name:* CS_Corrosion_Rate_a. *Location in TSPA-LA:* Tables 6.3.8-1 and 6.3.8-4.
CSNFMASS. Scale factor used to characterize uncertainty in radionuclide content of CSNF (dimensionless). *Distribution:* Uniform. *Range:* 0.85 to 1.4. *TSPA-LA Name:* CSNF_Mass_Uncert_a. *Location in TSPA-LA:* Sections 6.3.7.1.2, 6.3.7.1.3, and Table 6.3.7-7.
CSRINDDN. Grain density of CSNF rind (kg/m^3). *Distribution:* Uniform. *Range:* 5600 to 11500. *TSPA-LA Name:* Density_CSNF_Rind_a. *Location in TSPA-LA:* Table 6.3.8-4.
CSRINDPO. Porosity in CSNF rind (dimensionless). *Distribution:* Uniform. *Range:* 0.05 to 0.3. *TSPA-LA Name:* Rind_Porosity_CSNF_a. *Location in TSPA-LA:* Section 6.3.8.2.1 and Table 6.3.8-6.
CSRINDSA. Specific surface area of CSNF degradation rind (m^2/g). *Distribution:* Uniform. *Range:* 0.5 to 60. *TSPA-LA Name:* CSNF_Rind_SA_a. *Location in TSPA-LA:* Tables 6.3.8-2 and 6.3.8-4.
CSSPECSA. Logarithm of the effective specific surface area (m^2/mg) of the representative CSNF waste form (dimensionless). *Distribution:* Triangular. *Range:* -7.3 to -5.4. *Most Likely:* -6.7. *TSPA-LA Name:* Log_Specific_SA_CSNF_a. *Location in TSPA-LA:* Sections 6.3.7.4.1.2 and 6.3.7.4.1.3; Tables 6.3.7-30 and 6.3.7-31; and Equations 6.3.7-5 and 6.3.7-6.
CSWFA0AC. Correlated regression coefficient a0 in the abstracted rate model under acidic conditions (dimensionless). *Distribution:* Normal. *Mean/Median/Mode:* 0. *Standard Deviation:* 1. *TSPA-LA Name:* CSNF_WF_Uncert_a0_Acid_a. *Location in TSPA-LA:* Section 6.3.7.4.1.2; Equation 6.3.7-6.
CSWFA0AK. Correlated coefficient a0 in the abstracted rate model under alkaline conditions (dimensionless). *Distribution:* Normal. *Mean/Median/Mode:* 0. *Standard Deviation:* 1. *TSPA-LA Name:* CSNF_WF_Uncert_a0_Alk_a. *Location in TSPA-LA:* Section 6.3.7.4.1.2; Equation 6.3.7-5.
CSWFA1AK. Correlated coefficient a1 in the abstracted rate model under alkaline conditions (dimensionless). *Distribution:* Normal. *Mean/Median/Mode:* 0. *Standard Deviation:* 1. *TSPA-LA Name:* CSNF_WF_Uncert_a1_Alk_a. *Location in TSPA-LA:* Section 6.3.7.4.1.2 and Equation 6.3.7-5.
CSWFA2AK. Correlated coefficient a2 in the abstracted rate model under alkaline conditions (dimensionless). *Distribution:* Normal. *Mean/Median/Mode:* 0. *Standard Deviation:* 1. *TSPA-LA Name:* CSNF_WF_Uncert_a2_Alk_a. *Location in TSPA-LA:* Section 6.3.7.4.1.2 and Equation 6.3.7-5.
CSWFA3AK. Correlated coefficient a3 in the abstracted rate model under alkaline conditions (dimensionless). *Distribution:* Normal. *Mean/Median/Mode:* 0. *Standard Deviation:* 1. *TSPA-LA Name:* CSNF_WF_Uncert_a3_Alk_a. *Location in TSPA-LA:* Section 6.3.7.4.1.2 and Equation 6.3.7-5.
CSWFA4AC. Correlated coefficient a4 in the abstracted rate model under acid conditions (dimensionless). *Distribution:* Normal. *Mean/Median/Mode:* 0. *Standard Deviation:* 1. *TSPA-LA Name:* CSNF_WF_Uncert_a4_Acid_a. *Location in TSPA-LA :* Section 6.3.7.4.1.2 and Equation 6.3.7-6.
DASHAVG. Mass median ash particle diameter (cm). *Distribution:* Log triangular. *Range:* 0.001 to 0.1. *Mode:* 0.01. *TSPA-LA Name:* Dash_mean_a. *Location in TSPA-LA:* Table 6.5-4.
DASHSIG. Ash particle diameter standard deviation (log (cm)). *Distribution:* Uniform. *Range:* 0.301 to 0.903. *TSPA-LA Name:* Dash_sigma_a. *Location in TSPA-LA:* Table 6.5-4.
DCHANL. Diffusivity of radionuclides in channels of the Fortymile Wash fan (RMEI location) (cm^2/yr). *Distribution:* Uniform. *Range:* 0.035 to 0.266. *Mean:* 0.1505. *TSPA-LA Name:* D_Channels_a. *Location in TSPA-LA:* Table 6.5-5.
DDIVIDE. Diffusivity of radionuclides in divides of the Fortymile Wash fan (RMEI location) (cm^2/yr). *Distribution:* Uniform. *Range:* 0.001 to 0.095. *Mean* 0.048. *TSPA-LA Name:* D_Divides_a. *Location in TSPA-LA:* Table 6.5-5.

Table K3-1. High-Level Summary of Epistemically Uncertain Variables (i.e., elements of **e**) Considered in the TSPA-LA (Sensitivity Analysis Name) (Continued)

NOTE: * indicates variable not considered in sensitivity analysis due to correlations.

DELPPCO2. Selector variable for partial pressure of CO_2 (dimensionless). *Distribution:* Uniform. *Range:* -1 to 1. *TSPA-LA Name:* PCE_Delta_pCO2_a. *Location in TSPA-LA:* Sections 6.3.4.2 and 6.3.5.2.3; Table 6.3.5-4.
DIAMCOLL. Diameter of colloid particle (nm). *Distribution:* Uniform. *Range:* 50 to 300. *TSPA-LA Name:* Diameter_Colloid_a. *Location in TSPA-LA:* Tables 6.3.8-1 and 6.3.8-4.
DIFPATHL. Diffusive path length from waste package outer corrosion barrier to mid-point of invert (m). *Distribution:* Uniform. *Range:* 0.3 to 1.24. *TSPA-LA Name:* Diff_Path_Length_Invert_Top_a. *Location in TSPA-LA:* Section 6.3.8.2.4; Table 6.3.8-4.
DRAINDNS. Average drainage density for the Fortymile Wash drainage basin (1/km). *Distribution:* Uniform. *Range:* 20 to 33. *TSPA-LA Name:* Drainage_Density_a. *Location in TSPA-LA:* Table 6.5-5.
DSFLUX. Drip shield flux splitting factor (dimensionless). *Distribution:* Uniform. *Range:* 0 to 0.85. *TSPA-LA Name:* DS_Flux_Uncertainty_a. *Location in TSPA-LA:* Tables 6.3.6-1, 6.3.6-2 and 6.3.8-4; Sections 6.3.6.2 and 6.3.6.4.1; Equation 6.3.6-5.
DSNFMASS. Scale factor used to characterize uncertainty in radionuclide content of DSNF (dimensionless). *Distribution:* Triangular. *Range:* 0.45 to 2.9. *Most Likely:* 0.62. *TSPA-LA Name:* DSNF_Mass_Uncert_a. *Location in TSPA-LA:* Sections 6.3.7.1.2 and 6.3.7.1.3; Table 6.3.7-7.
DTDRHUNC. Selector variable used to determine the collapsed drift rubble thermal conductivity (dimensionless). *Distribution:* Discrete. *Range:* 1 to 2. *TSPA-LA Name:* dt_dRh_uncertainty. *Location in TSPA-LA:* Section 6.6.2.2.
DWCDISP. Selector variable used to determine the axial dispersion modeling case (dimensionless). *Distribution:* Discrete. *Range:* 0 to 1. *TSPA-LA Name:* DWC_Dispersivity_Cond_a. *Location in TSPA-LA:* Section 6.3.3.2.2; Table 6.3.3-5.
DWCSTERA. Multiplier for the standard deviation on the slope coefficient for determining the probability of condensation from percolation rate (dimensionless). *Distribution:* Normal. *Mean/Median/Mode:* 0. *Standard Deviation:* 1. *TSPA-LA Name:* DWC_Std_Error_a_a. *Location in TSPA-LA:* Section 6.3.3.2.2; Tables 6.3.3-4 and 6.3.3-5.
DWCSTERB. Multiplier for the standard deviation on the y-intercept coefficient for determining the probability of condensation from percolation rate (dimensionless). *Distribution:* Normal. *Mean/Median/Mode:* 0. *Standard Deviation:* 1. *TSPA-LA Name:* DWC_Std_Error_b_a. *Location in TSPA-LA:* Section 6.3.3.2.2; Tables 6.3.3-4 and 6.3.3-5.
DWCSTERC. Multiplier for the standard deviation on the slope coefficient for determining condensation rate from percolation rate (dimensionless). *Distribution:* Normal. *Mean/Median/Mode:* 0. *Standard Deviation:* 1. *TSPA-LA Name:* DWC_Std_Error_c_a. *Location in TSPA-LA:* Section 6.3.3.2.2; Tables 6.3.3-4 and 6.3.3-5.
DWCSTERD. Multiplier for the standard deviation on the y-intercept coefficient for determining the condensation rate from percolation rate (dimensionless). *Distribution:* Normal. *Mean/Median/Mode:* 0. *Standard Deviation:* 1. *TSPA-LA Name:* DWC_Std_Error_d_a. *Location in TSPA-LA:* Section 6.3.3.2.2; Tables 6.3.3-4 and 6.3.3-5.
DWCVENT. Selector variable specifying whether the ventilated or unventilated drip shield DWC modeling case is performed (dimensionless). *Distribution:* Discrete. *Range:* 0, 1. *TSPA-LA Name:* DWC_Ventilated_Cond_a. *Location in TSPA-LA:* Sections 6.3.3.2.2 and 6.3.3.2.3; Table 6.3.3-5.
EBSDIFCF. Exponential term representing uncertainty in the invert diffusion coefficient (dimensionless). *Distribution:* Truncated normal. *Range:* -0.621 to 0.687. *Mean:* 0.033. *Standard Deviation:* 0.218. *TSPA-LA Name:* Invert_Diff_Coeff_Uncert_a. *Location in TSPA-LA:* Section 6.3.8.2.4; Table 6.3.8-4; Equation 6.3.8-24.
EP1HINP2*. Logarithm of the scale factor used to characterize uncertainty in Np_2O_5 solubility for ionic strength values between 1 and 3 molal (dimensionless). *Distribution:* Truncated normal. *Range:* -1.7 to 1.7. *Mean:* 0. *Standard Deviation:* 0.85. *TSPA-LA Name:* Np2O5_Eps_1_high_a*. *Location in TSPA-LA:* Sections 6.3.7.5.1 and 6.3.7.5.2; Table 6.3.7-42; Equation 6.3.7-13a.
EP1HINPO2*. Logarithm of the scale factor used to characterize uncertainty in NpO_2 solubility at an ionic strength between 1 and 3 molal (dimensionless). *Distribution:* Truncated normal. *Range:* -1.34 to 1.34. *Mean:* 0. *Standard Deviation:* 0.67. *TSPA-LA Name:* NpO2_Eps_1_high_a*. *Location in TSPA-LA:* Sections 6.3.7.5.1, 6.3.7.5.2 and 6.3.7.5.3; Table 6.3.7-43; Equation 6.3.7-13a.

Table K3-1. High-Level Summary of Epistemically Uncertain Variables (i.e., elements of **e**) Considered in the TSPA-LA (Sensitivity Analysis Name) (Continued)

NOTE: * indicates variable not considered in sensitivity analysis due to correlations.

EP1HINU*. Logarithm of the scale factor used to characterize uncertainty in uranium solubility under nominal or seismic conditions at an ionic strength between 1and 3 molal (dimensionless). *Distribution:* Truncated normal. *Range:* -1.2 to 1.2. *Mean:* 0. *Standard Deviation:* 0.6. *TSPA-LA Name:* U_Eps_1_high_Nominal_a*. *Location in TSPA-LA:* Section 6.3.7.5.1, 6.3.7.5.2 and 6.3.7.5.3; Table 6.3.7-54; Equation 6.3.7-13a.
EP1HIOU*. Logarithm of the scale factor used to characterize uncertainty in uranium solubility under conditions other than nominal and seismic at an ionic strength between 1and 3 molal (dimensionless). *Distribution:* Truncated normal. *Range:* -1.2 to 1.2. *Mean:* 0. *Standard Deviation:* 0.6. *TSPA-LA Name:* U_Eps_1_high_Other_a*. *Location in TSPA-LA:* Sections 6.3.7.5.1, 6.3.7.5.2 and 6.3.7.5.3; Table 6.3.7-58; Equation 6.3.7-13a.
EP1HIPU*. Logarithm of the scale factor used to characterize uncertainty in plutonium solubility for ionic strength between 1 and 3 molal (dimensionless). *Distribution:* Truncated normal. *Range:* -1.52 to 1.52. *Mean:* 0. *Standard Deviation:* 0.76. *TSPA-LA Name:* Pu_Eps_1_high_a*. *Location in TSPA-LA:* Sections 6.3.7.5.1, 6.3.7.5.2 and 6.3.7.5.3; Table 6.3.7-44; Equation 6.3.7-13a.
EP1HISN*. Logarithm of the scale factor used to characterize uncertainty in tin solubility for high ionic strength conditions (dimensionless). *Distribution:* Truncated normal. *Range:* -1.08 to 1.08. *Mean:* 0. *Standard Deviation:* 0.54. *TSPA-LA Name:* Sn_Eps_high_a*. *Location in TSPA-LA:* Sections 6.3.7.5.2 and 6.3.7.5.3; Table 6.3.7-47; Equation 6.3.7-13a.
EP1HITH*. Logarithm of the scale factor used to characterize uncertainty in thorium solubility at ionic strength between 1 and 3 molal (dimensionless). *Distribution:* Truncated normal. *Range:* -1.52 to 1.52. *Mean:* 0. *Standard Deviation:* 0.76. *TSPA-LA Name:* Th_Eps_1_high_a*. *Location in TSPA-LA:* Sections 6.3.7.5.1, 6.3.7.5.2 and 6.3.7.5.3; Table 6.3.7-46; Equation 6.3.7-13a.
EP1LOWAM. Logarithm of the scale factor used to characterize uncertainty in americium solubility at an ionic strength below 1 molal (dimensionless). *Distribution:* Truncated normal. *Range:* -2 to 2. *Mean:* 0. *Standard Deviation:* 1. *TSPA-LA Name:* Am_Eps_1_low_a. *Location in TSPA-LA:* Sections 6.3.7.5.1, 6.3.7.5.2 and 6.3.7.5.3; Table 6.3.7-41; Equation 6.3.7-13a.
EP1LOWNU. Logarithm of the scale factor used to characterize uncertainty in uranium solubility under nominal or seismic conditions at an ionic strength below 1 molal (dimensionless). *Distribution:* Truncated normal. *Range:* -1 to 1. *Mean/Median/Mode:* 0. *Standard Deviation:* 0.5. *TSPA-LA Name:* U_Eps_1_low_Nominal_a. *Location in TSPA-LA:* Section 6.3.7.5.1, 6.3.7.5.2 and 6.3.7.5.3; Table 6.3.7-54; Equation 6.3.7-13a.
EP1LOWOU. Logarithm of the scale factor used to characterize uncertainty in uranium solubility under conditions other than nominal and seismic at an ionic strength below 1 molal (dimensionless). *Distribution:* Truncated normal. *Range:* -1 to 1. *Mean/Median/Mode:* 0. *Standard Deviation:* 0.5. *TSPA-LA Name:* U_Eps_1_low_Other_a. *Location in TSPA-LA:* Sections 6.3.7.5.1, 6.3.7.5.2 and 6.3.7.5.3; Table 6.3.7-58; Equation 6.3.7-13a.
EP1LOWPU. Logarithm of the scale factor used to characterize uncertainty in plutonium solubility at an ionic strength below 1 molal (dimensionless). *Distribution:* Truncated normal. *Range:* -1.4 to 1.4. *Mean/Median/Mode:* 0. *Standard Deviation:* 0.7. *TSPA-LA Name:* Pu_Eps_1_low_a. *Location in TSPA-LA:* Sections 6.3.7.5.1, 6.3.7.5.2 and 6.3.7.5.3; Table 6.3.7-44; Equation 6.3.7-13a.
EP1LOWSN. Logarithm of the scale factor used to characterize uncertainty in tin solubility for low ionic strength conditions (dimensionless). *Distribution:* Truncated normal. *Range:* -0.9 to 0.9. *Mean/Median/Mode:* 0. *Standard Deviation:* 0.45. *TSPA-LA Name:* Sn_Eps_low_a. *Location in TSPA-LA:* Sections 6.3.7.5.2 and 6.3.7.5.3; Table 6.3.7-47; Equation 6.3.7-13a.
EP1LOWTH. Logarithm of the scale factor used to characterize uncertainty in thorium solubility at an ionic strength below 1 molal (dimensionless). *Distribution:* Truncated normal. *Range:* -1.4 to 1.4. *Mean:* 0. *Standard Deviation:* 0.7. *TSPA-LA Name:* Th_Eps_1_low_a. *Location in TSPA-LA:* Sections 6.3.7.5.1, 6.3.7.5.2 and 6.3.7.5.3; Table 6.3.7-46; Equation 6.3.7-13a.
EP1NP2O5. Logarithm of the scale factor used to characterize uncertainty in Np_2O_5 solubility at an ionic strength below 1 molal (dimensionless). *Distribution:* Truncated normal. *Range:* -1.6 to 1.6. *Mean:* 0. *Standard Deviation:* 0.8. *TSPA-LA Name:* Np2O5_Eps_1_low_a. *Location in TSPA-LA:* Sections 6.3.7.5.1 and 6.3.7.5.2; Table 6.3.7-42; Equation 6.3.7-13a.
EP1NPO2. Logarithm of the scale factor used to characterize uncertainty in NpO_2 solubility at an ionic strength below 1 molal (dimensionless). *Distribution:* Truncated normal. *Range:* -1.2 to 1.2. *Mean:* 0. *Standard Deviation:* 0.6. *TSPA-LA Name:* NpO2_Eps_1_low_a. *Location in TSPA-LA:* Sections 6.3.7.5.1, 6.3.7.5.2 and 6.3.7.5.3; Table 6.3.7-43; Equation 6.3.7-13a.

Table K3-1. High-Level Summary of Epistemically Uncertain Variables (i.e., elements of **e**) Considered in the TSPA-LA (Sensitivity Analysis Name) (Continued)

NOTE: * indicates variable not considered in sensitivity analysis due to correlations.

EP1PA. Logarithm of the scale factor used to characterize uncertainty in protactinium solubility (dimensionless). *Distribution:* Uniform. *Range:* -4.42 to -0.05. *TSPA-LA Name:* Pa_Eps_1_a. *Location in TSPA-LA:* Sections 6.3.7.5.2 and 6.3.7.5.3; Table 6.3.7-45; Equation 6.3.7-13b.
EP2BCDHU*. Term associated with uncertainty in uranium solubility (controlled by boldwoodite saturation) due to variations in fluoride concentration for CDSP waste packages when ionic strength is greater than or equal to 0.004 molal and for the invert below CDSP waste packages (mg/L). *Distribution:* Triangular. *Range:* 0 to 272.3. *Most Likely:* 0. *TSPA-LA Name:* U_Eps_2_Boltwoodite_CDSP_Hig_a*. *Location in TSPA-LA:* Sections 6.3.7.5.1, 6.3.7.5.2 and 6.3.7.5.3; Table 6.3.7-58; Equation 6.3.7-13a.
EP2BCSHU*. Term associated with uncertainty in uranium solubility (controlled by boldwoodite saturation) due to variations in fluoride concentration for CSNF waste packages when ionic strength is greater than or equal to 0.2 molal and for the invert below CSNF waste packages (mg/L). *Distribution:* Triangular. *Range:* 0 to 57.01. *Most Likely:* 0. *TSPA-LA Name:* U_Eps_2_Boltwoodite_CSNF_Hig_a*. *Location in TSPA-LA:* Sections 6.3.7.5.1, 6.3.7.5.2 and 6.3.7.5.3; Table 6.3.7-58; Equation 6.3.7-13a.
EP2BLOWU*. Term associated with uncertainty in uranium solubility (controlled by boldwoodite saturation) due to variations in fluoride concentration for CDSP waste packages Cell 1a, Cell 1b when ionic strength is less than 0.004 molal, and CSNF waste packages when ionic strength is less than 0.2 molal (mg/L). *Distribution:* Triangular. *Range:* 0 to 6.13. *Most Likely:* 0. *TSPA-LA Name:* U_Eps_2_Boltwoodite_Glass_Lo_a*. *Location in TSPA-LA:* Sections 6.3.7.5.1, 6.3.7.5.2 and 6.3.7.5.3; Table 6.3.7-58; Equation 6.3.7-13a.
EP2CDNP2*. Term associated with uncertainty in Np_2O_5 solubility due to variations in fluoride concentration for CDSP waste packages when ionic strength is greater than or equal to 0.004 molal and for the invert below CDSP waste packages (mg/L). *Distribution:* Triangular. *Range:* 0 to 853. *Most Likely:* 0. *TSPA-LA Name:* Np2O5_Eps_2_CDSP_High_a*. *Location in TSPA-LA:* Sections 6.3.7.5.1 and 6.3.7.5.2; Table 6.3.7-42; Equation 6.3.7-13a.
EP2CDNPO2*. Term associated with uncertainty in NpO_2 solubility due to variations in fluoride concentration for CDSP waste packages when ionic strength is greater than or equal to 0.004 molal and for the invert below CDSP waste packages (mg/L). *Distribution:* Triangular. *Range:* 0 to 1093.5. *Most Likely:* 0. *TSPA-LA Name:* NpO2_Eps_2_CDSP_High_a*. *Location in TSPA-LA:* Sections 6.3.7.5.1, 6.3.7.5.2 and 6.3.7.5.3; Table 6.3.7-43; Equation 6.3.7-13a.
EP2CDPA*. Term associated with uncertainty in protactinium solubility due to variations in fluoride concentration for CDSP waste packages when ionic strength is greater than or equal to 0.004 molal and for the invert below CDSP waste packages (mg/L). *Distribution:* Triangular. *Range:* 0 to 853. *Most Likely:* 0. *TSPA-LA Name:* Pa_Eps_2_CDSP_High_a*. *Location in TSPA-LA:* Sections 6.3.7.5.2 and 6.3.7.5.3; Table 6.3.7-45; Equation 6.3.7-13b.
EP2CDPU*. Term associated with uncertainty in plutonium solubility due to variations in fluoride concentration for CDSP waste packages when ionic strength is greater than or equal to 0.004 molal and for the invert below CDSP waste packages (mg/L). *Distribution:* Triangular. *Range:* 0 to 5460. *Most Likely:* 0. *TSPA-LA Name:* Pu_Eps_2_CDSP_High_a*. *Location in TSPA-LA:* Sections 6.3.7.5.1, 6.3.7.5.2 and 6.3.7.5.3; Table 6.3.7-44; Equation 6.3.7-13a.
EP2CDTH*. Term associated with uncertainty in thorium solubility due to variations in fluoride concentration for CDSP waste packages when ionic strength is greater than or equal to 0.004 molal and for the invert below CDSP waste packages (mg/L). *Distribution:* Triangular. *Range:* 0 to 23723.2. *Most Likely:* 0. *TSPA-LA Name:* Th_Eps_2_CDSP_High_a*. *Location in TSPA-LA:* Sections 6.3.7.5.1, 6.3.7.5.2 and 6.3.7.5.3; Table 6.3.7-46; Equation 6.3.7-13a.
EP2CSHNU*. Term associated with uncertainty in uranium solubility (under nominal or seismic conditions) due to variations in fluoride concentration for CSNF waste packages when ionic strength is greater than or equal to 0.2 molal and for the invert below CSNF waste packages (mg/L). *Distribution:* Triangular. *Range:* 0 to 1361. *Most Likely:* 0. *TSPA-LA Name:* U_Eps_2_CSNF_High_Nominal_a*. *Location in TSPA-LA:* Section 6.3.7.5.1, 6.3.7.5.2 and 6.3.7.5.3; Table 6.3.7-54; Equation 6.3.7-13a.
EP2CSLNU*. Term associated with uncertainty in uranium solubility (under nominal or seismic conditions) due to variations in fluoride concentration for CSNF waste packages when ionic strength is less than 0.2 molal and for the invert below CSNF waste packages (mg/L). *Distribution:* Triangular. *Range:* 0 to 78. *Most Likely:* 0. *TSPA-LA Name:* U_Eps_2_CSNF_Low_Nominal_a*. *Location in TSPA-LA:* Section 6.3.7.5.1, 6.3.7.5.2 and 6.3.7.5.3; Table 6.3.7-54; Equation 6.3.7-13a.

Table K3-1. High-Level Summary of Epistemically Uncertain Variables (i.e., elements of **e**) Considered in the TSPA-LA (Sensitivity Analysis Name) (Continued)

NOTE: * indicates variable not considered in sensitivity analysis due to correlations.

EP2CSNP2*. Term associated with uncertainty in Np_2O_5 solubility due to variations in fluoride concentration for CSNF waste packages when ionic strength is greater than or equal to 0.2 molal and for the invert below CSNF waste packages (mg/L). *Distribution:* Triangular. *Range:* 0 to 197. *Most Likely:* 0. *TSPA-LA Name:* Np2O5_Eps_2_CSNF_High_a*. *Location in TSPA-LA:* Sections 6.3.7.5.1 and 6.3.7.5.2; Table 6.3.7-42; Equation 6.3.7-13a.
EP2CSNPO2*. Term associated with uncertainty in NpO_2 solubility due to variations in fluoride concentration for CSNF waste packages when ionic strength is greater than or equal to 0.2 molal and for the invert below CSNF waste packages (mg/L). *Distribution:* Triangular. *Range:* 0 to 255.8. *Most Likely:* 0. *TSPA-LA Name:* NpO2_Eps_2_CSNF_High_a*. *Location in TSPA-LA:* Sections 6.3.7.5.1, 6.3.7.5.2 and 6.3.7.5.3; Table 6.3.7-43; Equation 6.3.7-13a.
EP2CSPA*. Term associated with uncertainty in protactinium solubility due to variations in fluoride concentration for CSNF waste packages when ionic strength is greater than or equal to 0.2 molal and for the invert below CSNF waste packages (mg/L). *Distribution:* Triangular. *Range:* 0 to 197. *Most Likely:* 0. *TSPA-LA Name:* Pa_Eps_2_CSNF_High_a*. *Location in TSPA-LA:* Sections 6.3.7.5.2 and 6.3.7.5.3; Table 6.3.7-45; Equation 6.3.7-13b.
EP2CSPU*. Term associated with uncertainty in plutonium solubility due to variations in fluoride concentration for CSNF waste packages when ionic strength is greater than or equal to 0.2 molal and for the invert below CSNF waste packages (mg/L). *Distribution:* Triangular. *Range:* 0 to 1374. *Most Likely:* 0. *TSPA-LA Name:* Pu_Eps_2_CSNF_High_a*. *Location in TSPA-LA:* Sections 6.3.7.5.1, 6.3.7.5.2 and 6.3.7.5.3; Table 6.3.7-44; Equation 6.3.7-13a.
EP2CSTH*. Term associated with uncertainty in thorium solubility due to variations in fluoride concentration for CSNF waste packages when ionic strength is greater than or equal to 0.2 molal and for the invert below CSNF waste packages (mg/L). *Distribution:* Triangular. *Range:* 0 to 7848.3. *Most Likely:* 0. *TSPA-LA Name:* Th_Eps_2_CSNF_High_a*. *Location in TSPA-LA:* Sections 6.3.7.5.1, 6.3.7.5.2 and 6.3.7.5.3; Table 6.3.7-46; Equation 6.3.7-13a.
EP2HIAM*. Logarithm of the scale factor used to characterize uncertainty in americium solubility at ionic strength values between 1 and 3 molal (dimensionless). *Distribution:* Truncated normal. *Range:* -2.08 to 2.08. *Mean:* 0. *Standard Deviation:* 1.04. *TSPA-LA Name:* Am_Eps_1_high_a*. *Location in TSPA-LA:* Sections 6.3.7.5.1, 6.3.7.5.2 and 6.3.7.5.3; Equation 6.3.7-13a; Table 6.3.7-41.
EP2HICAM. Term associated with uncertainty in americium solubility due to variations in fluoride concentration for CSNF waste packages when ionic strength is greater than or equal to 0.2 molal and for the invert below CSNF waste packages (mg/L). *Distribution:* Triangular. *Range:* 0 to 109.03. *Most Likely:* 0. *TSPA-LA Name:* Am_Eps_2_CSNF_High_a. *Location in TSPA-LA:* Sections 6.3.7.5.2 and 6.3.7.5.3; Table 6.3.7-41; Equation 6.3.7-13a.
EP2HICDAM*. Term associated with uncertainty in americium solubility due to variations in fluoride concentration for CDSP waste packages when ionic strength is greater than or equal to 0.004 molal and for the invert below CDSP waste packages (mg/L). *Distribution:* Triangular. *Range:* 0 to 688.6. *Most Likely:* 0. *TSPA-LA Name:* Am_Eps_2_CDSP_High_a*. *Location in TSPA-LA:* Sections 6.3.7.5.2 and 6.3.7.5.3; Table 6.3.7-41; Equation 6.3.7-13a.
EP2LONP2*. Term associated with uncertainty in Np_2O_5 solubility due to variations in fluoride concentration for CDSP waste packages Cell 1a, Cell 1b when ionic strength is less than 0.004 molal, and CSNF waste packages when ionic strength is less than 0.2 molal (mg/L). *Distribution:* Triangular. *Range:* 0 to 11. *Most Likely:* 0. *TSPA-LA Name:* Np2O5_Eps_2_Glass_Low_a*. *Location in TSPA-LA:* Sections 6.3.7.5.1 and 6.3.7.5.2; Table 6.3.7-42; Equation 6.3.7-13a.
EP2LONPO2*. Term associated with uncertainty in NpO_2 solubility due to variations in fluoride concentration for CDSP waste packages Cell 1a, Cell 1b when ionic strength is less than 0.004 molal, and CSNF waste packages when ionic strength is less than 0.2 molal (mg/L). *Distribution:* Triangular. *Range:* 0 to 14.1. *Most Likely:* 0. *TSPA-LA Name:* NpO2_Eps_2_Glass_Low_a*. *Location in TSPA-LA:* Sections 6.3.7.5.1, 6.3.7.5.2 and 6.3.7.5.3; Table 6.3.7-43; Equation 6.3.7-13a.

Table K3-1. High-Level Summary of Epistemically Uncertain Variables (i.e., elements of **e**) Considered in the TSPA-LA (Sensitivity Analysis Name) (Continued)

NOTE: * indicates variable not considered in sensitivity analysis due to correlations.

EP2LOPA*. Term associated with uncertainty in protactinium solubility due to variations in fluoride concentration for CDSP waste packages Cell 1a, Cell 1b when ionic strength is less than 0.004 molal, and CSNF waste packages when ionic strength is less than 0.2 molal (mg/L). *Distribution:* Triangular. *Range:* 0 to 11. *Most Likely:* 0. *TSPA-LA Name:* Pa_Eps_2_Glass_Low_a*. *Location in TSPA-LA:* Sections 6.3.7.5.2 and 6.3.7.5.3; Table 6.3.7-45; Equation 6.3.7-13b.
EP2LOWAM*. Term associated with uncertainty in americium solubility due to variations in fluoride concentration for CDSP waste packages Cell 1a, Cell 1b when ionic strength is less than 0.004 molal, and CSNF waste packages when ionic strength is less than 0.2 molal (mg/L). *Distribution:* Triangular. *Range:* 0 to 4.42. *Most Likely:* 0. *TSPA-LA Name:* Am_Eps_2_Glass_Low_a*. *Location in TSPA-LA:* Sections 6.3.7.5.2 and 6.3.7.5.3; Table 6.3.7-41; Equation 6.3.7-13a.
EP2LOWPU*. Term associated with uncertainty in plutonium solubility due to variations in fluoride concentration for CDSP waste packages Cell 1a, Cell 1b when ionic strength is less than 0.004 molal, and CSNF waste packages when ionic strength is less than 0.2 molal (mg/L). *Distribution:* Triangular. *Range:* 0 to 79. *Most Likely:* 0. *TSPA-LA Name:* Pu_Eps_2_Glass_Low_a*. *Location in TSPA-LA:* Sections 6.3.7.5.1, 6.3.7.5.2 and 6.3.7.5.3; Table 6.3.7-44; Equation 6.3.7-13a.
EP2LOWTH*. Term associated with uncertainty in thorium solubility due to variations in fluoride concentration for CDSP waste packages Cell 1a, Cell 1b when ionic strength is less than 0.004 molal, and CSNF waste packages when ionic strength is less than 0.2 molal (mg/L). *Distribution:* Triangular. *Range:* 0 to 626.2. *Most Likely:* 0. *TSPA-LA Name:* Th_Eps_2_Glass_Low_a*. *Location in TSPA-LA:* Sections 6.3.7.5.1, 6.3.7.5.2 and 6.3.7.5.3; Table 6.3.7-46; Equation 6.3.7-13a.
EP2SCDHU*. Term associated with uncertainty in uranium solubility (controlled by schoepite saturation) due to variations in fluoride concentration for CDSP waste packages when ionic strength is greater than or equal to 0.004 molal and for the invert below CDSP waste packages (mg/L). *Distribution:* Triangular. *Range:* 0 to 5385. *Most Likely:* 0. *TSPA-LA Name:* U_Eps_2_Schoepite_CDSP_High_a*. *Location in TSPA-LA:* Sections 6.3.7.5.1, 6.3.7.5.2 and 6.3.7.5.3; Table 6.3.7-58; Equation 6.3.7-13a.
EP2SCSHU*. Term associated with uncertainty in uranium solubility (controlled by schoepite saturation) due to variations in fluoride concentration for CSNF waste packages when ionic strength is greater than or equal to 0.2 molal and for the invert below CSNF waste packages (mg/L). *Distribution:* Triangular. *Range:* 0 to 1361. *Most Likely:* 0. *TSPA-LA Name:* U_Eps_2_Schoepite_CSNF_High_a*. *Location in TSPA-LA:* Sections 6.3.7.5.1, 6.3.7.5.2 and 6.3.7.5.3; Table 6.3.7-58; Equation 6.3.7-13a.
EP2SLOWU*. Term associated with uncertainty in uranium solubility (controlled by schoepite saturation) due to variations in fluoride concentration for CDSP waste packages Cell 1a, Cell 1b when ionic strength is less than 0.004 molal, and CSNF waste packages when ionic strength is less than 0.2 molal (mg/L). *Distribution:* Triangular. *Range:* 0 to 78. *Most Likely:* 0. *TSPA-LA Name:* U_Eps_2_Schoepite_Glass_Low_a*. *Location in TSPA-LA:* Sections 6.3.7.5.1, 6.3.7.5.2 and 6.3.7.5.3; Table 6.3.7-58; Equation 6.3.7-13a.
FHHISKCP. Frenkel Halsey Hill water vapor adsorption isotherm parameter, *k*, for corrosion products (dimensionless). *Distribution:* Uniform. *Range:* 1.048 to 1.370 (see additional information). *TSPA-LA Name:* FHH_Isotherm_k_CP_a. *Location in TSPA-LA:* Table 6.3.8-4.
FHHISKCS. Frenkel Halsey Hill water vapor adsorption isotherm parameter, *k*, for CSNF rind (dimensionless). *Distribution:* Uniform. *Range:* 1.606 to 8.215. *TSPA-LA Name:* FHH_Isotherm_k_CSNF_Rind_a. *Location in TSPA-LA:* Table 6.3.8-4.
FHHISSCP. Frenkel Halsey Hill water vapor adsorption isotherm parameter, *s*, for corrosion products (dimensionless). *Distribution:* Uniform. *Range:* 1.525 to 1.852 (see additional information). *TSPA-LA Name:* FHH_Isotherm_s_CP_a. *Location in TSPA-LA:* Table 6.3.8-4.
FHHISSCS. Frenkel Halsey Hill water vapor adsorption isotherm parameter, *s*, for CSNF rind (dimensionless). *Distribution:* Uniform. *Range:* 1.656 to 3.038. *TSPA-LA Name:* FHH_Isotherm_s_CSNF_Rind_a. *Location in TSPA-LA:* Table 6.3.8-4.
FRACCHNL. Fraction of the RMEI location subject to fluvial deposition (dimensionless). *Distribution:* Uniform. *Range:* 0.088 to 0.54. *TSPA-LA Name:* Fraction_Channel_a. *Location in TSPA-LA:* Table 6.5-5.
FWDRAT. Default forward rate constant for irreversible sorption of plutonium and americium ($m^3/m^2/yr$). *Distribution:* Log uniform. *Range:* 0.002 to 0.05. *TSPA-LA Name:* Default_Fwd_Rate_Const_a. *Location in TSPA-LA:* Table 6.3.7-65.

Table K3-1. High-Level Summary of Epistemically Uncertain Variables (i.e., elements of **e**) Considered in the TSPA-LA (Sensitivity Analysis Name) (Continued)

NOTE: * indicates variable not considered in sensitivity analysis due to correlations.

GOERELAB. Fraction of total iron oxide that is goethite (dimensionless). *Distribution:* Uniform. *Range:* 0.45 to 0.8. *TSPA-LA Name:* Relative_Abundance_Goethite_a. *Location in TSPA-LA:* Section 6.3.8.2.3; Table 6.3.8-4.
GOESA. Specific surface area of goethite (m^2/g). *Distribution:* Truncated log normal. *Range:* 14.7 to 110. *Mean:* 51.42. *Standard Deviation:* 30.09. *TSPA-LA Name:* Goethite_SA_a. *Location in TSPA-LA:* Table 6.3.8-4; S_{CP} in Equation 6.3.8-19.
GOESITED. Density of sorption sites on goethite (1/nm^2). *Distribution:* Discrete. *Range:* 1.02 to 8.59. *TSPA-LA Name:* Goethite_Site_Density_a. *Location in TSPA-LA:* Table 6.3.8-3.
GP1NO3. Ratio of Cl to NO_3 (Cl:N) in Group 1 pore waters (dimensionless). *Distribution:* Discrete. *Range:* 0.783 to 6.1213. *TSPA-LA Name:* PCE_Gp1_Cl_NO3_CDF_a. *Location in TSPA-LA:* Section 6.3.4.3.2.
GP2NO3. Ratio of Cl to NO_3 (Cl:N) in Group 2 pore waters (dimensionless). *Distribution:* Discrete. *Range:* 2.359 to 3.187. *TSPA-LA Name:* PCE_Gp2_Cl_NO3_CDF_a. *Location in TSPA-LA:* Section 6.3.4.3.2.
GP3NO3. Ratio of Cl to NO_3 (Cl:N) in Group 3 pore waters (dimensionless). *Distribution:* Discrete. *Range:* 9.7782 to 64.128. *TSPA-LA Name:* PCE_Gp3_Cl_NO3_CDF_a. *Location in TSPA-LA:* Section 6.3.4.3.2.
GP4NO3. Ratio of Cl to NO_3 (Cl:N) in Group 4 pore waters (dimensionless). *Distribution:* Discrete. *Range:* 4.4485 to 8.2119. *TSPA-LA Name:* PCE_Gp4_Cl_NO3_CDF_a. *Location in TSPA-LA:* Section 6.3.4.3.2.
HFOSA. Hydrous ferric oxide (HFO) surface area (m^2/g). *Distribution:* Truncated log normal. *Range:* 68 to 600. *Mean:* 275.6. *Standard Deviation:* 113.4. *TSPA-LA Name:* HFO_SA_a. *Location in TSPA-LA:* Table 6.3.8-4; S_{CP} in Equation 6.3.8-19.
HFOSITED. Sorption site density for hydrous ferric oxide (HFO) (1/nm^2). *Distribution:* Discrete. *Range:* 0.56 to 5.65. *TSPA-LA Name:* HFO_Site_Density_a. *Location in TSPA-LA:* Table 6.3.8-3.
HLWDRACD. Effective rate coefficient (affinity term) for the dissolution of HLW glass in CDSP waste packages under low pH conditions (g/(m^2d)). *Distribution:* Triangular. *Range:* 8.41E+03 to 1.15E+07. *Mode:* 8.41E+03. *TSPA-LA Name:* HLW_Diss_kE_Acidic_a. *Location in TSPA-LA:* Sections 6.3.7.4.3.2 and 6.3.7.4.3.3; Table 6.3.7-32; Equation 6.3.7-8.
HLWDRALK. Effective rate coefficient (affinity term) for the dissolution of HLW glass in CDSP waste packages under high pH conditions (g/(m^2d)). *Distribution:* Triangular. *Range:* 2.82E+01 to 3.47E+04. *Mode:* 2.82E+01. *TSPA-LA Name:* HLW_Diss_kE_Alkaline_a. *Location in TSPA-LA:* Sections 6.3.7.4.3.2 and 6.3.7.4.3.3; Table 6.3.7-32; Equation 6.3.7-8.
HLWGRNDS. Specific surface area of HLWG degradation rind (m^2/g). *Distribution:* Uniform. *Range:* 10 to 38. *TSPA-LA Name:* HLWG_Rind_SA_a. *Location in TSPA-LA:* Table 6.3.8-4.
HLWMASS. Scale factor used to characterize uncertainty in radionuclide content of HLW glass (dimensionless). *Distribution:* Triangular. *Range:* 0.7 to 1.5. *Most Likely:* 1. *TSPA-LA Name:* HLW_Mass_Uncert_a. *Location in TSPA-LA:* Sections 6.3.7.1.2 and 6.3.7.1.3; Table 6.3.7-7.
IGERATE. Frequency of occurrence of volcanic eruptive events (yr^{-1}). *Calculated by:* Igneous_Event_Prob_a x 0.083. *Range:* 0 to 6.44E-08. *TSPA-LA Name:* IGERATE. *Location in TSPA-LA:* Section 6.5.2.1.1; Appendix J; Equation J7.5-3.
IGRATE. Frequency of intersection of the repository footprint by a volcanic event (yr^{-1}). *Distribution:* Piecewise uniform. *Range:* 0 to 7.76E-07. *TSPA-LA Name:* Igneous_Event_Prob_a. *Location in TSPA-LA:* Table 6.5-2.
ILTAC227. Volcanic Biosphere Dose Conversion Factor (BDCF) component for long-term inhalation of ^{227}Ac in modern interglacial climate ((Sv/yr)/(Bq/kg)). *Distribution:* Discrete. *Range:* 1.53E-07 to 4.5E-06. *Mean:* 9.0E-07. *Standard Deviation:* 5.75E-07. *TSPA-LA Name:* DE_BDCF_Inh_LT_Ac227. *Location in TSPA-LA:* Sections 6.3.11.1 and 6.3.11.2; Equation 6.3.11-4.
ILTAM241. Volcanic Biosphere Dose Conversion Factor (BDCF) component for long-term inhalation of ^{241}Am in modern interglacial climate ((Sv/yr)/(Bq/kg)). *Distribution:* Discrete. *Range:* 8.45E-08 to 2.48E-06. *Mean:* 4.96E-07. *Standard Deviation:* 3.17E-07. *TSPA-LA Name:* DE_BDCF_Inh_LT_Am241. *Location in TSPA-LA:* Sections 6.3.11.1 and 6.3.11.2; Equation 6.3.11-4.
ILTAM243. Volcanic Biosphere Dose Conversion Factor (BDCF) component for long-term inhalation of ^{243}Am in modern interglacial climate ((Sv/yr)/(Bq/kg)). *Distribution:* Discrete. *Range:* 8.38E-08 to 2.46E-06. *Mean:* 4.93E-07. *Standard Deviation:* 3.15E-07. *TSPA-LA Name:* DE_BDCF_Inh_LT_Am243. *Location in TSPA-LA:* Sections 6.3.11.1 and 6.3.11.2; Equation 6.3.11-4.

Table K3-1. High-Level Summary of Epistemically Uncertain Variables (i.e., elements of **e**) Considered in the TSPA-LA (Sensitivity Analysis Name) (Continued)

NOTE: * indicates variable not considered in sensitivity analysis due to correlations.

ILTCS137. Volcanic Biosphere Dose Conversion Factor (BDCF) component for long-term inhalation of ^{137}Cs in modern interglacial climate ((Sv/yr)/(Bq/kg)). *Distribution:* Discrete. *Range:* 3.43E-11 to 1.01E-09. *Mean:* 2.02E-10. *Standard Deviation:* 1.29E-10. *TSPA-LA Name:* DE_BDCF_Inh_LT_Cs137. *Location in TSPA-LA:* Sections 6.3.11.1 and 6.3.11.2; Equation 6.3.11-4.
ILTI129. Volcanic Biosphere Dose Conversion Factor (BDCF) component for long-term inhalation of ^{129}I in modern interglacial climate ((Sv/yr)/(Bq/kg)). *Distribution:* Discrete. *Range:* 3.15E-11 to 9.23E-10. *Mean:* 1.85E-10. *Standard Deviation:* 1.18E-10. *TSPA-LA Name:* DE_BDCF_Inh_LT_I129. *Location in TSPA-LA:* Sections 6.3.11.1 and 6.3.11.2; Equation 6.3.11-4.
ILTNP237. Volcanic Biosphere Dose Conversion Factor (BDCF) component for long-term inhalation of ^{237}Np in modern interglacial climate ((Sv/yr)/(Bq/kg)). *Distribution:* Discrete. *Range:* 4.35E-08 to 1.28E-06. *Mean:* 2.56E-07. *Standard Deviation:* 1.63E-07. *TSPA-LA Name:* DE_BDCF_Inh_LT_Np237. *Location in TSPA-LA:* Sections 6.3.11.1 and 6.3.11.2; Equation 6.3.11-4.
ILTPA231. Volcanic Biosphere Dose Conversion Factor (BDCF) component for long-term inhalation of ^{231}Pa in modern interglacial climate ((Sv/yr)/(Bq/kg)). *Distribution:* Discrete. *Range:* 2.02E-07 to 5.92E-06. *Mean:* 1.18E-06. *Standard Deviation:* 7.56E-07. *TSPA-LA Name:* DE_BDCF_Inh_LT_Pa231. *Location in TSPA-LA:* Sections 6.3.11.1 and 6.3.11.2; Equation 6.3.11-4.
ILTPU238. Volcanic Biosphere Dose Conversion Factor (BDCF) component for long-term inhalation of ^{238}Pu in modern interglacial climate ((Sv/yr)/(Bq/kg)). *Distribution:* Discrete. *Range:* 9.46E-08 to 2.78E-06. *Mean:* 5.56E-07. *Standard Deviation:* 3.55E-07. *TSPA-LA Name:* DE_BDCF_Inh_LT_Pu238. *Location in TSPA-LA:* Sections 6.3.11.1 and 6.3.11.2; Equation 6.3.11-4.
ILTPU239. Volcanic Biosphere Dose Conversion Factor (BDCF) component for long-term inhalation of ^{239}Pu in modern interglacial climate ((Sv/yr)/(Bq/kg)). *Distribution:* Discrete. *Range:* 1.04E-07 to 3.06E-06. *Mean:* 6.12E-07. *Standard Deviation:* 3.91E-07. *TSPA-LA Name:* DE_BDCF_Inh_LT_Pu239. *Location in TSPA-LA:* Sections 6.3.11.1 and 6.3.11.2; Equation 6.3.11-4.
ILTPU240. Volcanic Biosphere Dose Conversion Factor (BDCF) component for long-term inhalation of ^{240}Pu in modern interglacial climate ((Sv/yr)/(Bq/kg)). *Distribution:* Discrete. *Range:* 1.04E-07 to 3.06E-06. *Mean:* 6.12E-07. *Standard Deviation:* 3.91E-07. *TSPA-LA Name:* DE_BDCF_Inh_LT_Pu240. *Location in TSPA-LA:* Sections 6.3.11.1 and 6.3.11.2; Equation 6.3.11-4.
ILTPU242. Volcanic Biosphere Dose Conversion Factor (BDCF) component for long-term inhalation of ^{242}Pu in modern interglacial climate ((Sv/yr)/(Bq/kg)). *Distribution:* Discrete. *Range:* 9.90E-08 to 2.91E-06. *Mean:* 5.82E-07. *Standard Deviation:* 3.72E-07. *TSPA-LA Name:* DE_BDCF_Inh_LT_Pu242. *Location in TSPA-LA:* Sections 6.3.11.1 and 6.3.11.2; Equation 6.3.11-4.
ILTRA226. Volcanic Biosphere Dose Conversion Factor (BDCF) component for long-term inhalation of ^{226}Ra and ^{210}Pb in modern interglacial climate ((Sv/yr)/(Bq/kg)). *Distribution:* Discrete. *Range:* 1.71E-08 to 5.03E-07. *Mean:* 1.01E-07. *Standard Deviation:* 6.43E-08. *TSPA-LA Name:* DE_BDCF_ILT_Ra226_Pb210. *Location in TSPA-LA:* Sections 6.3.11.1 and 6.3.11.2; Equation 6.3.11-4.
ILTRA228. Volcanic Biosphere Dose Conversion Factor (BDCF) component for long-term inhalation of ^{228}Ra in modern interglacial climate ((Sv/yr)/(Bq/kg)). *Distribution:* Discrete. *Range:* 1.40E-08 to 4.12E-07. *Mean:* 8.24E-08. *Standard Deviation:* 5.27E-08. *TSPA-LA Name:* DE_BDCF_Inh_LT_Ra228. *Location in TSPA-LA:* Sections 6.3.11.1 and 6.3.11.2; Equation 6.3.11-4.
ILTSN126. Volcanic Biosphere Dose Conversion Factor (BDCF) component for long-term inhalation of ^{126}Sn in modern interglacial climate ((Sv/yr)/(Bq/kg)). *Distribution:* Discrete. *Range:* 1.36E-10 to 4.00E-09. *Mean:* 8.0E-10. *Standard Deviation:* 5.11E-10. *TSPA-LA Name:* DE_BDCF_Inh_LT_Sn126. *Location in TSPA-LA:* Sections 6.3.11.1 and 6.3.11.2; Equation 6.3.11-4.
ILTSR90. Volcanic Biosphere Dose Conversion Factor (BDCF) component for long-term inhalation of ^{90}Sr in modern interglacial climate ((Sv/yr)/(Bq/kg)). *Distribution:* Discrete. *Range:* 1.39E-10 to 4.08E-09. *Mean:* 8.16E-10. *Standard Deviation:* 5.21E-10. *TSPA-LA Name:* DE_BDCF_Inh_LT_Sr90. *Location in TSPA-LA:* Sections 6.3.11.1 and 6.3.11.2; Equation 6.3.11-4.
ILTTC99. Volcanic Biosphere Dose Conversion Factor (BDCF) component for long-term inhalation of ^{99}Tc in modern interglacial climate ((Sv/yr)/(Bq/kg)). *Distribution:* Discrete. *Range:* 1.17E-11 to 3.42E-10. *Mean:* 6.84E-11. *Standard Deviation:* 4.37E-11. *TSPA-LA Name:* DE_BDCF_Inh_LT_Tc99. *Location in TSPA-LA:* Sections 6.3.11.1 and 6.3.11.2; Equation 6.3.11-4.

Table K3-1. High-Level Summary of Epistemically Uncertain Variables (i.e., elements of **e**) Considered in the TSPA-LA (Sensitivity Analysis Name) (Continued)

NOTE: * indicates variable not considered in sensitivity analysis due to correlations.

ILTTH229. Volcanic Biosphere Dose Conversion Factor (BDCF) component for long-term inhalation of ^{229}Th in modern interglacial climate ((Sv/yr)/(Bq/kg)). *Distribution:* Discrete. *Range:* 2.24E-07 to 6.57E-06. *Mean:* 1.31E-06. *Standard Deviation:* 8.39E-07. *TSPA-LA Name:* DE_BDCF_Inh_LT_Th229. *Location in TSPA-LA:* Sections 6.3.11.1 and 6.3.11.2; Equation 6.3.11-4.
ILTTH230. Volcanic Biosphere Dose Conversion Factor (BDCF) component for long-term inhalation of ^{230}Th in modern interglacial climate ((Sv/yr)/(Bq/kg)). *Distribution:* Discrete. *Range:* 8.94E-08 to 2.62E-06. *Mean:* 5.25E-07. *Standard Deviation:* 3.35E-07. *TSPA-LA Name:* DE_BDCF_Inh_LT_Th230. *Location in TSPA-LA:* Sections 6.3.11.1 and 6.3.11.2; Equation 6.3.11-4.
ILTTH232. Volcanic Biosphere Dose Conversion Factor (BDCF) component for long-term inhalation of ^{232}Th in modern interglacial climate ((Sv/yr)/(Bq/kg)). *Distribution:* Discrete. *Range:* 9.64E-08 to 2.83E-06. *Mean:* 5.66E-07. *Standard Deviation:* 3.62E-07. *TSPA-LA Name:* DE_BDCF_Inh_LT_Th232. *Location in TSPA-LA:* Sections 6.3.11.1 and 6.3.11.2; Equation 6.3.11-4.
ILTU233. Volcanic Biosphere Dose Conversion Factor (BDCF) component for long-term inhalation of ^{233}U in modern interglacial climate ((Sv/yr)/(Bq/kg)). *Distribution:* Discrete. *Range:* 8.40E-09 to 2.47E-07. *Mean:* 4.94E-08. *Standard Deviation:* 3.15E-08. *TSPA-LA Name:* DE_BDCF_Inh_LT_U233. *Location in TSPA-LA:* Sections 6.3.11.1 and 6.3.11.2; Equation 6.3.11-4.
ILTU234. Volcanic Biosphere Dose Conversion Factor (BDCF) component for long-term inhalation of ^{234}U in modern interglacial climate ((Sv/yr)/(Bq/kg)). *Distribution:* Discrete. *Range:* 8.23E-09 to 2.42E-07. *Mean:* 4.84E-08. *Standard Deviation:* 3.09E-08. *TSPA-LA Name:* DE_BDCF_Inh_LT_U234. *Location in TSPA-LA:* Sections 6.3.11.1 and 6.3.11.2; Equation 6.3.11-4.
ILTU238. Volcanic Biosphere Dose Conversion Factor (BDCF) component for long-term inhalation of ^{238}U in modern interglacial climate ((Sv/yr)/(Bq/kg)). *Distribution:* Discrete. *Range:* 7.05E-09 to 2.07E-07. *Mean:* 4.14E-08. *Standard Deviation:* 2.65E-08. *TSPA-LA Name:* DE_BDCF_Inh_LT_U238. *Location in TSPA-LA:* Sections 6.3.11.1 and 6.3.11.2; Equation 6.3.11-4.
INFIL. Pointer variable for determining infiltration conditions: 10th, 30th, 50th or 90th percentile infiltration scenario (dimensionless). *Distribution:* Discrete. *Range:* 1 to 4. *TSPA-LA Name:* Infiltration_Scenario_a. *Location in TSPA-LA:* Section 6.3.1.2; Tables 6.3.1-2 and 6.3.5-4.
INGAC227. Volcanic Biosphere Dose Conversion Factor (BDCF) component for radon, external exposure and ingestion of ^{227}Ac in modern interglacial climate ((Sv/yr)/(Bq/m^2)). *Distribution:* Discrete. *Range:* 5.78E-09 to 7.76E-09. *Mean:* 6.16E-09. *Standard Deviation:* 1.8E-10. *TSPA-LA Name:* DE_BDCF_Ing_Exp_Radon_Ac227. *Location in TSPA-LA:* Sections 6.3.11.1 and 6.3.11.2; Equation 6.3.11-4.
INGAM241. Volcanic Biosphere Dose Conversion Factor (BDCF) component for radon, external exposure and ingestion of ^{241}Am in modern interglacial climate ((Sv/yr)/(Bq/m^2)). *Distribution:* Discrete. *Range:* 1.86E-10 to 1.00E-09. *Mean:* 2.51E-10. *Standard Deviation:* 7.00E-11. *TSPA-LA Name:* DE_BDCF_Ing_Exp_Radon_Am241. *Location in TSPA-LA:* Sections 6.3.11.1 and 6.3.11.2; Equation 6.3.11-4.
INGAM243. Volcanic Biosphere Dose Conversion Factor (BDCF) component for radon, external exposure and ingestion of ^{243}Am in modern interglacial climate ((Sv/yr)/(Bq/m^2)). *Distribution:* Discrete. *Range:* 2.51E-09 to 3.42E-09. *Mean:* 2.67E-09. *Standard Deviation:* 8.02E-11. *TSPA-LA Name:* DE_BDCF_Ing_Exp_Radon_Am243. *Location in TSPA-LA:* Sections 6.3.11.1 and 6.3.11.2; Equation 6.3.11-4.
INGCS137. Volcanic Biosphere Dose Conversion Factor (BDCF) component for radon, external exposure and ingestion of ^{137}Cs in modern interglacial climate ((Sv/yr)/(Bq/m^2)). *Distribution:* Discrete. *Range:* 6.75E-09 to 8.48E-09. *Mean:* 7.17E-09. *Standard Deviation:* 1.55E-10. *TSPA-LA Name:* DE_BDCF_Ing_Exp_Radon_Cs137. *Location in TSPA-LA:* Sections 6.3.11.1 and 6.3.11.2; Equation 6.3.11-4.
INGI129. Volcanic Biosphere Dose Conversion Factor (BDCF) component for radon, external exposure and ingestion of ^{129}I in modern interglacial climate ((Sv/yr)/(Bq/m^2)). *Distribution:* Discrete. *Range:* 1.39E-10 to 2.86E-08. *Mean:* 1.26E-09. *Standard Deviation:* 2.59E-09. *TSPA-LA Name:* DE_BDCF_Ing_Exp_Radon_I129. *Location in TSPA-LA:* Sections 6.3.11.1 and 6.3.11.2; Equation 6.3.11-4.
INGNP237. Volcanic Biosphere Dose Conversion Factor (BDCF) component for radon, external exposure and ingestion of ^{237}Np in modern interglacial climate ((Sv/yr)/(Bq/m^2)). *Distribution:* Discrete. *Range:* 2.62E-09 to 1.2E-08. *Mean:* 2.98E-09. *Standard Deviation:* 6.36E-10. *TSPA-LA Name:* DE_BDCF_Ing_Exp_Radon_Np237. *Location in TSPA-LA:* Sections 6.3.11.1 and 6.3.11.2; Equation 6.3.11-4.

Table K3-1. High-Level Summary of Epistemically Uncertain Variables (i.e., elements of **e**) Considered in the TSPA-LA (Sensitivity Analysis Name) (Continued)

NOTE: * indicates variable not considered in sensitivity analysis due to correlations.

INGPA231. Volcanic Biosphere Dose Conversion Factor (BDCF) component for radon, external exposure and ingestion of ^{231}Pa in modern interglacial climate ((Sv/yr)/(Bq/m^2)). *Distribution:* Discrete. *Range:* 5.02E-10 to 4.56E-09. *Mean:* 7.14E-10. *Standard Deviation:* 2.92E-10. *TSPA-LA Name:* DE_BDCF_Ing_Exp_Radon_Pa231. *Location in TSPA-LA:* Sections 6.3.11.1 and 6.3.11.2; Equation 6.3.11-4.
INGPU238. Volcanic Biosphere Dose Conversion Factor (BDCF) component for radon, external exposure and ingestion of ^{238}Pu in modern interglacial climate ((Sv/yr)/(Bq/m^2)). *Distribution:* Discrete. *Range:* 1.33E-11 to 9.18E-10. *Mean:* 7.78E-11. *Standard Deviation:* 7.72E-11. *TSPA-LA Name:* DE_BDCF_Ing_Exp_Radon_Pu238. *Location in TSPA-LA:* Sections 6.3.11.1 and 6.3.11.2; Equation 6.3.11-4.
INGPU239. Volcanic Biosphere Dose Conversion Factor (BDCF) component for radon, external exposure and ingestion of ^{239}Pu in modern interglacial climate ((Sv/yr)/(Bq/m^2)). *Distribution:* Discrete. *Range:* 1.40E-11 to 1.01E-09. *Mean:* 8.49E-11. *Standard Deviation:* 8.5E-11. *TSPA-LA Name:* DE_BDCF_Ing_Exp_Radon_Pu239. *Location in TSPA-LA:* Sections 6.3.11.1 and 6.3.11.2; Equation 6.3.11-4.
INGPU240. Volcanic Biosphere Dose Conversion Factor (BDCF) component for radon, external exposure and ingestion of ^{240}Pu in modern interglacial climate ((Sv/yr)/(Bq/m^2)). *Distribution:* Discrete. *Range:* 1.42E-11 to 1.01E-09. *Mean:* 8.52E-11. *Standard Deviation:* 8.5E-11. *TSPA-LA Name:* DE_BDCF_Ing_Exp_Radon_Pu240. *Location in TSPA-LA:* Sections 6.3.11.1 and 6.3.11.2; Equation 6.3.11-4.
INGPU242. Volcanic Biosphere Dose Conversion Factor (BDCF) component for radon, external exposure and ingestion of ^{242}Pu in modern interglacial climate ((Sv/yr)/(Bq/m^2)). *Distribution:* Discrete. *Range:* 1.31E-11 to 9.57E-10. *Mean:* 8.04E-11. *Standard Deviation:* 8.06E-11. *TSPA-LA Name:* DE_BDCF_Ing_Exp_Radon_Pu242. *Location in TSPA-LA:* Sections 6.3.11.1 and 6.3.11.2; Equation 6.3.11-4.
INGRA226. Volcanic Biosphere Dose Conversion Factor (BDCF) component for radon, external exposure and ingestion of ^{226}Ra and ^{210}Pb in modern interglacial climate ((Sv/yr)/(Bq/m^2)). *Distribution:* Discrete. *Range:* 3.07E-08 to 9.43E-08. *Mean:* 3.52E-08. *Standard Deviation:* 3.45E-09. *TSPA-LA Name:* DE_BDCF_IER_Ra226_Pb210. *Location in TSPA-LA:* Sections 6.3.11.1 and 6.3.11.2; Equation 6.3.11-4.
INGRA228. Volcanic Biosphere Dose Conversion Factor (BDCF) component for radon, external exposure and ingestion of ^{228}Ra in modern interglacial climate ((Sv/yr)/(Bq/m^2)). *Distribution:* Discrete. *Range:* 1.17E-08 to 2.62E-08. *Mean:* 1.27E-08. *Standard Deviation:* 7.44E-10. *TSPA-LA Name:* DE_BDCF_Ing_Exp_Radon_Ra228. *Location in TSPA-LA:* Sections 6.3.11.1 and 6.3.11.2; Equation 6.3.11-4.
INGSN126. Volcanic Biosphere Dose Conversion Factor (BDCF) component for radon, external exposure and ingestion of ^{126}Sn in modern interglacial climate ((Sv/yr)/(Bq/m^2)). *Distribution:* Discrete. *Range:* 2.38E-08 to 2.79E-08. *Mean:* 2.54E-08. *Standard Deviation:* 4.41E-10. *TSPA-LA Name:* DE_BDCF_Ing_Exp_Radon_Sn126. *Location in TSPA-LA:* Sections 6.3.11.1 and 6.3.11.2; Equation 6.3.11-4.
INGSR90. Volcanic Biosphere Dose Conversion Factor (BDCF) component for radon, external exposure and ingestion of ^{90}Sr in modern interglacial climate ((Sv/yr)/(Bq/m^2)). *Distribution:* Discrete. *Range:* 1.44E-09 to 6.10E-09. *Mean:* 1.81E-09. *Standard Deviation:* 3.67E-10. *TSPA-LA Name:* DE_BDCF_Ing_Exp_Radon_Sr90. *Location in TSPA-LA:* Sections 6.3.11.1 and 6.3.11.2; Equation 6.3.11-4.
INGTC99. Volcanic Biosphere Dose Conversion Factor (BDCF) component for radon, external exposure and ingestion of ^{99}Tc in modern interglacial climate ((Sv/yr)/(Bq/m^2)). *Distribution:* Discrete. *Range:* 5.08E-12 to 8.95E-09. *Mean:* 2.72E-10. *Standard Deviation:* 5.16E-10. *TSPA-LA Name:* DE_BDCF_Ing_Exp_Radon_Tc99. *Location in TSPA-LA:* Sections 6.3.11.1 and 6.3.11.2; Equation 6.3.11-4.
INGTH229. Volcanic Biosphere Dose Conversion Factor (BDCF) component for radon, external exposure and ingestion of ^{229}Th in modern interglacial climate ((Sv/yr)/(Bq/m^2)). *Distribution:* Discrete. *Range:* 4.33E-09 to 7.02E-09. *Mean:* 4.69E-09. *Standard Deviation:* 2.4E-10. *TSPA-LA Name:* DE_BDCF_Ing_Exp_Radon_Th229. *Location in TSPA-LA:* Sections 6.3.11.1 and 6.3.11.2; Equation 6.3.11-4.
INGTH230. Volcanic Biosphere Dose Conversion Factor (BDCF) component for radon, external exposure and ingestion of ^{230}Th in modern interglacial climate ((Sv/yr)/(Bq/m^2)). *Distribution:* Discrete. *Range:* 1.92E-11 to 8.68E-10. *Mean:* 8.51E-11. *Standard Deviation:* 7.82E-11. *TSPA-LA Name:* DE_BDCF_Ing_Exp_Radon_Th230. *Location in TSPA-LA:* Sections 6.3.11.1 and 6.3.11.2; Equation 6.3.11-4.
INGTH232. Volcanic Biosphere Dose Conversion Factor (BDCF) component for radon, external exposure and ingestion of ^{232}Th in modern interglacial climate ((Sv/yr)/(Bq/m^2)). *Distribution:* Discrete. *Range:* 1.72E-11 to 9.34E-10. *Mean:* 8.83E-11. *Standard Deviation:* 8.44E-11. *TSPA-LA Name:* DE_BDCF_Ing_Exp_Radon_Th232. *Location in TSPA-LA:* Sections 6.3.11.1 and 6.3.11.2; Equation 6.3.11-4.

Table K3-1. High-Level Summary of Epistemically Uncertain Variables (i.e., elements of **e**) Considered in the TSPA-LA (Sensitivity Analysis Name) (Continued)

NOTE: * indicates variable not considered in sensitivity analysis due to correlations.

INGU233. Volcanic Biosphere Dose Conversion Factor (BDCF) component for radon, external exposure and ingestion of ^{233}U in modern interglacial climate ((Sv/yr)/(Bq/m^2)). *Distribution:* Discrete. *Range:* 1.31E-11 to 9.04E-10. *Mean:* 6.48E-11. *Standard Deviation:* 6.12E-11. *TSPA-LA Name:* DE_BDCF_Ing_Exp_Radon_U233. *Location in TSPA-LA:* Sections 6.3.11.1 and 6.3.11.2; Equation 6.3.11-4.
INGU234. Volcanic Biosphere Dose Conversion Factor (BDCF) component for radon, external exposure and ingestion of ^{234}U in modern interglacial climate ((Sv/yr)/(Bq/m^2)). *Distribution:* Discrete. *Range:* 9.60E-12 to 8.7E-10. *Mean:* 5.96E-11. *Standard Deviation:* 5.9E-11. *TSPA-LA Name:* DE_BDCF_Ing_Exp_Radon_U234. *Location in TSPA-LA:* Sections 6.3.11.1 and 6.3.11.2; Equation 6.3.11-4.
INGU238. Volcanic Biosphere Dose Conversion Factor (BDCF) component for radon, external exposure and ingestion of ^{238}U in modern interglacial climate ((Sv/yr)/(Bq/m^2)). *Distribution:* Discrete. *Range:* 1.52E-09 to 2.41E-09. *Mean:* 1.62E-09. *Standard Deviation:* 6.16E-11. *TSPA-LA Name:* DE_BDCF_Ing_Exp_Radon_U238. *Location in TSPA-LA:* Sections 6.3.11.1 and 6.3.11.2; Equation 6.3.11-4.
INHLTPV. Pointer variable for long-term inhalation dose conversion factor for volcanic ash exposure (dimensionless). *Distribution:* Discrete. *Range:* 1 to 300. *TSPA-LA Name:* BDCF_Inh_LT. *Location in TSPA-LA:* Section 6.3.11; Equation 6.3.11-4.
INHSTPV. Pointer variable for short-term inhalation dose conversion factor for volcanic ash exposure (dimensionless). *Distribution:* Discrete. *Range:* 1 to 300. *TSPA-LA Name:* BDCF_Inh_ShT. *Location in TSPA-LA:* Section 6.3.11; Equation 6.3.11-4.
INRFRCCS. The initial release fraction of ^{137}Cs in a CSNF waste package (dimensionless). *Distribution:* Triangular. *Range:* 0.0039 to 0.1106. *Mode:* 0.0363. *TSPA-LA Name:* Initial_Release_Frac_Cs_a. *Location in TSPA-LA:* Sections 6.3.7.4.1.2 and 6.3.7.4.1.3; Table 6.3.7-29.
INRFRCI. The initial release fraction of ^{129}I in a CSNF waste package (dimensionless). *Distribution:* Triangular. *Range:* 0.0204 to 0.2675. *Mode:* 0.1124. *TSPA-LA Name:* Initial_Release_Frac_I_a. *Location in TSPA-LA:* Sections 6.3.7.4.1.2 and 6.3.7.4.1.3; Table 6.3.7-29.
INRFRCSR. The initial release fraction of ^{90}Sr in a CSNF waste package (dimensionless). *Distribution:* Triangular. *Range:* 0.0002 to 0.0025. *Mode:* 0.0009. *TSPA-LA Name:* Initial_Release_Frac_Sr_a. *Location in TSPA-LA:* Sections 6.3.7.4.1.2 and 6.3.7.4.1.3; Table 6.3.7-29.
INRFRCTC. The initial release fraction of ^{99}Tc in a CSNF waste package (dimensionless). *Distribution:* Triangular. *Range:* 0.0001 to 0.0026. *Mode:* 0.001. *TSPA-LA Name:* Initial_Release_Frac_Tc_a. *Location in TSPA-LA:* Sections 6.3.7.4.1.2 and 6.3.7.4.1.3; Table 6.3.7-29.
IS2DHLNS. Pointer variable used to determine ionic strength for 2DHLW Cell (Cell 1a) of CDSP waste packages under vapor influx conditions (dimensionless). *Distribution:* Uniform. *Range:* 0 to 1. *TSPA-LA Name:* Inpkg_IStr_2DHLW_NS_Rand_a. *Location in TSPA-LA:* Section 6.3.7.2.2 Part III.
IS2DHLS. Pointer variable used to determine ionic strength for 2DHLW Cell (Cell 1a) of CDSP waste packages under liquid influx conditions (dimensionless). *Distribution:* Uniform. *Range:* 0 to 1. *TSPA-LA Name:* Inpkg_IStr_2DHLW_S_Rand_a. *Location in TSPA-LA:* Section 6.3.7.2.2 Part III.
IS2MCONS. Pointer variable used to determine ionic strength for 2MCO Cell (Cell 1b) of CDSP waste packages under vapor influx conditions (dimensionless). *Distribution:* Uniform. *Range:* 0 to 1. *TSPA-LA Name:* Inpkg_IStr_2MCO_NS_Rand_a. *Location in TSPA-LA:* Section 6.3.7.2.2 Part III.
IS2MCOS. Pointer variable used to determine ionic strength for 2MCO Cell (Cell 1b) of CDSP waste packages under liquid influx conditions (dimensionless). *Distribution:* Uniform. *Range:* 0 to 1. *TSPA-LA Name:* Inpkg_IStr_2MCO_S_Rand_a. *Location in TSPA-LA:* Section 6.3.7.2.2 Part III.
ISCSNS. Pointer variable used to determine ionic strength for CSNF Cell under vapor influx conditions (dimensionless). *Distribution:* Uniform. *Range:* 0 to 1. *TSPA-LA Name:* Inpkg_IStr_CSNF_NS_Rand_a. *Location in TSPA-LA:* Section 6.3.7.2.2 Part III.
ISCSS. Pointer variable used to determine ionic strength for CSNF Cell under liquid influx conditions (dimensionless). *Distribution:* Uniform. *Range:* 0 to 1. *TSPA-LA Name:* Inpkg_IStr_CSNF_S_Rand_a. *Location in TSPA-LA:* Section 6.3.7.2.2 Part III.
ISTAC227. Volcanic Biosphere Dose Conversion Factor (BDCF) component for short-term inhalation of ^{227}Ac in modern interglacial climate ((Sv/yr)/(Bq/kg)). *Distribution:* Discrete. *Range:* 8.47E-08 to 2.14E-06. *Mean:* 5.85E-07. *Standard Deviation:* 3.32E-07. *TSPA-LA Name:* DE_BDCF_Inh_ShT_Ac227. *Location in TSPA-LA:* Sections 6.3.11.1 and 6.3.11.2; Equation 6.3.11-4.

Table K3-1. High-Level Summary of Epistemically Uncertain Variables (i.e., elements of **e**) Considered in the TSPA-LA (Sensitivity Analysis Name) (Continued)

NOTE: * indicates variable not considered in sensitivity analysis due to correlations.

ISTAM241. Volcanic Biosphere Dose Conversion Factor (BDCF) component for short-term inhalation of ^{241}Am in modern interglacial climate ((Sv/yr)/(Bq/kg)). *Distribution:* Discrete. *Range:* 4.67E-08 to 1.18E-06. *Mean:* 3.23E-07. *Standard Deviation:* 1.83E-07. *TSPA-LA Name:* DE_BDCF_Inh_ShT_Am241. *Location in TSPA-LA:* Sections 6.3.11.1 and 6.3.11.2; Equation 6.3.11-4.
ISTAM243. Volcanic Biosphere Dose Conversion Factor (BDCF) component for short-term inhalation of ^{243}Am in modern interglacial climate ((Sv/yr)/(Bq/kg)). *Distribution:* Discrete. *Range:* 4.64E-08 to 1.17E-06. *Mean:* 3.2E-07. *Standard Deviation:* 1.82E-07. *TSPA-LA Name:* DE_BDCF_Inh_ShT_Am243. *Location in TSPA-LA:* Sections 6.3.11.1 and 6.3.11.2; Equation 6.3.11-4.
ISTCS137. Volcanic Biosphere Dose Conversion Factor (BDCF) component for short-term inhalation of ^{137}Cs in modern interglacial climate ((Sv/yr)/(Bq/kg)). *Distribution:* Discrete. *Range:* 1.90E-11 to 4.80E-10. *Mean:* 1.31E-10. *Standard Deviation:* 7.44E-11. *TSPA-LA Name:* DE_BDCF_Inh_ShT_Cs137. *Location in TSPA-LA:* Sections 6.3.11.1 and 6.3.11.2; Equation 6.3.11-4.
ISTI129. Volcanic Biosphere Dose Conversion Factor (BDCF) component for short-term inhalation of ^{129}I in modern interglacial climate ((Sv/yr)/(Bq/kg)). *Distribution:* Discrete. *Range:* 1.74E-11 to 4.40E-10. *Mean:* 1.2E-10. *Standard Deviation:* 6.81E-11. *TSPA-LA Name:* DE_BDCF_Inh_ShT_I129. *Location in TSPA-LA:* Sections 6.3.11.1 and 6.3.11.2; Equation 6.3.11-4.
ISTNP237. Volcanic Biosphere Dose Conversion Factor (BDCF) component for short-term inhalation of ^{237}Np in modern interglacial climate ((Sv/yr)/(Bq/kg)). *Distribution:* Discrete. *Range:* 2.41E-08 to 6.08E-07. *Mean:* 1.66E-07. *Standard Deviation:* 9.43E-08. *TSPA-LA Name:* DE_BDCF_Inh_ShT_Np237. *Location in TSPA-LA:* Sections 6.3.11.1 and 6.3.11.2; Equation 6.3.11-4.
ISTPA231. Volcanic Biosphere Dose Conversion Factor (BDCF) component for short-term inhalation of ^{231}Pa in modern interglacial climate ((Sv/yr)/(Bq/kg)). *Distribution:* Discrete. *Range:* 1.11E-07 to 2.82E-06. *Mean:* 7.7E-07. *Standard Deviation:* 4.37E-07. *TSPA-LA Name:* DE_BDCF_Inh_ShT_Pa231. *Location in TSPA-LA:* Sections 6.3.11.1 and 6.3.11.2; Equation 6.3.11-4.
ISTPU238. Volcanic Biosphere Dose Conversion Factor (BDCF) component for short-term inhalation of ^{238}Pu in modern interglacial climate ((Sv/yr)/(Bq/kg)). *Distribution:* Discrete. *Range:* 5.23E-08 to 1.32E-06. *Mean:* 3.61E-07. *Standard Deviation:* 2.05E-07. *TSPA-LA Name:* DE_BDCF_Inh_ShT_Pu238. *Location in TSPA-LA:* Sections 6.3.11.1 and 6.3.11.2; Equation 6.3.11-4.
ISTPU239. Volcanic Biosphere Dose Conversion Factor (BDCF) component for short-term inhalation of ^{239}Pu in modern interglacial climate ((Sv/yr)/(Bq/kg)). *Distribution:* Discrete. *Range:* 5.76E-08 to 1.46E-06. *Mean:* 3.98E-07. *Standard Deviation:* 2.26E-07. *TSPA-LA Name:* DE_BDCF_Inh_ShT_Pu239. *Location in TSPA-LA:* Sections 6.3.11.1 and 6.3.11.2; Equation 6.3.11-4.
ISTPU240. Volcanic Biosphere Dose Conversion Factor (BDCF) component for short-term inhalation of ^{240}Pu in modern interglacial climate ((Sv/yr)/(Bq/kg)). *Distribution:* Discrete. *Range:* 5.76E-08 to 1.46E-06. *Mean:* 3.98E-07. *Standard Deviation:* 2.26E-07. *TSPA-LA Name:* DE_BDCF_Inh_ShT_Pu240. *Location in TSPA-LA:* Sections 6.3.11.1 and 6.3.11.2; Equation 6.3.11-4.
ISTPU242. Volcanic Biosphere Dose Conversion Factor (BDCF) component for short-term inhalation of ^{242}Pu in modern interglacial climate ((Sv/yr)/(Bq/kg)). *Distribution:* Discrete. *Range:* 5.47E-08 to 1.38E-06. *Mean:* 3.78E-07. *Standard Deviation:* 2.14E-07. *TSPA-LA Name:* DE_BDCF_Inh_ShT_Pu242. *Location in TSPA-LA:* Sections 6.3.11.1 and 6.3.11.2; Equation 6.3.11-4.
ISTRA226. Volcanic Biosphere Dose Conversion Factor (BDCF) component for short-term inhalation of ^{226}Ra and ^{210}Pb in modern interglacial climate ((Sv/yr)/(Bq/kg)). *Distribution:* Discrete. *Range:* 9.47E-09 to 2.39E-07. *Mean:* 6.54E-08. *Standard Deviation:* 3.71E-08. *TSPA-LA Name:* DE_BDCF_IST_Ra226_Pb210. *Location in TSPA-LA:* Sections 6.3.11.1 and 6.3.11.2; Equation 6.3.11-4.
ISTRA228. Volcanic Biosphere Dose Conversion Factor (BDCF) component for short-term inhalation of ^{228}Ra in modern interglacial climate ((Sv/yr)/(Bq/kg)). *Distribution:* Discrete. *Range:* 7.76E-09 to 1.96E-07. *Mean:* 5.36E-08. *Standard Deviation:* 3.04E-08. *TSPA-LA Name:* DE_BDCF_Inh_ShT_Ra228. *Location in TSPA-LA:* Sections 6.3.11.1 and 6.3.11.2; Equation 6.3.11-4.
ISTSN126. Volcanic Biosphere Dose Conversion Factor (BDCF) component for short-term inhalation of ^{126}Sn in modern interglacial climate ((Sv/yr)/(Bq/kg)). *Distribution:* Discrete. *Range:* 7.53E-11 to 1.90E-09. *Mean:* 5.2E-10. *Standard Deviation:* 2.95E-10. *TSPA-LA Name:* DE_BDCF_Inh_ShT_Sn126. *Location in TSPA-LA:* Sections 6.3.11.1 and 6.3.11.2; Equation 6.3.11-4.

Table K3-1. High-Level Summary of Epistemically Uncertain Variables (i.e., elements of **e**) Considered in the TSPA-LA (Sensitivity Analysis Name) (Continued)

NOTE: * indicates variable not considered in sensitivity analysis due to correlations.

ISTSR90. Volcanic Biosphere Dose Conversion Factor (BDCF) component for short-term inhalation of ^{90}Sr in modern interglacial climate ((Sv/yr)/(Bq/kg)). *Distribution:* Discrete. *Range:* 7.68E-11 to 1.94E-09. *Mean:* 5.3E-10. *Standard Deviation:* 3.01E-10. *TSPA-LA Name:* DE_BDCF_Inh_ShT_Sr90. *Location in TSPA-LA:* Sections 6.3.11.1 and 6.3.11.2; Equation 6.3.11-4.
ISTTC99. Volcanic Biosphere Dose Conversion Factor (BDCF) component for short-term inhalation of ^{99}Tc in modern interglacial climate ((Sv/yr)/(Bq/kg)). *Distribution:* Discrete. *Range:* 6.44E-12 to 1.63E-10. *Mean:* 4.45E-11. *Standard Deviation:* 2.52E-11. *TSPA-LA Name:* DE_BDCF_Inh_ShT_Tc99. *Location in TSPA-LA:* Sections 6.3.11.1 and 6.3.11.2; Equation 6.3.11-4.
ISTTH229. Volcanic Biosphere Dose Conversion Factor (BDCF) component for short-term inhalation of ^{229}Th in modern interglacial climate ((Sv/yr)/(Bq/kg)). *Distribution:* Discrete. *Range:* 1.24E-07 to 3.13E-06. *Mean:* 8.54E-07. *Standard Deviation:* 4.84E-07. *TSPA-LA Name:* DE_BDCF_Inh_ShT_Th229. *Location in TSPA-LA:* Sections 6.3.11.1 and 6.3.11.2; Equation 6.3.11-4.
ISTTH230. Volcanic Biosphere Dose Conversion Factor (BDCF) component for short-term inhalation of ^{230}Th in modern interglacial climate ((Sv/yr)/(Bq/kg)). *Distribution:* Discrete. *Range:* 4.94E-08 to 1.25E-06. *Mean:* 3.41E-07. *Standard Deviation:* 1.94E-07. *TSPA-LA Name:* DE_BDCF_Inh_ShT_Th230. *Location in TSPA-LA:* Sections 6.3.11.1 and 6.3.11.2; Equation 6.3.11-4.
ISTTH232. Volcanic Biosphere Dose Conversion Factor (BDCF) component for short-term inhalation of ^{232}Th in modern interglacial climate ((Sv/yr)/(Bq/kg)). *Distribution:* Discrete. *Range:* 5.33E-08 to 1.35E-06. *Mean:* 3.68E-07. *Standard Deviation:* 2.09E-07. *TSPA-LA Name:* DE_BDCF_Inh_ShT_Th232. *Location in TSPA-LA:* Sections 6.3.11.1 and 6.3.11.2; Equation 6.3.11-4.
ISTU233. Volcanic Biosphere Dose Conversion Factor (BDCF) component for short-term inhalation of ^{233}U in modern interglacial climate ((Sv/yr)/(Bq/kg)). *Distribution:* Discrete. *Range:* 4.65E-09 to 1.17E-07. *Mean:* 3.21E-08. *Standard Deviation:* 1.82E-08. *TSPA-LA Name:* DE_BDCF_Inh_ShT_U233. *Location in TSPA-LA:* Sections 6.3.11.1 and 6.3.11.2; Equation 6.3.11-4.
ISTU234. Volcanic Biosphere Dose Conversion Factor (BDCF) component for short-term inhalation of ^{234}U in modern interglacial climate ((Sv/yr)/(Bq/kg)). *Distribution:* Discrete. *Range:* 4.55E-09 to 1.15E-07. *Mean:* 3.15E-08. *Standard Deviation:* 1.78E-08. *TSPA-LA Name:* DE_BDCF_Inh_ShT_U234. *Location in TSPA-LA:* Sections 6.3.11.1 and 6.3.11.2; Equation 6.3.11-4.
ISTU238. Volcanic Biosphere Dose Conversion Factor (BDCF) component for short-term inhalation of ^{238}U in modern interglacial climate ((Sv/yr)/(Bq/kg)). *Distribution:* Discrete. *Range:* 3.90E-09 to 9.85E-08. *Mean:* 2.69E-08. *Standard Deviation:* 1.53E-08. *TSPA-LA Name:* DE_BDCF_Inh_ShT_U238. *Location in TSPA-LA:* Sections 6.3.11.1 and 6.3.11.2; Equation 6.3.11-4.
KDAMCOL. Distribution coefficient for reversible sorption of americium onto uranophane colloids (mL/g). *Distribution:* Log uniform. *Range:* 5 to 1.00E+04. *TSPA-LA Name:* Kd_Am_Rev_U_Col_a. *Location in TSPA-LA:* Sections 6.3.7.6.2 and 6.3.7.6.3; Equation 6.3.7-20; Table 6.3.7-64.
KDAMSMEC. Distribution coefficient for reversible sorption of americium to waste form (smectite) colloids (mL/g). *Distribution:* Piecewise uniform. *Range:* 1.00E+04 to 1.00E+07. *TSPA-LA Name:* Kd_Am_Rev_Smectite_a. *Location in TSPA-LA:* Sections 6.3.7.6.2 and 6.3.7.6.3; Equation 6.3.7-20; Tables 6.3.7-62 and 6.3.7-66.
KDCSCOL. Distribution coefficient for reversible sorption of cesium onto uranophane colloids (mL/g). *Distribution:* Log uniform. *Range:* 10 to 1000. *TSPA-LA Name:* Kd_Cs_Rev_U_Col_a. *Location in TSPA-LA:* Sections 6.3.7.6.2 and 6.3.7.6.3; Equation 6.3.7-20; Table 6.3.7-64.
KDCSSMEC. Distribution coefficient for reversible sorption of cesium to waste form (smectite) colloids (mL/g). *Distribution:* Piecewise uniform. *Range:* 50 to 5000. *TSPA-LA Name:* Kd_Cs_Rev_Smectite_a. *Location in TSPA-LA:* Sections 6.3.7.6.2 and 6.3.7.6.3; Equation 6.3.7-20; Tables 6.3.7-62 and 6.3.7-66.
KDNPCOL. Distribution coefficient for reversible sorption of neptunium onto uranophane colloids (mL/g). *Distribution:* Log uniform. *Range:* 1 to 500. *TSPA-LA Name:* Kd_Np_Rev_U_Col_a. *Location in TSPA-LA:* Sections 6.3.7.6.2 and 6.3.7.6.3; Equation 6.3.7-20; Table 6.3.7-64.
KDNPSMEC. Distribution coefficient for reversible sorption of neptunium to waste form (smectite) colloids (mL/g). *Distribution:* Log uniform. *Range:* 10 to 500. *TSPA-LA Name:* Kd_Np_Rev_Smectite_a. *Location in TSPA-LA:* Sections 6.3.7.6.2 and 6.3.7.6.3; Equation 6.3.7-20; Tables 6.3.7-62 and 6.3.7-66.

Table K3-1. High-Level Summary of Epistemically Uncertain Variables (i.e., elements of **e**) Considered in the TSPA-LA (Sensitivity Analysis Name) (Continued)

NOTE: * indicates variable not considered in sensitivity analysis due to correlations.

KDPACOL. Distribution coefficient for reversible sorption of protactinium onto uranophane colloids (mL/g). *Distribution:* Log uniform. *Range:* 5 to 1.00E+04. *TSPA-LA Name:* Kd_Pa_Rev_U_Col_a. *Location in TSPA-LA:* Sections 6.3.7.6.2 and 6.3.7.6.3; Equation 6.3.7-20; Table 6.3.7-64.
KDPASMEC. Distribution coefficient for reversible sorption of protactinium to waste form (smectite) colloids (mL/g). *Distribution:* Piecewise uniform. *Range:* 1.00E+04 to 1.00E+07. *TSPA-LA Name:* Kd_Pa_Rev_Smectite_a. *Location in TSPA-LA:* Sections 6.3.7.6.2 and 6.3.7.6.3; Equation 6.3.7-20; Tables 6.3.7-62 and 6.3.7-66.
KDPUCOL. Distribution coefficient for reversible sorption of plutonium onto uranophane colloids (mL/g). *Distribution:* Log uniform. *Range:* 5 to 1.00E+04. *TSPA-LA Name:* Kd_Pu_Rev_U_Col_a. *Location in TSPA-LA:* Sections 6.3.7.6.2 and 6.3.7.6.3; Equation 6.3.7-20; Table 6.3.7-64.
KDPUSMEC. Distribution coefficient for reversible sorption of plutonium to waste form (smectite) colloids (mL/g). *Distribution:* Piecewise uniform. *Range:* 1.00E+03 to 1.00E+05. *TSPA-LA Name:* Kd_Pu_Rev_Smectite_a. *Location in TSPA-LA:* Sections 6.3.7.6.2 and 6.3.7.6.3; Equation 6.3.7-20; Tables 6.3.7-62 and 6.3.7-66.
KDRACOL. Distribution coefficient for reversible sorption of radium onto uranophane colloids (mL/g). *Distribution:* Log uniform. *Range:* 10 to 1000. *TSPA-LA Name:* Kd_Ra_Rev_U_Col_a. *Location in TSPA-LA:* Sections 6.3.7.6.2 and 6.3.7.6.3; Equation 6.3.7-20; Table 6.3.7-64.
KDRASMEC. Distribution coefficient for reversible sorption of radium to waste form (smectite) colloids (mL/g). *Distribution:* Log uniform. *Range:* 100 to 5000. *TSPA-LA Name:* Kd_Ra_Rev_Smectite_a. *Location in TSPA-LA:* Sections 6.3.7.6.2 and 6.3.7.6.3; Equation 6.3.7-20; Tables 6.3.7-62 and 6.3.7-66.
KDSNCOL. Distribution coefficient for reversible sorption of tin onto uranophane colloids (mL/g). *Distribution:* Log uniform. *Range:* 1 to 100. *TSPA-LA Name:* Kd_Sn_Rev_U_Col_a. *Location in TSPA-LA:* Sections 6.3.7.6.2 and 6.3.7.6.3; Equation 6.3.7-20; Table 6.3.7-64.
KDSNSMEC. Distribution coefficient for reversible sorption of tin to waste form (smectite) colloids (mL/g). *Distribution:* Log uniform. *Range:* 1.00E+05 to 1.00E+06. *TSPA-LA Name:* Kd_Sn_Rev_Smectite_a. *Location in TSPA-LA:* Sections 6.3.7.6.2 and 6.3.7.6.3; Equation 6.3.7-20; Tables 6.3.7-62 and 6.3.7-66.
KDTHCOL. Distribution coefficient for reversible sorption of thorium onto uranophane colloids (mL/g). *Distribution:* Log uniform. *Range:* 5 to 1.00E+04. *TSPA-LA Name:* Kd_Th_Rev_U_Col_a. *Location in TSPA-LA:* Sections 6.3.7.6.2 and 6.3.7.6.3; Equation 6.3.7-20; Table 6.3.7-64.
KDTHSMEC. Distribution coefficient for reversible sorption of thorium to waste form (smectite) colloids (mL/g). *Distribution:* Piecewise uniform. *Range:* 1.00E+04 to 1.00E+07. *TSPA-LA Name:* Kd_Th_Rev_Smectite_a. *Location in TSPA-LA:* Sections 6.3.7.6.2 and 6.3.7.6.3; Equation 6.3.7-20; Tables 6.3.7-62 and 6.3.7-66.
KDUSMEC. Distribution coefficient for reversible sorption of uranium to waste form (smectite) colloids (mL/g). *Distribution:* Log uniform. *Range:* 5.00E+02 to 5.00E+04. *TSPA-LA Name:* Kd_U_Rev_Smectite_a. *Location in TSPA-LA:* Sections 6.3.7.6.2 and 6.3.7.6.3; Equation 6.3.7-20; Tables 6.3.7-62 and 6.3.7-66.
LDIVIDE. Depth of permeable soil on divides of the Fortymile Wash fan (RMEI location) (cm). *Distribution:* Uniform. *Range:* 102 to 140. *TSPA-LA Name:* L_Divides_a. *Location in TSPA-LA:* Table 6.5-5.
MASSDCRS. Mass loading decrease rate constant (1/yr). *Distribution:* Triangular. *Range:* 0.125 to 1. *Mode:* 0.2. *TSPA-LA Name:* Mass_Decrease_Const_GE10_a. *Location in TSPA-LA:* Equation 6.3.11-5.
MICAC227. Groundwater Biosphere Dose Conversion Factor (BDCF) for ^{227}Ac in modern interglacial climate ((Sv/year)/(Bq/m^3)). *Distribution:* Discrete. *Range:* 4.08E-07 to 4.32E-06. *Mean:* 1.3E-06. *Standard Deviation:* 5.28E-07. *TSPA-LA Name:* GW_BDCF_MIC_Ac227. *Location in TSPA-LA:* Sections 6.3.11.2 and 6.3.11.3; Table 6.3.11-3.
MICAM241. Groundwater Biosphere Dose Conversion Factor (BDCF) for ^{241}Am in modern interglacial climate ((Sv/year)/(Bq/m^3)). *Distribution:* Discrete. *Range:* 2.16E-07 to 3.30E-06. *Mean:* 8.34E-07. *Standard Deviation:* 4.03E-07. *TSPA-LA Name:* GW_BDCF_MIC_Am241. *Location in TSPA-LA:* Sections 6.3.11.2 and 6.3.11.3; Table 6.3.11-3.
MICAM243. Groundwater Biosphere Dose Conversion Factor (BDCF) for ^{243}Am in modern interglacial climate ((Sv/year)/(Bq/m^3)). *Distribution:* Discrete. *Range:* 2.21E-07 to 3.37E-06. *Mean:* 8.88E-07. *Standard Deviation:* 4.12E-07. *TSPA-LA Name:* GW_BDCF_MIC_Am243. *Location in TSPA-LA:* Sections 6.3.11.2 and 6.3.11.3; Table 6.3.11-3.

Table K3-1. High-Level Summary of Epistemically Uncertain Variables (i.e., elements of **e**) Considered in the TSPA-LA (Sensitivity Analysis Name) (Continued)

NOTE: * indicates variable not considered in sensitivity analysis due to correlations.

MICC14. Groundwater Biosphere Dose Conversion Factor (BDCF) for ^{14}C in modern interglacial climate ((Sv/year)/(Bq/m^3)). *Distribution:* Discrete. *Range:* 7.18E-10 to 2.56E-08. *Mean:* 1.93E-09. *Standard Deviation:* 1.85E-09. *TSPA-LA Name:* GW_BDCF_MIC_C14. *Location in TSPA-LA:* Sections 6.3.11.2 and 6.3.11.3; Table 6.3.11-3.
MICCl36. Groundwater Biosphere Dose Conversion Factor (BDCF) for ^{36}Cl in modern interglacial climate ((Sv/year)/(Bq/m^3)). *Distribution:* Discrete. *Range:* 1.28E-09 to 3.00E-07. *Mean:* 8.09E-09. *Standard Deviation:* 1.41E-08. *TSPA-LA Name:* GW_BDCF_MIC_Cl36. *Location in TSPA-LA:* Sections 6.3.11.2 and 6.3.11.3; Table 6.3.11-3.
MICCS135. Groundwater Biosphere Dose Conversion Factor (BDCF) for ^{135}Cs in modern interglacial climate ((Sv/year)/(Bq/m^3)). *Distribution:* Discrete. *Range:* 3.1E-09 to 8.48E-08. *Mean:* 1.45E-08. *Standard Deviation:* 1.02E-08. *TSPA-LA Name:* GW_BDCF_MIC_Cs135. *Location in TSPA-LA:* Sections 6.3.11.2 and 6.3.11.3; Table 6.3.11-3.
MICCS137. Groundwater Biosphere Dose Conversion Factor (BDCF) for ^{137}Cs in modern interglacial climate ((Sv/year)/(Bq/m^3)). *Distribution:* Discrete. *Range:* 3.87E-08 to 4.56E-07. *Mean:* 1.30E-07. *Standard Deviation:* 6.33E-08. *TSPA-LA Name:* GW_BDCF_MIC_Cs137. *Location in TSPA-LA:* Sections 6.3.11.2 and 6.3.11.3; Table 6.3.11-3.
MICI129. Groundwater Biosphere Dose Conversion Factor (BDCF) for ^{129}I in modern interglacial climate ((Sv/year)/(Bq/m^3)). *Distribution:* Discrete. *Range:* 8.59E-08 to 1.13E-06. *Mean:* 1.29E-07. *Standard Deviation:* 5.28E-08. *TSPA-LA Name:* GW_BDCF_MIC_I129. *Location in TSPA-LA:* Sections 6.3.11.2 and 6.3.11.3; Table 6.3.11-3.
MICNP237. Groundwater Biosphere Dose Conversion Factor (BDCF) for ^{237}Np in modern interglacial climate ((Sv/year)/(Bq/m^3)). *Distribution:* Discrete. *Range:* 1.06E-07 to 8.05E-07. *Mean:* 2.74E-07. *Standard Deviation:* 9.70E-08. *TSPA-LA Name:* GW_BDCF_MIC_Np237. *Location in TSPA-LA:* Sections 6.3.11.2 and 6.3.11.3; Table 6.3.11-3.
MICPA231. Groundwater Biosphere Dose Conversion Factor (BDCF) for ^{231}Pa in modern interglacial climate ((Sv/year)/(Bq/m^3)). *Distribution:* Discrete. *Range:* 6.58E-07 to 8.56E-06. *Mean:* 2.44E-06. *Standard Deviation:* 1.02E-06. *TSPA-LA Name:* GW_BDCF_MIC_Pa231. *Location in TSPA-LA:* Sections 6.3.11.2 and 6.3.11.3; Table 6.3.11-3.
MICPU238. Groundwater Biosphere Dose Conversion Factor (BDCF) for ^{238}Pu in modern interglacial climate ((Sv/year)/(Bq/m^3)). *Distribution:* Discrete. *Range:* 2.61E-07 to 2.09E-006. *Mean:* 7.61E-07. *Standard Deviation:* 2.78E-07. *TSPA-LA Name:* GW_BDCF_MIC_Pu238. *Location in TSPA-LA:* Sections 6.3.11.2 and 6.3.11.3; Table 6.3.11-3.
MICPU239. Groundwater Biosphere Dose Conversion Factor (BDCF) for ^{239}Pu in modern interglacial climate ((Sv/year)/(Bq/m^3)). *Distribution:* Discrete. *Range:* 3.49E-07 to 2.93E-06. *Mean:* 9.55E-07. *Standard Deviation:* 3.37E-07. *TSPA-LA Name:* GW_BDCF_MIC_Pu239. *Location in TSPA-LA:* Sections 6.3.11.2 and 6.3.11.3; Table 6.3.11-3.
MICPU240. Groundwater Biosphere Dose Conversion Factor (BDCF) for ^{240}Pu in modern interglacial climate ((Sv/year)/(Bq/m^3)). *Distribution:* Discrete. *Range:* 3.47E-07 to 2.90E-06. *Mean:* 9.51E-07. *Standard Deviation:* 3.35E-07. *TSPA-LA Name:* GW_BDCF_MIC_Pu240. *Location in TSPA-LA:* Sections 6.3.11.2 and 6.3.11.3; Table 6.3.11-3.
MICRA226. Groundwater Biosphere Dose Conversion Factor (BDCF) for ^{210}Pb summed into ^{226}Ra in modern interglacial climate ((Sv/year)/(Bq/m^3)). *Distribution:* Discrete. *Range:* 2.90E-06 to 2.82E-05. *Mean:* 6.52E-06. *Standard Deviation:* 2.58E-06. *TSPA-LA Name:* GW_BDCF_MIC_Ra226_Pb210. *Location in TSPA-LA:* Sections 6.3.11.2 and 6.3.11.3; Table 6.3.11-3.
MICSE79. Groundwater Biosphere Dose Conversion Factor (BDCF) for ^{79}Se in modern interglacial climate. ((Sv/year)/(Bq/m^3)). *Distribution:* Discrete. *Range:* 3.62E-09 to 1.51E-06. *Mean:* 2.42E-08. *Standard Deviation:* 7.48E-08. *TSPA-LA Name:* GW_BDCF_MIC_Se79. *Location in TSPA-LA:* Sections 6.3.11.2 and 6.3.11.3; Table-6.3.11-3.
MICSN126. Groundwater Biosphere Dose Conversion Factor (BDCF) for ^{126}Sn in modern interglacial climate ((Sv/year)/(Bq/m^3)). *Distribution:* Discrete. *Range:* 8.92E-08 to 1.68E-06. *Mean:* 4.33E-07. *Standard Deviation:* 2.39E-07. *TSPA-LA Name:* GW_BDCF_MIC_Sn126. *Location in TSPA-LA:* Sections 6.3.11.2 and 6.3.11.3; Table 6.3.11-3.

Table K3-1. High-Level Summary of Epistemically Uncertain Variables (i.e., elements of **e**) Considered in the TSPA-LA (Sensitivity Analysis Name) (Continued)

NOTE: * indicates variable not considered in sensitivity analysis due to correlations.

MICSR90. Groundwater Biosphere Dose Conversion Factor (BDCF) for ^{90}Sr in modern interglacial climate ((Sv/year)/(Bq/m^3)). *Distribution:* Discrete. *Range:* 2.51E-08 to 8.60E-08. *Mean:* 3.43E-08. *Standard Deviation:* 6.59E-09. *TSPA-LA Name:* GW_BDCF_MIC_Sr90. *Location in TSPA-LA:* Sections 6.3.11.2 and 6.3.11.3; Table 6.3.11-3.
MICTC99. Groundwater Biosphere Dose Conversion Factor (BDCF) for ^{99}Tc in modern interglacial climate ((Sv/year)/(Bq/m^3)). *Distribution:* Discrete. *Range:* 5.28E-10 to 2.85E-08. *Mean:* 1.12E-09. *Standard Deviation:* 1.26E-09. *TSPA-LA Name:* GW_BDCF_MIC_Tc99. *Location in TSPA-LA:* Sections 6.3.11.2 and 6.3.11.3; Table-6.3.11-3.
MICTH229. Groundwater Biosphere Dose Conversion Factor (BDCF) for ^{229}Th in modern interglacial climate ((Sv/year)/(Bq/m^3)). *Distribution:* Discrete. *Range:* 7.43E-07 to 8.05E-06. *Mean:* 2.58E-06. *Standard Deviation:* 1.03E-06. *TSPA-LA Name:* GW_BDCF_MIC_Th229. *Location in TSPA-LA:* Sections 6.3.11.2 and 6.3.11.3; Table 6.3.11-3.
MICU232. Groundwater Biosphere Dose Conversion Factor (BDCF) for 232U in modern interglacial climate ((Sv/year)/(Bq/m^3)). *Distribution:* Discrete. *Range:* 2.87E-07 to 1.86E-06. *Mean:* 6.04E-07. *Standard Deviation:* 2.17E-07. *TSPA-LA Name:* GW_BDCF_MIC_U232. *Location in TSPA-LA:* Sections 6.3.11.2 and 6.3.11.3; Table 6.3.11-3.
MICU233. Groundwater Biosphere Dose Conversion Factor (BDCF) for ^{233}U in modern interglacial climate ((Sv/year)/(Bq/m^3)). *Distribution:* Discrete. *Range:* 4.13E-08 to 3.13E-07. *Mean:* 8.97E-08. *Standard Deviation:* 3.35E-08. *TSPA-LA Name:* GW_BDCF_MIC_U233. *Location in TSPA-LA:* Sections 6.3.11.2 and 6.3.11.3; Table 6.3.11-3.
MICU234. Groundwater Biosphere Dose Conversion Factor (BDCF) for ^{234}U in modern interglacial climate ((Sv/year)/(Bq/m^3)). *Distribution:* Discrete. *Range:* 3.96E-08 to 2.20E-07. *Mean:* 8.19E-08. *Standard Deviation:* 2.81E-08. *TSPA-LA Name:* GW_BDCF_MIC_U234. *Location in TSPA-LA:* Sections 6.3.11.2 and 6.3.11.3; Table 6.3.11-3.
MICU238. Groundwater Biosphere Dose Conversion Factor (BDCF) for ^{238}U in modern interglacial climate ((Sv/year)/(Bq/m^3)). *Distribution:* Discrete. *Range:* 3.85E-08 to 2.07E-07. *Mean:* 7.87E-08. *Standard Deviation:* 2.62E-08. *TSPA-LA Name:* GW_BDCF_MIC_U238. *Location in TSPA-LA:* Sections 6.3.11.2 and 6.3.11.3; Table 6.3.11-3.
NIOSA. Specific surface area of NiO (m^2/g). *Distribution:* Uniform. *Range:* 1 to 30. *TSPA-LA Name:* NiO_SA_a. *Location in TSPA-LA:* Table 6.3.8-4; S_{CP} in Equation 6.3.8-19.
PH2DHLNS. Pointer variable used to determine pH in 2DHLW Cell (Cell 1a) of CDSP waste packages under vapor influx conditions (dimensionless). *Distribution:* Uniform. *Range:* 0 to 1. *TSPA-LA Name:* Inpkg_pH_2DHLW_NS_Rand_a. *Location in TSPA-LA:* Section 6.3.7.2.2 Part IV.
PH2DHLS. Pointer variable used to determine pH in 2DHLW Cell (Cell 1a) of CDSP waste packages under liquid influx conditions (dimensionless). *Distribution:* Uniform. *Range:* 0 to 1. *TSPA-LA Name:* Inpkg_pH_2DHLW_S_Rand_a. *Location in TSPA-LA:* Section 6.3.7.2.2 Part IV.
PH2MCONS. Pointer variable used to determine pH in 2MCO Cell (Cell 1b) of CDSP waste packages under vapor influx conditions (dimensionless). *Distribution:* Uniform. *Range:* 0 to 1. *TSPA-LA Name:* Inpkg_pH_2MCO_NS_Rand_a. *Location in TSPA-LA:* Section 6.3.7.2.2 Part IV.
PH2MCOS. Pointer variable used to determine pH in 2MCO Cell (Cell 1b) of CDSP waste packages under liquid influx conditions (dimensionless). *Distribution:* Uniform. *Range:* 0 to 1. *TSPA-LA Name:* Inpkg_pH_2MCO_S_Rand_a. *Location in TSPA-LA:* Section 6.3.7.2.2 Part IV.
PH2RGER. Error term in regression equation for pH of corrosion products domain (dimensionless). *Distribution:* Truncated normal. *Range:* -0.64 to 0.64. *Mean/Median/Mode:* 0. *Standard Deviation:* 0.32. *TSPA-LA Name:* pH_Cell2_Regression_Error_a. *Location in TSPA-LA:* Equation 6.3.8-27.
PHCSNS. Pointer variable used to determine pH in CSNF Cell1 under vapor influx conditions (dimensionless). *Distribution:* Uniform. *Range:* 0 to 1. *TSPA-LA Name:* Inpkg_pH_CSNF_NS_Rand_a. *Location in TSPA-LA:* Section 6.3.7.2.2 Part IV.
PHCSS. Pointer variable used to determine pH in CSNF Cell1 under liquid influx conditions (dimensionless). *Distribution:* Uniform. *Range:* 0 to 1. *TSPA-LA Name:* Inpkg_pH_CSNF_S_Rand_a. *Location in TSPA-LA:* Section 6.3.7.2.2 Part IV.

Table K3-1. High-Level Summary of Epistemically Uncertain Variables (i.e., elements of **e**) Considered in the TSPA-LA (Sensitivity Analysis Name) (Continued)

NOTE: * indicates variable not considered in sensitivity analysis due to correlations.

PROBDSEF. Probability for undetected defects in drip shields (dimensionless). *Distribution:* Log-normal. *Median:* 4.3E-07. *Error Factor:* 14. *TSPA-LA Name:* UNC_DS_EF_conv_from_ln. *Location in TSPA-LA:* Section 6.4.1; Tables 6.4-1 and 6.4-2.
PROBWPEF. Probability for the undetected defects in waste packages (dimensionless). *Distribution:* Log-normal. *Median:* 4.14E-05. *Error Factor:* 8.17. *TSPA-LA Name:* UNC_WP_EF_conv_from_ln. *Location in TSPA-LA:* Section 6.4.2; Tables 6.4-1 and 6.4-2.
RHI85. The in-drift precipitated/salts (IDPS) process model uncertainty factor for the logarithm of the ionic strength of the in-drift waters at high relative humidity (≥85%) (log molal). *Distribution:* Triangular. *Range:* -0.1 to 0.1. *Mean/Median/Mode:* 0. *TSPA-LA Name:* PCE_I_Uncert_RH_85_100_a. *Location in TSPA-LA:* Section 6.4.1; Tables 6.4-1 and 6.4-2; Figure 6.4-4.
RHMU0. The IDPS process model uncertainty factor for the logarithm of the chloride concentration of the in-drift waters at relative humidity ≤20% (dimensionless). *Distribution:* Triangular. *Range:* -0.7 to 0.7. *Most Likely:* 0. *TSPA-LA Name:* PCE_Cl_MU_RH_0_20_a. *Location in TSPA-LA:* Sections 6.3.4, 6.3.4.2, 6.3.4.3.1, 6.3.4.3.2 and 6.3.5.2.3; Tables 6.3.4-2, 6.3.4-3 and 6.3.5-4.
RHMU20. The IDPS process model uncertainty factor for the logarithm of the chloride concentration of the in-drift waters at relative humidity >20 and ≤40% (dimensionless). *Distribution:* Triangular. *Range:* -0.5 to 0.5. *Most Likely:* 0. *TSPA-LA Name:* PCE_Cl_MU_RH_20_40_a. *Location in TSPA-LA:* Sections 6.3.4, 6.3.4.2, 6.3.4.3.1, 6.3.4.3.2 and 6.3.5.2.3; Tables 6.3.4-2, 6.3.4-3 and 6.3.5-4.
RHMU40. The IDPS process model uncertainty factor for the logarithm of the chloride concentration of the in-drift waters at relative humidity >40 and ≤65% (dimensionless). *Distribution:* Triangular. *Range:* -0.4 to 0.4. *Most Likely:* 0. *TSPA-LA Name:* PCE_Cl_MU_RH_40_65_a. *Location in TSPA-LA:* Sections 6.3.4, 6.3.4.2, 6.3.4.3.1, 6.3.4.3.2 and 6.3.5.2.3; Tables 6.3.4-2, 6.3.4-3 and 6.3.5-4.
RHMU65. The IDPS process model uncertainty factor for the logarithm of the chloride concentration of the in-drift waters at relative humidity >65 and ≤85% (dimensionless). *Distribution:* Triangular. *Range:* -0.1 to 0.1. *Most Likely:* 0. *TSPA-LA Name:* PCE_Cl_MU_RH_65_85_a. *Location in TSPA-LA:* Sections 6.3.4, 6.3.4.2, 6.3.4.3.1, 6.3.4.3.2 and 6.3.5.2.3; Tables 6.3.4-2, 6.3.4-3 and 6.3.5-4.
RHMU85*. The IDPS process model uncertainty factor for the logarithm of the chloride concentration of the in-drift waters at relative humidity >85% (dimensionless). *Distribution:* Triangular. *Range:* 0 to 0. *Most Likely:* 0. *TSPA-LA Name:* PCE_Cl_MU_RH_85_100_a*. *Location in TSPA-LA:* Sections 6.3.4, 6.3.4.2, 6.3.4.3.1, 6.3.4.3.2 and 6.3.5.2.3; Tables 6.3.4-2, 6.3.4-3 and 6.3.5-4.
RHMUN40. The IDPS process model uncertainty factor for the logarithm of the chloride + nitrate concentration of the in-drift waters at relative humidity >40% and ≤65% (dimensionless). *Distribution:* Triangular. *Range:* -0.57 to 0.57. *Most Likely:* 0. *TSPA-LA Name:* PCE_Cl_N_MU_RH_40_65_a. *Location in TSPA-LA:* Sections 6.3.4.3.2 and 6.3.5.2.3; Tables 6.3.4-2, 6.3.4-3 and 6.3.5-4.
RHMUN65. The IDPS process model uncertainty factor for the logarithm of the chloride + nitrate concentration of the in-drift waters at relative humidity >65% and ≤85% (dimensionless). *Distribution:* Triangular. *Range:* -0.22 to 0.22. *Most Likely:* 0. *TSPA-LA Name:* PCE_Cl_N_MU_RH_65_85_a. *Location in TSPA-LA:* Sections 6.3.4.3.2 and 6.3.5.2.3; Tables 6.3.4-2, 6.3.4-3 and 6.3.5-4.
RHMUN85*. The IDPS process model uncertainty factor for the logarithm of the chloride + nitrate concentration of the in-drift waters at relative humidity >85% (dimensionless). *Distribution:* Triangular. *Range:* 0 to 0. *Most Likely:* 0. *TSPA-LA Name:* PCE_Cl_N_MU_RH_85_100_a*. *Location in TSPA-LA:* Sections 6.3.4.3.2 and 6.3.5.2.3; Tables 6.3.4-2, 6.3.4-3 and 6.3.5-4.
RHMUNO0. The IDPS process model uncertainty factor for the logarithm of the chloride to nitrate ratio of the in-drift waters at relative humidity ≤20% (dimensionless). *Distribution:* Triangular. *Range:* -1.4 to 1.4. *Most Likely:* 0. *TSPA-LA Name:* PCE_Cl_NO3_MU_RH_0_20_a. *Location in TSPA-LA:* Sections 6.3.4.3.1, 6.3.4.3.2 and 6.3.5.2.3; Tables 6.3.4-2, 6.3.4-3 and 6.3.5-4.
RHMUNO20. The IDPS process model uncertainty factor for the logarithm of the chloride to nitrate ratio of the in-drift waters at relative humidity >20% and ≤65% (dimensionless). *Distribution:* Triangular. *Range:* -0.5 to 0.5. *Most Likely:* 0. *TSPA-LA Name:* PCE_Cl_NO3_MU_RH_20_65_a. *Location in TSPA-LA:* Sections 6.3.4.3.1, 6.3.4.3.2 and 6.3.5.2.3; Tables 6.3.4-2, 6.3.4-3 and 6.3.5-4.

Table K3-1. High-Level Summary of Epistemically Uncertain Variables (i.e., elements of **e**) Considered in the TSPA-LA (Sensitivity Analysis Name) (Continued)

NOTE: * indicates variable not considered in sensitivity analysis due to correlations.

RHMUNO65. The IDPS process model uncertainty factor for the logarithm of the chloride to nitrate ratio of the in-drift waters at relative humidity >65% and ≤85% (dimensionless). *Distribution:* Triangular. *Range:* -0.2 to 0.2. *Most Likely:* 0. *TSPA-LA Name:* PCE_Cl_NO3_MU_RH_65_85_a. *Location in TSPA-LA:* Sections 6.3.4.3.1, 6.3.4.3.2 and 6.3.5.2.3; Tables 6.3.4-2, 6.3.4-3 and 6.3.5-4.
RHMUNO85*. The IDPS process model uncertainty factor for the logarithm of the chloride to nitrate ratio of the in-drift waters at low relative humidity >85% (dimensionless). *Distribution:* Triangular. *Range:* 0 to 0. *Most Likely:* 0. *TSPA-LA Name:* PCE_Cl_NO3_MU_RH_85_100_a*. *Location in TSPA-LA:* Sections 6.3.4.3.1, 6.3.4.3.2 and 6.3.5.2.3; Tables 6.3.4-2, 6.3.4-3 and 6.3.5-4.
RHPH0. The IDPS process model uncertainty factor for the pH of the in-drift waters at relative humidity ≤65% (dimensionless). *Distribution:* Triangular. *Range:* -2 to 2. *Most Likely:* 0. *TSPA-LA Name:* PCE_pH_Uncert_RH_0_65_a. *Location in TSPA-LA:* Table 6.3.5-4.
RHPH65. The IDPS process model uncertainty factor for the pH of the in-drift waters at relative humidity >65 and ≤75% (dimensionless). *Distribution:* Triangular. *Range:* -1 to 1. *Most Likely:* 0. *TSPA-LA Name:* PCE_pH_Uncert_RH_65_75_a. *Location in TSPA-LA:* Table 6.3.5-4.
RHPH75. The IDPS process model uncertainty factor for the pH of the in-drift waters at relative humidity >75% (dimensionless). *Distribution:* Discrete. *Range:* -0.3123 to 0.4288. *TSPA-LA Name:* PCE_pH_Uncert_RH_75_100_a. *Location in TSPA-LA:* Table 6.3.5-4.
RSUSTHIK. Thickness of combined ash/soil mixture available for resuspension (m). *Distribution:* Uniform. *Range:* 0.001 to 0.003. *Mean/Median/Mode:* 0.002. *TSPA-LA Name:* Resuspension_Thickness_a. *Location in TSPA-LA:* Equation 6.3.11-6.
RUBMAXL. Volume of lithophysal rock that must fall to fill the drift (m^3/m). *Distribution:* Uniform. *Range:* 30 to 120. *TSPA-LA Name:* Vol_Rubble_Max_Lith_a. *Location in TSPA-LA:* Sections 6.3.5.2.3 and 6.6.3.1; Tables 6.3.5-4 and 6.6-2.
RUBMAXNL. Volume of nonlithophysal rock that must fall to fill the drift (m^3/m). *Distribution:* Uniform. *Range:* 30 to 120. *TSPA-LA Name:* Vol_Rubble_Max_NonLith_a. *Location in TSPA-LA:* Section 6.3.5.2.3 and 6.6.3.1; Tables 6.3.5-4 and 6.6-2.
SC_DPTH. Scour depth in Fortymile Wash at the fan apex (cm). *Distribution:* Uniform. *Range:* 73 to 122. *TSPA-LA Name:* Scour_Depth_a. *Location in TSPA-LA:* Table 6.5-5.
SCCTHR. Stress threshold for stress corrosion cracking (MPa). *Distribution:* Uniform. *Range:* 315.9 to 368.55. *TSPA-LA Name:* Stress_Thresh_SCC_a. *Location in TSPA-LA:* Table 6.3.5-3.
SCCTHRP. Residual stress threshold for SCC nucleation of Alloy 22 (as a percentage of yield strength in MPa) (dimensionless). *Distribution:* Uniform. *Range:* 90 to 105. *TSPA-LA Name:* Stress_Thresh_A22_a. *Location in TSPA-LA:* Section 6.6.1.3.7; Table 6.6-2.
SCHOBOLT. Fractional value used to interpolate between Schoepite and Boltwoodite look-up tables (dimensionless). *Distribution:* Uniform. *Range:* 0 to 1. *TSPA-LA Name:* Schoepite_Boltwoodite_Interp_a. *Location in TSPA-LA:* Table 6.3.7-58.
SEEPCON*. Pointer variable to determine the seepage/condensation regime for the first failed waste package in a percolation subregion (dimensionless). *Distribution:* Uniform. *Range:* 0 to 1. *TSPA-LA Name:* Seepage_Condensation_Prob_a*.
SEEPPRM. Logarithm of the mean fracture permeability in lithophysal rock units (dimensionless). *Distribution:* Triangular. *Range:* -0.92 to 0.92. *Mode:* 0. *TSPA-LA Name:* LogK_Uncert_Lith_a. *Location in TSPA-LA:* Sections 6.3.5.2.3, 6.3.3.1.2 and 6.3.3.1.3; Tables 6.3.5-4, 6.3.3-2 and 6.3.3-3.
SEEPPRMN. Logarithm of the mean fracture permeability in non-lithophysal rock units (dimensionless). *Distribution:* Triangular. *Range:* -0.68 to 0.68. *Mode:* 0. *TSPA-LA Name:* LogK_Uncert_NonLith_a. *Location in TSPA-LA:* Sections 6.3.5.2.3, 6.3.3.1.2 and 6.3.3.1.3; Tables 6.3.5-4, 6.3.3-2 and 6.3.3-3.
SEEPUNC. Uncertainty factor to account for small-scale heterogeneity in fracture permeability (dimensionless). *Distribution:* Uniform. *Range:* 0 to 1. *TSPA-LA Name:* Seepage_Uncertainty_a. *Location in TSPA-LA:* Section 6.3.3.1.2; Tables 6.3.3-3 and 6.3.5-4.
SEEPWAT. Pointer variable used to select which seepage water type in used in the physical and chemical environment (P&CE) submodel calculations (dimensionless). *Distribution:* Discrete. *Range:* 1 to 4. *TSPA-LA Name:* Seepage_Water_Type_a. *Location in TSPA-LA:* Table 6.3.5-4.

Table K3-1. High-Level Summary of Epistemically Uncertain Variables (i.e., elements of **e**) Considered in the TSPA-LA (Sensitivity Analysis Name) (Continued)

NOTE: * indicates variable not considered in sensitivity analysis due to correlations.

SMECSA. Specific surface area for smectite colloids (m^2/g). *Distribution:* Uniform. *Range:* 10 to 100. *TSPA-LA Name:* Specific_SA_Smectite_Col_a. *Location in TSPA-LA:* Table 6.3.7-62.
SOILDENS. Density of surface soil correlated with the volcanic BDCFs (kg/m^3). *Distribution:* Triangular. *Range:* 1300 to 1700. *Mean/Median/Mode:* 1500. *TSPA-LA Name:* Soil_Density_a. *Location in TSPA-LA:* Equation 6.3.11-6.
SZCOLRAL. Logarithm of colloid retardation factor in alluvium (dimensionless). *Distribution:* Piecewise uniform. *Range:* 0.903 to 3.715. *TSPA-LA Name:* CORAL. *Location in TSPA-LA:* Sections 6.3.10.1, 6.3.10.2 and 6.3.10.4.2; Table 6.3.10-2.
SZCOLRVO. Logarithm of colloid retardation factor in volcanic units (dimensionless). *Distribution:* Piecewise uniform. *Range:* 0.778 to 2.903. *TSPA-LA Name:* CORVO. *Location in TSPA-LA:* Sections 6.3.10.1, 6.3.10.2 and 6.3.10.4.2; Table 6.3.10-2.
SZCONCOL. Logarithm of ambient concentration of colloids in groundwater (g/mL). *Distribution:* Piecewise uniform. *Range:* -9 to -3.6. *TSPA-LA Name:* Conc_Col. *Location in TSPA-LA:* Table 6.3.10-2.
SZDENAL. Bulk density of alluvium (kg/m^3). *Distribution:* Normal. *Mean/Median/Mode:* 1910. *Standard Deviation:* 78. *TSPA-LA Name:* Alluvium_Density. *Location in TSPA-LA:* Table 6.3.10-2.
SZDIFCVO. Logarithm of effective diffusion coefficient in fractured volcanic units (m^2/s). *Distribution:* Piecewise uniform. *Range:* -11.3 to -9.3. *TSPA-LA Name:* DCVO. *Location in TSPA-LA:* Sections 6.3.10.2 and 6.3.10.5; Table 6.3.10-2.
SZFIPOVO. Logarithm of flowing interval porosity in volcanic units (dimensionless). *Distribution:* Piecewise uniform. *Range:* -5 to -1. *Mean/Median/Mode:* -3. *TSPA-LA Name:* FPVO. *Location in TSPA-LA:* Table 6.3.10-2.
SZFISPVO. Flowing interval spacing in fractured volcanic units (m). *Distribution:* Piecewise uniform. *Range:* 1.86 to 80. *TSPA-LA Name:* FISVO. *Location in TSPA-LA:* Section 6.3.10.5; Table 6.3.10-2.
SZGWSPDM. Logarithm of the scale factor used to characterize uncertainty in groundwater specific discharge (dimensionless). *Distribution:* Piecewise uniform. *Range:* -0.951 to 0.951. *TSPA-LA Name:* GWSPD. *Location in TSPA-LA:* Section 6.3.10.2; Table 6.3.10-2.
SZKDAMAL. Americium sorption coefficient in alluvium (mL/g). *Distribution:* Truncated normal. *Range:* 1000 to 10000. *Mean/Median/Mode:* 5500. *Standard Deviation:* 1500. *TSPA-LA Name:* Kd_Am_Al. *Location in TSPA-LA:* Section 6.3.10.2; Table 6.3.10-2.
SZKDAMCO. Americium sorption coefficient onto smectite colloids (mL/g). *Distribution:* Piecewise uniform. *Range:* 1.00E+04 to 1.00E+07. *TSPA-LA Name:* Kd_Am_Col. *Location in TSPA-LA:* Section 6.3.10.2; Table 6.3.10-2.
SZKDAMVO. Americium sorption coefficient in volcanic units (mL/g). *Distribution:* Truncated normal. *Range:* 1000 to 10000. *Mean/Median/Mode:* 5500. *Standard Deviation:* 1500. *TSPA-LA Name:* Kd_Am_Vo. *Location in TSPA-LA:* Section 6.3.10.2; Table 6.3.10-2.
SZKDCSAL. Cesium sorption coefficient in alluvium (mL/g). *Distribution:* Truncated normal. *Range:* 100 to 1000. *Mean/Median/Mode:* 728. *Standard Deviation:* 464. *TSPA-LA Name:* Kd_Cs_Al. *Location in TSPA-LA:* Section 6.3.10.2; Table 6.3.10-2.
SZKDCSCO. Cesium sorption coefficient onto smectite colloids (mL/g). *Distribution:* Piecewise uniform. *Range:* 50 to 5000. *TSPA-LA Name:* Kd_Cs_Col. *Location in TSPA-LA:* Section 6.3.10.2; Table 6.3.10-2.
SZKDCSVO. Cesium sorption coefficient in volcanic units (mL/g). *Distribution:* Piecewise uniform. *Range:* 100 to 6783. *TSPA-LA Name:* Kd_Cs_Vo. *Location in TSPA-LA:* Section 6.3.10.2; Table 6.3.10-2.
SZKDNPAL. Neptunium sorption coefficient in alluvium (mL/g). *Distribution:* Piecewise uniform. *Range:* 1.8 to 13. *TSPA-LA Name:* Kd_Np_Al. *Location in TSPA-LA:* Section 6.3.10.2; Table 6.3.10-2.
SZKDNPVO. Neptunium sorption coefficient in volcanic units (mL/g). *Distribution:* Piecewise uniform. *Range:* 0 to 6. *TSPA-LA Name:* Kd_Np_Vo. *Location in TSPA-LA:* Section 6.3.10.2; Table 6.3.10-2.
SZKDPUAL. Plutonium sorption coefficient in alluvium (mL/g). *Distribution:* Beta. *Range:* 50 to 300. *Mean/Median/Mode:* 100. *Standard Deviation:* 15. *TSPA-LA Name:* Kd_Pu_Al. *Location in TSPA-LA:* Section 6.3.10.2; Table 6.3.10-2.

Table K3-1. High-Level Summary of Epistemically Uncertain Variables (i.e., elements of **e**) Considered in the TSPA-LA (Sensitivity Analysis Name) (Continued)

NOTE: * indicates variable not considered in sensitivity analysis due to correlations.

SZKDPUCO. Plutonium sorption coefficient onto smectite colloids (mL/g). *Distribution:* Piecewise uniform. *Range:* 1.00E+03 to 1.00E+05. *TSPA-LA Name:* Kd_Pu_Col. *Location in TSPA-LA:* Section 6.3.10.2; Table 6.3.10-2.
SZKDPUVO. Plutonium sorption coefficient in volcanic units (mL/g). *Distribution:* Piecewise uniform. *Range:* 10 to 300. *TSPA-LA Name:* Kd_Pu_Vo. *Location in TSPA-LA:* Section 6.3.10.2; Table 6.3.10-2.
SZKDRAAL. Radium sorption coefficient in alluvium (mL/g). *Distribution:* Uniform. *Range:* 100 to 1000. *TSPA-LA Name:* Kd_Ra_Al. *Location in TSPA-LA:* Section 6.3.10.2; Table 6.3.10-2.
SZKDRAVO*. Radium sorption coefficient in volcanic units (mL/g). *Distribution:* Uniform. *Range:* 100 to 1000. *TSPA-LA Name:* Kd_Ra_Vo*. *Location in TSPA-LA:* Section 6.3.10.2; Table 6.3.10-2.
SZKDSEAL. Selenium sorption coefficient in alluvium (mL/g). *Distribution:* Truncated log normal. *Range:* 1 to 50. *Mean/Median/Mode:* 14. *Standard Deviation:* 11.2. *TSPA-LA Name:* Kd_Se_Al. *Location in TSPA-LA:* Section 6.3.10.2; Table 6.3.10-2.
SZKDSEVO. Selenium sorption coefficient in volcanic units (mL/g). *Distribution:* Truncated log normal. *Range:* 1 to 50. *Mean/Median/Mode:* 14. *Standard Deviation:* 11.2. *TSPA-LA Name:* Kd_Se_Vo. *Location in TSPA-LA:* Section 6.3.10.2; Table 6.3.10-2.
SZKDSNAL. Tin sorption coefficient in alluvium (mL/g). *Distribution:* Log uniform. *Range:* 1.00E+02 to 1.00E+05. *TSPA-LA Name:* Kd_Sn_Al. *Location in TSPA-LA:* Section 6.3.10.2; Table 6.3.10-2.
SZKDSNCO. Tin sorption coefficient onto smectite colloids (mL/g). *Distribution:* Log uniform. *Range:* 1.00E+05 to 1.00E+06. *TSPA-LA Name:* Kd_Sn_Col. *Location in TSPA-LA:* Section 6.3.10.2; Table 6.3.10-2.
SZKDSNVO. Tin sorption coefficient in volcanic units (mL/g). *Distribution:* Log uniform. *Range:* 1.00E+02 to 1.00E+05. *TSPA-LA Name:* Kd_Sn_Vo. *Location in TSPA-LA:* Section 6.3.10.2; Table 6.3.10-2.
SZKDSRAL. Strontium sorption coefficient in alluvium (mL/g). *Distribution:* Uniform. *Range:* 20 to 400. *TSPA-LA Name:* Kd_Sr_Al. *Location in TSPA-LA:* Section 6.3.10.2; Table 6.3.10-2.
SZKDSRVO. Strontium sorption coefficient in volcanic units (mL/g). *Distribution:* Uniform. *Range:* 20 to 400. *TSPA-LA Name:* Kd_Sr_Vo. *Location in TSPA-LA:* Section 6.3.10.2; Table 6.3.10-2.
SZKDUAL. Uranium sorption coefficient in alluvium (mL/g). *Distribution:* Piecewise uniform. *Range:* 1.7 to 8.9. *TSPA-LA Name:* Kd_U_Al. *Location in TSPA-LA:* Section 6.3.10.2; Table 6.3.10-2.
SZKDUVO. Uranium sorption coefficient in volcanic units (mL/g). *Distribution:* Piecewise uniform. *Range:* 0 to 20. *TSPA-LA Name:* Kd_U_Vo. *Location in TSPA-LA:* Section 6.3.10.2; Table 6.3.10-2.
SZLODISP. Logarithm of longitudinal dispersivity (m). *Distribution:* Right-truncated normal. *Range*: $-\infty$ to 3.5. Mean*:* 2.0. *Standard Deviation:* 0.75. *TSPA-LA Name:* LDISP. *Location in TSPA-LA:* Section 6.3.10.2; Table 6.3.10-2.
SZPORSAL. Effective porosity in shallow alluvium (dimensionless). *Distribution:* Truncated normal. *Range:* 0 to 0.3. *Mean:* 0.18. *Standard Deviation:* 0.051. *TSPA-LA Name:* NVF26. *Location in TSPA-LA:* Table 6.3.10-2.
SZPORUAL. Effective porosity in undifferentiated alluvium (valley fill) (dimensionless). *Distribution:* Truncated normal. *Range:* 0 to 0.3. *Mean:* 0.18. *Standard Deviation:* 0.051. *TSPA-LA Name:* NVF11. *Location in TSPA-LA:* Table 6.3.10-2.
SZRAHAVO. Ratio of horizontal anisotropy (north-south over east-west) in the permeability of the SZ volcanic units (dimensionless). *Distribution:* Piecewise uniform. *Range:* 0.05 to 20. *TSPA-LA Name:* HAVO. *Location in TSPA-LA:* Sections 6.3.10.2 and 6.3.10.5; Table 6.3.10-2.
SZSREG1X. Relative x location of point source in source region 1 (dimensionless). *Distribution:* Uniform. *Range:* 0 to 1. *TSPA-LA Name:* SRC1X. *Location in TSPA-LA:* Section 6.3.10.2; Table 6.3.10-2.
SZSREG1Y. Relative y location of point source in source region 1 (dimensionless). *Distribution:* Uniform. *Range:* 0 to 1. *TSPA-LA Name:* SRC1Y. *Location in TSPA-LA:* Section 6.3.10.2; Table 6.3.10-2.
SZSREG2X. Relative x location of point source in source region 2 (dimensionless). *Distribution:* Uniform. *Range:* 0 to 1. *TSPA-LA Name:* SRC2X. *Location in TSPA-LA:* Section 6.3.10.2; Table 6.3.10-2.
SZSREG2Y. Relative y location of point source in source region 2 (dimensionless). *Distribution:* Uniform. *Range:* 0 to 1. *TSPA-LA Name:* SRC2Y. *Location in TSPA-LA:* Section 6.3.10.2; Table 6.3.10-2.
SZSREG3X. Relative x location of point source in source region 3 (dimensionless). *Distribution:* Uniform. *Range:* 0 to 1. *TSPA-LA Name:* SRC3X. *Location in TSPA-LA:* Section 6.3.10.2; Table 6.3.10-2.

Table K3-1. High-Level Summary of Epistemically Uncertain Variables (i.e., elements of **e**) Considered in the TSPA-LA (Sensitivity Analysis Name) (Continued)

NOTE: * indicates variable not considered in sensitivity analysis due to correlations.

SZSREG3Y. Relative y location of point source in source region 3 (dimensionless). *Distribution:* Uniform. *Range:* 0 to 1. *TSPA-LA Name:* SRC3Y. *Location in TSPA-LA:* Section 6.3.10.2; Table 6.3.10-2.
SZSREG4X. Relative x location of point source in source region 4 (dimensionless). *Distribution:* Uniform. *Range:* 0 to 1. *TSPA-LA Name:* SRC4X. *Location in TSPA-LA:* Section 6.3.10.2; Table 6.3.10-2.
SZSREG4Y. Relative y location of point source in source region 4 (dimensionless). *Distribution:* Uniform. *Range:* 0 to 1. *TSPA-LA Name:* SRC4Y. *Location in TSPA-LA:* Section 6.3.10.2; Table 6.3.10-2.
SZWBNDAL. Northwestern boundary of alluvial uncertainty zone (dimensionless). *Distribution:* Uniform. *Range:* 0 to 1. *TSPA-LA Name:* FPLANW. *Location in TSPA-LA:* Section 6.3.10.2; Table 6.3.10-2.
THERMCON. Selector variable for one of three host-rock thermal conductivity scenarios (low, mean, and high) (dimensionless). *Distribution:* Discrete. *Range:* 1 to 3. *TSPA-LA Name:* Thermal_Conductivity_Uncert_a. *Location in TSPA-LA:* Sections 6.3.2.2, 6.3.2.3, 6.3.5.1.3, 6.3.5.2.3 and 6.6.2.2; Tables 6.3.2-1, 6.3.2-3 and 6.3.5-4.
UZCOKDAM. Colloid sorption coefficient for americium (mg/mg). *Calculated by:* Colloidal_Kd_Am_uz*Colloidal_Concentration_uz. *TSPA-LA Name:* Colloidal_Kc_Am_UZP. *Location in TSPA-LA:* Section 6.3.9.2.
UZCOKDCS. Colloid sorption coefficient for cesium (mg/mg). *Calculated by:* Colloidal_Kd_Cs_uz*Colloidal_Concentration_uz. *TSPA-LA Name:* Colloidal_Kc_Cs_UZP. *Location in TSPA-LA:* Section 6.3.9.2.
UZCOKDPA. Colloid sorption coefficient for protactinium (mg/mg). *Calculated by:* Colloidal_Kd_Am_uz*Colloidal_Concentration_uz. *TSPA-LA Name:* Colloidal_Kc_Pa_UZP. *Location in TSPA-LA:* Section 6.3.9.2.
UZCOKDPU. Colloid sorption coefficient for plutonium (mg/mg). *Calculated by:* Colloidal_Kd_Pu_uz*Colloidal_Concentration_uz. *TSPA-LA Name:* Colloidal_Kc_Pu_UZP. *Location in TSPA-LA:* Section 6.3.9.2.
UZCOKDSN. Colloid sorption coefficient for tin (mg/mg). *Calculated by:* Colloidal_Kd_Sn_uz*Colloidal_Concentration_uz. *TSPA-LA Name:* Colloidal_Kc_Sn_UZP. *Location in TSPA-LA:* Section 6.3.9.2.
UZCOKDTH. Colloid sorption coefficient for thorium (mg/mg). *Calculated by:* Calculated by Colloidal_Kd_Am_uz*Colloidal_Concentration_uz. *TSPA-LA Name:* Colloidal_Kc_Th_UZP. *Location in TSPA-LA:* Section 6.3.9.2.
UZFAG1. Fracture aperture for group 1 rock unit (chnf) (m). *Calculated by:* Por_group1_a/ff_group1_a. *TSPA-LA Name:* fa_group1_a. *Location in TSPA-LA:* Section 6.3.9.2; Equation 6.3.9-2; Fracture porosity values and frequency values are shown in Tables 6.3.9-6 and 6.3.9-7.
UZFAG2. Fracture aperture for group 2 rock unit (tswf) (m). *Calculated by:* Por_group2_a/ff_group2_a. *TSPA-LA Name:* fa_group2_a. *Location in TSPA-LA:* Section 6.3.9.2; Equation 6.3.9-2; Fracture porosity values and frequency values are shown in Tables 6.3.9-6 and 6.3.9-7.
UZFAG3. Fracture aperture for group 3 rock units (ch[2,3,4,5]fz, pcf[2,5]z, pp4fz, pp1fz, bf2fz, tr2fz) (m). *Calculated by:* Por_group3_a/ff_group3_a. *TSPA-LA Name:* fa_group3_a. *Location in TSPA-LA:* Section 6.3.9.2; Equation 6.3.9-2; Fracture porosity values and frequency values are shown in Tables 6.3.9-6 and 6.3.9-7.
UZFAG4. Fracture aperture for group 4 rock units (pp3fd, pp2fd, bf3fd, tr3fd) (m). *Calculated by:* Por_group4_a/ff_group4_a. *TSPA-LA Name:* fa_group4_a. *Location in TSPA-LA:* Section 6.3.9.2; Equation 6.3.9-2; Fracture porosity values and frequency values are shown in Tables 6.3.9-6 and 6.3.9-7.
UZFAG5. Fracture aperture for group 5 rock units (ch1fz, pcf1z, ch6fz, pcf6z) (m). *Calculated by:* Por_group5_a/ff_group5_a. *TSPA-LA Name:* fa_group5_a. *Location in TSPA-LA:* Section 6.3.9.2; Equation 6.3.9-2; Fracture porosity values and frequency values are shown in Tables 6.3.9-6 and 6.3.9-7.
UZFAG6. Fracture aperture for group 6 rock units (ch[1,2,3,4,5,6]fv) (m). *Calculated by:* Por_group6_a/ff_group6_a. *TSPA-LA Name:* fa_group6_a. *Location in TSPA-LA:* Section 6.3.9.2; Equation 6.3.9-2; Fracture porosity values and frequency values are shown in Tables 6.3.9-6 and 6.3.9-7.
UZFAG7. Fracture aperture for group 7 rock units (tswf9, pcf39, tswfv, tswfz) (m). *Calculated by:* Por_group7_a/ff_group7_a. *TSPA-LA Name:* fa_group7_a. *Location in TSPA-LA:* Section 6.3.9.2; Equation 6.3.9-2; Fracture porosity values and frequency values are shown in Tables 6.3.9-6 and 6.3.9-7.

Table K3-1. High-Level Summary of Epistemically Uncertain Variables (i.e., elements of **e**) Considered in the TSPA-LA (Sensitivity Analysis Name) (Continued)

NOTE: * indicates variable not considered in sensitivity analysis due to correlations.

UZFAG8. Fracture aperture for group 8 rock units (tswf[4,5], tswf[6,7], tswf8, pcf38) (m). *Calculated by:* Por_group8_a/ff_group8_a. *TSPA-LA Name:* fa_group8_a. *Location in TSPA-LA:* Section 6.3.9.2; Equation 6.3.9-2; Fracture porosity values and frequency values are shown in Tables 6.3.9-6 and 6.3.9-7.
UZFAG9. Fracture aperture for group 9 rock units (tswf3) (m). *Calculated by:* Por_group9_a/ff_group9_a. *TSPA-LA Name:* fa_group9_a. *Location in TSPA-LA:* Section 6.3.9.2; Equation 6.3.9-2; Fracture porosity values and frequency values are shown in Tables 6.3.9-6 and 6.3.9-7.
UZGAM. Active fracture model (AFM) Gamma parameter (dimensionless). *Distribution:* Uniform. *Range:* 0.2 to 0.6. *TSPA-LA Name:* Gamma_AFM_a. *Location in TSPA-LA:* Sections 6.3.9.2, 6.3.9.3 and 6.3.9.4.1; Table 6.3.9-5.
UZKDAMDT. Sorption coefficient of americium in devitrified tuff units of UZ (mL/g). *Distribution:* Truncated normal. *Range:* 1000 to 10000. *Mean:* 5500. *Standard Deviation:* 1500. *TSPA-LA Name:* KdAm_Devit_a. *Location in TSPA-LA:* Sections 6.3.9.2 and 6.3.9.3; Equation 6.3.9-3; Table 6.3.9-2.
UZKDAMVT*. Sorption coefficient of americium in vitrified tuff units of UZ (mL/g). *Distribution:* Piecewise uniform. *Range:* 100 to 1000. *Median:* 400. *TSPA-LA Name:* KdAm_Vit_a*. *Location in TSPA-LA:* Sections 6.3.9.2 and 6.3.9.3; Equation 6.3.9-3; Table 6.3.9-2.
UZKDAMZT*. Sorption coefficient of americium in zeolitic tuff units of UZ (mL/g). *Distribution:* Truncated normal. *Range:* 1000 to 10000. *Mean:* 5500. *Standard Deviation:* 1500. *TSPA-LA Name:* KdAm_Zeo_a*. *Location in TSPA-LA:* Sections 6.3.9.2 and 6.3.9.3; Equation 6.3.9-3; Table 6.3.9-2.
UZKDCSDT. Sorption coefficient of cesium in devitrified tuff units of UZ (mL/g). *Distribution:* Uniform. *Range:* 1 to 15. *TSPA-LA Name:* KdCs_Devit_a. *Location in TSPA-LA:* Sections 6.3.9.2 and 6.3.9.3; Equation 6.3.9-3; Table 6.3.9-2.
UZKDCSVT*. Sorption coefficient of cesium in vitrified tuff units of UZ (mL/g). *Distribution:* Piecewise uniform. *Range:* 0 to 100. *Median:* 2. *TSPA-LA Name:* KdCs_Vit_a*. *Location in TSPA-LA:* Sections 6.3.9.2 and 6.3.9.3; Equation 6.3.9-3; Table 6.3.9-2.
UZKDCSZT. Sorption coefficient for cesium in zeolitic tuff units of UZ (mL/g). *Distribution:* Piecewise uniform. *Range:* 425 to 20000. *Median:* 5,000. *TSPA-LA Name:* KdCs_Zeo_a. *Location in TSPA-LA:* Sections 6.3.9.2 and 6.3.9.3; Equation 6.3.9-3; Table 6.3.9-2.
UZKDNPDT. Sorption coefficient for neptunium in devitrified tuff units of UZ (mL/g). *Distribution:* Piecewise uniform. *Range:* 0 to 6. *Median:* 0.5. *TSPA-LA Name:* KdNp_Devit_a. *Location in TSPA-LA:* Sections 6.3.9.2 and 6.3.9.3; Equation 6.3.9-3; Table 6.3.9-2.
UZKDNPVT*, Sorption coefficient for neptunium in vitrified tuff units of UZ (mL/g). *Distribution:* Piecewise uniform. *Range:* 0 to 3. *Median:* 1. *TSPA-LA Name:* KdNp_Vit_a*. *Location in TSPA-LA:* Sections 6.3.9.2 and 6.3.9.3; Equation 6.3.9-3; Table 6.3.9-2.
UZKDNPZT*. Sorption coefficient for neptunium in zeolitic tuff units of UZ (mL/g). *Distribution:* Piecewise uniform. *Range:* 0 to 6. *Median:* 0.5. *TSPA-LA Name:* KdNp_Zeo_a*. *Location in TSPA-LA:* Sections 6.3.9.2 and 6.3.9.3; Equation 6.3.9-3; Table 6.3.9-2.
UZKDPADT. Sorption coefficient for protactinium in devitrified tuff units of UZ (mL/g). *Distribution:* Truncated normal. *Range:* 1000 to 10000. *Mean:* 5500. *Standard Deviation:* 1500. *TSPA-LA Name:* KdPa_Devit_a. *Location in TSPA-LA:* Sections 6.3.9.2 and 6.3.9.3; Equation 6.3.9-3; Table 6.3.9-2.
UZKDPAVT*. Sorption coefficient for protactinium in vitrified tuff units of UZ (mL/g). *Distribution:* Truncated normal. *Range:* 1000 to 10000. *Mean:* 5500. *Standard Deviation:* 1500. *TSPA-LA Name:* KdPa_Vit_a*. *Location in TSPA-LA:* Sections 6.3.9.2 and 6.3.9.3; Equation 6.3.9-3; Table 6.3.9-2.
UZKDPAZT*. Sorption coefficient for protactinium in zeolitic tuff units of UZ (mL/g). *Distribution:* Truncated normal. *Range:* 1000 to 10000. *Mean:* 5500. *Standard Deviation:* 1500. *TSPA-LA Name:* KdPa_Zeo_a*. *Location in TSPA-LA:* Sections 6.3.9.2 and 6.3.9.3; Equation 6.3.9-3; Table 6.3.9-2.
UZKDPUDT. Sorption coefficient for plutonium in devitrified tuff units of UZ (mL/g). *Distribution:* Piecewise uniform. *Range:* 10 to 200. *Median:* 70. *TSPA-LA Name:* KdPu_Devit_a. *Location in TSPA-LA:* Sections 6.3.9.2 and 6.3.9.3; Equation 6.3.9-3; Table 6.3.9-2.
UZKDPUVT*. Sorption coefficient for plutonium in vitrified tuff units of UZ (mL/g). *Distribution:* Piecewise uniform. *Range:* 10 to 200. *Median:* 100. *TSPA-LA Name:* KdPu_Vit_a*. *Location in TSPA-LA:* Sections 6.3.9.2 and 6.3.9.3; Equation 6.3.9-3; Table 6.3.9-2.

Table K3-1. High-Level Summary of Epistemically Uncertain Variables (i.e., elements of **e**) Considered in the TSPA-LA (Sensitivity Analysis Name) (Continued)

NOTE: * indicates variable not considered in sensitivity analysis due to correlations.

UZKDPUZT*. Sorption coefficient for plutonium in zeolitic tuff units of UZ (mL/g). *Distribution:* Piecewise uniform. *Range:* 10 to 200. *Median:* 100. *TSPA-LA Name:* KdPu_Zeo_a*. *Location in TSPA-LA:* Sections 6.3.9.2 and 6.3.9.3; Equation 6.3.9-3; Table 6.3.9-2.
UZKDRADT*. Sorption coefficient for radium in devitrified tuff units of UZ (mL/g). *Distribution:* Uniform. *Range:* 100 to 1000. *TSPA-LA Name:* KdRa_Devit_a*. *Location in TSPA-LA:* Sections 6.3.9.2 and 6.3.9.3; Equation 6.3.9-3; Table 6.3.9-2.
UZKDRAVT*. Sorption coefficient for radium in vitrified tuff units of UZ (mL/g). *Distribution:* Uniform. *Range:* 50 to 600. *TSPA-LA Name:* KdRa_Vit_a*. *Location in TSPA-LA:* Sections 6.3.9.2 and 6.3.9.3; Equation 6.3.9-3; Table 6.3.9-2.
UZKDRAZT*. Sorption coefficient for radium in zeolitic tuff units of UZ (mL/g). *Distribution:* Uniform. *Range:* 1000 to 5000. *TSPA-LA Name:* KdRa_Zeo_a*. *Location in TSPA-LA:* Sections 6.3.9.2 and 6.3.9.3; Equation 6.3.9-3; Table 6.3.9-2.
UZKDSEDT. Sorption coefficient for selenium in devitrified tuff units of UZ (mL/g). *Distribution:* Truncated log normal. *Range:* 1 to 50. *Mean:* 14. *Standard Deviation:* 11.2. *TSPA-LA Name:* KdSe_Devit_a. *Location in TSPA-LA:* Sections 6.3.9.2 and 6.3.9.3; Equation 6.3.9-3; Table 6.3.9-2.
UZKDSEVT*. Sorption coefficient for selenium in vitrified tuff units of UZ (mL/g). *Distribution:* Truncated log normal. *Range:* 0 to 25. *Mean:* 8.6. *Standard Deviation:* 7.9. *TSPA-LA Name:* KdSe_Vit_a*. *Location in TSPA-LA:* Sections 6.3.9.2 and 6.3.9.3; Equation 6.3.9-3; Table 6.3.9-2.
UZKDSEZT*. Sorption coefficient for selenium in zeolitic tuff units of UZ (mL/g). *Distribution:* Truncated log normal. *Range:* 1 to 35. *Mean:* 14.3. *Standard Deviation:* 7.9. *TSPA-LA Name:* KdSe_Zeo_a*. *Location in TSPA-LA:* Sections 6.3.9.2 and 6.3.9.3; Equation 6.3.9-3; Table 6.3.9-2.
UZKDSNDT. Sorption coefficient for tin in devitrified tuff units of UZ (mL/g). *Distribution:* Log-uniform. *Range:* 100 to 100000. *TSPA-LA Name:* KdSn_Devit_a. *Location in TSPA-LA:* Sections 6.3.9.2 and 6.3.9.3; Equation 6.3.9-3; Table 6.3.9-2.
UZKDSNVT*. Sorption coefficient for tin in vitrified tuff units of UZ (mL/g). *Distribution:* Log-uniform. *Range:* 100 to 5000. *TSPA-LA Name:* KdSn_Vit_a*. *Location in TSPA-LA:* Sections 6.3.9.2 and 6.3.9.3; Equation 6.3.9-3; Table 6.3.9-2.
UZKDSNZT*. Sorption coefficient for tin in zeolitic tuff units of UZ (mL/g). *Distribution:* Log-uniform. *Range:* 100 to 5000. *TSPA-LA Name:* KdSn_Zeo_a*. *Location in TSPA-LA:* Sections 6.3.9.2 and 6.3.9.3; Equation 6.3.9-3; Table 6.3.9-2.
UZKDSRDT. Sorption coefficient for strontium in devitrified tuff units of UZ (mL/g). *Distribution:* Uniform. *Range:* 10 to 70. *TSPA-LA Name:* KdSr_Devit_a. *Location in TSPA-LA:* Sections 6.3.9.2 and 6.3.9.3; Equation 6.3.9-3; Table 6.3.9-2.
UZKDSRVT*. Sorption coefficient for strontium in vitrified tuff units of UZ (mL/g). *Distribution:* Uniform. *Range:* 0 to 50. *TSPA-LA Name:* KdSr_Vit_a*. *Location in TSPA-LA:* Sections 6.3.9.2 and 6.3.9.3; Equation 6.3.9-3; Table 6.3.9-2.
UZKDSRZT*. Sorption coefficient for strontium in zeolitic tuff units of UZ (mL/g). *Distribution:* Uniform. *Range:* 50 to 2000. *TSPA-LA Name:* KdSr_Zeo_a*. *Location in TSPA-LA:* Sections 6.3.9.2 and 6.3.9.3; Equation 6.3.9-3; Table 6.3.9-2.
UZKDTHDT. Sorption coefficient for thorium in devitrified tuff units of UZ (mL/g). *Distribution:* Uniform. *Range:* 1000 to 10000. *TSPA-LA Name:* KdTh_Devit_a. *Location in TSPA-LA:* Sections 6.3.9.2 and 6.3.9.3; Equation 6.3.9-3; Table 6.3.9-2.
UZKDTHVT*. Sorption coefficient for thorium in vitrified tuff units of UZ (mL/g). *Distribution:* Uniform. *Range:* 1000 to 10000. *TSPA-LA Name:* KdTh_Vit_a*. *Location in TSPA-LA:* Sections 6.3.9.2 and 6.3.9.3; Equation 6.3.9-3; Table 6.3.9-2.
UZKDTHZT*. Sorption coefficient for thorium in zeolitic tuff units of UZ (mL/g). *Distribution:* Uniform. *Range:* 1000 to 30000. *TSPA-LA Name:* KdTh_Zeo_a*. *Location in TSPA-LA:* Sections 6.3.9.2 and 6.3.9.3; Equation 6.3.9-3; Table 6.3.9-2.
UZKDUDT. Sorption coefficient for uranium in devitrified tuff units of UZ (mL/g). *Distribution:* Piecewise uniform. *Range:* 0 to 4. *Median:* 0.2. *TSPA-LA Name:* KdU_Devit_a. *Location in TSPA-LA:* Sections 6.3.9.2 and 6.3.9.3; Equation 6.3.9-3; Table 6.3.9-2.

Table K3-1. High-Level Summary of Epistemically Uncertain Variables (i.e., elements of **e**) Considered in the TSPA-LA (Sensitivity Analysis Name) (Continued)

NOTE: * indicates variable not considered in sensitivity analysis due to correlations.

UZKDUVT*. Sorption coefficient for uranium in vitrified tuff units of UZ (mL/g). *Distribution:* Piecewise uniform. *Range:* 0 to 3. *Median:* 0.2. *TSPA-LA Name:* KdU_Vit_a*. *Location in TSPA-LA:* Sections 6.3.9.2 and 6.3.9.3; Equation 6.3.9-3; Table 6.3.9-2.
UZKDUZT*. Sorption coefficient for uranium in zeolitic tuff units of UZ (mL/g). *Distribution:* Piecewise uniform. *Range:* 0 to 30. *Median:* 0.5. *TSPA-LA Name:* KdU_Zeo_a*. *Location in TSPA-LA:* Sections 6.3.9.2 and 6.3.9.3; Equation 6.3.9-3; Table 6.3.9-2.
UZRCOL. Colloid retardation factor (dimensionless). *Distribution:* Piecewise uniform. *Range:* 6 to 799.83. *TSPA-LA Name:* Colloidal_Retard_Factor_dist_a. *Location in TSPA-LA:* Sections 6.3.9.2 and 6.3.9.3; Table 6.3.9-12.
UZTORRG1. Logarithm of the tortuosity in rock group 1 (dimensionless). *Distribution:* Left truncated normal. *Range*: 0 to ∞. *Mean:* -1.15. *Standard Deviation:* 0.29. *TSPA-LA Name:* UZ_Tortuosity_RG1. *Location in TSPA-LA:* Section 6.3.9.2; Table 6.3.9-4.
UZTORRG2. Logarithm of the tortuosity in rock group 2 (dimensionless). *Distribution:* Left truncated normal. *Range*: 0 to ∞. *Mean:* -3.62. *Standard Deviation:* 0.29. *TSPA-LA Name:* UZ_Tortuosity_RG2. *Location in TSPA-LA:* Section 6.3.9.2; Table 6.3.9-4.
UZTORRG3. Logarithm of the tortuosity in rock group 3 (dimensionless). *Distribution:* Left truncated normal. *Range*: 0 to ∞. *Mean:* -1.84. *Standard Deviation:* 0.29. *TSPA-LA Name:* UZ_Tortuosity_RG3. *Location in TSPA-LA:* Section 6.3.9.2; Table 6.3.9-4.
WATRCKIN. Parameter used to correlate WRIP_beta so that it resamples at the same probability level throughout a realization (dimensionless). *Distribution:* Uniform. *Range:* 0 to 1. *TSPA-LA Name:* WRIP_beta_rand_a. *Location in TSPA-LA:* Section 6.3.4.2; Table 6.3.4-1.
WDCRCDEN. Ratio of SCC area to unit of seismic damaged area for a waste package (dimensionless). *Distribution:* Uniform. *Range:* 0.00327 to 0.0131. *TSPA-LA Name:* WP_Crack_Area_Density_a. *Location in TSPA-LA:* Table 6.6-2.
WDDEFCNT. Flaw density parameter (flaws per mm^3 of weld) (dimensionless). *Distribution:* Gamma. *Mean:* 4.529E-07. *Standard Deviation:* 1.654E-07. *TSPA-LA Name:* Defect_Count_a. *Location in TSPA-LA:* Section 6.3.5.1.2; Table 6.3.5-3.
WDDEFSZE. Flaw size parameter (flaw size per mm of weld) (dimensionless). *Distribution:* Gamma. *Mean:* 0.2205. *Standard Deviation:* 0.0833. *TSPA-LA Name:* Defect_Size_a. *Location in TSPA-LA:* Section 6.3.5.1.2; Table 6.3.5-3; Equation 6.3.5-10.
WDDSAGGC. Topside general corrosion rate of the drip shield (nm/yr). *Distribution:* Normal. *Mean:* 46.067. *Standard Deviation:* 1.187. *TSPA-LA Name:* WDDSAggrGC_Mean_a. *Location in TSPA-LA:* Sections 6.3.5.1.2 and 6.3.5.1.3; Table 6.3.5-3.
WDDSBEGC. Underside general corrosion rate of the drip shield (mm/yr). *Distribution:* Normal. *Mean:* 5.15E-06. *Standard Deviation:* 8.31E-07. *TSPA-LA Name:* WDDSBenignGC_Mean_a. *Location in TSPA-LA:* Sections 6.3.5.1.2 and 6.3.5.1.3; Table 6.3.5-3.
WDDSGC29. General corrosion rate ratio for drip shield support material (ratio of Titanium Grade 29 to Titanium Grade 7) (dimensionless). *Distribution:* Discrete. *Range:* 1 to 6.6786. *TSPA-LA Name:* WDDSGC_29_a. *Location in TSPA-LA:* Section 6.3.5.1.2.
WDGCA22. Temperature dependent slope term of Alloy 22 general corrosion rate (K). *Distribution:* Truncated normal. *Range:* 666 to 7731. *Mean:* 4905. *Standard Deviation:* 1413. *TSPA-LA Name:* C1_GenCorr_A22_a. *Location in TSPA-LA:* Sections 6.3.5.1.2 and 6.3.5.1.3; Tables 6.3.5-3 and 6.3.5-4; Equation 6.3.5-4.
WDGCUA22. Variable for selecting distribution for general corrosion rate (low, medium, or high) (dimensionless). *Distribution:* Discrete. *Range:* 1 to 3. *TSPA-LA Name:* GC_ULevel_A22_a. *Location in TSPA-LA:* Table 6.3.5-4.
WDLCRATE. Crevice corrosion (localized corrosion) propagation rate (mm/yr). *Distribution:* Log uniform. *Range:* 0.0127 to 1.27. *TSPA-LA Name:* LC_rate_a. *Location in TSPA-LA:* Sections 6.3.5.2.1, 6.3.5.2.2, 6.3.5.2.3, 6.3.5.3.2 and 6.3.5.4; Table 6.3.5-4.
WDMICRHT. Relative humidity threshold for initiating microbially induced corrosion (dimensionless). *Distribution:* Uniform. *Range:* 0.75 to 0.9. *TSPA-LA Name:* MIC_RHThresh_a. *Location in TSPA-LA:* Sections 6.3.5.1.2 and 6.3.5.1.3; Tables 6.3.5-3 and 6.3.5-4.

Table K3-1. High-Level Summary of Epistemically Uncertain Variables (i.e., elements of **e**) Considered in the TSPA-LA (Sensitivity Analysis Name) (Continued)

NOTE: * indicates variable not considered in sensitivity analysis due to correlations.

WDNSCC. Stress corrosion cracking growth rate exponent (repassivation slope) (dimensionless). *Distribution:* Truncated normal. *Range:* 0.935 to 1.395. *Mean:* 1.165. *Standard Deviation:* 0.115. *TSPA-LA Name:* n_SCC_a. *Location in TSPA-LA:* Sections 6.3.5.1.2 and 6.3.5.4; Table 6.3.5-3; Equations 6.3.5-13 and 6.3.5-14.
WDZOLID. Deviation from median yield strength range for outer lid (dimensionless). *Distribution:* Truncated normal. *Range:* -3 to 3. *Mean/Median/Mode:* 0. *Standard Deviation:* 1. *TSPA-LA Name:* z_OL_a. *Location in TSPA-LA:* Sections 6.3.5.1.2 and 6.3.5.1.3; Table 6.3.5-3.
WFDEGEXF. The surface area exposure factor for the amount of HLW glass contacted by water (dimensionless). *Distribution:* Triangular. *Range:* 4 to 17. *Mode:* 4. *TSPA-LA Name:* Exposure_Factor_a. *Location in TSPA-LA:* Sections 6.3.7.4.3.2 and 6.3.7.4.3.3; Equation 6.3.7-9; Table 6.3.7-32.
WPFLUX. Waste package flux splitting factor (dimensionless). *Distribution:* Uniform. *Range:* 0 to 2.41. *TSPA-LA Name:* WP_Flux_Uncertainty_a. *Location in TSPA-LA:* Sections 6.3.6.1, 6.3.6.2 and 6.3.6.3; Tables 6.3.6-1, 6.3.6-2 and 6.3.8-4; Equation 6.3.6-6.

Table K3-2. High-Level Summary of Epistemically Uncertain Variables (i.e., elements of **e**) Considered in the TSPA-LA (TSPA Parameter Name)

NOTE: * indicates variable not considered in sensitivity analysis due to correlations.

Alluvium_Density - Bulk density of alluvium (kg/m^3). *Distribution:* Normal. *Mean/Median/Mode:* 1910. *Standard Deviation:* 78. *Sensitivity Name:* SZDENAL. *Location in TSPA-LA:* Table 6.3.10-2.
Alpha_Uncert_Lith_a - van Genuchten capillary strength parameter in lithophysal rock units (Pa). *Distribution:* Triangular. *Range:* -105 to 105. *Mean/Median/Mode:* 0. *Sensitivity Name:* ALPHAL. *Location in TSPA-LA:* Sections 6.3.3.1.2 and 6.3.3.1.3; Tables 6.3.3-1, 6.3.3-3 and 6.3.5-4.
Alpha_Uncert_NonLith_a* - van Genuchten capillary strength parameter in nonlithophysal rock units (Pa). *Distribution:* Triangular. *Range:* -105 to 105. *Mean/Median/Mode:* 0. *Sensitivity Name:* ALPHANL*. *Location in TSPA-LA:* Section 6.3.3.1.2; Tables 6.3.3-1, 6.3.3-3 and 6.3.5-4.
Am_Eps_1_high_a* - Logarithm of the scale factor used to characterize uncertainty in americium solubility at ionic strength values between 1 and 3 molal (dimensionless). *Distribution:* Truncated normal. *Range:* -2.08 to 2.08. *Mean:* 0. *Standard Deviation:* 1.04. *Sensitivity Name:* EP2HIAM*. *Location in TSPA-LA:* Sections 6.3.7.5.1, 6.3.7.5.2 and 6.3.7.5.3; Equation 6.3.7-13a; Table 6.3.7-41.
Am_Eps_1_low_a - Logarithm of the scale factor used to characterize uncertainty in americium solubility at an ionic strength below 1 molal (dimensionless). *Distribution:* Truncated normal. *Range:* -2 to 2. *Mean:* 0. *Standard Deviation:* 1. *Sensitivity Name:* EP1LOWAM. *Location in TSPA-LA:* Sections 6.3.7.5.1, 6.3.7.5.2 and 6.3.7.5.3; Table 6.3.7-41; Equation 6.3.7-13a.
Am_Eps_2_CDSP_High_a* - Term associated with uncertainty in americium solubility due to variations in fluoride concentration for CDSP waste packages when ionic strength is greater than or equal to 0.004 molal and for the invert below CDSP waste packages (mg/L). *Distribution:* Triangular. *Range:* 0 to 688.6. *Most Likely:* 0. *Sensitivity Name:* EP2HICDAM*. *Location in TSPA-LA:* Sections 6.3.7.5.2 and 6.3.7.5.3; Table 6.3.7-41; Equation 6.3.7-13a.
Am_Eps_2_CSNF_High_a - Term associated with uncertainty in americium solubility due to variations in fluoride concentration for CSNF waste packages when ionic strength is greater than or equal to 0.2 molal and for the invert below CSNF waste packages (mg/L). *Distribution:* Triangular. *Range:* 0 to 109.03. *Most Likely:* 0. *Sensitivity Name:* EP2HICAM. *Location in TSPA-LA:* Sections 6.3.7.5.2 and 6.3.7.5.3; Table 6.3.7-41; Equation 6.3.7-13a.
Am_Eps_2_Glass_Low_a* - Term associated with uncertainty in americium solubility due to variations in fluoride concentration for CDSP waste packages Cell 1a, Cell 1b when ionic strength is less than 0.004 molal, and CSNF waste packages when ionic strength is less than 0.2 molal (mg/L). *Distribution:* Triangular. *Range:* 0 to 4.42. *Most Likely:* 0. *Sensitivity Name:* EP2LOWAM*. *Location in TSPA-LA:* Sections 6.3.7.5.2 and 6.3.7.5.3; Table 6.3.7-41; Equation 6.3.7-13a.
Ash_Density_a - Tephra settled density (kg/m^3). *Distribution:* Truncated normal. *Range:* 300 to 1500. *Mean:* 1000. *Standard Deviation:* 100. *Sensitivity Name:* ASHDENS. *Location in TSPA-LA:* Table 6.5-5.
b_Tillage_a - Depth of soil within which radionuclides contribute to dose from external exposure (m). *Distribution:* Uniform. *Range:* 0.05 to 0.3. *Sensitivity Name:* BTILLAGE. *Location in TSPA-LA:* Table 6.5-5.
Background_Alpha_a - Natural background levels of alpha emitters in groundwater (pCi/L). *Distribution:* Truncated normal. *Range:* 0 to 0.71. *Mean/Median/Mode:* 0.5. *Sensitivity Name:* BCKALPHA. *Location in TSPA-LA:* Sections 6.3.10.2 and 6.3.11.2; Table 6.3.10-6.
Background_Ra226_Ra228_a - Natural background levels of combined ^{226}Ra and ^{228}Ra in groundwater (pCi/L). *Distribution:* Truncated normal. *Range:* 0 to 0.71. *Mean/Median/Mode:* 0.5. *Sensitivity Name:* BCKRA226. *Location in TSPA-LA:* Sections 6.3.10.2 and 6.3.11.2; Table 6.3.10-6.
BDCF_Inh_LT - Pointer variable for long-term inhalation dose conversion factor for volcanic ash exposure (dimensionless). *Distribution:* Discrete. *Range:* 1 to 300. *Sensitivity Name:* INHLTPV. *Location in TSPA-LA:* Section 6.3.11; Equation 6.3.11-4.
BDCF_Inh_ShT - Pointer variable for short-term inhalation dose conversion factor for volcanic ash exposure (dimensionless). *Distribution:* Discrete. *Range:* 1 to 300. *Sensitivity Name:* INHSTPV. *Location in TSPA-LA:* Section 6.3.11; Equation 6.3.11-4.
Beta_Dist_a - Column diffusion constant (dimensionless). *Distribution:* Uniform. *Range:* 0.01 to 0.5. *Sensitivity Name:* BETA. *Location in TSPA-LA:* Table 6.5-4.
C1_GenCorr_A22_a - Temperature dependent slope term of Alloy 22 general corrosion rate (K). *Distribution:* Truncated normal. *Range:* 666 to 7731. *Mean:* 4905. *Standard Deviation:* 1413. *Sensitivity Name:* WDGCA22. *Location in TSPA-LA:* Sections 6.3.5.1.2 and 6.3.5.1.3; Tables 6.3.5-3 and 6.3.5-4; Equation 6.3.5-4.

Table K3-2. High-Level Summary of Epistemically Uncertain Variables (i.e., elements of **e**) Considered in the TSPA-LA (TSPA Parameter Name) (Continued)

NOTE: * indicates variable not considered in sensitivity analysis due to correlations.

Colloidal_Kc_Am_UZP - Colloid sorption coefficient for americium (mg/mg). *Calculated by:* Colloidal_Kd_Am_uz*Colloidal_Concentration_uz. *Sensitivity Name:* UZCOKDAM. *Location in TSPA-LA:* Section 6.3.9.2.
Colloidal_Kc_Cs_UZP - Colloid sorption coefficient for cesium (mg/mg). *Calculated by:* Colloidal_Kd_Cs_uz*Colloidal_Concentration_uz. *Sensitivity Name:* UZCOKDCS. *Location in TSPA-LA:* Section 6.3.9.2.
Colloidal_Kc_Pa_UZP - Colloid sorption coefficient for protactinium (mg/mg). *Calculated by:* Colloidal_Kd_Am_uz*Colloidal_Concentration_uz. *Sensitivity Name:* UZCOKDPA. *Location in TSPA-LA:* Section 6.3.9.2.
Colloidal_Kc_Pu_UZP - Colloid sorption coefficient for plutonium (mg/mg). *Calculated by:* Colloidal_Kd_Pu_uz*Colloidal_Concentration_uz. *Sensitivity Name:* UZCOKDPU. *Location in TSPA-LA:* Section 6.3.9.2.
Colloidal_Kc_Sn_UZP - Colloid sorption coefficient for tin (mg/mg). *Calculated by:* Colloidal_Kd_Sn_uz*Colloidal_Concentration_uz. *Sensitivity Name:* UZCOKDSN. *Location in TSPA-LA:* Section 6.3.9.2.
Colloidal_Kc_Th_UZP - Colloid sorption coefficient for thorium (mg/mg). *Calculated by:* Calculated by Colloidal_Kd_Am_uz*Colloidal_Concentration_uz. *Sensitivity Name:* UZCOKDTH. *Location in TSPA-LA:* Section 6.3.9.2.
Colloidal_Retard_Factor_dist_a - Colloid retardation factor (dimensionless). *Distribution:* Piecewise uniform. *Range:* 6 to 799.83. *Sensitivity Name:* UZRCOL. *Location in TSPA-LA:* Sections 6.3.9.2 and 6.3.9.3; Table 6.3.9-12.
Conc_Col – Logarithm of ambient concentration of colloids in groundwater (g/mL). *Distribution:* Piecewise uniform. *Range:* -9 to -3.6. *Sensitivity Name:* SZCONCOL. *Location in TSPA-LA:* Table 6.3.10-2.
Conc_Col_FeOx_CS_Sampled_a - FeOx colloid concentration when carbon steel is corroding (mg/L). *Distribution:* Truncated log normal. *Range:* 0.3 to 30. *Mean:* 3.69. *Standard Deviation:* 2.79. *Sensitivity Name:* COLFEOCS. *Location in TSPA-LA:* Table 6.3.7-65.
Conc_Col_FeOx_SS_Sampled_a - FeOx colloid concentration when degraded stainless steel is present, but no degrading carbon steel is present (mg/L). *Distribution:* Piecewise uniform. *Range:* 1.00E-03 to 3.00E+01. *Sensitivity Name:* COLFEOSS. *Location in TSPA-LA:* Table 6.3.7-65.
Conc_Col_Gw_Sampled_a - Concentration of groundwater colloids when colloids are stable (mg/L). *Distribution:* Piecewise uniform. *Range:* 0.001 to 200. *Median:* 0.1. *Sensitivity Name:* COLGW. *Location in TSPA-LA:* Table 6.3.7-66.
Conc_Col_U_Sampled_a - Concentration of uranophane colloids when colloids are stable (mg/L). *Distribution:* Piecewise uniform. *Range:* 0.001 to 200. *Median:* 0.1. *Sensitivity Name:* COLU. *Location in TSPA-LA:* Table 6.3.7-64.
CORAL – Logarithm of colloid retardation factor in alluvium (dimensionless). *Distribution:* Piecewise uniform. *Range:* 0.903 to 3.715. *Sensitivity Name:* SZCOLRAL. *Location in TSPA-LA:* Sections 6.3.10.1, 6.3.10.2 and 6.3.10.4.2; Table 6.3.10-2.
CORVO – Logarithm of colloid retardation factor in volcanic units (dimensionless). *Distribution:* Piecewise uniform. *Range:* 0.778 to 2.903. *Sensitivity Name:* SZCOLRVO. *Location in TSPA-LA:* Sections 6.3.10.1, 6.3.10.2 and 6.3.10.4.2; Table 6.3.10-2.
CPu_Col_CSNF_Sampled_a Concentration of irreversibly attached plutonium on CSNF colloids when colloids are stable (mol/L). *Distribution:* Piecewise uniform. *Range:* 1.00E-10 to 5.00E-06. *Median:* 1.00E-07. *Sensitivity Name:* CPUCOLCS. *Location in TSPA-LA:* Section 6.3.7.6.2; Table 6.3.7-63.
CPu_Col_Wf_Embed_Sampled_a - Concentration of irreversibly attached plutonium on glass/waste form colloids when colloids are stable (mol/L). *Distribution:* Uniform. *Range:* 1.00E-11 to 1.00E-08. *Sensitivity Name:* CPUCOLWF. *Location in TSPA-LA:* Section 6.3.7.6.2; Table 6.3.7-62.
CPu_Per_CSNF_Embed_Col_a - Concentration of irreversibly attached plutonium per concentration of CSNF colloids ((mol/L)/(mg/L)). *Distribution:* Uniform. *Range:* 5.00E-07 to 1.00E-06. *Sensitivity Name:* CPUPERCS. *Location in TSPA-LA:* Section 6.3.7.6.2; Table 6.3.7-63.

Table K3-2. High-Level Summary of Epistemically Uncertain Variables (i.e., elements of **e**) Considered in the TSPA-LA (TSPA Parameter Name) (Continued)

NOTE: * indicates variable not considered in sensitivity analysis due to correlations.

CPu_Per_WF_Embed_Col_a - Concentration of irreversibly attached plutonium per concentration of waste form colloids ((mol/L)/(mg/L)). *Distribution:* Triangular. *Range:* 5.00E-09 to 2.5E-08. *Most Likely:* 2.00E-08. *Sensitivity Name:* CPUPERWF. *Location in TSPA-LA:* Section 6.3.7.6.2; Table 6.3.7-62.
Cr2O3_SA_a - Specific surface area of Cr_2O_3 (m^2/g). *Distribution:* Uniform. *Range:* 1 to 20. *Sensitivity Name:* CR2O3SA. *Location in TSPA-LA:* Table 6.3.8-4, S_{CP} in Equation 6.3.8-19.
Critical_Slope_a - Critical gradient for tephra mobilization from hillslopes (dimensionless). *Distribution:* Uniform. *Range:* 0.21 to 0.47. *Sensitivity Name:* CRITSLOP. *Location in TSPA-LA:* Table 6.5-5.
CS_Corrosion_Rate_a - Carbon steel corrosion rate (□m/yr). *Distribution:* Truncated log normal. *Range:* 25 to 135. *Mean:* 78.5. *Standard Deviation:* 25. *Sensitivity Name:* CSCORRAT. *Location in TSPA-LA:* Tables 6.3.8-1 and 6.3.8-4.
CSNF_Mass_Uncert_a - Scale factor used to characterize uncertainty in radionuclide content of CSNF (dimensionless). *Distribution:* Uniform. *Range:* 0.85 to 1.4. *Sensitivity Name:* CSNFMASS. *Location in TSPA-LA:* Sections 6.3.7.1.2 and 6.3.7.1.3; Table 6.3.7-7.
CSNF_Rind_SA_a - Specific surface area of CSNF degradation rind (m^2/g). *Distribution:* Uniform. *Range:* 0.5 to 60. *Sensitivity Name:* CSRINDSA. *Location in TSPA-LA:* Tables 6.3.8-2 and 6.3.8-4.
CSNF_WF_Uncert_a0_Acid_a - Correlated regression coefficient a0 in the abstracted rate model under acidic conditions (dimensionless). *Distribution:* Normal. *Mean/Median/Mode:* 0. *Standard Deviation:* 1. *Sensitivity Name:* CSWFA0AC. *Location in TSPA-LA:* Section 6.3.7.4.1.2; Equation 6.3.7-6.
CSNF_WF_Uncert_a0_Alk_a - Correlated coefficient a0 in the abstracted rate model under alkaline conditions (dimensionless). *Distribution:* Normal. *Mean/Median/Mode:* 0. *Standard Deviation:* 1. *Sensitivity Name:* CSWFA0AK. *Location in TSPA-LA:* Section 6.3.7.4.1.2; Equation 6.3.7-5.
CSNF_WF_Uncert_a1_Alk_a - Correlated coefficient a1 in the abstracted rate model under alkaline conditions (dimensionless). *Distribution:* Normal. *Mean/Median/Mode:* 0. *Standard Deviation:* 1. *Sensitivity Name:* CSWFA1AK. *Location in TSPA-LA:* Section 6.3.7.4.1.2; Equation 6.3.7-5.
CSNF_WF_Uncert_a2_Alk_a - Correlated coefficient a2 in the abstracted rate model under alkaline conditions (dimensionless). *Distribution:* Normal. *Mean/Median/Mode:* 0. *Standard Deviation:* 1. *Sensitivity Name:* CSWFA2AK. *Location in TSPA-LA:* Section 6.3.7.4.1.2; Equation 6.3.7-5.
CSNF_WF_Uncert_a3_Alk_a - Correlated coefficient a3 in the abstracted rate model under alkaline conditions (dimensionless). *Distribution:* Normal. *Mean/Median/Mode:* 0. *Standard Deviation:* 1. *Sensitivity Name:* CSWFA3AK. *Location in TSPA-LA:* Section 6.3.7.4.1.2; Equation 6.3.7-5.
CSNF_WF_Uncert_a4_Acid_a - Correlated coefficient a4 in the abstracted rate model under acid conditions (dimensionless). *Distribution:* Normal. *Mean/Median/Mode:* 0. *Standard Deviation:* 1. *Sensitivity Name:* CSWFA4AC. *Location in TSPA-LA:* Section 6.3.7.4.1.2; Equation 6.3.7-6.
D_Channels_a - Diffusivity of radionuclides in channels of the Fortymile Wash fan (RMEI location) (cm^2/yr). *Distribution:* Uniform. *Range:* 0.035 to 0.266. *Mean:* 0.1505. *Sensitivity Name:* DCHANL. *Location in TSPA-LA:* Table 6.5-5.
D_Divides_a - Diffusivity of radionuclides in divides of the Fortymile Wash fan (RMEI location) (cm^2/yr). *Distribution:* Uniform. *Range:* 0.001 to 0.095. *Mean* 0.048. *Sensitivity Name:* DDIVIDE. *Location in TSPA-LA:* Table 6.5-5.
Dash_mean_a - Mass median ash particle diameter (cm). *Distribution:* Log triangular. *Range:* 0.001 to 0.1. *Mode:* 0.01. *Sensitivity Name:* DASHAVG. *Location in TSPA-LA:* Table 6.5-4.
Dash_sigma_a - Ash particle diameter standard deviation (log (cm)). *Distribution:* Uniform. *Range:* 0.301 to 0.903. *Sensitivity Name:* DASHSIG. *Location in TSPA-LA:* Table 6.5-4.
DCVO – Logarithm of effective diffusion coefficient in fractured volcanic units (m^2/s). *Distribution:* Piecewise uniform. *Range:* -11.3 to -9.3. *Sensitivity Name:* SZDIFCVO. *Location in TSPA-LA:* Sections 6.3.10.2 and 6.3.10.5; Table 6.3.10-2.
DE_BDCF_IER_Ra226_Pb210 - Volcanic Biosphere Dose Conversion Factor (BDCF) component for radon, external exposure and ingestion of ^{226}Ra and ^{210}Pb in modern interglacial climate ((Sv/yr)/(Bq/m^2)). *Distribution:* Discrete. *Range:* 3.07E-08 to 9.43E-08. *Mean:* 3.52E-08. *Standard Deviation:* 3.45E-09. *Sensitivity Name:* INGRA226. *Location in TSPA-LA:* Sections 6.3.11.1 and 6.3.11.2; Equation 6.3.11-4.

Table K3-2. High-Level Summary of Epistemically Uncertain Variables (i.e., elements of **e**) Considered in the TSPA-LA (TSPA Parameter Name) (Continued)

NOTE: * indicates variable not considered in sensitivity analysis due to correlations.

DE_BDCF_ILT_Ra226_Pb210 - Volcanic Biosphere Dose Conversion Factor (BDCF) component for long-term inhalation of ^{226}Ra and ^{210}Pb in modern interglacial climate ((Sv/yr)/(Bq/kg)). *Distribution:* Discrete. *Range:* 1.71E-08 to 5.03E-07. *Mean:* 1.01E-07. *Standard Deviation:* 6.43E-08. *Sensitivity Name:* ILTRA226. *Location in TSPA-LA:* Sections 6.3.11.1 and 6.3.11.2; Equation 6.3.11-4.
DE_BDCF_Ing_Exp_Radon_Ac227 - Volcanic Biosphere Dose Conversion Factor (BDCF) component for radon, external exposure and ingestion of ^{227}Ac in modern interglacial climate ((Sv/yr)/(Bq/m^2)). *Distribution:* Discrete. *Range:* 5.78E-09 to 7.76E-09. *Mean:* 6.16E-09. *Standard Deviation:* 1.8E-10. *Sensitivity Name:* INGAC227. *Location in TSPA-LA:* Sections 6.3.11.1 and 6.3.11.2; Equation 6.3.11-4.
DE_BDCF_Ing_Exp_Radon_Am241 - Volcanic Biosphere Dose Conversion Factor (BDCF) component for radon, external exposure and ingestion of ^{241}Am in modern interglacial climate ((Sv/yr)/(Bq/m^2)). *Distribution:* Discrete. *Range:* 1.86E-10 to 1.00E-09. *Mean:* 2.51E-10. *Standard Deviation:* 7.00E-11. *Sensitivity Name:* INGAM241. *Location in TSPA-LA:* Sections 6.3.11.1 and 6.3.11.2; Equation 6.3.11-4.
DE_BDCF_Ing_Exp_Radon_Am243 - Volcanic Biosphere Dose Conversion Factor (BDCF) component for radon, external exposure and ingestion of ^{243}Am in modern interglacial climate ((Sv/yr)/(Bq/m^2)). *Distribution:* Discrete. *Range:* 2.51E-09 to 3.42E-09. *Mean:* 2.67E-09. *Standard Deviation:* 8.02E-11. *Sensitivity Name:* INGAM243. *Location in TSPA-LA:* Sections 6.3.11.1 and 6.3.11.2; Equation 6.3.11-4.
DE_BDCF_Ing_Exp_Radon_Cs137 - Volcanic Biosphere Dose Conversion Factor (BDCF) component for radon, external exposure and ingestion of ^{137}Cs in modern interglacial climate ((Sv/yr)/(Bq/m^2)). *Distribution:* Discrete. *Range:* 6.75E-09 to 8.48E-09. *Mean:* 7.17E-09. *Standard Deviation:* 1.55E-10. *Sensitivity Name:* INGCS137. *Location in TSPA-LA:* Sections 6.3.11.1 and 6.3.11.2; Equation 6.3.11-4.
DE_BDCF_Ing_Exp_Radon_I129 - Volcanic Biosphere Dose Conversion Factor (BDCF) component for radon, external exposure and ingestion of ^{129}I in modern interglacial climate ((Sv/yr)/(Bq/m^2)). *Distribution:* Discrete. *Range:* 1.39E-10 to 2.86E-08. *Mean:* 1.26E-09. *Standard Deviation:* 2.59E-09. *Sensitivity Name:* INGI129. *Location in TSPA-LA:* Sections 6.3.11.1 and 6.3.11.2; Equation 6.3.11-4.
DE_BDCF_Ing_Exp_Radon_Np237 - Volcanic Biosphere Dose Conversion Factor (BDCF) component for radon, external exposure and ingestion of ^{237}Np in modern interglacial climate ((Sv/yr)/(Bq/m^2)). *Distribution:* Discrete. *Range:* 2.62E-09 to 1.2E-08. *Mean:* 2.98E-09. *Standard Deviation:* 6.36E-10. *Sensitivity Name:* INGNP237. *Location in TSPA-LA:* Sections 6.3.11.1 and 6.3.11.2; Equation 6.3.11-4.
DE_BDCF_Ing_Exp_Radon_Pa231 - Volcanic Biosphere Dose Conversion Factor (BDCF) component for radon, external exposure and ingestion of ^{231}Pa in modern interglacial climate ((Sv/yr)/(Bq/m^2)). *Distribution:* Discrete. *Range:* 5.02E-10 to 4.56E-09. *Mean:* 7.14E-10. *Standard Deviation:* 2.92E-10. *Sensitivity Name:* INGPA231. *Location in TSPA-LA:* Sections 6.3.11.1 and 6.3.11.2; Equation 6.3.11-4.
DE_BDCF_Ing_Exp_Radon_Pu238 - Volcanic Biosphere Dose Conversion Factor (BDCF) component for radon, external exposure and ingestion of ^{238}Pu in modern interglacial climate ((Sv/yr)/(Bq/m^2)). *Distribution:* Discrete. *Range:* 1.33E-11 to 9.18E-10. *Mean:* 7.78E-11. *Standard Deviation:* 7.72E-11. *Sensitivity Name:* INGPU238. *Location in TSPA-LA:* Sections 6.3.11.1 and 6.3.11.2; Equation 6.3.11-4.
DE_BDCF_Ing_Exp_Radon_Pu239 - Volcanic Biosphere Dose Conversion Factor (BDCF) component for radon, external exposure and ingestion of ^{239}Pu in modern interglacial climate ((Sv/yr)/(Bq/m^2)). *Distribution:* Discrete. *Range:* 1.40E-11 to 1.01E-09. *Mean:* 8.49E-11. *Standard Deviation:* 8.5E-11. *Sensitivity Name:* INGPU239. *Location in TSPA-LA:* Sections 6.3.11.1 and 6.3.11.2; Equation 6.3.11-4.
DE_BDCF_Ing_Exp_Radon_Pu240 - Volcanic Biosphere Dose Conversion Factor (BDCF) component for radon, external exposure and ingestion of ^{240}Pu in modern interglacial climate ((Sv/yr)/(Bq/m^2)). *Distribution:* Discrete. *Range:* 1.42E-11 to 1.01E-09. *Mean:* 8.52E-11. *Standard Deviation:* 8.5E-11. *Sensitivity Name:* INGPU240. *Location in TSPA-LA:* Sections 6.3.11.1 and 6.3.11.2; Equation 6.3.11-4.
DE_BDCF_Ing_Exp_Radon_Pu242 - Volcanic Biosphere Dose Conversion Factor (BDCF) component for radon, external exposure and ingestion of ^{242}Pu in modern interglacial climate ((Sv/yr)/(Bq/m^2)). *Distribution:* Discrete. *Range:* 1.31E-11 to 9.57E-10. *Mean:* 8.04E-11. *Standard Deviation:* 8.06E-11. *Sensitivity Name:* INGPU242. *Location in TSPA-LA:* Sections 6.3.11.1 and 6.3.11.2; Equation 6.3.11-4.
DE_BDCF_Ing_Exp_Radon_Ra228 - Volcanic Biosphere Dose Conversion Factor (BDCF) component for radon, external exposure and ingestion of ^{228}Ra in modern interglacial climate ((Sv/yr)/(Bq/m^2)). *Distribution:* Discrete. *Range:* 1.17E-08 to 2.62E-08. *Mean:* 1.27E-08. *Standard Deviation:* 7.44E-10. *Sensitivity Name:* INGRA228. *Location in TSPA-LA:* Sections 6.3.11.1 and 6.3.11.2; Equation 6.3.11-4.

Table K3-2. High-Level Summary of Epistemically Uncertain Variables (i.e., elements of **e**) Considered in the TSPA-LA (TSPA Parameter Name) (Continued)

NOTE: * indicates variable not considered in sensitivity analysis due to correlations.

DE_BDCF_Ing_Exp_Radon_Sn126 - Volcanic Biosphere Dose Conversion Factor (BDCF) component for radon, external exposure and ingestion of ^{126}Sn in modern interglacial climate ((Sv/yr)/(Bq/m^2)). *Distribution:* Discrete. *Range:* 2.38E-08 to 2.79E-08. *Mean:* 2.54E-08. *Standard Deviation:* 4.41E-10. *Sensitivity Name:* INGSN126. *Location in TSPA-LA:* Sections 6.3.11.1 and 6.3.11.2; Equation 6.3.11-4.
DE_BDCF_Ing_Exp_Radon_Sr90 - Volcanic Biosphere Dose Conversion Factor (BDCF) component for radon, external exposure and ingestion of ^{90}Sr in modern interglacial climate ((Sv/yr)/(Bq/m^2)). *Distribution:* Discrete. *Range:* 1.44E-09 to 6.10E-09. *Mean:* 1.81E-09. *Standard Deviation:* 3.67E-10. *Sensitivity Name:* INGSR90. *Location in TSPA-LA:* Sections 6.3.11.1 and 6.3.11.2; Equation 6.3.11-4.
DE_BDCF_Ing_Exp_Radon_Tc99 - Volcanic Biosphere Dose Conversion Factor (BDCF) component for radon, external exposure and ingestion of ^{99}Tc in modern interglacial climate ((Sv/yr)/(Bq/m^2)). *Distribution:* Discrete. *Range:* 5.08E-12 to 8.95E-09. *Mean:* 2.72E-10. *Standard Deviation:* 5.16E-10. *Sensitivity Name:* INGTC99. *Location in TSPA-LA:* Sections 6.3.11.1 and 6.3.11.2; Equation 6.3.11-4.
DE_BDCF_Ing_Exp_Radon_Th229 - Volcanic Biosphere Dose Conversion Factor (BDCF) component for radon, external exposure and ingestion of ^{229}Th in modern interglacial climate ((Sv/yr)/(Bq/m^2)). *Distribution:* Discrete. *Range:* 4.33E-09 to 7.02E-09. *Mean:* 4.69E-09. *Standard Deviation:* 2.4E-10. *Sensitivity Name:* INGTH229. *Location in TSPA-LA:* Sections 6.3.11.1 and 6.3.11.2; Equation 6.3.11-4.
DE_BDCF_Ing_Exp_Radon_Th230 - Volcanic Biosphere Dose Conversion Factor (BDCF) component for radon, external exposure and ingestion of ^{230}Th in modern interglacial climate ((Sv/yr)/(Bq/m^2)). *Distribution:* Discrete. *Range:* 1.92E-11 to 8.68E-10. *Mean:* 8.51E-11. *Standard Deviation:* 7.82E-11. *Sensitivity Name:* INGTH230. *Location in TSPA-LA:* Sections 6.3.11.1 and 6.3.11.2; Equation 6.3.11-4.
DE_BDCF_Ing_Exp_Radon_Th232 - Volcanic Biosphere Dose Conversion Factor (BDCF) component for radon, external exposure and ingestion of ^{232}Th in modern interglacial climate ((Sv/yr)/(Bq/m^2)). *Distribution:* Discrete. *Range:* 1.72E-11 to 9.34E-10. *Mean:* 8.83E-11. *Standard Deviation:* 8.44E-11. *Sensitivity Name:* INGTH232. *Location in TSPA-LA:* Sections 6.3.11.1 and 6.3.11.2; Equation 6.3.11-4.
DE_BDCF_Ing_Exp_Radon_U233 - Volcanic Biosphere Dose Conversion Factor (BDCF) component for radon, external exposure and ingestion of ^{233}U in modern interglacial climate ((Sv/yr)/(Bq/m^2)). *Distribution:* Discrete. *Range:* 1.31E-11 to 9.04E-10. *Mean:* 6.48E-11. *Standard Deviation:* 6.12E-11. *Sensitivity Name:* INGU233. *Location in TSPA-LA:* Sections 6.3.11.1 and 6.3.11.2; Equation 6.3.11-4.
DE_BDCF_Ing_Exp_Radon_U234 - Volcanic Biosphere Dose Conversion Factor (BDCF) component for radon, external exposure and ingestion of ^{234}U in modern interglacial climate ((Sv/yr)/(Bq/m^2)). *Distribution:* Discrete. *Range:* 9.60E-12 to 8.7E-10. *Mean:* 5.96E-11. *Standard Deviation:* 5.9E-11. *Sensitivity Name:* INGU234. *Location in TSPA-LA:* Sections 6.3.11.1 and 6.3.11.2; Equation 6.3.11-4.
DE_BDCF_Ing_Exp_Radon_U238 - Volcanic Biosphere Dose Conversion Factor (BDCF) component for radon, external exposure and ingestion of ^{238}U in modern interglacial climate ((Sv/yr)/(Bq/m^2)). *Distribution:* Discrete. *Range:* 1.52E-09 to 2.41E-09. *Mean:* 1.62E-09. *Standard Deviation:* 6.16E-11. *Sensitivity Name:* INGU238. *Location in TSPA-LA:* Sections 6.3.11.1 and 6.3.11.2; Equation 6.3.11-4.
DE_BDCF_Inh_LT_Ac227 - Volcanic Biosphere Dose Conversion Factor (BDCF) component for long-term inhalation of ^{227}Ac in modern interglacial climate ((Sv/yr)/(Bq/kg)). *Distribution:* Discrete. *Range:* 1.53E-07 to 4.5E-06. *Mean:* 9.0E-07. *Standard Deviation:* 5.75E-07. *Sensitivity Name:* ILTAC227. *Location in TSPA-LA:* Sections 6.3.11.1 and 6.3.11.2; Equation 6.3.11-4.
DE_BDCF_Inh_LT_Am241 - Volcanic Biosphere Dose Conversion Factor (BDCF) component for long-term inhalation of ^{241}Am in modern interglacial climate ((Sv/yr)/(Bq/kg)). *Distribution:* Discrete. *Range:* 8.45E-08 to 2.48E-06. *Mean:* 4.96E-07. *Standard Deviation:* 3.17E-07. *Sensitivity Name:* ILTAM241. *Location in TSPA-LA:* Sections 6.3.11.1 and 6.3.11.2; Equation 6.3.11-4.
DE_BDCF_Inh_LT_Am243 - Volcanic Biosphere Dose Conversion Factor (BDCF) component for long-term inhalation of ^{243}Am in modern interglacial climate ((Sv/yr)/(Bq/kg)). *Distribution:* Discrete. *Range:* 8.38E-08 to 2.46E-06. *Mean:* 4.93E-07. *Standard Deviation:* 3.15E-07. *Sensitivity Name:* ILTAM243. *Location in TSPA-LA:* Sections 6.3.11.1 and 6.3.11.2; Equation 6.3.11-4.
DE_BDCF_Inh_LT_Cs137 - Volcanic Biosphere Dose Conversion Factor (BDCF) component for long-term inhalation of ^{137}Cs in modern interglacial climate ((Sv/yr)/(Bq/kg)). *Distribution:* Discrete. *Range:* 3.43E-11 to 1.01E-09. *Mean:* 2.02E-10. *Standard Deviation:* 1.29E-10. *Sensitivity Name:* ILTCS137. *Location in TSPA-LA:* Sections 6.3.11.1 and 6.3.11.2; Equation 6.3.11-4.

Table K3-2. High-Level Summary of Epistemically Uncertain Variables (i.e., elements of **e**) Considered in the TSPA-LA (TSPA Parameter Name) (Continued)

NOTE: * indicates variable not considered in sensitivity analysis due to correlations.

DE_BDCF_Inh_LT_I129 - Volcanic Biosphere Dose Conversion Factor (BDCF) component for long-term inhalation of ^{129}I in modern interglacial climate ((Sv/yr)/(Bq/kg)). *Distribution:* Discrete. *Range:* 3.15E-11 to 9.23E-10. *Mean:* 1.85E-10. *Standard Deviation:* 1.18E-10. *Sensitivity Name:* ILTI129. *Location in TSPA-LA:* Sections 6.3.11.1 and 6.3.11.2; Equation 6.3.11-4.
DE_BDCF_Inh_LT_Np237 - Volcanic Biosphere Dose Conversion Factor (BDCF) component for long-term inhalation of ^{237}Np in modern interglacial climate ((Sv/yr)/(Bq/kg)). *Distribution:* Discrete. *Range:* 4.35E-08 to 1.28E-06. *Mean:* 2.56E-07. *Standard Deviation:* 1.63E-07. *Sensitivity Name:* ILTNP237. *Location in TSPA-LA:* Sections 6.3.11.1 and 6.3.11.2; Equation 6.3.11-4.
DE_BDCF_Inh_LT_Pa231 - Volcanic Biosphere Dose Conversion Factor (BDCF) component for long-term inhalation of ^{231}Pa in modern interglacial climate ((Sv/yr)/(Bq/kg)). *Distribution:* Discrete. *Range:* 2.02E-07 to 5.92E-06. *Mean:* 1.18E-06. *Standard Deviation:* 7.56E-07. *Sensitivity Name:* ILTPA231. *Location in TSPA-LA:* Sections 6.3.11.1 and 6.3.11.2; Equation 6.3.11-4.
DE_BDCF_Inh_LT_Pu238 - Volcanic Biosphere Dose Conversion Factor (BDCF) component for long-term inhalation of ^{238}Pu in modern interglacial climate ((Sv/yr)/(Bq/kg)). *Distribution:* Discrete. *Range:* 9.46E-08 to 2.78E-06. *Mean:* 5.56E-07. *Standard Deviation:* 3.55E-07. *Sensitivity Name:* ILTPU238. *Location in TSPA-LA:* Sections 6.3.11.1 and 6.3.11.2; Equation 6.3.11-4.
DE_BDCF_Inh_LT_Pu239 - Volcanic Biosphere Dose Conversion Factor (BDCF) component for long-term inhalation of ^{239}Pu in modern interglacial climate ((Sv/yr)/(Bq/kg)). *Distribution:* Discrete. *Range:* 1.04E-07 to 3.06E-06. *Mean:* 6.12E-07. *Standard Deviation:* 3.91E-07. *Sensitivity Name:* ILTPU239. *Location in TSPA-LA:* Sections 6.3.11.1 and 6.3.11.2; Equation 6.3.11-4.
DE_BDCF_Inh_LT_Pu240 - Volcanic Biosphere Dose Conversion Factor (BDCF) component for long-term inhalation of ^{240}Pu in modern interglacial climate ((Sv/yr)/(Bq/kg)). *Distribution:* Discrete. *Range:* 1.04E-07 to 3.06E-06. *Mean:* 6.12E-07. *Standard Deviation:* 3.91E-07. *Sensitivity Name:* ILTPU240. *Location in TSPA-LA:* Sections 6.3.11.1 and 6.3.11.2; Equation 6.3.11-4.
DE_BDCF_Inh_LT_Pu242 - Volcanic Biosphere Dose Conversion Factor (BDCF) component for long-term inhalation of ^{242}Pu in modern interglacial climate ((Sv/yr)/(Bq/kg)). *Distribution:* Discrete. *Range:* 9.90E-08 to 2.91E-06. *Mean:* 5.82E-07. *Standard Deviation:* 3.72E-07. *Sensitivity Name:* ILTPU242. *Location in TSPA-LA:* Sections 6.3.11.1 and 6.3.11.2; Equation 6.3.11-4.
DE_BDCF_Inh_LT_Ra228 - Volcanic Biosphere Dose Conversion Factor (BDCF) component for long-term inhalation of ^{228}Ra in modern interglacial climate ((Sv/yr)/(Bq/kg)). *Distribution:* Discrete. *Range:* 1.40E-08 to 4.12E-07. *Mean:* 8.24E-08. *Standard Deviation:* 5.27E-08. *Sensitivity Name:* ILTRA228. *Location in TSPA-LA:* Sections 6.3.11.1 and 6.3.11.2; Equation 6.3.11-4.
DE_BDCF_Inh_LT_Sn126 - Volcanic Biosphere Dose Conversion Factor (BDCF) component for long-term inhalation of ^{126}Sn in modern interglacial climate ((Sv/yr)/(Bq/kg)). *Distribution:* Discrete. *Range:* 1.36E-10 to 4.00E-09. *Mean:* 8.0E-10. *Standard Deviation:* 5.11E-10. *Sensitivity Name:* ILTSN126. *Location in TSPA-LA:* Sections 6.3.11.1 and 6.3.11.2; Equation 6.3.11-4.
DE_BDCF_Inh_LT_Sr90 - Volcanic Biosphere Dose Conversion Factor (BDCF) component for long-term inhalation of ^{90}Sr in modern interglacial climate ((Sv/yr)/(Bq/kg)). *Distribution:* Discrete. *Range:* 1.39E-10 to 4.08E-09. *Mean:* 8.16E-10. *Standard Deviation:* 5.21E-10. *Sensitivity Name:* ILTSR90. *Location in TSPA-LA:* Sections 6.3.11.1 and 6.3.11.2; Equation 6.3.11-4.
DE_BDCF_Inh_LT_Tc99 - Volcanic Biosphere Dose Conversion Factor (BDCF) component for long-term inhalation of ^{99}Tc in modern interglacial climate ((Sv/yr)/(Bq/kg)). *Distribution:* Discrete. *Range:* 1.17E-11 to 3.42E-10. *Mean:* 6.84E-11. *Standard Deviation:* 4.37E-11. *Sensitivity Name:* ILTTC99. *Location in TSPA-LA:* Sections 6.3.11.1 and 6.3.11.2; Equation 6.3.11-4.
DE_BDCF_Inh_LT_Th229 - Volcanic Biosphere Dose Conversion Factor (BDCF) component for long-term inhalation of ^{229}Th in modern interglacial climate ((Sv/yr)/(Bq/kg)). *Distribution:* Discrete. *Range:* 2.24E-07 to 6.57E-06. *Mean:* 1.31E-06. *Standard Deviation:* 8.39E-07. *Sensitivity Name:* ILTTH229. *Location in TSPA-LA:* Sections 6.3.11.1 and 6.3.11.2; Equation 6.3.11-4.
DE_BDCF_Inh_LT_Th230 - Volcanic Biosphere Dose Conversion Factor (BDCF) component for long-term inhalation of ^{230}Th in modern interglacial climate ((Sv/yr)/(Bq/kg)). *Distribution:* Discrete. *Range:* 8.94E-08 to 2.62E-06. *Mean:* 5.25E-07. *Standard Deviation:* 3.35E-07. *Sensitivity Name:* ILTTH230. *Location in TSPA-LA:* Sections 6.3.11.1 and 6.3.11.2; Equation 6.3.11-4.

Table K3-2. High-Level Summary of Epistemically Uncertain Variables (i.e., elements of **e**) Considered in the TSPA-LA (TSPA Parameter Name) (Continued)

NOTE: * indicates variable not considered in sensitivity analysis due to correlations.

DE_BDCF_Inh_LT_Th232 - Volcanic Biosphere Dose Conversion Factor (BDCF) component for long-term inhalation of ^{232}Th in modern interglacial climate ((Sv/yr)/(Bq/kg)). *Distribution:* Discrete. *Range:* 9.64E-08 to 2.83E-06. *Mean:* 5.66E-07. *Standard Deviation:* 3.62E-07. *Sensitivity Name:* ILTTH232. *Location in TSPA-LA:* Sections 6.3.11.1 and 6.3.11.2; Equation 6.3.11-4.
DE_BDCF_Inh_LT_U233 - Volcanic Biosphere Dose Conversion Factor (BDCF) component for long-term inhalation of ^{233}U in modern interglacial climate ((Sv/yr)/(Bq/kg)). *Distribution:* Discrete. *Range:* 8.40E-09 to 2.47E-07. *Mean:* 4.94E-08. *Standard Deviation:* 3.15E-08. *Sensitivity Name:* ILTU233. *Location in TSPA-LA:* Sections 6.3.11.1 and 6.3.11.2; Equation 6.3.11-4.
DE_BDCF_Inh_LT_U234 - Volcanic Biosphere Dose Conversion Factor (BDCF) component for long-term inhalation of ^{234}U in modern interglacial climate ((Sv/yr)/(Bq/kg)). *Distribution:* Discrete. *Range:* 8.23E-09 to 2.42E-07. *Mean:* 4.84E-08. *Standard Deviation:* 3.09E-08. *Sensitivity Name:* ILTU234. *Location in TSPA-LA:* Sections 6.3.11.1 and 6.3.11.2; Equation 6.3.11-4.
DE_BDCF_Inh_LT_U238 - Volcanic Biosphere Dose Conversion Factor (BDCF) component for long-term inhalation of ^{238}U in modern interglacial climate ((Sv/yr)/(Bq/kg)). *Distribution:* Discrete. *Range:* 7.05E-09 to 2.07E-07. *Mean:* 4.14E-08. *Standard Deviation:* 2.65E-08. *Sensitivity Name:* ILTU238. *Location in TSPA-LA:* Sections 6.3.11.1 and 6.3.11.2; Equation 6.3.11-4.
DE_BDCF_Inh_ShT_Ac227 - Volcanic Biosphere Dose Conversion Factor (BDCF) component for short-term inhalation of ^{227}Ac in modern interglacial climate ((Sv/yr)/(Bq/kg)). *Distribution:* Discrete. *Range:* 8.47E-08 to 2.14E-06. *Mean:* 5.85E-07. *Standard Deviation:* 3.32E-07. *Sensitivity Name:* ISTAC227. *Location in TSPA-LA:* Sections 6.3.11.1 and 6.3.11.2; Equation 6.3.11-4.
DE_BDCF_Inh_ShT_Am241 - Volcanic Biosphere Dose Conversion Factor (BDCF) component for short-term inhalation of ^{241}Am in modern interglacial climate ((Sv/yr)/(Bq/kg)). *Distribution:* Discrete. *Range:* 4.67E-08 to 1.18E-06. *Mean:* 3.23E-07. *Standard Deviation:* 1.83E-07. *Sensitivity Name:* ISTAM241. *Location in TSPA-LA:* Sections 6.3.11.1 and 6.3.11.2; Equation 6.3.11-4.
DE_BDCF_Inh_ShT_Am243 - Volcanic Biosphere Dose Conversion Factor (BDCF) component for short-term inhalation of ^{243}Am in modern interglacial climate ((Sv/yr)/(Bq/kg)). *Distribution:* Discrete. *Range:* 4.64E-08 to 1.17E-06. *Mean:* 3.2E-07. *Standard Deviation:* 1.82E-07. *Sensitivity Name:* ISTAM243. *Location in TSPA-LA:* Sections 6.3.11.1 and 6.3.11.2; Equation 6.3.11-4.
DE_BDCF_Inh_ShT_Cs137 - Volcanic Biosphere Dose Conversion Factor (BDCF) component for short-term inhalation of ^{137}Cs in modern interglacial climate ((Sv/yr)/(Bq/kg)). *Distribution:* Discrete. *Range:* 1.90E-11 to 4.80E-10. *Mean:* 1.31E-10. *Standard Deviation:* 7.44E-11. *Sensitivity Name:* ISTCS137. *Location in TSPA-LA:* Sections 6.3.11.1 and 6.3.11.2; Equation 6.3.11-4.
DE_BDCF_Inh_ShT_I129 - Volcanic Biosphere Dose Conversion Factor (BDCF) component for short-term inhalation of ^{129}I in modern interglacial climate ((Sv/yr)/(Bq/kg)). *Distribution:* Discrete. *Range:* 1.74E-11 to 4.40E-10. *Mean:* 1.2E-10. *Standard Deviation:* 6.81E-11. *Sensitivity Name:* ISTI129. *Location in TSPA-LA:* Sections 6.3.11.1 and 6.3.11.2; Equation 6.3.11-4.
DE_BDCF_Inh_ShT_Np237 - Volcanic Biosphere Dose Conversion Factor (BDCF) component for short-term inhalation of ^{237}Np in modern interglacial climate ((Sv/yr)/(Bq/kg)). *Distribution:* Discrete. *Range:* 2.41E-08 to 6.08E-07. *Mean:* 1.66E-07. *Standard Deviation:* 9.43E-08. *Sensitivity Name:* ISTNP237. *Location in TSPA-LA:* Sections 6.3.11.1 and 6.3.11.2; Equation 6.3.11-4.
DE_BDCF_Inh_ShT_Pa231 - Volcanic Biosphere Dose Conversion Factor (BDCF) component for short-term inhalation of ^{231}Pa in modern interglacial climate ((Sv/yr)/(Bq/kg)). *Distribution:* Discrete. *Range:* 1.11E-07 to 2.82E-06. *Mean:* 7.7E-07. *Standard Deviation:* 4.37E-07. *Sensitivity Name:* ISTPA231. *Location in TSPA-LA:* Sections 6.3.11.1 and 6.3.11.2; Equation 6.3.11-4.
DE_BDCF_Inh_ShT_Pu238 - Volcanic Biosphere Dose Conversion Factor (BDCF) component for short-term inhalation of ^{238}Pu in modern interglacial climate ((Sv/yr)/(Bq/kg)). *Distribution:* Discrete. *Range:* 5.23E-08 to 1.32E-06. *Mean:* 3.61E-07. *Standard Deviation:* 2.05E-07. *Sensitivity Name:* ISTPU238. *Location in TSPA-LA:* Sections 6.3.11.1 and 6.3.11.2; Equation 6.3.11-4.
DE_BDCF_Inh_ShT_Pu239 - Volcanic Biosphere Dose Conversion Factor (BDCF) component for short-term inhalation of ^{239}Pu in modern interglacial climate ((Sv/yr)/(Bq/kg)). *Distribution:* Discrete. *Range:* 5.76E-08 to 1.46E-06. *Mean:* 3.98E-07. *Standard Deviation:* 2.26E-07. *Sensitivity Name:* ISTPU239. *Location in TSPA-LA:* Sections 6.3.11.1 and 6.3.11.2; Equation 6.3.11-4.

Table K3-2. High-Level Summary of Epistemically Uncertain Variables (i.e., elements of **e**) Considered in the TSPA-LA (TSPA Parameter Name) (Continued)

NOTE: * indicates variable not considered in sensitivity analysis due to correlations.

DE_BDCF_Inh_ShT_Pu240 - Volcanic Biosphere Dose Conversion Factor (BDCF) component for short-term inhalation of ^{240}Pu in modern interglacial climate ((Sv/yr)/(Bq/kg)). *Distribution:* Discrete. *Range:* 5.76E-08 to 1.46E-06. *Mean:* 3.98E-07. *Standard Deviation:* 2.26E-07. *Sensitivity Name:* ISTPU240. *Location in TSPA-LA:* Sections 6.3.11.1 and 6.3.11.2; Equation 6.3.11-4.
DE_BDCF_Inh_ShT_Pu242 - Volcanic Biosphere Dose Conversion Factor (BDCF) component for short-term inhalation of ^{242}Pu in modern interglacial climate ((Sv/yr)/(Bq/kg)). *Distribution:* Discrete. *Range:* 5.47E-08 to 1.38E-06. *Mean:* 3.78E-07. *Standard Deviation:* 2.14E-07. *Sensitivity Name:* ISTPU242. *Location in TSPA-LA:* Sections 6.3.11.1 and 6.3.11.2; Equation 6.3.11-4.
DE_BDCF_Inh_ShT_Ra228 - Volcanic Biosphere Dose Conversion Factor (BDCF) component for short-term inhalation of ^{228}Ra in modern interglacial climate ((Sv/yr)/(Bq/kg)). *Distribution:* Discrete. *Range:* 7.76E-09 to 1.96E-07. *Mean:* 5.36E-08. *Standard Deviation:* 3.04E-08. *Sensitivity Name:* ISTRA228. *Location in TSPA-LA:* Sections 6.3.11.1 and 6.3.11.2; Equation 6.3.11-4.
DE_BDCF_Inh_ShT_Sn126 - Volcanic Biosphere Dose Conversion Factor (BDCF) component for short-term inhalation of ^{126}Sn in modern interglacial climate ((Sv/yr)/(Bq/kg)). *Distribution:* Discrete. *Range:* 7.53E-11 to 1.90E-09. *Mean:* 5.2E-10. *Standard Deviation:* 2.95E-10. *Sensitivity Name:* ISTSN126. *Location in TSPA-LA:* Sections 6.3.11.1 and 6.3.11.2; Equation 6.3.11-4.
DE_BDCF_Inh_ShT_Sr90 - Volcanic Biosphere Dose Conversion Factor (BDCF) component for short-term inhalation of ^{90}Sr in modern interglacial climate ((Sv/yr)/(Bq/kg)). *Distribution:* Discrete. *Range:* 7.68E-11 to 1.94E-09. *Mean:* 5.3E-10. *Standard Deviation:* 3.01E-10. *Sensitivity Name:* ISTSR90. *Location in TSPA-LA:* Sections 6.3.11.1 and 6.3.11.2; Equation 6.3.11-4.
DE_BDCF_Inh_ShT_Tc99 - Volcanic Biosphere Dose Conversion Factor (BDCF) component for short-term inhalation of ^{99}Tc in modern interglacial climate ((Sv/yr)/(Bq/kg)). *Distribution:* Discrete. *Range:* 6.44E-12 to 1.63E-10. *Mean:* 4.45E-11. *Standard Deviation:* 2.52E-11. *Sensitivity Name:* ISTTC99. *Location in TSPA-LA:* Sections 6.3.11.1 and 6.3.11.2; Equation 6.3.11-4.
DE_BDCF_Inh_ShT_Th229 - Volcanic Biosphere Dose Conversion Factor (BDCF) component for short-term inhalation of ^{229}Th in modern interglacial climate ((Sv/yr)/(Bq/kg)). *Distribution:* Discrete. *Range:* 1.24E-07 to 3.13E-06. *Mean:* 8.54E-07. *Standard Deviation:* 4.84E-07. *Sensitivity Name:* ISTTH229. *Location in TSPA-LA:* Sections 6.3.11.1 and 6.3.11.2; Equation 6.3.11-4.
DE_BDCF_Inh_ShT_Th230 - Volcanic Biosphere Dose Conversion Factor (BDCF) component for short-term inhalation of ^{230}Th in modern interglacial climate ((Sv/yr)/(Bq/kg)). *Distribution:* Discrete. *Range:* 4.94E-08 to 1.25E-06. *Mean:* 3.41E-07. *Standard Deviation:* 1.94E-07. *Sensitivity Name:* ISTTH230. *Location in TSPA-LA:* Sections 6.3.11.1 and 6.3.11.2; Equation 6.3.11-4.
DE_BDCF_Inh_ShT_Th232 - Volcanic Biosphere Dose Conversion Factor (BDCF) component for short-term inhalation of ^{232}Th in modern interglacial climate ((Sv/yr)/(Bq/kg)). *Distribution:* Discrete. *Range:* 5.33E-08 to 1.35E-06. *Mean:* 3.68E-07. *Standard Deviation:* 2.09E-07. *Sensitivity Name:* ISTTH232. *Location in TSPA-LA:* Sections 6.3.11.1 and 6.3.11.2; Equation 6.3.11-4.
DE_BDCF_Inh_ShT_U233 - Volcanic Biosphere Dose Conversion Factor (BDCF) component for short-term inhalation of ^{233}U in modern interglacial climate ((Sv/yr)/(Bq/kg)). *Distribution:* Discrete. *Range:* 4.65E-09 to 1.17E-07. *Mean:* 3.21E-08. *Standard Deviation:* 1.82E-08. *Sensitivity Name:* ISTU233. *Location in TSPA-LA:* Sections 6.3.11.1 and 6.3.11.2; Equation 6.3.11-4.
DE_BDCF_Inh_ShT_U234 - Volcanic Biosphere Dose Conversion Factor (BDCF) component for short-term inhalation of ^{234}U in modern interglacial climate ((Sv/yr)/(Bq/kg)). *Distribution:* Discrete. *Range:* 4.55E-09 to 1.15E-07. *Mean:* 3.15E-08. *Standard Deviation:* 1.78E-08. *Sensitivity Name:* ISTU234. *Location in TSPA-LA:* Sections 6.3.11.1 and 6.3.11.2; Equation 6.3.11-4.
DE_BDCF_Inh_ShT_U238 - Volcanic Biosphere Dose Conversion Factor (BDCF) component for short-term inhalation of ^{238}U in modern interglacial climate ((Sv/yr)/(Bq/kg)). *Distribution:* Discrete. *Range:* 3.90E-09 to 9.85E-08. *Mean:* 2.69E-08. *Standard Deviation:* 1.53E-08. *Sensitivity Name:* ISTU238. *Location in TSPA-LA:* Sections 6.3.11.1 and 6.3.11.2; Equation 6.3.11-4.
DE_BDCF_IST_Ra226_Pb210 - Volcanic Biosphere Dose Conversion Factor (BDCF) component for short-term inhalation of ^{226}Ra and ^{210}Pb in modern interglacial climate ((Sv/yr)/(Bq/kg)). *Distribution:* Discrete. *Range:* 9.47E-09 to 2.39E-07. *Mean:* 6.54E-08. *Standard Deviation:* 3.71E-08. *Sensitivity Name:* ISTRA226. *Location in TSPA-LA:* Sections 6.3.11.1 and 6.3.11.2; Equation 6.3.11-4.

Table K3-2. High-Level Summary of Epistemically Uncertain Variables (i.e., elements of **e**) Considered in the TSPA-LA (TSPA Parameter Name) (Continued)

NOTE: * indicates variable not considered in sensitivity analysis due to correlations.

Default_Fwd_Rate_Const_a - Default forward rate constant for irreversible sorption of plutonium and americium ($m^3/m^2/yr$). *Distribution:* Log uniform. *Range:* 0.002 to 0.05. *Sensitivity Name:* FWDRAT. *Location in TSPA-LA:* Table 6.3.7-65.
Defect_Count_a - Flaw density parameter (flaws per mm^3 of weld) (dimensionless). *Distribution:* Gamma. *Mean:* 4.529E-07. *Standard Deviation:* 1.654E-07. *Sensitivity Name:* WDDEFCNT. *Location in TSPA-LA:* Section 6.3.5.1.2; Table 6.3.5-3.
Defect_Size_a - Flaw size parameter (flaw size per mm of weld) (dimensionless). *Distribution:* Gamma. *Mean:* 0.2205. *Standard Deviation:* 0.0833. *Sensitivity Name:* WDDEFSZE. *Location in TSPA-LA:* Section 6.3.5.1.2; Table 6.3.5-3; Equation 6.3.5-10.
Density_CSNF_Rind_a - Grain density of CSNF rind (kg/m^3). *Distribution:* Uniform. *Range:* 5600 to 11500. *Sensitivity Name:* CSRINDDN. *Location in TSPA-LA:* Table 6.3.8-4.
Diameter_Colloid_a - Diameter of colloid particle (nm). *Distribution:* Uniform. *Range:* 50 to 300. *Sensitivity Name:* DIAMCOLL. *Location in TSPA-LA:* Tables 6.3.8-1 and 6.3.8-4.
Diff_Path_Length_Invert_Top_a - Diffusive path length from waste package outer corrosion barrier to mid-point of invert (m). *Distribution:* Uniform. *Range:* 0.3 to 1.24. *Sensitivity Name:* DIFPATHL. *Location in TSPA-LA:* Section 6.3.8.2.4; Table 6.3.8-4.
Drainage_Density_a - Average drainage density for the Fortymile Wash drainage basin (1/km). *Distribution:* Uniform. *Range:* 20 to 33. *Sensitivity Name:* DRAINDNS. *Location in TSPA-LA:* Table 6.5-5.
DS_Flux_Uncertainty_a - Drip shield flux splitting factor (dimensionless). *Distribution:* Uniform. *Range:* 0 to 0.85. *Sensitivity Name:* DSFLUX. *Location in TSPA-LA:* Tables 6.3.6-1, 6.3.6-2 and 6.3.8-4; Sections 6.3.6.2 and 6.3.6.4.1; Equation 6.3.6-5.
DSNF_Mass_Uncert_a - Scale factor used to characterize uncertainty in radionuclide content of DSNF (dimensionless). *Distribution:* Triangular. *Range:* 0.45 to 2.9. *Most Likely:* 0.62. *Sensitivity Name:* DSNFMASS. *Location in TSPA-LA:* Sections 6.3.7.1.2 and 6.3.7.1.3; Table 6.3.7-7.
dt_dRh_uncertainty - Selector variable used to determine the collapsed drift rubble thermal conductivity (dimensionless). *Distribution:* Discrete. *Range:* 1 to 2. *Sensitivity Name:* DTDRHUNC. *Location in TSPA-LA:* Section 6.6.2.2.
DWC_Dispersivity_Cond_a - Selector variable used to determine the axial dispersion modeling case (dimensionless). *Distribution:* Discrete. *Range:* 0 to 1. *Sensitivity Name:* DWCDISP. *Location in TSPA-LA:* Section 6.3.3.2.2; Table 6.3.3-5.
DWC_Std_Error_a_a - Multiplier for the standard deviation on the slope coefficient for determining the probability of condensation from percolation rate (dimensionless). *Distribution:* Normal. *Mean/Median/Mode:* 0. *Standard Deviation:* 1. *Sensitivity Name:* DWCSTERA. *Location in TSPA-LA:* Section 6.3.3.2.2; Tables 6.3.3-4 and 6.3.3-5.
DWC_Std_Error_b_a - Multiplier for the standard deviation on the y-intercept coefficient for determining the probability of condensation from percolation rate (dimensionless). *Distribution:* Normal. *Mean/Median/Mode:* 0. *Standard Deviation:* 1. *Sensitivity Name:* DWCSTERB. *Location in TSPA-LA:* Section 6.3.3.2.2; Tables 6.3.3-4 and 6.3.3-5.
DWC_Std_Error_c_a - Multiplier for the standard deviation on the slope coefficient for determining condensation rate from percolation rate (dimensionless). *Distribution:* Normal. *Mean/Median/Mode:* 0. *Standard Deviation:* 1. *Sensitivity Name:* DWCSTERC. *Location in TSPA-LA:* Section 6.3.3.2.2; Tables 6.3.3-4 and 6.3.3-5.
DWC_Std_Error_d_a - Multiplier for the standard deviation on the y-intercept coefficient for determining the condensation rate from percolation rate (dimensionless). *Distribution:* Normal. *Mean/Median/Mode:* 0. *Standard Deviation:* 1. *Sensitivity Name:* DWCSTERD. *Location in TSPA-LA:* Section 6.3.3.2.2; Tables 6.3.3-4 and 6.3.3-5.
DWC_Ventilated_Cond_a - Selector variable specifying whether the ventilated or unventilated drip shield DWC modeling case is performed (dimensionless). *Distribution:* Discrete. *Range:* 0, 1. *Sensitivity Name:* DWCVENT. *Location in TSPA-LA:* Sections 6.3.3.2.2 and 6.3.3.2.3; Table 6.3.3-5.
Exposure_Factor_a - The surface area exposure factor for the amount of HLW glass contacted by water (dimensionless). *Distribution:* Triangular. *Range:* 4 to 17. *Mode:* 4. *Sensitivity Name:* WFDEGEXF. *Location in TSPA-LA:* Sections 6.3.7.4.3.2 and 6.3.7.4.3.3; Equation 6.3.7-9; Table 6.3.7-32.

Table K3-2. High-Level Summary of Epistemically Uncertain Variables (i.e., elements of **e**) Considered in the TSPA-LA (TSPA Parameter Name) (Continued)

NOTE: * indicates variable not considered in sensitivity analysis due to correlations.

fa_group1_a - Fracture aperture for group 1 rock unit (chnf) (m). *Calculated by:* Por_group1_a/ff_group1_a. *Sensitivity Name:* UZFAG1. *Location in TSPA-LA:* Section 6.3.9.2; Equation 6.3.9-2; Fracture porosity values and frequency values are shown in Tables 6.3.9-6 and 6.3.9-7.
fa_group2_a - Fracture aperture for group 2 rock unit (tswf) (m). *Calculated by:* Por_group2_a/ff_group2_a. *Sensitivity Name:* UZFAG2. *Location in TSPA-LA:* Section 6.3.9.2; Equation 6.3.9-2; Fracture porosity values and frequency values are shown in Tables 6.3.9-6 and 6.3.9-7.
fa_group3_a - Fracture aperture for group 3 rock units (ch[2,3,4,5]fz, pcf[2,5]z, pp4fz, pp1fz, bf2fz, tr2fz) (m). *Calculated by:* Por_group3_a/ff_group3_a. *Sensitivity Name:* UZFAG3. *Location in TSPA-LA:* Section 6.3.9.2; Equation 6.3.9-2; Fracture porosity values and frequency values are shown in Tables 6.3.9-6 and 6.3.9-7.
fa_group4_a - Fracture aperture for group 4 rock units (pp3fd, pp2fd, bf3fd, tr3fd) (m). *Calculated by:* Por_group4_a/ff_group4_a. *Sensitivity Name:* UZFAG4. *Location in TSPA-LA:* Section 6.3.9.2; Equation 6.3.9-2; Fracture porosity values and frequency values are shown in Tables 6.3.9-6 and 6.3.9-7.
fa_group5_a - Fracture aperture for group 5 rock units (ch1fz, pcf1z, ch6fz, pcf6z) (m). *Calculated by:* Por_group5_a/ff_group5_a. *Sensitivity Name:* UZFAG5. *Location in TSPA-LA:* Section 6.3.9.2; Equation 6.3.9-2; Fracture porosity values and frequency values are shown in Tables 6.3.9-6 and 6.3.9-7.
fa_group6_a - Fracture aperture for group 6 rock units (ch[1,2,3,4,5,6]fv) (m). *Calculated by:* Por_group6_a/ff_group6_a. *Sensitivity Name:* UZFAG6. *Location in TSPA-LA:* Section 6.3.9.2; Equation 6.3.9-2; Fracture porosity values and frequency values are shown in Tables 6.3.9-6 and 6.3.9-7.
fa_group7_a - Fracture aperture for group 7 rock units (tswf9, pcf39, tswfv, tswfz) (m). *Calculated by:* Por_group7_a/ff_group7_a. *Sensitivity Name:* UZFAG7. *Location in TSPA-LA:* Section 6.3.9.2; Equation 6.3.9-2; Fracture porosity values and frequency values are shown in Tables 6.3.9-6 and 6.3.9-7.
fa_group8_a - Fracture aperture for group 8 rock units (tswf[4,5], tswf[6,7], tswf8, pcf38) (m). *Calculated by:* Por_group8_a/ff_group8_a. *Sensitivity Name:* UZFAG8. *Location in TSPA-LA:* Section 6.3.9.2; Equation 6.3.9-2; Fracture porosity values and frequency values are shown in Tables 6.3.9-6 and 6.3.9-7.
fa_group9_a - Fracture aperture for group 9 rock units (tswf3) (m). *Calculated by:* Por_group9_a/ff_group9_a. *Sensitivity Name:* UZFAG9. *Location in TSPA-LA:* Section 6.3.9.2; Equation 6.3.9-2; Fracture porosity values and frequency values are shown in Tables 6.3.9-6 and 6.3.9-7.
FHH_Isotherm_k_CP_a - Frenkel Halsey Hill water vapor adsorption isotherm parameter, *k*, for corrosion products (dimensionless). *Distribution:* Uniform. *Range:* 1.048 to 1.370 (see additional information). *Sensitivity Name:* FHHISKCP. *Location in TSPA-LA:* Table 6.3.8-4.
FHH_Isotherm_k_CSNF_Rind_a - Frenkel Halsey Hill water vapor adsorption isotherm parameter, *k*, for CSNF rind (dimensionless). *Distribution:* Uniform. *Range:* 1.606 to 8.215. *Sensitivity Name:* FHHISKCS. *Location in TSPA-LA:* Table 6.3.8-4.
FHH_Isotherm_s_CP_a - Frenkel Halsey Hill water vapor adsorption isotherm parameter, *s*, for corrosion products (dimensionless). *Distribution:* Uniform. *Range:* 1.525 to 1.852 (see additional information). *Sensitivity Name:* FHHISSCP. *Location in TSPA-LA:* Table 6.3.8-4.
FHH_Isotherm_s_CSNF_Rind_a - Frenkel Halsey Hill water vapor adsorption isotherm parameter, *s*, for CSNF rind (dimensionless). *Distribution:* Uniform. *Range:* 1.656 to 3.038. *Sensitivity Name:* FHHISSCS. *Location in TSPA-LA:* Table 6.3.8-4.
FISVO - Flowing interval spacing in fractured volcanic units (m). *Distribution:* Piecewise uniform. *Range:* 1.86 to 80. *Sensitivity Name:* SZFISPVO. *Location in TSPA-LA:* Section 6.3.10.5; Table 6.3.10-2.
FPLANW - Northwestern boundary of alluvial uncertainty zone (dimensionless). *Distribution:* Uniform. *Range:* 0 to 1. *Sensitivity Name:* SZWBNDAL. *Location in TSPA-LA:* Section 6.3.10.2; Table 6.3.10-2.
FPVO – Logarithm of flowing interval porosity in volcanic units (dimensionless). *Distribution:* Piecewise uniform. *Range:* -5 to -1. *Mean/Median/Mode:* -3. *Sensitivity Name:* SZFIPOVO. *Location in TSPA-LA:* Table 6.3.10-2.
Fraction_Channel_a - Fraction of the RMEI location subject to fluvial deposition (dimensionless). *Distribution:* Uniform. *Range:* 0.088 to 0.54. *Sensitivity Name:* FRACCHNL. *Location in TSPA-LA:* Table 6.5-5.
Gamma_AFM_a - Active fracture model (AFM) Gamma parameter (dimensionless). *Distribution:* Uniform. *Range:* 0.2 to 0.6. *Sensitivity Name:* UZGAM. *Location in TSPA-LA:* Sections 6.3.9.2, 6.3.9.3 and 6.3.9.4.1; Table 6.3.9-5.

Table K3-2. High-Level Summary of Epistemically Uncertain Variables (i.e., elements of **e**) Considered in the TSPA-LA (TSPA Parameter Name) (Continued)

NOTE: * indicates variable not considered in sensitivity analysis due to correlations.

GC_ULevel_A22_a - Variable for selecting distribution for general corrosion rate (low, medium, or high) (dimensionless). *Distribution:* Discrete. *Range:* 1 to 3. *Sensitivity Name:* WDGCUA22. *Location in TSPA-LA:* Table 6.3.5-4.
Goethite_SA_a - Specific surface area of goethite (m^2/g). *Distribution:* Truncated log normal. *Range:* 14.7 to 110. *Mean:* 51.42. *Standard Deviation:* 30.09. *Sensitivity Name:* GOESA. *Location in TSPA-LA:* Table 6.3.8-4; S_{CP} in Equation 6.3.8-19.
Goethite_Site_Density_a - Density of sorption sites on goethite (1/nm^2). *Distribution:* Discrete. *Range:* 1.02 to 8.59. *Sensitivity Name:* GOESITED. *Location in TSPA-LA:* Table 6.3.8-3.
GW_BDCF_MIC_Ac227 - Groundwater Biosphere Dose Conversion Factor (BDCF) for ^{227}Ac in modern interglacial climate ((Sv/year)/(Bq/m^3)). *Distribution:* Discrete. *Range:* 4.08E-07 to 4.32E-06. *Mean:* 1.3E-06. *Standard Deviation:* 5.28E-07. *Sensitivity Name:* MICAC227. *Location in TSPA-LA:* Sections 6.3.11.2 and 6.3.11.3; Table 6.3.11-3.
GW_BDCF_MIC_Am241 - Groundwater Biosphere Dose Conversion Factor (BDCF) for ^{241}Am in modern interglacial climate ((Sv/year)/(Bq/m^3)). *Distribution:* Discrete. *Range:* 2.16E-07 to 3.30E-06. *Mean:* 8.34E-07. *Standard Deviation:* 4.03E-07. *Sensitivity Name:* MICAM241. *Location in TSPA-LA:* Sections 6.3.11.2 and 6.3.11.3; Table 6.3.11-3.
GW_BDCF_MIC_Am243 - Groundwater Biosphere Dose Conversion Factor (BDCF) for ^{243}Am in modern interglacial climate ((Sv/year)/(Bq/m^3)). *Distribution:* Discrete. *Range:* 2.21E-07 to 3.37E-06. *Mean:* 8.88E-07. *Standard Deviation:* 4.12E-07. *Sensitivity Name:* MICAM243. *Location in TSPA-LA:* Sections 6.3.11.2 and 6.3.11.3; Table 6.3.11-3.
GW_BDCF_MIC_C14 - Groundwater Biosphere Dose Conversion Factor (BDCF) for ^{14}C in modern interglacial climate ((Sv/year)/(Bq/m^3)). *Distribution:* Discrete. *Range:* 7.18E-10 to 2.56E-08. *Mean:* 1.93E-09. *Standard Deviation:* 1.85E-09. *Sensitivity Name:* MICC14. *Location in TSPA-LA:* Sections 6.3.11.2 and 6.3.11.3; Table 6.3.11-3.
GW_BDCF_MIC_Cl36 - Groundwater Biosphere Dose Conversion Factor (BDCF) for ^{36}Cl in modern interglacial climate ((Sv/year)/(Bq/m^3)). *Distribution:* Discrete. *Range:* 1.28E-09 to 3.00E-07. *Mean:* 8.09E-09. *Standard Deviation:* 1.41E-08. *Sensitivity Name:* MICCl36. *Location in TSPA-LA:* Sections 6.3.11.2 and 6.3.11.3; Table 6.3.11-3.
GW_BDCF_MIC_Cs135 - Groundwater Biosphere Dose Conversion Factor (BDCF) for ^{135}Cs in modern interglacial climate ((Sv/year)/(Bq/m^3)). *Distribution:* Discrete. *Range:* 3.1E-09 to 8.48E-08. *Mean:* 1.45E-08. *Standard Deviation:* 1.02E-08. *Sensitivity Name:* MICCS135. *Location in TSPA-LA:* Sections 6.3.11.2 and 6.3.11.3; Table 6.3.11-3.
GW_BDCF_MIC_Cs137 - Groundwater Biosphere Dose Conversion Factor (BDCF) for ^{137}Cs in modern interglacial climate ((Sv/year)/(Bq/m^3)). *Distribution:* Discrete. *Range:* 3.87E-08 to 4.56E-07. *Mean:* 1.30E-07. *Standard Deviation:* 6.33E-08. *Sensitivity Name:* MICCS137. *Location in TSPA-LA:* Sections 6.3.11.2 and 6.3.11.3; Table 6.3.11-3.
GW_BDCF_MIC_I129 - Groundwater Biosphere Dose Conversion Factor (BDCF) for ^{129}I in modern interglacial climate ((Sv/year)/(Bq/m^3)). *Distribution:* Discrete. *Range:* 8.59E-08 to 1.13E-06. *Mean:* 1.29E-07. *Standard Deviation:* 5.28E-08. *Sensitivity Name:* MICI129. *Location in TSPA-LA:* Sections 6.3.11.2 and 6.3.11.3; Table 6.3.11-3.
GW_BDCF_MIC_Np237 - Groundwater Biosphere Dose Conversion Factor (BDCF) for ^{237}Np in modern interglacial climate ((Sv/year)/(Bq/m^3)). *Distribution:* Discrete. *Range:* 1.06E-07 to 8.05E-07. *Mean:* 2.74E-07. *Standard Deviation:* 9.70E-08. *Sensitivity Name:* MICNP237. *Location in TSPA-LA:* Sections 6.3.11.2 and 6.3.11.3; Table 6.3.11-3.
GW_BDCF_MIC_Pa231 - Groundwater Biosphere Dose Conversion Factor (BDCF) for ^{231}Pa in modern interglacial climate ((Sv/year)/(Bq/m^3)). *Distribution:* Discrete. *Range:* 6.58E-07 to 8.56E-06. *Mean:* 2.44E-06. *Standard Deviation:* 1.02E-06. *Sensitivity Name:* MICPA231. *Location in TSPA-LA:* Sections 6.3.11.2 and 6.3.11.3; Table 6.3.11-3.
GW_BDCF_MIC_Pu238 - Groundwater Biosphere Dose Conversion Factor (BDCF) for ^{238}Pu in modern interglacial climate ((Sv/year)/(Bq/m^3)). *Distribution:* Discrete. *Range:* 2.61E-07 to 2.09E-006. *Mean:* 7.61E-07. *Standard Deviation:* 2.78E-07. *Sensitivity Name:* MICPU238. *Location in TSPA-LA:* Sections 6.3.11.2 and 6.3.11.3; Table 6.3.11-3.

Table K3-2. High-Level Summary of Epistemically Uncertain Variables (i.e., elements of **e**) Considered in the TSPA-LA (TSPA Parameter Name) (Continued)

NOTE: * indicates variable not considered in sensitivity analysis due to correlations.

GW_BDCF_MIC_Pu239 - Groundwater Biosphere Dose Conversion Factor (BDCF) for ^{239}Pu in modern interglacial climate ((Sv/year)/(Bq/m^3)). *Distribution:* Discrete. *Range:* 3.49E-07 to 2.93E-06. *Mean:* 9.55E-07. *Standard Deviation:* 3.37E-07. *Sensitivity Name:* MICPU239. *Location in TSPA-LA:* Sections 6.3.11.2 and 6.3.11.3; Table 6.3.11-3.
GW_BDCF_MIC_Pu240 - Groundwater Biosphere Dose Conversion Factor (BDCF) for ^{240}Pu in modern interglacial climate ((Sv/year)/(Bq/m^3)). *Distribution:* Discrete. *Range:* 3.47E-07 to 2.90E-06. *Mean:* 9.51E-07. *Standard Deviation:* 3.35E-07. *Sensitivity Name:* MICPU240. *Location in TSPA-LA:* Sections 6.3.11.2 and 6.3.11.3; Table 6.3.11-3.
GW_BDCF_MIC_Ra226_Pb210 - Groundwater Biosphere Dose Conversion Factor (BDCF) for ^{210}Pb summed into ^{226}Ra in modern interglacial climate ((Sv/year)/(Bq/m^3)). *Distribution:* Discrete. *Range:* 2.90E-06 to 2.82E-05. *Mean:* 6.52E-06. *Standard Deviation:* 2.58E-06. *Sensitivity Name:* MICRA226. *Location in TSPA-LA:* Sections 6.3.11.2 and 6.3.11.3; Table 6.3.11-3.
GW_BDCF_MIC_Se79 - Groundwater Biosphere Dose Conversion Factor (BDCF) for ^{79}Se in modern interglacial climate ((Sv/year)/(Bq/m^3)). *Distribution:* Discrete. *Range:* 3.62E-09 to 1.51E-06. *Mean:* 2.42E-08. *Standard Deviation:* 7.48E-08. *Sensitivity Name:* MICSE79. *Location in TSPA-LA:* Sections 6.3.11.2 and 6.3.11.3; Table 6.3.11-3.
GW_BDCF_MIC_Sn126 - Groundwater Biosphere Dose Conversion Factor (BDCF) for ^{126}Sn in modern interglacial climate ((Sv/year)/(Bq/m^3)). *Distribution:* Discrete. *Range:* 8.92E-08 to 1.68E-06. *Mean:* 4.33E-07. *Standard Deviation:* 2.39E-07. *Sensitivity Name:* MICSN126. *Location in TSPA-LA:* Sections 6.3.11.2 and 6.3.11.3; Table 6.3.11-3.
GW_BDCF_MIC_Sr90 - Groundwater Biosphere Dose Conversion Factor (BDCF) for ^{90}Sr in modern interglacial climate ((Sv/year)/(Bq/m^3)). *Distribution:* Discrete. *Range:* 2.51E-08 to 8.60E-08. *Mean:* 3.43E-08. *Standard Deviation:* 6.59E-09. *Sensitivity Name:* MICSR90. *Location in TSPA-LA:* Sections 6.3.11.2 and 6.3.11.3; Table 6.3.11-3.
GW_BDCF_MIC_Tc99 - Groundwater Biosphere Dose Conversion Factor (BDCF) for ^{99}Tc in modern interglacial climate ((Sv/year)/(Bq/m^3)). *Distribution:* Discrete. *Range:* 5.28E-10 to 2.85E-08. *Mean:* 1.12E-09. *Standard Deviation:* 1.26E-09. *Sensitivity Name:* MICTC99. *Location in TSPA-LA:* Sections 6.3.11.2 and 6.3.11.3; Table 6.3.11-3.
GW_BDCF_MIC_Th229 - Groundwater Biosphere Dose Conversion Factor (BDCF) for ^{229}Th in modern interglacial climate ((Sv/year)/(Bq/m^3)). *Distribution:* Discrete. *Range:* 7.43E-07 to 8.05E-06. *Mean:* 2.58E-06. *Standard Deviation:* 1.03E-06. *Sensitivity Name:* MICTH229. *Location in TSPA-LA:* Sections 6.3.11.2 and 6.3.11.3; Table 6.3.11-3.
GW_BDCF_MIC_U232 - Groundwater Biosphere Dose Conversion Factor (BDCF) for 232U in modern interglacial climate ((Sv/year)/(Bq/m^3)). *Distribution:* Discrete. *Range:* 2.87E-07 to 1.86E-06. *Mean:* 6.04E-07. *Standard Deviation:* 2.17E-07. *Sensitivity Name:* MICU232. *Location in TSPA-LA:* Sections 6.3.11.2 and 6.3.11.3; Table 6.3.11-3.
GW_BDCF_MIC_U233 - Groundwater Biosphere Dose Conversion Factor (BDCF) for ^{233}U in modern interglacial climate ((Sv/year)/(Bq/m^3)). *Distribution:* Discrete. *Range:* 4.13E-08 to 3.13E-07. *Mean:* 8.97E-08. *Standard Deviation:* 3.35E-08. *Sensitivity Name:* MICU233. *Location in TSPA-LA:* Sections 6.3.11.2 and 6.3.11.3; Table 6.3.11-3.
GW_BDCF_MIC_U234 - Groundwater Biosphere Dose Conversion Factor (BDCF) for ^{234}U in modern interglacial climate ((Sv/year)/(Bq/m^3)). *Distribution:* Discrete. *Range:* 3.96E-08 to 2.20E-07. *Mean:* 8.19E-08. *Standard Deviation:* 2.81E-08. *Sensitivity Name:* MICU234. *Location in TSPA-LA:* Sections 6.3.11.2 and 6.3.11.3; Table 6.3.11-3.
GW_BDCF_MIC_U238 - Groundwater Biosphere Dose Conversion Factor (BDCF) for ^{238}U in modern interglacial climate ((Sv/year)/(Bq/m^3)). *Distribution:* Discrete. *Range:* 3.85E-08 to 2.07E-07. *Mean:* 7.87E-08. *Standard Deviation:* 2.62E-08. *Sensitivity Name:* MICU238. *Location in TSPA-LA:* Sections 6.3.11.2 and 6.3.11.3; Table 6.3.11-3.
GWSPD - Logarithm of the scale factor used to characterize uncertainty in groundwater specific discharge (dimensionless). *Distribution:* Piecewise uniform. *Range:* -0.951 to 0.951. *Sensitivity Name:* SZGWSPDM. *Location in TSPA-LA:* Section 6.3.10.2; Table 6.3.10-2.

Table K3-2. High-Level Summary of Epistemically Uncertain Variables (i.e., elements of **e**) Considered in the TSPA-LA (TSPA Parameter Name) (Continued)

NOTE: * indicates variable not considered in sensitivity analysis due to correlations.

HAVO - Ratio of horizontal anisotropy (north-south over east-west) in the permeability of the SZ volcanic units (dimensionless). *Distribution:* Piecewise uniform. *Range:* 0.05 to 20. *Sensitivity Name:* SZRAHAVO. *Location in TSPA-LA:* Sections 6.3.10.2 and 6.3.10.5; Table 6.3.10-2.
HFO_SA_a - Hydrous ferric oxide (HFO) surface area (m^2/g). *Distribution:* Truncated log normal. *Range:* 68 to 600. *Mean:* 275.6. *Standard Deviation:* 113.4. *Sensitivity Name:* HFOSA. *Location in TSPA-LA:* Table 6.3.8-4; S_{CP} in Equation 6.3.8-19.
HFO_Site_Density_a - Sorption site density for hydrous ferric oxide (HFO) (1/nm^2). *Distribution:* Discrete. *Range:* 0.56 to 5.65. *Sensitivity Name:* HFOSITED. *Location in TSPA-LA:* Table 6.3.8-3.
HLW_Diss_kE_Acidic_a - Effective rate coefficient (affinity term) for the dissolution of HLW glass in CDSP waste packages under low pH conditions (g/(m^2d)). *Distribution:* Triangular. *Range:* 8.41E+03 to 1.15E+07. *Mode:* 8.41E+03. *Sensitivity Name:* HLWDRACD. *Location in TSPA-LA:* Sections 6.3.7.4.3.2 and 6.3.7.4.3.3; Table 6.3.7-32; Equation 6.3.7-8.
HLW_Diss_kE_Alkaline_a - Effective rate coefficient (affinity term) for the dissolution of HLW glass in CDSP waste packages under high pH conditions (g/(m^2d)). *Distribution:* Triangular. *Range:* 2.82E+01 to 3.47E+04. *Mode:* 2.82E+01. *Sensitivity Name:* HLWDRALK. *Location in TSPA-LA:* Sections 6.3.7.4.3.2 and 6.3.7.4.3.3; Table 6.3.7-32; Equation 6.3.7-8.
HLW_Mass_Uncert_a - Scale factor used to characterize uncertainty in radionuclide content of HLW glass (dimensionless). *Distribution:* Triangular. *Range:* 0.7 to 1.5. *Most Likely:* 1. *Sensitivity Name:* HLWMASS. *Location in TSPA-LA:* Sections 6.3.7.1.2 and 6.3.7.1.3; Table 6.3.7-7.
HLWG_Rind_SA_a - Specific surface area of HLWG degradation rind (m^2/g). *Distribution:* Uniform. *Range:* 10 to 38. *Sensitivity Name:* HLWGRNDS. *Location in TSPA-LA:* Table 6.3.8-4.
IGERATE - Frequency of occurrence of volcanic eruptive events (yr^{-1}). *Calculated by:* Igneous_Event_Prob_a x 0.083. *Range:* 0 to 6.44E-08. *Sensitivity Name:* IGERATE. *Location in TSPA-LA:* Section 6.5.2.1.1; Appendix J; Equation J7.5-3.
Igneous_Event_Prob_a - Frequency of intersection of the repository footprint by a volcanic event (yr^{-1}). *Distribution:* Piecewise uniform. *Range:* 0 to 7.76E-07. *Sensitivity Name:* IGRATE. *Location in TSPA-LA:* Table 6.5-2.
Infiltration_Scenario_a - Pointer variable for determining infiltration conditions: 10^{th}, 30^{th}, 50^{th} or 90^{th} percentile infiltration scenario (dimensionless). *Distribution:* Discrete. *Range:* 1 to 4. *Sensitivity Name:* INFIL. *Location in TSPA-LA:* Section 6.3.1.2; Tables 6.3.1-2 and 6.3.5-4.
Initial_Release_Frac_Cs_a - The initial release fraction of ^{137}Cs in a CSNF waste package (dimensionless). *Distribution:* Triangular. *Range:* 0.0039 to 0.1106. *Mode:* 0.0363. *Sensitivity Name:* INRFRCCS. *Location in TSPA-LA:* Sections 6.3.7.4.1.2 and 6.3.7.4.1.3; Table 6.3.7-29.
Initial_Release_Frac_I_a - The initial release fraction of ^{129}I in a CSNF waste package (dimensionless). *Distribution:* Triangular. *Range:* 0.0204 to 0.2675. *Mode:* 0.1124. *Sensitivity Name:* INRFRCI. *Location in TSPA-LA:* Sections 6.3.7.4.1.2 and 6.3.7.4.1.3; Table 6.3.7-29.
Initial_Release_Frac_Sr_a - The initial release fraction of ^{90}Sr in a CSNF waste package (dimensionless). *Distribution:* Triangular. *Range:* 0.0002 to 0.0025. *Mode:* 0.0009. *Sensitivity Name:* INRFRCSR. *Location in TSPA-LA:* Sections 6.3.7.4.1.2 and 6.3.7.4.1.3; Table 6.3.7-29.
Initial_Release_Frac_Tc_a - The initial release fraction of ^{99}Tc in a CSNF waste package (dimensionless). *Distribution:* Triangular. *Range:* 0.0001 to 0.0026. *Mode:* 0.001. *Sensitivity Name:* INRFRCTC. *Location in TSPA-LA:* Sections 6.3.7.4.1.2 and 6.3.7.4.1.3; Table 6.3.7-29.
Inpkg_IStr_2DHLW_NS_Rand_a - Pointer variable used to determine ionic strength for 2DHLW Cell (Cell 1a) of CDSP waste packages under vapor influx conditions (dimensionless). *Distribution:* Uniform. *Range:* 0 to 1. *Sensitivity Name:* IS2DHLNS. *Location in TSPA-LA:* Section 6.3.7.2.2 Part III.
Inpkg_IStr_2DHLW_S_Rand_a - Pointer variable used to determine ionic strength for 2DHLW Cell (Cell 1a) of CDSP waste packages under liquid influx conditions (dimensionless). *Distribution:* Uniform. *Range:* 0 to 1. *Sensitivity Name:* IS2DHLS. *Location in TSPA-LA:* Section 6.3.7.2.2 Part III.
Inpkg_IStr_2MCO_NS_Rand_a - Pointer variable used to determine ionic strength for 2MCO Cell (Cell 1b) of CDSP waste packages under vapor influx conditions (dimensionless). *Distribution:* Uniform. *Range:* 0 to 1. *Sensitivity Name:* IS2MCONS. *Location in TSPA-LA:* Section 6.3.7.2.2 Part III.

Table K3-2. High-Level Summary of Epistemically Uncertain Variables (i.e., elements of **e**) Considered in the TSPA-LA (TSPA Parameter Name) (Continued)

NOTE: * indicates variable not considered in sensitivity analysis due to correlations.

lnpkg_IStr_2MCO_S_Rand_a - Pointer variable used to determine ionic strength for 2MCO Cell (Cell 1b) of CDSP waste packages under liquid influx conditions (dimensionless). *Distribution:* Uniform. *Range:* 0 to 1. *Sensitivity Name:* IS2MCOS. *Location in TSPA-LA:* Section 6.3.7.2.2 Part III.
lnpkg_IStr_CSNF_NS_Rand_a - Pointer variable used to determine ionic strength for CSNF Cell under vapor influx conditions (dimensionless). *Distribution:* Uniform. *Range:* 0 to 1. *Sensitivity Name:* ISCSNS. *Location in TSPA-LA:* Section 6.3.7.2.2 Part III.
lnpkg_IStr_CSNF_S_Rand_a - Pointer variable used to determine ionic strength for CSNF Cell under liquid influx conditions (dimensionless). *Distribution:* Uniform. *Range:* 0 to 1. *Sensitivity Name:* ISCSS. *Location in TSPA-LA:* Section 6.3.7.2.2 Part III.
lnpkg_pH_2DHLW_NS_Rand_a - Pointer variable used to determine pH in 2DHLW Cell (Cell 1a) of CDSP waste packages under vapor influx conditions (dimensionless). *Distribution:* Uniform. *Range:* 0 to 1. *Sensitivity Name:* PH2DHLNS. *Location in TSPA-LA:* Section 6.3.7.2.2 Part IV.
lnpkg_pH_2DHLW_S_Rand_a - Pointer variable used to determine pH in 2DHLW Cell (Cell 1a) of CDSP waste packages under liquid influx conditions (dimensionless). *Distribution:* Uniform. *Range:* 0 to 1. *Sensitivity Name:* PH2DHLS. *Location in TSPA-LA:* Section 6.3.7.2.2 Part IV.
lnpkg_pH_2MCO_NS_Rand_a - Pointer variable used to determine pH in 2MCO Cell (Cell 1b) of CDSP waste packages under vapor influx conditions (dimensionless). *Distribution:* Uniform. *Range:* 0 to 1. *Sensitivity Name:* PH2MCONS. *Location in TSPA-LA:* Section 6.3.7.2.2 Part IV.
lnpkg_pH_2MCO_S_Rand_a - Pointer variable used to determine pH in 2MCO Cell (Cell 1b) of CDSP waste packages under liquid influx conditions (dimensionless). *Distribution:* Uniform. *Range:* 0 to 1. *Sensitivity Name:* PH2MCOS. *Location in TSPA-LA:* Section 6.3.7.2.2 Part IV.
lnpkg_pH_CSNF_NS_Rand_a - Pointer variable used to determine pH in CSNF Cell1 under vapor influx conditions (dimensionless). *Distribution:* Uniform. *Range:* 0 to 1. *Sensitivity Name:* PHCSNS. *Location in TSPA-LA:* Section 6.3.7.2.2 Part IV.
lnpkg_pH_CSNF_S_Rand_a - Pointer variable used to determine pH in CSNF Cell1 under liquid influx conditions (dimensionless). *Distribution:* Uniform. *Range:* 0 to 1. *Sensitivity Name:* PHCSS. *Location in TSPA-LA:* Section 6.3.7.2.2 Part IV.
Invert_Diff_Coeff_Uncert_a - Exponential term representing uncertainty in the invert diffusion coefficient (dimensionless). *Distribution:* Truncated normal. *Range:* -0.621 to 0.687. *Mean:* 0.033. *Standard Deviation:* 0.218. *Sensitivity Name:* EBSDIFCF. *Location in TSPA-LA:* Section 6.3.8.2.4; Table 6.3.8-4; Equation 6.3.8-24.
Kd_Am_Al - Americium sorption coefficient in alluvium (mL/g). *Distribution:* Truncated normal. *Range:* 1000 to 10000. *Mean/Median/Mode:* 5500. *Standard Deviation:* 1500. *Sensitivity Name:* SZKDAMAL. *Location in TSPA-LA:* Section 6.3.10.2; Table 6.3.10-2.
Kd_Am_Col - Americium sorption coefficient onto smectite colloids (mL/g). *Distribution:* Piecewise uniform. *Range:* 1.00E+04 to 1.00E+07. *Sensitivity Name:* SZKDAMCO. *Location in TSPA-LA:* Section 6.3.10.2; Table 6.3.10-2.
Kd_Am_Rev_Smectite_a - Distribution coefficient for reversible sorption of americium to waste form (smectite) colloids (mL/g). *Distribution:* Piecewise uniform. *Range:* 1.00E+04 to 1.00E+07. *Sensitivity Name:* KDAMSMEC. *Location in TSPA-LA:* Sections 6.3.7.6.2 and 6.3.7.6.3; Equation 6.3.7-20; Tables 6.3.7-62 and 6.3.7-66.
Kd_Am_Rev_U_Col_a - Distribution coefficient for reversible sorption of americium onto uranophane colloids (mL/g). *Distribution:* Log uniform. *Range:* 5 to 1.00E+04. *Sensitivity Name:* KDAMCOL. *Location in TSPA-LA:* Sections 6.3.7.6.2 and 6.3.7.6.3; Equation 6.3.7-20; Table 6.3.7-64.
Kd_Am_Vo - Americium sorption coefficient in volcanic units (mL/g). *Distribution:* Truncated normal. *Range:* 1000 to 10000. *Mean/Median/Mode:* 5500. *Standard Deviation:* 1500. *Sensitivity Name:* SZKDAMVO. *Location in TSPA-LA:* Section 6.3.10.2; Table 6.3.10-2.
Kd_Cs_Al - Cesium sorption coefficient in alluvium (mL/g). *Distribution:* Truncated normal. *Range:* 100 to 1000. *Mean/Median/Mode:* 728. *Standard Deviation:* 464. *Sensitivity Name:* SZKDCSAL. *Location in TSPA-LA:* Section 6.3.10.2; Table 6.3.10-2.
Kd_Cs_Col - Cesium sorption coefficient onto smectite colloids (mL/g). *Distribution:* Piecewise uniform. *Range:* 50 to 5000. *Sensitivity Name:* SZKDCSCO. *Location in TSPA-LA:* Section 6.3.10.2; Table 6.3.10-2.

Table K3-2. High-Level Summary of Epistemically Uncertain Variables (i.e., elements of **e**) Considered in the TSPA-LA (TSPA Parameter Name) (Continued)

NOTE: * indicates variable not considered in sensitivity analysis due to correlations.

Kd_Cs_Rev_Smectite_a - Distribution coefficient for reversible sorption of cesium to waste form (smectite) colloids (mL/g). *Distribution:* Piecewise uniform. *Range:* 50 to 5000. *Sensitivity Name:* KDCSSMEC. *Location in TSPA-LA:* Sections 6.3.7.6.2 and 6.3.7.6.3; Equation 6.3.7-20; Tables 6.3.7-62 and 6.3.7-66.
Kd_Cs_Rev_U_Col_a - Distribution coefficient for reversible sorption of cesium onto uranophane colloids (mL/g). *Distribution:* Log uniform. *Range:* 10 to 1000. *Sensitivity Name:* KDCSCOL. *Location in TSPA-LA:* Sections 6.3.7.6.2 and 6.3.7.6.3; Equation 6.3.7-20; Table 6.3.7-64.
Kd_Cs_Vo - Cesium sorption coefficient in volcanic units (mL/g). *Distribution:* Piecewise uniform. *Range:* 100 to 6783. *Sensitivity Name:* SZKDCSVO. *Location in TSPA-LA:* Section 6.3.10.2; Table 6.3.10-2.
Kd_Np_Al - Neptunium sorption coefficient in alluvium (mL/g). *Distribution:* Piecewise uniform. *Range:* 1.8 to 13. *Sensitivity Name:* SZKDNPAL. *Location in TSPA-LA:* Section 6.3.10.2; Table 6.3.10-2.
Kd_Np_Rev_Smectite_a - Distribution coefficient for reversible sorption of neptunium to waste form (smectite) colloids (mL/g). *Distribution:* Log uniform. *Range:* 10 to 500. *Sensitivity Name:* KDNPSMEC. *Location in TSPA-LA:* Sections 6.3.7.6.2 and 6.3.7.6.3; Equation 6.3.7-20; Tables 6.3.7-62 and 6.3.7-66.
Kd_Np_Rev_U_Col_a - Distribution coefficient for reversible sorption of neptunium onto uranophane colloids (mL/g). *Distribution:* Log uniform. *Range:* 1 to 500. *Sensitivity Name:* KDNPCOL. *Location in TSPA-LA:* Sections 6.3.7.6.2 and 6.3.7.6.3; Equation 6.3.7-20; Table 6.3.7-64.
Kd_Np_Vo - Neptunium sorption coefficient in volcanic units (mL/g). *Distribution:* Piecewise uniform. *Range:* 0 to 6. *Sensitivity Name:* SZKDNPVO. *Location in TSPA-LA:* Section 6.3.10.2; Table 6.3.10-2.
Kd_Pa_Rev_Smectite_a - Distribution coefficient for reversible sorption of protactinium to waste form (smectite) colloids (mL/g). *Distribution:* Piecewise uniform. *Range:* 1.00E+04 to 1.00E+07. *Sensitivity Name:* KDPASMEC. *Location in TSPA-LA:* Sections 6.3.7.6.2 and 6.3.7.6.3; Equation 6.3.7-20; Tables 6.3.7-62 and 6.3.7-66.
Kd_Pa_Rev_U_Col_a - Distribution coefficient for reversible sorption of protactinium onto uranophane colloids (mL/g). *Distribution:* Log uniform. *Range:* 5 to 1.00E+04. *Sensitivity Name:* KDPACOL. *Location in TSPA-LA:* Sections 6.3.7.6.2 and 6.3.7.6.3; Equation 6.3.7-20; Table 6.3.7-64.
Kd_Pu_Al - Plutonium sorption coefficient in alluvium (mL/g). *Distribution:* Beta. *Range:* 50 to 300. *Mean/Median/Mode:* 100. *Standard Deviation:* 15. *Sensitivity Name:* SZKDPUAL. *Location in TSPA-LA:* Section 6.3.10.2; Table 6.3.10-2.
Kd_Pu_Col - Plutonium sorption coefficient onto smectite colloids (mL/g). *Distribution:* Piecewise uniform. *Range:* 1.00E+03 to 1.00E+05. *Sensitivity Name:* SZKDPUCO. *Location in TSPA-LA:* Section 6.3.10.2; Table 6.3.10-2.
Kd_Pu_Rev_Smectite_a - Distribution coefficient for reversible sorption of plutonium to waste form (smectite) colloids (mL/g). *Distribution:* Piecewise uniform. *Range:* 1.00E+03 to 1.00E+05. *Sensitivity Name:* KDPUSMEC. *Location in TSPA-LA:* Sections 6.3.7.6.2 and 6.3.7.6.3; Equation 6.3.7-20; Tables 6.3.7-62 and 6.3.7-66.
Kd_Pu_Rev_U_Col_a - Distribution coefficient for reversible sorption of plutonium onto uranophane colloids (mL/g). *Distribution:* Log uniform. *Range:* 5 to 1.00E+04. *Sensitivity Name:* KDPUCOL. *Location in TSPA-LA:* Sections 6.3.7.6.2 and 6.3.7.6.3; Equation 6.3.7-20; Table 6.3.7-64.
Kd_Pu_Vo - Plutonium sorption coefficient in volcanic units (mL/g). *Distribution:* Piecewise uniform. *Range:* 10 to 300. *Sensitivity Name:* SZKDPUVO. *Location in TSPA-LA:* Section 6.3.10.2; Table 6.3.10-2.
Kd_Ra_Al - Radium sorption coefficient in alluvium (mL/g). *Distribution:* Uniform. *Range:* 100 to 1000. *Sensitivity Name:* SZKDRAAL. *Location in TSPA-LA:* Section 6.3.10.2; Table 6.3.10-2.
Kd_Ra_Rev_Smectite_a - Distribution coefficient for reversible sorption of radium to waste form (smectite) colloids (mL/g). *Distribution:* Log uniform. *Range:* 100 to 5000. *Sensitivity Name:* KDRASMEC. *Location in TSPA-LA:* Sections 6.3.7.6.2 and 6.3.7.6.3; Equation 6.3.7-20; Tables 6.3.7-62 and 6.3.7-66.
Kd_Ra_Rev_U_Col_a - Distribution coefficient for reversible sorption of radium onto uranophane colloids (mL/g). *Distribution:* Log uniform. *Range:* 10 to 1000. *Sensitivity Name:* KDRACOL. *Location in TSPA-LA:* Sections 6.3.7.6.2 and 6.3.7.6.3; Equation 6.3.7-20; Table 6.3.7-64.
Kd_Ra_Vo* - Radium sorption coefficient in volcanic units (mL/g). *Distribution:* Uniform. *Range:* 100 to 1000. *Sensitivity Name:* SZKDRAVO*. *Location in TSPA-LA:* Section 6.3.10.2; Table 6.3.10-2.
Kd_Se_Al - Selenium sorption coefficient in alluvium (mL/g). *Distribution:* Truncated log normal. *Range:* 1 to 50. *Mean/Median/Mode:* 14. *Standard Deviation:* 11.2. *Sensitivity Name:* SZKDSEAL. *Location in TSPA-LA:* Section 6.3.10.2; Table 6.3.10-2.

Table K3-2. High-Level Summary of Epistemically Uncertain Variables (i.e., elements of **e**) Considered in the TSPA-LA (TSPA Parameter Name) (Continued)

NOTE: * indicates variable not considered in sensitivity analysis due to correlations.

Kd_Se_Vo - Selenium sorption coefficient in volcanic units (mL/g). *Distribution:* Truncated log normal. *Range:* 1 to 50. *Mean/Median/Mode:* 14. *Standard Deviation:* 11.2. *Sensitivity Name:* SZKDSEVO. *Location in TSPA-LA:* Section 6.3.10.2; Table 6.3.10-2.
Kd_Sn_Al - Tin sorption coefficient in alluvium (mL/g). *Distribution:* Log uniform. *Range:* 1.00E+02 to 1.00E+05. *Sensitivity Name:* SZKDSNAL. *Location in TSPA-LA:* Section 6.3.10.2; Table 6.3.10-2.
Kd_Sn_Col - Tin sorption coefficient onto smectite colloids (mL/g). *Distribution:* Log uniform. *Range:* 1.00E+05 to 1.00E+06. *Sensitivity Name:* SZKDSNCO. *Location in TSPA-LA:* Section 6.3.10.2; Table 6.3.10-2.
Kd_Sn_Rev_Smectite_a - Distribution coefficient for reversible sorption of tin to waste form (smectite) colloids (mL/g). *Distribution:* Log uniform. *Range:* 1.00E+05 to 1.00E+06. *Sensitivity Name:* KDSNSMEC. *Location in TSPA-LA:* Sections 6.3.7.6.2 and 6.3.7.6.3; Equation 6.3.7-20; Tables 6.3.7-62 and 6.3.7-66.
Kd_Sn_Rev_U_Col_a - Distribution coefficient for reversible sorption of tin onto uranophane colloids (mL/g). *Distribution:* Log uniform. *Range:* 1 to 100. *Sensitivity Name:* KDSNCOL. *Location in TSPA-LA:* Sections 6.3.7.6.2 and 6.3.7.6.3; Equation 6.3.7-20; Table 6.3.7-64.
Kd_Sn_Vo - Tin sorption coefficient in volcanic units (mL/g). *Distribution:* Log uniform. *Range:* 1.00E+02 to 1.00E+05. *Sensitivity Name:* SZKDSNVO. *Location in TSPA-LA:* Section 6.3.10.2; Table 6.3.10-2.
Kd_Sr_Al - Strontium sorption coefficient in alluvium (mL/g). *Distribution:* Uniform. *Range:* 20 to 400. *Sensitivity Name:* SZKDSRAL. *Location in TSPA-LA:* Section 6.3.10.2; Table 6.3.10-2.
Kd_Sr_Vo - Strontium sorption coefficient in volcanic units (mL/g). *Distribution:* Uniform. *Range:* 20 to 400. *Sensitivity Name:* SZKDSRVO. *Location in TSPA-LA:* Section 6.3.10.2; Table 6.3.10-2.
Kd_Th_Rev_Smectite_a - Distribution coefficient for reversible sorption of thorium to waste form (smectite) colloids (mL/g). *Distribution:* Piecewise uniform. *Range:* 1.00E+04 to 1.00E+07. *Sensitivity Name:* KDTHSMEC. *Location in TSPA-LA:* Sections 6.3.7.6.2 and 6.3.7.6.3; Equation 6.3.7-20; Tables 6.3.7-62 and 6.3.7-66.
Kd_Th_Rev_U_Col_a - Distribution coefficient for reversible sorption of thorium onto uranophane colloids (mL/g). *Distribution:* Log uniform. *Range:* 5 to 1.00E+04. *Sensitivity Name:* KDTHCOL. *Location in TSPA-LA:* Sections 6.3.7.6.2 and 6.3.7.6.3; Equation 6.3.7-20; Table 6.3.7-64.
Kd_U_Al - Uranium sorption coefficient in alluvium (mL/g). *Distribution:* Piecewise uniform. *Range:* 1.7 to 8.9. *Sensitivity Name:* SZKDUAL. *Location in TSPA-LA:* Section 6.3.10.2; Table 6.3.10-2.
Kd_U_Rev_Smectite_a - Distribution coefficient for reversible sorption of uranium to waste form (smectite) colloids (mL/g). *Distribution:* Log uniform. *Range:* 5.00E+02 to 5.00E+04. *Sensitivity Name:* KDUSMEC. *Location in TSPA-LA:* Sections 6.3.7.6.2 and 6.3.7.6.3; Equation 6.3.7-20; Tables 6.3.7-62 and 6.3.7-66.
Kd_U_Vo - Uranium sorption coefficient in volcanic units (mL/g). *Distribution:* Piecewise uniform. *Range:* 0 to 20. *Sensitivity Name:* SZKDUVO. *Location in TSPA-LA:* Section 6.3.10.2; Table 6.3.10-2.
KdAm_Devit_a - Sorption coefficient of americium in devitrified tuff units of UZ (mL/g). *Distribution:* Truncated normal. *Range:* 1000 to 10000. *Mean:* 5500. *Standard Deviation:* 1500. *Sensitivity Name:* UZKDAMDT. *Location in TSPA-LA:* Sections 6.3.9.2 and 6.3.9.3; Equation 6.3.9-3; Table 6.3.9-2.
KdAm_Vit_a* - Sorption coefficient of americium in vitrified tuff units of UZ (mL/g). *Distribution:* Piecewise uniform. *Range:* 100 to 1000. *Median:* 400. *Sensitivity Name:* UZKDAMVT*. *Location in TSPA-LA:* Sections 6.3.9.2 and 6.3.9.3; Equation 6.3.9-3; Table 6.3.9-2.
KdAm_Zeo_a* - Sorption coefficient of americium in zeolitic tuff units of UZ (mL/g). *Distribution:* Truncated normal. *Range:* 1000 to 10000. *Mean:* 5500. *Standard Deviation:* 1500. *Sensitivity Name:* UZKDAMZT*. *Location in TSPA-LA:* Sections 6.3.9.2 and 6.3.9.3; Equation 6.3.9-3; Table 6.3.9-2.
KdCs_Devit_a - Sorption coefficient of cesium in devitrified tuff units of UZ (mL/g). *Distribution:* Uniform. *Range:* 1 to 15. *Sensitivity Name:* UZKDCSDT. *Location in TSPA-LA:* Sections 6.3.9.2 and 6.3.9.3; Equation 6.3.9-3; Table 6.3.9-2.
KdCs_Vit_a* - Sorption coefficient of cesium in vitrified tuff units of UZ (mL/g). *Distribution:* Piecewise uniform. *Range:* 0 to 100. *Median:* 2. *Sensitivity Name:* UZKDCSVT*. *Location in TSPA-LA:* Sections 6.3.9.2 and 6.3.9.3; Equation 6.3.9-3; Table 6.3.9-2.
KdCs_Zeo_a - Sorption coefficient for cesium in zeolitic tuff units of UZ (mL/g). *Distribution:* Piecewise uniform. *Range:* 425 to 20000. *Median:* 5,000. *Sensitivity Name:* UZKDCSZT. *Location in TSPA-LA:* Sections 6.3.9.2 and 6.3.9.3; Equation 6.3.9-3; Table 6.3.9-2.

Table K3-2. High-Level Summary of Epistemically Uncertain Variables (i.e., elements of **e**) Considered in the TSPA-LA (TSPA Parameter Name) (Continued)

NOTE: * indicates variable not considered in sensitivity analysis due to correlations.

KdNp_Devit_a - Sorption coefficient for neptunium in devitrified tuff units of UZ (mL/g). *Distribution:* Piecewise uniform. *Range:* 0 to 6. *Median:* 0.5. *Sensitivity Name:* UZKDNPDT. *Location in TSPA-LA:* Sections 6.3.9.2 and 6.3.9.3; Equation 6.3.9-3; Table 6.3.9-2.
KdNp_Vit_a* - Sorption coefficient for neptunium in vitrified tuff units of UZ (mL/g). *Distribution:* Piecewise uniform. *Range:* 0 to 3. *Median:* 1. *Sensitivity Name:* UZKDNPVT*, *Location in TSPA-LA:* Sections 6.3.9.2 and 6.3.9.3; Equation 6.3.9-3; Table 6.3.9-2.
KdNp_Zeo_a* - Sorption coefficient for neptunium in zeolitic tuff units of UZ (mL/g). *Distribution:* Piecewise uniform. *Range:* 0 to 6. *Median:* 0.5. *Sensitivity Name:* UZKDNPZT*. *Location in TSPA-LA:* Sections 6.3.9.2 and 6.3.9.3; Equation 6.3.9-3; Table 6.3.9-2.
KdPa_Devit_a - Sorption coefficient for protactinium in devitrified tuff units of UZ (mL/g). *Distribution:* Truncated normal. *Range:* 1000 to 10000. *Mean:* 5500. *Standard Deviation:* 1500. *Sensitivity Name:* UZKDPADT. *Location in TSPA-LA:* Sections 6.3.9.2 and 6.3.9.3; Equation 6.3.9-3; Table 6.3.9-2.
KdPa_Vit_a* - Sorption coefficient for protactinium in vitrified tuff units of UZ (mL/g). *Distribution:* Truncated normal. *Range:* 1000 to 10000. *Mean:* 5500. *Standard Deviation:* 1500. *Sensitivity Name:* UZKDPAVT*. *Location in TSPA-LA:* Sections 6.3.9.2 and 6.3.9.3; Equation 6.3.9-3; Table 6.3.9-2.
KdPa_Zeo_a* - Sorption coefficient for protactinium in zeolitic tuff units of UZ (mL/g). *Distribution:* Truncated normal. *Range:* 1000 to 10000. *Mean:* 5500. *Standard Deviation:* 1500. *Sensitivity Name:* UZKDPAZT*. *Location in TSPA-LA:* Sections 6.3.9.2 and 6.3.9.3; Equation 6.3.9-3; Table 6.3.9-2.
KdPu_Devit_a - Sorption coefficient for plutonium in devitrified tuff units of UZ (mL/g). *Distribution:* Piecewise uniform. *Range:* 10 to 200. *Median:* 70. *Sensitivity Name:* UZKDPUDT. *Location in TSPA-LA:* Sections 6.3.9.2 and 6.3.9.3; Equation 6.3.9-3; Table 6.3.9-2.
KdPu_Vit_a* - Sorption coefficient for plutonium in vitrified tuff units of UZ (mL/g). *Distribution:* Piecewise uniform. *Range:* 10 to 200. *Median:* 100. *Sensitivity Name:* UZKDPUVT*. *Location in TSPA-LA:* Sections 6.3.9.2 and 6.3.9.3; Equation 6.3.9-3; Table 6.3.9-2.
KdPu_Zeo_a* - Sorption coefficient for plutonium in zeolitic tuff units of UZ (mL/g). *Distribution:* Piecewise uniform. *Range:* 10 to 200. *Median:* 100. *Sensitivity Name:* UZKDPUZT*. *Location in TSPA-LA:* Sections 6.3.9.2 and 6.3.9.3; Equation 6.3.9-3; Table 6.3.9-2.
KdRa_Devit_a* - Sorption coefficient for radium in devitrified tuff units of UZ (mL/g). *Distribution:* Uniform. *Range:* 100 to 1000. *Sensitivity Name:* UZKDRADT*. *Location in TSPA-LA:* Sections 6.3.9.2 and 6.3.9.3; Equation 6.3.9-3; Table 6.3.9-2.
KdRa_Vit_a* - Sorption coefficient for radium in vitrified tuff units of UZ (mL/g). *Distribution:* Uniform. *Range:* 50 to 600. *Sensitivity Name:* UZKDRAVT*. *Location in TSPA-LA:* Sections 6.3.9.2 and 6.3.9.3; Equation 6.3.9-3; Table 6.3.9-2.
KdRa_Zeo_a* - Sorption coefficient for radium in zeolitic tuff units of UZ (mL/g). *Distribution:* Uniform. *Range:* 1000 to 5000. *Sensitivity Name:* UZKDRAZT*. *Location in TSPA-LA:* Sections 6.3.9.2 and 6.3.9.3; Equation 6.3.9-3; Table 6.3.9-2.
KdSe_Devit_a - Sorption coefficient for selenium in devitrified tuff units of UZ (mL/g). *Distribution:* Truncated log normal. *Range:* 1 to 50. *Mean:* 14. *Standard Deviation:* 11.2. *Sensitivity Name:* UZKDSEDT. *Location in TSPA-LA:* Sections 6.3.9.2 and 6.3.9.3; Equation 6.3.9-3; Table 6.3.9-2.
KdSe_Vit_a* - Sorption coefficient for selenium in vitrified tuff units of UZ (mL/g). *Distribution:* Truncated log normal. *Range:* 0 to 25. *Mean:* 8.6. *Standard Deviation:* 7.9. *Sensitivity Name:* UZKDSEVT*. *Location in TSPA-LA:* Sections 6.3.9.2 and 6.3.9.3; Equation 6.3.9-3; Table 6.3.9-2.
KdSe_Zeo_a* - Sorption coefficient for selenium in zeolitic tuff units of UZ (mL/g). *Distribution:* Truncated log normal. *Range:* 1 to 35. *Mean:* 14.3. *Standard Deviation:* 7.9. *Sensitivity Name:* UZKDSEZT*. *Location in TSPA-LA:* Sections 6.3.9.2 and 6.3.9.3; Equation 6.3.9-3; Table 6.3.9-2.
KdSn_Devit_a - Sorption coefficient for tin in devitrified tuff units of UZ (mL/g). *Distribution:* Log-uniform. *Range:* 100 to 100000. *Sensitivity Name:* UZKDSNDT. *Location in TSPA-LA:* Sections 6.3.9.2 and 6.3.9.3; Equation 6.3.9-3; Table 6.3.9-2.
KdSn_Vit_a* - Sorption coefficient for tin in vitrified tuff units of UZ (mL/g). *Distribution:* Log-uniform. *Range:* 100 to 5000. *Sensitivity Name:* UZKDSNVT*. *Location in TSPA-LA:* Sections 6.3.9.2 and 6.3.9.3; Equation 6.3.9-3; Table 6.3.9-2.

Table K3-2. High-Level Summary of Epistemically Uncertain Variables (i.e., elements of **e**) Considered in the TSPA-LA (TSPA Parameter Name) (Continued)

NOTE: * indicates variable not considered in sensitivity analysis due to correlations.

KdSn_Zeo_a* - Sorption coefficient for tin in zeolitic tuff units of UZ (mL/g). *Distribution:* Log-uniform. *Range:* 100 to 5000. *Sensitivity Name:* UZKDSNZT*. *Location in TSPA-LA:* Sections 6.3.9.2 and 6.3.9.3; Equation 6.3.9-3; Table 6.3.9-2.
KdSr_Devit_a - Sorption coefficient for strontium in devitrified tuff units of UZ (mL/g). *Distribution:* Uniform. *Range:* 10 to 70. *Sensitivity Name:* UZKDSRDT. *Location in TSPA-LA:* Sections 6.3.9.2 and 6.3.9.3; Equation 6.3.9-3; Table 6.3.9-2.
KdSr_Vit_a* - Sorption coefficient for strontium in vitrified tuff units of UZ (mL/g). *Distribution:* Uniform. *Range:* 0 to 50. *Sensitivity Name:* UZKDSRVT*. *Location in TSPA-LA:* Sections 6.3.9.2 and 6.3.9.3; Equation 6.3.9-3; Table 6.3.9-2.
KdSr_Zeo_a* - Sorption coefficient for strontium in zeolitic tuff units of UZ (mL/g). *Distribution:* Uniform. *Range:* 50 to 2000. *Sensitivity Name:* UZKDSRZT*. *Location in TSPA-LA:* Sections 6.3.9.2 and 6.3.9.3; Equation 6.3.9-3; Table 6.3.9-2.
KdTh_Devit_a - Sorption coefficient for thorium in devitrified tuff units of UZ (mL/g). *Distribution:* Uniform. *Range:* 1000 to 10000. *Sensitivity Name:* UZKDTHDT. *Location in TSPA-LA:* Sections 6.3.9.2 and 6.3.9.3; Equation 6.3.9-3; Table 6.3.9-2.
KdTh_Vit_a* - Sorption coefficient for thorium in vitrified tuff units of UZ (mL/g). *Distribution:* Uniform. *Range:* 1000 to 10000. *Sensitivity Name:* UZKDTHVT*. *Location in TSPA-LA:* Sections 6.3.9.2 and 6.3.9.3; Equation 6.3.9-3; Table 6.3.9-2.
KdTh_Zeo_a* - Sorption coefficient for thorium in zeolitic tuff units of UZ (mL/g). *Distribution:* Uniform. *Range:* 1000 to 30000. *Sensitivity Name:* UZKDTHZT*. *Location in TSPA-LA:* Sections 6.3.9.2 and 6.3.9.3; Equation 6.3.9-3; Table 6.3.9-2.
KdU_Devit_a - Sorption coefficient for uranium in devitrified tuff units of UZ (mL/g). *Distribution:* Piecewise uniform. *Range:* 0 to 4. *Median:* 0.2. *Sensitivity Name:* UZKDUDT. *Location in TSPA-LA:* Sections 6.3.9.2 and 6.3.9.3; Equation 6.3.9-3; Table 6.3.9-2.
KdU_Vit_a* - Sorption coefficient for uranium in vitrified tuff units of UZ (mL/g). *Distribution:* Piecewise uniform. *Range:* 0 to 3. *Median:* 0.2. *Sensitivity Name:* UZKDUVT*. *Location in TSPA-LA:* Sections 6.3.9.2 and 6.3.9.3; Equation 6.3.9-3; Table 6.3.9-2.
KdU_Zeo_a* - Sorption coefficient for uranium in zeolitic tuff units of UZ (mL/g). *Distribution:* Piecewise uniform. *Range:* 0 to 30. *Median:* 0.5. *Sensitivity Name:* UZKDUZT*. *Location in TSPA-LA:* Sections 6.3.9.2 and 6.3.9.3; Equation 6.3.9-3; Table 6.3.9-2.
L_Divides_a - Depth of permeable soil on divides of the Fortymile Wash fan (RMEI location) (cm). *Distribution:* Uniform. *Range:* 102 to 140. *Sensitivity Name:* LDIVIDE. *Location in TSPA-LA:* Table 6.5-5.
LC_rate_a - Crevice corrosion (localized corrosion) propagation rate (mm/yr). *Distribution:* Log uniform. *Range:* 0.0127 to 1.27. *Sensitivity Name:* WDLCRATE. *Location in TSPA-LA:* Sections 6.3.5.2.1, 6.3.5.2.2, 6.3.5.2.3, 6.3.5.3.2 and 6.3.5.4; Table 6.3.5-4.
LDISP – Logarithm of longitudinal dispersivity (m). *Distribution:* Right truncated normal. *Range*: $-\infty$ to 3.5. *Mean:* 2.0. *Standard Deviation:* 0.75. *Sensitivity Name:* SZLODISP. *Location in TSPA-LA:* Section 6.3.10.2; Table 6.3.10-2.
Log_Specific_SA_CSNF_a - Logarithm of the effective specific surface area (m^2/mg) of the representative CSNF waste form (dimensionless). *Distribution:* Triangular. *Range:* -7.3 to -5.4. *Most Likely:* -6.7. *Sensitivity Name:* CSSPECSA. *Location in TSPA-LA:* Sections 6.3.7.4.1.2 and 6.3.7.4.1.3; Tables 6.3.7-30 and 6.3.7-31; Equations 6.3.7-5 and 6.3.7-6.
LogK_Uncert_Lith_a - Logarithm of the mean fracture permeability in lithophysal rock units (dimensionless). *Distribution:* Triangular. *Range:* -0.92 to 0.92. *Mode:* 0. *Sensitivity Name:* SEEPPRM. *Location in TSPA-LA:* Sections 6.3.5.2.3, 6.3.3.1.2 and 6.3.3.1.3; Tables 6.3.5-4, 6.3.3-2 and 6.3.3-3.
LogK_Uncert_NonLith_a - Logarithm of the mean fracture permeability in non-lithophysal rock units (dimensionless). *Distribution:* Triangular. *Range:* -0.68 to 0.68. *Mode:* 0. *Sensitivity Name:* SEEPPRMN. *Location in TSPA-LA:* Sections 6.3.5.2.3, 6.3.3.1.2 and 6.3.3.1.3; Tables 6.3.5-4, 6.3.3-2 and 6.3.3-3.
Mass_Decrease_Const_GE10_a - Mass loading decrease rate constant (1/yr). *Distribution:* Triangular. *Range:* 0.125 to 1. *Mode:* 0.2. *Sensitivity Name:* MASSDCRS. *Location in TSPA-LA:* Equation 6.3.11-5.

Table K3-2. High-Level Summary of Epistemically Uncertain Variables (i.e., elements of **e**) Considered in the TSPA-LA (TSPA Parameter Name) (Continued)

NOTE: * indicates variable not considered in sensitivity analysis due to correlations.

MIC_RHThresh_a - Relative humidity threshold for initiating microbially induced corrosion (dimensionless). *Distribution:* Uniform. *Range:* 0.75 to 0.9. *Sensitivity Name:* WDMICRHT. *Location in TSPA-LA:* Sections 6.3.5.1.2 and 6.3.5.1.3; Tables 6.3.5-3 and 6.3.5-4.
n_SCC_a - Stress corrosion cracking growth rate exponent (repassivation slope) (dimensionless). *Distribution:* Truncated normal. *Range:* 0.935 to 1.395. *Mean:* 1.165. *Standard Deviation:* 0.115. *Sensitivity Name:* WDNSCC. *Location in TSPA-LA:* Sections 6.3.5.1.2 and 6.3.5.4; Table 6.3.5-3; Equations 6.3.5-13 and 6.3.5-14.
NiO_SA_a - Specific surface area of NiO (m^2/g). *Distribution:* Uniform. *Range:* 1 to 30. *Sensitivity Name:* NIOSA. *Location in TSPA-LA:* Table 6.3.8-4; S_{CP} in Equation 6.3.8-19.
Np2O5_Eps_1_high_a* - Logarithm of the scale factor used to characterize uncertainty in Np_2O_5 solubility for ionic strength values between 1 and 3 molal (dimensionless). *Distribution:* Truncated normal. *Range:* -1.7 to 1.7. *Mean:* 0. *Standard Deviation:* 0.85. *Sensitivity Name:* EP1HINP2*. *Location in TSPA-LA:* Sections 6.3.7.5.1 and 6.3.7.5.2; Table 6.3.7-42; Equation 6.3.7-13a.
Np2O5_Eps_1_low_a - Logarithm of the scale factor used to characterize uncertainty in Np_2O_5 solubility at an ionic strength below 1 molal (dimensionless). *Distribution:* Truncated normal. *Range:* -1.6 to 1.6. *Mean:* 0. *Standard Deviation:* 0.8. *Sensitivity Name:* EP1NP2O5. *Location in TSPA-LA:* Sections 6.3.7.5.1 and 6.3.7.5.2; Table 6.3.7-42; Equation 6.3.7-13a.
Np2O5_Eps_2_CDSP_High_a* - Term associated with uncertainty in Np_2O_5 solubility due to variations in fluoride concentration for CDSP waste packages when ionic strength is greater than or equal to 0.004 molal and for the invert below CDSP waste packages (mg/L). *Distribution:* Triangular. *Range:* 0 to 853. *Most Likely:* 0. *Sensitivity Name:* EP2CDNP2*. *Location in TSPA-LA:* Sections 6.3.7.5.1 and 6.3.7.5.2; Table 6.3.7-42; Equation 6.3.7-13a.
Np2O5_Eps_2_CSNF_High_a* - Term associated with uncertainty in Np_2O_5 solubility due to variations in fluoride concentration for CSNF waste packages when ionic strength is greater than or equal to 0.2 molal and for the invert below CSNF waste packages (mg/L). *Distribution:* Triangular. *Range:* 0 to 197. *Most Likely:* 0. *Sensitivity Name:* EP2CSNP2*. *Location in TSPA-LA:* Sections 6.3.7.5.1 and 6.3.7.5.2; Table 6.3.7-42; Equation 6.3.7-13a.
Np2O5_Eps_2_Glass_Low_a* - Term associated with uncertainty in Np_2O_5 solubility due to variations in fluoride concentration for CDSP waste packages Cell 1a, Cell 1b when ionic strength is less than 0.004 molal, and CSNF waste packages when ionic strength is less than 0.2 molal (mg/L). *Distribution:* Triangular. *Range:* 0 to 11. *Most Likely:* 0. *Sensitivity Name:* EP2LONP2*. *Location in TSPA-LA:* Sections 6.3.7.5.1 and 6.3.7.5.2; Table 6.3.7-42; Equation 6.3.7-13a.
NpO2_Eps_1_high_a* - Logarithm of the scale factor used to characterize uncertainty in NpO_2 solubility at an ionic strength between 1 and 3 molal (dimensionless). *Distribution:* Truncated normal. *Range:* -1.34 to 1.34. *Mean:* 0. *Standard Deviation:* 0.67. *Sensitivity Name:* EP1HINPO2*. *Location in TSPA-LA:* Sections 6.3.7.5.1, 6.3.7.5.2 and 6.3.7.5.3; Table 6.3.7-43; Equation 6.3.7-13a.
NpO2_Eps_1_low_a - Logarithm of the scale factor used to characterize uncertainty in NpO_2 solubility at an ionic strength below 1 molal (dimensionless). *Distribution:* Truncated normal. *Range:* -1.2 to 1.2. *Mean:* 0. *Standard Deviation:* 0.6. *Sensitivity Name:* EP1NPO2. *Location in TSPA-LA:* Sections 6.3.7.5.1, 6.3.7.5.2 and 6.3.7.5.3; Table 6.3.7-43; Equation 6.3.7-13a.
NpO2_Eps_2_CDSP_High_a* - Term associated with uncertainty in NpO_2 solubility due to variations in fluoride concentration for CDSP waste packages when ionic strength is greater than or equal to 0.004 molal and for the invert below CDSP waste packages (mg/L). *Distribution:* Triangular. *Range:* 0 to 1093.5. *Most Likely:* 0. *Sensitivity Name:* EP2CDNPO2*. *Location in TSPA-LA:* Sections 6.3.7.5.1, 6.3.7.5.2 and 6.3.7.5.3; Table 6.3.7-43; Equation 6.3.7-13a.
NpO2_Eps_2_CSNF_High_a* - Term associated with uncertainty in NpO_2 solubility due to variations in fluoride concentration for CSNF waste packages when ionic strength is greater than or equal to 0.2 molal and for the invert below CSNF waste packages (mg/L). *Distribution:* Triangular. *Range:* 0 to 255.8. *Most Likely:* 0. *Sensitivity Name:* EP2CSNPO2*. *Location in TSPA-LA:* Sections 6.3.7.5.1, 6.3.7.5.2 and 6.3.7.5.3; Table 6.3.7-43; Equation 6.3.7-13a.
NpO2_Eps_2_Glass_Low_a* - Term associated with uncertainty in NpO_2 solubility due to variations in fluoride concentration for CDSP waste packages Cell 1a, Cell 1b when ionic strength is less than 0.004 molal, and CSNF waste packages when ionic strength is less than 0.2 molal (mg/L). *Distribution:* Triangular. *Range:* 0 to 14.1. *Most Likely:* 0. *Sensitivity Name:* EP2LONPO2*. *Location in TSPA-LA:* Sections 6.3.7.5.1, 6.3.7.5.2 and 6.3.7.5.3; Table 6.3.7-43; Equation 6.3.7-13a.

Table K3-2. High-Level Summary of Epistemically Uncertain Variables (i.e., elements of **e**) Considered in the TSPA-LA (TSPA Parameter Name) (Continued)

NOTE: * indicates variable not considered in sensitivity analysis due to correlations.

NVF11 - Effective porosity in undifferentiated alluvium (valley fill) (dimensionless). *Distribution:* Truncated normal. *Range:* 0 to 0.3. *Mean:* 0.18. *Standard Deviation:* 0.051. *Sensitivity Name:* SZPORUAL. *Location in TSPA-LA:* Table 6.3.10-2.
NVF26 - Effective porosity in shallow alluvium (dimensionless). *Distribution:* Truncated normal. *Range:* 0 to 0.3. *Mean:* 0.18. *Standard Deviation:* 0.051. *Sensitivity Name:* SZPORSAL. *Location in TSPA-LA:* Table 6.3.10-2.
Pa_Eps_1_a - Logarithm of the scale factor used to characterize uncertainty in protactinium solubility (dimensionless). *Distribution:* Uniform. *Range:* -4.42 to -0.05. *Sensitivity Name:* EP1PA. *Location in TSPA-LA:* Sections 6.3.7.5.2 and 6.3.7.5.3; Table 6.3.7-45; Equation 6.3.7-13b.
Pa_Eps_2_CDSP_High_a* - Term associated with uncertainty in protactinium solubility due to variations in fluoride concentration for CDSP waste packages when ionic strength is greater than or equal to 0.004 molal and for the invert below CDSP waste packages (mg/L). *Distribution:* Triangular. *Range:* 0 to 853. *Most Likely:* 0. *Sensitivity Name:* EP2CDPA*. *Location in TSPA-LA:* Sections 6.3.7.5.2 and 6.3.7.5.3; Table 6.3.7-45; Equation 6.3.7-13b.
Pa_Eps_2_CSNF_High_a* - Term associated with uncertainty in protactinium solubility due to variations in fluoride concentration for CSNF waste packages when ionic strength is greater than or equal to 0.2 molal and for the invert below CSNF waste packages (mg/L). *Distribution:* Triangular. *Range:* 0 to 197. *Most Likely:* 0. *Sensitivity Name:* EP2CSPA*. *Location in TSPA-LA:* Sections 6.3.7.5.2 and 6.3.7.5.3; Table 6.3.7-45; Equation 6.3.7-13b.
Pa_Eps_2_Glass_Low_a* - Term associated with uncertainty in protactinium solubility due to variations in fluoride concentration for CDSP waste packages Cell 1a, Cell 1b when ionic strength is less than 0.004 molal, and CSNF waste packages when ionic strength is less than 0.2 molal (mg/L). *Distribution:* Triangular. *Range:* 0 to 11. *Most Likely:* 0. *Sensitivity Name:* EP2LOPA*. *Location in TSPA-LA:* Sections 6.3.7.5.2 and 6.3.7.5.3; Table 6.3.7-45; Equation 6.3.7-13b.
PCE_Cl_MU_RH_0_20_a - The IDPS process model uncertainty factor for the logarithm of the chloride concentration of the in-drift waters at relative humidity ≤20% (dimensionless). *Distribution:* Triangular. *Range:* -0.7 to 0.7. *Most Likely:* 0. *Sensitivity Name:* RHMU0. *Location in TSPA-LA:* Sections 6.3.4, 6.3.4.2, 6.3.4.3.1, 6.3.4.3.2 and 6.3.5.2.3; Tables 6.3.4-2, 6.3.4-3 and 6.3.5-4.
PCE_Cl_MU_RH_20_40_a - The IDPS process model uncertainty factor for the logarithm of the chloride concentration of the in-drift waters at relative humidity >20 and ≤40% (dimensionless). *Distribution:* Triangular. *Range:* -0.5 to 0.5. *Most Likely:* 0. *Sensitivity Name:* RHMU20. *Location in TSPA-LA:* Sections 6.3.4, 6.3.4.2, 6.3.4.3.1, 6.3.4.3.2 and 6.3.5.2.3; Tables 6.3.4-2, 6.3.4-3 and 6.3.5-4.
PCE_Cl_MU_RH_40_65_a – The IDPS process model uncertainty factor for the logarithm of the chloride concentration of the in-drift waters at relative humidity >40 and ≤65% (dimensionless). *Distribution:* Triangular. *Range:* -0.4 to 0.4. *Most Likely:* 0. *Sensitivity Name:* RHMU40. *Location in TSPA-LA:* Sections 6.3.4, 6.3.4.2, 6.3.4.3.1, 6.3.4.3.2 and 6.3.5.2.3; Tables 6.3.4-2, 6.3.4-3 and 6.3.5-4.
PCE_Cl_MU_RH_65_85_a - The IDPS process model uncertainty factor for the logarithm of the chloride concentration of the in-drift waters at relative humidity >65 and ≤85% (dimensionless). *Distribution:* Triangular. *Range:* -0.1 to 0.1. *Most Likely:* 0. *Sensitivity Name:* RHMU65. *Location in TSPA-LA:* Sections 6.3.4, 6.3.4.2, 6.3.4.3.1, 6.3.4.3.2 and 6.3.5.2.3; Tables 6.3.4-2, 6.3.4-3 and 6.3.5-4.
PCE_Cl_MU_RH_85_100_a* - The IDPS process model uncertainty factor for the logarithm of the chloride concentration of the in-drift waters at relative humidity >85% (dimensionless). *Distribution:* Triangular. *Range:* 0 to 0. *Most Likely:* 0. *Sensitivity Name:* RHMU85*. *Location in TSPA-LA:* Sections 6.3.4, 6.3.4.2, 6.3.4.3.1, 6.3.4.3.2 and 6.3.5.2.3; Tables 6.3.4-2, 6.3.4-3 and 6.3.5-4.
PCE_Cl_N_MU_RH_40_65_a - The IDPS process model uncertainty factor for the logarithm of the chloride + nitrate concentration of the in-drift waters at relative humidity >40% and ≤65% (dimensionless). *Distribution:* Triangular. *Range:* -0.57 to 0.57. *Most Likely:* 0. *Sensitivity Name:* RHMUN40. *Location in TSPA-LA:* Sections 6.3.4.3.2 and 6.3.5.2.3; Tables 6.3.4-2, 6.3.4-3 and 6.3.5-4.
PCE_Cl_N_MU_RH_65_85_a - The IDPS process model uncertainty factor for the logarithm of the chloride + nitrate concentration of the in-drift waters at relative humidity >65% and ≤85% (dimensionless). *Distribution:* Triangular. *Range:* -0.22 to 0.22. *Most Likely:* 0. *Sensitivity Name:* RHMUN65. *Location in TSPA-LA:* Sections 6.3.4.3.2 and 6.3.5.2.3; Tables 6.3.4-2, 6.3.4-3 and 6.3.5-4.

Table K3-2. High-Level Summary of Epistemically Uncertain Variables (i.e., elements of **e**) Considered in the TSPA-LA (TSPA Parameter Name) (Continued)

NOTE: * indicates variable not considered in sensitivity analysis due to correlations.

PCE_Cl_N_MU_RH_85_100_a* - The in-drift precipitates/salts (IDPS) process model uncertainty factor for the logarithm of the chloride + nitrate concentration of the in-drift waters at relative humidity >85% (dimensionless). *Distribution:* Triangular. *Range:* 0 to 0. *Most Likely:* 0. *Sensitivity Name:* RHMUN85*. *Location in TSPA-LA:* Sections 6.3.4.3.2 and 6.3.5.2.3; Tables 6.3.4-2, 6.3.4-3 and 6.3.5-4.
PCE_Cl_NO3_MU_RH_0_20_a - The IDPS process model uncertainty factor for the logarithm of the chloride to nitrate ratio of the in-drift waters at relative humidity ≤20% (dimensionless). *Distribution:* Triangular. *Range:* -1.4 to 1.4. *Most Likely:* 0. *Sensitivity Name:* RHMUNO0. *Location in TSPA-LA:* Sections 6.3.4.3.1, 6.3.4.3.2 and 6.3.5.2.3; Tables 6.3.4-2, 6.3.4-3 and 6.3.5-4.
PCE_Cl_NO3_MU_RH_20_65_a - The IDPS process model uncertainty factor for the logarithm of the chloride to nitrate ratio of the in-drift waters at relative humidity >20% and ≤65% (dimensionless). *Distribution:* Triangular. *Range:* -0.5 to 0.5. *Most Likely:* 0. *Sensitivity Name:* RHMUNO20. *Location in TSPA-LA:* Sections 6.3.4.3.1, 6.3.4.3.2 and 6.3.5.2.3; Tables 6.3.4-2, 6.3.4-3 and 6.3.5-4.
PCE_Cl_NO3_MU_RH_65_85_a – The IDPS process model uncertainty factor for the logarithm of the chloride to nitrate ratio of the in-drift waters at relative humidity >65% and ≤85% (dimensionless). *Distribution:* Triangular. *Range:* -0.2 to 0.2. *Most Likely:* 0. *Sensitivity Name:* RHMUNO65. *Location in TSPA-LA:* Sections 6.3.4.3.1, 6.3.4.3.2 and 6.3.5.2.3; Tables 6.3.4-2, 6.3.4-3 and 6.3.5-4.
PCE_Cl_NO3_MU_RH_85_100_a* - The IDPS process model uncertainty factor for the logarithm of the chloride to nitrate ratio of the in-drift waters at low relative humidity >85% (dimensionless). *Distribution:* Triangular. *Range:* 0 to 0. *Most Likely:* 0. *Sensitivity Name:* RHMUNO85*. *Location in TSPA-LA:* Sections 6.3.4.3.1, 6.3.4.3.2 and 6.3.5.2.3; Tables 6.3.4-2, 6.3.4-3 and 6.3.5-4.
PCE_Delta_pCO2_a - Selector variable for partial pressure of CO_2 (dimensionless). *Distribution:* Uniform. *Range:* -1 to 1. *Sensitivity Name:* DELPPCO2. *Location in TSPA-LA:* Sections 6.3.4.2 and 6.3.5.2.3; Table 6.3.5-4.
PCE_Gp1_Cl_NO3_CDF_a - Ratio of Cl to NO_3 (Cl:N) in Group 1 pore waters (dimensionless). *Distribution:* Discrete. *Range:* 0.783 to 6.1213. *Sensitivity Name:* GP1NO3. *Location in TSPA-LA:* Section 6.3.4.3.2.
PCE_Gp2_Cl_NO3_CDF_a - Ratio of Cl to NO_3 (Cl:N) in Group 2 pore waters (dimensionless). *Distribution:* Discrete. *Range:* 2.359 to 3.187. *Sensitivity Name:* GP2NO3. *Location in TSPA-LA:* Section 6.3.4.3.2.
PCE_Gp3_Cl_NO3_CDF_a - Ratio of Cl to NO_3 (Cl:N) in Group 3 pore waters (dimensionless). *Distribution:* Discrete. *Range:* 9.7782 to 64.128. *Sensitivity Name:* GP3NO3. *Location in TSPA-LA:* Section 6.3.4.3.2.
PCE_Gp4_Cl_NO3_CDF_a - Ratio of Cl to NO_3 (Cl:N) in Group 4 pore waters (dimensionless). *Distribution:* Discrete. *Range:* 4.4485 to 8.2119. *Sensitivity Name:* GP4NO3. *Location in TSPA-LA:* Section 6.3.4.3.2.
PCE_I_Uncert_RH_85_100_a - The IDPS process model uncertainty factor for the logarithm of the ionic strength of the in-drift waters at high relative humidity (≥85%) (log molal). *Distribution:* Triangular. *Range:* -0.1 to 0.1. *Mean/Median/Mode:* 0. *Sensitivity Name:* RHI85. *Location in TSPA-LA:* Section 6.4.1; Tables 6.4-1 and 6.4-2; Figure 6.4-4.
PCE_pH_Uncert_RH_0_65_a - The IDPS process model uncertainty factor for the pH of the in-drift waters at relative humidity ≤65% (dimensionless). *Distribution:* Triangular. *Range:* -2 to 2. *Most Likely:* 0. *Sensitivity Name:* RHPH0. *Location in TSPA-LA:* Table 6.3.5-4.
PCE_pH_Uncert_RH_65_75_a - The IDPS process model uncertainty factor for the pH of the in-drift waters at relative humidity >65 and ≤75% (dimensionless). *Distribution:* Triangular. *Range:* -1 to 1. *Most Likely:* 0. *Sensitivity Name:* RHPH65. *Location in TSPA-LA:* Table 6.3.5-4
PCE_pH_Uncert_RH_75_100_a - The IDPS process model uncertainty factor for the pH of the in-drift waters at relative humidity >75% (dimensionless). *Distribution:* Discrete. *Range:* -0.3123 to 0.4288. *Sensitivity Name:* RHPH75. *Location in TSPA-LA:* Table 6.3.5-4
pH_CeII2_Regression_Error_a - Error term in regression equation for pH of corrosion products domain (dimensionless). *Distribution:* Truncated normal. *Range:* -0.64 to 0.64. *Mean/Median/Mode:* 0. *Standard Deviation:* 0.32. *Sensitivity Name:* PH2RGER. *Location in TSPA-LA:* Equation 6.3.8-27.
Pu_Eps_1_high_a* - Logarithm of the scale factor used to characterize uncertainty in plutonium solubility for ionic strength between 1 and 3 molal (dimensionless). *Distribution:* Truncated normal. *Range:* -1.52 to 1.52. *Mean:* 0. *Standard Deviation:* 0.76. *Sensitivity Name:* EP1HIPU*. *Location in TSPA-LA:* Sections 6.3.7.5.1, 6.3.7.5.2 and 6.3.7.5.3; Table 6.3.7-44; Equation 6.3.7-13a.

Table K3-2. High-Level Summary of Epistemically Uncertain Variables (i.e., elements of **e**) Considered in the TSPA-LA (TSPA Parameter Name) (Continued)

NOTE: * indicates variable not considered in sensitivity analysis due to correlations.

Pu_Eps_1_low_a - Logarithm of the scale factor used to characterize uncertainty in plutonium solubility at an ionic strength below 1 molal (dimensionless). *Distribution:* Truncated normal. *Range:* -1.4 to 1.4. *Mean/Median/Mode:* 0. *Standard Deviation:* 0.7. *Sensitivity Name:* EP1LOWPU. *Location in TSPA-LA:* Sections 6.3.7.5.1, 6.3.7.5.2 and 6.3.7.5.3; Table 6.3.7-44; Equation 6.3.7-13a.
Pu_Eps_2_CDSP_High_a* - Term associated with uncertainty in plutonium solubility due to variations in fluoride concentration for CDSP waste packages when ionic strength is greater than or equal to 0.004 molal and for the invert below CDSP waste packages (mg/L). *Distribution:* Triangular. *Range:* 0 to 5460. *Most Likely:* 0. *Sensitivity Name:* EP2CDPU*. *Location in TSPA-LA:* Sections 6.3.7.5.1, 6.3.7.5.2 and 6.3.7.5.3; Table 6.3.7-44; Equation 6.3.7-13a.
Pu_Eps_2_CSNF_High_a* - Term associated with uncertainty in plutonium solubility due to variations in fluoride concentration for CSNF waste packages when ionic strength is greater than or equal to 0.2 molal and for the invert below CSNF waste packages (mg/L). *Distribution:* Triangular. *Range:* 0 to 1374. *Most Likely:* 0. *Sensitivity Name:* EP2CSPU*. *Location in TSPA-LA:* Sections 6.3.7.5.1, 6.3.7.5.2 and 6.3.7.5.3; Table 6.3.7-44; Equation 6.3.7-13a.
Pu_Eps_2_Glass_Low_a* - Term associated with uncertainty in plutonium solubility due to variations in fluoride concentration for CDSP waste packages Cell 1a, Cell 1b when ionic strength is less than 0.004 molal, and CSNF waste packages when ionic strength is less than 0.2 molal (mg/L). *Distribution:* Triangular. *Range:* 0 to 79. *Most Likely:* 0. *Sensitivity Name:* EP2LOWPU*. *Location in TSPA-LA:* Sections 6.3.7.5.1, 6.3.7.5.2 and 6.3.7.5.3; Table 6.3.7-44; Equation 6.3.7-13a.
Relative_Abundance_Goethite_a - Fraction of total iron oxide that is goethite (dimensionless). *Distribution:* Uniform. *Range:* 0.45 to 0.8. *Sensitivity Name:* GOERELAB. *Location in TSPA-LA:* Section 6.3.8.2.3; Table 6.3.8-4.
Resuspension_Thickness_a - Thickness of combined ash/soil mixture available for resuspension (m). *Distribution:* Uniform. *Range:* 0.001 to 0.003. *Mean/Median/Mode:* 0.002. *Sensitivity Name:* RSUSTHIK. *Location in TSPA-LA:* Equation 6.3.11-6.
Rind_Porosity_CSNF_a - Porosity in CSNF rind (dimensionless). *Distribution:* Uniform. *Range:* 0.05 to 0.3. *Sensitivity Name:* CSRINDPO. *Location in TSPA-LA:* Section 6.3.8.2.1; Table 6.3.8-6.
Schoepite_Boltwoodite_Interp_a - Fractional value used to interpolate between Schoepite and Boltwoodite look-up tables (dimensionless). *Distribution:* Uniform. *Range:* 0 to 1. *Sensitivity Name:* SCHOBOLT. *Location in TSPA-LA:* Table 6.3.7-58.
Scour_Depth_a - Scour depth in Fortymile Wash at the fan apex (cm). *Distribution:* Uniform. *Range:* 73 to 122. *Sensitivity Name:* SC_DPTH. *Location in TSPA-LA:* Table 6.5-5.
Seepage_Condensation_Prob_a* - Pointer variable to determine the seepage/condensation regime for the first failed waste package in a percolation subregion (dimensionless). *Distribution:* Uniform. *Range:* 0 to 1. *Sensitivity Name:* SEEPCON*.
Seepage_Uncertainty_a - Uncertainty factor to account for small-scale heterogeneity in fracture permeability (dimensionless). *Distribution:* Uniform. *Range:* 0 to 1. *Sensitivity Name:* SEEPUNC. *Location in TSPA-LA:* Section 6.3.3.1.2; Tables 6.3.3-3 and 6.3.5-4.
Seepage_Water_Type_a - Pointer variable used to select which seepage water type in used in the physical and chemical environment (P&CE) submodel calculations (dimensionless). *Distribution:* Discrete. *Range:* 1 to 4. *Sensitivity Name:* SEEPWAT. *Location in TSPA-LA:* Table 6.3.5-4.
Sn_Eps_high_a* - Logarithm of the scale factor used to characterize uncertainty in tin solubility for high ionic strength conditions (dimensionless). *Distribution:* Truncated normal. *Range:* -1.08 to 1.08. *Mean:* 0. *Standard Deviation:* 0.54. *Sensitivity Name:* EP1HISN*. *Location in TSPA-LA:* Sections 6.3.7.5.2 and 6.3.7.5.3; Table 6.3.7-47; Equation 6.3.7-13a.
Sn_Eps_low_a - Logarithm of the scale factor used to characterize uncertainty in tin solubility for low ionic strength conditions (dimensionless). *Distribution:* Truncated normal. *Range:* -0.9 to 0.9. *Mean/Median/Mode:* 0. *Standard Deviation:* 0.45. *Sensitivity Name:* EP1LOWSN. *Location in TSPA-LA:* Sections 6.3.7.5.2 and 6.3.7.5.3; Table 6.3.7-47; Equation 6.3.7-13a.
Soil_Density_a - Density of surface soil correlated with the volcanic BDCFs (kg/m^3). *Distribution:* Triangular. *Range:* 1300 to 1700. *Mean/Median/Mode:* 1500. *Sensitivity Name:* SOILDENS. *Location in TSPA-LA:* Equation 6.3.11-6.

Table K3-2. High-Level Summary of Epistemically Uncertain Variables (i.e., elements of **e**) Considered in the TSPA-LA (TSPA Parameter Name) (Continued)

NOTE: * indicates variable not considered in sensitivity analysis due to correlations.

Specific_SA_Smectite_Col_a - Specific surface area for smectite colloids (m^2/g). *Distribution:* Uniform. *Range:* 10 to 100. *Sensitivity Name:* SMECSA. *Location in TSPA-LA:* Table 6.3.7-62.
SRC1X - Relative x location of point source in source region 1 (dimensionless). *Distribution:* Uniform. *Range:* 0 to 1. *Sensitivity Name:* SZSREG1X. *Location in TSPA-LA:* Section 6.3.10.2; Table 6.3.10-2.
SRC1Y - Relative y location of point source in source region 1 (dimensionless). *Distribution:* Uniform. *Range:* 0 to 1. *Sensitivity Name:* SZSREG1Y. *Location in TSPA-LA:* Section 6.3.10.2; Table 6.3.10-2.
SRC2X - Relative x location of point source in source region 2 (dimensionless). *Distribution:* Uniform. *Range:* 0 to 1. *Sensitivity Name:* SZSREG2X. *Location in TSPA-LA:* Section 6.3.10.2; Table 6.3.10-2.
SRC2Y - Relative y location of point source in source region 2 (dimensionless). *Distribution:* Uniform. *Range:* 0 to 1. *Sensitivity Name:* SZSREG2Y. *Location in TSPA-LA:* Section 6.3.10.2; Table 6.3.10-2.
SRC3X - Relative x location of point source in source region 3 (dimensionless). *Distribution:* Uniform. *Range:* 0 to 1. *Sensitivity Name:* SZSREG3X. *Location in TSPA-LA:* Section 6.3.10.2; Table 6.3.10-2.
SRC3Y - Relative y location of point source in source region 3 (dimensionless). *Distribution:* Uniform. *Range:* 0 to 1. *Sensitivity Name:* SZSREG3Y. *Location in TSPA-LA:* Section 6.3.10.2; Table 6.3.10-2.
SRC4X - Relative x location of point source in source region 4 (dimensionless). *Distribution:* Uniform. *Range:* 0 to 1. *Sensitivity Name:* SZSREG4X. *Location in TSPA-LA:* Section 6.3.10.2; Table 6.3.10-2.
SRC4Y - Relative y location of point source in source region 4 (dimensionless). *Distribution:* Uniform. *Range:* 0 to 1. *Sensitivity Name:* SZSREG4Y. *Location in TSPA-LA:* Section 6.3.10.2; Table 6.3.10-2.
SS_Corrosion_Rate_a - Stainless steel corrosion rate (□m/yr). *Distribution:* Truncated log normal. *Range:* 0.01 to 0.51. *Mean/Median/Mode:* 0.267. *Standard Deviation:* 0.209. *Sensitivity Name:* CORRATSS. *Location in TSPA-LA:* Tables 6.3.8-1 and 6.3.8-4.
Stress_Thresh_A22_a - Residual stress threshold for SCC nucleation of Alloy 22 (as a percentage of yield strength in MPa) (dimensionless). *Distribution:* Uniform. *Range:* 90 to 105. *Sensitivity Name:* SCCTHRP. *Location in TSPA-LA:* Section 6.6.1.3.7; Table 6.6-2.
Stress_Thresh_SCC_a - Stress threshold for stress corrosion cracking (MPa). *Distribution:* Uniform. *Range:* 315.9 to 368.55. *Sensitivity Name:* SCCTHR. *Location in TSPA-LA:* Table 6.3.5-3.
Target_Flux_Out_Ratio_a - Ratio of radionuclide mass associated with colloids (reversible and irreversible) to radionuclide mass associated with colloids and dissolved radionuclide mass (dimensionless). *Distribution:* Uniform. *Range:* 0.9 to 0.99. *Sensitivity Name:* CFLUXOUT. *Location in TSPA-LA:* Table 6.3.7-65.
Th_Eps_1_high_a* - Logarithm of the scale factor used to characterize uncertainty in thorium solubility at ionic strength between 1 and 3 molal (dimensionless). *Distribution:* Truncated normal. *Range:* -1.52 to 1.52. *Mean:* 0. *Standard Deviation:* 0.76. *Sensitivity Name:* EP1HITH*. *Location in TSPA-LA:* Sections 6.3.7.5.1, 6.3.7.5.2 and 6.3.7.5.3; Table 6.3.7-46; Equation 6.3.7-13a.
Th_Eps_1_low_a - Logarithm of the scale factor used to characterize uncertainty in thorium solubility at an ionic strength below 1 molal (dimensionless). *Distribution:* Truncated normal. *Range:* -1.4 to 1.4. *Mean:* 0. *Standard Deviation:* 0.7. *Sensitivity Name:* EP1LOWTH. *Location in TSPA-LA:* Sections 6.3.7.5.1, 6.3.7.5.2 and 6.3.7.5.3; Table 6.3.7-46; Equation 6.3.7-13a.
Th_Eps_2_CDSP_High_a* - Term associated with uncertainty in thorium solubility due to variations in fluoride concentration for CDSP waste packages when ionic strength is greater than or equal to 0.004 molal and for the invert below CDSP waste packages (mg/L). *Distribution:* Triangular. *Range:* 0 to 23723.2. *Most Likely:* 0. *Sensitivity Name:* EP2CDTH*. *Location in TSPA-LA:* Sections 6.3.7.5.1, 6.3.7.5.2 and 6.3.7.5.3; Table 6.3.7-46; Equation 6.3.7-13a.
Th_Eps_2_CSNF_High_a* - Term associated with uncertainty in thorium solubility due to variations in fluoride concentration for CSNF waste packages when ionic strength is greater than or equal to 0.2 molal and for the invert below CSNF waste packages (mg/L). *Distribution:* Triangular. *Range:* 0 to 7848.3. *Most Likely:* 0. *Sensitivity Name:* EP2CSTH*. *Location in TSPA-LA:* Sections 6.3.7.5.1, 6.3.7.5.2 and 6.3.7.5.3; Table 6.3.7-46; Equation 6.3.7-13a.

Table K3-2. High-Level Summary of Epistemically Uncertain Variables (i.e., elements of **e**) Considered in the TSPA-LA (TSPA Parameter Name) (Continued)

NOTE: * indicates variable not considered in sensitivity analysis due to correlations.

Th_Eps_2_Glass_Low_a* - Term associated with uncertainty in thorium solubility due to variations in fluoride concentration for CDSP waste packages Cell 1a, Cell 1b when ionic strength is less than 0.004 molal, and CSNF waste packages when ionic strength is less than 0.2 molal (mg/L). *Distribution:* Triangular. *Range:* 0 to 626.2. *Most Likely:* 0. *Sensitivity Name:* EP2LOWTH*. *Location in TSPA-LA:* Sections 6.3.7.5.1, 6.3.7.5.2 and 6.3.7.5.3; Table 6.3.7-46; Equation 6.3.7-13a.
Thermal_Conductivity_Uncert_a - Selector variable for one of three host-rock thermal conductivity scenarios (low, mean, and high) (dimensionless). *Distribution:* Discrete. *Range:* 1 to 3. *Sensitivity Name:* THERMCON. *Location in TSPA-LA:* Sections 6.3.2.2, 6.3.2.3, 6.3.5.1.3, 6.3.5.2.3 and 6.6.2.2; Tables 6.3.2-1, 6.3.2-3 and 6.3.5-4.
U_Eps_1_high_Nominal_a* - Logarithm of the scale factor used to characterize uncertainty in uranium solubility under nominal or seismic conditions at an ionic strength between 1and 3 molal (dimensionless). *Distribution:* Truncated normal. *Range:* -1.2 to 1.2. *Mean:* 0. *Standard Deviation:* 0.6. *Sensitivity Name:* EP1HINU*. *Location in TSPA-LA:* Section 6.3.7.5.1, 6.3.7.5.2 and 6.3.7.5.3; Table 6.3.7-54; Equation 6.3.7-13a.
U_Eps_1_high_Other_a* - Logarithm of the scale factor used to characterize uncertainty in uranium solubility under conditions other than nominal and seismic at an ionic strength between 1and 3 molal (dimensionless). *Distribution:* Truncated normal. *Range:* -1.2 to 1.2. *Mean:* 0. *Standard Deviation:* 0.6. *Sensitivity Name:* EP1HIOU*. *Location in TSPA-LA:* Sections 6.3.7.5.1, 6.3.7.5.2 and 6.3.7.5.3; Table 6.3.7-58; Equation 6.3.7-13a.
U_Eps_1_low_Nominal_a - Logarithm of the scale factor used to characterize uncertainty in uranium solubility under nominal or seismic conditions at an ionic strength below 1 molal (dimensionless). *Distribution:* Truncated normal. *Range:* -1 to 1. *Mean/Median/Mode:* 0. *Standard Deviation:* 0.5. *Sensitivity Name:* EP1LOWNU. *Location in TSPA-LA:* Section 6.3.7.5.1, 6.3.7.5.2 and 6.3.7.5.3; Table 6.3.7-54; Equation 6.3.7-13a.
U_Eps_1_low_Other_a - Logarithm of the scale factor used to characterize uncertainty in uranium solubility under conditions other than nominal and seismic at an ionic strength below 1 molal (dimensionless). *Distribution:* Truncated normal. *Range:* -1 to 1. *Mean/Median/Mode:* 0. *Standard Deviation:* 0.5. *Sensitivity Name:* EP1LOWOU. *Location in TSPA-LA:* Sections 6.3.7.5.1, 6.3.7.5.2 and 6.3.7.5.3; Table 6.3.7-58; Equation 6.3.7-13a.
U_Eps_2_Boltwoodite_CDSP_Hig_a* - Term associated with uncertainty in uranium solubility (controlled by boldwoodite saturation) due to variations in fluoride concentration for CDSP waste packages when ionic strength is greater than or equal to 0.004 molal and for the invert below CDSP waste packages (mg/L). *Distribution:* Triangular. *Range:* 0 to 272.3. *Most Likely:* 0. *Sensitivity Name:* EP2BCDHU*. *Location in TSPA-LA:* Sections 6.3.7.5.1, 6.3.7.5.2 and 6.3.7.5.3; Table 6.3.7-58; Equation 6.3.7-13a.
U_Eps_2_Boltwoodite_CSNF_Hig_a* - Term associated with uncertainty in uranium solubility (controlled by boldwoodite saturation) due to variations in fluoride concentration for CSNF waste packages when ionic strength is greater than or equal to 0.2 molal and for the invert below CSNF waste packages (mg/L). *Distribution:* Triangular. *Range:* 0 to 57.01. *Most Likely:* 0. *Sensitivity Name:* EP2BCSHU*. *Location in TSPA-LA:* Sections 6.3.7.5.1, 6.3.7.5.2 and 6.3.7.5.3; Table 6.3.7-58; Equation 6.3.7-13a.
U_Eps_2_Boltwoodite_Glass_Lo_a* - Term associated with uncertainty in uranium solubility (controlled by boldwoodite saturation) due to variations in fluoride concentration for CDSP waste packages Cell 1a, Cell 1b when ionic strength is less than 0.004 molal, and CSNF waste packages when ionic strength is less than 0.2 molal (mg/L). *Distribution:* Triangular. *Range:* 0 to 6.13. *Most Likely:* 0. *Sensitivity Name:* EP2BLOWU*. *Location in TSPA-LA:* Sections 6.3.7.5.1, 6.3.7.5.2 and 6.3.7.5.3; Table 6.3.7-58; Equation 6.3.7-13a.
U_Eps_2_CSNF_High_Nominal_a* - Term associated with uncertainty in uranium solubility (under nominal or seismic conditions) due to variations in fluoride concentration for CSNF waste packages when ionic strength is greater than or equal to 0.2 molal and for the invert below CSNF waste packages (mg/L). *Distribution:* Triangular. *Range:* 0 to 1361. *Most Likely:* 0. *Sensitivity Name:* EP2CSHNU*. *Location in TSPA-LA:* Section 6.3.7.5.1, 6.3.7.5.2 and 6.3.7.5.3; Table 6.3.7-54; Equation 6.3.7-13a.
U_Eps_2_CSNF_Low_Nominal_a* - Term associated with uncertainty in uranium solubility (under nominal or seismic conditions) due to variations in fluoride concentration for CSNF waste packages when ionic strength is less than 0.2 molal and for the invert below CSNF waste packages (mg/L). *Distribution:* Triangular. *Range:* 0 to 78. *Most Likely:* 0. *Sensitivity Name:* EP2CSLNU*. *Location in TSPA-LA:* Section 6.3.7.5.1, 6.3.7.5.2 and 6.3.7.5.3; Table 6.3.7-54; Equation 6.3.7-13a.

Table K3-2. High-Level Summary of Epistemically Uncertain Variables (i.e., elements of **e**) Considered in the TSPA-LA (TSPA Parameter Name) (Continued)

NOTE: * indicates variable not considered in sensitivity analysis due to correlations.

U_Eps_2_Schoepite_CDSP_High_a* - Term associated with uncertainty in uranium solubility (controlled by schoepite saturation) due to variations in fluoride concentration for CDSP waste packages when ionic strength is greater than or equal to 0.004 molal and for the invert below CDSP waste packages (mg/L). *Distribution:* Triangular. *Range:* 0 to 5385. *Most Likely:* 0. *Sensitivity Name:* EP2SCDHU*. *Location in TSPA-LA:* Sections 6.3.7.5.1, 6.3.7.5.2 and 6.3.7.5.3; Table 6.3.7-58; Equation 6.3.7-13a.
U_Eps_2_Schoepite_CSNF_High_a* - Term associated with uncertainty in uranium solubility (controlled by schoepite saturation) due to variations in fluoride concentration for CSNF waste packages when ionic strength is greater than or equal to 0.2 molal and for the invert below CSNF waste packages (mg/L). *Distribution:* Triangular. *Range:* 0 to 1361. *Most Likely:* 0. *Sensitivity Name:* EP2SCSHU*. *Location in TSPA-LA:* Sections 6.3.7.5.1, 6.3.7.5.2 and 6.3.7.5.3; Table 6.3.7-58; Equation 6.3.7-13a.
U_Eps_2_Schoepite_Glass_Low_a* - Term associated with uncertainty in uranium solubility (controlled by schoepite saturation) due to variations in fluoride concentration for CDSP waste packages Cell 1a, Cell 1b when ionic strength is less than 0.004 molal, and CSNF waste packages when ionic strength is less than 0.2 molal (mg/L). *Distribution:* Triangular. *Range:* 0 to 78. *Most Likely:* 0. *Sensitivity Name:* EP2SLOWU*. *Location in TSPA-LA:* Sections 6.3.7.5.1, 6.3.7.5.2 and 6.3.7.5.3; Table 6.3.7-58; Equation 6.3.7-13a.
UNC_DS_EF_conv_from_ln - Probability for undetected defects in drip shields (dimensionless). *Distribution:* Log-normal. *Median:* 4.3E-07. *Error Factor:* 14. *Sensitivity Name:* PROBDSEF. *Location in TSPA-LA:* Section 6.4.1; Tables 6.4-1 and 6.4-2.
UNC_WP_EF_conv_from_ln - Probability for the undetected defects in waste packages (dimensionless). *Distribution:* Log-normal. *Median:* 4.14E-05. *Error Factor:* 8.17. *Sensitivity Name:* PROBWPEF. *Location in TSPA-LA:* Section 6.4.2; Tables 6.4-1 and 6.4-2.
UZ_Tortuosity_RG1 - Logarithm of the tortuosity in rock group 1 (dimensionless). *Distribution:* Left truncated normal. *Range*: 0 to ∞. *Mean:* -1.15. *Standard Deviation:* 0.29. *Sensitivity Name:* UZTORRG1. *Location in TSPA-LA:* Section 6.3.9.2; Table 6.3.9-4.
UZ_Tortuosity_RG2 - Logarithm of the tortuosity in rock group 2 (dimensionless). *Distribution:* Left truncated normal. *Range*: 0 to ∞. *Mean:* -1.57. *Standard Deviation:* 0.29. *Sensitivity Name:* UZTORRG2. *Location in TSPA-LA:* Section 6.3.9.2; Table 6.3.9-4.
UZ_Tortuosity_RG3 - Logarithm of the tortuosity in rock group 3 (dimensionless). *Distribution:* Left truncated normal. *Range*: 0 to ∞. *Mean:* -1.84. *Standard Deviation:* 0.29. *Sensitivity Name:* UZTORRG3. *Location in TSPA-LA:* Section 6.3.9.2; Table 6.3.9-4.
Vol_Rubble_Max_Lith_a - Volume of lithophysal rock that must fall to fill the drift (m^3/m). *Distribution:* Uniform. *Range:* 30 to 120. *Sensitivity Name:* RUBMAXL. *Location in TSPA-LA:* Sections 6.3.5.2.3 and 6.6.3.1; Tables 6.3.5-4 and 6.6-2.
Vol_Rubble_Max_NonLith_a - Volume of nonlithophysal rock that must fall to fill the drift (m^3/m). *Distribution:* Uniform. *Range:* 30 to 120. *Sensitivity Name:* RUBMAXNL. *Location in TSPA-LA:* Section 6.3.5.2.3 and 6.6.3.1; Tables 6.3.5-4 and 6.6-2.
WDDSAggrGC_Mean_a - Topside general corrosion rate of the drip shield (nm/yr). *Distribution:* Normal. *Mean:* 46.067. *Standard Deviation:* 1.187. *Sensitivity Name:* WDDSAGGC. *Location in TSPA-LA:* Sections 6.3.5.1.2 and 6.3.5.1.3; Table 6.3.5-3.
WDDSBenignGC_Mean_a - Underside general corrosion rate of the drip shield (mm/yr). *Distribution:* Normal. *Mean:* 5.15E-06. *Standard Deviation:* 8.31E-07. *Sensitivity Name:* WDDSBEGC. *Location in TSPA-LA:* Sections 6.3.5.1.2 and 6.3.5.1.3; Table 6.3.5-3.
WDDSGC_29_a - General corrosion rate ratio for drip shield support material (ratio of Titanium Grade 29 to Titanium Grade 7) (dimensionless). *Distribution:* Discrete. *Range:* 1 to 6.6786. *Sensitivity Name:* WDDSGC29. *Location in TSPA-LA:* Section 6.3.5.1.2.
WP_Crack_Area_Density_a - Ratio of SCC crack area to unit of seismic damaged area for a waste package (dimensionless). *Distribution:* Uniform. *Range:* 0.00327 to 0.0131. *Sensitivity Name:* WDCRCDEN. *Location in TSPA-LA:* Table 6.6-2.
WP_Flux_Uncertainty_a - Waste package flux splitting factor (dimensionless). *Distribution:* Uniform. *Range:* 0 to 2.41. *Sensitivity Name:* WPFLUX. *Location in TSPA-LA:* Sections 6.3.6.1, 6.3.6.2 and 6.3.6.3; Tables 6.3.6-1, 6.3.6-2 and 6.3.8-4; Equation 6.3.6-6.

Table K3-2. High-Level Summary of Epistemically Uncertain Variables (i.e., elements of **e**) Considered in the TSPA-LA (TSPA Parameter Name) (Continued)

NOTE: * indicates variable not considered in sensitivity analysis due to correlations.

WRIP_beta_rand_a - Parameter used to correlate WRIP_beta so that it resamples at the same probability level throughout a realization (dimensionless). *Distribution:* Uniform. *Range:* 0 to 1. *Sensitivity Name:* WATRCKIN. *Location in TSPA-LA:* Section 6.3.4.2; Table 6.3.4-1.
z_OL_a - Deviation from median yield strength range for outer lid (dimensionless). *Distribution:* Truncated normal. *Range:* -3 to 3. *Mean/Median/Mode:* 0. *Standard Deviation:* 1. *Sensitivity Name:* WDZOLID. *Location in TSPA-LA:* Sections 6.3.5.1.2 and 6.3.5.1.3; Table 6.3.5-3.

Table K3-3. Detailed Summary of Epistemically Uncertain Variables (i.e., elements of **e**) Considered in the TSPA-LA (TSPA Parameter Name)

NOTE: * indicates variable not considered in sensitivity analysis due to correlations.

Alluvium_Density - Bulk density of alluvium (kg/m^3). *Distribution:* Normal. *Mean/Median/Mode:* 1910. *Standard Deviation:* 78. *Additional Information:* The volcanic fracture porosity, volcanic matrix porosity and volcanic density are constants, while alluvium density (i.e., bulk density of alluvium) is a stochastic parameter. These parameters are provided to the TSPA-LA Model to use in the one-dimensional simulations. The alluvium density is used in the calculation of the retardation of sorbing radionuclides. The dry bulk density of alluvium is a flow and transport parameter that is not radionuclide specific. It is related to the matrix retardation coefficient and is used in the computation of the retardation of sorbing radionuclides for irreversible colloidal transport. To treat the one- and three-dimensional transport through the SZ consistently, the sampled values used to generate the saturated zone breakthrough curves are also used in the TSPA-LA Model. These values are tabulated as 200 sets of values for the SZ parameters, accounting for appropriate correletions, and are entered into the TSPA model as a table of 200 values for each parameter. The TSPA-LA Model selects values from this table using the Goldsim variable SZ_index_a. *Sensitivity Name:* SZDENAL. *Location in TSPA-LA:* Table 6.3.10-2. *DTN:* SN0702PASZFTMA.002_R1 [DIRS 183471]. *References: Saturated Zone Flow and Transport Model Abstraction* (SNL 2008 [DIRS 183750], Section 6.5.2.7; Tables 6-8, 7-1[a] and A-1[a]; Figure 6-17).
Alpha_Uncert_Lith_a - van Genuchten capillary strength parameter in lithophysal rock units (Pa). *Distribution:* Triangular. *Range:* -105 to 105. *Mean/Median/Mode:* 0. *Correlation:* Correlated with Alpha_Uncert_NonLith_a. *Symbol:* 1/α. *Additional Information:* The van Genuchten capillary-strength parameter characterizes the strength of the fracture network to retain the water within the formation, reducing or preventing seepage. The values of local percolation flux, the sampled values of local permeability, and capillary strength parameters are used to interpolate from the look-up tables for the mean seepage rate into a 5.1-m-long drift section and the seepage rate standard deviation. The value of standard deviation is used to account for uncertainty in the estimation of seepage rates. Recorded in TSPA Input Database as three constants: Alpha_Uncert_A_min (minimum), Alpha_Uncert_A_mode (mode), and Alpha_Uncert_A_max (maximum). *Sensitivity Name:* ALPHAL. *Location in TSPA-LA:* Sections 6.3.3.1.2 and 6.3.3.1.3; Tables 6.3.3-1, 6.3.3-3 and 6.3.5-4. *DTN:* LB0407AMRU0120.001_R0 [DIRS 173280]. *References: Abstraction of Drift Seepage* (SNL 2007, DIRS [181244], Sections 6.3[a] and 6.6[a]; Figures 6-1[a], 6-12[a], 6-20[a] and 7-4[a]).
Alpha_Uncert_NonLith_a*. van Genuchten capillary strength parameter in nonlithophysal rock units (Pa). *Distribution:* Triangular. *Range:* -105 to 105. *Mean/Median/Mode:* 0. *Correlation:* Correlated to Alpha_Uncert_Lith_a. *Symbol:* 1/α. *Additional Information:* See Alpha_Uncert_Lith_a. This parameter is used to select the mean and standard deviation of seepage flow, from their respective response surfaces. Recorded in TSPA Input Database as three constants: Alpha_Uncert_A_min (minimum), Alpha_Uncert_A_mode (mode), and Alpha_Uncert_A_max (maximum). *Sensitivity Name:* ALPHANL*. *Location in TSPA-LA:* Section 6.3.3.1.2; Tables 6.3.3-1, 6.3.3-3 and 6.3.5-4. *DTN:* LB0407AMRU0120.001_R0 [DIRS 173280]. *References: Abstraction of Drift Seepage* (SNL 2007 [DIRS 181244], Sections 6.3[a] and 6.6[a]; Figures 6-1[a], 6-12[a], 6-20[a] and 7-4[a]).
Am_Eps_1_high_a*. Logarithm of the scale factor used to characterize uncertainty in americium solubility at ionic strength values between 1 and 3 molal (dimensionless). *Distribution:* Truncated normal. *Range:* -2.08 to 2.08. *Mean:* 0. *Standard Deviation:* 1.04. *Correlation:* Correlated to Am_Eps_1_low_a with a correlation factor of 1. *Symbol:* ε_1. *Additional Information:* See Am_Eps_1_low_a. *Sensitivity Name:* EP2HIAM*. *Location in TSPA-LA:* Sections 6.3.7.5.1, 6.3.7.5.2 and 6.3.7.5.3; Equation 6.3.7-13a; Table 6.3.7-41. *DTN:* MO0702PADISCON.001_R0 [DIRS 179358], Tables 8 & 19. *References: Dissolved Concentration Limits of Elements with Radioactive Isotopes* (SNL 2007 [DIRS 177418], Sections 6.9 and 8.1.2; Equations 6.9-1 and 8-1; Table 6.9-4).
Am_Eps_1_low_a. Logarithm of the scale factor used to characterize uncertainty in americium solubility at an ionic strength below 1 molal (dimensionless). *Distribution:* Truncated normal. *Range:* -2 to 2. *Mean:* 0. *Standard Deviation:* 1. *Correlation:* Correlated to Am_Eps_1_high_a with a correlation factor of 1. *Symbol:* ε_1. *Additional Information:* This is an exponential term associated with uncertainty in americium solubility (log k) below 1 molal ionic strength. Am_Eps_1_low defines uncertainty in the log K of the solubility limit for ionic strengths below 1 molal. Am_Eps_1_high defines log K uncertainty for ionic strength values between 1 and 3 molal. This parameter is referred to as ε_1 in the referenced. This parameter is used in calculation as: [Pu, Np, U, Am, Th, and Sn] = 10^S* 10^ε_1+ (ε_2 • N). *Sensitivity Name:* EP1LOWAM. *Location in TSPA-LA:* Sections 6.3.7.5.1, 6.3.7.5.2 and 6.3.7.5.3; Table 6.3.7-41; Equation 6.3.7-13a. *DTN:* MO0702PADISCON.001_R0 [DIRS 179358], Tables 8 & 19. *References: Dissolved Concentration Limits of Elements with Radioactive Isotopes* (SNL 2007 [DIRS 177418], Sections 6.9 and 8.1.2; Equations 6.9-1 and 8.1; Table 6.9-4).

Table K3-3. Detailed Summary of Epistemically Uncertain Variables (i.e., elements of **e**) Considered in the TSPA-LA (TSPA Parameter Name) (Continued)

NOTE: * indicates variable not considered in sensitivity analysis due to correlations.

Am_Eps_2_CDSP_High_a*. Term associated with uncertainty in americium solubility due to variations in fluoride concentration for CDSP waste packages when ionic strength is greater than or equal to 0.004 molal and for the invert below CDSP waste packages (mg/L). *Distribution:* Triangular. *Range:* 0 to 688.6. *Most Likely:* 0. *Correlation:* Correlated to Am_Eps_2_CSNF_High_a. *Symbol:* $\varepsilon_2^{\text{CDSP-F-high}}$, $\varepsilon_2^{\text{CDSP-invert}}$. *Additional Information:* See Am_Eps_2_CSNF_High_a. *Sensitivity Name:* EP2HICDAM*. *Location in TSPA-LA:* Sections 6.3.7.5.2 and 6.3.7.5.3; Table 6.3.7-41; Equation 6.3.7-13a. *DTN:* MO0702PAFLUORI.000_R1 [DIRS 181219], Table 13. *References: Dissolved Concentration Limits of Elements with Radioactive Isotopes* (SNL 2007 [DIRS 177418], Sections 6.9 and 8.1.2; Equations 6.9-1 and 8.1; Tables 6.9-4 and 8-2).
Am_Eps_2_CSNF_High_a. Term associated with uncertainty in americium solubility due to variations in fluoride concentration for CSNF waste packages when ionic strength is greater than or equal to 0.2 molal and for the invert below CSNF waste packages (mg/L). *Distribution:* Triangular. *Range:* 0 to 109.03. *Most Likely:* 0. *Correlation:* Correlated to all other Eps_2 parameters. *Symbol:* $\varepsilon_2^{\text{CSNF-high}}$, $\varepsilon_2^{\text{CSNF-invert}}$. *Additional Information:* The range of fluoride uncertainty for a given TSPA-LA run depends on the type of waste package being considered and the pH. This pH dependence can be implemented into the TSPA model through the use of a multiplication factor that is a function of pH. In TSPA-LA, the fluoride uncertainty for the actinides should be perfectly correlated during sampling. This parameter is calculated from the difference in base solubility (in mg/L). This parameter is referred to as ε_2 in the referenced AMR. *Sensitivity Name:* EP2HICAM. *Location in TSPA-LA:* Sections 6.3.7.5.2 and 6.3.7.5.3; Table 6.3.7-41; Equation 6.3.7-13a. *DTN:* MO0702PAFLUORI.000_R1 [DIRS 181219], Table 13. *References: Dissolved Concentration Limits of Elements with Radioactive Isotopes* (SNL 2007 [DIRS 177418], Sections 6.9 and 8.1.2; Equations 6.9-1 and 8.1; Tables 6.9-4 and 8-2).
Am_Eps_2_Glass_Low_a*. Term associated with uncertainty in americium solubility due to variations in fluoride concentration for CDSP waste packages Cell 1a, Cell 1b when ionic strength is less than 0.004 molal, and CSNF waste packages when ionic strength is less than 0.2 molal (mg/L). *Distribution:* Triangular. *Range:* 0 to 4.42. *Most Likely:* 0. *Correlation:* Correlated to Am_Eps_2_CSNF_High_a. *Symbol:* $\varepsilon_2^{\text{CSNF-low}}$, $\varepsilon_2^{\text{CDSP-Glass}}$, $\varepsilon_2^{\text{CDSP-F-low}}$. *Additional Information:* See Am_Eps_2_CSNF_High_a. *Sensitivity Name:* EP2LOWAM*. *Location in TSPA-LA:* Sections 6.3.7.5.2 and 6.3.7.5.3; Table 6.3.7-41; Equation 6.3.7-13a. *DTN:* MO0702PAFLUORI.000_R1 [DIRS 181219], Table 13. *References: Dissolved Concentration Limits of Elements with Radioactive Isotopes* (SNL 2007 [DIRS 177418], Sections 6.9 and 8.1.2; Equations 6.9-1 and 8.1; Tables 6.9-4 and 8-2).
Ash_Density_a. Tephra settled density (kg/m^3). *Distribution:* Truncated normal. *Range:* 300 to 1500. *Mean:* 1000. *Standard Deviation:* 100. *Symbol:* ψ_s. *Additional Information:* The ash settled density is the bulk density of the ash that settles on the ground after an eruption. Areal densities can be converted to deposit thickness by dividing the areal density by the value of settled (deposit) density. There are two reasonable ways of treating deposit density in TSPA calculations: 1) simply use 1,000 kg/m^3, or 2) use a sample from a normal distribution. Uncertainties are due to a lack of published data. *Sensitivity Name:* ASHDENS. *Location in TSPA-LA:* Table 6.5-5. *DTN:* LA0612DK831811.001_R1 [DIRS 179987]. *References: Characterize Eruptive Processes at Yucca Mountain, Nevada* (SNL 2007 [DIRS 174260], Table 7-1).
b_Tillage_a. Depth of soil within which radionuclides contribute to dose from external exposure (m). *Distribution:* Uniform. *Range:* 0.05 to 0.3. *Additional Information:* The tillage depth is a biosphere model parameter that is also provided as input to the TSPA model to allow calculation of soil depth-integrated radionuclide concentration per unit surface area of the soil. The time-dependent areal radionuclide concentration in surface soil represents radionuclide activity integrated over the tillage depth. All crop roots are considered to be in the soil layer extending down to the tilling depth. For many crops, the root systems can extend to below the tillage depth. This approach effectively assumes (conservatively) that all roots, the source of radionuclide uptake for plants, are exposed to a radionuclide concentration as calculated for the tillage region. Recorded as b_tillage_a in the TSPA Input Database as a table of values presampled in the Biosphere model. Values for the TSPA-LA Model selected from b_tillage_a by the parameter Bio_Index. *Sensitivity Name:* BTILLAGE. *Location in TSPA-LA:* Table 6.5-5. *DTN:* MO0702PAVBPDCF.000_R0 [DIRS 179330]. *References: Biosphere Model Report* (SNL 2007 [DIRS 177399], Sections 6.3.1.6, 6.3.2.2, 6.3.2.6, 6.4.1, 6.4.2.1, 6.5.1 and 7.4.2; Equation 6.5.1-2; Tables 6.6-3 and 6.7-1).

Table K3-3. Detailed Summary of Epistemically Uncertain Variables (i.e., elements of **e**) Considered in the TSPA-LA (TSPA Parameter Name) (Continued)

NOTE: * indicates variable not considered in sensitivity analysis due to correlations.

Background_Alpha_a. Natural background levels of alpha emitters in groundwater (pCi/L). *Distribution:* Truncated normal. *Range:* 0 to 0.71. *Mean/Median/Mode:* 0.5. *Additional Information:* Inputs to the Biosphere Model include background concentrations of ^{226}Ra and ^{228}Ra and alpha emitters in the groundwater. To demonstrate compliance with 10 CFR 63.331 natural background concentrations of ^{226}Ra, ^{228}Ra and alpha emitters will be included in the groundwater protection calculations. The values used in the TSPA-LA model are the means of the natural background distributions calculated in the *Saturated Zone Flow and Transport Model Abstraction*. The mean values are used so that variations in the groundwater protection calculations will reflect variations in releases from the repository and not be masked by variation in the natural background distributions. *Sensitivity Name:* BCKALPHA. *Location in TSPA-LA:* Sections 6.3.10.2 and 6.3.11.2; Table 6.3.10-6. *Output DTN:* MO0708TSPAGENT.000_R0 [DIRS 183000].
Background_Ra226_Ra228_a. Natural background levels of combined ^{226}Ra and ^{228}Ra in groundwater (pCi/L). *Distribution:* Truncated normal. *Range:* 0 to 0.71. *Mean/Median/Mode:* 0.5. *Additional Information:* See Background_Alpha_a. *Sensitivity Name:* BCKRA226. *Location in TSPA-LA:* Sections 6.3.10.2 and 6.3.11.2; Table 6.3.10-6. *Output DTN:* MO0708TSPAGENT.000_R0 [DIRS 183000].
BDCF_Inh_LT. Pointer variable for long-term inhalation dose conversion factor for volcanic ash exposure (dimensionless). *Distribution:* Discrete. *Range:* 1 to 300. *Symbol:* $BDCF_{inh,p,i}$ *Additional Information:* This is the vector of values for each radionuclide, selected from the pre-sampled BDCFs by Bio_Index. This pointer variable selects a value for each radionuclide, and the values for each radionuclide are correlated with a coefficient of 1. The minimum value of this variable (1) is associated with the lowest value of the BDCF set. The highest value (300) is associated with the highest value of the BDCF set. *Sensitivity Name:* INHLTPV. *Location in TSPA-LA:* Section 6.3.11; Equation 6.3.11-4. *DTN:* MO0702PAVBPDCF.000 _R0 [DIRS 179330]. *References: Biosphere Model Report* (SNL 2007 [DIRS 177399], Sections 6.12.2 and 6.14.5; Table 6.12-2; Figure 6.14-2).
BDCF_Inh_ShT. Pointer variable for short-term inhalation dose conversion factor for volcanic ash exposure (dimensionless). *Distribution:* Discrete. *Range:* 1 to 300. *Symbol:* $BDCF_{inh,v,i}$ *Additional Information:* See BDCF_Inh_ShT. *Sensitivity Name:* INHSTPV. *Location in TSPA-LA:* Section 6.3.11; Equation 6.3.11-4. *DTN:* MO0702PAVBPDCF.000 _R0 [DIRS 179330]. *References: Biosphere Model Report* (SNL 2007 [DIRS 177399], Sections 6.12.2 and 6.14.5; Table 6.12-2; Figure 6.14-2).
Beta_Dist_a. Column diffusion constant (dimensionless). *Distribution:* Uniform. *Range:* 0.01 to 0.5. *Symbol:* $\beta_{\tilde{}}$ *Additional Information:* This parameter affects the distribution of particles vertically in the ash column and helps determine where particles exit the column. ASHPLUME takes a beta value and determines the vertical profile of particle sizes in the erupted column that will then be transported down wind. The larger beta becomes, the more the particle distribution becomes skewed towards the top of the column. A value of 0.5 generates a column particle distribution that contains very few particles in the lower 70% of the column, whereas a beta value of 0.01 gives an upwardly decreasing distribution that contains the most particles lower in the column. The beta parameter is related to the buoyancy of particles in the eruptive column and determines how high most particles will travel before exiting the column. Based on comparisons of modeled and observed tephra distributions, beta values of 0.5 or greater are not representative of typical eruptions. Uncertainty in this value originates from the relationship between the mathematical coefficient and physical processes. *Sensitivity Name:* BETA. *Location in TSPA-LA:* Table 6.5-4. *DTN:* LA0702PADE03GK.002_R1 [DIRS 179980]. *References: Atmospheric Dispersal and Deposition of Tephra from a Potential Volcanic Eruption at Yucca Mountain, Nevada* (SNL 2007 [DIRS 177431], Sections 6.5.2.3, 7.2 and 8.2; Tables 4-1, 6-3, 8-2, C-1, C-5 and J-1; Figure C-4).
C1_GenCorr_A22_a. Temperature dependent slope term of Alloy 22 general corrosion rate (K). *Distribution:* Truncated normal. *Range:* 666 to 7731. *Mean:* 4905. *Standard Deviation:* 1413. *Symbol:* C_1. *Additional Information:* The temperature-dependence term represents the effect of temperature on corrosion rates of Alloy 22 based on polarization resistance measurements using a wide variety of specimen configurations, metallurgical conditions, and exposure environments (i.e., water chemistries). Truncation of the C_1 distribution at +2/-3 standard deviations is appropriate given that the resulting range in apparent activation energies spans a large range of values from extremely low temperature dependence to a high temperature dependence. The entire variance in the temperature dependence term is due to uncertainty. The higher the value of C_1, the greater the dependence of general corrosion rate on temperature. *Sensitivity Name:* WDGCA22. *Location in TSPA-LA:* Sections 6.3.5.1.2 and 6.3.5.1.3; Tables 6.3.5-3 and 6.3.5-4; Equation 6.3.5-4. *DTN:* MO0703PAGENCOR.001_R4 [DIRS 182029]. *References: General Corrosion and Localized Corrosion of the Waste Package Outer Barrier* (SNL 2007 [DIRS 178519], Sections 6.4.3 and 6.4.3.4).

Table K3-3. Detailed Summary of Epistemically Uncertain Variables (i.e., elements of **e**) Considered in the TSPA-LA (TSPA Parameter Name) (Continued)

NOTE: * indicates variable not considered in sensitivity analysis due to correlations.

Colloidal_Kc_Am_UZP. Colloid sorption coefficient for americium (mg/mg). *Calculated by:* Colloidal_Kd_Am_uz*Colloidal_Concentration_uz. *Correlation:* Correlated to Colloidal_Kc_Pa_UZP and Colloidal_Kc_Th_UZP with a correlation coefficient of 1. *Symbol:* K_c. *Additional Information:* Selector elements for colloidal K_cs. For colloid-facilitated radionuclide transport in which radionuclides are reversibly attached to colloids, a partition coefficient is defined to represent the potential for enhanced migration of radionuclides in association with colloids. For reversible radionuclide sorption on the colloids, the K_c values are calculated by multiplying a radionuclide's sorption coefficient for a species onto a colloid, K_d, by the colloid concentrations in the water. Used in FEHM as an input parameter for calculating the retardation factors for colloid facilitated radionuclide transport in the media. To address the uncertainty of colloid concentration on colloid facilitated transport, the colloid concentration is sampled at run time and provided to FEHM for the calculation of K_c. See Conc_Col_Gw_Sampled_a and Kd_Am_Col. *Sensitivity Name:* UZCOKDAM. *Location in TSPA-LA:* Section 6.3.9.2. *DTN:* LA0701PANS02BR.003_R2 [DIRS 180497] for Kds. *References: Particle Tracking Model and Abstraction of Transport Processes Addendum 002* (SNL 2008 [DIRS 184748], Sections 6.5.12 and 6.5.13; Tables 6.6.1-1 and 6-22).
Colloidal_Kc_Cs_UZP. Colloid sorption coefficient for cesium (mg/mg). *Calculated by:* Colloidal_Kd_Cs_uz*Colloidal_Concentration_uz. *Symbol:* K_c. *Additional Information:* Selector elements for colloidal K_cs. For colloid-facilitated radionuclide transport in which radionuclides are reversibly attached to colloids, a partition coefficient is defined to represent the potential for enhanced migration of radionuclides in association with colloids. For reversible radionuclide sorption on the colloids, the K_c values are calculated by multiplying a radionuclide's sorption coefficient for a species onto a colloid, K_d, by the colloid concentrations in the water. Used in FEHM as an input parameter for calculating the retardation factors for colloid facilitated radionuclide transport in the media. To address the uncertainty of colloid concentration on colloid facilitated transport, the colloid concentration is sampled at run time and provided to FEHM for the calculation of K_c. See Conc_Col_Gw_Sampled_a and Kd_Cs_Col. *Sensitivity Name:* UZCOKDCS. *Location in TSPA-LA:* Section 6.3.9.2. *DTN:* LA0701PANS02BR.003_R2 [DIRS 180497] for Kds. *References: Particle Tracking Model and Abstraction of Transport Processes Addendum 002* (SNL 2008 [DIRS 184748], Sections 6.5.12 and 6.5.13; Tables 6.6.1-1 and 6-22).
Colloidal_Kc_Pa_UZP. Colloid sorption coefficient for protactinium (mg/mg). *Calculated by:* Colloidal_Kd_Am_uz*Colloidal_Concentration_uz. *Correlation:* Correlated to Colloidal_Kc_Am_UZP and Colloidal_Kc_Th_UZP with a correlation coefficient of 1. *Symbol:* K_c. *Additional Information:* Selector elements for colloidal K_cs. For colloid-facilitated radionuclide transport in which radionuclides are reversibly attached to colloids, a partition coefficient is defined to represent the potential for enhanced migration of radionuclides in association with colloids. For reversible radionuclide sorption on the colloids, the K_c values are calculated by multiplying a radionuclide's sorption coefficient for a species onto a colloid, K_d, by the colloid concentrations in the water. Used in FEHM as an input parameter for calculating the retardation factors for colloid facilitated radionuclide transport in the media. To address the uncertainty of colloid concentration on colloid facilitated transport, the colloid concentration is sampled at run time and provided to FEHM for the calculation of K_c. See Conc_Col_Gw_Sampled_a and Kd_Am_Col. *Sensitivity Name:* UZCOKDPA. *Location in TSPA-LA:* Section 6.3.9.2. *DTN:* LA0701PANS02BR.003_R2 [DIRS 180497] for Kds. *References: Particle Tracking Model and Abstraction of Transport Processes Addendum 002* (SNL 2008 [DIRS 184748], Sections 6.5.12; Tables 6.6.1-1 and 6-22).
Colloidal_Kc_Pu_UZP. Colloid sorption coefficient for plutonium (mg/mg). *Calculated by:* Colloidal_Kd_Pu_uz*Colloidal_Concentration_uz. *Symbol:* K_c. *Additional Information:* Selector elements for colloidal K_cs. For colloid-facilitated radionuclide transport in which radionuclides are reversibly attached to colloids, a partition coefficient is defined to represent the potential for enhanced migration of radionuclides in association with colloids. For reversible radionuclide sorption on the colloids, the K_c values are calculated by multiplying a radionuclide's sorption coefficient for a species onto a colloid, K_d, by the colloid concentrations in the water. Used in FEHM as an input parameter for calculating the retardation factors for colloid facilitated radionuclide transport in the media. To address the uncertainty of colloid concentration on colloid facilitated transport, the colloid concentration is sampled at run time and provided to FEHM for the calculation of K_c. See Conc_Col_Gw_Sampled_a and Kd_Pu_Col. *Sensitivity Name:* UZCOKDPU. *Location in TSPA-LA:* Section 6.3.9.2. *DTN:* LA0701PANS02BR.003_R2 [DIRS 180497] for Kds. *References: Particle Tracking Model and Abstraction of Transport Processes Addendum 002* (SNL 2008 [DIRS 184748], Sections 6.5.12 and 6.5.13; Tables 6.6.1-1 and 6-22).

Table K3-3. Detailed Summary of Epistemically Uncertain Variables (i.e., elements of **e**) Considered in the TSPA-LA (TSPA Parameter Name) (Continued)

NOTE: * indicates variable not considered in sensitivity analysis due to correlations.

Colloidal_Kc_Sn_UZP. Colloid sorption coefficient for tin (mg/mg). *Calculated by:* Colloidal_Kd_Sn_uz*Colloidal_Concentration_uz. *Symbol:* K_c. *Additional Information:* Selector elements for colloidal K_cs. For colloid-facilitated radionuclide transport in which radionuclides are reversibly attached to colloids, a partition coefficient is defined to represent the potential for enhanced migration of radionuclides in association with colloids. For reversible radionuclide sorption on the colloids, the Kc values are calculated by multiplying a radionuclide's sorption coefficient for a species onto a colloid, Kd, by the colloid concentrations in the water. Used in FEHM as an input parameter for calculating the retardation factors for colloid facilitated radionuclide transport in the media. To address the uncertainty of colloid concentration on colloid facilitated transport, the colloid concentration is sampled at run time and provided to FEHM for the calculation of Kc. See Conc_Col_Gw_Sampled_a and Kd_Sn_Col. *Sensitivity Name:* UZCOKDSN. *Location in TSPA-LA:* Section 6.3.9.2. *DTN:* LA0701PANS02BR.003_R2 [DIRS 180497] for Kds. *References: Particle Tracking Model and Abstraction of Transport Processes Addendum 002* (SNL 2008 [DIRS 184748], Sections 6.5.12 and 6.5.13; Tables 6.6.1-1 and 6-22).
Colloidal_Kc_Th_UZP. Colloid sorption coefficient for thorium (mg/mg). *Calculated by:* Calculated by Colloidal_Kd_Am_uz*Colloidal_Concentration_uz. *Correlation:* Correlated to Colloidal_Kc_Am_UZP and Colloidal_Kc_Pa_UZP with a correlation coefficient of 1. *Symbol:* K_c. *Additional Information:* Selector elements for colloidal K_cs. For colloid-facilitated radionuclide transport in which radionuclides are reversibly attached to colloids, a partition coefficient is defined to represent the potential for enhanced migration of radionuclides in association with colloids. For reversible radionuclide sorption on the colloids, the K_c values are calculated by multiplying a radionuclide's sorption coefficient for a species onto a colloid, K_d, by the colloid concentrations in the water. Used in FEHM as an input parameter for calculating the retardation factors for colloid facilitated radionuclide transport in the media. To address the uncertainty of colloid concentration on colloid facilitated transport, the colloid concentration is sampled at run time and provided to FEHM for the calculation of K_c. See Conc_Col_Gw_Sampled_a and Kd_Am_Col. *Sensitivity Name:* UZCOKDTH. *Location in TSPA-LA:* Section 6.3.9.2. *DTN:* LA0701PANS02BR.003_R2 [DIRS 180497] for Kds. *References: Particle Tracking Model and Abstraction of Transport Processes Addendum 002* (SNL 2008 [DIRS 184748], Sections 6.5.12; Tables 6.6.1-1 and 6-22).
Colloidal_Retard_Factor_dist_a. Colloid retardation factor (dimensionless). *Distribution:* Piecewise uniform. *Range:* 6 to 799.83. *Symbol:* R_{coll}. *Additional Information:* The colloid retardation factor is used in the TSPA LA Model to simulate the impact of reversible filtration on colloids in the fractured media with respect to radionuclides irreversibly sorbed onto colloids. In TSPA-LA calculations, to investigate the uncertainty of colloid retardation factors on radionuclide transport, colloid retardation factors are sampled for each realization at run time. The colloid retardation factor is used by FEHM in simulating the effects of colloid retardation in fractured rock on colloid-facilitated radionuclide transport. *Sensitivity Name:* UZRCOL. *Location in TSPA-LA:* Sections 6.3.9.2 and 6.3.9.3; Table 6.3.9-12. *DTN:* LA0701PANS02BR.003_R2 [DIRS 180497], Table 5.doc. *References: Particle Tracking Model and Abstraction of Transport Processes Addendum 002* (SNL 2008 [DIRS 184748], Sections 4.1.9, 6.5.13 and 6.8.2.2; Table 8-2; Figures 6.8.2-23 and 6.8.2-24).
Conc_Col. Logarithm of ambient concentration of colloids in groundwater (g/mL). *Distribution:* Piecewise uniform. *Range:* -9 to -3.6. *Symbol:* C_{coll}. *Additional Information:* This parameter is used to calculate the retardation of radionuclides in colloidal transport. To treat the one- and three-dimensional transport through the SZ consistently, the sampled values used to generate the saturated zone breakthrough curves are also used in the TSPA-LA Model. These values are tabulated as 200 sets of values for the SZ parameters, accounting for appropriate correletions, and are entered into the TSPA model as a table of 200 values for each parameter. The TSPA-LA Model selects values from this table using the Goldsim variable SZ_index_a. *Sensitivity Name:* SZCONCOL. *Location in TSPA-LA:* Table 6.3.10-2. *DTN:* SN0702PASZFTMA.002_R1 [DIRS 183471]. *References: Saturated Zone Flow and Transport Model Abstraction* (SNL 2008 [DIRS 183750], Sections 6.3.1, 6.5.1.1 and 6.5.2.12; Tables 4-3, 6-8, A-1[a] and B-1; Equation 6-4).

Table K3-3. Detailed Summary of Epistemically Uncertain Variables (i.e., elements of **e**) Considered in the TSPA-LA (TSPA Parameter Name) (Continued)

NOTE: * indicates variable not considered in sensitivity analysis due to correlations.

Conc_Col_FeOx_CS_Sampled_a. FeOx colloid concentration when carbon steel is corroding (mg/L). *Distribution:* Truncated log normal. *Range:* 0.3 to 30. *Mean:* 3.69. *Standard Deviation:* 2.79. *Additional Information:* Iron oxyhydroxide colloids would be expected to form as a result of corrosion of the waste package and associated engineered barrier system components. The input data from carbon steel corrosion are short term tests with a less durable material; therefore, these are believed to be much higher than what will occur in the long term. Few peer-reviewed publications present information on iron oxide–oxyhydroxide colloid concentrations as a function of aqueous chemistry, therefore there is uncertainty in the amount of colloids produced from steel corrosion. The range of values for maximum iron oxide–oxyhydroxide colloids concentration was chosen so that it was greater than iron oxyhydroxide colloid levels found in groundwater, but high enough to reflect the masses of corroded ferrous metal anticipated in the repository. *Sensitivity Name:* COLFEOCS. *Location in TSPA-LA:* Table 6.3.7-65. *DTN:* MO0701PAIRONCO.000_R1 [DIRS 180440]. *References: Waste Form and In-Drift Colloids-Associated Radionuclide Concentrations: Abstraction and Summary* (SNL 2007 [DIRS 177423], Sections 6.3.2, 6.3.8, 6.5.1.4, 6.5.2, 6.3.12.1 and 6.6.5; Equations 6-13 and 6-15; Figure 6-20; Table 6-24).
Conc_Col_FeOx_SS_Sampled_a. FeOx colloid concentration when degraded stainless steel is present, but no degrading carbon steel is present (mg/L). *Distribution:* Piecewise uniform. *Range:* 1.00E-03 to 3.00E+01. *Additional Information:* The assessment of colloid concentrations from stainless steel is subjective as there is insufficient data available to make a reliable analysis. As stainless steel is less corrosive than carbon steel, the overall colloid mass distribution was reduced compared to carbon steel. *Sensitivity Name:* COLFEOSS. *Location in TSPA-LA:* Table 6.3.7-65. *DTN:* MO0701PAIRONCO.000_R1 [DIRS 180440]. *References: Waste Form and In-Drift Colloids-Associated Radionuclide Concentrations: Abstraction and Summary* (SNL 2007 [DIRS 177423], Sections 6.3.2, 6.3.8, 6.5.1.4, 6.5.2 and 6.6.5; Figure 6-21; Tables 6-11 and 6-24).
Conc_Col_Gw_Sampled_a. Concentration of groundwater colloids when colloids are stable (mg/L). *Distribution:* Piecewise uniform. *Range:* 0.001 to 200. *Median:* 0.1. *Additional Information:* At Yucca Mountain, inorganic groundwater colloids, primarily consisting of clay, silica, and iron oxyhydroxides, may be transported in seepage water into the repository from the vadose zone above it or may be formed due to changes in chemical conditions near the repository. Pseudocolloids may form due to the sorption onto these natural colloids of radionuclides mobilized from degradation of the waste form. Pseudocolloids thus formed in the waste and engineered barrier system may influence radionuclide transport. Several factors contribute to uncertainty in the concentrations of colloids in the groundwater samples used to establish parameters for use in the TSPA analysis including (1) field sampling techniques, including differences in pumping rates at each well during extraction of the water samples, (2) other unknown factors affecting the quantities of particles suspended in the water samples, including the types of additives introduced in the wells during the drilling process itself, and (3) errors inherent to the laboratory methods used to measure the quantities of colloids suspended in the water samples (e.g., filter ripening, interference and detection limitations for dynamic light scattering measurement techniques). A cumulative distribution function was developed to accommodate the variable colloid concentrations and the uncertainty in groundwater sample collection. This allowed for stochastic sampling, including high concentrations (i.e., ~100 mg/L) in at least 2% of the model iterations, while probabilistically allowing for the selection of lower mass concentrations (0.001 mg/L to 1.0 mg/L) 75% of the time. *Sensitivity Name:* COLGW. *Location in TSPA-LA:* Table 6.3.7-66. *DTN:* MO0701PAGROUND.000_R0 [DIRS 179310]. *References: Waste Form and In-Drift Colloids-Associated Radionuclide Concentrations: Abstraction and Summary* (SNL 2007 [DIRS 177423], Sections 6.3.1, 6.3.9, 6.3.11, 6.3.12, 6.5.1.5, 6.5.1.6, 6.5.3, 6.6.6, 7.1.4, 8.1 and Appendix I; Figures 6-22 and 6-24; Tables 6-13, 6-24, 7-1 and I-1).
Conc_Col_U_Sampled_a. Concentration of uranophane colloids when colloids are stable (mg/L). *Distribution:* Piecewise uniform. *Range:* 0.001 to 200. *Median:* 0.1. *Symbol:* $m_{coll,Uranophane,sampled}$. *Additional Information:* The selection of this distribution was based on comparison with commonly observed colloid population distributions of groundwater colloids that are dominated by smectite clay particles. To estimate the uncertainty, it is therefore recommended that the uranophane colloids have a distribution identical to that of the groundwater colloids because the dominant interfacial phase in the groundwater (smectite clay) has surface electrical properties that are similar to uranophane. As the K_d values for the uranophane are low, the probability of radionuclide transport, other than uranium, associated with these colloids is low. *Sensitivity Name:* COLU. *Location in TSPA-LA:* Table 6.3.7-64. *DTN:* MO0701PACSNFCP.000_R1 [DIRS 180439]. *References: Waste Form and In-Drift Colloids-Associated Radionuclide Concentrations: Abstraction and Summary* (SNL 2007 [DIRS 177423], Sections 5.6, 6.3.1, 6.3.2.5, 6.3.2.6, 6.5.1.3, 6.5.1.6, 6.5.2.1, 6.6.4 and 7.1.3; Figures 6-15, 6-28, 6-29 and 6-39; Tables 6-8 and 6-24).

Table K3-3. Detailed Summary of Epistemically Uncertain Variables (i.e., elements of **e**) Considered in the TSPA-LA (TSPA Parameter Name) (Continued)

NOTE: * indicates variable not considered in sensitivity analysis due to correlations.

CORAL. Logarithm of colloid retardation factor in alluvium (dimensionless). *Distribution:* Piecewise uniform. *Range:* 0.903 to 3.715. *Symbol:* R. *Additional Information:* This parameter specifies the retardation of colloids with irreversibly sorbed radionuclides in the alluvium. To treat the one- and three-dimensional transport through the SZ consistently, the sampled values used to generate the saturated zone breakthrough curves are also used in the TSPA-LA Model. These values are tabulated as 200 sets of values for the SZ parameters, accounting for appropriate correletions, and are entered into the TSPA model as a table of 200 values for each parameter. The TSPA-LA Model selects values from this table using the Goldsim variable SZ_index_a. *Sensitivity Name:* SZCOLRAL. *Location in TSPA-LA:* Sections 6.3.10.1, 6.3.10.2 and 6.3.10.4.2; Table 6.3.10-2. *DTN:* SN0702PASZFTMA.002_R1 [DIRS 183471]. *References: Saturated Zone Flow and Transport Model Abstraction* (SNL 2008 [DIRS 183750], Sections 6.3.1, 6.5.1.1 and 6.5.2.11; Tables 4-3, 6-8, A-1[a] and B-1; Equations 6-2 and 6-10; Figure 6-22).
CORVO. Logarithm of colloid retardation factor in volcanic units (dimensionless). *Distribution:* Piecewise uniform. *Range:* 0.778 to 2.903. *Symbol:* R. *Additional Information:* This parameter specifies retardation of colloids with irreversibly sorbed radionuclides in the volcanic units. To treat the one- and three-dimensional transport through the SZ consistently, the sampled values used to generate the saturated zone breakthrough curves are also used in the TSPA-LA Model. These values are tabulated as 200 sets of values for the SZ parameters, accounting for appropriate correletions, and are entered into the TSPA model as a table of 200 values for each parameter. The TSPA-LA Model selects values from this table using the Goldsim variable SZ_index_a. *Sensitivity Name:* SZCOLRVO. *Location in TSPA-LA:* Sections 6.3.10.1, 6.3.10.2 and 6.3.10.4.2; Table 6.3.10-2. *DTN:* SN0702PASZFTMA.002_R1 [DIRS 183471]. *References: Saturated Zone Flow and Transport Model Abstraction* (SNL 2008 [DIRS 183750], Sections 6.3.1, 6.5.1.1 and 6.5.2.11; Tables 4-3, 6-8, A-1[a] and B-1; Equations 6-2 and 6-10; Figure 6-22).
CPu_Col_CSNF_Sampled_a. Concentration of irreversibly attached plutonium on CSNF colloids when colloids are stable (mol/L). *Distribution:* Piecewise uniform. *Range:* 1.00E-10 to 5.00E-06. *Median:* 1.00E-07. *Symbol:* $C_{RN,coll,SNF,embed,sampled}$. *Additional Information:* This model looks exclusively at the irreversible attachment of radionuclides to CSNF colloids. The radionuclides Pu and Am are modeled as irreversibly embedded within CSNF colloids. An empirical cumulative distribution function was developed to accommodate the variable plutonium colloid concentrations and the uncertainty in testing configurations for CSNF corrosion tests. It is reasonable to assume that these CSNF plutonium colloid concentrations will persist for 1 Ma, if CSNF is still present and undergoing weathering, and the solution conditions are suitable for stable colloids. It is conservative to assume these colloids persist at late times after all waste forms are degraded and the initially suspended colloids are washed away. *Sensitivity Name:* CPUCOLCS. *Location in TSPA-LA:* Section 6.3.7.6.2; Table 6.3.7-63. *DTN:* MO0701PACSNFCP.000_R1 [DIRS 180439]. *References: Waste Form and In-Drift Colloids-Associated Radionuclide Concentrations: Abstraction and Summary* (SNL 2007 [DIRS 177423], Sections 6.3.1, 6.3.2.4, 6.3.4, 6.5, 6.5.1.2 and 6.6.3, Tables 6-6, 6-24 and 8-1, Figures 6-10, 6-28, 6-29 and 6-31).
CPu_Col_Wf_Embed_Sampled_a. Concentration of irreversibly attached plutonium on glass/waste form colloids when colloids are stable (mol/L). *Distribution:* Uniform. *Range:* 1.00E-11 to 1.00E-08. *Symbol:* $C_{RN,coll,DHLWG,embed,sampled}$. *Additional Information:* To obtain the plutonium concentration associated with DHLWG colloids, a range is sampled uniformly. Colloids from the corrosion of DHLWG are modeled as smectite particles with irreversibly associated (embedded) Pu and Am. In the case of DHLWG, modeling americium and plutonium as irreversible colloids is conservative and bounding. *Sensitivity Name:* CPUCOLWF. *Location in TSPA-LA:* Section 6.3.7.6.2; Table 6.3.7-62. *DTN:* MO0701PAGLASWF.000_R1 [DIRS 180393]. *References: Waste Form and In-Drift Colloids-Associated Radionuclide Concentrations: Abstraction and Summary* (SNL 2007 [DIRS 177423], Sections 6.3.1, 6.3.2.2, 6.3.3, 6.4.2, 6.5.1.1, 6.5.1.6, 6.5.2 and 6.6.2; Figures 6-6, 6-7, 6-18 and 6-28 to 6-31; Tables 6-4, 6-5, 6-24 and 8-1).
CPu_Per_CSNF_Embed_Col_a. Concentration of irreversibly attached plutonium per concentration of CSNF colloids ((mol/L)/(mg/L)). *Distribution:* Uniform. *Range:* 5.00E-07 to 1.00E-06. *Symbol:* $C_{coll,SNF,uniform}$. *Additional Information:* See CPu_Col_CSNF_Sampled_a. *Sensitivity Name:* CPUPERCS. *Location in TSPA-LA:* Section 6.3.7.6.2; Table 6.3.7-63. *DTN:* MO0701PACSNFCP.000_R1 [DIRS 180439]. *References: Waste Form and In-Drift Colloids-Associated Radionuclide Concentrations: Abstraction and Summary* (SNL 2007 [DIRS 177423], Table 6-24).
CPu_Per_WF_Embed_Col_a. Concentration of irreversibly attached plutonium per concentration of waste form colloids ((mol/L)/(mg/L)). *Distribution:* Triangular. *Range:* 5.00E-09 to 2.5E-08. *Most Likely:* 2.00E-08. *Symbol:* $C_{coll,DHLWG,sampled}$. *Additional Information:* See CPu_Col_CSNF_Sampled_a. *Sensitivity Name:* CPUPERWF. *Location in TSPA-LA:* Section 6.3.7.6.2; Table 6.3.7-62. *DTN:* MO0701PAGLASWF.000_R1 [DIRS 180393]. *References: Waste Form and In-Drift Colloids-Associated Radionuclide Concentrations: Abstraction and Summary* (MDL-EBS-PA-000004 REV 03, SNL 2007 [DIRS 177423], Figure 6-6; Table 6-24).

Table K3-3. Detailed Summary of Epistemically Uncertain Variables (i.e., elements of **e**) Considered in the TSPA-LA (TSPA Parameter Name) (Continued)

NOTE: * indicates variable not considered in sensitivity analysis due to correlations.

Cr2O3_SA_a. Specific surface area of Cr_2O_3 (m^2/g). *Distribution:* Uniform. *Range:* 1 to 20. *Symbol:* S_{CrOx}. *Additional Information:* For the water saturation calculation, the solid density of each of the four corrosion product components is multiplied by its respective specific surface area. *Sensitivity Name:* CR2O3SA. *Location in TSPA-LA:* Table 6.3.8-4, S_{CP} in Equation 6.3.8-19. *DTN:* SN0703PAEBSRTA.001_R3 [DIRS 183217]. *References: EBS Radionuclide Transport Abstraction* (ANL-WIS-PA-000001 REV 03, SNL 2007 [DIRS 177407], Sections 6.3.4.3.3 and 6.5.2.2.1; Tables 4.1-19, 6.3-7, and 8.2-4).
Critical_Slope_a. Critical gradient for tephra mobilization from hillslopes (dimensionless). *Distribution:* Uniform. *Range:* 0.21 to 0.47. *Symbol:* S. *Additional Information:* The critical slope is reported as a fraction of the vertical change in elevation over the horizontal change in distance and is dimensionless. It represents the steepest stable slope for tephra-blanketed hillslopes. The waste-contaminated tephra is mobilized from slopes greater than a specified critical slope. As the critical slope increases, the predicted mass of ash/fuel mobilized decreases. Capturing the lower bound of the critical slope is thus necessary to assure reasonable and conservative results. *Sensitivity Name:* CRITSLOP. *Location in TSPA-LA:* Table 6.5-5. *DTN:* MO0702PAFARDAT.001_R3 [DIRS 182578]. *References: Redistribution of Tephra and Waste by Geomorphic Processes Following a Potential Volcanic Eruption at Yucca Mountain, Nevada* (SNL 2007 [DIRS 179347], Sections 6.2.1, 6.3.2, 6.3.3, 6.5.2, 6.6.1 and 6.6.3; Tables 4.1-3, 6.4-1, 6.5.2-1 and 6.5.10-1; Figures 6.3.3-9 and 6.6.1-1).
CS_Corrosion_Rate_a. Carbon steel corrosion rate (μm/yr). *Distribution:* Truncated log normal. *Range:* 25 to 135. *Mean:* 78.5. *Standard Deviation:* 25. *Symbol:* r_{CS}. *Additional Information:* Carbon-steel corrosion rate is used in computing the mass of stationary corrosion products in the waste package. The corrosion rates for Carbon Steel A516 are known with some uncertainty. From these rates and the thicknesses of the steel components, the lifetime of each type of steel is computed. The extent of corrosion, specifically, the mass of corrosion products, is interpolated over the lifetime of each type of steel. *Sensitivity Name:* CSCORRAT. *Location in TSPA-LA:* Tables 6.3.8-1 and 6.3.8-4. *DTN:* SN0703PAEBSRTA.001_R3 [DIRS 183217]. *References: EBS Radionuclide Transport Abstraction* (SNL 2007 [DIRS 177407], Sections 6.3.4.3.4.3, 6.5.2.2.1 and Appendix F; Tables 4.1-1, 6.5-7, 8.2-4 and 8.2-7; Equation 6.5.2.2.1-1).
CSNF_Mass_Uncert_a. Scale factor used to characterize uncertainty in radionuclide content of CSNF (dimensionless). *Distribution:* Uniform. *Range:* 0.85 to 1.4. *Additional Information:* The sampled multiplier is applied to the nominal CSNF values for all radionuclides except ^{238}U. A radionuclide mass uncertainty multiplier is selected at the beginning of each realization and applied to each waste package that is assumed breached. The selected uncertainty multiplier is held constant during each realization run. CSNF, DSNF, and HLW glass each have their own uncertainty multiplier assigned at the beginning of each realization. *Sensitivity Name:* CSNFMASS. *Location in TSPA-LA:* Sections 6.3.7.1.2 and 6.3.7.1.3; Table 6.3.7-7. *DTN:* SN0310T0505503.004_R0 [DIRS 168761]. *References: Initial Radionuclides Inventory* (SNL 2007 [DIRS 180472], Section 6.6.1, 6.7 and 7; Table 7-2),
CSNF_Rind_SA_a. Specific surface area of CSNF degradation rind (m^2/g). *Distribution:* Uniform. *Range:* 0.5 to 60. *Symbol:* $s_{r,n}$ or s_{rind}. *Additional Information:* See Density_CSNF_Rind_a. The scatter in the data and use of several different materials lead to a range and distribution of parameter values for the FHH isotherm. The specific surface area is a sampled parameter, with a range given by the range of values for the surrogate materials used to generate the FHH adsorption isotherm. While the specific surface area does not necessarily affect the adsorption isotherm, the water saturation is directly proportional to specific surface area. The use of surrogate material properties, where both specific surface area and density are higher than the values estimated for schoepite and CSNF, will result in overestimating water saturation in and releases of radionuclides from the CSNF rind. Sampling from the range and distribution for rind specific surface area given above will enable TSPA to evaluate the sensitivity of estimates for releases of radionuclides to this parameter. To capture this large uncertainty, the specific surface area and density of the rind materials, as well as the porosity, will be sampled from uniform distributions over the ranges of the surrogate material properties. *Sensitivity Name:* CSRINDSA. *Location in TSPA-LA:* Tables 6.3.8-2 and 6.3.8-4. *DTN:* SN0703PAEBSRTA.001_R3 [DIRS 183217]. *References: EBS Radionuclide Transport Abstraction* (SNL 2007 [DIRS 177407], Section 6.3.4.6.1; Equation 6.3.4.6.1-4; Tables 6.5-9, 8.2-4 and 8.2-7).

Table K3-3. Detailed Summary of Epistemically Uncertain Variables (i.e., elements of **e**) Considered in the TSPA-LA (TSPA Parameter Name) (Continued)

NOTE: * indicates variable not considered in sensitivity analysis due to correlations.

CSNF_WF_Uncert_a0_Acid_a. Correlated regression coefficient a0 in the abstracted rate model under acidic conditions (dimensionless). *Distribution:* Normal. *Mean/Median/Mode:* 0. *Standard Deviation:* 1. *Additional Information:* The CSNF WF degradation rate is modeled with a regression model for the degradation rate with uncertain coefficients. The uncertainty in the regression coefficients is sampled by generating vectors from a multivariate normal population with a specified covariance matrix. For the acid-side determination, a random vector is comprised of sampled values for CSNF_WF_Uncert_a0_Acid_a and CSNF_WF_Uncert_a4_Acid_a. The uncertainty in the abstracted rate expression coefficients a0 and a4 is correlated as defined by a covariance matrix. The TSPA implementation of the covariance matrix utilizes the Cholesky Factorization of the covariance matrix and each realization of the random vector to compute the correlated coefficients a0 and a4 for each realization. *Sensitivity Name:* CSWFA0AC. *Location in TSPA-LA:* Section 6.3.7.4.1.2; Equation 6.3.7-6. *References: CSNF Waste Form Degradation: Summary Abstraction* (BSC 2004 [DIRS 169987], Sections 6.4.1.3 and 8.1; Equation 11).
CSNF_WF_Uncert_a0_Alk_a. Correlated coefficient a0 in the abstracted rate model under alkaline conditions (dimensionless). *Distribution:* Normal. *Mean/Median/Mode:* 0. *Standard Deviation:* 1. *Additional Information:* The CSNF WF degradation rate is modeled with a regression model for the degradation rate with uncertain coefficients. The uncertainty in the regression coefficients is sampled by generating vectors from a multivariate normal population with a specified covariance matrix. For the alkaline-side determination, the random vector is comprised of sampled values for CSNF_WF_Uncert_a0_Alk_a, CSNF_WF_Uncert_a1_Alk_a, CSNF_WF_Uncert_a2_Alk_a and CSNF_WF_Uncert_a3_Alk_a. The uncertainty in the abstracted rate expression coefficients a0, a1, a2, and a3 is correlated as defined by a covariance matrix. The TSPA implementation of the covariance matrix utilizes the Cholesky Factorization of the covariance matrix and each realization of the random vector to compute the correlated coefficients a0, a1, a2, and a3 for each realization. *Sensitivity Name:* CSWFA0AK. *Location in TSPA-LA:* Section 6.3.7.4.1.2; Equation 6.3.7-5. *References: CSNF Waste Form Degradation: Summary Abstraction* (BSC 2004 [DIRS 169987], Sections 6.4.1.2 and 8.1; Equation 10).
CSNF_WF_Uncert_a1_Alk_a. Correlated coefficient a1 in the abstracted rate model under alkaline conditions (dimensionless). *Distribution:* Normal. *Mean/Median/Mode:* 0. *Standard Deviation:* 1. *Additional Information:* See CSNF_WF_Uncert_a0_Alk_a. *Sensitivity Name:* CSWFA1AK. *Location in TSPA-LA:* Section 6.3.7.4.1.2; Equation 6.3.7-5. *References: CSNF Waste Form Degradation: Summary Abstraction* (BSC 2004 [DIRS 169987], Sections 6.4.1.2 and 8.1; Equation 10).
CSNF_WF_Uncert_a2_Alk_a. Correlated coefficient a2 in the abstracted rate model under alkaline conditions (dimensionless). *Distribution:* Normal. *Mean/Median/Mode:* 0. *Standard Deviation:* 1. *Additional Information:* See CSNF_WF_Uncert_a0_Alk_a. *Sensitivity Name:* CSWFA2AK. *Location in TSPA-LA:* Section 6.3.7.4.1.2; Equation 6.3.7-5. *References: CSNF Waste Form Degradation: Summary Abstraction* (BSC 2004 [DIRS 169987], Sections 6.4.1.2 and 8.1; Equation 10).
CSNF_WF_Uncert_a3_Alk_a. Correlated coefficient a3 in the abstracted rate model under alkaline conditions (dimensionless). *Distribution:* Normal. *Mean/Median/Mode:* 0. *Standard Deviation:* 1. *Additional Information:* See CSNF_WF_Uncert_a0_Alk_a. *Sensitivity Name:* CSWFA3AK. *Location in TSPA-LA:* Section 6.3.7.4.1.2; Equation 6.3.7-5. *References: CSNF Waste Form Degradation: Summary Abstraction* (BSC 2004 [DIRS 169987], Sections 6.4.1.2 and 8.1; Equation 10).
CSNF_WF_Uncert_a4_Acid_a. Correlated coefficient a4 in the abstracted rate model under acid conditions (dimensionless). *Distribution:* Normal. *Mean/Median/Mode:* 0. *Standard Deviation:* 1. *Additional Information:* See CSNF_WF_Uncert_a0_Acid_a. *Sensitivity Name:* CSWFA4AC. *Location in TSPA-LA:* Section 6.3.7.4.1.2; Equation 6.3.7-6. *References: CSNF Waste Form Degradation: Summary Abstraction* (BSC 2004 [DIRS 169987], Sections 6.4.1.3 and 8.1; Equation 11).
D_Channels_a. Diffusivity of radionuclides in channels of the Fortymile Wash fan (RMEI location) (cm^2/yr). *Distribution:* Uniform. *Range:* 0.035 to 0.266. *Mean:* 0.1505. *Symbol:* D_c. *Additional Information:* The uncertainty distribution for this parameter is based on measured ^{137}Cs profiles from channels and young terraces of the upper Fortymile Wash alluvial fan. The diffusivity model is used to calculate the waste concentration profile over time in the RMEI domain. As the diffusivity parameter increases, the rate of diffusion into the soil increases, decreasing the near surface contamination (and thus the calculated dose) at a more rapid rate. Capturing the low end of the diffusivity range is thus critical to assure reasonable and conservative results. *Sensitivity Name:* DCHANL. *Location in TSPA-LA:* Table 6.5-5. *DTN:* MO0702PAFARDAT.001_R3 [DIRS 182578]. *References: Redistribution of Tephra and Waste by Geomorphic Processes Following a Potential Volcanic Eruption at Yucca Mountain, Nevada* (SNL 2007 [DIRS 179347], Sections 6.5.8.2, 6.6.2 and 7.1.3; Tables 6.4-1, 6.5.8-2 and 6.6.2-1).

Table K3-3. Detailed Summary of Epistemically Uncertain Variables (i.e., elements of **e**) Considered in the TSPA-LA (TSPA Parameter Name) (Continued)

NOTE: * indicates variable not considered in sensitivity analysis due to correlations.

D_Divides_a. Diffusivity of radionuclides in divides of the Fortymile Wash fan (RMEI location) (cm^2/yr). *Distribution:* Uniform. *Range:* 0.001 to 0.095. *Mean* 0.048. *Symbol:* D_d. *Additional Information:* The uncertainty distribution for this parameter is based on measured ^{137}Cs profiles from interchannel divides (assumed to be older than 10,000 yr) on the upper Fortymile Wash alluvial fan. The diffusivity model is used to calculate the waste concentration profile over time in the RMEI domain. As the diffusivity parameter increases, the rate of diffusion into the soil increases, decreasing the near surface contamination (and thus the calculated dose) at a more rapid rate. Capturing the low end of the diffusivity range is thus critical to assure reasonable and conservative results. *Sensitivity Name:* DDIVIDE. *Location in TSPA-LA:* Table 6.5-5. *DTN:* MO0702PAFARDAT.001_R3 [DIRS 182578]. *References: Redistribution of Tephra and Waste by Geomorphic Processes Following a Potential Volcanic Eruption at Yucca Mountain, Nevada* (SNL 2007 [DIRS 179347], Sections 6.5.8.1, 6.6.2 and 7.1.3; Tables 6.4-1, 6.5.8-1 and 6.6.2-1).
Dash_mean_a. Mass median ash particle diameter (cm). *Distribution:* Log triangular. *Range:* 0.001 to 0.1. *Mode:* 0.01. *Symbol:* d. *Additional Information:* The ash particle diameter is defined within the ASHPLUME model by two parameters: the mean ash particle diameter and the ash particle diameter standard deviation. The mode honors the frequency of values near this value in samples from Lathrop Wells volcano, while the tails honor the variability in mean grain size observed at historical violent Strombolian eruptions. The size distribution of ash particles transported by the ASHPLUME code is generally much larger than the particle size used to calculate the inhalation BDCFs. Tephra concentrations show strong sensitivity (factor of 35) to mean ash particle diameter, and fuel concentrations show small sensitivity (factor of 2) to two orders of magnitude variation in mean ash particle diameter. *Sensitivity Name:* DASHAVG. *Location in TSPA-LA:* Table 6.5-4. *DTN:* LA0702PADE03GK.002_R1 [DIRS 179980]. *References: Atmospheric Dispersal and Deposition of Tephra from a Potential Volcanic Eruption at Yucca Mountain, Nevada* (SNL 2007 [DIRS 177431], Sections 6.5.2.4, 7.2, 7.7 and Appendix C; Tables 4-1, 6-3, 8-2 and C-3; Figure C-2).
Dash_sigma_a. Ash particle diameter standard deviation (log (cm)). *Distribution:* Uniform. *Range:* 0.301 to 0.903. *Symbol:* σ_d. *Additional Information:* The ash particle diameter is defined within the ASHPLUME model by two parameters: the mean ash particle diameter and the ash particle diameter standard deviation. The upper and lower bounds of the range were chosen based on scientific judgment to bracket the sparse observations, and the uniform distribution reflects sparseness of the data and the equal likelihood of any value within the range. *Sensitivity Name:* DASHSIG. *Location in TSPA-LA:* Table 6.5-4. *DTN:* LA0702PADE03GK.002_R1 [DIRS 179980]. *References:* Atmospheric Dispersal and Deposition of Tephra from a Potential Volcanic Eruption at Yucca Mountain, Nevada (MDL-MGR-GS-000002 REV 03, SNL 2007 [DIRS 177431], Section 6.5.2.5, 7.2 and Appendix C; Tables 4-1, 6-3, 8-2 and C-4; Figure C-3).
DCVO. Logarithm of effective diffusion coefficient in fractured volcanic units (m^2/s). *Distribution:* Piecewise uniform. *Range:* -11.3 to -9.3. *Symbol:* D_e. *Additional Information:* The uncertain input parameters influencing matrix diffusion include effective diffusion coefficient (DCVO), flowing interval spacing (FISVO), and flowing interval porosity (FPVO). For the SZ 1-D transport model the matrix diffusion coefficient for those radionuclides that do experience matrix diffusion is implemented by calculating an effective tortuosity, based on the sampled value of effective diffusion coefficient and the free water diffusion coefficient. To treat the one- and three-dimensional transport through the SZ consistently, the sampled values used to generate the saturated zone breakthrough curves are also used in the TSPA-LA Model. These values are tabulated as 200 sets of values for the SZ parameters, accounting for appropriate correletions, and are entered into the TSPA model as a table of 200 values for each parameter. The TSPA-LA Model selects values from this table using the Goldsim variable SZ_index_a. *Sensitivity Name:* SZDIFCVO. *Location in TSPA-LA:* Sections 6.3.10.2 and 6.3.10.5; Table 6.3.10-2. *DTN:* SN0702PASZFTMA.002_R1 [DIRS 183471]. *References: Saturated Zone Flow and Transport Model Abstraction* (SNL 2008 [DIRS 183750], Section 6.5.2.6; Tables 6-8, B-1, 7-1[a], A-1[a], B-2[a],; Equations 6-15 and 6-17; Figures 6-14 and 6-15).
DE_BDCF_IER_Ra226_Pb210. Volcanic Biosphere Dose Conversion Factor (BDCF) component for radon, external exposure and ingestion of ^{226}Ra and ^{210}Pb in modern interglacial climate ((Sv/yr)/(Bq/m^2)). *Distribution:* Discrete. *Range:* 3.07E-08 to 9.43E-08. *Mean:* 3.52E-08. *Standard Deviation:* 3.45E-09. *Symbol:* $BDCF_{ext,ing,Rn,i}$. *Additional Information:* See DE_BDCF_Inh_LT_Ac227. *Sensitivity Name:* INGRA226. *Location in TSPA-LA:* Sections 6.3.11.1 and 6.3.11.2; Equation 6.3.11-4. *DTN:* MO0702PAVBPDCF.000_R0 [DIRS 179330]. *References: Biosphere Model Report* SNL 2007 [DIRS 177399], Sections 6.12.2 and 6.12.3; Table 6.12-4; Equation 6.12-1).

Table K3-3. Detailed Summary of Epistemically Uncertain Variables (i.e., elements of **e**) Considered in the TSPA-LA (TSPA Parameter Name) (Continued)

NOTE: * indicates variable not considered in sensitivity analysis due to correlations.

DE_BDCF_ILT_Ra226_Pb210. Volcanic Biosphere Dose Conversion Factor (BDCF) component for long-term inhalation of ^{226}Ra and ^{210}Pb in modern interglacial climate ((Sv/yr)/(Bq/kg)). *Distribution:* Discrete. *Range:* 1.71E-08 to 5.03E-07. *Mean:* 1.01E-07. *Standard Deviation:* 6.43E-08. *Symbol:* $BDCF_{inh,p,i}$. *Additional Information:* See DE_BDCF_Inh_LT_Ac227. *Sensitivity Name:* ILTRA226. *Location in TSPA-LA:* Sections 6.3.11.1 and 6.3.11.2; Equation 6.3.11-4. *DTN:* MO0702PAVBPDCF.000_R0 [DIRS 179330]. *References: Biosphere Model Report* (SNL 2007 [DIRS 177399], Sections 6.12.2 and 6.12.3; Table 6.12-3; Equation 6.12-1).
DE_BDCF_Ing_Exp_Radon_Ac227. Volcanic Biosphere Dose Conversion Factor (BDCF) component for radon, external exposure and ingestion of ^{227}Ac in modern interglacial climate ((Sv/yr)/(Bq/m^2)). *Distribution:* Discrete. *Range:* 5.78E-09 to 7.76E-09. *Mean:* 6.16E-09. *Standard Deviation:* 1.8E-10. *Symbol:* $BDCF_{ext,ing,Rn,i}$. *Additional Information:* See DE_BDCF_Inh_LT_Ac227. *Sensitivity Name:* INGAC227. *Location in TSPA-LA:* Sections 6.3.11.1 and 6.3.11.2; Equation 6.3.11-4. *DTN:* MO0702PAVBPDCF.000_R0 [DIRS 179330]. *References: Biosphere Model Report* (MDL-MGR-MD-000001, SNL 2007 [DIRS 177399], Sections 6.12.2 and 6.12.3; Table 6.12-4; Equation 6.12-1).
DE_BDCF_Ing_Exp_Radon_Am241. Volcanic Biosphere Dose Conversion Factor (BDCF) component for radon, external exposure and ingestion of ^{241}Am in modern interglacial climate ((Sv/yr)/(Bq/m^2)). *Distribution:* Discrete. *Range:* 1.86E-10 to 1.00E-09. *Mean:* 2.51E-10. *Standard Deviation:* 7.00E-11. *Symbol:* $BDCF_{ext,ing,Rn,i}$. *Additional Information:* See DE_BDCF_Inh_LT_Ac227. *Sensitivity Name:* INGAM241. *Location in TSPA-LA:* Sections 6.3.11.1 and 6.3.11.2; Equation 6.3.11-4. *DTN:* MO0702PAVBPDCF.000_R0 [DIRS 179330]. *References: Biosphere Model Report* (MDL-MGR-MD-000001, SNL 2007 [DIRS 177399], Sections 6.12.2 and 6.12.3; Table 6.12-4; Equation 6.12-1).
DE_BDCF_Ing_Exp_Radon_Am243. Volcanic Biosphere Dose Conversion Factor (BDCF) component for radon, external exposure and ingestion of ^{243}Am in modern interglacial climate ((Sv/yr)/(Bq/m^2)). *Distribution:* Discrete. *Range:* 2.51E-09 to 3.42E-09. *Mean:* 2.67E-09. *Standard Deviation:* 8.02E-11. *Symbol:* $BDCF_{ext,ing,Rn,i}$. *Additional Information:* See DE_BDCF_Inh_LT_Ac227. *Sensitivity Name:* INGAM243. *Location in TSPA-LA:* Sections 6.3.11.1 and 6.3.11.2; Equation 6.3.11-4. *DTN:* MO0702PAVBPDCF.000_R0 [DIRS 179330]. *References: Biosphere Model Report* (SNL 2007 [DIRS 177399], Sections 6.12.2 and 6.12.3; Table 6.12-4; Equation 6.12-1).
DE_BDCF_Ing_Exp_Radon_Cs137. Volcanic Biosphere Dose Conversion Factor (BDCF) component for radon, external exposure and ingestion of ^{137}Cs in modern interglacial climate ((Sv/yr)/(Bq/m^2)). *Distribution:* Discrete. *Range:* 6.75E-09 to 8.48E-09. *Mean:* 7.17E-09. *Standard Deviation:* 1.55E-10. *Symbol:* $BDCF_{ext,ing,Rn,i}$. *Additional Information:* See DE_BDCF_Inh_LT_Ac227. *Sensitivity Name:* INGCS137. *Location in TSPA-LA:* Sections 6.3.11.1 and 6.3.11.2; Equation 6.3.11-4. *DTN:* MO0702PAVBPDCF.000_R0 [DIRS 179330]. *References: Biosphere Model Report* (SNL 2007 [DIRS 177399], Sections 6.12.2 and 6.12.3; Table 6.12-4; Equation 6.12-1).
DE_BDCF_Ing_Exp_Radon_I129. Volcanic Biosphere Dose Conversion Factor (BDCF) component for radon, external exposure and ingestion of ^{129}I in modern interglacial climate ((Sv/yr)/(Bq/m^2)). *Distribution:* Discrete. *Range:* 1.39E-10 to 2.86E-08. *Mean:* 1.26E-09. *Standard Deviation:* 2.59E-09. *Symbol:* $BDCF_{ext,ing,Rn,i}$. *Additional Information:* See DE_BDCF_Inh_LT_Ac227. *Sensitivity Name:* INGI129. *Location in TSPA-LA:* Sections 6.3.11.1 and 6.3.11.2; Equation 6.3.11-4. *DTN:* MO0702PAVBPDCF.000_R0 [DIRS 179330]. *References: Biosphere Model Report* (SNL 2007 [DIRS 177399], Sections 6.12.2 and 6.12.3; Table 6.12-4; Equation 6.12-1).
DE_BDCF_Ing_Exp_Radon_Np237. Volcanic Biosphere Dose Conversion Factor (BDCF) component for radon, external exposure and ingestion of ^{237}Np in modern interglacial climate ((Sv/yr)/(Bq/m^2)). *Distribution:* Discrete. *Range:* 2.62E-09 to 1.2E-08. *Mean:* 2.98E-09. *Standard Deviation:* 6.36E-10. *Symbol:* $BDCF_{ext,ing,Rn,i}$. *Additional Information:* See DE_BDCF_Inh_LT_Ac227. *Sensitivity Name:* INGNP237. *Location in TSPA-LA:* Sections 6.3.11.1 and 6.3.11.2; Equation 6.3.11-4. *DTN:* MO0702PAVBPDCF.000_R0 [DIRS 179330]. *References: Biosphere Model Report* (SNL 2007 [DIRS 177399], Sections 6.12.2 and 6.12.3; Table 6.12-4; Equation 6.12-1).
DE_BDCF_Ing_Exp_Radon_Pa231. Volcanic Biosphere Dose Conversion Factor (BDCF) component for radon, external exposure and ingestion of ^{231}Pa in modern interglacial climate ((Sv/yr)/(Bq/m^2)). *Distribution:* Discrete. *Range:* 5.02E-10 to 4.56E-09. *Mean:* 7.14E-10. *Standard Deviation:* 2.92E-10. *Symbol:* $BDCF_{ext,ing,Rn,i}$. *Additional Information:* See DE_BDCF_Inh_LT_Ac227. *Sensitivity Name:* INGPA231. *Location in TSPA-LA:* Sections 6.3.11.1 and 6.3.11.2; Equation 6.3.11-4. *DTN:* MO0702PAVBPDCF.000_R0 [DIRS 179330]. *References: Biosphere Model Report* (SNL 2007 [DIRS 177399], Sections 6.12.2 and 6.12.3; Table 6.12-4; Equation 6.12-1).

Table K3-3. Detailed Summary of Epistemically Uncertain Variables (i.e., elements of **e**) Considered in the TSPA-LA (TSPA Parameter Name) (Continued)

NOTE: * indicates variable not considered in sensitivity analysis due to correlations.

DE_BDCF_Ing_Exp_Radon_Pu238. Volcanic Biosphere Dose Conversion Factor (BDCF) component for radon, external exposure and ingestion of ^{238}Pu in modern interglacial climate ((Sv/yr)/(Bq/m^2)). *Distribution:* Discrete. *Range:* 1.33E-11 to 9.18E-10. *Mean:* 7.78E-11. *Standard Deviation:* 7.72E-11. *Symbol:* $BDCF_{ext,ing,Rn,i}$. *Additional Information:* See DE_BDCF_Inh_LT_Ac227. *Sensitivity Name:* INGPU238. *Location in TSPA-LA:* Sections 6.3.11.1 and 6.3.11.2; Equation 6.3.11-4. *DTN:* MO0702PAVBPDCF.000_R0 [DIRS 179330]. *References: Biosphere Model Report* (SNL 2007 [DIRS 177399], Sections 6.12.2 and 6.12.3; Table 6.12-4; Equation 6.12-1).
DE_BDCF_Ing_Exp_Radon_Pu239. Volcanic Biosphere Dose Conversion Factor (BDCF) component for radon, external exposure and ingestion of ^{239}Pu in modern interglacial climate ((Sv/yr)/(Bq/m^2)). *Distribution:* Discrete. *Range:* 1.40E-11 to 1.01E-09. *Mean:* 8.49E-11. *Standard Deviation:* 8.5E-11. *Symbol:* $BDCF_{ext,ing,Rn,i}$. *Additional Information:* See DE_BDCF_Inh_LT_Ac227. *Sensitivity Name:* INGPU239. *Location in TSPA-LA:* Sections 6.3.11.1 and 6.3.11.2; Equation 6.3.11-4. *DTN:* MO0702PAVBPDCF.000_R0 [DIRS 179330]. *References: Biosphere Model Report* (SNL 2007 [DIRS 177399], Sections 6.12.2 and 6.12.3; Table 6.12-4; Equation 6.12-1).
DE_BDCF_Ing_Exp_Radon_Pu240. Volcanic Biosphere Dose Conversion Factor (BDCF) component for radon, external exposure and ingestion of ^{240}Pu in modern interglacial climate ((Sv/yr)/(Bq/m^2)). *Distribution:* Discrete. *Range:* 1.42E-11 to 1.01E-09. *Mean:* 8.52E-11. *Standard Deviation:* 8.5E-11. *Symbol:* $BDCF_{ext,ing,Rn,i}$. *Additional Information:* See DE_BDCF_Inh_LT_Ac227. *Sensitivity Name:* INGPU240. *Location in TSPA-LA:* Sections 6.3.11.1 and 6.3.11.2; Equation 6.3.11-4. *DTN:* MO0702PAVBPDCF.000_R0 [DIRS 179330]. *References: Biosphere Model Report* (SNL 2007 [DIRS 177399], Sections 6.12.2 and 6.12.3; Table 6.12-4; Equation 6.12-1).
DE_BDCF_Ing_Exp_Radon_Pu242. Volcanic Biosphere Dose Conversion Factor (BDCF) component for radon, external exposure and ingestion of ^{242}Pu in modern interglacial climate ((Sv/yr)/(Bq/m^2)). *Distribution:* Discrete. *Range:* 1.31E-11 to 9.57E-10. *Mean:* 8.04E-11. *Standard Deviation:* 8.06E-11. *Symbol:* $BDCF_{ext,ing,Rn,i}$. *Additional Information:* See DE_BDCF_Inh_LT_Ac227. *Sensitivity Name:* INGPU242. *Location in TSPA-LA:* Sections 6.3.11.1 and 6.3.11.2; Equation 6.3.11-4. *DTN:* MO0702PAVBPDCF.000_R0 [DIRS 179330]. *References: Biosphere Model Report* (SNL 2007 [DIRS 177399], Sections 6.12.2 and 6.12.3; Table 6.12-4; Equation 6.12-1).
DE_BDCF_Ing_Exp_Radon_Ra228. Volcanic Biosphere Dose Conversion Factor (BDCF) component for radon, external exposure and ingestion of ^{228}Ra in modern interglacial climate ((Sv/yr)/(Bq/m^2)). *Distribution:* Discrete. *Range:* 1.17E-08 to 2.62E-08. *Mean:* 1.27E-08. *Standard Deviation:* 7.44E-10. *Symbol:* $BDCF_{ext,ing,Rn,i}$. *Additional Information:* See DE_BDCF_Inh_LT_Ac227. *Sensitivity Name:* INGRA228. *Location in TSPA-LA:* Sections 6.3.11.1 and 6.3.11.2; Equation 6.3.11-4. *DTN:* MO0702PAVBPDCF.000_R0 [DIRS 179330]. *References: Biosphere Model Report* (SNL 2007 [DIRS 177399], Sections 6.12.2 and 6.12.3; Table 6.12-4; Equation 6.12-1).
DE_BDCF_Ing_Exp_Radon_Sn126. Volcanic Biosphere Dose Conversion Factor (BDCF) component for radon, external exposure and ingestion of ^{126}Sn in modern interglacial climate ((Sv/yr)/(Bq/m^2)). *Distribution:* Discrete. *Range:* 2.38E-08 to 2.79E-08. *Mean:* 2.54E-08. *Standard Deviation:* 4.41E-10. *Symbol:* $BDCF_{ext,ing,Rn,i}$. *Additional Information:* See DE_BDCF_Inh_LT_Ac227. *Sensitivity Name:* INGSN126. *Location in TSPA-LA:* Sections 6.3.11.1 and 6.3.11.2; Equation 6.3.11-4. *DTN:* MO0702PAVBPDCF.000_R0 [DIRS 179330]. *References: Biosphere Model Report* (SNL 2007 [DIRS 177399], Sections 6.12.2 and 6.12.3; Table 6.12-4; Equation 6.12-1).
DE_BDCF_Ing_Exp_Radon_Sr90. Volcanic Biosphere Dose Conversion Factor (BDCF) component for radon, external exposure and ingestion of ^{90}Sr in modern interglacial climate ((Sv/yr)/(Bq/m^2)). *Distribution:* Discrete. *Range:* 1.44E-09 to 6.10E-09. *Mean:* 1.81E-09. *Standard Deviation:* 3.67E-10. *Symbol:* $BDCF_{ext,ing,Rn,i}$. *Additional Information:* See DE_BDCF_Inh_LT_Ac227. *Sensitivity Name:* INGSR90. *Location in TSPA-LA:* Sections 6.3.11.1 and 6.3.11.2; Equation 6.3.11-4. *DTN:* MO0702PAVBPDCF.000_R0 [DIRS 179330]. *References: Biosphere Model Report* (SNL 2007 [DIRS 177399], Sections 6.12.2 and 6.12.3; Table 6.12-4; Equation 6.12-1).
DE_BDCF_Ing_Exp_Radon_Tc99. Volcanic Biosphere Dose Conversion Factor (BDCF) component for radon, external exposure and ingestion of ^{99}Tc in modern interglacial climate ((Sv/yr)/(Bq/m^2)). *Distribution:* Discrete. *Range:* 5.08E-12 to 8.95E-09. *Mean:* 2.72E-10. *Standard Deviation:* 5.16E-10. *Symbol:* $BDCF_{ext,ing,Rn,i}$. *Additional Information:* See DE_BDCF_Inh_LT_Ac227. *Sensitivity Name:* INGTC99. *Location in TSPA-LA:* Sections 6.3.11.1 and 6.3.11.2; Equation 6.3.11-4. *DTN:* MO0702PAVBPDCF.000_R0 [DIRS 179330]. *References: Biosphere Model Report* (SNL 2007 [DIRS 177399], Sections 6.12.2 and 6.12.3; Table 6.12-4; Equation 6.12-1).
DE_BDCF_Ing_Exp_Radon_Th229. Volcanic Biosphere Dose Conversion Factor (BDCF) component for radon, external exposure and ingestion of ^{229}Th in modern interglacial climate ((Sv/yr)/(Bq/m^2)). *Distribution:* Discrete. *Range:* 4.33E-09 to 7.02E-09. *Mean:* 4.69E-09. *Standard Deviation:* 2.4E-10. *Symbol:* $BDCF_{ext,ing,Rn,i}$. *Additional Information:* See DE_BDCF_Inh_LT_Ac227. *Sensitivity Name:* INGTH229. *Location in TSPA-LA:* Sections 6.3.11.1 and 6.3.11.2; Equation 6.3.11-4. *DTN:* MO0702PAVBPDCF.000_R0 [DIRS 179330]. *References: Biosphere Model Report* (SNL 2007 [DIRS 177399], Sections 6.12.2 and 6.12.3; Table 6.12-4; Equation 6.12-1).

Table K3-3. Detailed Summary of Epistemically Uncertain Variables (i.e., elements of **e**) Considered in the TSPA-LA (TSPA Parameter Name) (Continued)

NOTE: * indicates variable not considered in sensitivity analysis due to correlations.

DE_BDCF_Ing_Exp_Radon_Th230. Volcanic Biosphere Dose Conversion Factor (BDCF) component for radon, external exposure and ingestion of ^{230}Th in modern interglacial climate ((Sv/yr)/(Bq/m^2)). *Distribution:* Discrete. *Range:* 1.92E-11 to 8.68E-10. *Mean:* 8.51E-11. *Standard Deviation:* 7.82E-11. *Symbol:* $BDCF_{ext,ing,Rn,i}$. *Additional Information:* See DE_BDCF_Inh_LT_Ac227. *Sensitivity Name:* INGTH230. *Location in TSPA-LA:* Sections 6.3.11.1 and 6.3.11.2; Equation 6.3.11-4. *DTN:* MO0702PAVBPDCF.000_R0 [DIRS 179330]. *References: Biosphere Model Report* (SNL 2007 [DIRS 177399], Sections 6.12.2 and 6.12.3; Table 6.12-4; Equation 6.12-1).
DE_BDCF_Ing_Exp_Radon_Th232. Volcanic Biosphere Dose Conversion Factor (BDCF) component for radon, external exposure and ingestion of ^{232}Th in modern interglacial climate ((Sv/yr)/(Bq/m^2)). *Distribution:* Discrete. *Range:* 1.72E-11 to 9.34E-10. *Mean:* 8.83E-11. *Standard Deviation:* 8.44E-11. *Symbol:* $BDCF_{ext,ing,Rn,i}$. *Additional Information:* See DE_BDCF_Inh_LT_Ac227. *Sensitivity Name:* INGTH232. *Location in TSPA-LA:* Sections 6.3.11.1 and 6.3.11.2; Equation 6.3.11-4. *DTN:* MO0702PAVBPDCF.000_R0 [DIRS 179330]. *References: Biosphere Model Report* (MDL-MGR-MD-000001, SNL 2007 [DIRS 177399], Sections 6.12.2 and 6.12.3; Table 6.12-4; Equation 6.12-1).
DE_BDCF_Ing_Exp_Radon_U233. Volcanic Biosphere Dose Conversion Factor (BDCF) component for radon, external exposure and ingestion of ^{233}U in modern interglacial climate ((Sv/yr)/(Bq/m^2)). *Distribution:* Discrete. *Range:* 1.31E-11 to 9.04E-10. *Mean:* 6.48E-11. *Standard Deviation:* 6.12E-11. *Symbol:* $BDCF_{ext,ing,Rn,i}$. *Additional Information:* See DE_BDCF_Inh_LT_Ac227. *Sensitivity Name:* INGU233. *Location in TSPA-LA:* Sections 6.3.11.1 and 6.3.11.2; Equation 6.3.11-4. *DTN:* MO0702PAVBPDCF.000_R0 [DIRS 179330]. *References: Biosphere Model Report* (MDL-MGR-MD-000001, SNL 2007 [DIRS 177399], Sections 6.12.2 and 6.12.3; Table 6.12-4; Equation 6.12-1).
DE_BDCF_Ing_Exp_Radon_U234. Volcanic Biosphere Dose Conversion Factor (BDCF) component for radon, external exposure and ingestion of ^{234}U in modern interglacial climate ((Sv/yr)/(Bq/m^2)). *Distribution:* Discrete. *Range:* 9.60E-12 to 8.7E-10. *Mean:* 5.96E-11. *Standard Deviation:* 5.9E-11. *Symbol:* $BDCF_{ext,ing,Rn,i}$. *Additional Information:* See DE_BDCF_Inh_LT_Ac227. *Sensitivity Name:* INGU234. *Location in TSPA-LA:* Sections 6.3.11.1 and 6.3.11.2; Equation 6.3.11-4. *DTN:* MO0702PAVBPDCF.000_R0 [DIRS 179330]. *References: Biosphere Model Report* (MDL-MGR-MD-000001, SNL 2007 [DIRS 177399], Sections 6.12.2 and 6.12.3; Table 6.12-4; Equation 6.12-1).
DE_BDCF_Ing_Exp_Radon_U238. Volcanic Biosphere Dose Conversion Factor (BDCF) component for radon, external exposure and ingestion of ^{238}U in modern interglacial climate ((Sv/yr)/(Bq/m^2)). *Distribution:* Discrete. *Range:* 1.52E-09 to 2.41E-09. *Mean:* 1.62E-09. *Standard Deviation:* 6.16E-11. *Symbol:* $BDCF_{ext,ing,Rn,i}$. *Additional Information:* See DE_BDCF_Inh_LT_Ac227. *Sensitivity Name:* INGU238. *Location in TSPA-LA:* Sections 6.3.11.1 and 6.3.11.2; Equation 6.3.11-4. *DTN:* MO0702PAVBPDCF.000_R0 [DIRS 179330]. *References: Biosphere Model Report* (MDL-MGR-MD-000001, SNL 2007 [DIRS 177399], Sections 6.12.2 and 6.12.3; Table 6.12-4; Equation 6.12-1).

Table K3-3. Detailed Summary of Epistemically Uncertain Variables (i.e., elements of **e**) Considered in the TSPA-LA (TSPA Parameter Name) (Continued)

NOTE: * indicates variable not considered in sensitivity analysis due to correlations.

DE_BDCF_Inh_LT_Ac227. Volcanic Biosphere Dose Conversion Factor (BDCF) component for long-term inhalation of ^{227}Ac in modern interglacial climate ((Sv/yr)/(Bq/kg)). *Distribution:* Discrete. *Range:* 1.53E-07 to 4.5E-06. *Mean:* 9.0E-07. *Standard Deviation:* 5.75E-07. *Symbol:* $BDCF_{inh,p,i}$. *Additional Information:* Volcanic BDCFs consist of three BDCF components for each primary radionuclide. The first component, called the ingestion component, $BDCF_{ext,ing,Rn,i}$, accounts for exposure to sources external to the body, ingestion, and inhalation of radon decay products. This component is numerically equal to the annual dose to the RMEI from these exposure pathways per unit of areal radionuclide concentration in the soil (Sv/yr per Bq/m^2). The second and third BDCF components, called the short-term and the long-term inhalation BDCF components, account for inhaling airborne particulates. The short-term inhalation component, $BDCF_{inh,v,i}$, is numerically equal to the early-time increase in inhalation dose (over and above the long-term inhalation dose described by the long-term inhalation BDCF component) during the first year following a volcanic eruption per unit of radionuclide concentration in the soil layer that can become resuspended (Sv/yr per Bq/kg). This term is used together with the time function, representing the decrease of the airborne particulate concentration with time, to calculate short-term increase in inhalation exposure due to elevated levels of airborne particulate matter after a volcanic eruption, relative to the conditions existing before and long after an eruption. With time, mass loading returns to the pre-eruption level. These exposure conditions are described by the long-term inhalation BDCF, $BDCF_{inh,p,i}$, which accounts for inhalation of resuspended particulates under nominal conditions, i.e., when the mass loading is not elevated as the result of volcanic eruption. This component is numerically equal to the annual dose to the RMEI from inhaling particulates at the nominal concentration in the air, per unit of radionuclide concentration in the soil that can be resuspended (Sv/yr per Bq/kg). To account for correlations between parameters used to compute BDCFs, the Biosphere Model generates a table of 1,000 sets of values for each BDCF. These values are entered into the TSPA Input Database as a table of 1,000 values for each parameter. The TSPA-LA Model selects values from this table using the Goldsim variable Bio_index_a. *Sensitivity Name:* ILTAC227. *Location in TSPA-LA:* Sections 6.3.11.1 and 6.3.11.2; Equation 6.3.11-4. *DTN:* MO0702PAVBPDCF.000_R0 [DIRS 179330]. *References: Biosphere Model Report* (MDL-MGR-MD-000001, SNL 2007 [DIRS 177399], Sections 6.12.2 and 6.12.3; Table 6.12-3; Equation 6.12-1).
DE_BDCF_Inh_LT_Am241. Volcanic Biosphere Dose Conversion Factor (BDCF) component for long-term inhalation of ^{241}Am in modern interglacial climate ((Sv/yr)/(Bq/kg)). *Distribution:* Discrete. *Range:* 8.45E-08 to 2.48E-06. *Mean:* 4.96E-07. *Standard Deviation:* 3.17E-07. *Symbol:* $BDCF_{inh,p,i}$. *Additional Information:* See DE_BDCF_Inh_LT_Ac227. *Sensitivity Name:* ILTAM241. *Location in TSPA-LA:* Sections 6.3.11.1 and 6.3.11.2; Equation 6.3.11-4. *DTN:* MO0702PAVBPDCF.000_R0 [DIRS 179330]. *References: Biosphere Model Report* (MDL-MGR-MD-000001, SNL 2007 [DIRS 177399], Sections 6.12.2 and 6.12.3; Table 6.12-3; Equation 6.12-1).
DE_BDCF_Inh_LT_Am243. Volcanic Biosphere Dose Conversion Factor (BDCF) component for long-term inhalation of ^{243}Am in modern interglacial climate ((Sv/yr)/(Bq/kg)). *Distribution:* Discrete. *Range:* 8.38E-08 to 2.46E-06. *Mean:* 4.93E-07. *Standard Deviation:* 3.15E-07. *Symbol:* $BDCF_{inh,p,i}$. *Additional Information:* See DE_BDCF_Inh_LT_Ac227. *Sensitivity Name:* ILTAM243. *Location in TSPA-LA:* Sections 6.3.11.1 and 6.3.11.2; Equation 6.3.11-4. *DTN:* MO0702PAVBPDCF.000_R0 [DIRS 179330]. *References: Biosphere Model Report* (SNL 2007 [DIRS 177399], Sections 6.12.2 and 6.12.3; Table 6.12-3; Equation 6.12-1).
DE_BDCF_Inh_LT_Cs137. Volcanic Biosphere Dose Conversion Factor (BDCF) component for long-term inhalation of ^{137}Cs in modern interglacial climate ((Sv/yr)/(Bq/kg)). *Distribution:* Discrete. *Range:* 3.43E-11 to 1.01E-09. *Mean:* 2.02E-10. *Standard Deviation:* 1.29E-10. *Symbol:* $BDCF_{inh,p,i}$. *Additional Information:* See DE_BDCF_Inh_LT_Ac227. *Sensitivity Name:* ILTCS137. *Location in TSPA-LA:* Sections 6.3.11.1 and 6.3.11.2; Equation 6.3.11-4. *DTN:* MO0702PAVBPDCF.000_R0 [DIRS 179330]. *References: Biosphere Model Report* (SNL 2007 [DIRS 177399], Sections 6.12.2 and 6.12.3; Table 6.12-3; Equation 6.12-1).
DE_BDCF_Inh_LT_I129. Volcanic Biosphere Dose Conversion Factor (BDCF) component for long-term inhalation of ^{129}I in modern interglacial climate ((Sv/yr)/(Bq/kg)). *Distribution:* Discrete. *Range:* 3.15E-11 to 9.23E-10. *Mean:* 1.85E-10. *Standard Deviation:* 1.18E-10. *Symbol:* $BDCF_{inh,p,i}$. *Additional Information:* See DE_BDCF_Inh_LT_Ac227. *Sensitivity Name:* ILTI129. *Location in TSPA-LA:* Sections 6.3.11.1 and 6.3.11.2; Equation 6.3.11-4. *DTN:* MO0702PAVBPDCF.000_R0 [DIRS 179330]. *References: Biosphere Model Report* (SNL 2007 [DIRS 177399], Sections 6.12.2 and 6.12.3; Table 6.12-3; Equation 6.12-1).
DE_BDCF_Inh_LT_Np237. Volcanic Biosphere Dose Conversion Factor (BDCF) component for long-term inhalation of ^{237}Np in modern interglacial climate ((Sv/yr)/(Bq/kg)). *Distribution:* Discrete. *Range:* 4.35E-08 to 1.28E-06. *Mean:* 2.56E-07. *Standard Deviation:* 1.63E-07. *Symbol:* $BDCF_{inh,p,i}$. *Additional Information:* See DE_BDCF_Inh_LT_Ac227. *Sensitivity Name:* ILTNP237. *Location in TSPA-LA:* Sections 6.3.11.1 and 6.3.11.2; Equation 6.3.11-4. *DTN:* MO0702PAVBPDCF.000_R0 [DIRS 179330]. *References: Biosphere Model Report* (SNL 2007 [DIRS 177399], Sections 6.12.2 and 6.12.3; Table 6.12-3; Equation 6.12-1).

Table K3-3. Detailed Summary of Epistemically Uncertain Variables (i.e., elements of **e**) Considered in the TSPA-LA (TSPA Parameter Name) (Continued)

NOTE: * indicates variable not considered in sensitivity analysis due to correlations.

DE_BDCF_Inh_LT_Pa231. Volcanic Biosphere Dose Conversion Factor (BDCF) component for long-term inhalation of ^{231}Pa in modern interglacial climate ((Sv/yr)/(Bq/kg)). *Distribution:* Discrete. *Range:* 2.02E-07 to 5.92E-06. *Mean:* 1.18E-06. *Standard Deviation:* 7.56E-07. *Symbol:* $BDCF_{inh,p,i}$. *Additional Information:* See DE_BDCF_Inh_LT_Ac227. *Sensitivity Name:* ILTPA231. *Location in TSPA-LA:* Sections 6.3.11.1 and 6.3.11.2; Equation 6.3.11-4. *DTN:* MO0702PAVBPDCF.000_R0 [DIRS 179330]. *References: Biosphere Model Report* (SNL 2007 [DIRS 177399], Sections 6.12.2 and 6.12.3; Table 6.12-3; Equation 6.12-1).
DE_BDCF_Inh_LT_Pu238. Volcanic Biosphere Dose Conversion Factor (BDCF) component for long-term inhalation of ^{238}Pu in modern interglacial climate ((Sv/yr)/(Bq/kg)). *Distribution:* Discrete. *Range:* 9.46E-08 to 2.78E-06. *Mean:* 5.56E-07. *Standard Deviation:* 3.55E-07. *Symbol:* $BDCF_{inh,p,i}$. *Additional Information:* See DE_BDCF_Inh_LT_Ac227. *Sensitivity Name:* ILTPU238. *Location in TSPA-LA:* Sections 6.3.11.1 and 6.3.11.2; Equation 6.3.11-4. *DTN:* MO0702PAVBPDCF.000_R0 [DIRS 179330]. *References: Biosphere Model Report* (SNL 2007 [DIRS 177399], Sections 6.12.2 and 6.12.3; Table 6.12-3; Equation 6.12-1).
DE_BDCF_Inh_LT_Pu239. Volcanic Biosphere Dose Conversion Factor (BDCF) component for long-term inhalation of ^{239}Pu in modern interglacial climate ((Sv/yr)/(Bq/kg)). *Distribution:* Discrete. *Range:* 1.04E-07 to 3.06E-06. *Mean:* 6.12E-07. *Standard Deviation:* 3.91E-07. *Symbol:* $BDCF_{inh,p,i}$. *Additional Information:* See DE_BDCF_Inh_LT_Ac227. *Sensitivity Name:* ILTPU239. *Location in TSPA-LA:* Sections 6.3.11.1 and 6.3.11.2; Equation 6.3.11-4. *DTN:* MO0702PAVBPDCF.000_R0 [DIRS 179330]. *References: Biosphere Model Report* (SNL 2007 [DIRS 177399], Sections 6.12.2 and 6.12.3; Table 6.12-3; Equation 6.12-1).
DE_BDCF_Inh_LT_Pu240. Volcanic Biosphere Dose Conversion Factor (BDCF) component for long-term inhalation of ^{240}Pu in modern interglacial climate ((Sv/yr)/(Bq/kg)). *Distribution:* Discrete. *Range:* 1.04E-07 to 3.06E-06. *Mean:* 6.12E-07. *Standard Deviation:* 3.91E-07. *Symbol:* $BDCF_{inh,p,i}$. *Additional Information:* See DE_BDCF_Inh_LT_Ac227. *Sensitivity Name:* ILTPU240. *Location in TSPA-LA:* Sections 6.3.11.1 and 6.3.11.2; Equation 6.3.11-4. *DTN:* MO0702PAVBPDCF.000_R0 [DIRS 179330]. *References: Biosphere Model Report* (SNL 2007 [DIRS 177399], Sections 6.12.2 and 6.12.3; Table 6.12-3; Equation 6.12-1).
DE_BDCF_Inh_LT_Pu242. Volcanic Biosphere Dose Conversion Factor (BDCF) component for long-term inhalation of ^{242}Pu in modern interglacial climate ((Sv/yr)/(Bq/kg)). *Distribution:* Discrete. *Range:* 9.90E-08 to 2.91E-06. *Mean:* 5.82E-07. *Standard Deviation:* 3.72E-07. *Symbol:* $BDCF_{inh,p,i}$. *Additional Information:* See DE_BDCF_Inh_LT_Ac227. *Sensitivity Name:* ILTPU242. *Location in TSPA-LA:* Sections 6.3.11.1 and 6.3.11.2; Equation 6.3.11-4. *DTN:* MO0702PAVBPDCF.000_R0 [DIRS 179330]. *References: Biosphere Model Report* (SNL 2007 [DIRS 177399], Sections 6.12.2 and 6.12.3; Table 6.12-3; Equation 6.12-1).
DE_BDCF_Inh_LT_Ra228. Volcanic Biosphere Dose Conversion Factor (BDCF) component for long-term inhalation of ^{228}Ra in modern interglacial climate ((Sv/yr)/(Bq/kg)). *Distribution:* Discrete. *Range:* 1.40E-08 to 4.12E-07. *Mean:* 8.24E-08. *Standard Deviation:* 5.27E-08. *Symbol:* $BDCF_{inh,p,i}$. *Additional Information:* See DE_BDCF_Inh_LT_Ac227. *Sensitivity Name:* ILTRA228. *Location in TSPA-LA:* Sections 6.3.11.1 and 6.3.11.2; Equation 6.3.11-4. *DTN:* MO0702PAVBPDCF.000_R0 [DIRS 179330]. *References: Biosphere Model Report* (SNL 2007 [DIRS 177399], Sections 6.12.2 and 6.12.3; Table 6.12-3; Equation 6.12-1).
DE_BDCF_Inh_LT_Sn126. Volcanic Biosphere Dose Conversion Factor (BDCF) component for long-term inhalation of ^{126}Sn in modern interglacial climate ((Sv/yr)/(Bq/kg)). *Distribution:* Discrete. *Range:* 1.36E-10 to 4.00E-09. *Mean:* 8.0E-10. *Standard Deviation:* 5.11E-10. *Symbol:* $BDCF_{inh,p,i}$. *Additional Information:* See DE_BDCF_Inh_LT_Ac227. *Sensitivity Name:* ILTSN126. *Location in TSPA-LA:* Sections 6.3.11.1 and 6.3.11.2; Equation 6.3.11-4. *DTN:* MO0702PAVBPDCF.000_R0 [DIRS 179330]. *References: Biosphere Model Report* (SNL 2007 [DIRS 177399], Sections 6.12.2 and 6.12.3; Table 6.12-3; Equation 6.12-1).
DE_BDCF_Inh_LT_Sr90. Volcanic Biosphere Dose Conversion Factor (BDCF) component for long-term inhalation of ^{90}Sr in modern interglacial climate ((Sv/yr)/(Bq/kg)). *Distribution:* Discrete. *Range:* 1.39E-10 to 4.08E-09. *Mean:* 8.16E-10. *Standard Deviation:* 5.21E-10. *Symbol:* $BDCF_{inh,p,i}$. *Additional Information:* See DE_BDCF_Inh_LT_Ac227. *Sensitivity Name:* ILTSR90. *Location in TSPA-LA:* Sections 6.3.11.1 and 6.3.11.2; Equation 6.3.11-4. *DTN:* MO0702PAVBPDCF.000_R0 [DIRS 179330]. *References: Biosphere Model Report* (SNL 2007 [DIRS 177399], Sections 6.12.2 and 6.12.3; Table 6.12-3; Equation 6.12-1).
DE_BDCF_Inh_LT_Tc99. Volcanic Biosphere Dose Conversion Factor (BDCF) component for long-term inhalation of ^{99}Tc in modern interglacial climate ((Sv/yr)/(Bq/kg)). *Distribution:* Discrete. *Range:* 1.17E-11 to 3.42E-10. *Mean:* 6.84E-11. *Standard Deviation:* 4.37E-11. *Symbol:* $BDCF_{inh,p,i}$. *Additional Information:* See DE_BDCF_Inh_LT_Ac227. *Sensitivity Name:* ILTTC99. *Location in TSPA-LA:* Sections 6.3.11.1 and 6.3.11.2; Equation 6.3.11-4. *DTN:* MO0702PAVBPDCF.000_R0 [DIRS 179330]. *References: Biosphere Model Report* (SNL 2007 [DIRS 177399], Sections 6.12.2 and 6.12.3; Table 6.12-3; Equation 6.12-1).

Table K3-3. Detailed Summary of Epistemically Uncertain Variables (i.e., elements of **e**) Considered in the TSPA-LA (TSPA Parameter Name) (Continued)

NOTE: * indicates variable not considered in sensitivity analysis due to correlations.

DE_BDCF_Inh_LT_Th229. Volcanic Biosphere Dose Conversion Factor (BDCF) component for long-term inhalation of ^{229}Th in modern interglacial climate ((Sv/yr)/(Bq/kg)). *Distribution:* Discrete. *Range:* 2.24E-07 to 6.57E-06. *Mean:* 1.31E-06. *Standard Deviation:* 8.39E-07. *Symbol:* $BDCF_{inh,p,i}$. *Additional Information:* See DE_BDCF_Inh_LT_Ac227. *Sensitivity Name:* ILTTH229. *Location in TSPA-LA:* Sections 6.3.11.1 and 6.3.11.2; Equation 6.3.11-4. *DTN:* MO0702PAVBPDCF.000_R0 [DIRS 179330]. *References: Biosphere Model Report* (SNL 2007 [DIRS 177399], Sections 6.12.2 and 6.12.3; Table 6.12-3; Equation 6.12-1).
DE_BDCF_Inh_LT_Th230. Volcanic Biosphere Dose Conversion Factor (BDCF) component for long-term inhalation of ^{230}Th in modern interglacial climate ((Sv/yr)/(Bq/kg)). *Distribution:* Discrete. *Range:* 8.94E-08 to 2.62E-06. *Mean:* 5.25E-07. *Standard Deviation:* 3.35E-07. *Symbol:* $BDCF_{inh,p,i}$. *Additional Information:* See DE_BDCF_Inh_LT_Ac227. *Sensitivity Name:* ILTTH230. *Location in TSPA-LA:* Sections 6.3.11.1 and 6.3.11.2; Equation 6.3.11-4. *DTN:* MO0702PAVBPDCF.000_R0 [DIRS 179330]. *References: Biosphere Model Report* (SNL 2007 [DIRS 177399], Sections 6.12.2 and 6.12.3; Table 6.12-3; Equation 6.12-1).
DE_BDCF_Inh_LT_Th232. Volcanic Biosphere Dose Conversion Factor (BDCF) component for long-term inhalation of ^{232}Th in modern interglacial climate ((Sv/yr)/(Bq/kg)). *Distribution:* Discrete. *Range:* 9.64E-08 to 2.83E-06. *Mean:* 5.66E-07. *Standard Deviation:* 3.62E-07. *Symbol:* $BDCF_{inh,p,i}$. *Additional Information:* See DE_BDCF_Inh_LT_Ac227. *Sensitivity Name:* ILTTH232. *Location in TSPA-LA:* Sections 6.3.11.1 and 6.3.11.2; Equation 6.3.11-4. *DTN:* MO0702PAVBPDCF.000_R0 [DIRS 179330]. *References: Biosphere Model Report* (SNL 2007 [DIRS 177399], Sections 6.12.2 and 6.12.3; Table 6.12-3; Equation 6.12-1).
DE_BDCF_Inh_LT_U233. Volcanic Biosphere Dose Conversion Factor (BDCF) component for long-term inhalation of ^{233}U in modern interglacial climate ((Sv/yr)/(Bq/kg)). *Distribution:* Discrete. *Range:* 8.40E-09 to 2.47E-07. *Mean:* 4.94E-08. *Standard Deviation:* 3.15E-08. *Symbol:* $BDCF_{inh,p,i}$. *Additional Information:* See DE_BDCF_Inh_LT_Ac227. *Sensitivity Name:* ILTU233. *Location in TSPA-LA:* Sections 6.3.11.1 and 6.3.11.2; Equation 6.3.11-4. *DTN:* MO0702PAVBPDCF.000_R0 [DIRS 179330]. *References: Biosphere Model Report* (SNL 2007 [DIRS 177399], Sections 6.12.2 and 6.12.3; Table 6.12-3; Equation 6.12-1).
DE_BDCF_Inh_LT_U234. Volcanic Biosphere Dose Conversion Factor (BDCF) component for long-term inhalation of ^{234}U in modern interglacial climate ((Sv/yr)/(Bq/kg)). *Distribution:* Discrete. *Range:* 8.23E-09 to 2.42E-07. *Mean:* 4.84E-08. *Standard Deviation:* 3.09E-08. *Symbol:* $BDCF_{inh,p,i}$. *Additional Information:* See DE_BDCF_Inh_LT_Ac227. *Sensitivity Name:* ILTU234. *Location in TSPA-LA:* Sections 6.3.11.1 and 6.3.11.2; Equation 6.3.11-4. *DTN:* MO0702PAVBPDCF.000_R0 [DIRS 179330]. *References: Biosphere Model Report* (SNL 2007 [DIRS 177399], Sections 6.12.2 and 6.12.3; Table 6.12-3; Equation 6.12-1).
DE_BDCF_Inh_LT_U238. Volcanic Biosphere Dose Conversion Factor (BDCF) component for long-term inhalation of ^{238}U in modern interglacial climate ((Sv/yr)/(Bq/kg)). *Distribution:* Discrete. *Range:* 7.05E-09 to 2.07E-07. *Mean:* 4.14E-08. *Standard Deviation:* 2.65E-08. *Symbol:* $BDCF_{inh,p,i}$. *Additional Information:* See DE_BDCF_Inh_LT_Ac227. *Sensitivity Name:* ILTU238. *Location in TSPA-LA:* Sections 6.3.11.1 and 6.3.11.2; Equation 6.3.11-4. *DTN:* MO0702PAVBPDCF.000_R0 [DIRS 179330]. *References: Biosphere Model Report* (SNL 2007 [DIRS 177399], Sections 6.12.2 and 6.12.3; Table 6.12-3; Equation 6.12-1).
DE_BDCF_Inh_ShT_Ac227. Volcanic Biosphere Dose Conversion Factor (BDCF) component for short-term inhalation of ^{227}Ac in modern interglacial climate ((Sv/yr)/(Bq/kg)). *Distribution:* Discrete. *Range:* 8.47E-08 to 2.14E-06. *Mean:* 5.85E-07. *Standard Deviation:* 3.32E-07. *Symbol:* $BDCF_{inh,v,i}$. *Additional Information:* See DE_BDCF_Inh_LT_Ac227. *Sensitivity Name:* ISTAC227. *Location in TSPA-LA:* Sections 6.3.11.1 and 6.3.11.2; Equation 6.3.11-4. *DTN:* MO0702PAVBPDCF.000_R0 [DIRS 179330]. *References: Biosphere Model Report* (SNL 2007 [DIRS 177399], Sections 6.12.2 and 6.12.3; Table 6.12-2; Equation 6.12-1).
DE_BDCF_Inh_ShT_Am241. Volcanic Biosphere Dose Conversion Factor (BDCF) component for short-term inhalation of ^{241}Am in modern interglacial climate ((Sv/yr)/(Bq/kg)). *Distribution:* Discrete. *Range:* 4.67E-08 to 1.18E-06. *Mean:* 3.23E-07. *Standard Deviation:* 1.83E-07. *Symbol:* $BDCF_{inh,v,i}$. *Additional Information:* See DE_BDCF_Inh_LT_Ac227. *Sensitivity Name:* ISTAM241. *Location in TSPA-LA:* Sections 6.3.11.1 and 6.3.11.2; Equation 6.3.11-4. *DTN:* MO0702PAVBPDCF.000_R0 [DIRS 179330]. *References: Biosphere Model Report* (SNL 2007 [DIRS 177399], Sections 6.12.2 and 6.12.3; Table 6.12-2; Equation 6.12-1).
DE_BDCF_Inh_ShT_Am243. Volcanic Biosphere Dose Conversion Factor (BDCF) component for short-term inhalation of ^{243}Am in modern interglacial climate ((Sv/yr)/(Bq/kg)). *Distribution:* Discrete. *Range:* 4.64E-08 to 1.17E-06. *Mean:* 3.2E-07. *Standard Deviation:* 1.82E-07. *Symbol:* $BDCF_{inh,v,i}$. *Additional Information:* See DE_BDCF_Inh_LT_Ac227. *Sensitivity Name:* ISTAM243. *Location in TSPA-LA:* Sections 6.3.11.1 and 6.3.11.2; Equation 6.3.11-4. *DTN:* MO0702PAVBPDCF.000_R0 [DIRS 179330]. *References: Biosphere Model Report* (SNL 2007 [DIRS 177399], Sections 6.12.2 and 6.12.3; Table 6.12-2; Equation 6.12-1).

Table K3-3. Detailed Summary of Epistemically Uncertain Variables (i.e., elements of **e**) Considered in the TSPA-LA (TSPA Parameter Name) (Continued)

NOTE: * indicates variable not considered in sensitivity analysis due to correlations.

DE_BDCF_Inh_ShT_Cs137. Volcanic Biosphere Dose Conversion Factor (BDCF) component for short-term inhalation of ^{137}Cs in modern interglacial climate ((Sv/yr)/(Bq/kg)). *Distribution:* Discrete. *Range:* 1.90E-11 to 4.80E-10. *Mean:* 1.31E-10. *Standard Deviation:* 7.44E-11. *Symbol:* $BDCF_{inh,v,i}$. *Additional Information:* See DE_BDCF_Inh_LT_Ac227. *Sensitivity Name:* ISTCS137. *Location in TSPA-LA:* Sections 6.3.11.1 and 6.3.11.2; Equation 6.3.11-4. *DTN:* MO0702PAVBPDCF.000_R0 [DIRS 179330]. *References: Biosphere Model Report* (SNL 2007 [DIRS 177399], Sections 6.12.2 and 6.12.3; Table 6.12-2; Equation 6.12-1).
DE_BDCF_Inh_ShT_I129. Volcanic Biosphere Dose Conversion Factor (BDCF) component for short-term inhalation of ^{129}I in modern interglacial climate ((Sv/yr)/(Bq/kg)). *Distribution:* Discrete. *Range:* 1.74E-11 to 4.40E-10. *Mean:* 1.2E-10. *Standard Deviation:* 6.81E-11. *Symbol:* $BDCF_{inh,v,i}$. *Additional Information:* See DE_BDCF_Inh_LT_Ac227. *Sensitivity Name:* ISTI129. *Location in TSPA-LA:* Sections 6.3.11.1 and 6.3.11.2; Equation 6.3.11-4. *DTN:* MO0702PAVBPDCF.000_R0 [DIRS 179330]. *References: Biosphere Model Report* (SNL 2007 [DIRS 177399], Sections 6.12.2 and 6.12.3; Table 6.12-2; Equation 6.12-1).
DE_BDCF_Inh_ShT_Np237. Volcanic Biosphere Dose Conversion Factor (BDCF) component for short-term inhalation of ^{237}Np in modern interglacial climate ((Sv/yr)/(Bq/kg)). *Distribution:* Discrete. *Range:* 2.41E-08 to 6.08E-07. *Mean:* 1.66E-07. *Standard Deviation:* 9.43E-08. *Symbol:* $BDCF_{inh,v,i}$. *Additional Information:* See DE_BDCF_Inh_LT_Ac227. *Sensitivity Name:* ISTNP237. *Location in TSPA-LA:* Sections 6.3.11.1 and 6.3.11.2; Equation 6.3.11-4. *DTN:* MO0702PAVBPDCF.000_R0 [DIRS 179330]. *References: Biosphere Model Report* (SNL 2007 [DIRS 177399], Sections 6.12.2 and 6.12.3; Table 6.12-2; Equation 6.12-1).
DE_BDCF_Inh_ShT_Pa231. Volcanic Biosphere Dose Conversion Factor (BDCF) component for short-term inhalation of ^{231}Pa in modern interglacial climate ((Sv/yr)/(Bq/kg)). *Distribution:* Discrete. *Range:* 1.11E-07 to 2.82E-06. *Mean:* 7.7E-07. *Standard Deviation:* 4.37E-07. *Symbol:* $BDCF_{inh,v,i}$. *Additional Information:* See DE_BDCF_Inh_LT_Ac227. *Sensitivity Name:* ISTPA231. *Location in TSPA-LA:* Sections 6.3.11.1 and 6.3.11.2; Equation 6.3.11-4. *DTN:* MO0702PAVBPDCF.000_R0 [DIRS 179330]. *References: Biosphere Model Report* (SNL 2007 [DIRS 177399], Sections 6.12.2 and 6.12.3; Table 6.12-2; Equation 6.12-1).
DE_BDCF_Inh_ShT_Pu238. Volcanic Biosphere Dose Conversion Factor (BDCF) component for short-term inhalation of ^{238}Pu in modern interglacial climate ((Sv/yr)/(Bq/kg)). *Distribution:* Discrete. *Range:* 5.23E-08 to 1.32E-06. *Mean:* 3.61E-07. *Standard Deviation:* 2.05E-07. *Symbol:* $BDCF_{inh,v,i}$. *Additional Information:* See DE_BDCF_Inh_LT_Ac227. *Sensitivity Name:* ISTPU238. *Location in TSPA-LA:* Sections 6.3.11.1 and 6.3.11.2; Equation 6.3.11-4. *DTN:* MO0702PAVBPDCF.000_R0 [DIRS 179330]. *References: Biosphere Model Report* (SNL 2007 [DIRS 177399], Sections 6.12.2 and 6.12.3; Table 6.12-2; Equation 6.12-1).
DE_BDCF_Inh_ShT_Pu239. Volcanic Biosphere Dose Conversion Factor (BDCF) component for short-term inhalation of ^{239}Pu in modern interglacial climate ((Sv/yr)/(Bq/kg)). *Distribution:* Discrete. *Range:* 5.76E-08 to 1.46E-06. *Mean:* 3.98E-07. *Standard Deviation:* 2.26E-07. *Symbol:* $BDCF_{inh,v,i}$. *Additional Information:* See DE_BDCF_Inh_LT_Ac227. *Sensitivity Name:* ISTPU239. *Location in TSPA-LA:* Sections 6.3.11.1 and 6.3.11.2; Equation 6.3.11-4. *DTN:* MO0702PAVBPDCF.000_R0 [DIRS 179330]. *References: Biosphere Model Report* (SNL 2007 [DIRS 177399], Sections 6.12.2 and 6.12.3; Table 6.12-2; Equation 6.12-1).
DE_BDCF_Inh_ShT_Pu240. Volcanic Biosphere Dose Conversion Factor (BDCF) component for short-term inhalation of ^{240}Pu in modern interglacial climate ((Sv/yr)/(Bq/kg)). *Distribution:* Discrete. *Range:* 5.76E-08 to 1.46E-06. *Mean:* 3.98E-07. *Standard Deviation:* 2.26E-07. *Symbol:* $BDCF_{inh,v,i}$. *Additional Information:* See DE_BDCF_Inh_LT_Ac227. *Sensitivity Name:* ISTPU240. *Location in TSPA-LA:* Sections 6.3.11.1 and 6.3.11.2; Equation 6.3.11-4. *DTN:* MO0702PAVBPDCF.000_R0 [DIRS 179330]. *References: Biosphere Model Report* (SNL 2007 [DIRS 177399], Sections 6.12.2 and 6.12.3; Table 6.12-2; Equation 6.12-1).
DE_BDCF_Inh_ShT_Pu242. Volcanic Biosphere Dose Conversion Factor (BDCF) component for short-term inhalation of ^{242}Pu in modern interglacial climate ((Sv/yr)/(Bq/kg)). *Distribution:* Discrete. *Range:* 5.47E-08 to 1.38E-06. *Mean:* 3.78E-07. *Standard Deviation:* 2.14E-07. *Symbol:* $BDCF_{inh,v,i}$. *Additional Information:* See DE_BDCF_Inh_LT_Ac227. *Sensitivity Name:* ISTPU242. *Location in TSPA-LA:* Sections 6.3.11.1 and 6.3.11.2; Equation 6.3.11-4. *DTN:* MO0702PAVBPDCF.000_R0 [DIRS 179330]. *References: Biosphere Model Report* (SNL 2007 [DIRS 177399], Sections 6.12.2 and 6.12.3; Table 6.12-2; Equation 6.12-1).
DE_BDCF_Inh_ShT_Ra228. Volcanic Biosphere Dose Conversion Factor (BDCF) component for short-term inhalation of ^{228}Ra in modern interglacial climate ((Sv/yr)/(Bq/kg)). *Distribution:* Discrete. *Range:* 7.76E-09 to 1.96E-07. *Mean:* 5.36E-08. *Standard Deviation:* 3.04E-08. *Symbol:* $BDCF_{inh,v,i}$. *Additional Information:* See DE_BDCF_Inh_LT_Ac227. *Sensitivity Name:* ISTRA228. *Location in TSPA-LA:* Sections 6.3.11.1 and 6.3.11.2; Equation 6.3.11-4. *DTN:* MO0702PAVBPDCF.000_R0 [DIRS 179330]. *References: Biosphere Model Report* (SNL 2007 [DIRS 177399], Sections 6.12.2 and 6.12.3; Table 6.12-2; Equation 6.12-1).

Table K3-3. Detailed Summary of Epistemically Uncertain Variables (i.e., elements of **e**) Considered in the TSPA-LA (TSPA Parameter Name) (Continued)

NOTE: * indicates variable not considered in sensitivity analysis due to correlations.

DE_BDCF_Inh_ShT_Sn126. Volcanic Biosphere Dose Conversion Factor (BDCF) component for short-term inhalation of ^{126}Sn in modern interglacial climate ((Sv/yr)/(Bq/kg)). *Distribution:* Discrete. *Range:* 7.53E-11 to 1.90E-09. *Mean:* 5.2E-10. *Standard Deviation:* 2.95E-10. *Symbol:* $BDCF_{inh,v,i}$. *Additional Information:* See DE_BDCF_Inh_LT_Ac227. *Sensitivity Name:* ISTSN126. *Location in TSPA-LA:* Sections 6.3.11.1 and 6.3.11.2; Equation 6.3.11-4. *DTN:* MO0702PAVBPDCF.000_R0 [DIRS 179330]. *References: Biosphere Model Report* (SNL 2007 [DIRS 177399], Sections 6.12.2 and 6.12.3; Table 6.12-2; Equation 6.12-1).
DE_BDCF_Inh_ShT_Sr90. Volcanic Biosphere Dose Conversion Factor (BDCF) component for short-term inhalation of ^{90}Sr in modern interglacial climate ((Sv/yr)/(Bq/kg)). *Distribution:* Discrete. *Range:* 7.68E-11 to 1.94E-09. *Mean:* 5.3E-10. *Standard Deviation:* 3.01E-10. *Symbol:* $BDCF_{inh,v,i}$. *Additional Information:* See DE_BDCF_Inh_LT_Ac227. *Sensitivity Name:* ISTSR90. *Location in TSPA-LA:* Sections 6.3.11.1 and 6.3.11.2; Equation 6.3.11-4. *DTN:* MO0702PAVBPDCF.000_R0 [DIRS 179330]. *References: Biosphere Model Report* (SNL 2007 [DIRS 177399], Sections 6.12.2 and 6.12.3; Table 6.12-2; Equation 6.12-1).
DE_BDCF_Inh_ShT_Tc99. Volcanic Biosphere Dose Conversion Factor (BDCF) component for short-term inhalation of ^{99}Tc in modern interglacial climate ((Sv/yr)/(Bq/kg)). *Distribution:* Discrete. *Range:* 6.44E-12 to 1.63E-10. *Mean:* 4.45E-11. *Standard Deviation:* 2.52E-11. *Symbol:* $BDCF_{inh,v,i}$. *Additional Information:* See DE_BDCF_Inh_LT_Ac227. *Sensitivity Name:* ISTTC99. *Location in TSPA-LA:* Sections 6.3.11.1 and 6.3.11.2; Equation 6.3.11-4. *DTN:* MO0702PAVBPDCF.000_R0 [DIRS 179330]. *References: Biosphere Model Report* (SNL 2007 [DIRS 177399], Sections 6.12.2 and 6.12.3; Table 6.12-2; Equation 6.12-1).
DE_BDCF_Inh_ShT_Th229. Volcanic Biosphere Dose Conversion Factor (BDCF) component for short-term inhalation of ^{229}Th in modern interglacial climate ((Sv/yr)/(Bq/kg)). *Distribution:* Discrete. *Range:* 1.24E-07 to 3.13E-06. *Mean:* 8.54E-07. *Standard Deviation:* 4.84E-07. *Symbol:* $BDCF_{inh,v,i}$. *Additional Information:* See DE_BDCF_Inh_LT_Ac227. *Sensitivity Name:* ISTTH229. *Location in TSPA-LA:* Sections 6.3.11.1 and 6.3.11.2; Equation 6.3.11-4. *DTN:* MO0702PAVBPDCF.000_R0 [DIRS 179330]. *References: Biosphere Model Report* (SNL 2007 [DIRS 177399], Sections 6.12.2 and 6.12.3; Table 6.12-2; Equation 6.12-1).
DE_BDCF_Inh_ShT_Th230. Volcanic Biosphere Dose Conversion Factor (BDCF) component for short-term inhalation of ^{230}Th in modern interglacial climate ((Sv/yr)/(Bq/kg)). *Distribution:* Discrete. *Range:* 4.94E-08 to 1.25E-06. *Mean:* 3.41E-07. *Standard Deviation:* 1.94E-07. *Symbol:* $BDCF_{inh,v,i}$. *Additional Information:* See DE_BDCF_Inh_LT_Ac227. *Sensitivity Name:* ISTTH230. *Location in TSPA-LA:* Sections 6.3.11.1 and 6.3.11.2; Equation 6.3.11-4. *DTN:* MO0702PAVBPDCF.000_R0 [DIRS 179330]. *References: Biosphere Model Report* (SNL 2007 [DIRS 177399], Sections 6.12.2 and 6.12.3; Table 6.12-2; Equation 6.12-1).
DE_BDCF_Inh_ShT_Th232. Volcanic Biosphere Dose Conversion Factor (BDCF) component for short-term inhalation of ^{232}Th in modern interglacial climate ((Sv/yr)/(Bq/kg)). *Distribution:* Discrete. *Range:* 5.33E-08 to 1.35E-06. *Mean:* 3.68E-07. *Standard Deviation:* 2.09E-07. *Symbol:* $BDCF_{inh,v,i}$. *Additional Information:* See DE_BDCF_Inh_LT_Ac227. *Sensitivity Name:* ISTTH232. *Location in TSPA-LA:* Sections 6.3.11.1 and 6.3.11.2; Equation 6.3.11-4. *DTN:* MO0702PAVBPDCF.000_R0 [DIRS 179330]. *References: Biosphere Model Report* (SNL 2007 [DIRS 177399], Sections 6.12.2 and 6.12.3; Table 6.12-2; Equation 6.12-1).
DE_BDCF_Inh_ShT_U233. Volcanic Biosphere Dose Conversion Factor (BDCF) component for short-term inhalation of ^{233}U in modern interglacial climate ((Sv/yr)/(Bq/kg)). *Distribution:* Discrete. *Range:* 4.65E-09 to 1.17E-07. *Mean:* 3.21E-08. *Standard Deviation:* 1.82E-08. *Symbol:* $BDCF_{inh,v,i}$. *Additional Information:* See DE_BDCF_Inh_LT_Ac227. *Sensitivity Name:* ISTU233. *Location in TSPA-LA:* Sections 6.3.11.1 and 6.3.11.2; Equation 6.3.11-4. *DTN:* MO0702PAVBPDCF.000_R0 [DIRS 179330]. *References: Biosphere Model Report* (SNL 2007 [DIRS 177399], Sections 6.12.2 and 6.12.3; Table 6.12-2; Equation 6.12-1).
DE_BDCF_Inh_ShT_U234. Volcanic Biosphere Dose Conversion Factor (BDCF) component for short-term inhalation of ^{234}U in modern interglacial climate ((Sv/yr)/(Bq/kg)). *Distribution:* Discrete. *Range:* 4.55E-09 to 1.15E-07. *Mean:* 3.15E-08. *Standard Deviation:* 1.78E-08. *Symbol:* $BDCF_{inh,v,i}$. *Additional Information:* See DE_BDCF_Inh_LT_Ac227. *Sensitivity Name:* ISTU234. *Location in TSPA-LA:* Sections 6.3.11.1 and 6.3.11.2; Equation 6.3.11-4. *DTN:* MO0702PAVBPDCF.000_R0 [DIRS 179330]. *References: Biosphere Model Report* (SNL 2007 [DIRS 177399], Sections 6.12.2 and 6.12.3; Table 6.12-2; Equation 6.12-1).
DE_BDCF_Inh_ShT_U238. Volcanic Biosphere Dose Conversion Factor (BDCF) component for short-term inhalation of ^{238}U in modern interglacial climate ((Sv/yr)/(Bq/kg)). *Distribution:* Discrete. *Range:* 3.90E-09 to 9.85E-08. *Mean:* 2.69E-08. *Standard Deviation:* 1.53E-08. *Symbol:* $BDCF_{inh,v,i}$. *Additional Information:* See DE_BDCF_Inh_LT_Ac227. *Sensitivity Name:* ISTU238. *Location in TSPA-LA:* Sections 6.3.11.1 and 6.3.11.2; Equation 6.3.11-4. *DTN:* MO0702PAVBPDCF.000_R0 [DIRS 179330]. *References: Biosphere Model Report* (SNL 2007 [DIRS 177399], Sections 6.12.2 and 6.12.3; Table 6.12-2; Equation 6.12-1).

Table K3-3. Detailed Summary of Epistemically Uncertain Variables (i.e., elements of **e**) Considered in the TSPA-LA (TSPA Parameter Name) (Continued)

NOTE: * indicates variable not considered in sensitivity analysis due to correlations.

DE_BDCF_IST_Ra226_Pb210. Volcanic Biosphere Dose Conversion Factor (BDCF) component for short-term inhalation of ^{226}Ra and ^{210}Pb in modern interglacial climate ((Sv/yr)/(Bq/kg)). *Distribution:* Discrete. *Range:* 9.47E-09 to 2.39E-07. *Mean:* 6.54E-08. *Standard Deviation:* 3.71E-08. *Symbol:* $BDCF_{inh,v,i}$. *Additional Information:* See DE_BDCF_Inh_LT_Ac227. *Sensitivity Name:* ISTRA226. *Location in TSPA-LA:* Sections 6.3.11.1 and 6.3.11.2; Equation 6.3.11-4. *DTN:* MO0702PAVBPDCF.000_R0 [DIRS 179330]. *References: Biosphere Model Report* (SNL 2007 [DIRS 177399], Sections 6.12.2 and 6.12.3; Table 6.12-2; Equation 6.12-1).
Default_Fwd_Rate_Const_a. Default forward rate constant for irreversible sorption of plutonium and americium ($m^3/m^2/yr$). *Distribution:* Log uniform. *Range:* 0.002 to 0.05. *Symbol:* k. *Additional Information:* A sampled parameter that defines the default forward rate constant for irreversible sorption of Pu and Am onto iron oxyhydroxide colloids and stationary corrosion products for zero or near zero advective flux conditions. The log-uniform distribution and range used for sampling Default_Fwd_Rate_Const_a is from the *Waste Form and In-Drift Colloids-Associated Radionuclide Concentrations: Abstraction and Summary* (SNL 2007 [DIRS 177423], Sections 6.3.12.2). Recorded in TSPA Input Database as Max_Default_Fwd_Rate_Const and Min_Default_Fwd_Rate_Const. *Sensitivity Name:* FWDRAT. *Location in TSPA-LA:* Table 6.3.7-65. *DTN:* MO0701PAIRONCO.000_R1 [DIRS 180440]. *References: Waste Form and In-Drift Colloids-Associated Radionuclide Concentrations: Abstraction and Summary* (SNL 2007 [DIRS 177423], Sections 6.3.12.2, 6.5.1.4 and 8.1; Equations 6-18 and 6-19; Table 6-24).
Defect_Count_a. Flaw density parameter (flaws per mm^3 of weld) (dimensionless). *Distribution:* Gamma. *Mean:* 4.529E-07. *Standard Deviation:* 1.654E-07. *Symbol:* λ_c. *Additional Information:* This parameter is used to compute the cumulative probability of a manufacturing defect based on the probability for the nondetection of weld flaws. Inputs to this calculation are the weld thickness, the weld volume, the defect fraction considered, a detection threshold, a characteristic flaw size, a shape factor, a defect count parameter, and a defect size parameter. The variation in the number of weld defects parameter is a function of the flaw size and count parameters that are sampled as uncertain for each realization. *Sensitivity Name:* WDDEFCNT. *Location in TSPA-LA:* Section 6.3.5.1.2; Table 6.3.5-3. *DTN:* MO0701PASHIELD.000_R2 [DIRS 180508]. *References: Analysis of Mechanisms for Early Waste Package / Drip Shield Failure* (SNL 2007 [DIRS 178765], Sections 6.3.1.3, 6.3.1.8 and A.3; Figure 6-4; Tables 6-4 and 7-1; Equations 11, 12 and 23).
Defect_Size_a. Flaw size parameter (flaw size per mm of weld) (dimensionless). *Distribution:* Gamma. *Mean:* 0.2205. *Standard Deviation:* 0.0833. *Symbol:* λ_s. *Additional Information:* See Defect_Count_a. The variation in weld flaw sizes is expressed as aleatory uncertainty at the WP level, given by a CDF dependent on an uncertain flaw size parameter that is sampled for each realization. *Sensitivity Name:* WDDEFSZE. *Location in TSPA-LA:* Section 6.3.5.1.2; Table 6.3.5-3; Equation 6.3.5-10. *DTN:* MO0701PASHIELD.000_R2 [DIRS 180508]. *References: Analysis of Mechanisms for Early Waste Package / Drip Shield Failure* (SNL 2007 [DIRS 178765], Sections 6.3.1.2 and A.2; Table 7-1; Equations 5 to 7).
Density_CSNF_Rind_a. Grain density of CSNF rind (kg/m^3). *Distribution:* Uniform. *Range:* 5600 to 11500. *Symbol:* ρ_r. *Additional Information:* The water saturation in waste form rind (for CSNF and HLWG waste forms) is dependent on the relative humidity, which varies over time, on the rind specific surface area and on the rind grain density. Density_CSNF_Rind_a is a sampled parameter whose range covers the range of values obtained from the literature for the surrogate materials used to create the adsorption isotherm. Sparse data do not show any trends to justify any distribution except uniform. To capture this large uncertainty, the specific surface area and density of the rind materials, as well as the porosity, will be sampled from uniform distributions over the ranges of the surrogate material properties. *Sensitivity Name:* CSRINDDN. *Location in TSPA-LA:* Table 6.3.8-4. *DTN:* SN0703PAEBSRTA.001_R3 [DIRS 183217]. *References: EBS Radionuclide Transport Abstraction* (SNL 2007 [DIRS 177407], Section 6.5.2.2.2.1; Equation 6.5.2.2.2.1-1; Tables 6.5-9 and 8.2-4).
Diameter_Colloid_a. Diameter of colloid particle (nm). *Distribution:* Uniform. *Range:* 50 to 300. *Symbol:* d_{coll}. *Additional Information:* The effect of colloid particle size, and thus the colloid diffusion coefficient, on releases of radionuclides from the EBS can be evaluated by sampling on the colloid particle size in TSPA. Because transport associated with individual colloid particles cannot be modeled in TSPA, a representative value of the colloid size is chosen from the population of colloid particles. This representative value is expected to be uncertain and can be represented by an epistemic uncertainty distribution that will be sampled in TSPA. The uncertainty range in the representative value is going to be narrower than the size range in the colloid population. At the same time, the representative value must be representative of all three types of colloids that are considered in the EBS transport model. For each TSPA realization, a single size (diameter) is sampled. *Sensitivity Name:* DIAMCOLL. *Location in TSPA-LA:* Tables 6.3.8-1 and 6.3.8-4. *DTN:* SN0703PAEBSRTA.001_R3 [DIRS 183217]. *References: EBS Radionuclide Transport Abstraction* (SNL 2007 [DIRS 177407], Section 6.3.4.4; Equation 6.3.4.4-1; Tables 8.2-4 and 8.2-7).

Table K3-3. Detailed Summary of Epistemically Uncertain Variables (i.e., elements of **e**) Considered in the TSPA-LA (TSPA Parameter Name) (Continued)

NOTE: * indicates variable not considered in sensitivity analysis due to correlations.

Diff_Path_Length_Invert_Top_a. Diffusive path length from waste package outer corrosion barrier to mid-point of invert (m). *Distribution:* Uniform. *Range:* 0.3 to 1.24. *Additional Information:* The lower end of the range is the distance from the center of the invert to the top of the invert; the upper end is the distance from the center of the invert up to a representative breach location up the side of the waste package. Uncertainty in breach locations in different waste packages over time precludes defining any distribution other than uniform. *Sensitivity Name:* DIFPATHL. *Location in TSPA-LA:* Section 6.3.8.2.4; Table 6.3.8-4. *DTN:* SN0703PAEBSRTA.001_R3 [DIRS 183217]. *References: EBS Radionuclide Transport Abstraction* (SNL 2007 [DIRS 177407], Table 8.2-4).
Drainage_Density_a. Average drainage density for the Fortymile Wash drainage basin (1/km). *Distribution:* Uniform. *Range:* 20 to 33. *Symbol:* X. *Additional Information:* The drainage density is the ratio of the total length of all channels within a drainage basin to the area of that basin. The drainage density parameter is used to define the channel system in the Fortymile Wash drainage basin. Since the drainage density parameter influences the amount of tephra that may be mobilized, it is important to define this parameter in such a way that adequately addresses the uncertainty in the extent of channels and their ability to redistribute and transport tephra. The value of the drainage density that yields the lowest value for the average distance between the observed and predicted channel heads is considered the optimal value for the drainage density input into the tephra redistribution model. This parameter is used in order to distinguish hillslopes from channels within the FAR software code. *Sensitivity Name:* DRAINDNS. *Location in TSPA-LA:* Table 6.5-5. *DTN:* MO0702PAFARDAT.001_R3 [DIRS 182578]. *References: Redistribution of Tephra and Waste by Geomorphic Processes Following a Potential Volcanic Eruption at Yucca Mountain, Nevada* (SNL 2007 [DIRS 179347], Sections 6.2.1, 6.3.2, 6.5.3, 6.6.1, 6.6.3, 7.2.4 and 8.1; Figures 6.3.3-9 and 6.6.1-1; Table 6.5.3-1).
DS_Flux_Uncertainty_a. Drip shield flux splitting factor (dimensionless). *Distribution:* Uniform. *Range:* 0 to 0.85. *Symbol:* f'_{DS}. *Additional Information:* Uncertainty in the drip shield flux splitting algorithm is given by DS_Flux_Uncertainty_a. The range is derived from analyses of breached drip shield experimental results. There is insufficient data to show trends on which to base any distribution other than uniform. *Sensitivity Name:* DSFLUX. *Location in TSPA-LA:* Tables 6.3.6-1, 6.3.6-2 and 6.3.8-4; Sections 6.3.6.2 and 6.3.6.4.1; Equation 6.3.6-5. *DTN:* SN0703PAEBSRTA.001_R3 [DIRS 183217]. *References: EBS Radionuclide Transport Abstraction* (SNL 2007 [DIRS 177407], Sections 6.3.1.1, 6.3.2.4, 6.5.1.1.1, 6.5.1.1.2.4, 7.1.1.1, Appendix C and Appendix E; Tables 6.3-1, 7.1-7, 8.1-1 and 8.2-4; Equations 6.3.2.4-2, 6.5.1.1.2.4-2 and 6.5.1.1.2.4-3).
DSNF_Mass_Uncert_a. Scale factor used to characterize uncertainty in radionuclide content of DSNF (dimensionless). *Distribution:* Triangular. *Range:* 0.45 to 2.9. *Most Likely:* 0.62. *Additional Information:* See CSNF_Mass_Uncert_a. *Sensitivity Name:* DSNFMASS. *Location in TSPA-LA:* Sections 6.3.7.1.2 and 6.3.7.1.3; Table 6.3.7-7. *DTN:* SN0310T0505503.004_R0 [DIRS 168761]. *References: Initial Radionuclides Inventory* (SNL 2007 [DIRS 180472], Sections 6.6.2, 6.7 and 7; Table 7-2),
dt_dRh_uncertainty. Selector variable used to determine the collapsed drift rubble thermal conductivity (dimensionless). *Distribution:* Discrete. *Range:* 1 to 2. *Additional Information:* There is epistemic uncertainty in the thermal conductivity (K_{th}) of the rubble resulting from a seismic event. A value of 1 indicates the low K_{th} case, while a value of 2 indicates the high K_{th} case. Neither the high-K_{th} case nor low-K_{th} case is more or less likely to be the appropriate value to be applied for effective thermal conductivity of the host-rock rubble. As a result of this argument, each alternative, the high- and low-K_{th} cases, can be assigned the same probability (of 50 percent). *Sensitivity Name:* DTDRHUNC. *Location in TSPA-LA:* Section 6.6.2.2. *DTN:* MO0505SPAROCKM.000_R0 [DIRS 173893]. *References: Multiscale Thermohydrologic Model* (SNL 2007 [DIRS 181383], Sections 6.2.10.3, 6.3.7 and 6.3.17[a]).
DWC_Dispersivity_Cond_a. Selector variable used to determine the axial dispersion modeling case (dimensionless). *Distribution:* Discrete. *Range:* 0 to 1. *Additional Information:* This TSPA implementation parameter specifies whether the high dispersivity (DWC_Dispersivity_Cond_a = 1) or low dispersivity (DWC_Dispersivity_Cond_a = 0) modeling case is used to calculate drift-wall condensation. The probability of encountering each of the two modeling cases is 0.5. *Sensitivity Name:* DWCDISP. *Location in TSPA-LA:* Section 6.3.3.2.2; Table 6.3.3-5. *References: In Drift Natural Convection and Condensation* (SNL 2007 [DIRS 181648], Sections 6.1 [a], 6.1.3[a], Appendix A[a] and B[a]; Tables 6-2[a] and 6-3[a].

Table K3-3. Detailed Summary of Epistemically Uncertain Variables (i.e., elements of **e**) Considered in the TSPA-LA (TSPA Parameter Name) (Continued)

NOTE: * indicates variable not considered in sensitivity analysis due to correlations.

DWC_Std_Error_a_a. Multiplier for the standard deviation on the slope coefficient for determining the probability of condensation from percolation rate (dimensionless). *Distribution:* Normal. *Mean/Median/Mode:* 0. *Standard Deviation:* 1. *Additional Information:* The standard errors applied to the coefficients used in the correlation between the percolation rate and the condensation rate/probability for the four drift wall condensation (DWC) modeling cases (high and low dispersivity, ventilated or unventilated drip shields) are applied as the product of the sampled value from a truncated normal distribution and the value of the standard error specifically defined for each modeling case. A unique distribution is sampled for the slope and y-intercept for both the condensation rate and probability. The standard errors can be used as uncertainty ranges around the slope and intercept parameters. Sampling for the standard error values should be independent. *Sensitivity Name:* DWCSTERA. *Location in TSPA-LA:* Section 6.3.3.2.2; Tables 6.3.3-4 and 6.3.3-5. *References: In Drift Natural Convection and Condensation* (SNL 2007 [DIRS 181648], Sections 6.1.3 [a], Appendix A[a] and B[a]; Tables A-1[a] to A-3[a] and B-1[a] to B-3[a]).
DWC_Std_Error_b_a. Multiplier for the standard deviation on the y-intercept coefficient for determining the probability of condensation from percolation rate (dimensionless). *Distribution:* Normal. *Mean/Median/Mode:* 0. *Standard Deviation:* 1. *Additional Information:* See DWC_Std_Error_a_a. *Sensitivity Name:* DWCSTERB. *Location in TSPA-LA:* Section 6.3.3.2.2; Tables 6.3.3-4 and 6.3.3-5. *References:* In Drift Natural Convection and Condensation (MDL-EBS-MD-000001 REV 00 AD 01, SNL 2007 [DIRS 181648], Section 6.1.3 [a], Appendix A[a] and B[a]; Tables A-1[a] to A-3[a] and B-1[a] to B-3[a]).
DWC_Std_Error_c_a. Multiplier for the standard deviation on the slope coefficient for determining condensation rate from percolation rate (dimensionless). *Distribution:* Normal. *Mean/Median/Mode:* 0. *Standard Deviation:* 1. *Additional Information:* See DWC_Std_Error_a_a. *Sensitivity Name:* DWCSTERC. *Location in TSPA-LA:* Section 6.3.3.2.2; Tables 6.3.3-4 and 6.3.3-5. *References: In Drift Natural Convection and Condensation* (SNL 2007 [DIRS 181648], Sections 6.1.3[a], Appendix A[a] and B [a]; Tables A-1[a] to A-3[a] and B-1[a] to B-3[a]).
DWC_Std_Error_d_a. Multiplier for the standard deviation on the y-intercept coefficient for determining the condensation rate from percolation rate (dimensionless). *Distribution:* Normal. *Mean/Median/Mode:* 0. *Standard Deviation:* 1. *Additional Information:* See DWC_Std_Error_a_a. *Sensitivity Name:* DWCSTERD. *Location in TSPA-LA:* Section 6.3.3.2.2; Tables 6.3.3-4 and 6.3.3-5. *References:* I*n Drift Natural Convection and Condensation* (SNL 2007 [DIRS 181648], Sections 6.1.3[a], Appendix A[a] and B [a]; Tables A-1[a] to A-3[a] and B-1[a] to B-3[a]).
DWC_Ventilated_Cond_a. Selector variable specifying whether the ventilated or unventilated drip shield DWC modeling case is performed (dimensionless). *Distribution:* Discrete. *Range:* 0, 1. *Additional Information:* This TSPA implementation parameter specifies whether the ventilated drip shield (DWC_Ventilated_Cond_a = 1) or unventilated drip shield (DWC_Ventilated_Cond_a = 0) modeling case is used to calculate drift-wall condensation. The probability of encountering each of the two modeling cases is 0.5. *Sensitivity Name:* DWCVENT. *Location in TSPA-LA:* Sections 6.3.3.2.2 and 6.3.3.2.3; Table 6.3.3-5. *References:* I*n Drift Natural Convection and Condensation* (SNL 2007 [DIRS 181648], Sections 6.1.2[a], 6.1.3 [a], Appendix A[a] and B [a]; Tables 6-2[a], 6-3[a] and 8-1[a]).
Exposure_Factor_a. The surface area exposure factor for the amount of HLW glass contacted by water (dimensionless). *Distribution:* Triangular. *Range:* 4 to 17. *Mode:* 4. *Symbol:* $f_{exposure}$. *Additional Information:* The exposure factor is used to account for several uncertainties regarding the glass surface area that is used to calculate the glass degradation rate and, ultimately, the radionuclide release rate. The upper limit of the range represents the case where glass in cracks has the same reactivity as glass at free surfaces. The lower limit of the range accounts for the limited access of water to glass in interior cracks and the lower reactivity of glass in the cracks. The exposure factor accounts for the thermal cracking anticipated for all glass and impact cracking anticipated for about 1% of the glass. *Sensitivity Name:* WFDEGEXF. *Location in TSPA-LA:* Sections 6.3.7.4.3.2 and 6.3.7.4.3.3; Equation 6.3.7-9; Table 6.3.7-32. *DTN:* MO0502ANLGAMR1.016_R0 [DIRS 172830]. *References: Defense HLW Glass Degradation Model* (BSC 2004 [DIRS 169988], Sections 4.1, 6.5.4, 6.6, 6.7, 6.8.1, 6.8.5, 8.1 and 8.2.1; Equations 44, 45, 48 and 49; Tables 6-14 and 8-1).

Table K3-3. Detailed Summary of Epistemically Uncertain Variables (i.e., elements of **e**) Considered in the TSPA-LA (TSPA Parameter Name) (Continued)

NOTE: * indicates variable not considered in sensitivity analysis due to correlations.

fa_group1_a. Fracture aperture for group 1 rock unit (chnf) (m). *Calculated by:* Por_group1_a/ff_group1_a. *Symbol:* 2b. *Additional Information:* This is the ratio of porosity (Por_group#_a) to fracture frequency (ff_group#_a). There is only one standard deviation for fracture porosity, so the other groups are assigned a fracture porosity standard deviation such that the ratio of the standard deviation to the mean is constant for all the groups. This is based on the relationship between fracture frequency and the standard deviation of fracture frequency found for model units above the proposed repository. In this way, the mean and standard deviation for each parameter in each group were computed. As porosity must lie within the finite range of 0 to 1, a beta distribution with these bounds is suitable for studying the influence of porosity uncertainty on radionuclide transport. The logarithm of the fracture frequency has a normal distribution with a mean of.2.33 and a standard deviation of 0.724. The fracture porosity has beta distribution with a minimum of 0, a maximum of 1, a mean of 0.001 and a standard deviation of 0.000309. *Sensitivity Name:* UZFAG1. *Location in TSPA-LA:* Section 6.3.9.2; Equation 6.3.9-2; Fracture porosity values and frequency values are shown in Tables 6.3.9-6 and 6.3.9-7. *DTN:* Fracture frequency, porosity and aperture found in: LA0701PANS02BR.003_R2 [DIRS 180497], Table 1.doc. *References: Particle Tracking Model and Abstraction of Transport Processes Addendum 002* (SNL 2008 [DIRS 184748], Sections 4.1.2 and 6.5.7; Tables 6.6.1-1, 7-1 and 8-2).
fa_group2_a. Fracture aperture for group 2 rock unit (tswf) (m). *Calculated by:* Por_group2_a/ff_group2_a. *Symbol:* 2b. *Additional Information:* See fa_group1_a. The logarithm of the fracture frequency has a normal distribution with a mean of 0.296 and a standard deviation of 0.724. The fracture porosity has a beta distribution with a minimum of 0, a maximum of 1, a mean of 0.025 and a standard deviation of 0.00725. *Sensitivity Name:* UZFAG2. *Location in TSPA-LA:* Section 6.3.9.2; Equation 6.3.9-2; Fracture porosity values and frequency values are shown in Tables 6.3.9-6 and 6.3.9-7. *DTN:* Fracture frequency, porosity and aperture found in: LA0701PANS02BR.003_R2 [DIRS 180497], Table 1.doc. *References: Particle Tracking Model and Abstraction of Transport Processes Addendum 002* (SNL 2008 [DIRS 184748], Sections 4.1.2 and 6.5.7; Tables 6.6.1-1, 7-1 and 8-2).
fa_group3_a. Fracture aperture for group 3 rock units (ch[2,3,4,5]fz, pcf[2,5]z, pp4fz, pp1fz, bf2fz, tr2fz) (m). *Calculated by:* Por_group3_a/ff_group3_a. *Symbol:* 2b. *Additional Information:* See fa_group1_a. The logarithm of the fracture frequency has a normal distribution with a mean of -2.23 and a standard deviation of 0.724. The fracture porosity has a beta distribution with a minimum of 0, a maximum of 1, a mean of 0.00037 and a standard deviation of 0.000109. *Sensitivity Name:* UZFAG3. *Location in TSPA-LA:* Section 6.3.9.2; Equation 6.3.9-2; Fracture porosity values and frequency values are shown in Tables 6.3.9-6 and 6.3.9-7. *DTN:* Fracture frequency, porosity and aperture found in: LA0701PANS02BR.003_R2 [DIRS 180497], Table 1.doc. *References: Particle Tracking Model and Abstraction of Transport Processes Addendum 002* (SNL 2008 [DIRS 184748], Sections 4.1.2 and 6.5.7; Tables 6.6.1-1, 7-1 and 8-2).
fa_group4_a. Fracture aperture for group 4 rock units (pp3fd, pp2fd, bf3fd, tr3fd) (m). *Calculated by:* Por_group4_a/ff_group4_a. *Symbol:* 2b. *Additional Information:* See fa_group1_a. The logarithm of the fracture frequency has a normal distribution with a mean of -1.87 and a standard deviation of 0.724. The fracture porosity has a beta distribution with a minimum of 0, a maximum of 1, a mean of 0.00097 and a standard deviation of 0.000285. *Sensitivity Name:* UZFAG4. *Location in TSPA-LA:* Section 6.3.9.2; Equation 6.3.9-2; Fracture porosity values and frequency values are shown in Tables 6.3.9-6 and 6.3.9-7. *DTN:* Fracture frequency, porosity and aperture found in: LA0701PANS02BR.003_R2 [DIRS 180497], Table 1.doc. *References: Particle Tracking Model and Abstraction of Transport Processes Addendum 002* (SNL 2008 [DIRS 184748], Sections 4.1.2 and 6.5.7; Tables 6.6.1-1, 7-1 and 8-2).
fa_group5_a. Fracture aperture for group 5 rock units (ch1fz, pcf1z, ch6fz, pcf6z) (m). *Calculated by:* Por_group5_a/ff_group5_a. *Symbol:* 2b. *Additional Information:* See fa_group1_a. The logarithm of the fracture frequency has a normal distribution with a mean of -3.48 and a standard deviation of 0.724. The fracture porosity has a beta distribution with a minimum of 0, a maximum of 1, a mean of 0.00016 and a standard deviation of 4.71E-05. *Sensitivity Name:* UZFAG5. *Location in TSPA-LA:* Section 6.3.9.2; Equation 6.3.9-2; Fracture porosity values and frequency values are shown in Tables 6.3.9-6 and 6.3.9-7. *DTN:* Fracture frequency, porosity and aperture found in: LA0701PANS02BR.003_R2 [DIRS 180497], Table 1.doc. *References: Particle Tracking Model and Abstraction of Transport Processes Addendum 002* (SNL 2008 [DIRS 184748], Sections 4.1.2 and 6.5.7; Tables 6.6.1-1, 7-1 and 8-2).

Table K3-3. Detailed Summary of Epistemically Uncertain Variables (i.e., elements of **e**) Considered in the TSPA-LA (TSPA Parameter Name) (Continued)

NOTE: * indicates variable not considered in sensitivity analysis due to correlations.

fa_group6_a. Fracture aperture for group 6 rock units (ch[1,2,3,4,5,6]fv) (m). *Calculated by:* Por_group6_a/ff_group6_a. *Symbol:* 2b. *Additional Information:* See fa_group1_a. The logarithm of the fracture frequency has a normal distribution with a mean of -2.38 and a standard deviation of 0.724. The fracture porosity has a beta distribution with a minimum of 0, a maximum of 1, a mean of 0.00069 and a standard deviation of 0.000203. *Sensitivity Name:* UZFAG6. *Location in TSPA-LA:* Section 6.3.9.2; Equation 6.3.9-2; Fracture porosity values and frequency values are shown in Tables 6.3.9-6 and 6.3.9-7. *DTN:* Fracture frequency, porosity and aperture found in: LA0701PANS02BR.003_R2 [DIRS 180497], Table 1.doc. *References: Particle Tracking Model and Abstraction of Transport Processes Addendum 002* (SNL 2008 [DIRS 184748], Sections 4.1.2 and 6.5.7; Tables 6.6.1-1, 7-1 and 8-2).
fa_group7_a. Fracture aperture for group 7 rock units (tswf9, pcf39, tswfv, tswfz) (m). *Calculated by:* Por_group7_a/ff_group7_a. *Symbol:* 2b. *Additional Information:* See fa_group1_a. The logarithm of the fracture frequency has a normal distribution with a mean of -0.303 and a standard deviation of 0.724. The fracture porosity has a beta distribution with a minimum of 0, a maximum of 1, a mean of 0.0043 and a standard deviation of 0.00126. *Sensitivity Name:* UZFAG7. *Location in TSPA-LA:* Section 6.3.9.2; Equation 6.3.9-2; Fracture porosity values and frequency values are shown in Tables 6.3.9-6 and 6.3.9-7. *DTN:* Fracture frequency, porosity and aperture found in: LA0701PANS02BR.003_R2 [DIRS 180497], Table 1.doc. *References: Particle Tracking Model and Abstraction of Transport Processes Addendum 002* (SNL 2008 [DIRS 184748], Sections 4.1.2 and 6.5.7; Tables 6.6.1-1, 7-1 and 8-2).
fa_group8_a. Fracture aperture for group 8 rock units (tswf[4,5], tswf[6,7], tswf8, pcf38) (m). *Calculated by:* Por_group8_a/ff_group8_a. *Symbol:* 2b. *Additional Information:* See fa_group1_a. The logarithm of the fracture frequency has a normal distribution with a mean of 1.12 and a standard deviation of 0.724. The fracture porosity has a beta distribution with a minimum of 0, a maximum of 1, a mean of 0.0105 and a standard deviation of 0.0031. *Sensitivity Name:* UZFAG8. *Location in TSPA-LA:* Section 6.3.9.2; Equation 6.3.9-2; Fracture porosity values and frequency values are shown in Tables 6.3.9-6 and 6.3.9-7. *DTN:* Fracture frequency, porosity and aperture found in: LA0701PANS02BR.003_R2 [DIRS 180497], Table 1.doc. *References: Particle Tracking Model and Abstraction of Transport Processes Addendum 002* (SNL 2008 [DIRS 184748], Sections 4.1.2 and 6.5.7; Tables 6.6.1-1, 7-1 and 8-2).
fa_group9_a. Fracture aperture for group 9 rock units (tswf3) (m). *Calculated by:* Por_group9_a/ff_group9_a. *Symbol:* 2b. *Additional Information:* See fa_group1_a. Group 9 (tswf3) has its own standard deviation for fracture frequency, which is used. As porosity must lie within the finite range of 0 to 1, a beta distribution with these bounds is suitable for studying the influence of porosity uncertainty on radionuclide transport. The logarithm of the fracture frequency has a normal distribution with a mean of -0.692 and a standard deviation of 0.981. The fracture porosity has a beta distribution with a minimum of 0, a maximum of 1, a mean of 0.0058 and a standard deviation of 0.00171. *Sensitivity Name:* UZFAG9. *Location in TSPA-LA:* Section 6.3.9.2; Equation 6.3.9-2; Fracture porosity values and frequency values are shown in Tables 6.3.9-6 and 6.3.9-7. *DTN:* Fracture frequency, porosity and aperture found in: LA0701PANS02BR.003_R2 [DIRS 180497], Table 1.doc. *References: Particle Tracking Model and Abstraction of Transport Processes Addendum 002* (SNL 2008 [DIRS 184748], Sections 4.1.2 and 6.5.7; Tables 6.6.1-1, 7-1 and 8-2).
FHH_Isotherm_k_CP_a. Frenkel Halsey Hill water vapor adsorption isotherm parameter, *k*, for corrosion products (dimensionless). *Distribution:* Uniform. *Range:* 1.048 to 1.370 (see additional information). *Symbol:* k_{CP}. *Additional Information: k* and *s* are parameters that in principle are calculable from properties of the absorbent and substrate but in practice are empirical. Because the adsorption isotherms for each corrosion product component (goethite, HFO, and chromium and nickel oxides) overlap and include uncertainty, data for all the components are lumped together to form a single isotherm, with the uncertainty accounted for using a range and uniform distribution for the corrosion product FHH parameters. Analysis of available water vapor adsorption isotherm data fit to the FHH function for the isotherm produced a mean and standard deviation for parameter *k*. A uniform distribution is used due to lack of trends in the empirical data to suggest any other distributions. In the TSPA-LA Model the incorrect range of values was used for this parameter. The correct range is 1.030 to 1.326. See Appendix P, Table P-6 for a discussion of the effects of this error. *Sensitivity Name:* FHHISKCP. *Location in TSPA-LA:* Table 6.3.8-4. *DTN:* SN0703PAEBSRTA.001_R3 [DIRS 183217]. *References: EBS Radionuclide Transport Abstraction* (ANL-WIS-PA-000001 REV 03, SNL 2007 [DIRS 177407], Sections 6.3.4.3.2 and 6.5.2.2.1; Tables 6.5-7 and 8.2-4; Equations 6.3.4.3.2-1 to 6.3.4.3.2-3).

Table K3-3. Detailed Summary of Epistemically Uncertain Variables (i.e., elements of **e**) Considered in the TSPA-LA (TSPA Parameter Name) (Continued)

NOTE: * indicates variable not considered in sensitivity analysis due to correlations.

FHH_Isotherm_k_CSNF_Rind_a. Frenkel Halsey Hill water vapor adsorption isotherm parameter, *k*, for CSNF rind (dimensionless). *Distribution:* Uniform. *Range:* 1.606 to 8.215. *Symbol:* k_{rind}. *Additional Information:* The water adsorption isotherm for waste form rind is of the same functional form as for corrosion products. The CSNF rind saturation calculation uses the FHH adsorption isotherm (a function of relative humidity). Uncertainty is accounted for using a range and uniform distribution for the CSNF rind FHH empirical parameters, *k* and *s*. See FHH_Isotherm_k_CP_a. *Sensitivity Name:* FHHISKCS. *Location in TSPA-LA:* Table 6.3.8-4. *DTN:* SN0703PAEBSRTA.001_R3 [DIRS 183217]. *References: EBS Radionuclide Transport Abstraction* (SNL 2007 [DIRS 177407], Sections 6.3.4.6.1 and 6.5.2.2.2; Tables 6.5-9 and 8.2-4; Equations 6.3.4.6.1-1 to 6.3.4.6.1-3).
FHH_Isotherm_s_CP_a. Frenkel Halsey Hill water vapor adsorption isotherm parameter, *s*, for corrosion products (dimensionless). *Distribution:* Uniform. *Range:* 1.525 to 1.852 (see additional information). *Symbol:* s_{CP}. *Additional Information:* See FHH_Isotherm_k_CP_a. Analysis of available water vapor adsorption isotherm data fit to FHH functional for of the isotherm produced a mean and standard deviation for parameter *s*. In the TSPA-LA Model the incorrect range of values was used for this parameter. The correct range is 1.493 to 1.799. See Appendix P, Table P-6, for a discussion of the effects of this error. *Sensitivity Name:* FHHISSCP. *Location in TSPA-LA:* Table 6.3.8-4. *DTN:* SN0703PAEBSRTA.001_R3 [DIRS 183217]. *References: EBS Radionuclide Transport Abstraction* (SNL 2007 [DIRS 177407], Sections 6.3.4.3.2 and 6.5.2.2.1; Tables 6.5-7 and 8.2-4; Equations 6.3.4.3.2-1 to 6.3.4.3.2-3).
FHH_Isotherm_s_CSNF_Rind_a. Frenkel Halsey Hill water vapor adsorption isotherm parameter, *s*, for CSNF rind (dimensionless). *Distribution:* Uniform. *Range:* 1.656 to 3.038. *Symbol:* s_{rind}. *Additional Information:* See FHH_Isotherm_k_CSNF_Rind_a. *Sensitivity Name:* FHHISSCS. *Location in TSPA-LA:* Table 6.3.8-4. *DTN:* SN0703PAEBSRTA.001_R3 [DIRS 183217]. *References: EBS Radionuclide Transport Abstraction* (SNL 2007 [DIRS 177407], Sections 6.3.4.6.1 and 6.5.2.2.2; Tables 6.5-9 and 8.2-4; Equations 6.3.4.6.1-1 to 6.3.4.6.1-3).
FISVO. Flowing interval spacing in fractured volcanic units (m). *Distribution:* Piecewise uniform. *Range:* 1.86 to 80. *Additional Information:* The uncertain input parameters influencing matrix diffusion in the SZ Flow and Transport Model Submodel include effective diffusion coefficient, flowing interval spacing, and flowing interval porosity. The flowing interval spacing and flowing interval porosity are used to define the effective area to flow in the fractured volcanic units. To treat the one- and three-dimensional transport through the SZ consistently, the sampled values used to generate the saturated zone breakthrough curves are also used in the TSPA-LA Model. These values are tabulated as 200 sets of values for the SZ parameters, accounting for appropriate correletions, and are entered into the TSPA model as a table of 200 values for each parameter. The TSPA-LA Model selects values from this table using the Goldsim variable SZ_index_a. *Sensitivity Name:* SZFISPVO. *Location in TSPA-LA:* Section 6.3.10.5; Table 6.3.10-2. *DTN:* SN0702PASZFTMA.002_R1 [DIRS 183471]. *References: Saturated Zone Flow and Transport Model Abstraction* (SNL 2008 [DIRS 183750], Sections 6.5.1.2, 6.5.2.3[a] B-2[a], 7-1[b], and A-1[b]; Tables 4-3, 6-7[a], 6-8, 7-1[a], A-1[a] and B-1; Figure 6-5[a]).
FPLANW. Northwestern boundary of alluvial uncertainty zone (dimensionless). *Distribution:* Uniform. *Range:* 0 to 1. *Additional Information:* This parameter is used to determine the lengths of the flow paths in the volcanic units and alluvium. Implemented as a uniform distribution where a value of 0.0 corresponds to the minimum extent of the uncertainty zone, and 1.0 corresponds to the maximum extent of the uncertainty zone in a westerly direction. FPLANW defines the location where the pathlines may cross from the fracture-dominated flow in the volcanic units to the higher-porosity alluvium. To treat the one- and three-dimensional transport through the SZ consistently, the sampled values used to generate the saturated zone breakthrough curves are also used in the TSPA-LA Model. These values are tabulated as 200 sets of values for the SZ parameters, accounting for appropriate correletions, and are entered into the TSPA model as a table of 200 values for each parameter. The TSPA-LA Model selects values from this table using the Goldsim variable SZ_index_a. *Sensitivity Name:* SZWBNDAL. *Location in TSPA-LA:* Section 6.3.10.2; Table 6.3.10-2. *DTN:* SN0702PASZFTMA.002_R1 [DIRS 183471]. *References: Saturated Zone Flow and Transport Model Abstraction* (SNL 2008 [DIRS 183750], Sections 6.5.1.2[a] and 6.5.2.2[a]; Tables 6-7[a], 7-1[a] and A-1[a]).

Table K3-3. Detailed Summary of Epistemically Uncertain Variables (i.e., elements of **e**) Considered in the TSPA-LA (TSPA Parameter Name) (Continued)

NOTE: * indicates variable not considered in sensitivity analysis due to correlations.

FPVO. Logarithm of lowing interval porosity in volcanic units (dimensionless). *Distribution:* Piecewise uniform. *Range:* -5 to -1. *Median:* -3. *Additional Information:* The flowing interval spacing and flowing interval porosity are used to define the effective area to flow in the fractured volcanic units. To treat the one- and three-dimensional transport through the SZ consistently, the sampled values used to generate the saturated zone breakthrough curves are also used in the TSPA-LA Model. These values are tabulated as 200 sets of values for the SZ parameters, accounting for appropriate correletions, and are entered into the TSPA model as a table of 200 values for each parameter. The TSPA-LA Model selects values from this table using the Goldsim variable SZ_index_a. *Sensitivity Name:* SZFIPOVO. *Location in TSPA-LA:* Table 6.3.10-2. *DTN:* SN0702PASZFTMA.002_R1 [DIRS 183471]. *References: Saturated Zone Flow and Transport Model Abstraction* (SNL 2008 [DIRS 183750], Sections 6.5.1.1, 6.5.1.2, 6.5.2.5, 6.5.2.15, B-2[a], 7-1[b], and A-1[b]; Tables 6-8, 7-1[a], A-1[a] and B-1).
Fraction_Channel_a. Fraction of the RMEI location subject to fluvial deposition (dimensionless). *Distribution:* Uniform. *Range:* 0.09 to 0.54. *Symbol:* F. *Additional Information:* The concentrations on divides and channels are combined using the weighting factor for the fraction of the alluvial fan composed of channels to yield one concentration for the resuspendable surface layer and one concentration for the tillage depth for use by the Volcanic Ash Exposure Submodel in dose calculations. The fraction of the Fortymile Wash alluvial fan area is estimated by measuring the fractional area of the current fan that has been active over the past 10,000 years. *Sensitivity Name:* FRACCHNL. *Location in TSPA-LA:* Table 6.5-5. *DTN:* MO0702PAFARDAT.001_R3 [DIRS 182578]. *References: Redistribution of Tephra and Waste by Geomorphic Processes Following a Potential Volcanic Eruption at Yucca Mountain, Nevada* (SNL 2007 [DIRS 179347], Section 6.3.2, 6.5.4.2 and 7.1.3; Tables 6.4-1 and 6.5.10-1).
Gamma_AFM_a. Active fracture model (AFM) Gamma parameter (dimensionless). *Distribution:* Uniform. *Range:* 0.2 to 0.6. *Additional Information:* The parameter will be sampled from a range to incorporate this uncertainty into the model. Process flow model results have demonstrated that the AFM parameters have very little influence on the relevant flow model parameters for transport, namely the fluid saturations and flow rates in the fracture and matrix continua. Smaller values of the gamma parameter reduce the effective size of the matrix block, and therefore increase the strength of the fracture-matrix flux term. A single, uncertain value of gamma will be provided for rock units below the repository. A reasonable upper bound is the value used in the development of the flow model, approximately 0.6. A range that extends down to 0.2 provides an overall range that is equally distributed above and below the nominal value of 0.4. With no additional information available to define this parameter uncertainty distribution, the parameter will be sampled from a uniform distribution from 0.2 to 0.6. This range is consistent with the available data, and maintains the model within a range in which preferential flow through a subset of fractures will occur for all realizations. *Sensitivity Name:* UZGAM. *Location in TSPA-LA:* Sections 6.3.9.2, 6.3.9.3 and 6.3.9.4.1; Table 6.3.9-5. *DTN:* LA0701PANS02BR.003_R2 [DIRS 180497], Readme.doc. *References: Particle Tracking Model and Abstraction of Transport Processes Addendum 002* (SNL 2008 [DIRS 184748], Section 6.5.6; Tables 6.6.1-1 and 8-2).
GC_ULevel_A22_a. Variable for selecting distribution for general corrosion rate (low, medium, or high) (dimensionless). *Distribution:* Discrete. *Range:* 1 to 3. *Additional Information:* In TSPA, the low, medium, and high general corrosion rate distribution for Alloy 22 is randomly selected in such a way that the low and high general corrosion rate distributions are each used for 5% of realizations and the medium general corrosion rate distribution is used for the remaining 90% of realizations. *Sensitivity Name:* WDGCUA22. *Location in TSPA-LA:* Table 6.3.5-4. *DTN:* MO0703PAGENCOR.001_R4 [DIRS 182029]. *References: General Corrosion and Localized Corrosion of the Waste Package Outer Barrier* (SNL 2007 [DIRS 178519], Sections 6.4.3 and 6.4.3.3; Table 6-7; Figure 6-23).
Goethite_SA_a. Specific surface area of goethite (m^2/g). *Distribution:* Truncated log normal. *Range:* 14.7 to 110. *Mean:* 51.42. *Standard Deviation:* 30.09. *Symbol:* S_G. *Additional Information:* For the water saturation calculation, the solid density of each of the four corrosion product components is multiplied by its respective specific surface area. Specific surface areas for goethite and HFO are used for the competitive radionuclide sorption model as well as for the water sorption and saturation model. *Sensitivity Name:* GOESA. *Location in TSPA-LA:* Table 6.3.8-4; S_{CP} in Equation 6.3.8-19. *DTN:* SN0703PAEBSRTA.001_R3 [DIRS 183217]. *References: EBS Radionuclide Transport Abstraction* (SNL 2007 [DIRS 177407], Sections 4.1.2, 6.3.4.2.3.1, 6.3.4.3.3, 6.5.2.2.1, J.6.3 and Appendix K; Equation 6.3.4.2.3.1-1; Tables 4.1-12, 4.1-19, 6.3-7, 6.5-7 and 8.2-4).
Goethite_Site_Density_a. Density of sorption sites on goethite ($1/nm^2$). *Distribution:* Discrete. *Range:* 1.02 to 8.59. *Symbol:* $N_{S,G}$. *Additional Information:* Range and distribution are those of the input data and adequately capture the behavior of the parameter without further analysis. *Sensitivity Name:* GOESITED. *Location in TSPA-LA:* Table 6.3.8-3. *DTN:* SN0703PAEBSRTA.001_R3 [DIRS 183217]. *References: EBS Radionuclide Transport Abstraction* (SNL 2007 [DIRS 177407], Sections 4.1.2, 6.3.4.2.3.1, J.6.3 and J.6.5.1; Equation 6.3.4.2.3.1-1; Tables 4.1-12, 6.3-4, 6.3-5 and 8.2-2).

Table K3-3. Detailed Summary of Epistemically Uncertain Variables (i.e., elements of **e**) Considered in the TSPA-LA (TSPA Parameter Name) (Continued)

NOTE: * indicates variable not considered in sensitivity analysis due to correlations.

GW_BDCF_MIC_Ac227. Groundwater Biosphere Dose Conversion Factor (BDCF) for ^{227}Ac in modern interglacial climate ((Sv/year)/(Bq/m^3)). *Distribution:* Discrete. *Range:* 4.08E-07 to 4.32E-06. *Mean:* 1.3E-06. *Standard Deviation:* 5.28E-07. *Additional Information:* The groundwater BDCFs predict, in a stochastic manner to allow for parametric uncertainty, the annual dose (Sv/yr) to the reasonably maximally exposed individual for a unit activity concentration (1 Bq/m^3) in the groundwater for each radionuclide considered by TSPA. BDCFs were developed for three climate states: the present-day climate, monsoon climate, and glacial transition climate. Some BDCFs include contributions from their short-lived decay products. To account for correlations between parameters used to compute BDCFs, the Biosphere Model generates a table of 1,000 sets of values for each BDCF. These values are entered into the TSPA Input Database as a table of 1,000 values for each parameter. The TSPA-LA Model selects values from this table using the Goldsim variable Bio_index_a. *Sensitivity Name:* MICAC227. *Location in TSPA-LA:* Sections 6.3.11.2 and 6.3.11.3; Table 6.3.11-3. *DTN:* MO0702PAGBDCFS.001_R0 [DIRS 179327]. *References: Biosphere Model Report* (SNL 2007 [DIRS 177399], Sections 1, 6.1, 6.4, 6.4.10, 6.8.10, 6.11 and 6.13; Equations 6.4.10-2, 6.4.10-4, 6.2.10-5 and 6.11-5; Tables 6.11-8 and 6.11-12).
GW_BDCF_MIC_Am241. Groundwater Biosphere Dose Conversion Factor (BDCF) for ^{241}Am in modern interglacial climate ((Sv/year)/(Bq/m^3)). *Distribution:* Discrete. *Range:* 2.16E-07 to 3.30E-06. *Mean:* 8.34E-07. *Standard Deviation:* 4.03E-07. *Additional Information:* See GW_BDCF_MIC_Ac227. *Sensitivity Name:* MICAM241. *Location in TSPA-LA:* Sections 6.3.11.2 and 6.3.11.3; Table 6.3.11-3. *DTN:* MO0702PAGBDCFS.001_R0 [DIRS 179327]. *References: Biosphere Model Report* (SNL 2007 [DIRS 177399], Sections 1, 6.1, 6.4, 6.4.10, 6.8.10, 6.11 and 6.13; Equations 6.4.10-2, 6.4.10-4, 6.2.10-5 and 6.11-5; Tables 6.11-8 and 6.11-12).
GW_BDCF_MIC_Am243. Groundwater Biosphere Dose Conversion Factor (BDCF) for ^{243}Am in modern interglacial climate ((Sv/year)/(Bq/m^3)). *Distribution:* Discrete. *Range:* 2.21E-07 to 3.37E-06. *Mean:* 8.88E-07. *Standard Deviation:* 4.12E-07. *Additional Information:* See GW_BDCF_MIC_Ac227. *Sensitivity Name:* MICAM243. *Location in TSPA-LA:* Sections 6.3.11.2 and 6.3.11.3; Table 6.3.11-3. *DTN:* MO0702PAGBDCFS.001_R0 [DIRS 179327]. *References: Biosphere Model Report* (SNL 2007 [DIRS 177399], Sections 1, 6.1, 6.4, 6.4.10, 6.8.10, 6.11 and 6.13; Equations 6.4.10-2, 6.4.10-4, 6.2.10-5 and 6.11-5; Tables 6.11-8 and 6.11-12).
GW_BDCF_MIC_C14. Groundwater Biosphere Dose Conversion Factor (BDCF) for ^{14}C in modern interglacial climate ((Sv/year)/(Bq/m^3)). *Distribution:* Discrete. *Range:* 7.18E-10 to 2.56E-08. *Mean:* 1.93E-09. *Standard Deviation:* 1.85E-09. *Additional Information:* See GW_BDCF_MIC_Ac227. *Sensitivity Name:* MICC14. *Location in TSPA-LA:* Sections 6.3.11.2 and 6.3.11.3; Table 6.3.11-3. *DTN:* MO0702PAGBDCFS.001_R0 [DIRS 179327]. *References: Biosphere Model Report* (SNL 2007 [DIRS 177399], Sections 1, 6.1, 6.4, 6.4.10, 6.8.10, 6.11 and 6.13; Equations 6.4.10-2, 6.4.10-4, 6.2.10-5 and 6.11-5; Tables 6.11-8 and 6.11-12).
GW_BDCF_MIC_Cl36. Groundwater Biosphere Dose Conversion Factor (BDCF) for ^{36}Cl in modern interglacial climate ((Sv/year)/(Bq/m^3)). *Distribution:* Discrete. *Range:* 1.28E-09 to 3.00E-07. *Mean:* 8.09E-09. *Standard Deviation:* 1.41E-08. *Additional Information:* See GW_BDCF_MIC_Ac227. *Sensitivity Name:* MICCl36. *Location in TSPA-LA:* Sections 6.3.11.2 and 6.3.11.3; Table 6.3.11-3. *DTN:* MO0702PAGBDCFS.001_R0 [DIRS 179327]. *References: Biosphere Model Report* (SNL 2007 [DIRS 177399], Sections 1, 6.1, 6.4, 6.4.10, 6.8.10, 6.11 and 6.13; Equations 6.4.10-2, 6.4.10-4, 6.2.10-5 and 6.11-5; Tables 6.11-8 and 6.11-12).
GW_BDCF_MIC_Cs135. Groundwater Biosphere Dose Conversion Factor (BDCF) for ^{135}Cs in modern interglacial climate ((Sv/year)/(Bq/m^3)). *Distribution:* Discrete. *Range:* 3.1E-09 to 8.48E-08. *Mean:* 1.45E-08. *Standard Deviation:* 1.02E-08. *Additional Information:* See GW_BDCF_MIC_Ac227. *Sensitivity Name:* MICCS135. *Location in TSPA-LA:* Sections 6.3.11.2 and 6.3.11.3; Table 6.3.11-3. *DTN:* MO0702PAGBDCFS.001_R0 [DIRS 179327]. *References: Biosphere Model Report* (SNL 2007 [DIRS 177399], Sections 1, 6.1, 6.4, 6.4.10, 6.8.10, 6.11 and 6.13; Equations 6.4.10-2, 6.4.10-4, 6.2.10-5 and 6.11-5; Tables 6.11-8 and 6.11-12).
GW_BDCF_MIC_Cs137. Groundwater Biosphere Dose Conversion Factor (BDCF) for ^{137}Cs in modern interglacial climate ((Sv/year)/(Bq/m^3)). *Distribution:* Discrete. *Range:* 3.87E-08 to 4.56E-07. *Mean:* 1.30E-07. *Standard Deviation:* 6.33E-08. *Additional Information:* See GW_BDCF_MIC_Ac227. *Sensitivity Name:* MICCS137. *Location in TSPA-LA:* Sections 6.3.11.2 and 6.3.11.3; Table 6.3.11-3. *DTN:* MO0702PAGBDCFS.001_R0 [DIRS 179327]. *References: Biosphere Model Report* (SNL 2007 [DIRS 177399], Sections 1, 6.1, 6.4, 6.4.10, 6.8.10, 6.11 and 6.13; Equations 6.4.10-2, 6.4.10-4, 6.2.10-5 and 6.11-5; Tables 6.11-8 and 6.11-12).

Table K3-3. Detailed Summary of Epistemically Uncertain Variables (i.e., elements of **e**) Considered in the TSPA-LA (TSPA Parameter Name) (Continued)

NOTE: * indicates variable not considered in sensitivity analysis due to correlations.

GW_BDCF_MIC_I129. Groundwater Biosphere Dose Conversion Factor (BDCF) for ^{129}I in modern interglacial climate ((Sv/year)/(Bq/m^3)). *Distribution:* Discrete. *Range:* 8.59E-08 to 1.13E-06. *Mean:* 1.29E-07. *Standard Deviation:* 5.28E-08. *Additional Information:* See GW_BDCF_MIC_Ac227. *Sensitivity Name:* MICI129. *Location in TSPA-LA:* Sections 6.3.11.2 and 6.3.11.3; Table 6.3.11-3. *DTN:* MO0702PAGBDCFS.001_R0 [DIRS 179327]. *References: Biosphere Model Report* (SNL 2007 [DIRS 177399], Sections 1, 6.1, 6.4, 6.4.10, 6.8.10, 6.11 and 6.13; Equations 6.4.10-2, 6.4.10-4, 6.2.10-5 and 6.11-5; Tables 6.11-8 and 6.11-12).
GW_BDCF_MIC_Np237. Groundwater Biosphere Dose Conversion Factor (BDCF) for ^{237}Np in modern interglacial climate ((Sv/year)/(Bq/m^3)). *Distribution:* Discrete. *Range:* 1.06E-07 to 8.05E-07. *Mean:* 2.74E-07. *Standard Deviation:* 9.70E-08. *Additional Information:* See GW_BDCF_MIC_Ac227. *Sensitivity Name:* MICNP237. *Location in TSPA-LA:* Sections 6.3.11.2 and 6.3.11.3; Table 6.3.11-3. *DTN:* MO0702PAGBDCFS.001_R0 [DIRS 179327]. *References: Biosphere Model Report* (SNL 2007 [DIRS 177399], Sections 1, 6.1, 6.4, 6.4.10, 6.8.10, 6.11 and 6.13; Equations 6.4.10-2, 6.4.10-4, 6.2.10-5 and 6.11-5; Tables 6.11-8 and 6.11-12).
GW_BDCF_MIC_Pa231. Groundwater Biosphere Dose Conversion Factor (BDCF) for ^{231}Pa in modern interglacial climate ((Sv/year)/(Bq/m^3)). *Distribution:* Discrete. *Range:* 6.58E-07 to 8.56E-06. *Mean:* 2.44E-06. *Standard Deviation:* 1.02E-06. *Additional Information:* See GW_BDCF_MIC_Ac227. *Sensitivity Name:* MICPA231. *Location in TSPA-LA:* Sections 6.3.11.2 and 6.3.11.3; Table 6.3.11-3. *DTN:* MO0702PAGBDCFS.001_R0 [DIRS 179327]. *References: Biosphere Model Report* (SNL 2007 [DIRS 177399], Sections 1, 6.1, 6.4, 6.4.10, 6.8.10, 6.11 and 6.13; Equations 6.4.10-2, 6.4.10-4, 6.2.10-5 and 6.11-5; Tables 6.11-8 and 6.11-12).
GW_BDCF_MIC_Pu238. Groundwater Biosphere Dose Conversion Factor (BDCF) for ^{238}Pu in modern interglacial climate ((Sv/year)/(Bq/m^3)). *Distribution:* Discrete. *Range:* 2.61E-07 to 2.09E-006. *Mean:* 7.61E-07. *Standard Deviation:* 2.78E-07. *Additional Information:* See GW_BDCF_MIC_Ac227. *Sensitivity Name:* MICPU238. *Location in TSPA-LA:* Sections 6.3.11.2 and 6.3.11.3; Table 6.3.11-3. *DTN:* MO0702PAGBDCFS.001_R0 [DIRS 179327]. *References: Biosphere Model Report* (SNL 2007 [DIRS 177399], Sections 1, 6.1, 6.4, 6.4.10, 6.8.10, 6.11 and 6.13; Equations 6.4.10-2, 6.4.10-4, 6.2.10-5 and 6.11-5; Tables 6.11-8 and 6.11-12).
GW_BDCF_MIC_Pu239. Groundwater Biosphere Dose Conversion Factor (BDCF) for ^{239}Pu in modern interglacial climate ((Sv/year)/(Bq/m^3)). *Distribution:* Discrete. *Range:* 3.49E-07 to 2.93E-06. *Mean:* 9.55E-07. *Standard Deviation:* 3.37E-07. *Additional Information:* See GW_BDCF_MIC_Ac227. *Sensitivity Name:* MICPU239. *Location in TSPA-LA:* Sections 6.3.11.2 and 6.3.11.3; Table 6.3.11-3. *DTN:* MO0702PAGBDCFS.001_R0 [DIRS 179327]. *References: Biosphere Model Report* (SNL 2007 [DIRS 177399], Sections 1, 6.1, 6.4, 6.4.10, 6.8.10, 6.11 and 6.13; Equations 6.4.10-2, 6.4.10-4, 6.2.10-5 and 6.11-5; Tables 6.11-8 and 6.11-12).
GW_BDCF_MIC_Pu240. Groundwater Biosphere Dose Conversion Factor (BDCF) for ^{240}Pu in modern interglacial climate ((Sv/year)/(Bq/m^3)). *Distribution:* Discrete. *Range:* 3.47E-07 to 2.90E-06. *Mean:* 9.51E-07. *Standard Deviation:* 3.35E-07. *Additional Information:* See GW_BDCF_MIC_Ac227. *Sensitivity Name:* MICPU240. *Location in TSPA-LA:* Sections 6.3.11.2 and 6.3.11.3; Table 6.3.11-3. *DTN:* MO0702PAGBDCFS.001_R0 [DIRS 179327]. *References: Biosphere Model Report* (SNL 2007 [DIRS 177399], Sections 1, 6.1, 6.4, 6.4.10, 6.8.10, 6.11 and 6.13; Equations 6.4.10-2, 6.4.10-4, 6.2.10-5 and 6.11-5; Tables 6.11-8 and 6.11-12).
GW_BDCF_MIC_Ra226_Pb210. Groundwater Biosphere Dose Conversion Factor (BDCF) for ^{210}Pb summed into ^{226}Ra in modern interglacial climate ((Sv/year)/(Bq/m^3)). *Distribution:* Discrete. *Range:* 2.90E-06 to 2.82E-05. *Mean:* 6.52E-06. *Standard Deviation:* 2.58E-06. *Additional Information:* BDCF sums were produced for the three primary radionuclides, ^{226}Ra, ^{232}Th and ^{232}U, to include the contribution from their long-lived decay products, which themselves are primary radionuclides, in the case the concentrations of these decay products were not calculated in the TSPA model. BDCFs sums included the following radionuclides: ^{226}Ra + ^{210}Pb; ^{232}Th + ^{228}Ra + ^{228}Th; and ^{232}U + ^{228}Th, assuming radioactive equilibrium with a parent radionuclide. Also see GW_BDCF_MIC_Ac227. *Sensitivity Name:* MICRA226. *Location in TSPA-LA:* Sections 6.3.11.2 and 6.3.11.3; Table 6.3.11-3. *DTN:* MO0702PAGBDCFS.001_R0 [DIRS 179327]. *References: Biosphere Model Report* (SNL 2007 [DIRS 177399], Sections 1, 6.1, 6.4, 6.4.10, 6.8.10, 6.11 and 6.13; Equations 6.4.10-2, 6.4.10-4, 6.2.10-5 and 6.11-5; Tables 6.11-8 and 6.11-12).
GW_BDCF_MIC_Se79. Groundwater Biosphere Dose Conversion Factor (BDCF) for ^{79}Se in modern interglacial climate. ((Sv/year)/(Bq/m^3)). *Distribution:* Discrete. *Range:* 3.62E-09 to 1.51E-06. *Mean:* 2.42E-08. *Standard Deviation:* 7.48E-08. *Additional Information:* See GW_BDCF_MIC_Ac227. *Sensitivity Name:* MICSE79. *Location in TSPA-LA:* Sections 6.3.11.2 and 6.3.11.3; Table 6.3.11-3. *DTN:* MO0702PAGBDCFS.001_R0 [DIRS 179327]. *References: Biosphere Model Report* (SNL 2007 [DIRS 177399], Sections 1, 6.1, 6.4, 6.4.10, 6.8.10, 6.11 and 6.13; Equations 6.4.10-2, 6.4.10-4, 6.2.10-5 and 6.11-5; Tables 6.11-8 and 6.11-12).

Table K3-3. Detailed Summary of Epistemically Uncertain Variables (i.e., elements of **e**) Considered in the TSPA-LA (TSPA Parameter Name) (Continued)

NOTE: * indicates variable not considered in sensitivity analysis due to correlations.

GW_BDCF_MIC_Sn126. Groundwater Biosphere Dose Conversion Factor (BDCF) for ^{126}Sn in modern interglacial climate ((Sv/year)/(Bq/m^3)). *Distribution:* Discrete. *Range:* 8.92E-08 to 1.68E-06. *Mean:* 4.33E-07. *Standard Deviation:* 2.39E-07. *Additional Information:* See GW_BDCF_MIC_Ac227. *Sensitivity Name:* MICSN126. *Location in TSPA-LA:* Sections 6.3.11.2 and 6.3.11.3; Table 6.3.11-3. *DTN:* MO0702PAGBDCFS.001_R0 [DIRS 179327]. *References: Biosphere Model Report* (SNL 2007 [DIRS 177399], Sections 1, 6.1, 6.4, 6.4.10, 6.8.10, 6.11 and 6.13; Equations 6.4.10-2, 6.4.10-4, 6.2.10-5 and 6.11-5; Tables 6.11-8 and 6.11-12).
GW_BDCF_MIC_Sr90. Groundwater Biosphere Dose Conversion Factor (BDCF) for ^{90}Sr in modern interglacial climate ((Sv/year)/(Bq/m^3)). *Distribution:* Discrete. *Range:* 2.51E-08 to 8.60E-08. *Mean:* 3.43E-08. *Standard Deviation:* 6.59E-09. *Additional Information:* See GW_BDCF_MIC_Ac227. *Sensitivity Name:* MICSR90. *Location in TSPA-LA:* Sections 6.3.11.2 and 6.3.11.3; Table 6.3.11-3. *DTN:* MO0702PAGBDCFS.001_R0 [DIRS 179327]. *References: Biosphere Model Report* (SNL 2007 [DIRS 177399], Sections 1, 6.1, 6.4, 6.4.10, 6.8.10, 6.11 and 6.13; Equations 6.4.10-2, 6.4.10-4, 6.2.10-5 and 6.11-5; Tables 6.11-8 and 6.11-12).
GW_BDCF_MIC_Tc99. Groundwater Biosphere Dose Conversion Factor (BDCF) for ^{99}Tc in modern interglacial climate ((Sv/year)/(Bq/m^3)). *Distribution:* Discrete. *Range:* 5.28E-10 to 2.85E-08. *Mean:* 1.12E-09. *Standard Deviation:* 1.26E-09. *Additional Information:* See GW_BDCF_MIC_Ac227. *Sensitivity Name:* MICTC99. *Location in TSPA-LA:* Sections 6.3.11.2 and 6.3.11.3; Table 6.3.11-3. *DTN:* MO0702PAGBDCFS.001_R0 [DIRS 179327]. *References: Biosphere Model Report* (SNL 2007 [DIRS 177399], Sections 1, 6.1, 6.4, 6.4.10, 6.8.10, 6.11 and 6.13; Equations 6.4.10-2, 6.4.10-4, 6.2.10-5 and 6.11-5; Tables 6.11-8 and 6.11-12).
GW_BDCF_MIC_Th229. Groundwater Biosphere Dose Conversion Factor (BDCF) for ^{229}Th in modern interglacial climate ((Sv/year)/(Bq/m^3)). *Distribution:* Discrete. *Range:* 7.43E-07 to 8.05E-06. *Mean:* 2.58E-06. *Standard Deviation:* 1.03E-06. *Additional Information:* See GW_BDCF_MIC_Ac227. *Sensitivity Name:* MICTH229. *Location in TSPA-LA:* Sections 6.3.11.2 and 6.3.11.3; Table 6.3.11-3. *DTN:* MO0702PAGBDCFS.001_R0 [DIRS 179327]. *References: Biosphere Model Report* (MDL-MGR-MD-000001 REV 02, SNL 2007 [DIRS 177399], Sections 1, 6.1, 6.4, 6.4.10, 6.8.10, 6.11 and 6.13; Equations 6.4.10-2, 6.4.10-4, 6.2.10-5 and 6.11-5; Tables 6.11-8 and 6.11-12).
GW_BDCF_MIC_U232. Groundwater Biosphere Dose Conversion Factor (BDCF) for 232U in modern interglacial climate ((Sv/year)/(Bq/m^3)). *Distribution:* Discrete. *Range:* 2.87E-07 to 1.86E-06. *Mean:* 6.04E-07. *Standard Deviation:* 2.17E-07. *Additional Information:* See GW_BDCF_MIC_Ac227. *Sensitivity Name:* MICU232. *Location in TSPA-LA:* Sections 6.3.11.2 and 6.3.11.3; Table 6.3.11-3. *DTN:* MO0702PAGBDCFS.001_R0 [DIRS 179327]. *References: Biosphere Model Report* (SNL 2007 [DIRS 177399], Sections 1, 6.1, 6.4, 6.4.10, 6.8.10, 6.11 and 6.13; Equations 6.4.10-2, 6.4.10-4, 6.2.10-5 and 6.11-5; Tables 6.11-8 and 6.11-12).
GW_BDCF_MIC_U233. Groundwater Biosphere Dose Conversion Factor (BDCF) for ^{233}U in modern interglacial climate ((Sv/year)/(Bq/m^3)). *Distribution:* Discrete. *Range:* 4.13E-08 to 3.13E-07. *Mean:* 8.97E-08. *Standard Deviation:* 3.35E-08. *Additional Information:* See GW_BDCF_MIC_Ac227. *Sensitivity Name:* MICU233. *Location in TSPA-LA:* Sections 6.3.11.2 and 6.3.11.3; Table 6.3.11-3. *DTN:* MO0702PAGBDCFS.001_R0 [DIRS 179327]. *References: Biosphere Model Report* (SNL 2007 [DIRS 177399], Sections 1, 6.1, 6.4, 6.4.10, 6.8.10, 6.11 and 6.13; Equations 6.4.10-2, 6.4.10-4, 6.2.10-5 and 6.11-5; Tables 6.11-8 and 6.11-12).
GW_BDCF_MIC_U234. Groundwater Biosphere Dose Conversion Factor (BDCF) for ^{234}U in modern interglacial climate ((Sv/year)/(Bq/m^3)). *Distribution:* Discrete. *Range:* 3.96E-08 to 2.20E-07. *Mean:* 8.19E-08. *Standard Deviation:* 2.81E-08. *Additional Information:* See GW_BDCF_MIC_Ac227. *Sensitivity Name:* MICU234. *Location in TSPA-LA:* Sections 6.3.11.2 and 6.3.11.3; Table 6.3.11-3. *DTN:* MO0702PAGBDCFS.001_R0 [DIRS 179327]. *References: Biosphere Model Report* (SNL 2007 [DIRS 177399], Sections 1, 6.1, 6.4, 6.4.10, 6.8.10, 6.11 and 6.13; Equations 6.4.10-2, 6.4.10-4, 6.2.10-5 and 6.11-5; Tables 6.11-8 and 6.11-12).
GW_BDCF_MIC_U238. Groundwater Biosphere Dose Conversion Factor (BDCF) for ^{238}U in modern interglacial climate ((Sv/year)/(Bq/m^3)). *Distribution:* Discrete. *Range:* 3.85E-08 to 2.07E-07. *Mean:* 7.87E-08. *Standard Deviation:* 2.62E-08. *Additional Information:* See GW_BDCF_MIC_Ac227. *Sensitivity Name:* MICU238. *Location in TSPA-LA:* Sections 6.3.11.2 and 6.3.11.3; Table 6.3.11-3. *DTN:* MO0702PAGBDCFS.001_R0 [DIRS 179327]. *References: Biosphere Model Report* (SNL 2007 [DIRS 177399], Sections 1, 6.1, 6.4, 6.4.10, 6.8.10, 6.11 and 6.13; Equations 6.4.10-2, 6.4.10-4, 6.2.10-5 and 6.11-5; Tables 6.11-8 and 6.11-12).

Table K3-3. Detailed Summary of Epistemically Uncertain Variables (i.e., elements of **e**) Considered in the TSPA-LA (TSPA Parameter Name) (Continued)

NOTE: * indicates variable not considered in sensitivity analysis due to correlations.

GWSPD. Logarithm of the scale factor used to characterize uncertainty in groundwater specific discharge (dimensionless). *Distribution:* Piecewise uniform. *Range:* -0.951 to 0.951. *Additional Information:* Uncertainty exists in the groundwater specific discharge in the SZ. The uncertainty is captured by the groundwater specific discharge multiplier. The uncertainty in GWSPD is applied to all of the climate states. To treat the one- and three-dimensional transport through the SZ consistently, the sampled values used to generate the saturated zone breakthrough curves are also used in the TSPA-LA Model. These values are tabulated as 200 sets of values for the SZ parameters, accounting for appropriate correletions, and are entered into the TSPA model as a table of 200 values for each parameter. The TSPA-LA Model selects values from this table using the Goldsim variable SZ_index_a. *Sensitivity Name:* SZGWSPDM. *Location in TSPA-LA:* Section 6.3.10.2; Table 6.3.10-2. *DTN:* SN0702PASZFTMA.002_R1 [DIRS 183471]. *References: Saturated Zone Flow and Transport Model Abstraction* (SNL 2008 [DIRS 183750], Sections 6.5.1.2[a], 6.5.2.1[a], 6.5.3[a] and 8.1[a]; Tables 6-7[a], 7-1[a] and A-1[a]; Figure 6-2[a]).
HAVO. Ratio of horizontal anisotropy (north-south over east-west) in the permeability of the SZ volcanic units (dimensionless). *Distribution:* Piecewise uniform. *Range:* 0.05 to 20. *Additional Information:* The average specific discharge varies as a function of the horizontal anisotropy. The values of flow path lengths are given for each of the four source regions beneath the repository, as functions of the parameter HAVO. To treat the one- and three-dimensional transport through the SZ consistently, the sampled values used to generate the saturated zone breakthrough curves are also used in the TSPA-LA Model. These values are tabulated as 200 sets of values for the SZ parameters, accounting for appropriate correletions, and are entered into the TSPA model as a table of 200 values for each parameter. The TSPA-LA Model selects values from this table using the Goldsim variable SZ_index_a. *Sensitivity Name:* SZRAHAVO. *Location in TSPA-LA:* Sections 6.3.10.2 and 6.3.10.5; Table 6.3.10-2. *DTN:* SN0702PASZFTMA.002_R1 [DIRS 183471]. *References: Saturated Zone Flow and Transport Model Abstraction* (SNL 2008 [DIRS 183750], Sections 6.4, 6.5.1.2[a], 6.5.2.1 and 6.5.2.10; Tables 4-3, 6-5[a], 6-6[a], 6-8, 7-1[a] and A-1[a]; Figure 6-5[a]).
HFO_SA_a. Hydrous ferric oxide (HFO) surface area (m^2/g). *Distribution:* Truncated log normal. *Range:* 68 to 600. *Mean:* 275.6. *Standard Deviation:* 113.4. *Symbol:* s_{HFO}. *Additional Information:* See Goethite_SA_a. *Sensitivity Name:* HFOSA. *Location in TSPA-LA:* Table 6.3.8-4; S_{CP} in Equation 6.3.8-19. *DTN:* SN0703PAEBSRTA.001_R3 [DIRS 183217]. *References: EBS Radionuclide Transport Abstraction* (SNL 2007 [DIRS 177407], Sections 4.1.2, 6.3.4.2.3.1, 6.3.4.3.3, 6.5.2.2.1 and Appendix K; Equation 6.3.4.2.3.1-1; Tables 4.1-14, 4.1-19, 6.3-7, 6.5-7 and 8.2-4).
HFO_Site_Density_a. Sorption site density for hydrous ferric oxide (HFO) ($1/nm^2$). *Distribution:* Discrete. *Range:* 0.56 to 5.65. *Symbol:* $N_{S,HFO}$. *Additional Information:* The sorption density and specific surface area data for goethite and for HFO were compiled from many laboratory studies mainly addressing the single metal sorption from aqueous solutions. The sorption density data for HFO were compiled from Dzombak and Morel (1990 [DIRS 105483]), which is widely referenced in the sorption modeling literature. *Sensitivity Name:* HFOSITED. *Location in TSPA-LA:* Table 6.3.8-3. *DTN:* SN0703PAEBSRTA.001_R3 [DIRS 183217]. *References: EBS Radionuclide Transport Abstraction* (SNL 2007 [DIRS 177407], Sections 4.1.2 and 6.3.4.2.3.1; Equation 6.3.4.2.3.1-1; Tables 4.1-13, 6.3-6 and 8.2-2).
HLW_Diss_kE_Acidic_a. Effective rate coefficient (affinity term) for the dissolution of HLW glass in CDSP waste packages under low pH conditions ($g/(m^2d)$). *Distribution:* Triangular. *Range:* 8.41E+03 to 1.15E+07. *Mode:* 8.41E+03. *Symbol:* k_{E_acid}, k_{E_acidic}, k_E. *Additional Information:* HLW_Diss_kE_Acidic_a and HLW_Diss_kE_Alkaline_a define the uncertain parameters for k_{eff} in the rate equation under acidic and alkaline conditions, respectively. *Sensitivity Name:* HLWDRACD. *Location in TSPA-LA:* Sections 6.3.7.4.3.2 and 6.3.7.4.3.3; Table 6.3.7-32; Equation 6.3.7-8. *DTN:* MO0502ANLGAMR1.016_R0 [DIRS 172830]. *References: Defense HLW Glass Degradation Model* (BSC 2004 [DIRS 169988], Sections 6.5.1, 6.5.2.5, 6.5.2.6, 6.6, 6.7, 8.1 and 8.2.2; Equations 13, 31, 32 and 50; Tables 6-14 and 8-1).
HLW_Diss_kE_Alkaline_a. Effective rate coefficient (affinity term) for the dissolution of HLW glass in CDSP waste packages under high pH conditions ($g/(m^2d)$). *Distribution:* Triangular. *Range:* 2.82E+01 to 3.47E+04. *Mode:* 2.82E+01. *Symbol:* $k_{E\_alkaline}$, k_E. *Additional Information:* See HLW_Diss_kE_Acidic_a. *Sensitivity Name:* HLWDRALK. *Location in TSPA-LA:* Sections 6.3.7.4.3.2 and 6.3.7.4.3.3; Table 6.3.7-32; Equation 6.3.7-8. *DTN:* MO0502ANLGAMR1.016_R0 [DIRS 172830]. *References: Defense HLW Glass Degradation Model* (BSC 2004 [DIRS 169988], Sections 6.4.2, 6.5.1, 6.5.2.4, 6.5.2.6, 6.6, 6.7, 8.1 and 8.2.2; Equations 13 and 51; Tables 6-14 and 8-1).

Table K3-3. Detailed Summary of Epistemically Uncertain Variables (i.e., elements of **e**) Considered in the TSPA-LA (TSPA Parameter Name) (Continued)

NOTE: * indicates variable not considered in sensitivity analysis due to correlations.

HLW_Mass_Uncert_a. Scale factor used to characterize uncertainty in radionuclide content of HLW glass (dimensionless). *Distribution:* Triangular. *Range:* 0.7 to 1.5. *Most Likely:* 1. *Additional Information:* See CSNF_Mass_Uncert_a. *Sensitivity Name:* HLWMASS. *Location in TSPA-LA:* Sections 6.3.7.1.2 and 6.3.7.1.3; Table 6.3.7-7. *DTN:* SN0310T0505503.004_R0 [DIRS 168761]. *References: Initial Radionuclides Inventory* (SNL 2007 [DIRS 180472], Sections 6.6.3, 6.7 and 7; Table 7-2),
HLWG_Rind_SA_a. Specific surface area of HLWG degradation rind (m^2/g). *Distribution:* Uniform. *Range:* 10 to 38. *Symbol:* S_{HLWG}. *Additional Information:* See Density_CSNF_Rind_a. The HLW glass rind specific surface area is a new sampled parameter whose range is based on that of kaolinite, since glass degradation products are clay-like in nature. *Sensitivity Name:* HLWGRNDS. *Location in TSPA-LA:* Table 6.3.8-4. *DTN:* SN0703PAEBSRTA.001_R3 [DIRS 183217]. *References: EBS Radionuclide Transport Abstraction* (SNL 2007 [DIRS 177407], Sections 6.3.4.6.2, 6.5.2.2.2 and 6.5.2.2.2.2; Equation 6.3.4.6.2-2; Tables 6.5-9 and 8.2-4).
IGERATE. Frequency of occurrence of volcanic eruptive events (yr^{-1}). *Calculated by:* Igneous_Event_Prob_a x 0.083. *Range:* 0 to 6.44E-08. *Correlation:* Correlated to Igneous_Event_Prob_a with a correlation coefficient of 1. *Additional Information:* Volcanic eruptive events may occur in conjunction with an igneous intrusion event. The frequency of eruptive events that intersect waste is estimated as described in Appendix J, Equation J7.5-3. *Sensitivity Name:* IGERATE. *Location in TSPA-LA:* Section 6.5.2.1.1; Appendix J; Equation J7.5-3. *Output DTN:* MO0708TSPAGENT.000_R0 [DIRS 183000]. *References: Number of Waste Packages Hit by Igneous Events* (SNL 2007 [DIRS 177432], Table 6-5; Figure 7-2).
Igneous_Event_Prob_a. Frequency of intersection of the repository footprint by a volcanic event (yr^{-1}). *Distribution:* Piecewise uniform. *Range:* 0 to 7.76E-07. *Additional Information:* The probability of an igneous event is the annual frequency of an intersection of the repository by a volcanic dike. The parameter Igneous_Event_Prob_a is used in the TSPA model to determine the probability of an igneous event intersecting the repository footprint. An igneous event includes an intrusion by magma and may also include eruptive conduits intersecting the repository. Igneous_Event_Prob_a is treated as an epistemic uncertainty and is sampled from the distribution for each TSPA model realization. The resulting value is used as the annual frequency of igneous events in the calculation of expected value of dose resulting from igneous intrusion and igneous eruptive events. *Sensitivity Name:* IGRATE. *Location in TSPA-LA:* Table 6.5-2. *DTN:* LA0307BY831811.001_R0 [DIRS 164713], output data file PVHA-4PA.DST. *References: Characterize Framework for Igneous Activity at Yucca Mountain, Nevada* (BSC 2004 [DIRS 169989], Sections 6.1, 6.1.1, 6.3, 6.3.1.5, 6.3.1.8, 6.4.2, 6.5, 6.5.1.1, 6.5.2.1 and Appendix A; Figures 6-8, 6-23 and 6-24; Tables 6-5 and 7-1).
Infiltration_Scenario_a. Pointer variable for determining infiltration conditions: 10th, 30th, 50th or 90th percentile infiltration scenario (dimensionless). *Distribution:* Discrete. *Range:* 1 to 4. *Additional Information:* This parameter provides the weighting factors for the three infiltration scenarios used in the TSPA-LA analysis. The parameters contained within the TSPA parameter of Infiltration_Scenario_a correspond to infiltration uncertainty scenarios 1 through 4, going from the lowest infiltration scenario to the highest infiltration scenario. The use of the different percentile infiltration values is intended to cover the uncertainties associated with the infiltration for each climate. The two future climatic scenarios, the monsoon and glacial-transition periods, are used to account for possible climate-induced changes in precipitation and net infiltration. *Sensitivity Name:* INFIL. *Location in TSPA-LA:* Section 6.3.1.2; Tables 6.3.1-2 and 6.3.5-4. *DTN:* LB0701PAWFINFM.001_R0 [DIRS 179283]. *References: UZ Flow Models and Submodels* (SNL 2007 [DIRS 184614], Sections 6.1.4, 6.2.3, 6.2.5, 6.3.4, 6.6.1, 6.8.4 and 6.10.1; Tables 6.1-2 and 6.1-3).
Initial_Release_Frac_Cs_a. The initial release fraction of ^{137}Cs in a CSNF waste package (dimensionless). *Distribution:* Triangular. *Range:* 0.0039 to 0.1106. *Mode:* 0.0363. *Symbol:* f_i. *Additional Information:* Only a fraction of the inventory is immediately available for release upon the failure of the cladding within a failed waste package. Furthermore, only Cs, I, Tc and Sr are immediately available for release. The initial release fraction is set at the beginning of each realization and held constant during each realization. *Sensitivity Name:* INRFRCCS. *Location in TSPA-LA:* Sections 6.3.7.4.1.2 and 6.3.7.4.1.3; Table 6.3.7-29. *DTN:* MO0404ANLSF001.001R0 [DIRS 169007]. *References: CSNF Waste Form Degradation: Summary Abstraction* (BSC 2004 [DIRS 169987], Sections 1, 4.1.1, 6.3, 7.1.1 and 8.2; Equations 1 and 3; Tables 6-3, 7-2, 7-3, 8-1 and 8-4).
Initial_Release_Frac_I_a. The initial release fraction of ^{129}I in a CSNF waste package (dimensionless). *Distribution:* Triangular. *Range:* 0.0204 to 0.2675. *Mode:* 0.1124. *Symbol:* f_i. *Additional Information:* See Initial_Release_Frac_Cs_a. *Sensitivity Name:* INRFRCI. *Location in TSPA-LA:* Sections 6.3.7.4.1.2 and 6.3.7.4.1.3; Table 6.3.7-29. *DTN:* MO0404ANLSF001.001_R0 [DIRS 169007]. *References: CSNF Waste Form Degradation: Summary Abstraction* (BSC 2004 [DIRS 169987], Sections 1, 4.1.1, 6.3, 7.1.1 and 8.2; Equations 1 and 3; Tables 6-3, 7-2, 7-3, 8-1 and 8-4).

Table K3-3. Detailed Summary of Epistemically Uncertain Variables (i.e., elements of **e**) Considered in the TSPA-LA (TSPA Parameter Name) (Continued)

NOTE: * indicates variable not considered in sensitivity analysis due to correlations.

Initial_Release_Frac_Sr_a. The initial release fraction of ^{90}Sr in a CSNF waste package (dimensionless). *Distribution:* Triangular. *Range:* 0.0002 to 0.0025. *Mode:* 0.0009. *Symbol:* f_i. *Additional Information:* See Initial_Release_Frac_Cs_a. *Sensitivity Name:* INRFRCSR. *Location in TSPA-LA:* Sections 6.3.7.4.1.2 and 6.3.7.4.1.3; Table 6.3.7-29. *DTN:* MO0404ANLSF001.001_R0 [DIRS 169007]. *References: CSNF Waste Form Degradation: Summary Abstraction* (BSC 2004 [DIRS 169987], Sections 1, 4.1.1, 6.3, 7.1.1 and 8.2; Equations 1 and 3; Tables 6-3, 7-2, 7-3, 8-1 and 8-4).
Initial_Release_Frac_Tc_a. The initial release fraction of ^{99}Tc in a CSNF waste package (dimensionless). *Distribution:* Triangular. *Range:* 0.0001 to 0.0026. *Mode:* 0.001. *Symbol:* f_i. *Additional Information:* See Initial_Release_Frac_Cs_a. *Sensitivity Name:* INRFRCTC. *Location in TSPA-LA:* Sections 6.3.7.4.1.2 and 6.3.7.4.1.3; Table 6.3.7-29. *DTN:* MO0404ANLSF001.001_R0 [DIRS 169007]. *References: CSNF Waste Form Degradation: Summary Abstraction* (BSC 2004 [DIRS 169987], Sections 1, 4.1.1, 6.3, 7.1.1 and 8.2; Equations 1 and 3; Tables 6-3, 7-2, 7-3, 8-1 and 8-4).
Inpkg_IStr_2DHLW_NS_Rand_a. Pointer variable used to determine ionic strength for 2DHLW Cell (Cell 1a) of CDSP waste packages under vapor influx conditions (dimensionless). *Distribution:* Uniform. *Range:* 0 to 1. *Additional Information:* The parameter Inpkg_IStr_2DHLW_NS_Rand_a selects a percentile for the distribution of uncertainty in ionic strength in DHLW waste packages for vapor influx conditions. In the vapor influx environment, the distribution of uncertainty the ionic strength is a log-triangular distribution with vertices that are a function of the vapor flux rate through the failed waste package. The vapor flux rate into the failed waste package is sampled by IPC_NDB_Vapor_Flux_a. *Sensitivity Name:* IS2DHLNS. *Location in TSPA-LA:* Section 6.3.7.2.2 Part III. *DTN:* SN0702PAIPC1CA.001_R2 [DIRS 180451], Spreadsheet: Abstr 2DHLW No Drip Ion Str.xls. *References: In-Package Chemistry Abstraction* (SNL 2007 [DIRS 180506], Sections 6.5.2[a], 6.10.8.2[a], 6.10.9.3[a] and 8.2.2[a]).
Inpkg_IStr_2DHLW_S_Rand_a. Pointer variable used to determine ionic strength for 2DHLW Cell (Cell 1a) of CDSP waste packages under liquid influx conditions (dimensionless). *Distribution:* Uniform. *Range:* 0 to 1. *Additional Information:* The parameter Inpkg_IStr_2DHLW_S_Rand_a selects a percentile for the distribution of uncertainty in ionic strength in DHLW waste packages for liquid influx conditions. Under liquid influx conditions, the distribution of uncertainty the ionic strength is a log-triangular distribution the vertices of which are a function of the flow rate through the failed waste package and hence may change with time. *Sensitivity Name:* IS2DHLS. *Location in TSPA-LA:* Section 6.3.7.2.2 Part III. *DTN:* SN0702PAIPC1CA.001_R2 [DIRS 180451], Spreadsheet: Abstr 2DHLW Seepage Ion Str 2.xls. *References: In-Package Chemistry Abstraction* (SNL 2007 [DIRS 180506], Sections 6.5.1[a], 6.10.2[a], 6.10.9.2[a] and 8.2.2[a]).
Inpkg_IStr_2MCO_NS_Rand_a. Pointer variable used to determine ionic strength for 2MCO Cell (Cell 1b) of CDSP waste packages under vapor influx conditions (dimensionless). *Distribution:* Uniform. *Range:* 0 to 1. *Additional Information:* See Inpkg_IStr_2DHLW_NS_Rand_a. *Sensitivity Name:* IS2MCONS. *Location in TSPA-LA:* Section 6.3.7.2.2 Part III. *DTN:* SN0702PAIPC1CA.001_R2 [DIRS 180451], Spreadsheet: Abstr 2MCO No Drip Ion Str.xls. *References: In-Package Chemistry Abstraction* (SNL 2007 [DIRS 180506], Sections 6.5.2[a], 6.10.8.2[a], 6.10.9.3[a] and 8.2.2[a]).
Inpkg_IStr_2MCO_S_Rand_a. Pointer variable used to determine ionic strength for 2MCO Cell (Cell 1b) of CDSP waste packages under liquid influx conditions (dimensionless). *Distribution:* Uniform. *Range:* 0 to 1. *Additional Information:* See Inpkg_IStr_2DHLW_S_Rand_a. *Sensitivity Name:* IS2MCOS. *Location in TSPA-LA:* Section 6.3.7.2.2 Part III. *DTN:* SN0702PAIPC1CA.001_R2 [DIRS 180451], Spreadsheet: Abstr 2MCO Seepage Ion Str 2.xls. *References: In-Package Chemistry Abstraction* (SNL 2007 [DIRS 180506], Sections 6.5.1[a], 6.10.2[a], 6.10.9.2[a] and 8.2.2[a]).
Inpkg_IStr_CSNF_NS_Rand_a. Pointer variable used to determine ionic strength for CSNF Cell under vapor influx conditions (dimensionless). *Distribution:* Uniform. *Range:* 0 to 1. *Additional Information:* See discussion forInpkg_IStr_2DHLW_NS_Rand_a. *Sensitivity Name:* ISCSNS. *Location in TSPA-LA:* Section 6.3.7.2.2 Part III. *DTN:* SN0702PAIPC1CA.001_R2 [DIRS 180451], Spreadsheet: Abstr CSNF No Drip Ion Str.xls. *References: In-Package Chemistry Abstraction* (SNL 2007 [DIRS 180506], Sections 6.5.2[a], 6.10.8.2[a], 6.10.9.3[a] and 8.2.2[a]).
Inpkg_IStr_CSNF_S_Rand_a. Pointer variable used to determine ionic strength for CSNF Cell under liquid influx conditions (dimensionless). *Distribution:* Uniform. *Range:* 0 to 1. *Additional Information:* See Inpkg_IStr_2DHLW_S_Rand_a. *Sensitivity Name:* ISCSS. *Location in TSPA-LA:* Section 6.3.7.2.2 Part III. *DTN:* SN0702PAIPC1CA.001_R2 [DIRS 180451], Spreadsheet: Abstr CSNF Seepage Ion Str 2.xls. *References: In-Package Chemistry Abstraction* (SNL 2007 [DIRS 180506], Sections 6.5.1[a], 6.10.2[a], 6.10.9.2[a] and 8.2.2[a]).

Table K3-3. Detailed Summary of Epistemically Uncertain Variables (i.e., elements of **e**) Considered in the TSPA-LA (TSPA Parameter Name) (Continued)

NOTE: * indicates variable not considered in sensitivity analysis due to correlations.

lnpkg_pH_2DHLW_NS_Rand_a. Pointer variable used to determine pH in 2DHLW Cell (Cell 1a) of CDSP waste packages under vapor influx conditions (dimensionless). *Distribution:* Uniform. *Range:* 0 to 1. *Additional Information:* The TSPA implementation of the pH abstraction is discretized into three models, one for CSNF waste packages and two for CDSP waste packages (DHLW and 2MCO). The pH is a function of pCO_2 and the logarithm of ionic strength in the package. Two dimensional look-up tables provide values for the maximum and minimum pH as a function of pCO_2 and the logarithm of ionic strength, for three waste types (DHLW, 2MCO and CSNF) and for liquid influx and vapor influx conditions. Linear interpolation is used to determine maximum and minimum pH. Then, a sampled value between 0 and 1 selects a pH value between the minimum and maximum pH values, using linear interpolation between the minimum and the maximum. The pH selection is performed within each percolation subregion environment. The parameter lnpkg_pH_2DHLW_NS_Rand_a selects the value between 0 and 1 that is used to determine pH for DHLW waste packages in vapor influx conditions. *Sensitivity Name:* PH2DHLNS. *Location in TSPA-LA:* Section 6.3.7.2.2 Part IV. *DTN:* SN0702PAIPC1CA.001_R2 [DIRS 180451], Spreadsheet: Abstr 2DHLW No Drip pH.xls. *References: In-Package Chemistry Abstraction* (SNL 2007 [DIRS 180506], Sections 6.3.4[a], 6.10.1[a] and 8.2.1[a]).
lnpkg_pH_2DHLW_S_Rand_a. Pointer variable used to determine pH in 2DHLW Cell (Cell 1a) of CDSP waste packages under liquid influx conditions (dimensionless). *Distribution:* Uniform. *Range:* 0 to 1. *Additional Information:* See lnpkg_pH_2DHLW_NS_Rand_a. *Sensitivity Name:* PH2DHLS. *Location in TSPA-LA:* Section 6.3.7.2.2 Part IV. *DTN:* SN0702PAIPC1CA.001_R2 [DIRS 180451], Spreadsheet: Abstr 2DHLW Seepage pH.xls. *References: In-Package Chemistry Abstraction* (SNL 2007 [DIRS 180506], Sections 6.3.4[a], 6.10.1[a] and 8.2.1[a]).
lnpkg_pH_2MCO_NS_Rand_a. Pointer variable used to determine pH in 2MCO Cell (Cell 1b) of CDSP waste packages under vapor influx conditions (dimensionless). *Distribution:* Uniform. *Range:* 0 to 1. *Additional Information:* See lnpkg_pH_2DHLW_NS_Rand_a. *Sensitivity Name:* PH2MCONS. *Location in TSPA-LA:* Section 6.3.7.2.2 Part IV. *DTN:* SN0702PAIPC1CA.001_R2 [DIRS 180451], Spreadsheet: Abstr 2MCO No Drip pH.xls. *References: In-Package Chemistry Abstraction* (SNL 2007 [DIRS 180506], Sections 6.3.4[a], 6.10.1[a] and 8.2.1[a]).
lnpkg_pH_2MCO_S_Rand_a. Pointer variable used to determine pH in 2MCO Cell (Cell 1b) of CDSP waste packages under liquid influx conditions (dimensionless). *Distribution:* Uniform. *Range:* 0 to 1. *Additional Information:* See lnpkg_pH_2DHLW_NS_Rand_a. *Sensitivity Name:* PH2MCOS. *Location in TSPA-LA:* Section 6.3.7.2.2 Part IV. *DTN:* SN0702PAIPC1CA.001_R2 [DIRS 180451], Spreadsheet: Abstr 2MCO Seepage pH.xls. *References: In-Package Chemistry Abstraction* (SNL 2007 [DIRS 180506], Sections 6.3.4[a], 6.10.1[a] and 8.2.1[a]; Table 6-21[a]).
lnpkg_pH_CSNF_NS_Rand_a. Pointer variable used to determine pH in CSNF Cell1 under vapor influx conditions (dimensionless). *Distribution:* Uniform. *Range:* 0 to 1. *Additional Information:* See lnpkg_pH_2DHLW_NS_Rand_a. *Sensitivity Name:* PHCSNS. *Location in TSPA-LA:* Section 6.3.7.2.2 Part IV. *DTN:* SN0702PAIPC1CA.001_R2 [DIRS 180451], Spreadsheet: Abstr CSNF No Drip pH.xls. *References: In-Package Chemistry Abstraction* (SNL 2007 [DIRS 180506], Sections 6.3.4[a], 6.10.1[a] and 8.2.1[a]).
lnpkg_pH_CSNF_S_Rand_a. Pointer variable used to determine pH in CSNF Cell1 under liquid influx conditions (dimensionless). *Distribution:* Uniform. *Range:* 0 to 1. *Additional Information:* See lnpkg_pH_2DHLW_NS_Rand_a. *Sensitivity Name:* PHCSS. *Location in TSPA-LA:* Section 6.3.7.2.2 Part IV. *DTN:* SN0702PAIPC1CA.001_R2 [DIRS 180451], Spreadsheet: Abstr CSNF Seepage pH.xls. *References: In-Package Chemistry Abstraction* (SNL 2007 [DIRS 180506], Sections 6.3.4[a], 6.10.1[a] and 8.2.1[a]).
Invert_Diff_Coeff_Uncert_a. Exponential term representing uncertainty in the invert diffusion coefficient (dimensionless). *Distribution:* Truncated normal. *Range:* -0.621 to 0.687. *Mean:* 0.033. *Standard Deviation:* 0.218. *Symbol:* ND. *Additional Information:* ND is in the exponent because the residuals are calculated in the log-log space of the statistical fit. This statistical fit is the submodel for the invert diffusion coefficient to be used for the TSPA. The uncertainty in the invert diffusion coefficient ranges over a factor of 20 and essentially encompasses the variable breakthrough times that could occur from including the longitudinal dispersion. *Sensitivity Name:* EBSDIFCF. *Location in TSPA-LA:* Section 6.3.8.2.4; Table 6.3.8-4; Equation 6.3.8-24. *DTN:* SN0703PAEBSRTA.001_R3 [DIRS 183217]. *References: EBS Radionuclide Transport Abstraction* (SNL 2007 [DIRS 177407], Sections 6.3.1.2, 6.3.4.1.1, 7.2.2 and Appendix G; Table 8.2-4; Equation 6.3.4.1.1-22).

Table K3-3. Detailed Summary of Epistemically Uncertain Variables (i.e., elements of **e**) Considered in the TSPA-LA (TSPA Parameter Name) (Continued)

NOTE: * indicates variable not considered in sensitivity analysis due to correlations.

Kd_Am_Al. Americium sorption coefficient in alluvium (mL/g). *Distribution:* Truncated normal. *Range:* 1000 to 10000. *Mean/Median/Mode:* 5500. *Standard Deviation:* 1500. *Correlation:* See SN0702PASZFTMA.001 [DIRS 179504]. *Additional Information:* A linear, equilibrium, sorption coefficient, K_d, is considered appropriate for the radionuclides that exhibit sorption during transport because of experimental observations that establish the adequacy of this approach. The K_d model also depends on chemical equilibrium between the aqueous phase and sorbed phase of a given species. The K_d model determines transport retardation. To treat the one- and three-dimensional transport through the SZ consistently, the sampled values used to generate the saturated zone breakthrough curves are also used in the TSPA-LA Model. These values are tabulated as 200 sets of values for the SZ parameters, accounting for appropriate correletions, and are entered into the TSPA model as a table of 200 values for each parameter. The TSPA-LA Model selects values from this table using the Goldsim variable SZ_index_a. *Sensitivity Name:* SZKDAMAL. *Location in TSPA-LA:* Section 6.3.10.2; Table 6.3.10-2. *DTN:* SN0702PASZFTMA.002_R1 [DIRS 183471]. *References: Saturated Zone Flow and Transport Model Abstraction* (SNL 2008 [DIRS 183750], Sections 6.3.1, 6.5.1.1, 6.5.1.2 and 6.5.2.8; Tables 4-3, 6-8, A-1[a] and B-1; Equations 6-2, 6-3 and 6-26).
Kd_Am_Col. Americium sorption coefficient onto smectite colloids (mL/g). *Distribution:* Piecewise uniform. *Range:* 1.00E+04 to 1.00E+07. *Additional Information:* In addition to the transport of radionuclides as solutes in groundwater, radionuclides may also be sorbed onto colloids and travel through the SZ to the accessible environment. The radionuclides may be reversibly or irreversibly sorbed onto colloids. A retardation factor is established for radionuclides that are irreversibly sorbed onto colloids. Implied in the use of a retardation factor to describe colloid transport is that colloid filtration and detachment rates are fast relative to groundwater transport times through the system. In addition, a small fraction of colloids, also called the "fast fraction," is transported unretarded through the SZ, based on groundwater transport times. Radionuclides that are reversibly sorbed onto colloids are in equilibrium with the aqueous phase and the geologic medium. In this mode of transport, the effective retardation of these radionuclides during transport in the SZ depends on the sorption of radionuclides to colloids, the concentration of colloids in the groundwater, and the sorption coefficient of the radionuclide onto the geologic medium. To treat the one- and three-dimensional transport through the SZ consistently, the sampled values used to generate the saturated zone breakthrough curves are also used in the TSPA-LA Model. These values are tabulated as 200 sets of values for the SZ parameters, accounting for appropriate correletions, and are entered into the TSPA model as a table of 200 values for each parameter. The TSPA-LA Model selects values from this table using the Goldsim variable SZ_index_a. *Sensitivity Name:* SZKDAMCO. *Location in TSPA-LA:* Section 6.3.10.2; Table 6.3.10-2. *DTN:* SN0702PASZFTMA.002_R1 [DIRS 183471]. *References: Saturated Zone Flow and Transport Model Abstraction* (SNL 2008 [DIRS 183750], Sections 6.5.1.1, 6.5.1.2, 6.5.2.8 and 6.5.2.12; Tables 4-3, 6-8, A-1[a] and B-1; Equations 6-4 and 6-26; Figure 6-24).
Kd_Am_Rev_Smectite_a. Distribution coefficient for reversible sorption of americium to waste form (smectite) colloids (mL/g). *Distribution:* Piecewise uniform. *Range:* 1.00E+04 to 1.00E+07. *Symbol:* $Kd_{,Am,coll,wf}$. *Additional Information:* K_d value for combined adsorption and desorption of americium on waste form, iron oxide–oxyhydroxide, and groundwater colloids. This value is used to determine effective reversibility of the radionuclides on colloids according to the relationship: $RN_{adsorbed/desorbed} = RN_{dissolved} \times K_{d,RN} \times M_{colloid}$, where RN = radionuclide, $K_{d,RN}$ = sorption coefficient (ml/g) for radionuclide RN, and $M_{colloid}$ = concentration of colloids in moles/L. *Sensitivity Name:* KDAMSMEC. *Location in TSPA-LA:* Sections 6.3.7.6.2 and 6.3.7.6.3; Equation 6.3.7-20; Tables 6.3.7-62 and 6.3.7-66. *DTN:* MO0701PASORPTN.000_R1 [DIRS 180391]. *References: Waste Form and In-Drift Colloids-Associated Radionuclide Concentrations: Abstraction and Summary* (SNL 2007 [DIRS 177423], Sections 4.1.1, 6.3.2.2, 6.3.12.1 and 6.6.8; Equations 6-13 and 6-15; Figure 6-24c; Tables 6-15 and 6-24).
Kd_Am_Rev_U_Col_a. Distribution coefficient for reversible sorption of americium onto uranophane colloids (mL/g). *Distribution:* Log uniform. *Range:* 5 to 1.00E+04. *Symbol:* $Kd_{Am,coll,uranophane}$. *Additional Information:* K_d is an equilibrium sorption coefficient used to approximate the partitioning of dissolved radionuclide between colloids and fluid. Values are based on analogue sorption studies on closely related phases. Reversible sorption is calculated from the sampled mass concentration of uranophane colloids, K_d values describing the distribution of radionuclides between the fluid and the U(VI) phase (uranophane) colloids, and the dissolved concentration of radionuclides as calculated by the TSPA-LA model. *Sensitivity Name:* KDAMCOL. *Location in TSPA-LA:* Sections 6.3.7.6.2 and 6.3.7.6.3; Equation 6.3.7-20; Table 6.3.7-64. *DTN:* MO0701PACSNFCP.000_R1 [DIRS 180439]. *References: Waste Form and In-Drift Colloids-Associated Radionuclide Concentrations: Abstraction and Summary* (SNL 2007 [DIRS 177423], Sections 4.1.1, 6.3.2.2, 6.3.2.6, 6.3.12.1, 6.5.1.3, 6.6.4 and 6.6.8; Equations 6-13 and 6-15; Tables 6-9 and 6-24).

Table K3-3. Detailed Summary of Epistemically Uncertain Variables (i.e., elements of **e**) Considered in the TSPA-LA (TSPA Parameter Name) (Continued)

NOTE: * indicates variable not considered in sensitivity analysis due to correlations.

Kd_Am_Vo. Americium sorption coefficient in volcanic units (mL/g). *Distribution:* Truncated normal. *Range:* 1000 to 10000. *Mean/Median/Mode:* 5500. *Standard Deviation:* 1500. *Correlation:* See SN0702PASZFTMA.001 [DIRS 179504]. *Additional Information:* A linear equilibrium sorption coefficient, K_d, is considered appropriate for the radionuclides that exhibit sorption during transport because of experimental observations that establish the adequacy of this approach. The K_d model also depends on chemical equilibrium between the aqueous phase and sorbed phase of a given species. The K_d model determines transport retardation. To treat the one- and three-dimensional transport through the SZ consistently, the sampled values used to generate the saturated zone breakthrough curves are also used in the TSPA-LA Model. These values are tabulated as 200 sets of values for the SZ parameters, accounting for appropriate correletions, and are entered into the TSPA model as a table of 200 values for each parameter. The TSPA-LA Model selects values from this table using the Goldsim variable SZ_index_a. *Sensitivity Name:* SZKDAMVO. *Location in TSPA-LA:* Section 6.3.10.2; Table 6.3.10-2. *DTN:* SN0702PASZFTMA.002_R1 [DIRS 183471]. *References: Saturated Zone Flow and Transport Model Abstraction* (SNL 2008 [DIRS 183750], Sections 6.3.1, 6.5.1.1, 6.5.1.2 and 6.5.2.8; Tables 4-3, 6-8, A-1[a] and B-1; Equations 6-2, 6-3 and 6-26).
Kd_Cs_Al. Cesium sorption coefficient in alluvium (mL/g). *Distribution:* Truncated normal. *Range:* 100 to 1000. *Mean/Median/Mode:* 728. *Standard Deviation:* 464. *Correlation:* See SN0702PASZFTMA.001 [DIRS 179504]. *Additional Information:* See Kd_Am_Al. *Sensitivity Name:* SZKDCSAL. *Location in TSPA-LA:* Section 6.3.10.2; Table 6.3.10-2. *DTN:* SN0702PASZFTMA.002_R1 [DIRS 183471]. *References: Saturated Zone Flow and Transport Model Abstraction* (SNL 2008 [DIRS 183750], Sections 6.3.1, 6.5.1.1, 6.5.1.2 and 6.5.2.8; Tables 4-3, 6-8, A-1[a] and B-1; Equations 6-2, 6-3 and 6-26).
Kd_Cs_Col. Cesium sorption coefficient onto smectite colloids (mL/g). *Distribution:* Piecewise uniform. *Range:* 50 to 5000. *Additional Information:* See Kd_Am_Col. *Sensitivity Name:* SZKDCSCO. *Location in TSPA-LA:* Section 6.3.10.2; Table 6.3.10-2. *DTN:* SN0702PASZFTMA.002_R1 [DIRS 183471]. *References: Saturated Zone Flow and Transport Model Abstraction* (SNL 2008 [DIRS 183750], Sections 6.5.1.1, 6.5.1.2, 6.5.2.8, 6.5.2.12 and 6.5.4.2[a]; Tables 4-3[a], 6-7[a], A-1[a] and B-1; Equations 6-4 and 6-26; Figure 6-25).
Kd_Cs_Rev_Smectite_a. Distribution coefficient for reversible sorption of cesium to waste form (smectite) colloids (mL/g). *Distribution:* Piecewise uniform. *Range:* 50 to 5000. *Symbol:* $Kd_{Cs,coll,wf}$. *Additional Information:* See Kd_Am_Rev_Smectite_a. *Sensitivity Name:* KDCSSMEC. *Location in TSPA-LA:* Sections 6.3.7.6.2 and 6.3.7.6.3; Equation 6.3.7-20; Tables 6.3.7-62 and 6.3.7-66. *DTN:* MO0701PASORPTN.000_R1 [DIRS 180391]. *References: Waste Form and In-Drift Colloids-Associated Radionuclide Concentrations: Abstraction and Summary* (SNL 2007 [DIRS 177423], Sections 4.1.1, 6.3.2.2, 6.3.12.1 and 6.6.8; Equations 6-13 and 6-15; Figure 6-24b; Tables 6-15 and 6-24).
Kd_Cs_Rev_U_Col_a. Distribution coefficient for reversible sorption of cesium onto uranophane colloids (mL/g). *Distribution:* Log uniform. *Range:* 10 to 1000. *Symbol:* $Kd_{Cs,coll,uranophane}$. *Additional Information:* See Kd_Am_Rev_U_Col_a. *Sensitivity Name:* KDCSCOL. *Location in TSPA-LA:* Sections 6.3.7.6.2 and 6.3.7.6.3; Equation 6.3.7-20; Table 6.3.7-64. *DTN:* MO0701PACSNFCP.000_R1 [DIRS 180439]. *References: Waste Form and In-Drift Colloids-Associated Radionuclide Concentrations: Abstraction and Summary* (SNL 2007 [DIRS 177423], Sections 4.1.1, 6.3.2.2, 6.3.2.6, 6.3.12.1, 6.5.1.3, 6.6.4 and 6.6.8; Equations 6-13 and 6-15; Tables 6-9 and 6-24).
Kd_Cs_Vo. Cesium sorption coefficient in volcanic units (mL/g). *Distribution:* Piecewise uniform. *Range:* 100 to 6783. *Correlation:* See SN0702PASZFTMA.001 [DIRS 179504]. *Additional Information:* See Kd_Am_Vo. *Sensitivity Name:* SZKDCSVO. *Location in TSPA-LA:* Section 6.3.10.2; Table 6.3.10-2. *DTN:* SN0702PASZFTMA.002_R1 [DIRS 183471]. *References: Saturated Zone Flow and Transport Model Abstraction* (SNL 2008 [DIRS 183750], Sections 6.3.1, 6.5.1.1, 6.5.1.2 and 6.5.2.8; Tables 4-3, 6-8, A-1[a] and B-1; Equations 6-2, 6-3 and 6-26).
Kd_Np_Al. Neptunium sorption coefficient in alluvium (mL/g). *Distribution:* Piecewise uniform. *Range:* 1.8 to 13. *Correlation:* See SN0702PASZFTMA.001 [DIRS 179504]. *Additional Information:* See Kd_Am_Al. *Sensitivity Name:* SZKDNPAL. *Location in TSPA-LA:* Section 6.3.10.2; Table 6.3.10-2. *DTN:* SN0702PASZFTMA.002_R1 [DIRS 183471]. *References: Saturated Zone Flow and Transport Model Abstraction* (SNL 2008 [DIRS 183750], Sections 6.3.1, 6.5.1.1, 6.5.1.2, 6.5.2.8 and 8.1; Tables 4-3, 6-8, 7-1[a], A-1[a] and B-1; Equations 6-2, 6-3 and 6-26).

Table K3-3. Detailed Summary of Epistemically Uncertain Variables (i.e., elements of **e**) Considered in the TSPA-LA (TSPA Parameter Name) (Continued)

NOTE: * indicates variable not considered in sensitivity analysis due to correlations.

Kd_Np_Rev_Smectite_a. Distribution coefficient for reversible sorption of neptunium to waste form (smectite) colloids (mL/g). *Distribution:* Log uniform. *Range:* 10 to 500. *Symbol:* $Kd_{Np,coll,smectite}$. *Additional Information:* See Kd_Am_Rev_Smectite_a. *Sensitivity Name:* KDNPSMEC. *Location in TSPA-LA:* Sections 6.3.7.6.2 and 6.3.7.6.3; Equation 6.3.7-20; Tables 6.3.7-62 and 6.3.7-66. *DTN:* MO0701PAKDSUNP.000_R1 [DIRS 180392]. *References: Waste Form and In-Drift Colloids-Associated Radionuclide Concentrations: Abstraction and Summary* (SNL 2007 [DIRS 177423], Sections 4.1.1, 6.3.2.2, 6.3.12.1 and 6.6.8; Equations 6-13 and 6-15; Figure 6-24a; Tables 6-15 and 6-24).
Kd_Np_Rev_U_Col_a. Distribution coefficient for reversible sorption of neptunium onto uranophane colloids (mL/g). *Distribution:* Log uniform. *Range:* 1 to 500. *Symbol:* $Kd_{Np,coll,uranophane}$. *Additional Information:* See Kd_Am_Rev_U_Col_a. In the TSPA-LA Model the lower bound for this parameter was entered erroneously as 1. The correct lower bound is 10. See Appendix P, Table P-6, for a discussion of the effect of this error. *Sensitivity Name:* KDNPCOL. *Location in TSPA-LA:* Sections 6.3.7.6.2 and 6.3.7.6.3; Equation 6.3.7-20; Table 6.3.7-64. *DTN:* MO0701PACSNFCP.000_R1 [DIRS 180439]. *References: Waste Form and In-Drift Colloids-Associated Radionuclide Concentrations: Abstraction and Summary* (SNL 2007 [DIRS 177423], Sections 4.1.1, 6.3.2.2, 6.3.2.6, 6.3.12.1, 6.5.1.3, 6.6.4 and 6.6.8; Equations 6-13 and 6-15; Tables 6-9 and 6-24).
Kd_Np_Vo. Neptunium sorption coefficient in volcanic units (mL/g). *Distribution:* Piecewise uniform. *Range:* 0 to 6. *Correlation:* See SN0702PASZFTMA.001 [DIRS 179504]. *Additional Information:* See Kd_Am_Vo. *Sensitivity Name:* SZKDNPVO. *Location in TSPA-LA:* Section 6.3.10.2; Table 6.3.10-2. *DTN:* SN0702PASZFTMA.002_R1 [DIRS 183471]. *References: Saturated Zone Flow and Transport Model Abstraction* (SNL 2008 [DIRS 183750], Sections 6.3.1, 6.5.1.1, 6.5.1.2, 6.5.2.8 and 8.1; Tables 4-3, 6-8, 7-1[a], A-1[a] and B-1; Equations 6-2, 6-3 and 6-26).
Kd_Pa_Rev_Smectite_a. Distribution coefficient for reversible sorption of protactinium to waste form (smectite) colloids (mL/g). *Distribution:* Piecewise uniform. *Range:* 1.00E+04 to 1.00E+07. *Symbol:* $Kd_{Pa,coll,wf}$. *Additional Information:* See Kd_Am_Rev_Smectite_a. *Sensitivity Name:* KDPASMEC. *Location in TSPA-LA:* Sections 6.3.7.6.2 and 6.3.7.6.3; Equation 6.3.7-20; Tables 6.3.7-62 and 6.3.7-66. *DTN:* MO0701PASORPTN.000_R1 [DIRS 180391]. *References: Waste Form and In-Drift Colloids-Associated Radionuclide Concentrations: Abstraction and Summary* (SNL 2007 [DIRS 177423], Sections 4.1.1, 6.3.2.2, 6.3.12.1 and 6.6.8; Equations 6-13 and 6-15; Figure 6-24c; Tables 6-15 and 6-24).
Kd_Pa_Rev_U_Col_a. Distribution coefficient for reversible sorption of protactinium onto uranophane colloids (mL/g). *Distribution:* Log uniform. *Range:* 5 to 1.00E+04. *Symbol:* $Kd_{Pa,coll,uranophane}$. *Additional Information:* See Kd_Am_Rev_U_Col_a. *Sensitivity Name:* KDPACOL. *Location in TSPA-LA:* Sections 6.3.7.6.2 and 6.3.7.6.3; Equation 6.3.7-20; Table 6.3.7-64. *DTN:* MO0701PACSNFCP.000_R1 [DIRS 180439]. *References: Waste Form and In-Drift Colloids-Associated Radionuclide Concentrations: Abstraction and Summary* (SNL 2007 [DIRS 177423], Sections 4.1.1, 6.3.2.2, 6.3.2.6, 6.3.12.1, 6.5.1.3, 6.6.4 and 6.6.8; Equations 6-13 and 6-15; Tables 6-9 and 6-24).
Kd_Pu_Al. Plutonium sorption coefficient in alluvium (mL/g). *Distribution:* Beta. *Range:* 50 to 300. *Mean/Median/Mode:* 100. *Standard Deviation:* 15. *Correlation:* See SN0702PASZFTMA.001 [DIRS 179504]. *Additional Information:* See Kd_Am_Al. *Sensitivity Name:* SZKDPUAL. *Location in TSPA-LA:* Section 6.3.10.2; Table 6.3.10-2. *DTN:* SN0702PASZFTMA.002_R1 [DIRS 183471]. *References: Saturated Zone Flow and Transport Model Abstraction* (SNL 2008 [DIRS 183750], Sections 6.3.1, 6.5.1.1, 6.5.1.2, 6.5.2.8 and 8.1; Tables 4-3, 6-8, A-1[a] and B-1; Equations 6-2, 6-3 and 6-26).
Kd_Pu_Col. Plutonium sorption coefficient onto smectite colloids (mL/g). *Distribution:* Piecewise uniform. *Range:* 1.00E+03 to 1.00E+05. *Additional Information:* See Kd_Am_Col. *Sensitivity Name:* SZKDPUCO. *Location in TSPA-LA:* Section 6.3.10.2; Table 6.3.10-2. *DTN:* SN0702PASZFTMA.002_R1 [DIRS 183471]. *References: Saturated Zone Flow and Transport Model Abstraction* (SNL 2008 [DIRS 183750], Sections 6.5.1.1, 6.5.1.2, 6.5.2.8, 6.5.2.12 and 6.5.4.2[a]; Tables 4-3[a], 6-7[a], A-1[a] and B-1; Equations 6-4 and 6-26; Figure 6-23).
Kd_Pu_Rev_Smectite_a. Distribution coefficient for reversible sorption of plutonium to waste form (smectite) colloids (mL/g). *Distribution:* Piecewise uniform. *Range:* 1.00E+03 to 1.00E+05. *Symbol:* $Kd_{Pu,coll,wf}$. *Additional Information:* See Kd_Am_Rev_Smectite_a. *Sensitivity Name:* KDPUSMEC. *Location in TSPA-LA:* Sections 6.3.7.6.2 and 6.3.7.6.3; Equation 6.3.7-20; Tables 6.3.7-62 and 6.3.7-66. *DTN:* MO0701PASORPTN.000_R1 [DIRS 180391]. *References: Waste Form and In-Drift Colloids-Associated Radionuclide Concentrations: Abstraction and Summary* (SNL 2007 [DIRS 177423], Sections 4.1.1, 6.3.2.2, 6.3.12.1 and 6.6.8; Equations 6-13 and 6-15; Figure 6-24c; Tables 6-15 and 6-24).

Table K3-3. Detailed Summary of Epistemically Uncertain Variables (i.e., elements of **e**) Considered in the TSPA-LA (TSPA Parameter Name) (Continued)

NOTE: * indicates variable not considered in sensitivity analysis due to correlations.

Kd_Pu_Rev_U_Col_a. Distribution coefficient for reversible sorption of plutonium onto uranophane colloids (mL/g). *Distribution:* Log uniform. *Range:* 5 to 1.00E+04. *Symbol:* $Kd_{Pu,coll,uranophane}$. *Additional Information:* See Kd_Am_Rev_U_Col_a. *Sensitivity Name:* KDPUCOL. *Location in TSPA-LA:* Sections 6.3.7.6.2 and 6.3.7.6.3; Equation 6.3.7-20; Table 6.3.7-64. *DTN:* MO0701PACSNFCP.000_R1 [DIRS 180439]. *References: Waste Form and In-Drift Colloids-Associated Radionuclide Concentrations: Abstraction and Summary* (SNL 2007 [DIRS 177423], Sections 4.1.1, 6.3.2.2, 6.3.2.6, 6.3.12.1, 6.5.1.3, 6.6.4 and 6.6.8; Equations 6-13 and 6-15; Tables 6-9 and 6-24).
Kd_Pu_Vo. Plutonium sorption coefficient in volcanic units (mL/g). *Distribution:* Piecewise uniform. *Range:* 10 to 300. *Correlation:* See SN0702PASZFTMA.001 [DIRS 179504]. *Additional Information:* See Kd_Am_Vo. *Sensitivity Name:* SZKDPUVO. *Location in TSPA-LA:* Section 6.3.10.2; Table 6.3.10-2. *DTN:* SN0702PASZFTMA.002_R1 [DIRS 183471]. *References: Saturated Zone Flow and Transport Model Abstraction* (SNL 2008 [DIRS 183750], Sections 6.3.1, 6.5.1.1, 6.5.1.2 and 6.5.2.8; Tables 4-3, 6-8, A-1[a] and B-1; Equations 6-2, 6-3 and 6-26).
Kd_Ra_Al. Radium sorption coefficient in alluvium (mL/g). *Distribution:* Uniform. *Range:* 100 to 1000. *Correlation:* See SN0702PASZFTMA.001 [DIRS 179504]. *Additional Information:* See Kd_Am_Al. *Sensitivity Name:* SZKDRAAL. *Location in TSPA-LA:* Section 6.3.10.2; Table 6.3.10-2. *DTN:* SN0702PASZFTMA.002_R1 [DIRS 183471]. *References: Saturated Zone Flow and Transport Model Abstraction* (SNL 2008 [DIRS 183750], Sections 6.3.1, 6.5.1.1, 6.5.1.2 and 6.5.2.8; Tables 4-3, 6-8, A-1[a] and B-1; Equations 6-2, 6-3 and 6-26).
Kd_Ra_Rev_Smectite_a. Distribution coefficient for reversible sorption of radium to waste form (smectite) colloids (mL/g). *Distribution:* Log uniform. *Range:* 100 to 5000. *Symbol:* $Kd_{Ra,coll,smectite}$. *Additional Information:* See Kd_Am_Rev_Smectite_a. Waste glass derived smectite colloids, corrosion-generated colloids, and seepage water–groundwater colloids may become pseudocolloids through reversible sorption of aqueous radionuclides onto them. *Sensitivity Name:* KDRASMEC. *Location in TSPA-LA:* Sections 6.3.7.6.2 and 6.3.7.6.3; Equation 6.3.7-20; Tables 6.3.7-62 and 6.3.7-66. *DTN:* MO0701PAKDSUNP.000_R1 [DIRS 180392]. *References: Waste Form and In-Drift Colloids-Associated Radionuclide Concentrations: Abstraction and Summary* (SNL 2007 [DIRS 177423], Sections 4.1.1, 6.3.2.2, 6.3.12.1 and 6.6.8; Equations 6-13 and 6-15; Figure 6-24b; Tables 6-15 and 6-24).
Kd_Ra_Rev_U_Col_a. Distribution coefficient for reversible sorption of radium onto uranophane colloids (mL/g). *Distribution:* Log uniform. *Range:* 10 to 1000. *Symbol:* $Kd_{Ra,coll,uranophane}$. *Additional Information:* See Kd_Am_Rev_U_Col_a. *Sensitivity Name:* KDRACOL. *Location in TSPA-LA:* Sections 6.3.7.6.2 and 6.3.7.6.3; Equation 6.3.7-20; Table 6.3.7-64. *DTN:* MO0701PACSNFCP.000_R1 [DIRS 180439]. *References: Waste Form and In-Drift Colloids-Associated Radionuclide Concentrations: Abstraction and Summary* (SNL 2007 [DIRS 177423], Sections 4.1.1, 6.3.2.2, 6.3.2.6, 6.3.12.1, 6.5.1.3, 6.6.4 and 6.6.8; Equations 6-13 and 6-15; Tables 6-9 and 6-24).
Kd_Ra_Vo*. Radium sorption coefficient in volcanic units (mL/g). *Distribution:* Uniform. *Range:* 100 to 1000. *Correlation:* See SN0702PASZFTMA.001 [DIRS 179504]. *Additional Information:* See Kd_Am_Vo. *Sensitivity Name:* SZKDRAVO*. *Location in TSPA-LA:* Section 6.3.10.2; Table 6.3.10-2. *DTN:* SN0702PASZFTMA.002_R1 [DIRS 183471]. *References: Saturated Zone Flow and Transport Model Abstraction* (SNL 2008 [DIRS 183750], Sections 6.3.1, 6.5.1.1, 6.5.1.2 and 6.5.2.8; Tables 4-3, 6-8, A-1[a] and B-1; Equations 6-2, 6-3 and 6-26).
Kd_Se_Al. Selenium sorption coefficient in alluvium (mL/g). *Distribution:* Truncated log normal. *Range:* 1 to 50. *Mean/Median/Mode:* 14. *Standard Deviation:* 11.2. *Correlation:* See SN0702PASZFTMA.001 [DIRS 179504]. *Additional Information:* See Kd_Am_Al. Two new nuclides have been added, namely radionuclide tin reversibly attached to colloids and sorbing radionuclide selenium. Uncertainty distributions for sorption coefficients of selenium and tin have recently been developed based on the need to simulate the migration of associated radionuclides in the TSPA model. *Sensitivity Name:* SZKDSEAL. *Location in TSPA-LA:* Section 6.3.10.2; Table 6.3.10-2. *DTN:* SN0702PASZFTMA.002_R1 [DIRS 183471]. *References: Saturated Zone Flow and Transport Model Abstraction* (SNL 2008 [DIRS 183750], Sections 6.5.3[a] and 8.1[a]; Tables 4-3[a], 6-7[a] and A-1[a]).
Kd_Se_Vo. Selenium sorption coefficient in volcanic units (mL/g). *Distribution:* Truncated log normal. *Range:* 1 to 50. *Mean/Median/Mode:* 14. *Standard Deviation:* 11.2. *Correlation:* See SN0702PASZFTMA.001 [DIRS 179504]. *Additional Information:* See Kd_Am_Vo. Two new nuclides have been added, namely radionuclide tin reversibly attached to colloids and sorbing radionuclide selenium. Uncertainty distributions for sorption coefficients of selenium and tin have recently been developed based on the need to simulate the migration of associated radionuclides in the TSPA model. *Sensitivity Name:* SZKDSEVO. *Location in TSPA-LA:* Section 6.3.10.2; Table 6.3.10-2. *DTN:* SN0702PASZFTMA.002_R1 [DIRS 183471]. *References: Saturated Zone Flow and Transport Model Abstraction* (SNL 2008 [DIRS 183750], Sections 6.5.3[a] and 8.1[a]; Tables 4-3[a], 6-7[a] and A-1[a]).

Table K3-3. Detailed Summary of Epistemically Uncertain Variables (i.e., elements of **e**) Considered in the TSPA-LA (TSPA Parameter Name) (Continued)

NOTE: * indicates variable not considered in sensitivity analysis due to correlations.

Kd_Sn_Al. Tin sorption coefficient in alluvium (mL/g). *Distribution:* Log uniform. *Range:* 1.00E+02 to 1.00E+05. *Correlation:* See SN0702PASZFTMA.001 [DIRS 179504]. *Additional Information:* See Kd_Am_Al. Two new nuclides have been added, namely radionuclide tin reversibly attached to colloids and sorbing radionuclide selenium. Uncertainty distributions for sorption coefficients of selenium and tin have recently been developed based on the need to simulate the migration of associated radionuclides in the TSPA model. *Sensitivity Name:* SZKDSNAL. *Location in TSPA-LA:* Section 6.3.10.2; Table 6.3.10-2. *DTN:* SN0702PASZFTMA.002_R1 [DIRS 183471]. *References: Saturated Zone Flow and Transport Model Abstraction* (SNL 2008 [DIRS 183750], Sections 6.5.3[a] and 8.1[a]; Tables 4-3[a], 6-7[a] and A-1[a]).
Kd_Sn_Col. Tin sorption coefficient onto smectite colloids (mL/g). *Distribution:* Log uniform. *Range:* 1.00E+05 to 1.00E+06. *Additional Information:* See Kd_Am_Col. Two new nuclides have been added, namely radionuclide tin reversibly attached to colloids and sorbing radionuclide selenium. Uncertainty distributions for sorption coefficients of selenium and tin have recently been developed based on the need to simulate the migration of associated radionuclides in the TSPA model. *Sensitivity Name:* SZKDSNCO. *Location in TSPA-LA:* Section 6.3.10.2; Table 6.3.10-2. *DTN:* SN0702PASZFTMA.002_R1 [DIRS 183471]. *References: Saturated Zone Flow and Transport Model Abstraction* (SNL 2008 [DIRS 183750], Sections 6.5.2.4[a], 6.5.3[a] and 8.1[a]; Tables 4-3[a], 6-7[a] and A-1[a]).
Kd_Sn_Rev_Smectite_a. Distribution coefficient for reversible sorption of tin to waste form (smectite) colloids (mL/g). *Distribution:* Log uniform. *Range:* 1.00E+05 to 1.00E+06. *Symbol:* $Kd_{Sn,coll,smectite}$. *Additional Information:* See Kd_Am_Rev_Smectite_a. Waste glass derived smectite colloids, corrosion-generated colloids, and seepage water–groundwater colloids may become pseudocolloids through reversible sorption of aqueous radionuclides onto them. *Sensitivity Name:* KDSNSMEC. *Location in TSPA-LA:* Sections 6.3.7.6.2 and 6.3.7.6.3; Equation 6.3.7-20; Tables 6.3.7-62 and 6.3.7-66. *DTN:* MO0701PAKDSUNP.000_R1 [DIRS 180392]. *References: Waste Form and In-Drift Colloids-Associated Radionuclide Concentrations: Abstraction and Summary* (SNL 2007 [DIRS 177423], Sections 4.1.1, 6.3.2.2, 6.3.12.1 and 6.6.8; Equations 6-13 and 6-15; Figure 6-24b; Tables 6-15 and 6-24).
Kd_Sn_Rev_U_Col_a. Distribution coefficient for reversible sorption of tin onto uranophane colloids (mL/g). *Distribution:* Log uniform. *Range:* 1 to 100. *Symbol:* $Kd_{Sn,coll,uranophane}$. *Additional Information:* See Kd_Am_Rev_U_Col_a. *Sensitivity Name:* KDSNCOL. *Location in TSPA-LA:* Sections 6.3.7.6.2 and 6.3.7.6.3; Equation 6.3.7-20; Table 6.3.7-64. *DTN:* MO0701PACSNFCP.000_R1 [DIRS 180439]. *References: Waste Form and In-Drift Colloids-Associated Radionuclide Concentrations: Abstraction and Summary* (SNL 2007 [DIRS 177423], Sections 4.1.1, 6.3.2.2, 6.3.2.6, 6.3.12.1, 6.5.1.3, 6.6.4 and 6.6.8; Equations 6-13 and 6-15; Tables 6-9 and 6-24).
Kd_Sn_Vo. Tin sorption coefficient in volcanic units (mL/g). *Distribution:* Log uniform. *Range:* 1.00E+02 to 1.00E+05. *Correlation:* See SN0702PASZFTMA.001 [DIRS 179504]. *Additional Information:* See Kd_Am_Vo. Two new nuclides have been added, namely radionuclide tin reversibly attached to colloids and sorbing radionuclide selenium. Uncertainty distributions for sorption coefficients of selenium and tin have recently been developed based on the need to simulate the migration of associated radionuclides in the TSPA model. *Sensitivity Name:* SZKDSNVO. *Location in TSPA-LA:* Section 6.3.10.2; Table 6.3.10-2. *DTN:* SN0702PASZFTMA.002_R1 [DIRS 183471]. *References: Saturated Zone Flow and Transport Model Abstraction* (SNL 2008 [DIRS 183750], Sections 6.5.3[a] and 8.1[a]; Tables 4-3[a], 6-7[a] and A-1[a]).
Kd_Sr_Al. Strontium sorption coefficient in alluvium (mL/g). *Distribution:* Uniform. *Range:* 20 to 400. *Correlation:* See SN0702PASZFTMA.001 [DIRS 179504]. *Additional Information:* See Kd_Am_Al. *Sensitivity Name:* SZKDSRAL. *Location in TSPA-LA:* Section 6.3.10.2; Table 6.3.10-2. *DTN:* SN0702PASZFTMA.002_R1 [DIRS 183471]. *References: Saturated Zone Flow and Transport Model Abstraction* (SNL 2008 [DIRS 183750], Sections 6.3.1, 6.5.1.1, 6.5.1.2 and 6.5.2.8; Tables 4-3, 6-8, A-1[a] and B-1; Equations 6-2, 6-3 and 6-26).
Kd_Sr_Vo. Strontium sorption coefficient in volcanic units (mL/g). *Distribution:* Uniform. *Range:* 20 to 400. *Correlation:* See SN0702PASZFTMA.001 [DIRS 179504]. *Additional Information:* See Kd_Am_Vo. *Sensitivity Name:* SZKDSRVO. *Location in TSPA-LA:* Section 6.3.10.2; Table 6.3.10-2. *DTN:* SN0702PASZFTMA.002_R1 [DIRS 183471]. *References: Saturated Zone Flow and Transport Model Abstraction* (SNL 2008 [DIRS 183750], Sections 6.3.1, 6.5.1.1, 6.5.1.2 and 6.5.2.8; Tables 4-3, 6-8, A-1[a] and B-1; Equations 6-2, 6-3 and 6-26).

Table K3-3. Detailed Summary of Epistemically Uncertain Variables (i.e., elements of **e**) Considered in the TSPA-LA (TSPA Parameter Name) (Continued)

NOTE: * indicates variable not considered in sensitivity analysis due to correlations.

Kd_Th_Rev_Smectite_a. Distribution coefficient for reversible sorption of thorium to waste form (smectite) colloids (mL/g). *Distribution:* Piecewise uniform. *Range:* 1.00E+04 to 1.00E+07. *Symbol:* $Kd_{Th,coll,wf}$. *Additional Information:* See Kd_Am_Rev_Smectite_a. *Sensitivity Name:* KDTHSMEC. *Location in TSPA-LA:* Sections 6.3.7.6.2 and 6.3.7.6.3; Equation 6.3.7-20; Tables 6.3.7-62 and 6.3.7-66. *DTN:* MO0701PASORPTN.000_R1 [DIRS 180391]. *References: Waste Form and In-Drift Colloids-Associated Radionuclide Concentrations: Abstraction and Summary* (SNL 2007 [DIRS 177423], Sections 4.1.1, 6.3.2.2, 6.3.12.1 and 6.6.8; Equations 6-13 and 6-15; Figure 6-24c; Tables 6-15 and 6-24).
Kd_Th_Rev_U_Col_a. Distribution coefficient for reversible sorption of thorium onto uranophane colloids (mL/g). *Distribution:* Log uniform. *Range:* 5 to 1.00E+04. *Symbol:* $Kd_{Th,coll,uranophane}$. *Additional Information:* See Kd_Am_Rev_U_Col_a. *Sensitivity Name:* KDTHCOL. *Location in TSPA-LA:* Sections 6.3.7.6.2 and 6.3.7.6.3; Equation 6.3.7-20; Table 6.3.7-64. *DTN:* MO0701PACSNFCP.000_R1 [DIRS 180439]. *References: Waste Form and In-Drift Colloids-Associated Radionuclide Concentrations: Abstraction and Summary* (SNL 2007 [DIRS 177423], Sections 4.1.1, 6.3.2.2, 6.3.2.6, 6.3.12.1, 6.5.1.3, 6.6.4 and 6.6.8; Equations 6-13 and 6-15; Tables 6-9 and 6-24).
Kd_U_Al. Uranium sorption coefficient in alluvium (mL/g). *Distribution:* Piecewise uniform. *Range:* 1.7 to 8.9. *Correlation:* See SN0702PASZFTMA.001 [DIRS 179504]. *Additional Information:* See Kd_Am_Al. *Sensitivity Name:* SZKDUAL. *Location in TSPA-LA:* Section 6.3.10.2; Table 6.3.10-2. *DTN:* SN0702PASZFTMA.002_R1 [DIRS 183471]. *References: Saturated Zone Flow and Transport Model Abstraction* (SNL 2008 [DIRS 183750], Sections 6.3.1, 6.5.1.1, 6.5.1.2 and 6.5.2.8; Tables 4-3, 6-8, A-1[a] and B-1; Equations 6-2, 6-3 and 6-26).
Kd_U_Rev_Smectite_a. Distribution coefficient for reversible sorption of uranium to waste form (smectite) colloids (mL/g). *Distribution:* Log uniform. *Range:* 5.00E+02 to 5.00E+04. *Symbol:* $Kd_{U,coll,smectite}$. *Additional Information:* See Kd_Am_Rev_Smectite_a. Waste glass derived smectite colloids, corrosion-generated colloids, and seepage water–groundwater colloids may become pseudocolloids through reversible sorption of aqueous radionuclides onto them. *Sensitivity Name:* KDUSMEC. *Location in TSPA-LA:* Sections 6.3.7.6.2 and 6.3.7.6.3; Equation 6.3.7-20; Tables 6.3.7-62 and 6.3.7-66. *DTN:* MO0701PAKDSUNP.000_R1 [DIRS 180392]. *References: Waste Form and In-Drift Colloids-Associated Radionuclide Concentrations: Abstraction and Summary* (SNL 2007 [DIRS 177423], Section 4.1.1, 6.3.2.2, 6.3.12.1 and 6.6.8; Equations 6-13 and 6-15; Figure 6-24a; Tables 6-15 and 6-24).
Kd_U_Vo. Uranium sorption coefficient in volcanic units (mL/g). *Distribution:* Piecewise uniform. *Range:* 0 to 20. *Correlation:* See SN0702PASZFTMA.001 [DIRS 179504]. *Additional Information:* See Kd_Am_Vo. *Sensitivity Name:* SZKDUVO. *Location in TSPA-LA:* Section 6.3.10.2; Table 6.3.10-2. *DTN:* SN0702PASZFTMA.002_R1 [DIRS 183471]. *References: Saturated Zone Flow and Transport Model Abstraction* (SNL 2008 [DIRS 183750], Sections 6.3.1, 6.5.1.1, 6.5.1.2 and 6.5.2.8; Tables 4-3, 6-8, A-1[a] and B-1; Equations 6-2, 6-3 and 6-26).
KdAm_Devit_a. Sorption coefficient of americium in devitrified tuff units of UZ (mL/g). *Distribution:* Truncated normal. *Range:* 1000 to 10000. *Mean:* 5500. *Standard Deviation:* 1500. *Correlation:* See *Radionuclide Transport Models Under Ambient Conditions* (SNL 2007 [DIRS 177396], Appendix B[a], Table B-2[a]). *Additional Information:* The matrix K_d adsorption coefficient is used in conjunction with bulk density, matrix porosity, and matrix saturation to derive the retardation coefficient used to determine the effective transport rate for sorbed species. A correlated set of K_ds are generated for radionuclides transported through the different rock types (zeolitic, vitric and devitrified tuffs) in the UZ. The generated set of Kds is used in the FEHM external input file and by the EBS model to describe radionuclide concentrations at the contact between the EBS-invert and the UZ. Recorded in the TSPA Input Database as four constants: UZ_Kd_Am_D_max, UZ_Kd_Am_D_mean, UZ_Kd_Am_D_SD, and UZ_Kd_Am_D_min. *Sensitivity Name:* UZKDAMDT. *Location in TSPA-LA:* Sections 6.3.9.2 and 6.3.9.3; Equation 6.3.9-3; Table 6.3.9-2. *DTN(s):* UZ_Kd_Am_D_max, UZ_Kd_Am_D_mean, UZ_Kd_Am_D_SD, and UZ_Kd_Am_D_min found in LA0408AM831341.001_R0 [DIRS 171584]. Kd values found in MO0506SPAROCKU.000 [DIRS 173958], Table 1. *References: Radionuclide Transport Models Under Ambient Conditions* (SNL 2007 [DIRS 177396], Sections 6.5 and A8.1; Table 6-1[a]).
KdAm_Vit_a*. Sorption coefficient of americium in vitrified tuff units of UZ (mL/g). *Distribution:* Piecewise uniform. *Range:* 100 to 1000. *Median:* 400. *Correlation:* See *Radionuclide Transport Models Under Ambient Conditions* (SNL 2007 [DIRS 177396], Appendix B[a], Table B-2[a]). *Additional Information:* See KdAm_Devit_a. Recorded in the TSPA Input Database as three constants: UZ_Kd_Am_V_c1, UZ_Kd_Am_V_c2, UZ_Kd_Am_V_c3. *Sensitivity Name:* UZKDAMVT*. *Location in TSPA-LA:* Sections 6.3.9.2 and 6.3.9.3; Equation 6.3.9-3; Table 6.3.9-2. *DTN(s):* UZ_Kd_Am_V_c1, UZ_Kd_Am_V_c2 and UZ_Kd_Am_V_c3 found in LA0408AM831341.001_R0 [DIRS 171584]. Kd values found in MO0506SPAROCKU.000 [DIRS 173958], Table 1.. *References: Radionuclide Transport Models Under Ambient Conditions* (SNL 2007 [DIRS 177396], Sections 6.5 and A8.1; Table 6-1[a]).

Table K3-3. Detailed Summary of Epistemically Uncertain Variables (i.e., elements of **e**) Considered in the TSPA-LA (TSPA Parameter Name) (Continued)

NOTE: * indicates variable not considered in sensitivity analysis due to correlations.

KdAm_Zeo_a*. Sorption coefficient of americium in zeolitic tuff units of UZ (mL/g). *Distribution:* Truncated normal. *Range:* 1000 to 10000. *Mean:* 5500. *Standard Deviation:* 1500. *Correlation:* See *Radionuclide Transport Models Under Ambient Conditions* (SNL 2007 [DIRS 177396], Appendix B[a], Table B-2[a]). *Additional Information:* See KdAm_Devit_a. Recorded in the TSPA Input Database as four constants: UZ_Kd_Am_Z_max, UZ_Kd_Am_Z_mean, UZ_Kd_Am_Z_SD, and UZ_Kd_Am_Z_min. *Sensitivity Name:* UZKDAMZT*. *Location in TSPA-LA:* Sections 6.3.9.2 and 6.3.9.3; Equation 6.3.9-3; Table 6.3.9-2. *DTN(s):* UZ_Kd_Am_Z_max, UZ_Kd_Am_Z_mean, UZ_Kd_Am_Z_SD, and UZ_Kd_Am_Z_min found in LA0408AM831341.001_R0 [DIRS 171584]. Kd values found in MO0506SPAROCKU.000 [DIRS 173958], Table 1. *References: Radionuclide Transport Models Under Ambient Conditions* (SNL 2007 [DIRS 177396], Sections 6.5 and A8.1; Table 6-1[a]).
KdCs_Devit_a. Sorption coefficient of cesium in devitrified tuff units of UZ (mL/g). *Distribution:* Uniform. *Range:* 1 to 15. *Correlation:* See *Radionuclide Transport Models Under Ambient Conditions* (SNL 2007 [DIRS 177396], Appendix B[a], Table B-2[a]). *Additional Information:* See KdAm_Devit_a. Recorded in the TSPA Input Database as UZ_Kd_Cs_D_max and UZ_Kd_Cs_D_min. *Sensitivity Name:* UZKDCSDT. *Location in TSPA-LA:* Sections 6.3.9.2 and 6.3.9.3; Equation 6.3.9-3; Table 6.3.9-2. *DTN(s):* UZ_Kd_Cs_D_max and UZ_Kd_Cs_D_min found in LA0408AM831341.001_R0 [DIRS 171584]. Kd values found in MO0506SPAROCKU.000 [DIRS 173958], Table 1. *References: Radionuclide Transport Models Under Ambient Conditions* (SNL 2007 [DIRS 177396], Section 6.5; Table 6-1[a]).
KdCs_Vit_a*. Sorption coefficient of cesium in vitrified tuff units of UZ (mL/g). *Distribution:* Piecewise uniform. *Range:* 0 to 100. *Median:* 2. *Correlation:* See *Radionuclide Transport Models Under Ambient Conditions* (SNL 2007 [DIRS 177396], Appendix B[a], Table B-2[a]). *Additional Information:* See KdAm_Devit_a. Recorded in the TSPA Input Database as three constants: UZ_Kd_Cs_V_c1, UZ_Kd_Cs_V_c2, and UZ_Kd_Cs_V_c3. *Sensitivity Name:* UZKDCSVT*. *Location in TSPA-LA:* Sections 6.3.9.2 and 6.3.9.3; Equation 6.3.9-3; Table 6.3.9-2. *DTN(s):* UZ_Kd_Cs_V_c1, UZ_Kd_Cs_V_c2, and UZ_Kd_Cs_V_c3 found in LA0408AM831341.001_R0 [DIRS 171584]. Kd values found in MO0506SPAROCKU.000 [DIRS 173958], Table 1. *References: Radionuclide Transport Models Under Ambient Conditions* (SNL 2007 [DIRS 177396], Section 6.5; Table 6-1[a]).
KdCs_Zeo_a. Sorption coefficient for cesium in zeolitic tuff units of UZ (mL/g). *Distribution:* Piecewise uniform. *Range:* 425 to 20000. *Median:* 5,000. *Correlation:* See *Radionuclide Transport Models Under Ambient Conditions* (SNL 2007 [DIRS 177396], Appendix B[a], Table B-2[a]). *Additional Information:* See KdAm_Devit_a. Recorded in the TSPA Input Database as three constants: UZ_Kd_Cs_Z_c1, UZ_Kd_Cs_Z_c2, and UZ_Kd_Cs_Z_c3. *Sensitivity Name:* UZKDCSZT. *Location in TSPA-LA:* Sections 6.3.9.2 and 6.3.9.3; Equation 6.3.9-3; Table 6.3.9-2. *DTN(s): UZ_Kd_Cs_Z_c1, UZ_Kd_Cs_Z_c2, and UZ_Kd_Cs_Z_c3 found in LA0408AM831341.001_R0 [DIRS 171584]. Kd values found in MO0506SPAROCKU.000 [DIRS 173958], Table 1. References: Radionuclide Transport Models Under Ambient Conditions* (SNL 2007 [DIRS 177396], Section 6.5; Table 6-1[a]).
KdNp_Devit_a. Sorption coefficient for neptunium in devitrified tuff units of UZ (mL/g). *Distribution:* Piecewise uniform. *Range:* 0 to 6. *Median:* 0.5. *Correlation:* See *Radionuclide Transport Models Under Ambient Conditions* (SNL 2007 [DIRS 177396], Appendix B[a], Table B-2[a]). *Additional Information:* See KdAm_Devit_a. Recorded in the TSPA Input Database as three constants: UZ_Kd_Np_D_c1, UZ_Kd_Np_D_c2, and UZ_Kd_Np_D_c3. *Sensitivity Name:* UZKDNPDT. *Location in TSPA-LA:* Sections 6.3.9.2 and 6.3.9.3; Equation 6.3.9-3; Table 6.3.9-2. *DTN(s):* UZ_Kd_Np_D_c1, UZ_Kd_Np_D_c2, and UZ_Kd_Np_D_c3 found in LA0408AM831341.001_R0 [DIRS 171584]. Kd values found in MO0506SPAROCKU.000 [DIRS 173958], Table 1. *References: Radionuclide Transport Models Under Ambient Conditions* (SNL 2007 [DIRS 177396], Section 6.5; Table 6-1[a]).
KdNp_Vit_a*. Sorption coefficient for neptunium in vitrified tuff units of UZ (mL/g). *Distribution:* Piecewise uniform. *Range:* 0 to 3. *Median:* 1. *Correlation:* See *Radionuclide Transport Models Under Ambient Conditions* (SNL 2007 [DIRS 177396], Appendix B[a], Table B-2[a]). *Additional Information:* See KdAm_Devit_a. Recorded in the TSPA Input Database as three constants: UZ_Kd_Np_V_c1, UZ_Kd_Np_V_c2, and UZ_Kd_Np_V_c3. *Sensitivity Name:* UZKDNPVT*, *Location in TSPA-LA:* Sections 6.3.9.2 and 6.3.9.3; Equation 6.3.9-3; Table 6.3.9-2. *DTN(s):* UZ_Kd_Np_V_c1, UZ_Kd_Np_V_c2, and UZ_Kd_Np_V_c3 found in LA0408AM831341.001_R0 [DIRS 171584]. Kd values found in MO0506SPAROCKU.000 [DIRS 173958], Table 1. *References: Radionuclide Transport Models Under Ambient Conditions* (SNL 2007 [DIRS 177396], Section 6.5; Table 6-1[a]).

Table K3-3. Detailed Summary of Epistemically Uncertain Variables (i.e., elements of **e**) Considered in the TSPA-LA (TSPA Parameter Name) (Continued)

NOTE: * indicates variable not considered in sensitivity analysis due to correlations.

KdNp_Zeo_a*. Sorption coefficient for neptunium in zeolitic tuff units of UZ (mL/g). *Distribution:* Piecewise uniform. *Range:* 0 to 6. *Median:* 0.5. *Correlation:* See *Radionuclide Transport Models Under Ambient Conditions* (SNL 2007 [DIRS 177396], Appendix B[a], Table B-2[a]). *Additional Information:* See KdAm_Devit_a. Recorded in the TSPA Input Database as three constants: UZ_Kd_Np_Z_c1, UZ_Kd_Np_Z_c2, and UZ_Kd_Np_Z_c3. *Sensitivity Name:* UZKDNPZT*. *Location in TSPA-LA:* Sections 6.3.9.2 and 6.3.9.3; Equation 6.3.9-3; Table 6.3.9-2. *DTN(s):* UZ_Kd_Np_Z_c1, UZ_Kd_Np_Z_c2, and UZ_Kd_Np_Z_c3 found in LA0408AM831341.001_R0 [DIRS 171584]. Kd values found in MO0506SPAROCKU.000 [DIRS 173958], Table 1. *References: Radionuclide Transport Models Under Ambient Conditions* (SNL 2007 [DIRS 177396], Section 6.5; Table 6-1[a]).
KdPa_Devit_a. Sorption coefficient for protactinium in devitrified tuff units of UZ (mL/g). *Distribution:* Truncated normal. *Range:* 1000 to 10000. *Mean:* 5500. *Standard Deviation:* 1500. *Correlation:* See *Radionuclide Transport Models Under Ambient Conditions* (SNL 2007 [DIRS 177396], Appendix B[a], Table B-2[a]). *Additional Information:* See KdAm_Devit_a. Recorded in the TSPA Input Database as four constants: UZ_Kd_Pa_D_max, UZ_Kd_Pa_D_mean, UZ_Kd_Pa_D_SD, and UZ_Kd_Pa_D_min. *Sensitivity Name:* UZKDPADT. *Location in TSPA-LA:* Sections 6.3.9.2 and 6.3.9.3; Equation 6.3.9-3; Table 6.3.9-2. *DTN(s):* UZ_Kd_Pa_D_max, UZ_Kd_Pa_D_mean, UZ_Kd_Pa_D_SD, and UZ_Kd_Pa_D_min found in LA0408AM831341.001_R0 [DIRS 171584]. Kd values found in MO0506SPAROCKU.000 [DIRS 173958], Table 1. *References: Radionuclide Transport Models Under Ambient Conditions* (SNL 2007 [DIRS 177396], Section 6.5; Table 6-1[a]).
KdPa_Vit_a*. Sorption coefficient for protactinium in vitrified tuff units of UZ (mL/g). *Distribution:* Truncated normal. *Range:* 1000 to 10000. *Mean:* 5500. *Standard Deviation:* 1500. *Correlation:* See *Radionuclide Transport Models Under Ambient Conditions* (SNL 2007 [DIRS 177396], Appendix B[a], Table B-2[a]). *Additional Information:* See KdAm_Devit_a. Recorded in the TSPA Input Database as four constants: UZ_Kd_Pa_V_max, UZ_Kd_Pa_V_mean, UZ_Kd_Pa_V_SD, and UZ_Kd_Pa_V_min. *Sensitivity Name:* UZKDPAVT*. *Location in TSPA-LA:* Sections 6.3.9.2 and 6.3.9.3; Equation 6.3.9-3; Table 6.3.9-2. *DTN(s):* UZ_Kd_Pa_V_max, UZ_Kd_Pa_V_mean, UZ_Kd_Pa_V_SD, and UZ_Kd_Pa_V_min found in LA0408AM831341.001_R0 [DIRS 171584]. Kd values found in MO0506SPAROCKU.000 [DIRS 173958], Table 1. *References: Radionuclide Transport Models Under Ambient Conditions* (SNL 2007 [DIRS 177396], Section 6.5; Table 6-1[a]).
KdPa_Zeo_a*. Sorption coefficient for protactinium in zeolitic tuff units of UZ (mL/g). *Distribution:* Truncated normal. *Range:* 1000 to 10000. *Mean:* 5500. *Standard Deviation:* 1500. *Correlation:* See *Radionuclide Transport Models Under Ambient Conditions* (SNL 2007 [DIRS 177396], Appendix B[a], Table B-2[a]). *Additional Information:* See KdAm_Devit_a. Recorded in the TSPA Input Database as four constants: UZ_Kd_Pa_Z_max, UZ_Kd_Pa_Z_mean, UZ_Kd_Pa_Z_SD, and UZ_Kd_Pa_Z_min. *Sensitivity Name:* UZKDPAZT*. *Location in TSPA-LA:* Sections 6.3.9.2 and 6.3.9.3; Equation 6.3.9-3; Table 6.3.9-2. *DTN(s):* UZ_Kd_Pa_Z_max, UZ_Kd_Pa_Z_mean, UZ_Kd_Pa_Z_SD, and UZ_Kd_Pa_Z_min found in LA0408AM831341.001_R0 [DIRS 171584]. Kd values found in MO0506SPAROCKU.000 [DIRS 173958], Table 1. *References: Radionuclide Transport Models Under Ambient Conditions* (SNL 2007 [DIRS 177396], Section 6.5; Table 6-1[a]).
KdPu_Devit_a. Sorption coefficient for plutonium in devitrified tuff units of UZ (mL/g). *Distribution:* Piecewise uniform. *Range:* 10 to 200. *Median:* 70. *Correlation:* See *Radionuclide Transport Models Under Ambient Conditions* (SNL 2007 [DIRS 177396], Appendix B[a], Table B-2[a]). *Additional Information:* See KdAm_Devit_a. Recorded in the TSPA Input Database as three constants: UZ_Kd_Pu_D_c1, UZ_Kd_Pu_D_c2, and UZ_Kd_Pu_D_c3. *Sensitivity Name:* UZKDPUDT. *Location in TSPA-LA:* Sections 6.3.9.2 and 6.3.9.3; Equation 6.3.9-3; Table 6.3.9-2. *DTN(s):* UZ_Kd_Pu_D_c1, UZ_Kd_Pu_D_c2, and UZ_Kd_Pu_D_c3 found in LA0408AM831341.001_R0 [DIRS 171584]. Kd values found in MO0506SPAROCKU.000 [DIRS 173958], Table 1. *References: Radionuclide Transport Models Under Ambient Conditions* (SNL 2007 [DIRS 177396], Section 6.5; Table 6-1[a]).
KdPu_Vit_a*. Sorption coefficient for plutonium in vitrified tuff units of UZ (mL/g). *Distribution:* Piecewise uniform. *Range:* 10 to 200. *Median:* 100. *Correlation:* See *Radionuclide Transport Models Under Ambient Conditions* (SNL 2007 [DIRS 177396], Appendix B[a], Table B-2[a]). *Additional Information:* See KdAm_Devit_a. Recorded in the TSPA Input Database as three constants: UZ_Kd_Pu_V_c1, UZ_Kd_Pu_V_c2, and UZ_Kd_Pu_V_c3. *Sensitivity Name:* UZKDPUVT*. *Location in TSPA-LA:* Sections 6.3.9.2 and 6.3.9.3; Equation 6.3.9-3; Table 6.3.9-2. *DTN(s):* UZ_Kd_Pu_V_c1, UZ_Kd_Pu_V_c2, and UZ_Kd_Pu_V_c3 found in LA0408AM831341.001_R0 [DIRS 171584]. Kd values found in MO0506SPAROCKU.000 [DIRS 173958], Table 1. *References: Radionuclide Transport Models Under Ambient Conditions* (SNL 2007 [DIRS 177396], Section 6.5; Table 6-1[a]).

Table K3-3. Detailed Summary of Epistemically Uncertain Variables (i.e., elements of **e**) Considered in the TSPA-LA (TSPA Parameter Name) (Continued)

NOTE: * indicates variable not considered in sensitivity analysis due to correlations.

KdPu_Zeo_a*. Sorption coefficient for plutonium in zeolitic tuff units of UZ (mL/g). *Distribution:* Piecewise uniform. *Range:* 10 to 200. *Median:* 100. *Correlation:* See *Radionuclide Transport Models Under Ambient Conditions* (SNL 2007 [DIRS 177396], Appendix B[a], Table B-2[a]). *Additional Information:* See KdAm_Devit_a. Recorded in the TSPA Input Database as three constants: UZ_Kd_Pu_Z_c1, UZ_Kd_Pu_Z_c2, and UZ_Kd_Pu_Z_c3. *Sensitivity Name:* UZKDPUZT*. *Location in TSPA-LA:* Sections 6.3.9.2 and 6.3.9.3; Equation 6.3.9-3; Table 6.3.9-2. *DTN(s):* UZ_Kd_Pu_Z_c1, UZ_Kd_Pu_Z_c2, and UZ_Kd_Pu_Z_c3 found in LA0408AM831341.001_R0 [DIRS 171584]. Kd values found in MO0506SPAROCKU.000 [DIRS 173958], Table 1. *References: Radionuclide Transport Models Under Ambient Conditions* (SNL 2007 [DIRS 177396], Section 6.5; Table 6-1[a]).
KdRa_Devit_a*. Sorption coefficient for radium in devitrified tuff units of UZ (mL/g). *Distribution:* Uniform. *Range:* 100 to 1000. *Correlation:* See *Radionuclide Transport Models Under Ambient Conditions* (SNL 2007 [DIRS 177396], Appendix B[a], Table B-2[a]). *Additional Information:* See KdAm_Devit_a. Recorded in the TSPA Input Database as UZ_Kd_Ra_D_max and UZ_Kd_Ra_D_min. *Sensitivity Name:* UZKDRADT*. *Location in TSPA-LA:* Sections 6.3.9.2 and 6.3.9.3; Equation 6.3.9-3; Table 6.3.9-2. *DTN(s):* UZ_Kd_Ra_D_max and UZ_Kd_Ra_D_min found in LA0408AM831341.001_R0 [DIRS 171584]. Kd values found in MO0506SPAROCKU.000 [DIRS 173958], Table 1. *References: Radionuclide Transport Models Under Ambient Conditions* (SNL 2007 [DIRS 177396], Section 6.5; Table 6-1[a]).
KdRa_Vit_a*. Sorption coefficient for radium in vitrified tuff units of UZ (mL/g). *Distribution:* Uniform. *Range:* 50 to 600. *Correlation:* See *Radionuclide Transport Models Under Ambient Conditions* (SNL 2007 [DIRS 177396], Appendix B[a], Table B-2[a]). *Additional Information:* See KdAm_Devit_a. Recorded in the TSPA Input Database as UZ_Kd_Ra_V_max and UZ_Kd_Ra_V_min. *Sensitivity Name:* UZKDRAVT*. *Location in TSPA-LA:* Sections 6.3.9.2 and 6.3.9.3; Equation 6.3.9-3; Table 6.3.9-2. *DTN(s):* UZ_Kd_Ra_V_max and UZ_Kd_Ra_V_min found in LA0408AM831341.001_R0 [DIRS 171584]. Kd values found in MO0506SPAROCKU.000 [DIRS 173958], Table 1. *References: Radionuclide Transport Models Under Ambient Conditions* (SNL 2007 [DIRS 177396], Section 6.5; Table 6-1[a]).
KdRa_Zeo_a*. Sorption coefficient for radium in zeolitic tuff units of UZ (mL/g). *Distribution:* Uniform. *Range:* 1000 to 5000. *Correlation:* See *Radionuclide Transport Models Under Ambient Conditions* (SNL 2007 [DIRS 177396], Appendix B[a], Table B-2[a]). *Additional Information:* See KdAm_Devit_a. Recorded in the TSPA Input Database as UZ_Kd_Ra_Z_max and UZ_Kd_Ra_Z_min. *Sensitivity Name:* UZKDRAZT*. *Location in TSPA-LA:* Sections 6.3.9.2 and 6.3.9.3; Equation 6.3.9-3; Table 6.3.9-2. *DTN(s):* UZ_Kd_Ra_Z_max and UZ_Kd_Ra_Z_min found in LA0408AM831341.001_R0 [DIRS 171584]. Kd values found in MO0506SPAROCKU.000 [DIRS 173958], Table 1. *References: Radionuclide Transport Models Under Ambient Conditions* (SNL 2007 [DIRS 177396], Section 6.5; Table 6-1[a]).
KdSe_Devit_a. Sorption coefficient for selenium in devitrified tuff units of UZ (mL/g). *Distribution:* Truncated log normal. *Range:* 1 to 50. *Mean:* 14. *Standard Deviation:* 11.2. *Correlation:* See *Radionuclide Transport Models Under Ambient Conditions* (SNL 2007 [DIRS 177396], Appendix B[a], Table B-2[a]). *Additional Information:* See KdAm_Devit_a. Recorded in the TSPA Input Database as four constants: UZ_Kd_Se_D_max, UZ_Kd_Se_D_mean, UZ_Kd_Se_D_SD, and UZ_Kd_Se_D_min. *Sensitivity Name:* UZKDSEDT. *Location in TSPA-LA:* Sections 6.3.9.2 and 6.3.9.3; Equation 6.3.9-3; Table 6.3.9-2. *DTN:* UZ_Kd_Se_D_max, UZ_Kd_Se_D_mean, UZ_Kd_Se_D_SD, and UZ_Kd_Se_D_min found in LB0701PAKDSESN.001_R0 [DIRS 179299]. *References: Radionuclide Transport Models Under Ambient Conditions* (SNL 2007 [DIRS 177396], Sections 6.5 and A8.10; Table 6-3; Figure A-73).
KdSe_Vit_a*. Sorption coefficient for selenium in vitrified tuff units of UZ (mL/g). *Distribution:* Truncated log normal. *Range:* 0 to 25. *Mean:* 8.6. *Standard Deviation:* 7.9. *Correlation:* See *Radionuclide Transport Models Under Ambient Conditions* (SNL 2007 [DIRS 177396], Appendix B[a], Table B-2[a]). *Additional Information:* See KdAm_Devit_a. Recorded in the TSPA Input Database as four constants: UZ_Kd_Se_V_max, UZ_Kd_Se_V_mean, UZ_Kd_Se_V_SD, UZ_Kd_Se_V_min, and UZ_Kd_Se_V_min_5004. *Sensitivity Name:* UZKDSEVT*. *Location in TSPA-LA:* Sections 6.3.9.2 and 6.3.9.3; Equation 6.3.9-3; Table 6.3.9-2. *DTN:* UZ_Kd_Se_V_max, UZ_Kd_Se_V_mean, UZ_Kd_Se_V_SD, UZ_Kd_Se_V_min, and UZ_Kd_Se_V_min_5004 found in LB0701PAKDSESN.001_R0 [DIRS 179299]. *References: Radionuclide Transport Models Under Ambient Conditions* (SNL 2007 [DIRS 177396], Section 6.5; Table 6-1[a]).

Table K3-3. Detailed Summary of Epistemically Uncertain Variables (i.e., elements of **e**) Considered in the TSPA-LA (TSPA Parameter Name) (Continued)

NOTE: * indicates variable not considered in sensitivity analysis due to correlations.

KdSe_Zeo_a*. Sorption coefficient for selenium in zeolitic tuff units of UZ (mL/g). *Distribution:* Truncated log normal. *Range:* 1 to 35. *Mean:* 14.3. *Standard Deviation:* 7.9. *Correlation:* See *Radionuclide Transport Models Under Ambient Conditions* (SNL 2007 [DIRS 177396], Appendix B[a], Table B-2[a]). *Additional Information:* See KdAm_Devit_a. Recorded in the TSPA Input Database as four constants: UZ_Kd_Se_Z_max, UZ_Kd_Se_Z_mean, UZ_Kd_Se_Z_SD, and UZ_Kd_Se_Z_min. *Sensitivity Name:* UZKDSEZT*. *Location in TSPA-LA:* Sections 6.3.9.2 and 6.3.9.3; Equation 6.3.9-3; Table 6.3.9-2. *DTN:* UZ_Kd_Se_Z_max, UZ_Kd_Se_Z_mean, UZ_Kd_Se_Z_SD, and UZ_Kd_Se_Z_min found in LB0701PAKDSESN.001_R0 [DIRS 179299]. *References: Radionuclide Transport Models Under Ambient Conditions* (SNL 2007 [DIRS 177396], Section 6.5; Table 6-1[a]).
KdSn_Devit_a. Sorption coefficient for tin in devitrified tuff units of UZ (mL/g). *Distribution:* Log-uniform. *Range:* 100 to 100000. *Correlation:* See *Radionuclide Transport Models Under Ambient Conditions* (SNL 2007 [DIRS 177396], Appendix B[a], Table B-2[a]). *Additional Information:* See KdAm_Devit_a. See discussion for KdAm_Devit_a. Recorded in the TSPA Input Database as four constants: UZ_Kd_Sn_D_min and UZ_Kd_Sn_D_max. *Sensitivity Name:* UZKDSNDT. *Location in TSPA-LA:* Sections 6.3.9.2 and 6.3.9.3; Equation 6.3.9-3; Table 6.3.9-2. *DTN:* UZ_Kd_Sn_D_min and UZ_Kd_Sn_D_max found in LB0701PAKDSESN.001_R0 [DIRS 179299]. *References: Radionuclide Transport Models Under Ambient Conditions* (SNL 2007 [DIRS 177396], Section 6.5; Table 6-1[a]).
KdSn_Vit_a*. Sorption coefficient for tin in vitrified tuff units of UZ (mL/g). *Distribution:* Log-uniform. *Range:* 100 to 5000. *Correlation:* See *Radionuclide Transport Models Under Ambient Conditions* (SNL 2007 [DIRS 177396], Appendix B[a], Table B-2[a]). *Additional Information:* See KdAm_Devit_a. Recorded in the TSPA Input Database as four constants: UZ_Kd_Sn_V_min and UZ_Kd_Sn_V_max. *Sensitivity Name:* UZKDSNVT*. *Location in TSPA-LA:* Sections 6.3.9.2 and 6.3.9.3; Equation 6.3.9-3; Table 6.3.9-2. *DTN:* UZ_Kd_Sn_V_min and UZ_Kd_Sn_V_max found in LB0701PAKDSESN.001_R0 [DIRS 179299]. *References: Radionuclide Transport Models Under Ambient Conditions* (SNL 2007 [DIRS 177396], Section 6.5; Table 6-1[a]).
KdSn_Zeo_a*. Sorption coefficient for tin in zeolitic tuff units of UZ (mL/g). *Distribution:* Log-uniform. *Range:* 100 to 5000. *Correlation:* See *Radionuclide Transport Models Under Ambient Conditions* (SNL 2007 [DIRS 177396], Appendix B[a], Table B-2[a]). *Additional Information:* See KdAm_Devit_a. Recorded in the TSPA Input Database as four constants: UZ_Kd_Sn_Z_min and UZ_Kd_Sn_Z_max. *Sensitivity Name:* UZKDSNZT*. *Location in TSPA-LA:* Sections 6.3.9.2 and 6.3.9.3; Equation 6.3.9-3; Table 6.3.9-2. *DTN:* UZ_Kd_Sn_Z_min and UZ_Kd_Sn_Z_max found in LB0701PAKDSESN.001_R0 [DIRS 179299]. *References: Radionuclide Transport Models Under Ambient Conditions* (SNL 2007 [DIRS 177396], Section 6.5; Table 6-1[a]).
KdSr_Devit_a. Sorption coefficient for strontium in devitrified tuff units of UZ (mL/g). *Distribution:* Uniform. *Range:* 10 to 70. *Correlation:* See *Radionuclide Transport Models Under Ambient Conditions* (SNL 2007 [DIRS 177396], Appendix B[a], Table B-2[a]). *Additional Information:* See KdAm_Devit_a. Recorded in the TSPA Input Database as four constants: UZ_Kd_Sr_D_max and UZ_Kd_Sr_D_min. *Sensitivity Name:* UZKDSRDT. *Location in TSPA-LA:* Sections 6.3.9.2 and 6.3.9.3; Equation 6.3.9-3; Table 6.3.9-2. *DTN:* UZ_Kd_Sr_D_max and UZ_Kd_Sr_D_min found in LA0408AM831341.001_R0 [DIRS 171584]. *References: Radionuclide Transport Models Under Ambient Conditions* (SNL 2007 [DIRS 177396], Section 6.5; Table 6-1[a]).
KdSr_Vit_a*. Sorption coefficient for strontium in vitrified tuff units of UZ (mL/g). *Distribution:* Uniform. *Range:* 0 to 50. *Correlation:* See *Radionuclide Transport Models Under Ambient Conditions* (SNL 2007 [DIRS 177396], Appendix B[a], Table B-2[a]). *Additional Information:* See KdAm_Devit_a. Recorded in the TSPA Input Database as four constants: UZ_Kd_Sr_V_max and UZ_Kd_Sr_V_min. *Sensitivity Name:* UZKDSRVT*. *Location in TSPA-LA:* Sections 6.3.9.2 and 6.3.9.3; Equation 6.3.9-3; Table 6.3.9-2. *DTN:* UZ_Kd_Sr_V_max and UZ_Kd_Sr_V_min found in LA0408AM831341.001_R0 [DIRS 171584]. *References: Radionuclide Transport Models Under Ambient Conditions* (SNL 2007 [DIRS 177396], Section 6.5; Table 6-1[a]).
KdSr_Zeo_a*. Sorption coefficient for strontium in zeolitic tuff units of UZ (mL/g). *Distribution:* Uniform. *Range:* 50 to 2000. *Correlation:* See *Radionuclide Transport Models Under Ambient Conditions* (SNL 2007 [DIRS 177396], Appendix B[a], Table B-2[a]). *Additional Information:* See KdAm_Devit_a. Recorded in the TSPA Input Database as four constants: UZ_Kd_Sr_Z_max and UZ_Kd_Sr_Z_min. *Sensitivity Name:* UZKDSRZT*. *Location in TSPA-LA:* Sections 6.3.9.2 and 6.3.9.3; Equation 6.3.9-3; Table 6.3.9-2. *DTN:* UZ_Kd_Sr_Z_max and UZ_Kd_Sr_Z_min found in LA0408AM831341.001_R0 [DIRS 171584]. *References: Radionuclide Transport Models Under Ambient Conditions* (SNL 2007 [DIRS 177396], Section 6.5; Table 6-1[a]).

Table K3-3. Detailed Summary of Epistemically Uncertain Variables (i.e., elements of **e**) Considered in the TSPA-LA (TSPA Parameter Name) (Continued)

NOTE: * indicates variable not considered in sensitivity analysis due to correlations.

KdTh_Devit_a. Sorption coefficient for thorium in devitrified tuff units of UZ (mL/g). *Distribution:* Uniform. *Range:* 1000 to 10000. *Correlation:* See *Radionuclide Transport Models Under Ambient Conditions* (SNL 2007 [DIRS 177396], Appendix B[a], Table B-2[a]). *Additional Information:* See KdAm_Devit_a. Recorded in the TSPA Input Database as four constants: UZ_Kd_Th_D_max and UZ_Kd_Th_D_min. *Sensitivity Name:* UZKDTHDT. *Location in TSPA-LA:* Sections 6.3.9.2 and 6.3.9.3; Equation 6.3.9-3; Table 6.3.9-2. *DTN:* UZ_Kd_Th_D_max and UZ_Kd_Th_D_min found in LA0408AM831341.001_R0 [DIRS 171584]. *References: Radionuclide Transport Models Under Ambient Conditions* (SNL 2007 [DIRS 177396], Section 6.5; Table 6-1[a]).
KdTh_Vit_a*. Sorption coefficient for thorium in vitrified tuff units of UZ (mL/g). *Distribution:* Uniform. *Range:* 1000 to 10000. *Correlation:* See *Radionuclide Transport Models Under Ambient Conditions* (SNL 2007 [DIRS 177396], Appendix B[a], Table B-2[a]). *Additional Information:* See KdAm_Devit_a. Recorded in the TSPA Input Database as four constants: UZ_Kd_Th_V_max and UZ_Kd_Th_V_min. *Sensitivity Name:* UZKDTHVT*. *Location in TSPA-LA:* Sections 6.3.9.2 and 6.3.9.3; Equation 6.3.9-3; Table 6.3.9-2. *DTN:* UZ_Kd_Th_V_max and UZ_Kd_Th_V_min found in LA0408AM831341.001_R0 [DIRS 171584]. *References: Radionuclide Transport Models Under Ambient Conditions* (SNL 2007 [DIRS 177396], Section 6.5; Table 6-1[a]).
KdTh_Zeo_a*. Sorption coefficient for thorium in zeolitic tuff units of UZ (mL/g). *Distribution:* Uniform. *Range:* 1000 to 30000. *Correlation:* See *Radionuclide Transport Models Under Ambient Conditions* (SNL 2007 [DIRS 177396], Appendix B[a], Table B-2[a]). *Additional Information:* See KdAm_Devit_a. Recorded in the TSPA Input Database as four constants: UZ_Kd_Th_Z_max and UZ_Kd_Th_Z_min. *Sensitivity Name:* UZKDTHZT*. *Location in TSPA-LA:* Sections 6.3.9.2 and 6.3.9.3; Equation 6.3.9-3; Table 6.3.9-2. *DTN:* UZ_Kd_Th_Z_max and UZ_Kd_Th_Z_min found in LA0408AM831341.001_R0 [DIRS 171584]. *References: Radionuclide Transport Models Under Ambient Conditions* (SNL 2007 [DIRS 177396], Section 6.5; Table 6-1[a]).
KdU_Devit_a. Sorption coefficient for uranium in devitrified tuff units of UZ (mL/g). *Distribution:* Piecewise uniform. *Range:* 0 to 4. *Median:* 0.2. *Correlation:* See *Radionuclide Transport Models Under Ambient Conditions* (SNL 2007 [DIRS 177396], Appendix B[a], Table B-2[a]). *Additional Information:* See KdAm_Devit_a. Recorded in the TSPA Input Database as four constants: UZ_Kd_U_D_c1, UZ_Kd_U_D_c2 and UZ_Kd_U_D_c3. *Sensitivity Name:* UZKDUDT. *Location in TSPA-LA:* Sections 6.3.9.2 and 6.3.9.3; Equation 6.3.9-3; Table 6.3.9-2. *DTN:* UZ_Kd_U_D_c1, UZ_Kd_U_D_c2 and UZ_Kd_U_D_c3 found in LA0408AM831341.001_R0 [DIRS 171584]. *References: Radionuclide Transport Models Under Ambient Conditions* (SNL 2007 [DIRS 177396], Section 6.5; Table 6-1[a]).
KdU_Vit_a*. Sorption coefficient for uranium in vitrified tuff units of UZ (mL/g). *Distribution:* Piecewise uniform. *Range:* 0 to 3. *Median:* 0.2. *Correlation:* See *Radionuclide Transport Models Under Ambient Conditions* (SNL 2007 [DIRS 177396], Appendix B[a], Table B-2[a]). *Additional Information:* See KdAm_Devit_a. Recorded in the TSPA Input Database as four constants: UZ_Kd_U_V_c1, UZ_Kd_U_V_c2 and UZ_Kd_U_V_c3. *Sensitivity Name:* UZKDUVT*. *Location in TSPA-LA:* Sections 6.3.9.2 and 6.3.9.3; Equation 6.3.9-3; Table 6.3.9-2. *DTN:* UZ_Kd_U_V_c1, UZ_Kd_U_V_c2 and UZ_Kd_U_V_c3 found in LA0408AM831341.001_R0 [DIRS 171584]. *References: Radionuclide Transport Models Under Ambient Conditions* (SNL 2007 [DIRS 177396], Section 6.5; Table 6-1[a]).
KdU_Zeo_a*. Sorption coefficient for uranium in zeolitic tuff units of UZ (mL/g). *Distribution:* Piecewise uniform. *Range:* 0 to 30. *Median:* 0.5. *Correlation:* See *Radionuclide Transport Models Under Ambient Conditions* (SNL 2007 [DIRS 177396], Appendix B[a], Table B-2[a]). *Additional Information:* See KdAm_Devit_a. Recorded in the TSPA Input Database as four constants: UZ_Kd_U_V_c1, UZ_Kd_U_V_c2, UZ_Kd_U_V_c3 and UZ_Kd_U_V_c3_5004. *Sensitivity Name:* UZKDUZT*. *Location in TSPA-LA:* Sections 6.3.9.2 and 6.3.9.3; Equation 6.3.9-3; Table 6.3.9-2. *DTN:* UZ_Kd_U_V_c1, UZ_Kd_U_V_c2, UZ_Kd_U_V_c3 and UZ_Kd_U_V_c3_5004 found in LA0408AM831341.001_R0 [DIRS 171584]. *References: Radionuclide Transport Models Under Ambient Conditions* (SNL 2007 [DIRS 177396], Section 6.5; Table 6-1[a]).

Table K3-3. Detailed Summary of Epistemically Uncertain Variables (i.e., elements of **e**) Considered in the TSPA-LA (TSPA Parameter Name) (Continued)

NOTE: * indicates variable not considered in sensitivity analysis due to correlations.

L_Divides_a. Depth of permeable soil on divides of the Fortymile Wash fan (RMEI location) (cm). *Distribution:* Uniform. *Range:* 102 to 140. *Symbol:* L_d. *Additional Information:* This parameter is constrained using field measurements from soil pits dug into inter-channel divides of the Fortymile Wash alluvial fan. Permeable soil depths were measured at several locations on the Fortymile Wash alluvial fan. The model uses a different depth for each of the two sub-domains in the RMEI location (channels and divides). As the permeable depth increases, the mass of radionuclides that will diffuse into the soil over time (and thus move below the biosphere depth) increases. Capturing the lower bound of the possible permeable depth is necessary to assure conservative model results. The permeable depth in the channel subdomain was inferred from the measurements made on the divides. *Sensitivity Name:* LDIVIDE. *Location in TSPA-LA:* Table 6.5-5. *DTN:* MO0702PAFARDAT.001_R3 [DIRS 182578]. *References: Redistribution of Tephra and Waste by Geomorphic Processes Following a Potential Volcanic Eruption at Yucca Mountain, Nevada* (SNL 2007 [DIRS 179347], Section 6.3.2, 6.5.5.1 and 7.1.3; Tables 4.1-4, 6.4-1 and 6.5.5-1).
LC_rate_a. Crevice corrosion (localized corrosion) propagation rate (mm/yr). *Distribution:* Log uniform. *Range:* 0.0127 to 1.27. *Additional Information:* Localized corrosion rate or crevice corrosion propagation rate. The crevice corrosion penetration model assumes that, when it occurs, crevice corrosion propagates at a (time-independent) constant rate. Variation in this parameter values is attributed to uncertainty. *Sensitivity Name:* WDLCRATE. *Location in TSPA-LA:* Sections 6.3.5.2.1, 6.3.5.2.2, 6.3.5.2.3, 6.3.5.3.2 and 6.3.5.4; Table 6.3.5-4. *DTN:* MO0703PAGENCOR.001_R4 [DIRS 182029]. *References: General Corrosion and Localized Corrosion of Waste Package Outer Barrier* (SNL 2007 [DIRS 178519], Sections 6.4.4.7 and 7.2.5; Table 8-3).
LDISP. Logarithm of longitudinal dispersivity (m). *Distribution:* Right truncated normal. *Range*: $-\infty$ to 3.5. *Mean:* 2.0. *Standard Deviation:* 0.75. *Symbol:* α_L. *Additional Information:* Represents variation in the longitudinal dispersivity of all the saturated zone units. Longitudinal dispersivity will be important only at the leading edge of the advancing plume; transverse dispersivity (horizontal transverse and vertical transverse) is the strongest control on plume spreading and possible dilution within the aquifer. To treat the one- and three-dimensional transport through the SZ consistently, the sampled values used to generate the saturated zone breakthrough curves are also used in the TSPA-LA Model. These values are tabulated as 200 sets of values for the SZ parameters, accounting for appropriate correletions, and are entered into the TSPA model as a table of 200 values for each parameter. The TSPA-LA Model selects values from this table using the Goldsim variable SZ_index_a. *Sensitivity Name:* SZLODISP. *Location in TSPA-LA:* Section 6.3.10.2; Table 6.3.10-2. *DTN:* SN0702PASZFTMA.002_R1 [DIRS 183471]. *References: Saturated Zone Flow and Transport Model Abstraction* (SNL 2008 [DIRS 183750], Sections 6.3.1 and 6.5.2.9; Tables 4-3, 6-8, 7-1[a], A-1[a] and B-1; Equations 6-27 to 6-29; Figures 6-18 and 6-19).
Log_Specific_SA_CSNF_a. Logarithm of the effective specific surface area (m^2/mg) of the representative CSNF waste form (dimensionless). *Distribution:* Triangular. *Range:* -7.3 to -5.4. *Most Likely:* -6.7. *Symbol:* $Log_{10}(A)$. *Additional Information:* The radionuclide release rate form the CSNF matrix under alkaline conditions (pH ≥ 6.8) is modeled as the fractional matrix dissolution rate (d^{-1}) which has the following mathematical form: Log (F) = Log (A) + a0 + a1 * IT + a2 * pCO_3 + a3 * pO_2. Where Log (F) = Base 10 log of the fractional dissolution rate of the fuel (d^{-1}), IT = Inverse temperature (K^{-1}), pCO_3 = Negative base 10 log of total carbonate (molar). pO_2 = Negative base 10 log of oxygen pressure (atmospheres), Log (A) = Base 10 log of the fuel effective specific surface area (m^2/mg), and a0, a1, a2, a3 = Regression parameters for the dissolution rate per unit area. *Sensitivity Name:* CSSPECSA. *Location in TSPA-LA:* Sections 6.3.7.4.1.2 and 6.3.7.4.1.3; Tables 6.3.7-30 and 6.3.7-31; Equations 6.3.7-5 and 6.3.7-6. *DTN:* MO0404ANLSF001.001_R0 [DIRS 169007]. *References: CSNF Waste Form Degradation: Summary Abstraction* (BSC 2004 [DIRS 169987], Sections 4.1.3, 5.2, 6.2.2.3, 6.4.1, 8.1 and 8.2; Equations 13 and 14; Tables 8-2 and 8-3).
LogK_Uncert_Lith_a. Logarithm of the mean fracture permeability in lithophysal rock units (dimensionless). *Distribution:* Triangular. *Range:* -0.92 to 0.92. *Mode:* 0. *Symbol:* log k. *Additional Information:* Ambient seepage is a function of three key parameters: capillary strength, permeability, and percolation flux. The ambient seepage results derived from the seepage model for performance assessment provide the basis for the quantitative evaluation of seepage as a function of these key hydrological properties. The log(k) is used to select the mean and standard deviation of seepage flow. The units for the value of k must be m^2 prior to calculating the logarithm. *Sensitivity Name:* SEEPPRM. *Location in TSPA-LA:* Sections 6.3.5.2.3, 6.3.3.1.2 and 6.3.3.1.3; Tables 6.3.5-4, 6.3.3-2 and 6.3.3-3. *DTN:* LB0407AMRU0120.001_R0 [DIRS 173280], *Summary_seepage_abstraction.doc. References: Abstraction of Drift Seepage* (SNL 2007 [DIRS 181244], Section 6.6.3).

Table K3-3. Detailed Summary of Epistemically Uncertain Variables (i.e., elements of **e**) Considered in the TSPA-LA (TSPA Parameter Name) (Continued)

NOTE: * indicates variable not considered in sensitivity analysis due to correlations.

LogK_Uncert_NonLith_a. Logarithm of the mean fracture permeability in non-lithophysal rock units (dimensionless). *Distribution:* Triangular. *Range:* -0.68 to 0.68. *Mode:* 0. *Symbol:* log k. *Additional Information:* See LogK_Uncert_Lith_a. *Sensitivity Name:* SEEPPRMN. *Location in TSPA-LA:* Sections 6.3.5.2.3, 6.3.3.1.2 and 6.3.3.1.3; Tables 6.3.5-4, 6.3.3-2 and 6.3.3-3. *DTN:* LB0407AMRU0120.001_R0 [DIRS 173280], *Summary_seepage_abstraction.doc. References: Abstraction of Drift Seepage* (SNL 2007 [DIRS 181244], Section 6.6.3).
Mass_Decrease_Const_GE10_a. Mass loading decrease rate constant (1/yr). *Distribution:* Triangular. *Range:* 0.125 to 1. *Mode:* 0.2. *Symbol:* λ. *Additional Information:* Mass loading decreases exponentially with time after the eruption. The mass loading decrease rate constant depends on the ash thickness. Selected distribution is based in part on the influence of ash redistribution on changes in mass loading through time. The ash redistribution model considers the interchannel divides separately from the distributary channels that carry redistributed ash. These areas can have a different thickness of ash or ash mixed with soil, and thus different mass loading decrease rate constants. To account for these differences, it is recommended that the mass loading decrease rate constant used in the TSPA model is that for the greater of the contaminated soil thickness in the distributary channels and interchannel divides. Because the thickness of the redistributed ash in the channels is likely to be greater than the threshold depth of 10 mm, it is reasonable to always use the mass loading decrease rate constant for the thicker contaminated layer. *Sensitivity Name:* MASSDCRS. *Location in TSPA-LA:* Equation 6.3.11-5. *DTN:* MO0702PAVBPDCF.000_R0 [DIRS 179330]. *References: Biosphere Model Report* (SNL 2007 [DIRS 177399], Section 6.12.3; Tables 6.6-3 and 6.7-1; Equation 6.12-3).
MIC_RHThresh_a. Relative humidity threshold for initiating microbially induced corrosion (dimensionless). *Distribution:* Uniform. *Range:* 0.75 to 0.9. *Additional Information:* MIC effects are applied when the relative humidity at the waste package surface is greater than a threshold relative humidity sampled from a uniform distribution between 75% and 90%. A uniform distribution has been chosen for the MIC relative humidity threshold because this statistical distribution is recommended when the upper and lower bounds of the distribution are reasonably well known, but only a low state of knowledge exists about how the MIC relative humidity threshold varies between these bounds. Consistent with the aforementioned low state of knowledge, the variation in the MIC relative humidity threshold is considered solely due to uncertainty. *Sensitivity Name:* WDMICRHT. *Location in TSPA-LA:* Sections 6.3.5.1.2 and 6.3.5.1.3; Tables 6.3.5-3 and 6.3.5-4. *DTN:* MO0703PAGENCOR.001_R4 [DIRS 182029]. *References: General Corrosion and Localized Corrosion of Waste Package Outer Barrier* (SNL 2007 [DIRS 178519], Sections 1.2, 4.1.1.7, 6.3.3, 6.4.5.1 and 8.2; Table 8-1).
n_SCC_a. Stress corrosion cracking growth rate exponent (repassivation slope) (dimensionless). *Distribution:* Truncated normal. *Range:* 0.935 to 1.395. *Mean:* 1.165. *Standard Deviation:* 0.115. *Symbol:* n. *Additional Information:* The threshold stress intensity factor is a function of the repassivation slope and mean general corrosion rate. Crack growth velocity is a function of the stress-intensity factor and repassivation slope. Uncertainty in the crack growth and in the stress-intensity factor threshold is represented by the uncertainty in the repassivation slope. The repassivation slope is sampled once for every realization in the TSPA model. *Sensitivity Name:* WDNSCC. *Location in TSPA-LA:* Sections 6.3.5.1.2 and 6.3.5.4; Table 6.3.5-3; Equations 6.3.5-13 and 6.3.5-14. *DTN:* MO0702PASTRESS.002_R2 [DIRS 180514], File: Model Output DTN.doc. *References: Stress Corrosion Cracking of Waste Package Outer Barrier and Drip Shield Materials* (SNL 2007 [DIRS 181953], Sections 6.4.4.4, 8.4.2.3 and 8.4.3; Tables 6-7, 8-1, 8-5, 8-6 and 8-15; Equations 4, 5, 70 and 71).
NiO_SA_a. Specific surface area of NiO (m^2/g). *Distribution:* Uniform. *Range:* 1 to 30. *Symbol:* S_{NiO}. *Additional Information:* See Cr2O3_SA_a. The properties of hematite (Fe_2O_3), goethite (FeOOH), hydrous ferric oxide (HFO), Cr_2O_3, and NiO are used for calculating the amount of water adsorbed onto stationary corrosion product surfaces. *Sensitivity Name:* NIOSA. *Location in TSPA-LA:* Table 6.3.8-4; S_{CP} in Equation 6.3.8-19. *DTN:* SN0703PAEBSRTA.001_R3 [DIRS 183217]. *References: EBS Radionuclide Transport Abstraction* (SNL 2007 [DIRS 177407], Sections 6.3.4.3.3 and 6.5.2.2; Tables 6.5-7 and 8.2-4).
Np2O5_Eps_1_high_a*. Logarithm of the scale factor used to characterize uncertainty in Np_2O_5 solubility for ionic strength values between 1 and 3 molal (dimensionless). *Distribution:* Truncated normal. *Range:* -1.7 to 1.7. *Mean:* 0. *Standard Deviation:* 0.85. *Correlation:* Correlated to Np2O5_Eps_1_low_a. *Symbol:* ε_1. *Additional Information:* See Am_Eps_1_low_a. *Sensitivity Name:* EP1HINP2*. *Location in TSPA-LA:* Sections 6.3.7.5.1 and 6.3.7.5.2; Table 6.3.7-42; Equation 6.3.7-13a. *DTN: MO0702PADISCON.001_R0* [DIRS 179358], Tables 3 & 19. *References: Dissolved Concentration Limits of Elements with Radioactive Isotopes* (SNL 2007 [DIRS 177418], Sections 6.6 and 8.1.2; Equations 6.6-5 and 8-1; Table 6.6-11).

Table K3-3. Detailed Summary of Epistemically Uncertain Variables (i.e., elements of **e**) Considered in the TSPA-LA (TSPA Parameter Name) (Continued)

NOTE: * indicates variable not considered in sensitivity analysis due to correlations.

Np2O5_Eps_1_low_a. Logarithm of the scale factor used to characterize uncertainty in Np_2O_5 solubility at an ionic strength below 1 molal (dimensionless). *Distribution:* Truncated normal. *Range:* -1.6 to 1.6. *Mean:* 0. *Standard Deviation:* 0.8. *Correlation:* Correlated to Np2O5_Eps_1_high_a with a correlation factor of 1. *Symbol:* ε_1. *Additional Information:* See Am_Eps_1_low_a. This model is applied only in the invert. *Sensitivity Name:* EP1NP2O5. *Location in TSPA-LA:* Sections 6.3.7.5.1 and 6.3.7.5.2; Table 6.3.7-42; Equation 6.3.7-13a. *DTN: MO0702PADISCON.001_R0* [DIRS 179358], Tables 3 & 19. *References: Dissolved Concentration Limits of Elements with Radioactive Isotopes* (SNL 2007 [DIRS 177418], Sections 6.6 and 8.1.2; Equations 6.6-5 and 8-1; Table 6.6-11).
Np2O5_Eps_2_CDSP_High_a*. Term associated with uncertainty in Np_2O_5 solubility due to variations in fluoride concentration for CDSP waste packages when ionic strength is greater than or equal to 0.004 molal and for the invert below CDSP waste packages (mg/L). *Distribution:* Triangular. *Range:* 0 to 853. *Most Likely:* 0. *Correlation:* Correlated to Am_Eps_2_CSNF_High_a. *Symbol:* $\varepsilon_2^{\text{CDSP-F-high}}$, $\varepsilon_2^{\text{CDSP-invert}}$. *Additional Information:* See Am_Eps_2_CSNF_High_a. *Sensitivity Name:* EP2CDNP2*. *Location in TSPA-LA:* Sections 6.3.7.5.1 and 6.3.7.5.2; Table 6.3.7-42; Equation 6.3.7-13a. *DTN:* MO0702PAFLUORI.000_R1 [DIRS 181219], Table 5. *References: Dissolved Concentration Limits of Elements with Radioactive Isotopes* (SNL 2007 [DIRS 177418], Sections 6.6 and 8.1.2; Equations 6.6-5 and 8-1; Table 6.6-11).
Np2O5_Eps_2_CSNF_High_a*. Term associated with uncertainty in Np_2O_5 solubility due to variations in fluoride concentration for CSNF waste packages when ionic strength is greater than or equal to 0.2 molal and for the invert below CSNF waste packages (mg/L). *Distribution:* Triangular. *Range:* 0 to 197. *Most Likely:* 0. *Correlation:* Correlated to Am_Eps_2_CSNF_High_a. *Symbol:* $\varepsilon_2^{\text{CSNF-high}}$, $\varepsilon_2^{\text{CSNF-invert}}$. *Additional Information:* See Am_Eps_2_CSNF_High_a. *Sensitivity Name:* EP2CSNP2*. *Location in TSPA-LA:* Sections 6.3.7.5.1 and 6.3.7.5.2; Table 6.3.7-42; Equation 6.3.7-13a. *DTN:* MO0702PAFLUORI.000_R1 [DIRS 181219], Table 5. *References: Dissolved Concentration Limits of Elements with Radioactive Isotopes* (SNL 2007 [DIRS 177418], Sections 6.6 and 8.1.2; Equations 6.6-5 and 8-1; Table 6.6-11).
Np2O5_Eps_2_Glass_Low_a*. Term associated with uncertainty in Np_2O_5 solubility due to variations in fluoride concentration for CDSP waste packages Cell 1a, Cell 1b when ionic strength is less than 0.004 molal, and CSNF waste packages when ionic strength is less than 0.2 molal (mg/L). *Distribution:* Triangular. *Range:* 0 to 11. *Most Likely:* 0. *Correlation:* Correlated to Am_Eps_2_CSNF_High_a. *Symbol:* $\varepsilon_2^{\text{CSNF-low}}$, $\varepsilon_2^{\text{CDSP-Glass}}$, $\varepsilon_2^{\text{CDSP-F-low}}$. *Additional Information:* See Am_Eps_2_CSNF_High_a. *Sensitivity Name:* EP2LONP2*. *Location in TSPA-LA:* Sections 6.3.7.5.1 and 6.3.7.5.2; Table 6.3.7-42; Equation 6.3.7-13a. *DTN:* MO0702PAFLUORI.000_R1 [DIRS 181219], Table 5. *References: Dissolved Concentration Limits of Elements with Radioactive Isotopes* (SNL 2007 [DIRS 177418], Sections 6.6 and 8.1.2; Equations 6.6-5 and 8-1; Table 6.6-11).
NpO2_Eps_1_high_a*. Logarithm of the scale factor used to characterize uncertainty in NpO_2 solubility at an ionic strength between 1 and 3 molal (dimensionless). *Distribution:* Truncated normal. *Range:* -1.34 to 1.34. *Mean:* 0. *Standard Deviation:* 0.67. *Correlation:* Correlated to NpO2_Eps_1_low_a. *Symbol:* ε_1. *Additional Information:* See Am_Eps_1_low_a. *Sensitivity Name:* EP1HINPO2*. *Location in TSPA-LA:* Sections 6.3.7.5.1, 6.3.7.5.2 and 6.3.7.5.3; Table 6.3.7-43; Equation 6.3.7-13a. *DTN: MO0702PADISCON.001_R0* [DIRS 179358], Tables 2 & 19. *References: Dissolved Concentration Limits of Elements with Radioactive Isotopes* (SNL 2007 [DIRS 177418], Sections 6.6 and 8.1.2; Equations 6.6-2 and 8-1; Table 6.6-5).
NpO2_Eps_1_low_a. Logarithm of the scale factor used to characterize uncertainty in NpO_2 solubility at an ionic strength below 1 molal (dimensionless). *Distribution:* Truncated normal. *Range:* -1.2 to 1.2. *Mean:* 0. *Standard Deviation:* 0.6. *Correlation:* Correlated to NpO2_Eps_1_high_a with a correlation factor of 1. *Symbol:* ε_1. *Additional Information:* See Am_Eps_1_low_a. This model is applied only within the waste package. *Sensitivity Name:* EP1NPO2. *Location in TSPA-LA:* Sections 6.3.7.5.1, 6.3.7.5.2 and 6.3.7.5.3; Table 6.3.7-43; Equation 6.3.7-13a. *DTN: MO0702PADISCON.001_R0* [DIRS 179358], Tables 2 & 19. *References: Dissolved Concentration Limits of Elements with Radioactive Isotopes* (SNL 2007 [DIRS 177418], Sections 6.6 and 8.1.2; Equations 6.6-2 and 8-1; Table 6.6-5).
NpO2_Eps_2_CDSP_High_a*. Term associated with uncertainty in NpO_2 solubility due to variations in fluoride concentration for CDSP waste packages when ionic strength is greater than or equal to 0.004 molal and for the invert below CDSP waste packages (mg/L). *Distribution:* Triangular. *Range:* 0 to 1093.5. *Most Likely:* 0. *Correlation:* Correlated to Am_Eps_2_CSNF_High_a. *Symbol:* $\varepsilon_2^{\text{CDSP-F-high}}$, $\varepsilon_2^{\text{CDSP-invert}}$. *Additional Information:* See Am_Eps_2_CSNF_High_a. *Sensitivity Name:* EP2CDNPO2*. *Location in TSPA-LA:* Sections 6.3.7.5.1, 6.3.7.5.2 and 6.3.7.5.3; Table 6.3.7-43; Equation 6.3.7-13a. *DTN:* MO0702PAFLUORI.000_R1 [DIRS 181219], Table 3. *References: Dissolved Concentration Limits of Elements with Radioactive Isotopes* (SNL 2007 [DIRS 177418], Sections 6.6 and 8.1.2; Equations 6.6-2 and 8-1; Table 6.6-5).

Table K3-3. Detailed Summary of Epistemically Uncertain Variables (i.e., elements of **e**) Considered in the TSPA-LA (TSPA Parameter Name) (Continued)

NOTE: * indicates variable not considered in sensitivity analysis due to correlations.

NpO2_Eps_2_CSNF_High_a*. Term associated with uncertainty in NpO_2 solubility due to variations in fluoride concentration for CSNF waste packages when ionic strength is greater than or equal to 0.2 molal and for the invert below CSNF waste packages (mg/L). *Distribution:* Triangular. *Range:* 0 to 255.8. *Most Likely:* 0. *Correlation:* Correlated to Am_Eps_2_CSNF_High_a. *Symbol:* $\varepsilon_2^{\text{CSNF-high}}$, $\varepsilon_2^{\text{CSNF-invert}}$. *Additional Information:* See Am_Eps_2_CSNF_High_a. *Sensitivity Name:* EP2CSNPO2*. *Location in TSPA-LA:* Sections 6.3.7.5.1, 6.3.7.5.2 and 6.3.7.5.3; Table 6.3.7-43; Equation 6.3.7-13a. *DTN:* MO0702PAFLUORI.000_R1 [DIRS 181219], Table 3. *References: Dissolved Concentration Limits of Elements with Radioactive Isotopes* (SNL 2007 [DIRS 177418], Sections 6.6 and 8.1.2; Equations 6.6-2 and 8-1; Table 6.6-5).
NpO2_Eps_2_Glass_Low_a*. Term associated with uncertainty in NpO_2 solubility due to variations in fluoride concentration for CDSP waste packages Cell 1a, Cell 1b when ionic strength is less than 0.004 molal, and CSNF waste packages when ionic strength is less than 0.2 molal (mg/L). *Distribution:* Triangular. *Range:* 0 to 14.1. *Most Likely:* 0. *Correlation:* Correlated to Am_Eps_2_CSNF_High_a. *Symbol:* $\varepsilon_2^{\text{CSNF-low}}$, $\varepsilon_2^{\text{CDSP-Glass}}$, $\varepsilon_2^{\text{CDSP-F-low}}$. *Additional Information:* See Am_Eps_2_CSNF_High_a. *Sensitivity Name:* EP2LONPO2*. *Location in TSPA-LA:* Sections 6.3.7.5.1, 6.3.7.5.2 and 6.3.7.5.3; Table 6.3.7-43; Equation 6.3.7-13a. *DTN:* MO0702PAFLUORI.000_R1 [DIRS 181219], Table 3. *References: Dissolved Concentration Limits of Elements with Radioactive Isotopes* (SNL 2007 [DIRS 177418], Sections 6.6 and 8.1.2; Equations 6.6-2 and 8-1; Table 6.6-5).
NVF11. Effective porosity in undifferentiated alluvium (valley fill) (dimensionless). *Distribution:* Truncated normal. *Range:* 0 to 0.3. *Mean:* 0.18. *Standard Deviation:* 0.051. *Additional Information:* See NVF26. *Sensitivity Name:* SZPORUAL. *Location in TSPA-LA:* Table 6.3.10-2. *DTN:* SN0702PASZFTMA.002_R1 [DIRS 183471]. *References: Saturated Zone Flow and Transport Model Abstraction* (SNL 2008 [DIRS 183750], Sections 6.5.2.3 and 6.5.2.14; Tables 7-1[a] and A-1[a]; Figures 6-9 and 6-10).
NVF26. Effective porosity in shallow alluvium (dimensionless). *Distribution:* Truncated normal. *Range:* 0 to 0.3. *Mean:* 0.18. *Standard Deviation:* 0.051. *Additional Information:* In the porous media of the alluvium, sorption is conceptualized to occur in that portion of the aquifer corresponding to the effective porosity of the alluvium. The effective porosity is defined as the fraction of the total volume of the medium through which significant groundwater flow occurs. The effective porosity parameter in the alluvium is used to correctly calculate the pore velocity of groundwater. Effective porosity is important for determining the average linear groundwater velocities used in the simulation of radionuclide transport. Groundwater velocities are rendered more accurate when dead-end pores are eliminated from consideration because they do not transmit water. The effective porosity results from that elimination. To treat the one- and three-dimensional transport through the SZ consistently, the sampled values used to generate the saturated zone breakthrough curves are also used in the TSPA-LA Model. These values are tabulated as 200 sets of values for the SZ parameters, accounting for appropriate correletions, and are entered into the TSPA model as a table of 200 values for each parameter. The TSPA-LA Model selects values from this table using the Goldsim variable SZ_index_a. Parameters NVF26 and NVF11 are new names for parameters NVF19 and NVF7. *Sensitivity Name:* SZPORSAL. *Location in TSPA-LA:* Table 6.3.10-2. *DTN:* SN0702PASZFTMA.002_R1 [DIRS 183471]. *References: Saturated Zone Flow and Transport Model Abstraction* (SNL 2008 [DIRS 183750], Sections 6.5.2.3 and 6.5.2.14; Tables 7-1[a] and A-1[a]; Figures 6-9 and 6-10).
Pa_Eps_1_a. Logarithm of the scale factor used to characterize uncertainty in protactinium solubility (dimensionless). *Distribution:* Uniform. *Range:* -4.42 to -0.05. *Symbol:* ε_1. *Additional Information:* This defines uncertainty in the choice of an analogue for protactinium solubilities. The uncertainty range for protactinium solubility is taken as the difference between the solubilities of neptunium and thorium. For protactinium, no multiplication factor is used in conjunction with □2. *Sensitivity Name:* EP1PA. *Location in TSPA-LA:* Sections 6.3.7.5.2 and 6.3.7.5.3; Table 6.3.7-45; Equation 6.3.7-13b. *DTN: MO0702PADISCON.001_R0*_R0 [DIRS 179358], Tables 9 & 19. *References: Dissolved Concentration Limits of Elements with Radioactive Isotopes* (SNL 2007 [DIRS 177418], Sections 6.11 and 8.1.2; Equations 6.11-2 and 8-2; Table 6.11-4).
Pa_Eps_2_CDSP_High_a*. Term associated with uncertainty in protactinium solubility due to variations in fluoride concentration for CDSP waste packages when ionic strength is greater than or equal to 0.004 molal and for the invert below CDSP waste packages (mg/L). *Distribution:* Triangular. *Range:* 0 to 853. *Most Likely:* 0. *Correlation:* Correlated to Am_Eps_2_CSNF_High_a. *Symbol:* $\varepsilon_2^{\text{CDSP-F-high}}$, $\varepsilon_2^{\text{CDSP-invert}}$. *Additional Information:* See Am_Eps_2_CSNF_High_a. *Sensitivity Name:* EP2CDPA*. *Location in TSPA-LA:* Sections 6.3.7.5.2 and 6.3.7.5.3; Table 6.3.7-45; Equation 6.3.7-13b. *DTN:* MO0702PAFLUORI.000_R1 [DIRS 181219], Table 15. *References: Dissolved Concentration Limits of Elements with Radioactive Isotopes* (SNL 2007 [DIRS 177418], Sections 6.11 and 8.1.2; Equations 6.11-2 and 8-2; Table 6.11-4).

Table K3-3. Detailed Summary of Epistemically Uncertain Variables (i.e., elements of **e**) Considered in the TSPA-LA (TSPA Parameter Name) (Continued)

NOTE: * indicates variable not considered in sensitivity analysis due to correlations.

Pa_Eps_2_CSNF_High_a*. Term associated with uncertainty in protactinium solubility due to variations in fluoride concentration for CSNF waste packages when ionic strength is greater than or equal to 0.2 molal and for the invert below CSNF waste packages (mg/L). *Distribution:* Triangular. *Range:* 0 to 197. *Most Likely:* 0. *Correlation:* Correlated to Am_Eps_2_CSNF_High_a. *Symbol:* $\varepsilon_2^{\text{CSNF-high}}$, $\varepsilon_2^{\text{CSNF-invert}}$. *Additional Information:* See Am_Eps_2_CSNF_High_a. *Sensitivity Name:* EP2CSPA*. *Location in TSPA-LA:* Sections 6.3.7.5.2 and 6.3.7.5.3; Table 6.3.7-45; Equation 6.3.7-13b. *DTN:* MO0702PAFLUORI.000_R1 [DIRS 181219], Table 15. *References: Dissolved Concentration Limits of Elements with Radioactive Isotopes* (SNL 2007 [DIRS 177418], Sections 6.11 and 8.1.2; Equations 6.11-2 and 8-2; Table 6.11-4).
Pa_Eps_2_Glass_Low_a*. Term associated with uncertainty in protactinium solubility due to variations in fluoride concentration for CDSP waste packages Cell 1a, Cell 1b when ionic strength is less than 0.004 molal, and CSNF waste packages when ionic strength is less than 0.2 molal (mg/L). *Distribution:* Triangular. *Range:* 0 to 11. *Most Likely:* 0. *Correlation:* Correlated to Am_Eps_2_CSNF_High_a. *Symbol:* $\varepsilon_2^{\text{CSNF-low}}$, $\varepsilon_2^{\text{CDSP-Glass}}$, $\varepsilon_2^{\text{CDSP-F-low}}$. *Additional Information:* See Am_Eps_2_CSNF_High_a. *Sensitivity Name:* EP2LOPA*. *Location in TSPA-LA:* Sections 6.3.7.5.2 and 6.3.7.5.3; Table 6.3.7-45; Equation 6.3.7-13b. *DTN:* MO0702PAFLUORI.000_R1 [DIRS 181219], Table 15. *References: Dissolved Concentration Limits of Elements with Radioactive Isotopes* (SNL 2007 [DIRS 177418], Sections 6.11 and 8.1.2; Equations 6.11-2 and 8-2; Table 6.11-4).
PCE_Cl_MU_RH_0_20_a. The in-drift precipitated/salts (IDPS) process model uncertainty factor for the logarithm of the chloride concentration of the in-drift waters at relative humidity ≤20% (dimensionless). *Distribution:* Triangular. *Range:* -0.7 to 0.7. *Most Likely:* 0. *Additional Information:* The P&CE seepage dilution/evaporation abstraction instructs TSPA to apply IDPS uncertainties on key chemical parameters. IDPS uncertainty factors for the Cl, N, Cl:N, and I of in-drift water are used directly by the P&CE abstraction models. Four values are extracted from the seepage evaporation/dilution lookup tables: pH, I, Cl, and N. Cl, N, and Cl:N are assumed to be correlated. The P&CE abstraction models use the molal concentrations of Cl and N to represent Cl^- and NO_3^- concentrations. *Sensitivity Name:* RHMU0. *Location in TSPA-LA:* Sections 6.3.4, 6.3.4.2, 6.3.4.3.1, 6.3.4.3.2 and 6.3.5.2.3; Tables 6.3.4-2, 6.3.4-3 and 6.3.5-4. *DTN:* SN0703PAEBSPCE.007_R2 [DIRS 184141]. *References: Engineered Barrier System: Physical and Chemical Environment* (SNL 2007 [DIRS 177412], Sections 4.1.17.1 and 6.12.3; Tables 4.1-10 and 6.12-1; Figure 6.6-18).
PCE_Cl_MU_RH_20_40_a. The IDPS process model uncertainty factor for the logarithm of the chloride concentration of the in-drift waters at relative humidity >20 and ≤40% (dimensionless). *Distribution:* Triangular. *Range:* -0.5 to 0.5. *Most Likely:* 0. *Additional Information:* See PCE_Cl_MU_RH_0_20_a. *Sensitivity Name:* RHMU20. *Location in TSPA-LA:* Sections 6.3.4, 6.3.4.2, 6.3.4.3.1, 6.3.4.3.2 and 6.3.5.2.3; Tables 6.3.4-2, 6.3.4-3 and 6.3.5-4. *DTN:* SN0703PAEBSPCE.007_R2 [DIRS 184141]. *References: Engineered Barrier System: Physical and Chemical Environment* (SNL 2007 [DIRS 177412], Sections 4.1.17.1 and 6.12.3; Tables 4.1-10 and 6.12-1; Figure 6.6-18).
PCE_Cl_MU_RH_40_65_a. The IDPS process model uncertainty factor for the logarithm of the chloride concentration of the in-drift waters at relative humidity >40 and ≤65% (dimensionless). *Distribution:* Triangular. *Range:* -0.4 to 0.4. *Most Likely:* 0. *Additional Information:* See PCE_Cl_MU_RH_0_20_a. *Sensitivity Name:* RHMU40. *Location in TSPA-LA:* Sections 6.3.4, 6.3.4.2, 6.3.4.3.1, 6.3.4.3.2 and 6.3.5.2.3; Tables 6.3.4-2, 6.3.4-3 and 6.3.5-4. *DTN:* SN0703PAEBSPCE.007_R2 [DIRS 184141]. *References: Engineered Barrier System: Physical and Chemical Environment* (SNL 2007 [DIRS 177412], Sections 4.1.17.1 and 6.12.3; Tables 4.1-10 and 6.12-1; Figure 6.6-18).
PCE_Cl_MU_RH_65_85_a. The IDPS process model uncertainty factor for the logarithm of the chloride concentration of the in-drift waters at relative humidity >65 and ≤85% (dimensionless). *Distribution:* Triangular. *Range:* -0.1 to 0.1. *Most Likely:* 0. *Additional Information:* See PCE_Cl_MU_RH_0_20_a. *Sensitivity Name:* RHMU65. *Location in TSPA-LA:* Sections 6.3.4, 6.3.4.2, 6.3.4.3.1, 6.3.4.3.2 and 6.3.5.2.3; Tables 6.3.4-2, 6.3.4-3 and 6.3.5-4. *DTN:* SN0703PAEBSPCE.007_R2 [DIRS 184141]. *References: Engineered Barrier System: Physical and Chemical Environment* (SNL 2007 [DIRS 177412], Sections 4.1.17.1 and 6.12.3; Tables 4.1-10 and 6.12-1; Figure 6.6-18).
PCE_Cl_MU_RH_85_100_a*. The IDPS process model uncertainty factor for the logarithm of the chloride concentration of the in-drift waters at relative humidity >85% (dimensionless). *Distribution:* Triangular. *Range:* 0 to 0. *Most Likely:* 0. *Additional Information:* See PCE_Cl_MU_RH_0_20_a. *Sensitivity Name:* RHMU85*. *Location in TSPA-LA:* Sections 6.3.4, 6.3.4.2, 6.3.4.3.1, 6.3.4.3.2 and 6.3.5.2.3; Tables 6.3.4-2, 6.3.4-3 and 6.3.5-4. *DTN:* SN0703PAEBSPCE.007_R2 [DIRS 184141]. *References: Engineered Barrier System: Physical and Chemical Environment* (SNL 2007 [DIRS 177412], Sections 4.1.17.1 and 6.12.3; Tables 4.1-10 and 6.12-1; Figure 6.6-18).

Table K3-3. Detailed Summary of Epistemically Uncertain Variables (i.e., elements of **e**) Considered in the TSPA-LA (TSPA Parameter Name) (Continued)

NOTE: * indicates variable not considered in sensitivity analysis due to correlations.

PCE_Cl_N_MU_RH_40_65_a. The IDPS process model uncertainty factor for the logarithm of the chloride + nitrate concentration of the in-drift waters at relative humidity >40% and ≤65% (dimensionless). *Distribution:* Triangular. *Range:* -0.57 to 0.57. *Most Likely:* 0. *Additional Information:* The P&CE seepage dilution/evaporation abstraction instructs TSPA to apply IDPS uncertainties on key chemical parameters. The uncertainty associated with Cl+N is calculated assuming linear combinations of the uncertainties on Cl and N provided by the IDPS model. Four values are extracted from the seepage evaporation/dilution lookup tables: pH, I, Cl, and N. .The P&CE abstraction models use the molal concentrations of Cl and N to represent Cl^- and NO_3^- concentrations. In the event of no salt separation, take the Cl+N concentrations from the lookup tables, sample the [Cl+N] uncertainty using the appropriate relative humidity range by applying a triangular distribution, and calculate ([Cl+N] + uncertainty). *Sensitivity Name:* RHMUN40. *Location in TSPA-LA:* Sections 6.3.4.3.2 and 6.3.5.2.3; Tables 6.3.4-2, 6.3.4-3 and 6.3.5-4. *DTN:* SN0703PAEBSPCE.007_R2 [DIRS 184141], Spreadsheet: PCE_IDPS_Uncertainties.xls. *References: Engineered Barrier System: Physical and Chemical Environment* (SNL 2007 [DIRS 177412], Sections 4.1.17.1 and 6.12.3; Tables 4.1-10 and 6.12-1; Figure 6.6-18).
PCE_Cl_N_MU_RH_65_85_a. The IDPS process model uncertainty factor for the logarithm of the chloride + nitrate concentration of the in-drift waters at relative humidity >65% and ≤85% (dimensionless). *Distribution:* Triangular. *Range:* -0.22 to 0.22. *Most Likely:* 0. *Additional Information:* See PCE_Cl_N_MU_RH_40_65_a. *Sensitivity Name:* RHMUN65. *Location in TSPA-LA:* Sections 6.3.4.3.2 and 6.3.5.2.3; Tables 6.3.4-2, 6.3.4-3 and 6.3.5-4. *DTN:* SN0703PAEBSPCE.007_R2 [DIRS 184141], Spreadsheet: PCE_IDPS_Uncertainties.xls. *References: Engineered Barrier System: Physical and Chemical Environment* (SNL 2007 [DIRS 177412], Sections 4.1.17.1 and 6.12.3; Tables 4.1-10 and 6.12-1; Figure 6.6-18).
PCE_Cl_N_MU_RH_85_100_a*. The IDPS process model uncertainty factor for the logarithm of the chloride + nitrate concentration of the in-drift waters at relative humidity >85% (dimensionless). *Distribution:* Triangular. *Range:* 0 to 0. *Most Likely:* 0. *Additional Information:* See PCE_Cl_N_MU_RH_40_65_a. *Sensitivity Name:* RHMUN85*. *Location in TSPA-LA:* Sections 6.3.4.3.2 and 6.3.5.2.3; Tables 6.3.4-2, 6.3.4-3 and 6.3.5-4. *DTN:* SN0703PAEBSPCE.007_R2 [DIRS 184141], Spreadsheet: PCE_IDPS_Uncertainties.xls. *References: Engineered Barrier System: Physical and Chemical Environment* (SNL 2007 [DIRS 177412], Sections 4.1.17.1 and 6.12.3; Tables 4.1-10 and 6.12-1; Figure 6.6-18).
PCE_Cl_NO3_MU_RH_0_20_a. The IDPS process model uncertainty factor for the logarithm of the chloride to nitrate ratio of the in-drift waters at relative humidity ≤20% (dimensionless). *Distribution:* Triangular. *Range:* -1.4 to 1.4. *Most Likely:* 0. *Additional Information:* See PCE_Cl_MU_RH_0_20_a. *Sensitivity Name:* RHMUNO0. *Location in TSPA-LA:* Sections 6.3.4.3.1, 6.3.4.3.2 and 6.3.5.2.3; Tables 6.3.4-2, 6.3.4-3 and 6.3.5-4. *DTN:* SN0703PAEBSPCE.007_R2 [DIRS 184141], Spreadsheet: PCE_IDPS_Uncertainties.xls. *References: Engineered Barrier System: Physical and Chemical Environment* (SNL 2007 [DIRS 177412], Sections 4.1.17.1 and 6.12.3; Tables 4.1-10 and 6.12-1; Figure 6.6-18).
PCE_Cl_NO3_MU_RH_20_65_a. The IDPS process model uncertainty factor for the logarithm of the chloride to nitrate ratio of the in-drift waters at relative humidity >20% and ≤65% (dimensionless). *Distribution:* Triangular. *Range:* -0.5 to 0.5. *Most Likely:* 0. *Additional Information:* See PCE_Cl_MU_RH_0_20_a. *Sensitivity Name:* RHMUNO20. *Location in TSPA-LA:* Sections 6.3.4.3.1, 6.3.4.3.2 and 6.3.5.2.3; Tables 6.3.4-2, 6.3.4-3 and 6.3.5-4. *DTN:* SN0703PAEBSPCE.007_R2 [DIRS 184141], Spreadsheet: PCE_IDPS_Uncertainties.xls. *References: Engineered Barrier System: Physical and Chemical Environment* (SNL 2007 [DIRS 177412], Sections 4.1.17.1 and 6.12.3; Tables 4.1-10 and 6.12-1; Figure 6.6-18).
PCE_Cl_NO3_MU_RH_65_85_a. The IDPS process model uncertainty factor for the logarithm of the chloride to nitrate ratio of the in-drift waters at relative humidity >65% and ≤85% (dimensionless). *Distribution:* Triangular. *Range:* -0.2 to 0.2. *Most Likely:* 0. *Additional Information:* See PCE_Cl_MU_RH_0_20_a. *Sensitivity Name:* RHMUNO65. *Location in TSPA-LA:* Sections 6.3.4.3.1, 6.3.4.3.2 and 6.3.5.2.3; Tables 6.3.4-2, 6.3.4-3 and 6.3.5-4. *DTN:* SN0703PAEBSPCE.007_R2 [DIRS 184141], Spreadsheet: PCE_IDPS_Uncertainties.xls. *References: Engineered Barrier System: Physical and Chemical Environment* (SNL 2007 [DIRS 177412], Sections 4.1.17.1 and 6.12.3; Tables 4.1-10 and 6.12-1; Figure 6.6-18).
PCE_Cl_NO3_MU_RH_85_100_a*. The IDPS process model uncertainty factor for the logarithm of the chloride to nitrate ratio of the in-drift waters at low relative humidity >85% (dimensionless). *Distribution:* Triangular. *Range:* 0 to 0. *Most Likely:* 0. *Additional Information:* See PCE_Cl_MU_RH_0_20_a. *Sensitivity Name:* RHMUNO85*. *Location in TSPA-LA:* Sections 6.3.4.3.1, 6.3.4.3.2 and 6.3.5.2.3; Tables 6.3.4-2, 6.3.4-3 and 6.3.5-4. *DTN:* SN0703PAEBSPCE.007_R2 [DIRS 184141], Spreadsheet: PCE_IDPS_Uncertainties.xls. *References: Engineered Barrier System: Physical and Chemical Environment* (SNL 2007 [DIRS 177412], Sections 4.1.17.1 and 6.12.3; Tables 4.1-10 and 6.12-1; Figure 6.6-18).

Table K3-3. Detailed Summary of Epistemically Uncertain Variables (i.e., elements of **e**) Considered in the TSPA-LA (TSPA Parameter Name) (Continued)

NOTE: * indicates variable not considered in sensitivity analysis due to correlations.

PCE_Delta_pCO2_a. Selector variable for partial pressure of CO_2 (dimensionless). *Distribution:* Uniform. *Range:* -1 to 1. *Additional Information:* Calculating the pCO_2 in the drift is difficult because it is the result of competing processes such as degassing, precipitation, and diffusion and advection of gas in the fractures. The minimum potential pCO_2 is calculated from the bounding case of high gas flow through fractures. The maximum potential pCO_2 could occur if the drift were a completely closed system and the water moved down through the temperature field without degassing. TSPA uses this uniform stochastic variable to choose which case to use in each realization. A negative value of the variable implies using the minimum pCO_2 case and a positive value implies the maximum pCO_2 case. The actual pCO_2 in the drift is calculated by scaling between ambient (0.001 bars) and the minimum or maximum, using the absolute value of PCE_Delta_pCO2_a as the scaling factor. This scaling accounts for the uncertainty in the in-drift pCO_2. pCO_2 is determined at the beginning of each TSPA realization. *Sensitivity Name:* DELPPCO2. *Location in TSPA-LA:* Sections 6.3.4.2 and 6.3.5.2.3; Table 6.3.5-4. *References: Engineered Barrier System: Physical and Chemical Environment* (SNL 2007 [DIRS 177412], Sections 6.1, 6.7.2, 6.9.1, 6.12.2.1, 6.12.4.2, 6.13, 6.15.1, 7.1.2.2, 7.1.3.3, 7.1.4.2 and 7.2.3).
PCE_Gp1_Cl_NO3_CDF_a. Ratio of Cl to NO_3 (Cl:N) in Group 1 pore waters (dimensionless). *Distribution:* Discrete. *Range:* 0.783 to 6.1213. *Additional Information:* Elemental ratios such as Cl:N are important in assessing the potential for localized corrosion of the waste package in the EBS environment. The localized corrosion model is one of the most important downstream models, and it is based on an empirical fit to the pH, temperature, chloride concentration, and Cl:N values of the solutions used in the corrosion experiments. There is uncertainty associated with the distribution of Cl:N ratios among all the available waters. *Sensitivity Name:* GP1NO3. *Location in TSPA-LA:* Section 6.3.4.3.2. *DTN:* SN0703PAEBSPCE.007_R2 [DIRS 184141], Spreadsheet Cl_NO3_CDFs.xls. *References: Engineered Barrier System: Physical and Chemical Environment* (SNL 2007 [DIRS 177412], Sections 4.1.2, 4.1.17.1, 6.12.2.1 and 6.12.3; Tables 4.1-1, 4.1-4, 4.1-10 and 6.12-1; Figure 6.6-18).
PCE_Gp2_Cl_NO3_CDF_a. Ratio of Cl to NO_3 (Cl:N) in Group 2 pore waters (dimensionless). *Distribution:* Discrete. *Range:* 2.359 to 3.187. *Additional Information:* See PCE_Gp1_Cl_NO3_CDF_a. *Sensitivity Name:* GP2NO3. *Location in TSPA-LA:* Section 6.3.4.3.2. *DTN:* SN0703PAEBSPCE.007_R2 [DIRS 184141], Spreadsheet Cl_NO3_CDFs.xls. *References: Engineered Barrier System: Physical and Chemical Environment* (SNL 2007 [DIRS 177412], Sections 4.1.2, 4.1.17.1, 6.12.2.1 and 6.12.3, Tables 4.1-1, 4.1-4, 4.1-10 and 6.12-1, Figure 6.6-18).
PCE_Gp3_Cl_NO3_CDF_a. Ratio of Cl to NO_3 (Cl:N) in Group 3 pore waters (dimensionless). *Distribution:* Discrete. *Range:* 9.7782 to 64.128. *Additional Information:* See PCE_Gp1_Cl_NO3_CDF_a. *Sensitivity Name:* GP3NO3. *Location in TSPA-LA:* Section 6.3.4.3.2. *DTN:* SN0703PAEBSPCE.007_R2 [DIRS 184141], Spreadsheet Cl_NO3_CDFs.xls. *References: Engineered Barrier System: Physical and Chemical Environment* (SNL 2007 [DIRS 177412], Sections 4.1.2, 4.1.17.1, 6.12.2.1 and 6.12.3; Tables 4.1-1, 4.1-4, 4.1-10 and 6.12-1; Figure 6.6-18).
PCE_Gp4_Cl_NO3_CDF_a. Ratio of Cl to NO_3 (Cl:N) in Group 4 pore waters (dimensionless). *Distribution:* Discrete. *Range:* 4.4485 to 8.2119. *Additional Information:* See PCE_Gp1_Cl_NO3_CDF_a. *Sensitivity Name:* GP4NO3. *Location in TSPA-LA:* Section 6.3.4.3.2. *DTN:* SN0703PAEBSPCE.007_R2 [DIRS 184141], Spreadsheet Cl_NO3_CDFs.xls *References: Engineered Barrier System: Physical and Chemical Environment* (SNL 2007 [DIRS 177412], Sections 4.1.2, 4.1.17.1, 6.12.2.1 and 6.12.3; Tables 4.1-1, 4.1-4, 4.1-10 and 6.12-1; Figure 6.6-18).
PCE_I_Uncert_RH_85_100_a. The IDPS process model uncertainty factor for the logarithm of the ionic strength of the in-drift waters at high relative humidity (≥85%) (log molal). *Distribution:* Triangular. *Range:* -0.1 to 0.1. *Mean/Median/Mode:* 0. *Additional Information:* IDPS uncertainty factors for the Cl, N, Cl:N, and I of in-drift water are used directly by the Physical and Chemical Environment (P&CE) abstraction models. Four values are extracted from the seepage evaporation/dilution lookup tables. No uncertainty is associated with the ionic strength below 85 percent relative humidity from the lookup tables because the ionic strength is not used by TSPA at these concentrations. Between 85 percent and 100 percent relative humidity the ionic strength is adjusted for uncertainty by applying a triangular distribution. Between 100 and 95 percent relative humidity in the drift, the ionic strength of the evaporating solutions exceeds 1 molal. At the lower relative humidity conditions, concentrations of well over 10 molal are possible. The key chemical parameters that are provided to TSPA-LA by the P&CE dilution/evaporation abstraction model are pH, ionic strength, Cl^- and NO_3^- as a function of relative humidity. *Sensitivity Name:* RHI85. *Location in TSPA-LA:* Section 6.4.1; Tables 6.4-1 and 6.4-2; Figure 6.4-4. *DTN:* SN0703PAEBSPCE.007_R2 [DIRS 184141]. *References: Engineered Barrier System: Physical and Chemical Environment* (SNL 2007 [DIRS 177412], Sections 4.1.17.1, 6.2.1.1.2, 6.12.3 and 6.13.3; Tables 4.1-10, 6.9-1 and 6.12-1; Equation 6.2-8).

Table K3-3. Detailed Summary of Epistemically Uncertain Variables (i.e., elements of **e**) Considered in the TSPA-LA (TSPA Parameter Name) (Continued)

NOTE: * indicates variable not considered in sensitivity analysis due to correlations.

PCE_pH_Uncert_RH_0_65_a. The IDPS process model uncertainty factor for the pH of the in-drift waters at relative humidity ≤65% (dimensionless). *Distribution:* Triangular. *Range:* -2 to 2. *Most Likely:* 0. *Additional Information:* The uncertainties for pH represent uncertainties in the evaporative evolution of pH in unbuffered systems. The uncertainty in pH may be reduced by considering pH buffering reactions in specific systems. The pH value is taken directly from the lookup tables and is adjusted by the uncertainties using a triangular distribution for relative humidity values below 75 percent. The IDPS process model provides feeds to the P&CE model, which in turn provides water chemistries, including pH, for evaluating the occurrence of localized corrosion of the waste package outer barrier and the solubility of radionuclides in the invert. Included in the IDPS feeds are estimated model uncertainties in water compositional parameters, including the predicted pH. *Sensitivity Name:* RHPH0. *Location in TSPA-LA:* Table 6.3.5-4. *DTN:* SN0703PAEBSPCE.007_R2 [DIRS 184141], Spreadsheet: PCE_IDPS_Uncertainties.xls. *References: Engineered Barrier System: Physical and Chemical Environment* (SNL 2007 [DIRS 177412], Sections 4.1.17.1, 6.9.5, 6.12.3 and 6.13; Tables 4.1-11, 6.12-2 and 7.2-1; Figures 6.9-1 and 6.9-3).
PCE_pH_Uncert_RH_65_75_a. The IDPS process model uncertainty factor for the pH of the in-drift waters at relative humidity >65 and ≤75% (dimensionless). *Distribution:* Triangular. *Range:* -1 to 1. *Most Likely:* 0. *Additional Information:* See PCE_pH_Uncert_RH_0_65_a. *Sensitivity Name:* RHPH65. *Location in TSPA-LA:* Table 6.3.5-4 *DTN:* SN0703PAEBSPCE.007_R2 [DIRS 184141], Spreadsheet: PCE_IDPS_Uncertainties.xls. *References: Engineered Barrier System: Physical and Chemical Environment* (SNL 2007 [DIRS 177412], Sections 4.1.17.1, 6.9.5, 6.12.3 and 6.13; Tables 4.1-11, 6.12-2 and 7.2-1; Figures 6.9-1 and 6.9-3).
PCE_pH_Uncert_RH_75_100_a. The IDPS process model uncertainty factor for the pH of the in-drift waters at relative humidity >75% (dimensionless). *Distribution:* Discrete. *Range:* -0.3123 to 0.4288. *Additional Information:* See PCE_pH_Uncert_RH_0_65_a. Between 100 perecent to 75 percent relative humidity, pH uncertainties are sampled from a discrete CDF. *Sensitivity Name:* RHPH75. *Location in TSPA-LA:* Table 6.3.5-4 *DTN:* SN0703PAEBSPCE.007_R2 [DIRS 184141], Spreadsheet: Re-evaluation of pH uncertainty.xls, tab: CDF of pH uncertainty. *References: Engineered Barrier System: Physical and Chemical Environment* (SNL 2007 [DIRS 177412], Sections 4.1.17.1, 6.9.5, 6.12.3 and 6.13; Tables 4.1-11, 6.12-2 and 7.2-1; Figures 6.9-1 and 6.9-3).
pH_Cell2_Regression_Error_a. Error term in regression equation for pH of corrosion products domain (dimensionless). *Distribution:* Truncated normal. *Range:* -0.64 to 0.64. *Mean/Median/Mode:* 0. *Standard Deviation:* 0.32. *Symbol:* E. *Additional Information:* The pH for the corrosion products domain (Cell 2) is computed by applying the following equation: $pH = 4.5342 + 0.6132\ pCO_2 - 0.3805\ \log_{10}[U] - 0.0254\ (\log_{10}[U])^2 + E$, where E is the error term (pH_Cell2_Regression_Error_a). *Sensitivity Name:* PH2RGER. *Location in TSPA-LA:* Equation 6.3.8-27. *DTN:* SN0703PAEBSRTA.001_R3 [DIRS 183217]. *References: EBS Radionuclide Transport Abstraction* (SNL 2007 [DIRS 177407], Sections 6.5.2.4.5 and 6.5.2.4.6; Equation 6.5.2.4.6-2).
Pu_Eps_1_high_a*. Logarithm of the scale factor used to characterize uncertainty in plutonium solubility for ionic strength between 1 and 3 molal (dimensionless). *Distribution:* Truncated normal. *Range:* -1.52 to 1.52. *Mean:* 0. *Standard Deviation:* 0.76. *Correlation:* Correlated to Pu_Eps_1_low_a with a correlation factor of 1. *Symbol:* ε_1. *Additional Information:* See Am_Eps_1_low_a. *Sensitivity Name:* EP1HIPU*. *Location in TSPA-LA:* Sections 6.3.7.5.1, 6.3.7.5.2 and 6.3.7.5.3; Table 6.3.7-44; Equation 6.3.7-13a. *DTN: MO0702PADISCON.001_R0* [DIRS 179358], Tables 1 & 19. *References: Dissolved Concentration Limits of Elements with Radioactive Isotopes* (SNL 2007 [DIRS 177418], Sections 6.5 and 8.1.2; Equations 6.5-1, 6.5-2 and 8.1; Table 6.5-5).
Pu_Eps_1_low_a. Logarithm of the scale factor used to characterize uncertainty in plutonium solubility at an ionic strength below 1 molal (dimensionless). *Distribution:* Truncated normal. *Range:* -1.4 to 1.4. *Mean/Median/Mode:* 0. *Standard Deviation:* 0.7. *Correlation:* Correlated to Pu_Eps_1_high_a with a correlation factor of 1. *Symbol:* ε_1. *Additional Information:* See Am_Eps_1_low_a. *Sensitivity Name:* EP1LOWPU. *Location in TSPA-LA:* Sections 6.3.7.5.1, 6.3.7.5.2 and 6.3.7.5.3; Table 6.3.7-44; Equation 6.3.7-13a. *DTN: MO0702PADISCON.001_R0* [DIRS 179358], Tables 1 & 19. *References: Dissolved Concentration Limits of Elements with Radioactive Isotopes* (SNL 2007 [DIRS 177418], Sections 6.5 and 8.1.2; Equations 6.5-1, 6.5-2 and 8-1; Table 6.5-5).
Pu_Eps_2_CDSP_High_a*. Term associated with uncertainty in plutonium solubility due to variations in fluoride concentration for CDSP waste packages when ionic strength is greater than or equal to 0.004 molal and for the invert below CDSP waste packages (mg/L). *Distribution:* Triangular. *Range:* 0 to 5460. *Most Likely:* 0. *Correlation:* Correlated to Am_Eps_2_CSNF_High_a. *Symbol:* $\varepsilon_2^{\text{CDSP-F-high}}$, $\varepsilon_2^{\text{CDSP-invert}}$. *Additional Information:* See Am_Eps_2_CSNF_High_a. *Sensitivity Name:* EP2CDPU*. *Location in TSPA-LA:* Sections 6.3.7.5.1, 6.3.7.5.2 and 6.3.7.5.3; Table 6.3.7-44; Equation 6.3.7-13a. *DTN:* MO0702PAFLUORI.000_R1 [DIRS 181219], Table 1. *References: Dissolved Concentration Limits of Elements with Radioactive Isotopes* (SNL 2007 [DIRS 177418], Sections 6.5 and 8.1.2; Equations 6.5-1, 6.5-2 and 8-1; Table 6.5-5).

Table K3-3. Detailed Summary of Epistemically Uncertain Variables (i.e., elements of **e**) Considered in the TSPA-LA (TSPA Parameter Name) (Continued)

NOTE: * indicates variable not considered in sensitivity analysis due to correlations.

Pu_Eps_2_CSNF_High_a*. Term associated with uncertainty in plutonium solubility due to variations in fluoride concentration for CSNF waste packages when ionic strength is greater than or equal to 0.2 molal and for the invert below CSNF waste packages (mg/L). *Distribution:* Triangular. *Range:* 0 to 1374. *Most Likely:* 0. *Correlation:* Correlated to Am_Eps_2_CSNF_High_a. *Symbol:* $\varepsilon_2^{\text{CSNF-high}}$, $\varepsilon_2^{\text{CSNF-invert}}$. *Additional Information:* See Am_Eps_2_CSNF_High_a. *Sensitivity Name:* EP2CSPU*. *Location in TSPA-LA:* Sections 6.3.7.5.1, 6.3.7.5.2 and 6.3.7.5.3; Table 6.3.7-44; Equation 6.3.7-13a. *DTN:* MO0702PAFLUORI.000_R1 [DIRS 181219], Table 1. *References: Dissolved Concentration Limits of Elements with Radioactive Isotopes* (SNL 2007 [DIRS 177418], Sections 6.5 and 8.1.2; Equations 6.5-1, 6.5-2 and 8-1; Table 6.5-5).
Pu_Eps_2_Glass_Low_a*. Term associated with uncertainty in plutonium solubility due to variations in fluoride concentration for CDSP waste packages Cell 1a, Cell 1b when ionic strength is less than 0.004 molal, and CSNF waste packages when ionic strength is less than 0.2 molal (mg/L). *Distribution:* Triangular. *Range:* 0 to 79. *Most Likely:* 0. *Correlation:* Correlated to Am_Eps_2_CSNF_High_a. *Symbol:* $\varepsilon_2^{\text{CSNF-low}}$, $\varepsilon_2^{\text{CDSP-Glass}}$, $\varepsilon_2^{\text{CDSP-F-low}}$. *Additional Information:* See Am_Eps_2_CSNF_High_a. *Sensitivity Name:* EP2LOWPU*. *Location in TSPA-LA:* Sections 6.3.7.5.1, 6.3.7.5.2 and 6.3.7.5.3; Table 6.3.7-44; Equation 6.3.7-13a. *DTN:* MO0702PAFLUORI.000_R1 [DIRS 181219], Table 1. *References: Dissolved Concentration Limits of Elements with Radioactive Isotopes* (SNL 2007 [DIRS 177418], Sections 6.5 and 8.1.2; Equations 6.5-1, 6.5-2 and 8-1; Table 6.5-5).
Relative_Abundance_Goethite_a. Fraction of total iron oxide that is goethite (dimensionless). *Distribution:* Uniform. *Range:* 0.45 to 0.8. *Additional Information:* Mass fraction of iron oxide that is goethite. The relative abundance of goethite and hydrous ferric oxide (HFO) is uncertain and affects the sorption sites per unit water volume for both the stationary corrosion products and iron oxyhydroxide colloids. A uniform distribution is used due to lack of data. *Sensitivity Name:* GOERELAB. *Location in TSPA-LA:* Section 6.3.8.2.3; Table 6.3.8-4. *DTN:* SN0703PAEBSRTA.001_R3 [DIRS 183217]. *References: EBS Radionuclide Transport Abstraction* (SNL 2007 [DIRS 177407], Sections 6.3.4.2.3.1 and 6.5.2.4.1; Tables 6.3-5, 6.5-7 and 8.2-4).
Resuspension_Thickness_a. Thickness of combined ash/soil mixture available for resuspension (m). *Distribution:* Uniform. *Range:* 0.001 to 0.003. *Mean/Median/Mode:* 0.002. *Symbol:* d_c. *Additional Information:* This parameter is also known as the critical depth, which the depth of surface soil layer that is available for resuspension. This thin top layer of the surface soil is assumed to always have radionuclide concentrations at equilibrium. Radionuclide concentration in this layer, with dimensions of activity per unit mass, is calculated outside the biosphere model and is the source term for the dose calculations. The mass radionuclide concentration in the resuspendable layer of soil for noncultivated land is used to calculate the radionuclide concentration in air, which then is used to estimate the human inhalation dose. *Sensitivity Name:* RSUSTHIK. *Location in TSPA-LA:* Equation 6.3.11-6. *DTN:* MO0702PAVBPDCF.000_R0 [DIRS 179330]. *References: Biosphere Model Report* (SNL 2007 [DIRS 177399], Equations 6.4.1-6, 6.4.1-29, 6.4.1-30, 6.4.1-32 and 6.12-2).
Rind_Porosity_CSNF_a. Porosity in CSNF rind (dimensionless). *Distribution:* Uniform. *Range:* 0.05 to 0.3. *Additional Information:* In addition to the adsorption isotherm, the density of rind solids, the rind specific surface area, and the rind porosity are needed to evaluate the water saturation. *Sensitivity Name:* CSRINDPO. *Location in TSPA-LA:* Section 6.3.8.2.1; Table 6.3.8-6. *DTN:* MO0411SPACLDDG.003_R1 [DIRS 180755]. *References: Cladding Degradation Summary for LA* (SNL 2007 [DIRS 180616], Section 6.5; Table 7-1[a]).
Schoepite_Boltwoodite_Interp_a. Fractional value used to interpolate between Schoepite and Boltwoodite look-up tables (dimensionless). *Distribution:* Uniform. *Range:* 0 to 1. *Additional Information:* This parameter was developed by TSPA and is used in the TSPA-LA Model to determine the fractional value that is used to interpolate between schoepite and Na-Boltwoodite look-up tables. This fractional value is sampled at the beginning of a realization and is used for the entire pH and log fCO_2 range throughout an entire realization. *Sensitivity Name:* SCHOBOLT. *Location in TSPA-LA:* Table 6.3.7-58. *DTN:* MO0702PADISCON.001_R0 [DIRS 179358]. *References: Dissolved Concentration Limits of Elements with Radioactive Isotopes* (SNL 2007 [DIRS 177418]).

Table K3-3. Detailed Summary of Epistemically Uncertain Variables (i.e., elements of **e**) Considered in the TSPA-LA (TSPA Parameter Name) (Continued)

NOTE: * indicates variable not considered in sensitivity analysis due to correlations.

Scour_Depth_a. Scour depth in Fortymile Wash at the fan apex (cm). *Distribution:* Uniform. *Range:* 73 to 122. *Symbol:* H. *Additional Information:* This parameter represents an effective scour depth within the channels at and below the apex of the Fortymile Wash alluvial fan. This input parameter is used as an estimate of the tephra mixing depth at the RMEI location and as a calibration for scour depth estimated throughout the upper drainage basin. The depth to which tephra and channel sediment are mixed is the scour depth. The ratio of the tephra thickness to the scour depth at the fan apex, just upstream from the RMEI location, is used as the fraction of channel-bed material composed of tephra when the redistributed tephra and waste reach the RMEI location. The scour depth at the fan apex is directly proportional to the amount of dilution (and to initial waste concentration) predicted in the channel domain by the model. In the upper drainage domain, as the scour depth across the grid increases (e.g., due to larger flood events) the amount of dilution will increase and the waste concentration within the channels of the upper drainage basin domain will tend to decrease. The concentration calculated at the fan apex is applied (in addition to direct deposition) throughout the RMEI channel subdomain, so a decrease in concentration will translate into a lower dose rate. Therefore, it is especially important to capture the lower end of the scour depth range. The greater the scour depth the greater the overall mass stored in the channels, and the higher the potential associated dose. As the scour depth increases, the normalized concentration increases. Deeper scour depth results in a lower initial concentration, and slower diffusion into the medium. At equilibrium conditions, the competing effects of scour depth on the lower and upper drainage basins cancel each other out, and the resulting concentration in the channel is independent of scour depth. Thus scour depth only influences the dose for non-equilibrium times. Until the concentration equilibrates, the calculated concentrations in the channels will be higher for shallower scour depths, making it essential to capture the lower bound of scour depth range. *Sensitivity Name:* SC_DPTH. *Location in TSPA-LA:* Table 6.5-5. *DTN:* MO0704PASCOURD.000_R1 [DIRS 182149]. *References: Redistribution of Tephra and Waste by Geomorphic Processes Following a Potential Volcanic Eruption at Yucca Mountain, Nevada* (SNL 2007 [DIRS 179347], Sections 6.2.2, 6.3.2, 6.5.6, 6.6.1 and 7.1.3; Figure 6.6.1-1; Tables 6.4-1 and 6.5.6-1).
Seepage_Condensation_Prob_a*. Pointer variable to determine the seepage/condensation regime for the first failed waste package in a percolation subregion (dimensionless). *Distribution:* Uniform. *Range:* 0 to 1. *Additional Information:* Parameter determined within TSPA. *Sensitivity Name:* SEEPCON*. *Output DTN:* MO0708TSPAGENT.000_R0 [DIRS 183000].
Seepage_Uncertainty_a. Uncertainty factor to account for small-scale heterogeneity in fracture permeability (dimensionless). *Distribution:* Uniform. *Range:* 0 to 1. *Additional Information:* At each location in the UZ flow grid, the Seepage Model for PA (SMPA) computes a distribution of seepage rates - at this stage the uncertainty arises from small-scale parameters (capillary strength and permeability). Once the distributions are known at each location, Seepage_Uncertainty_a determines the actual seepage value. The percentile indicated by the sampled value of Seepage_Uncertainty_a is applied to all grid locations. Ambient seepage is derived in a random process using predictive seepage simulations that provide seepage results as a function of the seepage-relevant parameters. For a particular set of these parameters, randomly sampled from the respective distributions, the mean seepage rate and its inherent estimation uncertainty, expressed by the standard deviation over the 20 realizations conducted, are linearly interpolated between the table values. The standard deviation is used to define a uniform uncertainty distribution. A seepage uncertainty value is then randomly sampled from this distribution and used to adjust the mean seepage values, giving the final ambient seepage rate for the considered parameter set. Conducting this procedure over a large number of random parameter sets results in the final distribution of ambient seepage. *Sensitivity Name:* SEEPUNC. *Location in TSPA-LA:* Section 6.3.3.1.2; Tables 6.3.3-3 and 6.3.5-4. *DTN:* LB0407AMRU0120.001_R0 [DIRS 173280]. *References: Abstraction of Drift Seepage* (SNL 2007 [DIRS 181244], Sections 6.5.1.3, 6.5.2.2, 6.8 and 8.1; Tables 6.8-3 and 6-12[a]).
Seepage_Water_Type_a. Pointer variable used to select which seepage water type in used in the physical and chemical environment (P&CE) submodel calculations (dimensionless). *Distribution:* Discrete. *Range:* 1 to 4. *Additional Information:* This parameter randomly selects which seepage water type is used in P&CE submodel calculations. The starting water type determines which CO_2 profile and which P&CE Water Bin map is used in the TSPA chemical environment calculations. *Sensitivity Name:* SEEPWAT. *Location in TSPA-LA:* Table 6.3.5-4. *References: Engineered Barrier System: Physical and Chemical Environment* (SNL 2007 [DIRS 177412], Sections 5.2.2, 6.3, 6.6, 6.6.5, 6.9, 6.12.3 and 6.15.1; Tables 6.13-5).

Table K3-3. Detailed Summary of Epistemically Uncertain Variables (i.e., elements of **e**) Considered in the TSPA-LA (TSPA Parameter Name) (Continued)

NOTE: * indicates variable not considered in sensitivity analysis due to correlations.

Sn_Eps_high_a*. Logarithm of the scale factor used to characterize uncertainty in tin solubility for high ionic strength conditions (dimensionless). *Distribution:* Truncated normal. *Range:* -1.08 to 1.08. *Mean:* 0. *Standard Deviation:* 0.54. *Correlation:* Correlated to Sn_Eps_low_a with a correlation factor of 1. *Symbol:* ε_1. *Additional Information:* See Am_Eps_1_low_a. *Sensitivity Name:* EP1HISN*. *Location in TSPA-LA:* Sections 6.3.7.5.2 and 6.3.7.5.3; Table 6.3.7-47; Equation 6.3.7-13a. *DTN:* MO0702PADISCON.001_R0 [DIRS 179358], Tables 16 & 19. *References: Dissolved Concentration Limits of Elements with Radioactive Isotopes* (SNL 2007 [DIRS 177418], Sections 6.19 and 8.1.2; Equations 6.19-12 and 8-1; Table 6.19-5).
Sn_Eps_low_a. Logarithm of the scale factor used to characterize uncertainty in tin solubility for low ionic strength conditions (dimensionless). *Distribution:* Truncated normal. *Range:* -0.9 to 0.9. *Mean/Median/Mode:* 0. *Standard Deviation:* 0.45. *Correlation:* Correlated to Sn_Eps_high_a with a correlation factor of 1. *Symbol:* ε_1. *Additional Information:* See Am_Eps_1_low_a. *Sensitivity Name:* EP1LOWSN. *Location in TSPA-LA:* Sections 6.3.7.5.2 and 6.3.7.5.3; Table 6.3.7-47; Equation 6.3.7-13a. *DTN:* MO0702PADISCON.001_R0 [DIRS 179358], Tables 16 & 19. *References: Dissolved Concentration Limits of Elements with Radioactive Isotopes* (SNL 2007 [DIRS 177418], Sections 6.19 and 8.1.2; Equations 6.19-12 and 8-1; Table 6.19-5).
Soil_Density_a. Density of surface soil correlated with the volcanic BDCFs (kg/m^3). *Distribution:* Triangular. *Range:* 1300 to 1700. *Mean/Median/Mode:* 1500. *Additional Information:* In the channels, where the ash is mixed with soil and diluted, the density of resuspendable layer, ρ_c, can be approximated by the density of soil, ρ_s. The waste volumetric concentration can be converted to waste mass concentration in the soil by dividing it by the density of the resuspendable layer, ρ_c. In the interchannel divides, the density of the resuspendable layer, ρ_c, can be calculated from the known tephra thickness, d_a, and density, ρ_a, and surface soil density, ρ_s. Provided to TSPA-LA as a table of 1000 values sampled in correlation with the volcanic BDCFs. *Sensitivity Name:* SOILDENS. *Location in TSPA-LA:* Equation 6.3.11-6. *DTN:* MO0702PAVBPDCF.000_R0 [DIRS 179330]. *References: Biosphere Model Report* (SNL 2007 [DIRS 177399], Sections 6.4.1.1, 6.5.1.1 and 6.12.3; Equations 6.4.1-6, 6.5.1-2 and 6.13-2; Tables 6.6.3 and 6.8-2);).
Specific_SA_Smectite_Col_a. Specific surface area for smectite colloids (m^2/g). *Distribution:* Uniform. *Range:* 10 to 100. *Symbol:* $SA_{Smectite,\ coll}$. *Additional Information:* The surface area and site density values provide a means for limiting total sorption. Available surface area will depend on conditions of secondary mineral precipitation that depend on multiple factors. *Sensitivity Name:* SMECSA. *Location in TSPA-LA:* Table 6.3.7-62. *DTN:* MO0701PAGLASWF.000_R1 [DIRS 180393]. *References: Waste Form and In-Drift Colloids-Associated Radionuclide Concentrations: Abstraction and Summary* (SNL 2007 [DIRS 177423], Section 6.3.2.4.1; Table 6-24).
SRC1X. Relative x location of point source in source region 1 (dimensionless). *Distribution:* Uniform. *Range:* 0 to 1. *Additional Information:* This parameter is used to determine the point source locations for three dimensional discharge from the unsaturated zone to the saturated zone. Point source locations are directly correlated to the saturated zone breakthrough curves. The parameter values are drawn from an independent, uniform distribution and tabulated into a one-dimensional look-up table of 200 random values for input to the TSPA model. The result is a randomly located point source within each of the four source regions for each realization of the SZ flow and transport abstraction model. To treat the one- and three-dimensional transport through the SZ consistently, the sampled values used to generate the saturated zone breakthrough curves are also used in the TSPA-LA Model. These values are tabulated as 200 sets of values for the SZ parameters, accounting for appropriate correletions, and are entered into the TSPA model as a table of 200 values for each parameter. The TSPA-LA Model selects values from this table using the Goldsim variable SZ_index_a. *Sensitivity Name:* SZSREG1X. *Location in TSPA-LA:* Section 6.3.10.2; Table 6.3.10-2. *DTN:* SN0702PASZFTMA.002_R1 [DIRS 183471]. *References: Saturated Zone Flow and Transport Model Abstraction* (SNL 2008 [DIRS 183750], Sections 6.5.2.13 and 7.4.2[a]; Tables 6-8, A-1[a] and B-1).
SRC1Y. Relative y location of point source in source region 1 (dimensionless). *Distribution:* Uniform. *Range:* 0 to 1. *Additional Information:* See SRC1X. *Sensitivity Name:* SZSREG1Y. *Location in TSPA-LA:* Section 6.3.10.2; Table 6.3.10-2. *DTN:* SN0702PASZFTMA.002_R1 [DIRS 183471]. *References: Saturated Zone Flow and Transport Model Abstraction* (SNL 2008 [DIRS 183750], Sections 6.5.2.13 and 7.4.2[a]; Tables 6-8, A-1[a] and B-1).
SRC2X. Relative x location of point source in source region 2 (dimensionless). *Distribution:* Uniform. *Range:* 0 to 1. *Additional Information:* See SRC1X. *Sensitivity Name:* SZSREG2X. *Location in TSPA-LA:* Section 6.3.10.2; Table 6.3.10-2. *DTN:* SN0702PASZFTMA.002_R1 [DIRS 183471]. *References: Saturated Zone Flow and Transport Model Abstraction* (SNL 2008 [DIRS 183750], Sections 6.5.2.13 and 7.4.2[a]; Tables 6-8, A-1[a] and B-1).

Table K3-3. Detailed Summary of Epistemically Uncertain Variables (i.e., elements of **e**) Considered in the TSPA-LA (TSPA Parameter Name) (Continued)

NOTE: * indicates variable not considered in sensitivity analysis due to correlations.

SRC2Y. Relative y location of point source in source region 2 (dimensionless). *Distribution:* Uniform. *Range:* 0 to 1. *Additional Information:* See SRC1X. *Sensitivity Name:* SZSREG2Y. *Location in TSPA-LA:* Section 6.3.10.2; Table 6.3.10-2. *DTN:* SN0702PASZFTMA.002_R1 [DIRS 183471]. *References: Saturated Zone Flow and Transport Model Abstraction* (SNL 2008 [DIRS 183750], Sections 6.5.2.13 and 7.4.2[a]; Tables 6-8, A-1[a] and B-1).
SRC3X. Relative x location of point source in source region 3 (dimensionless). *Distribution:* Uniform. *Range:* 0 to 1. *Additional Information:* See SRC1X. *Sensitivity Name:* SZSREG3X. *Location in TSPA-LA:* Section 6.3.10.2; Table 6.3.10-2. *DTN:* SN0702PASZFTMA.002_R1 [DIRS 183471]. *References: Saturated Zone Flow and Transport Model Abstraction* (SNL 2008 [DIRS 183750], Sections 6.5.2.13 and 7.4.2[a]; Tables 6-8, A-1[a] and B-1).
SRC3Y. Relative y location of point source in source region 3 (dimensionless). *Distribution:* Uniform. *Range:* 0 to 1. *Additional Information:* See SRC1X. *Sensitivity Name:* SZSREG3Y. *Location in TSPA-LA:* Section 6.3.10.2; Table 6.3.10-2. *DTN:* SN0702PASZFTMA.002_R1 [DIRS 183471]. *References: Saturated Zone Flow and Transport Model Abstraction* (SNL 2008 [DIRS 183750], Sections 6.5.2.13 and 7.4.2[a]; Tables 6-8, A-1[a] and B-1).
SRC4X. Relative x location of point source in source region 4 (dimensionless). *Distribution:* Uniform. *Range:* 0 to 1. *Additional Information:* See SRC1X. *Sensitivity Name:* SZSREG4X. *Location in TSPA-LA:* Section 6.3.10.2; Table 6.3.10-2. *DTN:* SN0702PASZFTMA.002_R1 [DIRS 183471]. *References: Saturated Zone Flow and Transport Model Abstraction* (SNL 2008 [DIRS 183750], Sections 6.5.2.13 and 7.4.2[a]; Tables 6-8, A-1[a] and B-1).
SRC4Y. Relative y location of point source in source region 4 (dimensionless). *Distribution:* Uniform. *Range:* 0 to 1. *Additional Information:* See SRC1X. *Sensitivity Name:* SZSREG4Y. *Location in TSPA-LA:* Section 6.3.10.2; Table 6.3.10-2. *DTN:* SN0702PASZFTMA.002_R1 [DIRS 183471]. *References: Saturated Zone Flow and Transport Model Abstraction* (SNL 2008 [DIRS 183750], Sections 6.5.2.13 and 7.4.2[a]; Tables 6-8, A-1[a] and B-1).
SS_Corrosion_Rate_a. Stainless steel corrosion rate (μm/yr). *Distribution:* Truncated log normal. *Range:* 0.01 to 0.51. *Mean/Median/Mode:* 0.267. *Standard Deviation:* 0.209. *Symbol:* r_{SS}. *Additional Information:* This value is used for computing the mass of stationary corrosion products in the waste package. To characterize the uncertainty in stainless steel corrosion rates, a truncated lognormal distribution was developed applying Bayesian updating. The lower bound was chosen to be the approximate mean general corrosion rate of Alloy 22 on the basis that Stainless Steel Type 316 is recognized to corrode faster than Alloy 22. The upper bound is chosen the largest measured rate so as not to extend the already high rates any higher. From these rates and the thicknesses of the steel components, the lifetime of each type of steel is computed. The extent of corrosion, specifically, the mass of corrosion products, is interpolated over the lifetime of each type of steel. Although this interpolation provides a reasonable means for approximating the mass of corrosion product in the interior of a waste package over time as it degrades, there is still uncertainty as to the actual mass of corrosion product. *Sensitivity Name:* CORRATSS. *Location in TSPA-LA:* Tables 6.3.8-1 and 6.3.8-4. *DTN:* SN0703PAEBSRTA.001_R3 [DIRS 183217]. *References: EBS Radionuclide Transport Abstraction*, (SNL 2007 [DIRS 177407], Sections 6.3.4.3.4.3, 6.5.2.2.1 and Appendix F; Tables 4.1-1, 6.5-7, 8.2-4 and 8.2-7; Equation 6.5.2.2.1-2).
Stress_Thresh_A22_a. Residual stress threshold for SCC nucleation of Alloy 22 (as a percentage of yield strength in MPa) (dimensionless). *Distribution:* Uniform. *Range:* 90 to 105. *Correlation:* Correlated to Stress_Thresh_SCC_a with a correlation factor of 1. *Additional Information:* The threshold stress (Stress_Thresh_A22) is taken to be 90% to 105% of the yield strength. Inputs to the slip dissolution mechanism include threshold stress, threshold stress intensity factor, an incipient crack size, and crack-growth-rate parameters. *Sensitivity Name:* SCCTHRP. *Location in TSPA-LA:* Section 6.6.1.3.7; Table 6.6-2. *DTN:* MO070PASTRESS.002_R2 [DIRS 180514]. *References:* Stress Corrosion Cracking of Waste Package Outer Barrier and Drip Shield Materials (SNL 2007 [DIRS 181953], Sections 6.1.1, 6.2.2, and 8.1.1; Tables 6-3, 8-3 and 8-15).
Stress_Thresh_SCC_a. Stress threshold for stress corrosion cracking (MPa). *Distribution:* Uniform. *Range:* 315.9 to 368.55. *Additional Information:* See Stress_Thresh_A22. *Sensitivity Name:* SCCTHR. *Location in TSPA-LA:* Table 6.3.5-3. *DTN:* MO0702PASTRESS.002_R2 [DIRS 180514]. *References:* Stress Corrosion Cracking of Waste Package Outer Barrier and Drip Shield Materials (SNL 2007 [DIRS 181953], Sections 6.1.1, 6.2.2, and 8.1.1; Tables 6-3, 8-3 and 8-15).

Table K3-3. Detailed Summary of Epistemically Uncertain Variables (i.e., elements of **e**) Considered in the TSPA-LA (TSPA Parameter Name) (Continued)

NOTE: * indicates variable not considered in sensitivity analysis due to correlations.

Target_Flux_Out_Ratio_a. Ratio of radionuclide mass associated with colloids (reversible and irreversible) to radionuclide mass associated with colloids and dissolved radionuclide mass (dimensionless). *Distribution:* Uniform. *Range:* 0.9 to 0.99. *Symbol:* F_{RN}. *Additional Information:* The target flux out ratio is a parameter used in the TSPA model calculation of irreversible sorption of Pu and Am onto iron oxyhydroxide colloids in the waste package. This is one of three parameters used to describe limits on the formation of colloids. F_{RN} is defined as: (RN reversibly sorbed to iron oxyhydroxide + RN irreversibly sorbed to iron oxyhydroxide)/(RN reversibly sorbed to iron oxyhydroxide + RN irreversibly sorbed to iron oxyhydroxide + dissolved RN). Can also be written as (concentration of Pu/Am on colloids / (concentration of Pu/Am on colloids + concentration of Pu/Am in water)). *Sensitivity Name:* CFLUXOUT. *Location in TSPA-LA:* Table 6.3.7-65. *DTN:* MO0701PAIRONCO.000_R1 [DIRS 180440]. *References: EBS Radionuclide Transport Abstraction* (SNL 2007 [DIRS 177407], Equations B-27 to B-30); *Waste Form and In-Drift Colloids-Associated Radionuclide Concentrations: Abstraction and Summary* (SNL 2007 [DIRS 177423], Sections 6.3.12.2 and 8.1; Table 6-24).
Th_Eps_1_high_a*. Logarithm of the scale factor used to characterize uncertainty in thorium solubility at ionic strength between 1 and 3 molal (dimensionless). *Distribution:* Truncated normal. *Range:* -1.52 to 1.52. *Mean:* 0. *Standard Deviation:* 0.76. *Correlation:* Correlated to Th_Eps_1_low_a with a correlation factor of 1. *Symbol:* ε_1. *Additional Information:* See Am_Eps_1_low_a. *Sensitivity Name:* EP1HITH*. *Location in TSPA-LA:* Sections 6.3.7.5.1, 6.3.7.5.2 and 6.3.7.5.3; Table 6.3.7-46; Equation 6.3.7-13a. *DTN:* MO0702PADISCON.001_R0 [DIRS 179358], Tables 7 & 19. *References: Dissolved Concentration Limits of Elements with Radioactive Isotopes* (SNL 2007 [DIRS 177418], Sections 6.8 and 8.1.2; Equations 6.8-2 and 8-1; Table 6.8-4).
Th_Eps_1_low_a. Logarithm of the scale factor used to characterize uncertainty in thorium solubility at an ionic strength below 1 molal (dimensionless). *Distribution:* Truncated normal. *Range:* -1.4 to 1.4. *Mean:* 0. *Standard Deviation:* 0.7. *Correlation:* Correlated to Th_Eps_1_high_a with a correlation factor of 1. *Symbol:* ε_1. *Additional Information:* See Am_Eps_1_low_a. *Sensitivity Name:* EP1LOWTH. *Location in TSPA-LA:* Sections 6.3.7.5.1, 6.3.7.5.2 and 6.3.7.5.3; Table 6.3.7-46; Equation 6.3.7-13a. *DTN:* MO0702PADISCON.001_R0 [DIRS 179358], Tables 7 & 19. *References: Dissolved Concentration Limits of Elements with Radioactive Isotopes* (SNL 2007 [DIRS 177418], Sections 6.8 and 8.1.2; Equations 6.8-2 and 8-1; Table 6.8-4).
Th_Eps_2_CDSP_High_a*. Term associated with uncertainty in thorium solubility due to variations in fluoride concentration for CDSP waste packages when ionic strength is greater than or equal to 0.004 molal and for the invert below CDSP waste packages (mg/L). *Distribution:* Triangular. *Range:* 0 to 23723.2. *Most Likely:* 0. *Correlation:* Correlated to Am_Eps_2_CSNF_High_a. *Symbol:* $\varepsilon_2^{\text{CDSP-F-high}}$, $\varepsilon_2^{\text{CDSP-invert}}$. *Additional Information:* See Am_Eps_2_CSNF_High_a. *Sensitivity Name:* EP2CDTH*. *Location in TSPA-LA:* Sections 6.3.7.5.1, 6.3.7.5.2 and 6.3.7.5.3; Table 6.3.7-46; Equation 6.3.7-13a. *DTN:* MO0702PAFLUORI.000_R1 [DIRS 181219], Table 11. *References: Dissolved Concentration Limits of Elements with Radioactive Isotopes* (SNL 2007 [DIRS 177418], Sections 6.8 and 8.1.2; Equations 6.8-2 and 8.1; Table 6.8-4).
Th_Eps_2_CSNF_High_a*. Term associated with uncertainty in thorium solubility due to variations in fluoride concentration for CSNF waste packages when ionic strength is greater than or equal to 0.2 molal and for the invert below CSNF waste packages (mg/L). *Distribution:* Triangular. *Range:* 0 to 7848.3. *Most Likely:* 0. *Correlation:* Correlated to Am_Eps_2_CSNF_High_a. *Symbol:* $\varepsilon_2^{\text{CSNF-high}}$, $\varepsilon_2^{\text{CSNF-invert}}$. *Additional Information:* See Am_Eps_2_CSNF_High_a. *Sensitivity Name:* EP2CSTH*. *Location in TSPA-LA:* Sections 6.3.7.5.1, 6.3.7.5.2 and 6.3.7.5.3; Table 6.3.7-46; Equation 6.3.7-13a. *DTN:* MO0702PAFLUORI.000_R1 [DIRS 181219], Table 11. *References: Dissolved Concentration Limits of Elements with Radioactive Isotopes* (SNL 2007 [DIRS 177418], Sections 6.8 and 8.1.2; Equations 6.8-2 and 8.1; Table 6.8-4).
Th_Eps_2_Glass_Low_a*. Term associated with uncertainty in thorium solubility due to variations in fluoride concentration for CDSP waste packages Cell 1a, Cell 1b when ionic strength is less than 0.004 molal, and CSNF waste packages when ionic strength is less than 0.2 molal (mg/L). *Distribution:* Triangular. *Range:* 0 to 626.2. *Most Likely:* 0. *Correlation:* Correlated to Am_Eps_2_CSNF_High_a. *Symbol:* $\varepsilon_2^{\text{CSNF-low}}$, $\varepsilon_2^{\text{CDSP-Glass}}$, $\varepsilon_2^{\text{CDSP-F-low}}$. *Additional Information:* See Am_Eps_2_CSNF_High_a. *Sensitivity Name:* EP2LOWTH*. *Location in TSPA-LA:* Sections 6.3.7.5.1, 6.3.7.5.2 and 6.3.7.5.3; Table 6.3.7-46; Equation 6.3.7-13a. *DTN:* MO0702PAFLUORI.000_R1 [DIRS 181219], Table 11. *References: Dissolved Concentration Limits of Elements with Radioactive Isotopes* (SNL 2007 [DIRS 177418], Sections 6.8 and 8.1.2; Equations 6.8-2 and 8.1; Table 6.8-4).

Table K3-3. Detailed Summary of Epistemically Uncertain Variables (i.e., elements of **e**) Considered in the TSPA-LA (TSPA Parameter Name) (Continued)

NOTE: * indicates variable not considered in sensitivity analysis due to correlations.

Thermal_Conductivity_Uncert_a. Selector variable for one of three host-rock thermal conductivity scenarios (low, mean, and high) (dimensionless). *Distribution:* Discrete. *Range:* 1 to 3. *Additional Information:* The thermal conductivity uncertainty model provides a discrete distribution between the three conductivity scenarios: Low, Mean, and High thermal conductivity. The three probability weightings for thermal conductivity uncertainty and the three probability weightings for infiltration scenario uncertainty are used to determine the aggregate probability weightings for the five MSTHM Process Model data sets provided as input to the TSPA LA Model. *Sensitivity Name:* THERMCON. *Location in TSPA-LA:* Sections 6.3.2.2, 6.3.2.3, 6.3.5.1.3, 6.3.5.2.3 and 6.6.2.2; Tables 6.3.2-1, 6.3.2-3 and 6.3.5-4. *DTN:* LL0703PA026MST.013_R0 [DIRS 179981]. *References: Multiscale Thermohydrologic Model* (SNL 2007 [DIRS 181383], Sections 6.2.13.3[a], 6.3.4[a] and 6.3.16[a]; Tables 6.3-47[a], 6.3-48[a]).
U_Eps_1_high_Nominal_a*. Logarithm of the scale factor used to characterize uncertainty in uranium solubility under nominal or seismic conditions at an ionic strength between 1and 3 molal (dimensionless). *Distribution:* Truncated normal. *Range:* -1.2 to 1.2. *Mean:* 0. *Standard Deviation:* 0.6. *Correlation:* Correlated to U_Eps_1_low_Nominal_a. *Symbol:* ε_1. *Additional Information:* There are two uranium solubility models: one for CSNF waste packages in nominal and seismic scenarios, and another for CDSP waste packages in all scenarios, CSNF packages breached during an igneous intrusion, and the invert. See Am_Eps_1_low_a. *Sensitivity Name:* EP1HINU*. *Location in TSPA-LA:* Section 6.3.7.5.1, 6.3.7.5.2 and 6.3.7.5.3; Table 6.3.7-54; Equation 6.3.7-13a. *DTN:* MO0702PADISCON.001_R0 [DIRS 179358], Tables 4 & 19. *References: Dissolved Concentration Limits of Elements with Radioactive Isotopes* (SNL 2007 [DIRS 177418], Sections 6.7 and 8.1.2; Equations 6.7-4 and 8.1; Table 6.7-9).
U_Eps_1_high_Other_a*. Logarithm of the scale factor used to characterize uncertainty in uranium solubility under conditions other than nominal and seismic at an ionic strength between 1and 3 molal (dimensionless). *Distribution:* Truncated normal. *Range:* -1.2 to 1.2. *Mean:* 0. *Standard Deviation:* 0.6. *Correlation:* Correlated to U_Eps_1_low_Other_a. *Symbol:* ε_1. *Additional Information:* This is the exponential term associated with uncertainty in uranium solubility below 1 molal ionic strength under conditions of igneous intrusion, all scenarios, and in the invert. Used for CDSP fuel types (all scenarios), CSNF fuel in the igneous scenario and all invert locations. See U_Eps_1_low_Nominal_a. *Sensitivity Name:* EP1HIOU*. *Location in TSPA-LA:* Sections 6.3.7.5.1, 6.3.7.5.2 and 6.3.7.5.3; Table 6.3.7-58; Equation 6.3.7-13a. *DTN:* MO0702PADISCON.001_R0 [DIRS 179358], Tables 5, 6 and 19. *References: Dissolved Concentration Limits of Elements with Radioactive Isotopes* (SNL 2007 [DIRS 177418], Sections 6.7 and 8.1.2; Equations 6.7-4 and 8.1; Table 6.7-11).
U_Eps_1_low_Nominal_a. Logarithm of the scale factor used to characterize uncertainty in uranium solubility under nominal or seismic conditions at an ionic strength below 1 molal (dimensionless). *Distribution:* Truncated normal. *Range:* -1 to 1. *Mean/Median/Mode:* 0. *Standard Deviation:* 0.5. *Correlation:* Correlated to U_Eps_1_high_Nominal_a with a correlation factor of 1. *Symbol:* ε_1. *Additional Information:* There are two uranium solubility models: one for CSNF waste packages in nominal and seismic scenarios, and another for CDSP waste packages in all scenarios, CSNF packages breached during an igneous intrusion, and the invert. See Am_Eps_1_low_a. *Sensitivity Name:* EP1LOWNU. *Location in TSPA-LA:* Section 6.3.7.5.1, 6.3.7.5.2 and 6.3.7.5.3; Table 6.3.7-54; Equation 6.3.7-13a. *DTN:* MO0702PADISCON.001_R0 [DIRS 179358], Tables 4 & 19. *References: Dissolved Concentration Limits of Elements with Radioactive Isotopes* (SNL 2007 [DIRS 177418], Sections 6.7 and 8.1.2; Equations 6.7-4 and 8-1; Table 6.7-9).
U_Eps_1_low_Other_a. Logarithm of the scale factor used to characterize uncertainty in uranium solubility under conditions other than nominal and seismic at an ionic strength below 1 molal (dimensionless). *Distribution:* Truncated normal. *Range:* -1 to 1. *Mean/Median/Mode:* 0. *Standard Deviation:* 0.5. *Correlation:* Correlated to U_Eps_1_high_Nominal_a with a correlation factor of 1. *Symbol:* ε_1. *Additional Information:* This is the exponential term associated with uncertainty in uranium solubility below 1 molal ionic strength under conditions of igneous intrusion, all scenarios, and in the invert. Used for CDSP fuel types (all scenarios), CSNF fuel in the igneous scenario and all invert locations. See U_Eps_1_low_Nominal_a. *Sensitivity Name:* EP1LOWOU. *Location in TSPA-LA:* Sections 6.3.7.5.1, 6.3.7.5.2 and 6.3.7.5.3; Table 6.3.7-58; Equation 6.3.7-13a. *DTN:* MO0702PADISCON.001_R0 [DIRS 179358], Tables 5, 6 and 19. *References: Dissolved Concentration Limits of Elements with Radioactive Isotopes* (SNL 2007 [DIRS 177418], Sections 6.7 and 8.1.2; Equations 6.7-4 and 8-1; Table 6.7-11).

Table K3-3. Detailed Summary of Epistemically Uncertain Variables (i.e., elements of **e**) Considered in the TSPA-LA (TSPA Parameter Name) (Continued)

NOTE: * indicates variable not considered in sensitivity analysis due to correlations.

U_Eps_2_Boltwoodite_CDSP_High_a*. Term associated with uncertainty in uranium solubility (controlled by boldwoodite saturation) due to variations in fluoride concentration for CDSP waste packages when ionic strength is greater than or equal to 0.004 molal and for the invert below CDSP waste packages (mg/L). *Distribution:* Triangular. *Range:* 0 to 272.3. *Most Likely:* 0. *Correlation:* Correlated to Am_Eps_2_CSNF_High_a. *Symbol:* $\varepsilon_2^{\text{CDSP-F-high}}$, $\varepsilon_2^{\text{CDSP-invert}}$. *Additional Information:* See Am_Eps_2_CSNF_High_a. *Sensitivity Name:* EP2BCDHU*. *Location in TSPA-LA:* Sections 6.3.7.5.1, 6.3.7.5.2 and 6.3.7.5.3; Table 6.3.7-58; Equation 6.3.7-13a. *DTN:* MO0702PAFLUORI.000_R1 [DIRS 181219], Table 9. *References: Dissolved Concentration Limits of Elements with Radioactive Isotopes* (SNL 2007 [DIRS 177418], Sections 6.7 and 8.1.2; Equations 6.7-4 and 8-1; Table 6.7-11).
U_Eps_2_Boltwoodite_CSNF_High_a*. Term associated with uncertainty in uranium solubility (controlled by boldwoodite saturation) due to variations in fluoride concentration for CSNF waste packages when ionic strength is greater than or equal to 0.2 molal and for the invert below CSNF waste packages (mg/L). *Distribution:* Triangular. *Range:* 0 to 57.01. *Most Likely:* 0. *Correlation:* Correlated to Am_Eps_2_CSNF_High_a. *Symbol:* $\varepsilon_2^{\text{CSNF-high}}$, $\varepsilon_2^{\text{CSNF-invert}}$. *Additional Information:* See Am_Eps_2_CSNF_High_a. *Sensitivity Name:* EP2BCSHU*. *Location in TSPA-LA AMR:* Sections 6.3.7.5.1, 6.3.7.5.2 and 6.3.7.5.3; Table 6.3.7-58; Equation 6.3.7-13a. *DTN:* MO0702PAFLUORI.000_R1 [DIRS 181219], Table 9. *References: Dissolved Concentration Limits of Elements with Radioactive Isotopes* (ANL-WIS-MD-000010 REV 06 [DIRS 177418], Sections 6.7 and 8.1.2; Equations 6.7-4 and 8-1; Table 6.7-11).
U_Eps_2_Boltwoodite_Glass_Low_a*. Term associated with uncertainty in uranium solubility (controlled by boldwoodite saturation) due to variations in fluoride concentration for CDSP waste packages Cell 1a, Cell 1b when ionic strength is less than 0.004 molal, and CSNF waste packages when ionic strength is less than 0.2 molal (mg/L). *Distribution:* Triangular. *Range:* 0 to 6.13. *Most Likely:* 0. *Correlation:* Correlated to Am_Eps_2_CSNF_High_a. *Symbol:* $\varepsilon_2^{\text{CSNF-low}}$, $\varepsilon_2^{\text{CDSP-Glass}}$, $\varepsilon_2^{\text{CDSP-F-low}}$. *Additional Information:* See Am_Eps_2_CSNF_High_a. *Sensitivity Name:* EP2BLOWU*. *Location in TSPA-LA:* Sections 6.3.7.5.1, 6.3.7.5.2 and 6.3.7.5.3; Table 6.3.7-58; Equation 6.3.7-13a. *DTN:* MO0702PAFLUORI.000_R1 [DIRS 181219], Table 9. *References: Dissolved Concentration Limits of Elements with Radioactive Isotopes* (SNL 2007 [DIRS 177418], Sections 6.7 and 8.1.2; Equations 6.7-4 and 8-1; Table 6.7-11).
U_Eps_2_CSNF_High_Nominal_a*. Term associated with uncertainty in uranium solubility (under nominal or seismic conditions) due to variations in fluoride concentration for CSNF waste packages when ionic strength is greater than or equal to 0.2 molal and for the invert below CSNF waste packages (mg/L). *Distribution:* Triangular. *Range:* 0 to 1361. *Most Likely:* 0. *Correlation:* Correlated to Am_Eps_2_CSNF_High_a. *Symbol:* $\varepsilon_2^{\text{CSNF-high}}$, $\varepsilon_2^{\text{CSNF-invert}}$. *Additional Information:* See Am_Eps_2_CSNF_High_a. *Sensitivity Name:* EP2CSHNU*. *Location in TSPA-LA:* Section 6.3.7.5.1, 6.3.7.5.2 and 6.3.7.5.3; Table 6.3.7-54; Equation 6.3.7-13a. *DTN:* MO0702PAFLUORI.000_R1 [DIRS 181219], Table 7. *References: Dissolved Concentration Limits of Elements with Radioactive Isotopes* (SNL 2007 [DIRS 177418], Sections 6.7 and 8.1.2; Equations 6.7-4 and 8-1; Table 6.7-9).
U_Eps_2_CSNF_Low_Nominal_a*. Term associated with uncertainty in uranium solubility (under nominal or seismic conditions) due to variations in fluoride concentration for CSNF waste packages when ionic strength is less than 0.2 molal and for the invert below CSNF waste packages (mg/L). *Distribution:* Triangular. *Range:* 0 to 78. *Most Likely:* 0. *Correlation:* Correlated to Am_Eps_2_CSNF_High_a. *Symbol:* $\varepsilon_2^{\text{CSNF-low}}$. *Additional Information:* See Am_Eps_2_CSNF_High_a. *Sensitivity Name:* EP2CSLNU*. *Location in TSPA-LA:* Section 6.3.7.5.1, 6.3.7.5.2 and 6.3.7.5.3; Table 6.3.7-54; Equation 6.3.7-13a. *DTN:* MO0702PAFLUORI.000_R1 [DIRS 181219], Table 7. *References: Dissolved Concentration Limits of Elements with Radioactive Isotopes* (SNL 2007 [DIRS 177418], Sections 6.7 and 8.1.2; Equations 6.7-4 and 8-1; Table 6.7-9).
U_Eps_2_Schoepite_CDSP_High_a*. Term associated with uncertainty in uranium solubility (controlled by schoepite saturation) due to variations in fluoride concentration for CDSP waste packages when ionic strength is greater than or equal to 0.004 molal and for the invert below CDSP waste packages (mg/L). *Distribution:* Triangular. *Range:* 0 to 5,385. *Most Likely:* 0. *Correlation:* Correlated to Am_Eps_2_CSNF_High_a. *Symbol:* $\varepsilon_2^{\text{CDSP-F-high}}$, $\varepsilon_2^{\text{CDSP-invert}}$. *Additional Information:* See Am_Eps_2_CSNF_High_a. *Sensitivity Name:* EP2SCDHU*. *Location in TSPA-LA:* Sections 6.3.7.5.1, 6.3.7.5.2 and 6.3.7.5.3; Table 6.3.7-58; Equation 6.3.7-13a. *DTN:* MO0702PAFLUORI.000_R1 [DIRS 181219], Table 9. *References: Dissolved Concentration Limits of Elements with Radioactive Isotopes* (SNL 2007 [DIRS 177418], Sections 6.7 and 8.1.2; Equations 6.7-4 and 8-1; Table 6.7-11).

Table K3-3. Detailed Summary of Epistemically Uncertain Variables (i.e., elements of **e**) Considered in the TSPA-LA (TSPA Parameter Name) (Continued)

NOTE: * indicates variable not considered in sensitivity analysis due to correlations.

U_Eps_2_Schoepite_CSNF_High_a*. Term associated with uncertainty in uranium solubility (controlled by schoepite saturation) due to variations in fluoride concentration for CSNF waste packages when ionic strength is greater than or equal to 0.2 molal and for the invert below CSNF waste packages (mg/L). *Distribution:* Triangular. *Range:* 0 to 1,361. *Most Likely:* 0. *Correlation:* Correlated to m_Eps_2_CSNF_High_a. *Symbol:* $\varepsilon_2^{\text{CSNF-high}}$, $\varepsilon_2^{\text{CSNF-invert}}$. *Additional Information:* See Am_Eps_2_CSNF_High_a. *Sensitivity Name:* EP2SCSHU*. *Location in TSPA-LA:* Sections 6.3.7.5.1, 6.3.7.5.2 and 6.3.7.5.3; Table 6.3.7-58; Equation 6.3.7-13a. *DTN:* MO0702PAFLUORI.000_R1 [DIRS 181219], Table 9. *References: Dissolved Concentration Limits of Elements with Radioactive Isotopes* (SNL 2007 [DIRS 177418], Sections 6.7 and 8.1.2; Equations 6.7-4 and 8-1; Table 6.7-11).
U_Eps_2_Schoepite_Glass_Low_a*. Term associated with uncertainty in uranium solubility (controlled by schoepite saturation) due to variations in fluoride concentration for CDSP waste packages Cell 1a, Cell 1b when ionic strength is less than 0.004 molal, and CSNF waste packages when ionic strength is less than 0.2 molal (mg/L). *Distribution:* Triangular. *Range:* 0 to 78. *Most Likely:* 0. *Correlation:* Correlated to Am_Eps_2_CSNF_High_a. *Symbol:* $\varepsilon_2^{\text{CSNF-low}}$, $\varepsilon_2^{\text{CDSP-Glass}}$, $\varepsilon_2^{\text{CDSP-F-low}}$. *Additional Information:* See Am_Eps_2_CSNF_High_a. *Sensitivity Name:* EP2SLOWU*. *Location in TSPA-LA:* Sections 6.3.7.5.1, 6.3.7.5.2 and 6.3.7.5.3; Table 6.3.7-58; Equation 6.3.7-13a. *DTN:* MO0702PAFLUORI.000_R1 [DIRS 181219], Table 9. *References: Dissolved Concentration Limits of Elements with Radioactive Isotopes* (SNL 2007 [DIRS 177418], Sections 6.7 and 8.1.2; Equations 6.7-4 and 8-1; Table 6.7-11).
UNC_DS_EF_conv_from_ln. Probability for undetected defects in drip shields (dimensionless). *Distribution:* Log-normal. *Median:* 4.3E-07. *Error Factor:* 14., *Additional Information:* For TSPA purposes, this distribution is the probability that a drip shield will fail soon after emplacement. The mechanisms of early failure implementation consists of specifying the likelihood (probability) that waste packages and drip shields can be considered as potentially subject to early failure (i.e., have undetected defects). Computed from TSPA Input Database parameter UNC_DS_EF by UNC_DS_EF_conv_from_ln = exp(UNC_DS_EF). *Sensitivity Name:* PROBDSEF. *Location in TSPA-LA:* Section 6.4.1; Tables 6.4-1 and 6.4-2. *DTN:* MO0701PASHIELD.000_R2 [DIRS 180508]. *References:* Analysis of Mechanisms for Early Waste Package / Drip Shield Failure (SNL 2007 [DIRS 178765], Sections 6.4, 6.5 and 7.1; Tables 6-10 and 7-1; Figure 6-21).
UNC_WP_EF_conv_from_ln. Probability for the undetected defects in waste packages (dimensionless). *Distribution:* Log-normal. *Median:* 4.14E-05. *Error Factor:* 8.17. *Additional Information:* For TSPA purposes, this distribution is the probability that a waste package will fail soon after emplacement. The mechanisms of early failure implementation consists of specifying the likelihood (probability) that waste packages and drip shields can be considered as potentially subject to early failure (i.e., have undetected defects). Computed from TSPA Input Database parameter UNC_WP_EF by UNC_WP_EF_conv_from_ln = exp(UNC_WP_EF). *Sensitivity Name:* PROBWPEF. *Location in TSPA-LA:* Section 6.4.2; Tables 6.4-1 and 6.4-2. *DTN:* MO0701PASHIELD.000_R2 [DIRS 180508]. *References:* Analysis of Mechanisms for Early Waste Package / Drip Shield Failure (SNL 2007 [DIRS 178765], Sections 6.3, 6.5 and 7.1; Tables 6-9 and 7-1; Figure 6-20).
UZ_Tortuosity_RG1. Logarithm of the tortuosity in rock group 1 (dimensionless). *Distribution:* Left truncated normal. *Range*: 0 to ∞. *Mean:* -1.15. *Standard Deviation:* 0.29. *Additional Information:* The tortuosity is computed from water content and base 10 log of the effective permeability. The uncertainty is implemented in the TSPA-LA Model for each rock group by selecting a standard normal random number and adding the product of the standard normal random number and standard deviation (in log10 space) to the log10 value of the mean tortuosity, taking the antilog of the value to derive the tortuosity for the present realization and multiplying each element-specific free-water diffusion coefficient by the tortuosity to derive 15 element-specific effective diffusion coefficients. In the UZ transport abstraction model, there are three tortuosity coefficient distributions for the three rock types (groups of layers with similar properties) specified in the compliance model. The range of tortuosity values is subdivided into three subranges called tortuosity rock groups, based on the tortuosity characteristics of the rock types in the unsaturated zone. Recorded in TSPA Input Database as UZDC_Mean_RG1 (mean) and UZ_DC_SD_RG1 (standard deviation). *Sensitivity Name:* UZTORRG1. *Location in TSPA-LA:* Section 6.3.9.2; Table 6.3.9-4. *DTN:* LB0702PAUZMTDF.001_R1 [DIRS 180776]. *References: Particle Tracking Model and Abstraction of Transport Processes Addendum 002* (SNL 2008 [DIRS 184748], Sections 4.1.4, 6.5.5 and Appendix A; Equation 6.5.5-1; Table 6.5.5-1).

Table K3-3. Detailed Summary of Epistemically Uncertain Variables (i.e., elements of **e**) Considered in the TSPA-LA (TSPA Parameter Name) (Continued)

NOTE: * indicates variable not considered in sensitivity analysis due to correlations.

UZ_Tortuosity_RG2. Logarithm of the tortuosity in rock group 2 (dimensionless). *Distribution:* Left truncated normal. *Range*: 0 to ∞. *Mean:* -1.57. *Standard Deviation:* 0.29. *Additional Information:* See UZ_Tortuosity_RG1. Recorded in TSPA Input Database as UZDC_Mean_RG2 (mean) and UZ_DC_SD_RG2 (standard deviation). *Sensitivity Name:* UZTORRG2. *Location in TSPA-LA:* Section 6.3.9.2; Table 6.3.9-4. *DTN:* LB0702PAUZMTDF.001_R1 [DIRS 180776]. *References: Particle Tracking Model and Abstraction of Transport Processes Addendum 002* (SNL 2008 [DIRS 184748], Sections 4.1.4, 6.5.5 and Appendix A; Equation 6.5.5-1; Table 6.5.5-1).
UZ_Tortuosity_RG3. Logarithm of the tortuosity in rock group 3 (dimensionless). *Distribution:* Left truncated normal. *Range*: 0 to ∞. *Mean:* -1.84. *Standard Deviation:* 0.29. *Additional Information:* See UZ_Tortuosity_RG1. Recorded in TSPA Input Database as UZDC_Mean_RG3 (mean) and UZ_DC_SD_RG3 (standard deviation). *Sensitivity Name:* UZTORRG3. *Location in TSPA-LA:* Section 6.3.9.2; Table 6.3.9-4. *DTN:* LB0702PAUZMTDF.001_R1 [DIRS 180776]. *References: Particle Tracking Model and Abstraction of Transport Processes Addendum 002* (SNL 2008 [DIRS 184748], Sections 4.1.4, 6.5.5 and Appendix A; Equation 6.5.5-1; Table 6.5.5-1).
Vol_Rubble_Max_Lith_a. Volume of lithophysal rock that must fall to fill the drift (m^3/m). *Distribution:* Uniform. *Range:* 30 to 120. *Additional Information:* This parameter represents epistemic uncertainty and spatial variability within the lithophysal zones. This distribution is sampled once per realization to determine the volume of intact lithophysal rock corresponding to complete drift collapse. A uniform distribution is appropriate here because the end points of the range are known, but the distribution of values within the range is not known. *Sensitivity Name:* RUBMAXL. *Location in TSPA-LA:* Sections 6.3.5.2.3 and 6.6.3.1; Tables 6.3.5-4 and 6.6-2. *DTN:* MO0703PASEISDA.002_R4 [DIRS 183156]. *References: Seismic Consequence Abstraction* (SNL 2007 [DIRS 176828], Sections 6.7.1 and 6.12.2; Tables 4-1, 6-28, 6-30, 6-32 and 6-88; Figures 6-52 to 6-54 and 6-57; Equations 5.3-1 and 6.7-2).
Vol_Rubble_Max_NonLith_a. Volume of nonlithophysal rock that must fall to fill the drift (m^3/m). *Distribution:* Uniform. *Range:* 30 to 120. *Additional Information:* See Vol_Rubble_Max_Lith_a. This parameter represents epistemic uncertainty and spatial variability within the nonlithophysal zones. *Sensitivity Name:* RUBMAXNL. *Location in TSPA-LA:* Section 6.3.5.2.3 and 6.6.3.1; Tables 6.3.5-4 and 6.6-2. *DTN:* MO0703PASEISDA.002_R4 [DIRS 183156]. *References: Seismic Consequence Abstraction* (SNL 2007 [DIRS 176828], Sections 6.7.2 and 6.12.2; Tables 6-31, 6-32 and 6-88; Figures 6-58 to 6-61; Equation 5.3-1).
WDDSAggrGC_Mean_a. Topside general corrosion rate of the drip shield (nm/yr). *Distribution:* Normal. *Mean:* 46.067. *Standard Deviation:* 1.187. *Additional Information:* The corrosion of the underside surface of the drip shield is more likely to be dry oxidation and humid-air corrosion, while the topside surface of the drip shield is more likely to undergo dry oxidation, humid-air and aqueous-phase corrosion. The topside surfaces that are subject to seepage dripping may be exposed to more aggressive chemical environment and conditions than those not subject to seepage dripping. The underside surfaces, where seepage cannot physically contact and dust cannot settle and accumulate, are not expected to be exposed to seepage water, and therefore corrosion will proceed under benign conditions. For the modeling purpose, the entire variation in the data is assumed to be due to the variability in the corrosion process. The resulting normal probability model represents the variability in the drip shield general corrosion rates for the aggressive conditions. The variability in the general corrosion rate is likely due to the randomness of the corrosion process under the conditions in the exposure environment. Recorded in the TSPA Input Database as two constants: WDDSAggrGC_Uncert_Mean and WDDSAggrGC_Uncert_SD. *Sensitivity Name:* WDDSAGGC. *Location in TSPA-LA:* Sections 6.3.5.1.2 and 6.3.5.1.3; Table 6.3.5-3. *DTN:* SN0704PADSGCMT.001_R2 [DIRS 182122]. *References: General Corrosion and Localized Corrosion of the Drip Shield* (SNL 2007 [DIRS 180778], Sections 1.3[a], 6.1.6.2[a] and 8.1[a]; Table 8-1[a]).
WDDSBenignGC_Mean_a. Underside general corrosion rate of the drip shield (mm/yr). *Distribution:* Normal. *Mean:* 5.15E-06. *Standard Deviation:* 8.31E-07. *Additional Information:* The description of the general corrosion model for the benign condition is split into two parts. First is the characterization and quantification of the uncertainty in the general corrosion model for the benign environmental condition. Second is the description of the corrosion rate variability model that represents the data. The variability in the general corrosion rate for the benign condition is due mainly to the randomness of the corrosion process under the conditions in the exposure environment. The experimental variability (e.g., variations in sample preparation and cleaning) also contributes to the variability in the corrosion rate. *Sensitivity Name:* WDDSBEGC. *Location in TSPA-LA:* Sections 6.3.5.1.2 and 6.3.5.1.3; Table 6.3.5-3. *DTN:* SN0704PADSGCMT.001_R2 [DIRS 182122]. *References: General Corrosion and Localized Corrosion of the Drip Shield* (SNL 2007 [DIRS 180778], Sections 1.3[a], 6.1.7.1[a] and 8.1[a]; Table 8-1[a]).

Table K3-3. Detailed Summary of Epistemically Uncertain Variables (i.e., elements of **e**) Considered in the TSPA-LA (TSPA Parameter Name) (Continued)

NOTE: * indicates variable not considered in sensitivity analysis due to correlations.

WDDSGC_29_a. General corrosion rate ratio for drip shield support material (ratio of Titanium Grade 29 to Titanium Grade 7) (dimensionless). *Distribution:* Discrete. *Range:* 1 to 6.6786. *Additional Information:* The general corrosion rate of Titanium Grade 29 is the value of Titanium Grade 7 multiplied by sampled value from the rate ratio distribution. For each realization of the TSPA-LA model, one general corrosion rate ratio is sampled from the distribution for general corrosion rate ratio, and one general corrosion rate for Titanium Grade 7 is sampled from the topside surface distribution of general corrosion rates of Titanium Grade 7 for an aggressive condition. In this way, the corrosion rate of the Titanium Grade 29 components will conservatively be independent of whether they are on the inside or outside of the drip shield Titanium Grade 7 plates. Only one sampled value of the general corrosion rate ratio is used per realization, assuming that the ratio is constant for the entire simulation period. *Sensitivity Name:* WDDSGC29. *Location in TSPA-LA:* Section 6.3.5.1.2. *DTN:* SN0704PADSGCMT.002_R1 [DIRS 182188]. *References: General Corrosion and Localized Corrosion of the Drip Shield* (SNL 2007 [DIRS 180778], Sections 6.2.2[a], 6.2.3[a] and 8.1[a]; Tables 6-8[a] and 8-1[a]; Figure 6-21[a]).
WP_Crack_Area_Density_a. Ratio of SCC crack area to unit of seismic damaged area for a waste package (dimensionless). *Distribution:* Uniform. *Range:* 0.00327 to 0.0131. *Additional Information:* WP_Crack_Area_Density_a is a scaling factor applied to the seismically damaged area to obtain the total area of the crack network. The use of a uniform distribution is reasonable as it accurately reflects the lack of knowledge of the exact value of the crack area density. *Sensitivity Name:* WDCRCDEN. *Location in TSPA-LA:* Table 6.6-2. *DTN:* MO0702PASTRESS.002_R2 [DIRS 180514]. *References: Stress Corrosion Cracking of Waste Package Outer Barrier and Drip Shield Materials* (SNL 2007 [DIRS 181953], Sections 6.7.2 to 6.7.4, 8.4.2.4 and 8.4.3; Tables 6-18, 8-1 and 8-15; Equations 32 and 73).
WP_Flux_Uncertainty_a. Waste package flux splitting factor (dimensionless). *Distribution:* Uniform. *Range:* 0 to 2.41. *Symbol:* f'_{WP}. *Additional Information:* See DS_Flux_Uncertainty_a. Uncertainty in the waste package flux splitting algorithm is given by WP_Flux_Uncertainty_a. As with the corresponding factor f_{DS} for the drip shield, bounds can be established for f_{WP} based on the dimensions of the patches, the waste package and the uncertain rivulet spread angle. A lower bound of zero is necessary to account for the possibility that seepage through the drip shield is completely diverted by an intact portion of the waste package outer corrosion barrier. An upper bound on f_{WP} is developed based on results of the breached drip shield experiments. The range for f_{WP} based entirely on experimental results is used in TSPA. *Sensitivity Name:* WPFLUX. *Location in TSPA-LA:* Sections 6.3.6.1, 6.3.6.2 and 6.3.6.3; Tables 6.3.6-1, 6.3.6-2 and 6.3.8-4; Equation 6.3.6-6. *DTN:* SN0703PAEBSRTA.001_R3 [DIRS 183217]. *References: EBS Radionuclide Transport Abstraction* (SNL 2007 [DIRS 177407], Sections 6.3.3.2.5, 6.5.1.1.3, 7.1.1.2, Appendix D and Appendix E; Tables 6.3-1, 7.1-12, 8.1-1 and 8.2-4; Equations 6.3.3.2.5 and 6.5.1.1.3).
WRIP_beta_rand_a. Parameter used to correlate WRIP_beta so that it resamples at the same probability level throughout a realization (dimensionless). *Distribution:* Uniform. *Range:* 0 to 1. *Additional Information:* The WRIP is sampled from beta distribution. WRIP_beta is sampled at every time step and perfectly correlated with WRIP_beta_rand_a. The WRIP value in the look-up table does not contain any uncertainty. It is specified as the mean of a beta distribution with a maximum equal to 2.838 times the mean, the minimum equal to 0.2039 times the mean, and the standard deviation equal to 0.4251 times the mean. This uncertainty accounts for uncertainty in the feldspar dissolution rate. This parameter is determined within TSPA. *Sensitivity Name:* WATRCKIN. *Location in TSPA-LA:* Section 6.3.4.2; Table 6.3.4-1. Output *DTN:* MO0708TSPAGENT.000_R0 [DIRS 183000].
z_OL_a. Deviation from median yield strength range for outer lid (dimensionless). *Distribution:* Truncated normal. *Range:* -3 to 3. *Mean/Median/Mode:* 0. *Standard Deviation:* 1. *Symbol:* z. *Additional Information:* Stress and stress-intensity factor profile model output parameters are to be used as inputs into the TSPA model. These parameters include the stress intensity versus depth for outer lid, the outer lid stress coefficients, the outer lid yield strength scaling factor, the uncertain deviation from median yield strength range for outer lid, the number of angles at which the stress intensity factor for the outer lid will be evaluated by SCCD, and the amplitude of the stress variation with angle for the outer lid. *Sensitivity Name:* WDZOLID. *Location in TSPA-LA:* Sections 6.3.5.1.2 and 6.3.5.1.3; Table 6.3.5-3. *DTN:* MO0702PASTRESS.002_R2 [DIRS 180514]. *References: Stress Corrosion Cracking of Waste Package Outer Barrier and Drip Shield Materials* (SNL 2007 [DIRS 181953], Sections 6.5.6.5 and 8.4.2.2; Table 8-15; Equation 67).

INTENTIONALLY LEFT BLANK

Table K3-4. Alphabetic Listing of the Various TSPA-LA Model Results Considered in Uncertainty and Sensitivity Analyses for Nominal (N), Drip Shield Early Failure (ED), Waste Package Early Failure (EW), Igneous Intrusive (II), Igneous Eruptive (IE), Seismic Ground Motion (SG), and Seismic Fault Displacement (SF) Modeling Cases in Appendix K4, K5, K6, and K7

Output Variable	Definition
BACDFLAD	Average breached area (m^2) on failed CDSP WPs under dripping conditions
BACDFLND	Average breached area (m^2) on failed CDSP WPs under nondripping conditions
BACSFLAD	Average breached area (m^2) on failed CSNF WPs under dripping conditions
BACSFLND	Average breached area (m^2) on failed CSNF WPs under nondripping conditions
DOIC239	Dose to RMEI (mrem/yr) from ^{239}Pu irreversibly attached to slow (i.e., Ic) colloids
DOIF239	Dose to RMEI (mrem/yr) from ^{239}Pu irreversibly attached to fast (i.e., If) colloids
DONP237	Dose to RMEI (mrem/yr) from dissolved ^{237}Np
DOPU239	Dose to RMEI (mrem/yr) from dissolved ^{239}Pu
DOSTOT	Dose to RMEI (mrem/yr) from all radioactive species
DOTC99	Dose to RMEI (mrem/yr) from dissolved ^{99}Tc
DSFLTM	Drip Shield failure time (yr)
ESFA239C	Cumulative release (g) for the movement of ^{239}Pu irreversibly attached to fast (i.e., If) colloids from the EBS to the UZ
ESIC239	Release rate (g/yr) for the movement of ^{239}Pu irreversibly attached to waste form (i.e., Ic) colloids from the EBS to the UZ
ESIC239C	Cumulative release (g) for the movement of ^{239}Pu irreversibly attached to waste form (i.e., Ic) colloids from the EBS to the UZ
ESIF239	Release rate (g/yr) for the movement of ^{239}Pu irreversibly attached to ferrous (i.e., If) colloids from the EBS to the UZ
ESIF239C	Cumulative release (g) for the movement of ^{239}Pu irreversibly attached to ferrous (i.e., If) colloids from the EBS to the UZ
ESNP237	Release rate (g/yr) for the movement of dissolved ^{237}Np from the EBS to the UZ
ESNP237C	Cumulative release (g) for the movement of dissolved ^{237}Np from the EBS to the UZ
ESPU239	Release rate (g/yr) for the movement of dissolved ^{239}Pu from the EBS to the UZ
ESPU239C	Cumulative release (g) for the movement of dissolved ^{239}Pu from the EBS to the UZ
ESSL239C	Cumulative release (g) for the movement of ^{239}Pu irreversibly attached to slow colloids from the EBS to the UZ

Table K3-4. Alphabetic Listing of the Various TSPA-LA Model Results Considered in Uncertainty and Sensitivity Analyses for Nominal (N), Drip Shield Early Failure (ED), Waste Package Early Failure (EW), Igneous Intrusive (II), Igneous Eruptive (IE), Seismic Ground Motion (SG), and Seismic Fault Displacement (SF) Modeling Cases in Appendix K4, K5, K6, and K7 (Continued)

Output Variable	Definition
ESTC99	Release rate (g/yr) for the movement of dissolved ^{99}Tc from the EBS to the UZ
ESTC99C	Cumulative release (g) for the movement of dissolved ^{99}Tc from the EBS to the UZ
EXPDOSE	Expected dose to RMEI (mrem/yr) from all radioactive species
ISCDINAD	Ionic strength (molal) in the invert beneath the WP for CDSP WPs under dripping conditions
ISCDINND	Ionic strength (molal) in the invert beneath the WP for CDSP WPs under nondripping conditions
ISCSINAD	Ionic strength (molal) in the invert beneath the WP for CSNF WPs under dripping conditions
ISCSINND	Ionic strength (molal) in the invert beneath the WP for CSNF WPs under nondripping conditions
NCDFL	Number of failed CDSP WPs
NCDFLAD	Number of failed CDSP WPs under dripping conditions
NCDFLND	Number of failed CDSP WPs under nondripping conditions
NCSFL	Number of failed CSNF WPs
NCSFLAD	Number of failed CSNF WPs under dripping conditions
NCSFLND	Number of failed CSNF WPs under nondripping conditions
PCO2CDIA	Partial pressure of CO_2 (bars) in the invert for CDSP WPs under dripping conditions
PCO2CDIN	Partial pressure of CO_2 (bars) in the invert for CDSP WPs under nondripping conditions
PCO2CSIA	Partial pressure of CO_2 (bars) in the invert for CSNF WPs under dripping conditions
PCO2CSIN	Partial pressure of CO_2 (bars) in the invert for CSNF WPs under nondripping conditions
PHCDINAD	pH in the invert beneath the WP for CDSP WPs under dripping conditions
PHCDINND	pH in the invert beneath the WP for CDSP WPs under nondripping conditions
PHCSINAD	pH in the invert beneath the WP for CSNF WPs under dripping conditions
PHCSINND	pH in the invert beneath the WP for CSNF WPs under nondripping conditions
RHCDINV	Relative humidity for CDSP WPs in the invert beneath the WP

Table K3-4. Alphabetic Listing of the Various TSPA-LA Model Results Considered in Uncertainty and Sensitivity Analyses for Nominal (N), Drip Shield Early Failure (ED), Waste Package Early Failure (EW), Igneous Intrusive (II), Igneous Eruptive (IE), Seismic Ground Motion (SG), and Seismic Fault Displacement (SF) Modeling Cases in Appendix K4, K5, K6, and K7 (Continued)

Output Variable	Definition
RHCDWP	Relative humidity for CDSP WPs on the WP
RHCSINV	Relative humidity for CSNF WPs in the invert beneath the WP
RHCSWP	Relative humidity for CSNF WPs on the WP
SPRATECD	Seepage rate (m^3/yr/WP) into the repository above CDSP WPs
SPRATECS	Seepage rate (m^3/yr/WP) into the repository above CSNF WPs
SZIC239	Release rate (g/yr) for the movement of ^{239}Pu irreversibly attached to slow (i.e., Ic) colloids across a subsurface plane at the location of the RMEI
SZIC239C	Cumulative release (g) for the movement of ^{239}Pu irreversibly attached to slow (i.e., Ic) colloids across a subsurface plane at the location of the RMEI
SZIF239	Release rate (g/yr) for the movement of ^{239}Pu irreversibly attached to fast (i.e., If) colloids across a subsurface plane at the location of the RMEI
SZIF239C	Cumulative release (g) for the movement of ^{239}Pu irreversibly attached to fast (i.e., If) colloids across a subsurface plane at the location of the RMEI
SZNP237	Release rate (g/yr) for the movement of dissolved ^{237}Np across a subsurface plane at the location of the RMEI
SZNP237C	Cumulative release (g) for the movement of dissolved ^{237}Np across a subsurface plane at the location of the RMEI
SZPU239	Release rate (g/yr) for the movement of dissolved ^{239}Pu across a subsurface plane at the location of the RMEI
SZPU239C	Cumulative release (g) for the movement of dissolved ^{239}Pu across a subsurface plane at the location of the RMEI
SZTC99	Release rate (g/yr) for the movement of dissolved ^{99}Tc across a subsurface plane at the location of the RMEI
SZTC99C	Cumulative release (g) for the movement of dissolved ^{99}Tc across a subsurface plane at the location of the RMEI
TMPCDINV	Drift temperature (C) for CDSP WPs in the invert beneath the WP
TMPCDWL	Drift temperature (C) for CDSP WPs at the drift wall
TMPCDWP	Drift temperature (C) for CDSP WPs on the WP
TMPCSINV	Drift temperature (C) for CSNF WPs in the invert beneath the WP
TMPCSWL	Drift temperature (C) for CSNF WPs at the drift wall
TMPCSWP	Drift temperature (C) for CSNF WPs on the WP
UZIC239	Release rate (g/yr) for the movement of ^{239}Pu irreversibly attached to slow (i.e., Ic) colloids from the UZ to the SZ

Table K3-4. Alphabetic Listing of the Various TSPA-LA Model Results Considered in Uncertainty and Sensitivity Analyses for Nominal (N), Drip Shield Early Failure (ED), Waste Package Early Failure (EW), Igneous Intrusive (II), Igneous Eruptive (IE), Seismic Ground Motion (SG), and Seismic Fault Displacement (SF) Modeling Cases in Appendix K4, K5, K6, and K7 (Continued)

Output Variable	Definition
UZIC239C	Cumulative release (g) for the movement of ^{239}Pu irreversibly attached to slow (i.e., Ic) colloids from the UZ to the SZ
UZIF239	Release rate (g/yr) for the movement of ^{239}Pu irreversibly attached to fast (i.e., If) colloids from the UZ to the SZ
UZIF239C	Cumulative release (g) for the movement of ^{239}Pu irreversibly attached to fast (i.e., If) colloids from the UZ to the SZ
UZNP237	Release rate (g/yr) for the movement of dissolved ^{237}Np from the UZ to the SZ
UZNP237C	Cumulative release (g) for the movement of dissolved ^{237}Np from the UZ to the SZ
UZPU239	Release rate (g/yr) for the movement of dissolved ^{239}Pu from the UZ to the SZ
UZPU239C	Cumulative release (g) for the movement of dissolved ^{239}Pu from the UZ to the SZ
UZTC99	Release rate (g/yr) for the movement of dissolved ^{99}Tc from the UZ to the SZ
UZTC99C	Cumulative release (g) for the movement of dissolved ^{99}Tc from the UZ to the SZ

Table K4.1-1. Summary of TSPA-LA Model Results Considered in Uncertainty and Sensitivity Analyses for the Nominal Scenario Class

BACSFLAD	Average breached area (m^2) on failed CSNF WPs under dripping conditions (Figures K.4.2-6, K.4.2-7)
BACSFLND	Average breached area (m^2) on failed CSNF WPs under nondripping conditions (Figures K.4.2-6, K.4.2-7)
DOSTOT	Dose to RMEI (mrem/yr) from all radioactive species (Figure K.4.5-1, K.4.5-2, K.4.5-3)
DSFLTM	Drip Shield failure time (yr) (Figure K.4.2-1)
ESNP237	Release rate (g/yr) for the movement of dissolved ^{237}Np from the EBS to the UZ (Figures K.4.4-1, K.4.4-2)
ESNP237C	Cumulative release (g) for the movement of dissolved ^{237}Np from the EBS to the UZ (Figures K.4.4-1, K.4.4-2)
ISCDINAD	Ionic strength (molal) in the invert beneath the WP for CDSP WPs under dripping conditions (Figure K.4.3-10)
ISCDINND	Ionic strength (molal) in the invert beneath the WP for CDSP WPs under nondripping conditions (Figure K.4.3-10)
ISCSINAD	Ionic strength (molal) in the invert beneath the WP for CSNF WPs under dripping conditions (Figures K.4.3-9, K.4.3-11)
ISCSINND	Ionic strength (molal) in the invert beneath the WP for CSNF WPs under nondripping conditions (Figure K.4.3-9)
NCDFL	Number of failed CDSP WPs (Figure K.4.2-2)
NCSFL	Number of failed CSNF WPs (Figures K.2-1, K.4.2-3)
NCSFLAD	Number of failed CSNF WPs under dripping conditions (Figures K.4.2-4, K.4.2-5)
NCSFLND	Number of failed CSNF WPs under nondripping conditions (Figures K.4.2-4, K.4.2-5)
PCO2CDIA	Partial pressure of CO_2 (bars) in the invert for CDSP WPs under dripping conditions (Figure K.4.3-7)
PCO2CSIA	Partial pressure of CO_2 (bars) in the invert for CSNF WPs under dripping conditions (Figures K.4.3-7, K.4.3-8)
PHCDINAD	pH in the invert beneath the WP for CDSP WPs under dripping conditions (Figure K.4.3-14)
PHCDINND	pH in the invert beneath the WP for CDSP WPs under nondripping conditions (Figure K.4.3-14)
PHCSINAD	pH in the invert beneath the WP for CSNF WPs under dripping conditions (Figures K.4.3-12, K.4.3-13)
PHCSINND	pH in the invert beneath the WP for CSNF WPs under nondripping conditions (Figures K.4.3-12, K.4.3-13)
RHCDINV	Relative humidity for CDSP WPs in the invert beneath the WP (Figure K.4.3-6)

Table K4.1-1. Summary of TSPA-LA Model Results Considered in Uncertainty and Sensitivity Analyses for the Nominal Scenario Class (Continued)

RHCDWP	Relative humidity for CDSP WPs on the WP (Figure K.4.3-6)
RHCSINV	Relative humidity for CSNF WPs in the invert beneath the WP (Figure K.4.3-6)
RHCSWP	Relative humidity for CSNF WPs on the WP (Figure K.4.3-6)
SPRATECD	Seepage rate (m^3/yr/WP) into the repository above CDSP WPs (Figures K.4.3-1, K.4.3-4)
SPRATECS	Seepage rate (m^3/yr/WP) into the repository above CSNF WPs (Figures K.4.3-1, K.4.3-2, K.4.3-3)
TMPCDINV	Drift temperature (C) for CDSP WPs in the invert beneath the WP (Figure K.4.3-5)
TMPCDWL	Drift temperature (C) for CDSP WPs at the drift wall (Figure K.4.3-5)
TMPCDWP	Drift temperature (C) for CDSP WPs on the WP (Figure K.4.3-5)
TMPCSINV	Drift temperature (C) for CSNF WPs in the invert beneath the WP (Figure K.4.3-5)
TMPCSWL	Drift temperature (C) for CSNF WPs at the drift wall (Figure K.4.3-5)
TMPCSWP	Drift temperature (C) for CSNF WPs on the WP (Figure K.4.3-5)

Table K5.1-1. Summary of TSPA-LA Model Results Considered in Uncertainty and Sensitivity Analyses for the Early Failure Scenario Classes

Output Variable	Definition
DOIC239	Dose to RMEI (mrem/yr) from ^{239}Pu irreversibly attached to slow (i.e., Ic) colloids (Figure K.5.6.1-1)
DOIF239	Dose to RMEI (mrem/yr) from ^{239}Pu irreversibly attached to fast (i.e., If) colloids (Figure K.5.6.1-2)
DONP237	Dose to RMEI (mrem/yr) from dissolved ^{237}Np (Figure K.5.6.1-3)
DOPU239	Dose to RMEI (mrem/yr) from dissolved ^{239}Pu (Figure K.5.6.1-4)
DOTC99	Dose to RMEI (mrem/yr) from dissolved ^{99}Tc (Figure K.5.6.1-5)
ESFA239C	Cumulative release (g) for the movement of ^{239}Pu irreversibly attached to fast (i.e., If) colloids from the EBS to the UZ (Figure K.5.4.1-6)
ESIC239	Release rate (g/yr) for the movement of ^{239}Pu irreversibly attached to waste form (i.e., Ic) colloids from the EBS to the UZ (Figures K.5.3.1-1, K.5.3.1-2, K.5.3.2-1, K.5.3.3-1, K.5.3.5-1)
ESIC239C	Cumulative release (g) for the movement of ^{239}Pu irreversibly attached to waste form (i.e., Ic) colloids from the EBS to the UZ (Figures K.5.3.1-1, K.5.3.1-2, K.5.3.2-1, K.5.3.3-1, K.5.3.5-1)
ESIF239	Release rate (g/yr) for the movement of ^{239}Pu irreversibly attached to ferrous (i.e., If) colloids from the EBS to the UZ (Figures K.5.3.1-3, K.5.3.1-4, K.5.3.2-2, K.5.3.3-2, K.5.3.5-2)
ESIF239C	Cumulative release (g) for the movement of ^{239}Pu irreversibly attached to ferrous (i.e., If) colloids from the EBS to the UZ (Figures K.5.3.1-3, K.5.3.1-4, K.5.3.2-2, K.5.3.3-2, K.5.3.5-2)
ESNP237	Release rate (g/yr) for the movement of dissolved ^{237}Np from the EBS to the UZ (Figures K.5.3.1-5, K.5.3.1-6, K.5.3.2-3, K.5.3.3-3, K.5.3.5-3, K.5.3.7-1, K.5.3.8-1, K.5.3.9-1, K.5.3.10-1, K.5.3.11-1, K.5.3.12-1)
ESNP237C	Cumulative release (g) for the movement of dissolved ^{237}Np from the EBS to the UZ (Figures K.5.3.1-5, K.5.3.1-6, K.5.3.2-3, K.5.3.3-3, K.5.3.5-3, K.5.3.7-1, K.5.3.8-1, K.5.3.9-1, K.5.3.10-1, K.5.3.11-1, K.5.3.12-1, K.5.4.1-9)
ESPU239	Release rate (g/yr) for the movement of dissolved ^{239}Pu from the EBS to the UZ (Figures K.5.3.1-7, K.5.3.1-8, K.5.3.2-4, K.5.3.3-4, K.5.3.5-4, K.5.3.7-2, K.5.3.8-2, K.5.3.9-2, K.5.3.10-2, K.5.3.11-2, K.5.3.12-2)
ESPU239C	Cumulative release (g) for the movement of dissolved ^{239}Pu from the EBS to the UZ (Figures K.5.3.1-7, K.5.3.1-8, K.5.3.2-4, K.5.3.3-4, K.5.3.5-4, K.5.3.7-2, K.5.3.8-2, K.5.3.9-2, K.5.3.10-2, K.5.3.11-2, K.5.3.12-2, K.5.4.1-12)
ESSL239C	Cumulative release (g) for the movement of ^{239}Pu irreversibly attached to slow colloids from the EBS to the UZ (Figure K.5.4.1-3)
ESTC99	Release rate (g/yr) for the movement of dissolved ^{99}Tc from the EBS to the UZ (Figures K.5.3.1-9, K.5.3.1-10, K.5.3.2-5, K.5.3.3-5, K.5.3.5-5)
ESTC99C	Cumulative release (g) for the movement of dissolved ^{99}Tc from the EBS to the UZ (Figures K.5.3.1-9, K.5.3.1-10, K.5.3.2-5, K.5.3.3-5, K.5.3.5-5, K.5.4.1-15)
EXPDOSE	Expected dose to RMEI (mrem/yr) from all radioactive species (Figure K.5.7.1-1, K.5.7.1-2, K.5.7.1-3, K.5.7.1-4, K.5.7.2-1, K.5.7.2-2, K.5.7.2-3, K.5.7.2-4, K.5.7.3-1, K.5.7.3-2, K.5.7.3-3, K.5.7.3-4, K.5.7.4-1, K.5.7.4-2)
ISCDINAD	Ionic strength (molal) in the invert beneath the WP for CDSP WPs under dripping conditions (Figure K.5.2-1)
ISCSINAD	Ionic strength (molal) in the invert beneath the WP for CSNF WPs under dripping conditions (Figure K.5.2-1)

Table K5.1-1. Summary of TSPA-LA Model Results Considered in Uncertainty and Sensitivity Analyses for the Early Failure Scenario Classes (Continued)

Output Variable	Definition
PHCDINAD	pH in the invert beneath the WP for CDSP WPs under dripping conditions (Figure K.5.2-2)
PHCSINAD	pH in the invert beneath the WP for CSNF WPs under dripping conditions (Figure K.5.2-2)
SZIC239	Release rate (g/yr) for the movement of ^{239}Pu irreversibly attached to slow (i.e., Ic) colloids across a subsurface plane at the location of the RMEI (Figure K.5.5.1-1)
SZIC239C	Cumulative release (g) for the movement of ^{239}Pu irreversibly attached to slow (i.e., Ic) colloids across a subsurface plane at the location of the RMEI (Figure K.5.5.1-1)
SZIF239	Release rate (g/yr) for the movement of ^{239}Pu irreversibly attached to fast (i.e., If) colloids across a subsurface plane at the location of the RMEI (Figure K.5.5.1-2)
SZIF239C	Cumulative release (g) for the movement of ^{239}Pu irreversibly attached to fast (i.e., If) colloids across a subsurface plane at the location of the RMEI (Figure K.5.5.1-2)
SZNP237	Release rate (g/yr) for the movement of dissolved ^{237}Np across a subsurface plane at the location of the RMEI (Figure K.5.5.1-3)
SZNP237C	Cumulative release (g) for the movement of dissolved ^{237}Np across a subsurface plane at the location of the RMEI (Figure K.5.5.1-3)
SZPU239	Release rate (g/yr) for the movement of dissolved ^{239}Pu across a subsurface plane at the location of the RMEI (Figure K.5.5.1-4)
SZPU239C	Cumulative release (g) for the movement of dissolved ^{239}Pu across a subsurface plane at the location of the RMEI (Figure K.5.5.1-4)
SZTC99	Release rate (g/yr) for the movement of dissolved ^{99}Tc across a subsurface plane at the location of the RMEI (Figure K.5.5.1-5)
SZTC99C	Cumulative release (g) for the movement of dissolved ^{99}Tc across a subsurface plane at the location of the RMEI (Figure K.5.5.1-5)
UZIC239	Release rate (g/yr) for the movement of ^{239}Pu irreversibly attached to slow (i.e., Ic) colloids from the UZ to the SZ (Figures K.5.4.1-1, K.5.4.1-2)
UZIC239C	Cumulative release (g) for the movement of ^{239}Pu irreversibly attached to slow (i.e., Ic) colloids from the UZ to the SZ (Figures K.5.4.1-1, K.5.4.1-2, K.5.4.1-3)
UZIF239	Release rate (g/yr) for the movement of ^{239}Pu irreversibly attached to fast (i.e., If) colloids from the UZ to the SZ (Figures K.5.4.1-4, K.5.4.1-5)
UZIF239C	Cumulative release (g) for the movement of ^{239}Pu irreversibly attached to fast (i.e., If) colloids from the UZ to the SZ (Figures K.5.4.1-4, K.5.4.1-5, K.5.4.1-6)
UZNP237	Release rate (g/yr) for the movement of dissolved ^{237}Np from the UZ to the SZ (Figures K.5.4.1-7, K.5.4.1-8)
UZNP237C	Cumulative release (g) for the movement of dissolved ^{237}Np from the UZ to the SZ (Figures K.5.4.1-7, K.5.4.1-8, K.5.4.1-9)
UZPU239	Release rate (g/yr) for the movement of dissolved ^{239}Pu from the UZ to the SZ (Figures K.5.4.1-10, K.5.4.1-11)
UZPU239C	Cumulative release (g) for the movement of dissolved ^{239}Pu from the UZ to the SZ (Figures K.5.4.1-10, K.5.4.1-11, K.5.4.1-12)

Table K5.1-1. Summary of TSPA-LA Model Results Considered in Uncertainty and Sensitivity Analyses for the Early Failure Scenario Classes (Continued)

Output Variable	Definition
UZTC99	Release rate (g/yr) for the movement of dissolved ^{99}Tc from the UZ to the SZ (Figures K.5.4.1-13, K.5.4.1-14)
UZTC99C	Cumulative release (g) for the movement of dissolved ^{99}Tc from the UZ to the SZ (Figures K.5.4.1-13, K.5.4.1-14, K.5.4.1-15)

Table K5.1-2 Summary of Uncertainty and Sensitivity Analysis Results for the Early Failure Scenario Class for Release from the Engineered Barrier System

Output Variable[a]	Time Interval[b]	Range[c]	Dominant Input Variable[d]	Figures[e]
Time-Dependent Release Rate (*ESIC239*, g/yr) and Cumulative Release (*ESIC239C*, g) for ^{239}Pu Irreversibly Attached to Waste Form Colloids				
Early DS Failure Above a CDSP WP Under Dripping Conditions				
ESIC239	[0, 10^4, 2×10^4 yr]	[2×10^{-7}, 10^{-3} g/yr]	*INFIL*(+) *CPUCOLWF*(+) *SEEPPRM*(–)	K5.3.1-1 K5.3.1-2
ESIC239C	[0, 10^4, 2×10^4 yr]	[3×10^{-3}, 10 g]	*CPUCOLWF*(+) *INFIL*(+) *SEEPPRM*(–)	K5.3.1-1 K5.3.1-2
Early DS Failure Above a CSNF WP Under Dripping Conditions				
ESIC239	[0, 10^4, 2×10^4 yr]	[3×10^{-11}, 10^{-8} g/yr]	*INFIL*(+)	K5.3.2-1
ESIC239C	[0, 10^4, 2×10^4 yr]	[3×10^{-7}, 10^{-1} g]	*INFIL*(+)	K5.3.2-1
Early CDSP WP Failure Under Dripping Conditions				
ESIC239	[0, 10^4, 2×10^4 yr]	Results removed due to model error		K5.3.3-1
ESIC239C	[0, 10^4, 2×10^4 yr]	Results removed due to model error		K5.3.3-1
Early CSNF WP Failure Under Dripping Conditions				
ESIC239	[0, 1.5×10^4, 2×10^4 yr]	Results removed due to model error		K5.3.5-1
ESIC239C	[0, 1.5×10^4, 2×10^4 yr]	Results removed due to model error		K5.3.5-1
Comment: *ESIC239* is zero prior to 10^4 yr.				
Time-Dependent Release Rate (*ESIF239*, g/yr) and Cumulative Release (*ESIF239C*, g) for ^{239}Pu Irreversibly Attached to Ferrous Colloids				
Early DS Failure Above a CDSP WP Under Dripping Conditions				
ESIF239	[0, 10^4, 2×10^4 yr]	Results removed due to model error		K5.3.1-3 K5.3.1-4
ESIF239C	[0, 10^4, 2×10^4 yr]	Results removed due to model error		K5.3.1-3 K5.3.1-4

Table K5.1-2 Summary of Uncertainty and Sensitivity Analysis Results for the Early Failure Scenario Class for Release from the Engineered Barrier System (Continued)

Variable[a]	Time Interval[b]	Range[c]	Dominant Input Variables[d]	Figures[e]
Early DS Failure Above a CSNF WP Under Dripping Conditions				
ESIF239	[0, 10^4, 2 × 10^4 yr]	Results removed due to model error		K5.3.2-2
ESIF239C	[0, 10^4, 2 × 10^4 yr]	Results removed due to model error		K5.3.2-2
Early CDSP WP Failure Under Dripping Conditions				
ESIF239	[0, 10^4, 2 × 10^4 yr]	Results removed due to model error		K5.3.3-2
ESIF239C	[0, 10^4, 2 × 10^4 yr]	Results removed due to model error		K5.3.2-2
Early CSNF WP Failure Under Dripping Conditions				
ESIF239	[0, 1.5 × 10^4, 2 × 10^4 yr]	Results removed due to model error		K5.3.5-2
ESIF239C	[0, 1.5 × 10^4, 2 × 10^4 yr]	Results removed due to model error		K5.3.5-2
Comment: *ESIF239* zero prior to 10^4 yr and values for some sample elements remain zero after 10^4 yr.				
Time-Dependent Release Rate (*ESNP237*, g/yr) and Cumulative Release (*ESNP237C*, g) for Dissolved ^{237}Np				
Early DS Failure Above a CDSP WP Under Dripping Conditions				
ESNP237	[0, 10^4, 2 × 10^4 yr]	[3 × 10^{-6}, 10^{-2} g/yr]	*INFIL*(+) *GOESITED*(–) *DSNFMASS*(+) *HFOSA*(–)	K5.3.1-5 K5.3.1-6
ESNP237C	[0, 10^4, 2 × 10^4 yr]	[2 × 10^{-2}, 10^2 g]	*DELPPCO2*(+) *PH2MCOS*(–) *INFIL*(+) *GOESITED*(–)	K5.3.1-5 K5.3.1-6
ESNP237	[0, 5 × 10^5, 10^6 yr]	[10^{-5}, 3 × 10^{-4} g/yr]	*GOESITED*(–) *INFIL*(+) *DSNFMASS*(+) *HFOSA*(–)	K5.3.7-1
ESNP237C	[0, 5 × 10^5, 10^6, yr]	[6, 800 g]	*GOESITED*(–) *INFIL*(+) *DSNFMASS*(+) *HFOSA*(–)	K5.3.7-1
Comment: Many variables have small effects on *ESNP237* and *ESNP237C*; see Figure K5.3.1-6				
Early DS Failure Above a CSNF WP Under Dripping Conditions				
ESNP237	[0, 10^4, 2 × 10^4 yr]	[7 × 10^{-7}, 10^{-1} g/yr]	*PHCSS*(–) *CORRATSS*(–) *INFIL*(+) *EP1NPO2*(+)	K5.3.2-3

Table K5.1-2 Summary of Uncertainty and Sensitivity Analysis Results for the Early Failure Scenario Class for Release from the Engineered Barrier System (Continued)

Variable[a]	Time Interval[b]	Range[c]	Dominant Input Variables[d]	Figures[e]
ESNP237C	[0, 10^4, 2 × 10^4 yr]	[8 × 10^{-3}, 4 × 10^3 g]	*PHCSS*(–) *INFIL*(+) *EP1NPO2*(+) *EP1LOWAM*(+) *CORRATSS*(–)	K5.3.2-3
ESNP237	[0, 5 × 10^5, 10^6 yr]	[7 × 10^{-5}, 2 × 10^{-2} g/yr]	*GOESITED*(–) *INFIL*(+) *PHCSS*(+)	K5.3.8-1
ESNP237C	[0, 5 × 10^5, 10^6, yr]	[10, 2 × 10^4 g]	*INFIL*(+) *GOESITED*(–)	K5.3.8-1
Early CDSP WP Failure Under Dripping Conditions				
ESNP237	[0, 10^4, 2 × 10^4 yr]	[10^{-7}, 2 × 10^{-2} g/yr]	*GOESITED*(–) *EBSDIFCF*(+)	K5.3.3-3
ESNP237C	[0, 10^4, 2 × 10^4 yr]	[4 × 10^{-3}, 7 g]	*GOESITED*(–) *DELPPCO2*(+) *PH2MCONS*(–) *INFIL*(+)	K5.3.3-3
ESNP237	[0, 5 × 10^5, 10^6 yr]	[8 × 10^{-6}, 10^{-3} g/yr]	*GOESITED*(–) *INFIL*(+)	K5.3.9-1
ESNP237C	[0, 5 × 10^5, 10^6, yr]	[2, 500 g]	*INFIL*(+) *GOESITED*(–) *HFOSA*(–)	K5.3.9-1
Early CSNF WP Failure Under Dripping Conditions				
ESNP237	[0, 1.5 × 10^4, 2 × 10^4 yr]	[0, 1 g/yr]	*INFIL*(–) *ISCSNS*(+)	K5.3.5-3
ESNP237C	[0, 1.5 × 10^4, 2 × 10^4 yr]	[0, 7 × 10^3, 7 g]	*INFIL*(–) *ISCSNS*(+)	K5.3.5-3
ESNP237	[0, 5 × 10^5, 10^6 yr]	[4 × 10^{-5}, 4 × 10^{-2} g/yr]	*GOESITED*(–) *INFIL*(+)	K5.3.11-1
ESNP237C	[0, 5 × 10^5, 10^6, yr]	[2, 2 × 10^4 g]	*ISCSNS*(+) *GOESITED*(–)	K5.3.11-1
Early CDSP WP Failure Under Nondripping Conditions				
ESNP237	[0, 5 × 10^5, 10^6 yr]	[10^{-7}, 2 × 10^{-5} g/yr]	*GOESITED*(–) *HFOSA*(–) *DSNFMASS*(+)	K5.3.10-1
ESNP237C	[0, 5 × 10^5, 10^6 yr]	[7 × 10^{-2}, 10 g]	*GOESITED*(–) *HFOSA*(–) *DSNFMASS*(+)	K5.3.10-1
Early CSNF WP Failure Under Nondripping Conditions				
ESNP237	[0, 5 × 10^5, 10^6 yr]	[10^{-7}, 8 × 10^{-3} g/yr]	*ISCSNS*(+)	K5.3.12-1

Table K5.1-2 Summary of Uncertainty and Sensitivity Analysis Results for the Early Failure Scenario Class for Release from the Engineered Barrier System (Continued)

Variable[a]	Time Interval[b]	Range[c]	Dominant Input Variables[d]	Figures[e]
			GOESITED(–)	
ESNP237C	[0, 5×10^5, 10^6 yr]	[10^{-1}, 7×10^3 g]	*ISCSNS*(+) *GOESITED*(–)	K5.3.12-1
Time-Dependent Release Rate (*ESPU239*, g/yr) and Cumulative Release (*ESPU239C*, g) for Dissolved ^{239}Pu				
Early DS Failure Above a CDSP WP Under Dripping Conditions				
ESPU239	[0, 10^4, 2×10^4 yr]	[2×10^{-7}, 2×10^{-2} g/yr]	*EP1LOWPU*(+) *INFIL*(+) *DELPPCO2*(+)	K5.3.1-7 K5.3.1-8
ESPU239C	[0, 10^4, 2×10^4 yr]	[10^{-3}, 300 g]	*EP1LOWPU*(+) *INFIL*(+) *DELPPCO2*(+)	K5.3.1-7 K5.3.1-8
ESPU239	[0, 10^5, 2×10^5 yr]	[4×10^{-6}, 5×10^{-3} g/yr]	*EP1LOWPU*(+) *INFIL*(+) *GOESITED*(–)	K5.3.7-2
ESPU239C	[0, 10^5, 2×10^5, yr]	[0.5, 3×10^3 g]	*EP1LOWPU*(+) *INFIL*(+) *GOESITED*(+)	K5.3.7-2
Early DS Failure Above a CSNF WP Under Dripping Conditions				
ESPU239	[0, 10^4, 2×10^4 yr]	[4×10^{-7}, 3×10^{-2} g/yr]	*EP1LOWPU*(+) *INFIL*(+) *DELPPCO2*(+) *PHCSS*(–)	K5.3.2-4
ESPU239C	[0, 10^4, 2×10^4 yr]	[3×10^{-3}, 200 g]	*INFIL*(+) *EP1LOWPU*(+) *DELPPCO2*(+) *PHCSS*(–)	K5.3.2-4
ESPU239	[0, 10^5, 2×10^5 yr]	[3×10^{-6}, 10^{-2} g/yr]	*EP1LOWPU*(+) *INFIL*(+) *GOESITED*(–) *PHCSS*(–)	K5.3.8-2
ESPU239C	[0, 10^5, 2×10^5, yr]	[0.8, 4×10^4 g/yr]	*EP1LOWPU*(+) *INFIL*(+) *PHCSS*(–) *DELPPCO2*(+)	K5.3.8-2
Early CDSP WP Failure Under Dripping Conditions				
ESPU239	[0, 10^4, 2×10^4 yr]	[10^{-7}, 2×10^{-2} g/yr]	*EP1LOWPU*(+) *INFIL*(+) *DELPPCO2*(+) *PH2MCONS*(–)	K5.3.3-4
ESPU239C	[0, 10^4, 2×10^4 yr]	[3×10^{-4}, 100 g]	*EP1LOWPU*(+) *DELPPCO2*(+)	K5.3.3-4

Table K5.1-2 Summary of Uncertainty and Sensitivity Analysis Results for the Early Failure Scenario Class for Release from the Engineered Barrier System (Continued)

Variable[a]	Time Interval[b]	Range[c]	Dominant Input Variables[d]	Figures[e]
			INFIL(+) *PH2MCONS*(–)	
ESPU239	[0, 10^5, 2 × 10^5 yr]	[3 × 10^{-6}, 10^{-3} g/yr]	*EP1LOWPU*(+) *EBSDIFCF*(+) *GOESITED*(–) *INFIL*(+)	K5.3.9-2
ESPU239C	[0, 10^5, 2 × 10^5, yr]	[0.3, 10^3 g]	*EP1LOWPU*(+) *EBSDIFCF*(+) *DIFPATHL*(–) *INFIL*(+)	K5.3.9-2
Early CSNF WP Failure Under Dripping Conditions				
ESPU239	[0, 1.5 × 10^4, 2 × 10^4 yr]	[0, 2 × 10^{-2} g/yr]	*ISCSNS*(+) *INFIL*(–)	K5.3.5-4
ESPU239C	[0, .5 × 10^4, 2 × 10^4 yr]	[0, 100 g]	*ISCSNS*(+) *INFIL*(–)	K5.3.5-4
ESPU239	[0, 10^5, 2 × 10^5 yr]	[10^{-6}, 5 × 10^{-3} g/yr]	*EP1LOWPU*(+) *ISCSNS*(+) *PHCSNS*(–)	K5.3.11-2
ESPU239C	[0, 10^5, 2 × 10^5, yr]	[0.1, 10^3 g]	*EP1LOWPU*(+) *ISCSNS*(+) *PHCSNS*(–)	K5.3.11-2
Early CDSP WP Failure Under Nondripping Conditions				
ESPU239	[0, 10^5, 2 × 10^5 yr]	[2 × 10^{-8}, 7 × 10^{-5} g/yr]	*EP1LOWPU*(+) *EBSDIFCF*(+) *GOESITED*(–)	K5.3.10-2
ESPU239C	[0, 10^5, 2 × 10^5 yr]	[10^{-3}, 30 g]	*EP1LOWPU*(+) *EBSDIFCF*(+) *PH2MCONS*(–)	K5.3.10-2
Early CSNF WP Failure Under Nondripping Conditions				
ESPU239	[0, 10^5, 2 × 10^5 yr]	[2 × 10^{-8}, 8 × 10^{-5}]	*EP1LOWPU*(+) *ISCSNS*(+) *PHCSNS*(–)	K5.3.12-2
ESPU239C	[0, 10^5, 2 × 10^5 yr]	[10^{-3}, 20 g]	*EP1LOWPU*(+) *ISCSNS*(+) *PHCSNS*(–)	K5.3.12-2
Time-Dependent Release Rate (*ESTC99*, g/yr) and Cumulative Release (*ESTC99C*, g) for Dissolved ^{99}Tc				
Early DS Failure Above CDSP WP Under Dripping Conditions				
ESTC99	[0, 3 × 10^3, 2 × 10^4 yr]	[3 × 10^{-5}, 0.2 g/yr]	*HLWDRALK*(–) *WFDEGEXF*(–) *HLWDRACD*(+) *PH2DHLS*(–)	K5.3.1-9 K5.3.1-10

Table K5.1-2 Summary of Uncertainty and Sensitivity Analysis Results for the Early Failure Scenario Class for Release from the Engineered Barrier System (Continued)

Variable[a]	Time Interval[b]	Range[c]	Dominant Input Variables[d]	Figures[e]
ESTC99C	[0, 3×10^3, 2×10^4 yr]	[200, 1700 g]	*HLWDRALK*(+) *HLWMASS*(+) *WFDEGEXF*(+) *HLWDRACD*(+) *DSNFMASS*(+)	K5.3.1-9 K5.3.1-10
Note: Most ^{99}Tc released by 3000 yr after DS failure.				
Early DS Failure Above CSNF WP Under Dripping Conditions				
ESTC99	[0, 3×10^3, 2×10^4 yr]	[3×10^{-9}, 0.1 g/yr]	*INFIL*(–) *SEEPPRMN*(+)	K5.3.2-5
ESTC99C	[0, 3×10^3, 2×10^4 yr]	[6500, 10,600 g]	*CSNFMASS*(+)	K5.3.2-5
Note: Effectively all ^{99}Tc released by 1500 yr after DS failure.				
Early CDSP WP Failure Under Dripping Conditions				
ESTC99	[0, 3×10^3, 2×10^4 yr]	[7×10^{-6}, 0.3 g/yr]	*HLWDRALK*(–) *INFIL*(–) *WFDEGEXF*(–)	K5.3.3-5
ESTC99C	[0, 3×10^3, 2×10^4 yr]	[200, 1700 g]	*HLWDRALK*(+) *HLWMASS*(+) *DSNFMASS*(+) *WFDEGEXF*(+)	K5.3.3-5
NOTE: Most ^{99}Tc released by 3000 yr after WP failure.				
Early CSNF WP Failure Under Dripping Conditions				
Release rate *ESTC99* zero until after 10^4 yr; then, release very rapid (Figure K.5.3.5-5a). Nonzero values for *ESTC99C* rapidly approach an asymptote with values between 6200 and 10,300 g, which is approximately the same range (i.e., 6500 to 10,600 g) obtained for *ESTC99C* for early failure of a DS above a CSNF WP under dripping conditions.				

[a] Dependent variable under consideration.
[b] Time interval [t_1, t_2, t_3], where t_1 is initial or event time, t_2 is time at which variable range (Column c) and dominant input variables (Column d) are determined, and t_3 is the end time for the analysis.
[c] Range of values at time t_2.
[d] Dominant input variables at time t_2 with "+" and "–" indicating positive and negative effects respectively.
[e] Figures presenting detailed analyses.

Table K5.1-3 Summary of Uncertainty and Sensitivity Analysis Results for Radionuclide Movement from the UZ to the SZ Resulting from Early DS Failure Above a CDSP WP Under Dripping Conditions

Variable[a]	Time Interval[b]	Range[c]	Dominant Variables[d]	Figures[e]
Release Rate (*UZIC239*, g/yr) and Cumulative Release (*UZIC239C*, g) for ^{239}Pu Irreversibly Attached to Slow Colloids				
UZIC239	[0, 10^4, 2 × 10^4 yr]	[2 × 10^{-7}, 10^{-3} g/yr]	*INFIL*(+) *CPUCOLWF*(+)	K5.4.1-1 K5.4.1-2
UZIC239C	[0, 10^4, 2 × 10^4 yr]	[3 × 10^{-3}, 10 g]	*CPUCOLWF*(+) *INFIL*(+)	K5.4.1-1 K5.4.1-2 K5.4.1-3
Release Rate (*UZIF239*, g/yr) and cumulative release (*UZIF239C*, g) for ^{239}Pu Irreversibly Attached to Fast Colloids				
UZIF239	[0, 10^4, 2 × 10^4 yr]	[4 × 10^{-10}, 2 × 10^{-6} g/yr]	*INFIL*(+) *CPUCOLWF*(+)	K5.4.1-4 K5.4.1-5
UZIF239C	[0, 10^4, 2 × 10^4 yr]	[4 × 10^{-6}, 0.02 g]	*CPUCOLWF*(+) *INFIL*(+)	K5.4.1-4 K5.4.1-5 K5.4.1-6
Release Rate (*UZNP237*, g/yr) and cumulative release (*UZNP237C*, g) for Dissolved ^{237}Np				
UZNP237	[0, 10^4, 2 × 10^4 yr]	[2 × 10^{-6}, 0.01 g/yr]	*INFIL*(+) *GOESITED*(–) *DEPPCO2*(+) *DSNFMASS*(+)	K5.4.1-7 K5.4.1-8
UZNP237C	[0, 10^4, 2 × 10^4 yr]	[0.01, 100 g]	*DELPPCO2*(+) *INFIL*(+) *PH2MCOS*(–) *GOESITED*(–)	K5.4.1-7 K5.4.1-8 K5.4.1-9
Release Rate (*UZPU239*, g/yr) and cumulative release (*UZPUP239C*, g) for Dissolved ^{237}Np				
UZPU239	[0, 10^9, 2 × 10^4 yr]	[10^{-7}, 0.02 g/yr]	*EP1LOWPU*(+) *INFIL*(+) *DELPPCO2*(+) *UZKDPUDT*(–)	K5.4.1-10 K5.4.1-11
UZPU239C	[0, 10^4, 2 × 10^4 yr]	[3 × 10^{-4}, 100 g]	*INFIL*(+) *EP1LOWPU*(+) *DELPPCO2*(+) *UZKDPUDT*(–)	K5.4.1-10 K5.4.1-11 K5.4.1-12

Table K5.1-3 Summary of Uncertainty and Sensitivity Analysis Results for Radionuclide Movement from the UZ to the SZ Resulting from Early DS Failure Above a CDSP WP Under Dripping Conditions (Continued)

Variable[a]	Time Interval[b]	Range[c]	Dominant Variables[d]	Figures[e]
Release Rate (*UZTC99*, g/yr) and cumulative release (*UZTC99C*, g) for Dissolved ^{99}Tc				
UZTC99	[0, 3×10^3, 2×10^4 yr]	[0.01, 0.3 g/yr]	*INFIL*(–) *HLWMASS*(+) *HLWDRACD*(+)	K5.4.1-13 K5.4.1-14
UZTC99C	[0, 2×10^3, 2×10^4 yr]	[100, 1.5×10^3g]	*INFIL*(+) *HLWDRALK*(+) *HLWMASS*(+) *WFDEGEXF*(+) *HLWDRACD*(+) *DSNFMASS*(+)	K5.4.1-13 K5.4.1-14 K5.4.1-15

[a] Dependent variable under consideration.
[b] Time interval [t_1, t_2, t_3], where t_1 is initial or event time, t_2 is time at which variable range (Column c) and dominant input variables (Column d) are determined, and t_3 is the end time for the analysis.
[c] Range of values at time t_2.
[d] Dominant input variables at time t_2 with "+" and "–" indicating positive and negative effects respectively.
[e] Figures presenting detailed analyses.

Table K5.1-4 Summary of Uncertainty and Sensitivity Analysis Results for Radionuclide Movement in the SZ Across a Subsurface Plane at the Location of the RMEI Resulting from Early DS Failure Above a CDSP WP Under Dripping Conditions

Variable[a]	Time Interval[b]	Range[c]	Dominant Input Variables[d]	Figures[e]
Release Rate (*SZIC239*, g/yr) and cumulative release (*SZIC239C*, g) for ^{239}Pu Irreversibly Attached to Waste Form Colloids				
SZIC239	[0, 10^4, 2 × 10^4 yr]	[?, 10^{-3} g/yr]	*SZCOLRAL*(–) *SZGWSPDM*(+) *SZF1POVO*(–) *SZLODISP*(+) *CPUCOLWF*(+)	K5.5.1-1
SZIC239C	[0, 10^4, 2 × 10^4 yr]	[?, 8 g]	*SZCOLRAL*(–) *SZGWSPDM*(+) *SZF1POVO*(–) *SZLODISP*(+)	K5.5.1-1
Release Rate (*SZIF239*, g/yr) and cumulative release (*SZIF239C*, g) for ^{239}Pu Irreversibly Attached to Fast Colloids				
SZIF239	[0, 10^4, 2 × 10^4 yr]	[4 × 10^{-10}, 2 × 10^{-6} g/yr]	*CPUCOLWF*(+) *INFIL*(+) *SEEPPRM*(–)	K5.5.1-2
SZIF239C	[0, 10^4, 2 × 10^4 yr]	[4 × 10^{-6}, 0.02 g]	*CPUCOLWF*(+) *INFIL*(+)	K5.5.1-2
Release Rate (*SZNP237*, g/yr) and cumulative release (*SZNP237C*, g) for Dissolved ^{237}Np				
SZNP237	[0, 10^4, 2 × 10^4 yr]	[10^{-7}, 8 × 10^{-3} g/yr]	*DELPPCO2*(+) *HFOSA*(–) *GOESITED*(–) *SZGWSPDM*(+)	K5.5.1-3
SZNP237C	[0, 10^4, 2 × 10^4 yr]	[?, 100 g]	*DELPPCO2*(+) *SZGWSPDM*(+) *SZFISPVO*(+)	K5.5.1-3
Release Rate (*SZPU239*, g/yr) and cumulative release (*SZPU239C*, g) for Dissolved ^{239}Pu				
SZPU239	[0, 10^4, 2 × 10^4 yr]	[0, 8 ×10^{-3} g/yr]	*SZGWSPDM*(+) *SZFISPVO*(+) SZCONCOL(+)	K5.5.1-4
SZPU239C	[0, 10^4, 2 × 10^4 yr]	[0, 20 g]	*SZGWSPDM*(+) *SZFISPVO*(+) SZCONCOL(+)	K5.5.1-4

Table K5.1-4 Summary of Uncertainty and Sensitivity Analysis Results for Radionuclide Movement in the SZ Across a Subsurface Plane at the Location of the RMEI Resulting from Early DS Failure Above a CDSP WP Under Dripping Conditions (Continued)

Variable[a]	Time Interval[b]	Range[c]	Dominant Variables[d]	Figures[e]
Release Rate (*SZTC99*, g/yr) and cumulative release (*SZTC99C*, g) for Dissolved ^{99}Tc				
SZTC99	[0, 2×10^3, 2×10^4 yr]	[5×10^{-3}, 0.4 g/yr]	*INFIL*(–) *SZFISPVO*(–) *SZGWSPDM*(–)	K5.5.1-5
SZTC99C	[0, 2×10^3, 2×10^4 yr]	[?, 1.4×10^3g]	*SZGWSPDM*(+) *INFIL*(+) *SZFISPOVO*(–) *DSNFMASS*(+) *HLWMASS*(+)	K5.5.1-5

[a] Dependent variable under consideration.
[b] Time interval [t_1, t_2, t_3], where t_1 is initial or event time, t_2 is time at which variable range (Column c) and dominant input variables (Column d) are determined, and t_3 is the end time for the analysis.
[c] Range of values at time t_2.
[d] Dominant input variables at time t_2 with "+" and "–" indicating positive and negative effects respectively.
[e] Figures presenting detailed analyses.

Table K5.1-5 Summary of Uncertainty and Sensitivity Analysis Results for Dose to the RMEI from Selected Radionuclides Resulting from Early DS Failure Above a CDSP WP Under Dripping Conditions

Variable[a]	Time Interval[b]	Range[c]	Dominant Input Variables[d]	Figures[e]
Dose from ^{239}Pu Irreversibly Attached to Slow Colloids (*DOIC239*, mrem/yr)				
DOIC239	[0, 10^4, 2×10^4 yr]	[10^{-8}, 0.1 mrem/yr]	*SZCOLRAL*(–) *SZGWSPDM*(+) *SZFIPOVO*(–) *SZLODISP*(+) *CPUCOLWF*(+)	K5.6.1-1
Dose from ^{239}Pu Irreversibly Attached to Fast Colloids (*DOIF239*, mrem/yr)				
DOIF239	[0, 10^4, 2×10^4 yr]	[2×10^{-8}, 2×10^{-4} mrem/yr]	*CPUCOLWF*(+) *INFIL*(+) *MICPU239*(+)	K5.6.1-2
Dose from Dissolved ^{237}Np (*DONP237*, mrem/yr)				
DONP237	[0, 10^4, 2×10^4 yr]	[10^{-8}, 10^{-3} mrem/yr]	*DELPPCO2*(+) *HFOSA*(–) *SEEPWAT*(+) *SZGWSPDM*(+)	K5.6.1-3
Dose from Dissolved ^{239}Pu (*DOPU239*, mrem/yr)				
DOPU239	[0, 10^4, 2×10^4 yr]	[0, 0.4 mrem/yr]	*SZGWSPDM*(+) *SZFISPVO*(+) *SZCONCOL*(+)	K5.6.1-4
Dose from Dissolved ^{99}Tc (*DOTC99*, mrem/yr)				
DOTC99	[0, 3×10^3, 2×10^4 yr]	[5×10^{-5}, 0.06 mrem/yr]	*MICTC99*(+) *INFIL*(–) *SZFIPOVO*(+)	K5.6.1-5

[a] Dependent variable under consideration.
[b] Time interval [t_1, t_2, t_3], where t_1 is initial or event time, t_2 is time at which variable range (Column c) and dominant input variables (Column d) are determined, and t_3 is the end time for the analysis.
[c] Range of values at time t_2.
[d] Dominant input variables at time t_2 with "+" and "–" indicating positive and negative effects respectively.
[e] Figures presenting detailed analyses.

Table K5.1-6 Summary of Uncertainty and Sensitivity Analysis Results for Expected Dose to the RMEI (*EXPDOSE*, mrem/yr) Resulting from Early Failures

Variable[a]	Time Interval[b]	Range[c]	Dominant Input Variables[d]	Figures[e]
Expected Dose for Early DS Failures (*EXPDOSE*, mrem/yr)				
EXPDOSE	[0, 10^4, 2×10^4 yr]	[10^{-8}, 4×10^{-3} mrem/yr]	*PROBDSEF*(+) *SEEPUNC*(+)	K5.7.1-1 K5.7.1-2
EXPDOSE	[0, 5×10^5, 10^6 yr]	[10^{-8}, 8×10^{-4} mrem/yr]	*PROBDSEF*(+) *INFIL*(+) *SZGWSPDM*(+) *SEEPUNC*(+) *SEEPRM*(–)	K5.7.1-3 K5.7.1-4
Expected Dose for Early WP Failures (*EXPDOSE*, mrem/yr)				
EXPDOSE	[0, 10^4, 2×10^4 yr]	[3×10^{-6}, 0.5 mrem/yr]	*PROBWPEF*(+) *INFIL*(–) *THERMCON*(+)	K5.7.2-1 K5.7.2-2
EXPDOSE	[10, 5×10^5, 10^6 yr]	[10^{-6}, 0.08 mrem/yr]	*PROBWPEF*(+) *INFIL*(+) *SZGWSPDM*(+) *SEEPRM*(–)	K5.7.2-3 K5.7.2-4
Expected Dose from Both Early DS Failure and Early WP Failure (*EXPDOSE*, mrem/yr)				
EXPDOSE	[0, 10^4, 2×10^4 yr]	[4×10^{-6}, 0.5 mrem/yr]	*PROBWPEF*(+) *INFIL*(–) *THERMCON*(+) *PPOBDSEF*(+)	K5.7.3-1 K5.7.3-2
EXPDOSE	[0, 5×10^5, 10^6 yr]	[10^{-6}, 0.09 mrem/yr]	*PROBWPEF*(+) *INFIL*(+) *SZGWSPDM*(+) *SEEPUNC*(+)	K5.7.3-3 K5.7.3-4
Expected Dose from Early DS Failure, Early WP Failure and Nominal Process WP Failure (*EXPDOSE*, mrem/yr)				
EXPDOSE	[0, 5×10^5, 10^6 yr]	[10^{-6}, 7 mrem/yr]	*WDGCA22*(–)	K5.7.4-1 K5.7.4-2

[a] Dependent variable under consideration.
[b] Time interval [t_1, t_2, t_3], where t_1 is initial or event time, t_2 is time at which variable range (Column c) and dominant input variables (Column d) are determined, and t_3 is the end time for the analysis.
[c] Range of values at time t_2.
[d] Dominant input variables at time t_2 with "+" and "–" indicating positive and negative effects respectively.
[e] Figures presenting detailed analyses.

INTENTIONALLY LEFT BLANK

Table K6.1-1. Summary of TSPA-LA Model Results Considered in Uncertainty and Sensitivity Analyses for the Igneous Scenario Classes

Output Variable	Definition
DOIC239	Dose to RMEI (mrem/yr) from ^{239}Pu irreversibly attached to slow (i.e., Ic) colloids (Figures K.6.6.1-1, K.6.6.1-2, K.6.6.2-1)
DOIF239	Dose to RMEI (mrem/yr) from ^{239}Pu irreversibly attached to fast (i.e., If) colloids (Figures K.6.6.1-3, K.6.6.1-4, K.6.6.2-2)
DONP237	Dose to RMEI (mrem/yr) from dissolved ^{237}Np (Figures K.6.6.1-5, K.6.6.1-6, K.6.6.2-3)
DOPU239	Dose to RMEI (mrem/yr) from dissolved ^{239}Pu (Figures K.6.6.1-7, K.6.6.1-8, K.6.6.2-4)
DOTC99	Dose to RMEI (mrem/yr) from dissolved ^{99}Tc (Figures K.6.6.1-9, K.6.6.1-10)
ESFA239C	Cumulative release (g) for the movement of ^{239}Pu irreversibly attached to fast (i.e., If) colloids from the EBS to the UZ (Figure K.6.4.1-6)
ESIC239	Release rate (g/yr) for the movement of ^{239}Pu irreversibly attached to waste form (i.e., Ic) colloids from the EBS to the UZ (Figures K.6.3.1-1, K.6.3.1-2, K.6.3.2-1)
ESIC239C	Cumulative release (g) for the movement of ^{239}Pu irreversibly attached to waste form (i.e., Ic) colloids from the EBS to the UZ (Figures K.6.3.1-1, K.6.3.1-2, K.6.3.2-1)
ESIF239	Release rate (g/yr) for the movement of ^{239}Pu irreversibly attached to ferrous (i.e., If) colloids from the EBS to the UZ (Figures K.6.3.1-3, K.6.3.1-4, K.6.3.2-2)
ESIF239C	Cumulative release (g) for the movement of ^{239}Pu irreversibly attached to ferrous (i.e., If) colloids from the EBS to the UZ (Figures K.6.3.1-3, K.6.3.1-4, K.6.3.2-2)
ESNP237	Release rate (g/yr) for the movement of dissolved ^{237}Np from the EBS to the UZ (Figures K.6.3.1-5, K.6.3.1-6, K.6.3.2-3)
ESNP237C	Cumulative release (g) for the movement of dissolved ^{237}Np from the EBS to the UZ (Figures K.6.3.1-5, K.6.3.1-6, K.6.3.2-3, K.6.4.1-9)
ESPU239	Release rate (g/yr) for the movement of dissolved ^{239}Pu from the EBS to the UZ (Figures K.6.3.1-7, K.6.3.1-8, K.6.3.2-4)
ESPU239C	Cumulative release (g) for the movement of dissolved ^{239}Pu from the EBS to the UZ (Figures K.6.3.1-7, K.6.3.1-8, K.6.3.2-4, K.6.4.1-12)
ESSL239C	Cumulative release (g) for the movement of ^{239}Pu irreversibly attached to slow colloids from the EBS to the UZ (Figure K.6.4.1-3)
ESTC99	Release rate (g/yr) for the movement of dissolved ^{99}Tc from the EBS to the UZ (Figures K.6.3.1-9, K.6.3.1-10)
ESTC99C	Cumulative release (g) for the movement of dissolved ^{99}Tc from the EBS to the UZ (Figures K.6.3.1-9, K.6.3.1-10, K.6.4.1-15)
EXPDOSE	Expected dose to RMEI (mrem/yr) from all radioactive species (Figures K.6.7.1-1, K.6.7.1-2, K.6.7.2-1, K.6.7.2-2, K.6.8.1-1, K.6.8.1-2, K.6.8.2-1, K.6.8.2-2)
ISCDINAD	Ionic strength (molal) in the invert beneath the WP for CDSP WPs under dripping conditions (Figure K.6.2-3)
ISCSINAD	Ionic strength (molal) in the invert beneath the WP for CSNF WPs under dripping conditions (Figure K.6.2-3)

Table K6.1-1. Summary of TSPA-LA Model Results Considered in Uncertainty and Sensitivity Analyses for the Igneous Scenario Classes (Continued)

Output Variable	Definition
PHCDINAD	pH in the invert beneath the WP for CDSP WPs under dripping conditions (Figure K.6.2-4)
PHCSINAD	pH in the invert beneath the WP for CSNF WPs under dripping conditions (Figure K.6.2-4)
SPRATECS	Seepage rate (m^3/yr/WP) into the repository above CSNF WPs (Figure K.6.2-2)
SZIC239	Release rate (g/yr) for the movement of ^{239}Pu irreversibly attached to slow (i.e., Ic) colloids across a subsurface plane at the location of the RMEI (Figures K.6.5.1-1, K.6.5.1-2, K.6.5.2-1)
SZIC239C	Cumulative release (g) for the movement of ^{239}Pu irreversibly attached to slow (i.e., Ic) colloids across a subsurface plane at the location of the RMEI (Figures K.6.5.1-1, K.6.5.1-2, K.6.5.1-3, K.6.5.2-1)
SZIF239	Release rate (g/yr) for the movement of ^{239}Pu irreversibly attached to fast (i.e., If) colloids across a subsurface plane at the location of the RMEI (Figures K.6.5.1-4, K.6.5.1-5, K.6.5.2-2)
SZIF239C	Cumulative release (g) for the movement of ^{239}Pu irreversibly attached to fast (i.e., If) colloids across a subsurface plane at the location of the RMEI (Figures K.6.5.1-4, K.6.5.1-5, K.6.5.1-6, K.6.5.2-2)
SZNP237	Release rate (g/yr) for the movement of dissolved ^{237}Np across a subsurface plane at the location of the RMEI (Figures K.6.5.1-7, K.6.5.1-8, K.6.5.2-3)
SZNP237C	Cumulative release (g) for the movement of dissolved ^{237}Np across a subsurface plane at the location of the RMEI (Figures K.6.5.1-7, K.6.5.1-8, K.6.5.1-9, K.6.5.2-3)
SZPU239	Release rate (g/yr) for the movement of dissolved ^{239}Pu across a subsurface plane at the location of the RMEI (Figures K.6.5.1-10, K.6.5.1-11, K.6.5.2-4)
SZPU239C	Cumulative release (g) for the movement of dissolved ^{239}Pu across a subsurface plane at the location of the RMEI (Figures K.6.5.1-10, K.6.5.1-11, K.6.5.1-12, K.6.5.2-4)
SZTC99	Release rate (g/yr) for the movement of dissolved ^{99}Tc across a subsurface plane at the location of the RMEI (Figures K.6.5.1-13, K.6.5.1-14)
SZTC99C	Cumulative release (g) for the movement of dissolved ^{99}Tc across a subsurface plane at the location of the RMEI (Figures K.6.5.1-13, K.6.5.1-14, K.6.5.1-15)
TMPCDINV	Drift temperature (C) for CDSP WPs in the invert beneath the WP (Figure K.6.2-1)
TMPCDWL	Drift temperature (C) for CDSP WPs at the drift wall (Figure K.6.2-1)
TMPCDWP	Drift temperature (C) for CDSP WPs on the WP (Figure K.6.2-1)
TMPCSINV	Drift temperature (C) for CSNF WPs in the invert beneath the WP (Figure K.6.2-1)
TMPCSWL	Drift temperature (C) for CSNF WPs at the drift wall (Figure K.6.2-1)
TMPCSWP	Drift temperature (C) for CSNF WPs on the WP (Figure K.6.2-1)
UZIC239	Release rate (g/yr) for the movement of ^{239}Pu irreversibly attached to slow (i.e., Ic) colloids from the UZ to the SZ (Figures K.6.4.1-1, K.6.4.1-2)
UZIC239C	Cumulative release (g) for the movement of ^{239}Pu irreversibly attached to slow (i.e., Ic) colloids from the UZ to the SZ (Figures K.6.4.1-1, K.6.4.1-2, K.6.4.1-3,

Table K6.1-1. Summary of TSPA-LA Model Results Considered in Uncertainty and Sensitivity Analyses for the Igneous Scenario Classes (Continued)

Output Variable	Definition
	K.6.5.1-3)
UZIF239	Release rate (g/yr) for the movement of ^{239}Pu irreversibly attached to fast (i.e., If) colloids from the UZ to the SZ (Figures K.6.4.1-4, K.6.4.1-5)
UZIF239C	Cumulative release (g) for the movement of ^{239}Pu irreversibly attached to fast (i.e., If) colloids from the UZ to the SZ (Figures K.6.4.1-4, K.6.4.1-5, K.6.4.1-6, K.6.5.1-6)
UZNP237	Release rate (g/yr) for the movement of dissolved ^{237}Np from the UZ to the SZ (Figures K.6.4.1-7, K.6.4.1-8)
UZNP237C	Cumulative release (g) for the movement of dissolved ^{237}Np from the UZ to the SZ (Figures K.6.4.1-7, K.6.4.1-8, K.6.4.1-9, K.6.5.1-9)
UZPU239	Release rate (g/yr) for the movement of dissolved ^{239}Pu from the UZ to the SZ (Figures K.6.4.1-10, K.6.4.1-11)
UZPU239C	Cumulative release (g) for the movement of dissolved ^{239}Pu from the UZ to the SZ (Figures K.6.4.1-10, K.6.4.1-11, K.6.4.1-12, K.6.5.1-12)
UZTC99	Release rate (g/yr) for the movement of dissolved ^{99}Tc from the UZ to the SZ (Figures K.6.4.1-13, K.6.4.1-14)
UZTC99C	Cumulative release (g) for the movement of dissolved ^{99}Tc from the UZ to the SZ (Figures K.6.4.1-13, K.6.4.1-14, K.6.4.1-15, K.6.5.1-15)

Table K6.1-2 Summary of Uncertainty and Sensitivity Analysis Results for Radionuclide Movement from the EBS to the UZ Resulting from an Igneous Intrusive Event that Destroys All WPs in the Repository

Output Variable[a]	Time Interval[b]	Range[c]	Dominant Input Variables[d]	Figures[e]
Release Rate (*ESIC239*, g/yr) and Cumulative Release (*ESIC239C*, g) for ^{239}Pu Irreversibly Attached to WP Colloids				
ESIC239	[10, 10^4, 2×10^4 yr]	[9×10^{-3}, 20 g/yr]	*CPUCOLWF*(+) *INFIL*(+)	K6.3.1-1 K6.3.1-2
ESIC239C	[10, 10^4, 2×10^4 yr]	[80, 2×10^5 g]	*CPUCOLWF*(+) *INFIL*(+)	K6.3.1-1 K6.3.1-2
ESIC239	[250, 10^5, 2×10^5 yr]	[0.02, 10 g/yr]	*EP1LOWPU*(–) *CPUCOLWF*(+)	K6.3.2-1
ESIC239C	[250, 10^5, 2×10^5 yr]	[2×10^3, 10^6 g]	*CPUCOLWF*(+) *EP1LOWPU*(–)	K6.3.2-1
Release Rate (*ESIF239*, g/yr) and Cumulative Release (*ESIF239C*, g) for ^{239}Pu Irreversibly Attached to Ferrous Colloids				
ESIF239	[10, 10^4, 2×10^4 yr]	Results removed due to model error		K6.3.1-3 K6.3.1-4

Table K6.1-2 Summary of Uncertainty and Sensitivity Analysis Results for Radionuclide Movement from the EBS to the UZ Resulting from an Igneous Intrusive Event that Destroys All WPs in the Repository (Continued)

Ouput Variable[a]	Time Interval[b]	Range[c]	Dominant Input Variables[d]	Figures[e]
ESIF239C	[10, 10^4, 2 × 10^4 yr]	Results removed due to model error		K6.3.1-3 K6.3.1-4
ESIF239	[250, 10^5, 2 × 10^5 yr]	Results removed due to model error		K6.3.2-2
ESIF239C	[250, 10^5, 2 × 10^5 yr]	Results removed due to model error		K6.3.2-2
Release Rate (*ESNP237*, g/yr) and Cumulative Release (*ESNP237C*, g) of Dissolved ^{237}Np				
ESNP237	[10, 10^4, 2 × 10^4 yr]	[0.3, 4 × 10^3 g/yr]	*EP1NP02*(+) *PHCSS*(–) *INFIL*(+) *CORRATSS*(–)	K6.3.1-5 K6.3.1-6
ESNP237C	[10, 10^4, 2 × 10^4 yr]	[3 × 10^3, 8 × 10^7 g]	*PHCSS*(–) *INFIL*(+) *EP1NP02*(+) *DELPPC02*(+) *EP1LOWAM*(+)	K6.3.1-5 K6.3.1-6
ESNP237	[250, 5 × 10^5, 10^6 yr]	[3, 200 g/yr]	*EPINPO2*(–) *PHCSS*(+) *GOESITED*(–)	K6.3.2-3
ESNP237C	[250, 5 × 10^5, 10^6 yr]	[2 × 10^6, 10^8 g]	*GOESITED*(–) *INFIL*(+) *EP1NPO2*(+)	K6.3.2-3
Release Rate (*ESPU239*, g/yr) and Cumulative Release (*ESPU239C*, g) of Dissolved ^{239}Pu				
ESPU239	[10, 10^4, 2 × 10^4 yr]	[1, 2 × 10^3 g/yr]	*EP1LOWPU*(+) *INFIL*(+) *DELPPCO2*(+)	K6.3.1-7 K6.3.1-8
ESPU239C	[10, 10^4, 2 × 10^4 yr]	[7 × 10^3, 2 × 10^7 g]	*EP1LOWPU*(+) *INFIL*(+) *DELPPCO2*(+)	K6.3.1-7 K6.3.1-8
ESPU239	[250, 10^5, 2 × 10^5 yr]	[1, 300 g/yr]	*EP1LOWPU*(+) *GOESITED*(–) *INFIL*(+)	K6.3.2-4
ESPU239C	[250, 10^5, 2 × 10^5 yr]	[2 × 10^5, 10^8 g]	*EP1LOWPU*(+) *INFIL*(+) *DELPPCO2*(+)	K6.3.2-4
Release Rate (*ESTC99*, g/yr) and Cumulative Release (*ESTC99C*, g) of Dissolved ^{99}Tc				
ESTC99	[10, 3 × 10^3, 2 × 10^4 yr]	[10^{-3}, 200 g/yr]	*HLWDRALK*(–) *INFIL*(–)	K6.3.1-9 K6.3.1-10

Table K6.1-2 Summary of Uncertainty and Sensitivity Analysis Results for Radionuclide Movement from the EBS to the UZ Resulting from an Igneous Intrusive Event that Destroys All WPs in the Repository (Continued)

Ouput Variable[a]	Time Interval[b]	Range[c]	Dominant Input Variables[d]	Figures[e]
ESTC99C	[10, 3×10^3, 2×10^4 yr]	[5.6×10^7, 9.3×10^7 g]	*CSNFMASS*(+)	K6.3.1-9 K6.3.1-10

[a] Dependent variable under consideration.
[b] Time interval [t_1, t_2, t_3], where t_1 is initial or event time, t_2 is time at which variable range (Column c) and dominant input variables (Column d) are determined, and t_3 is the end time for the analysis.
[c] Range of values at time t_2.
[d] Dominant input variables at time t_2 with "+" and "–" indicating positive and negative effects, respectively.
[e] Figures presenting detailed analyses.

Table K6.1-3 Summary of Uncertainty and Sensitivity Analysis Results for Radionuclide Movement from the UZ to the SZ Resulting from an Igneous Intrusive Event that Destroys all WPs in the Repository.

Output Variable[a]	Time Interval[b]	Range[c]	Dominant Input Variables[d]	Figures[e]
Release Rate (*UZIC239*, g/yr) and Cumulative Release (*UZIC239C*, g) for ^{239}Pu Irreversibly Attached to Slow Colloids				
UZIC239	[10, 10^4, 2×10^4 yr]	[9×10^{-3}, 20 g/yr]	*CPUCOLWF*(+) *INFIL*(+)	K6.4.1-1 K6.4.1-2
UZIC239C	[10, 10^4, 2×10^4 yr]	[70, 2×10^5 g]	*CPUCOLWF*(+) *INFIL*(+)	K6.4.1-1 K6.4.1-2 K6.4.1-3
Release Rate (*UZIF239*, g/yr) and Cumulative Release (*UZIF239C*, g) for ^{239}Pu Irreversibly Attached to Slow Colloids				
UZIF239	[10, 10^4, 2×10^4 yr]	[10^{-5}, 0.02 g/yr]	*CPUCOLWF*(+) *INFIL*(+)	K6.4.1-4 K6.4.1-5
UZIF239C	[10, 10^4, 2×10^4 yr]	[0.1, 300 g]	*CPUCOLWF*(+) *INFIL*(+)	K6.4.1-4 K6.4.1-5 K6.4.1-6
Release Rate (*UZNP237*, g/yr) and Cumulative Release (*UZIF239C*, g) for Dissolved ^{237}Np				
UZNP237	[10, 10^4, 2×10^4 yr]	[0.2, 4×10^3 g/yr]	*PHCSS*(–) *INFIL*(+) *DELPPCO2*(+) *EP1LOWAM*(+) *EP1NPO2*(+)	K6.4.1-7 K6.4.1-8

Table K6.1-3 Summary of Uncertainty and Sensitivity Analysis Results for Radionuclide Movement from the UZ to the SZ Resulting from an Igneous Intrusive Event that Destroys all WPs in the Repository. (Continued)

Output Variable[a]	Time Interval[b]	Range[c]	Dominant Input Variables[d]	Figures[e]
UZNP237C	[10, 10^4, 2 × 10^4 yr]	[10^3, 8 × 10^7 g]	*PHCSS*(–) *INFIL*(+) *EP1NP02*(+) *EP1LOWAM*(+) *DELPPC02*(+)	K6.4.1-7 K6.4.1-8 K6.4.1-9
Release Rate (*UZPU239*, g/yr) and Cumulative Release (*UZPU239C*, g) for Dissolved ^{239}Pu				
UZPU239	[10, 10^4, 2 × 10^4 yr]	[0.5, 10^3 g/yr]	*EP1LOWPU*(+) *INFIL*(+) *DELPPCO2*(+)	K6.4.1-10 K6.4.1-11
UZPU239C	[10, 10^4, 2 × 10^4 yr]	[2 × 10^3, 10^7 g]	*EP1LOWPU*(+) *INFIL*(+) *DELPPCO2*(+)	K6.4.1-10 K6.4.1-11 K6.4.1-12
Release Rate (*UZTC99*, g/yr) and Cumulative Release (*UZTC99C*, g) for Dissolved ^{99}Tc				
UZTC99	[10, 3 × 10^3, 2 × 10^4 yr]	[200, 10^4 g/yr]	*INFIL*(–) *CSNFMASS*(+)	K6.4.1-13 K6.4.1-14
UZTC99C	[10, 3 × 10^3, 2 × 10^4 yr]	[4.8 × 10^7, 8.9 × 10^7 g]	*CSNFMASS*(+) *INFIL(+)*	K6.4.1-13 K6.4.1-14 K6.4.1-15

[a] Dependent variable under consideration.
[b] Time interval [t_1, t_2, t_3], where t_1 is initial or event time, t_2 is time at which variable range (Column c) and dominant input variables (Column d) are determined, and t_3 is the end time for the analysis.
[c] Range of values at time t_2.
[d] Dominant input variables at time t_2 with "+" and "–" indicating positive and negative effects, respectively.
[e] Figures presenting detailed analyses.

Table K6.1-4 Summary of Uncertainty and Sensitivity Analysis Results for Radionuclide Movement in the SZ Across a Subsurface Plane at the Location of the RMEI Resulting from an Igneous Intrusive Event That Destroys all WPs in the Repository.

Output Variable[a]	Time Interval[b]	Range[c]	Dominant Input Variables[d]	Figures[e]
Release Rate (*SZIC239*, g/yr) and Cumulative Release (*SZIC239C*, g) for ^{239}Pu Irreversibly Attached to Slow Colloids				
SZIC239	[10, 10^4, 2 × 10^4 yr]	[0, 10 g/yr]	*SZCOLRAL*(–) CPUCOLWF(+) *SZGWSPDM*(+) *SZFIPOVO*(–) *INFIL*(+)	K6.5.1-1 K6.5.1-2
SZIC239C	[10, 10^4, 2 × 10^4 yr]	[0, 10^5 g]	*SZCOLRAL*(–) *SZFIPOVO*(–) *SZGWSPDM*(+) CPUCOLWF(+) *INFIL*(+)	K6.5.1-1 K6.5.1-2 K6.5.1-3
SZIC239	[250, 10^5, 2 × 10^5 yr]	[10^{-3}, 10 g/yr]	CPUCOLWF(+) *EP1LOWPU*(–) *SZCOLRAL*(–)	K6.5.2-1
SZIC239C	[250, 10^5, 2 × 10^5 yr]	[10, 10^6 g]	*SZCOLRAL*(–) *CPUCOLWF*(+) *SZGWSPDM*(+) *INFIL*(+)	K6.5.2-1
Release Rate (*SZIF239*, g/yr) and Cumulative Release (*SZIF239C*, g) for ^{239}Pu Irreversibly Attached to Fast Colloids				
SZIF239	[10, 10^4, 2 × 10^4 yr]	[10^{-5}, 0.02 g/yr]	*CPUCOLWF*(+) *INFIL*(+)	K6.5.1-4 K6.5.1-5
SZIF239C	[10, 10^4, 2 × 10^4 yr]	[0.1, 200 g]	*CPUCOLWF*(+) *INFIL*(+)	K6.5.1-4 K6.5.1-5 K.6.5.1-6
SZIF239	[250, 10^5, 2 × 10^5 yr]	[3 × 10^{-5}, 0.02 g/yr]	*EP1LOWPU*(–) *CPUCOLWF*(+)	K6.5.2-2
SZIF239C	[250, 10^5, 2 × 10^5 yr]	[3, 2 × 10^3 g]	*CPUCOLWF*(+) *EP1LOWPU*(–) *INFIL*(+)	K6.5.2-2
Release Rate (*SZNP237*, g/yr) and Cumulative Release (*SZNP237C*, g) of Dissolved ^{237}Np				
SZNP237	[10, 10^4, 2 × 10^4 yr]	[0, 10^3 g/yr]	*PHCSS*(–) *INFIL*(+) *EP1NP02*(+) *SZGWSPDM*(+)	K6.5.1-7 K6.5.1-8
SZNP237C	[10, 10^4, 2 × 10^4 yr]	[10^{-8}, 3 × 10^7 g]	*PHCSS*(–) *INFIL*(+) *SZGWSPDM*(+) *SZFISPVO*(+)	K6.5.1-7 K6.5.1-8 K6.5.1-9

Table K6.1-4 Summary of Uncertainty and Sensitivity Analysis Results for Radionuclide Movement in the SZ Across a Subsurface Plane at the Location of the RMEI Resulting from an Igneous Intrusive Event That Destroys all WPs in the Repository. (Continued)

Output Variable[a]	Time Interval[b]	Range[c]	Dominant Input Variables[d]	Figures[e]
SZNP237	[250, 5×10^5, 10^6 yr]	[3, 300 g/yr]	*GOESITED*(–) *PHCSS*(+) *EP1NP02*(–)	K6.5.2-3
SZNP237C	[250, 5×10^5, 10^6 yr]	[10^6, 10^8 g]	*GOESITED*(–) *INFIL*(+) *EP1NP02*(+)	K6.5.2-3
Release Rate (*SZPU239*, g/yr) and Cumulative Release (*SZPU239C*, g) of Dissolved ^{239}Pu				
SZPU239	[10, 10^4, 2×10^4 yr]	[0, 800 g/yr]	*SZGWSPDM*(+) *SZFISPVO*(+) *SZKDPUVO*(–)	K6.5.1-10 K6.5.1-11
SZPU239C	[10, 10^4, 2×10^4 yr]	[0, 3×10^6 g]	*SZGWSPDM*(+) *INFIL*(+) *SZFISPVO*(+)	K6.5.1-10 K6.5.1-11 K6.5.1-12
SZPU239	[250, 10^5, 2×10^5 yr]	[10^{-3}, 100 g/yr]	*SZGWSPDM*(+) *EP1LOWPU*(+) *SZFISPVO*(+) *SZDIFCVO*(–)	K6.5.2-4
SZPU239C	[250, 10^5, 2×10^5 yr]	[100, 4×10^7 g]	*SZGWSPDM*(+) *SZFISPVO*(+) *SZDIFCVO*(–) *EP1LOWPU*(+)	K6.5.2-4
Release Rate (*SZTC99*, g/yr) and Cumulative Release (*SZTC99C*, g) for Dissolved ^{99}Tc				
SZTC99	[10, 3×10^3, 2×10^4 yr]	[300, 3×10^4 g/yr]	*INFIL*(–) *CNSFMASS*(+) *UZFAG8*(–) *SZFIPOVO*(+)	K6.5.1-13 K6.5.1-14
SZTC99C	[10, 3×10^3, 2×10^4 yr]	[1.8×10^7, 8.2×10^7g]	*INFIL(+)* *SZGWSPDM*(+) *SZFISPVO*(+) *CSNFMASS*(+) *SZDIFCVO*(–)	K6.5.1-13 K6.5.1-14 K6.4.1-15

[a] Dependent variable under consideration.
[b] Time interval [t_1, t_2, t_3], where t_1 is initial or event time, t_2 is time at which variable range (Column c) and dominant input variables (Column d) are determined, and t_3 is the end time for the analysis.
[c] Range of values at time t_2.
[d] Dominant input variables at time t_2 with "+" and "–" indicating positive and negative effects, respectively.
[e] Figures presenting detailed analyses.

Table K6.1-5 Summary of Uncertainty and Sensitivity Analysis Results for Dose to the RMEI from Selected Radionuclides Resulting from an Igneous Intrusive Event that Destroys All WPs in the Repository.

Output Variable[a]	Time Interval[b]	Range[c]	Dominant Input Variables[d]	Figures[e]
Dose from ^{239}Pu Irreversibly Attached to Slow Colloids (*DOIC239*, mrem/yr)				
DOIC239	[10, 10^4, 2 × 10^4 yr]	[0.1, 10^3 mrem/yr]	*SZCOLRAL*(–) *CPUCOLWF*(+) *SZGWSPDM*(+) *SZFIPOVO*(–) *INFIL*(+)	K6.6.1-1 K6.6.1-2
DOIC239	[250, 10^5, 2 × 10^5 yr]	[0.1, 500 mrem/yr]	*CPUCOLWF*(+) *EP1LOWPU*(–) *SZCOLRAL*(–)	K6.6.2-1
Dose from ^{239}Pu Irreversibly Attached to Fast Colloids (*DOIF239*, mrem/yr)				
DOIF239	[10, 10^4, 2 × 10^4 yr]	[10^{-3}, 2 mrem/yr]	*CPUCOLWF*(+) *INFIL*(+) *MICPU239*(+)	K6.6.1-3 K6.6.1-4
DOIF239	[250, 10^5, 2 × 10^5 yr]	[10^{-3}, 1 mrem/yr]	*EP1LOWPU*(–) *CPUCOLWF*(+) *MICPU239*(+)	K6.6.2-2
Dose from Dissolved ^{237}Np (*DONP237*, mrem/yr)				
DONP237	[10, 10^4, 2 × 10^4 yr]	[10^{-2}, 700 mrem/yr]	*PHCSS*(–) *INFIL*(+) *EP1NP02*(+) *SZGWSPDM*(+)	K6.6.1-5 K6.6.1-6
DONP237	[250, 5 × 10^5, 10^6 yr]	[0.6, 50 mrem/yr]	*PHCSS*(+) *GOESITED*(–) *INFIL*(+) *EP1NP02*(+)	K6.6.2-3
Dose from Dissolved ^{239}Pu (*DOPU239*, mrem/yr)				
DOPU239	[10, 10^4, 2 × 10^4 yr]	[0, 3 × 10^4 mrem/yr]	*SZGWSPDM*(+) *SZFISPVO*(+) *SCKDPUVO*(–)	K6.6.1-7 K6.6.1-8
DOPU239	[250, 10^5, 2 × 10^5 yr]	[1, 5 × 10^3 mrem/yr]	*SZGWSPDM*(+) *EP1LOWPU*(+) *SZFISPOV*(+) *SZDIFCVO*(–)	K6.6.1-9 K6.6.1-10

Table K6.1-5 Summary of Uncertainty and Sensitivity Analysis Results for Dose to the RMEI from Selected Radionuclides Resulting from an Igneous Intrusive Event that Destroys All WPs in the Repository. (Continued)

Output Variable[a]	Time Interval[b]	Range[c]	Dominant Input Variables[d]	Figures[e]
Dose from Dissolved ^{99}Tc (*DOTC99*, mrem/yr)				
DOTC99	[10, 3 × 10^3, 2 × 10^4 yr]	[4, 3 × 10^3 mrem/yr]	*MICTC99*(+) *INFIL*(+) *CSNFMASS*(+)	K6.6.1-9 K6.6.1-10

[a] Dependent variable under consideration.
[b] Time interval [t_1, t_2, t_3], where t_1 is initial or event time, t_2 is time at which variable range (Column c) and dominant input variables (Column d) are determined, and t_3 is the end time for the analysis.
[c] Range of values at time t_2.
[d] Dominant input variables at time t_2 with "+" and "–" indicating positive and negative effects, respectively.
[e] Figures presenting detailed analyses.

Table K6.1-6 Summary of Uncertainty and Sensitivity Analysis Results for Effected Dose to the RMEI (*EXPDOSE*, mrem/yr) Resulting from Igneous Events

Output Variable[a]	Time Interval[b]	Range[c]	Dominant Input Variables[d]	Figures[e]
Expected Dose for Igneous Intrusive Events (*EXPDOSE*, mrem/yr)				
EXPDOSE	[0, 10^4, 2 × 10^4 yr]	[10^{-4}, 3 mrem/yr]	*IGRATE*(+) *SZGWSPDM*(+)	K6.7.1-1 K6.7.1-2
EXPDOSE	[0, 5 × 10^5, 10^6 yr]	[2 × 10^{-3}, 100 mrem/yr]	*IGRATE*(+) *SZGWSPDM*(+) *INFIL*(+)	K6.7.2-1 K6.7.2-2
Expected Dose for Igneous Eruptive Events (*EXPDOSE*, mrem/yr)				
EXPDOSE	[0, 10^4, 2 × 10^4 yr]	[3 × 10^{-7}, 2 × 10^{-2} mrem/yr]	*IGERATE*(+) *INHLTPV*(+) *DDIVIDE*(-)	K6.8.1-1 K6.8.1-2
EXPDOSE	[0, 5 × 10^5, 10^6 yr]	[7 × 10^{-7}, 10^{-3} mrem/yr]	*IGERATE*(+) *BTILLAGE*(+)	K6.8.2-1 K6.8.2-2

[a] Dependent variable under consideration.
[b] Time interval [t_1, t_2, t_3], where t_1 is initial or event time, t_2 is time at which variable range (Column c) and dominant input variables (Column d) are determined, and t_3 is the end time for the analysis.
[c] Range of values at time t_2.
[d] Dominant input variables at time t_2 with "+" and "–" indicating positive and negative effects, respectively.
[e] Figures presenting detailed analyses.

Table K7.1-1. Summary of TSPA-LA Model Results Considered in Uncertainty and Sensitivity Analyses for the Seismic Scenario Classes

Ouput Variable	Definition
DOIC239	Dose to RMEI (mrem/yr) from ^{239}Pu irreversibly attached to slow (i.e., Ic) colloids (Figure K.7.6-1)
DOIF239	Dose to RMEI (mrem/yr) from ^{239}Pu irreversibly attached to fast (i.e., If) colloids (Figure K.7.6-2)
DONP237	Dose to RMEI (mrem/yr) from dissolved ^{237}Np (Figure K.7.6-3)
DOPU239	Dose to RMEI (mrem/yr) from dissolved ^{239}Pu (Figure K.7.6-4)
DOTC99	Dose to RMEI (mrem/yr) from dissolved ^{99}Tc (Figure K.7.6-5)
ESIC239	Release rate (g/yr) for the movement of ^{239}Pu irreversibly attached to waste form (i.e., Ic) colloids from the EBS to the UZ (Figures K.7.3-1, K.7.3-2)
ESIC239C	Cumulative release (g) for the movement of ^{239}Pu irreversibly attached to waste form (i.e., Ic) colloids from the EBS to the UZ (Figures K.7.3-1, K.7.3-2)
ESIF239	Release rate (g/yr) for the movement of ^{239}Pu irreversibly attached to ferrous (i.e., If) colloids from the EBS to the UZ (Figures K.7.3-3, K.7.3-4)
ESIF239C	Cumulative release (g) for the movement of ^{239}Pu irreversibly attached to ferrous (i.e., If) colloids from the EBS to the UZ (Figures K.7.3-3, K.7.3-4)
ESNP237	Release rate (g/yr) for the movement of dissolved ^{237}Np from the EBS to the UZ (Figures K.7.3-5, K.7.3-6)
ESNP237C	Cumulative release (g) for the movement of dissolved ^{237}Np from the EBS to the UZ (Figures K.7.3-5, K.7.3-6)
ESPU239	Release rate (g/yr) for the movement of dissolved ^{239}Pu from the EBS to the UZ (Figures K.7.3-7, K.7.3-8)
ESPU239C	Cumulative release (g) for the movement of dissolved ^{239}Pu from the EBS to the UZ (Figures K.7.3-7, K.7.3-8)
ESTC99	Release rate (g/yr) for the movement of dissolved ^{99}Tc from the EBS to the UZ (Figures K.7.3-9, K.7.3-10)
ESTC99C	Cumulative release (g) for the movement of dissolved ^{99}Tc from the EBS to the UZ (Figures K.7.3-9, K.7.3-10)
EXPDOSE	Expected dose to RMEI (mrem/yr) from all radioactive species (Figures K.7.7.1-1, K.7.7.1-2, K.7.7.2-1, K.7.7.2-2, K.7.8.1-1, K.7.8.1-2, K.7.8.2-1, K.7.8.2-2)
SZIC239	Release rate (g/yr) for the movement of ^{239}Pu irreversibly attached to slow (i.e., Ic) colloids across a subsurface plane at the location of the RMEI (Figure K.7.5-1)
SZIC239C	Cumulative release (g) for the movement of ^{239}Pu irreversibly attached to slow (i.e., Ic) colloids across a subsurface plane at the location of the RMEI (Figure K.7.5-1)
SZIF239	Release rate (g/yr) for the movement of ^{239}Pu irreversibly attached to fast (i.e., If) colloids across a subsurface plane at the location of the RMEI (Figure K.7.5-2)
SZIF239C	Cumulative release (g) for the movement of ^{239}Pu irreversibly attached to fast (i.e., If) colloids across a subsurface plane at the location of the RMEI (Figure K.7.5-2)

Table K7.1-1. Summary of TSPA-LA Model Results Considered in Uncertainty and Sensitivity Analyses for the Seismic Scenario Classes (Continued)

Output Variable	Definition
SZNP237	Release rate (g/yr) for the movement of dissolved ^{237}Np across a subsurface plane at the location of the RMEI (Figure K.7.5-3)
SZNP237C	Cumulative release (g) for the movement of dissolved ^{237}Np across a subsurface plane at the location of the RMEI (Figure K.7.5-3)
SZPU239	Release rate (g/yr) for the movement of dissolved ^{239}Pu across a subsurface plane at the location of the RMEI (Figure K.7.5-4)
SZPU239C	Cumulative release (g) for the movement of dissolved ^{239}Pu across a subsurface plane at the location of the RMEI (Figure K.7.5-4)
SZTC99	Release rate (g/yr) for the movement of dissolved ^{99}Tc across a subsurface plane at the location of the RMEI (Figure K.7.5-5)
SZTC99C	Cumulative release (g) for the movement of dissolved ^{99}Tc across a subsurface plane at the location of the RMEI (Figure K.7.5-5)
UZIC239	Release rate (g/yr) for the movement of ^{239}Pu irreversibly attached to slow (i.e., Ic) colloids from the UZ to the SZ (Figure K.7.4-1)
UZIC239C	Cumulative release (g) for the movement of ^{239}Pu irreversibly attached to slow (i.e., Ic) colloids from the UZ to the SZ (Figure K.7.4-1)
UZIF239	Release rate (g/yr) for the movement of ^{239}Pu irreversibly attached to fast (i.e., If) colloids from the UZ to the SZ (Figure K.7.4-2)
UZIF239C	Cumulative release (g) for the movement of ^{239}Pu irreversibly attached to fast (i.e., If) colloids from the UZ to the SZ (Figure K.7.4-2)
UZNP237	Release rate (g/yr) for the movement of dissolved ^{237}Np from the UZ to the SZ (Figure K.7.4-3)
UZNP237C	Cumulative release (g) for the movement of dissolved ^{237}Np from the UZ to the SZ (Figure K.7.4-3)
UZPU239	Release rate (g/yr) for the movement of dissolved ^{239}Pu from the UZ to the SZ (Figure K.7.4-4)
UZPU239C	Cumulative release (g) for the movement of dissolved ^{239}Pu from the UZ to the SZ (Figure K.7.4-4)
UZTC99	Release rate (g/yr) for the movement of dissolved ^{99}Tc from the UZ to the SZ (Figure K.7.4-5)
UZTC99C	Cumulative release (g) for the movement of dissolved ^{99}Tc from the UZ to the SZ (Figure K.7.4-5)

Table K7.1-2 Summary of Uncertainty and Sensitivity Analysis Results for Radionuclide Movement from the EBS to the UZ Resulting from a Seismically Induced Damaged Area of 10^{-6} (32.6 m^2) at 10 yrs to All CDSP WPs in the Repository

Output Variable[a]	Time Interval[b]	Range[c]	Dominant Input Variables[d]	Figures[e]
Release Rate (*ESIC239*, g/yr) and Cumulative Release (*ESIC239C*, g) for ^{239}Pu Irreversibly Attached to WP Colloids				
ESIC239	[10, 10^4, 2×10^4 yr]	Results removed due to model error		K7.3-1 K7.3-2
ESIC239C	[10, 10^4, 2×10^4 yr]	Results removed due to model error		K7.3-1 K7.3-2
Release Rate (*ESIF239*, g/yr) and Cumulative Release (*ESIF239C*, g) for ^{239}Pu Irreversibly Attached to Ferrous Colloids				
ESIF239	[10, 10^4, 2×10^4 yr]	Results removed due to model error		K7.3-3 K7.3-4
ESIF239C	[10, 10^4, 2×10^4 yr]	Results removed due to model error		K7.3-3 K7.3-4
Release Rate (*ESNP237*, g/yr) and Cumulative Release (*ESNP237C*, g) for Dissolved ^{237}Np				
ESNP237	[10, 10^4, 2×10^4 yr]	[4×10^{-7}, 7×10^{-4} g/yr]	*GOESITED*(–) *EP1LOWNU*(+) *DSNFMASS*(+) *HFOSA*(–)	K7.3-5 K7.3-6
ESNP237C	[10, 10^4, 2×10^4 yr]	[2×10^{-4}, 7 g]	*GOESITED*(–) *DSNFMASS*(+) *DELPPC02*(+) *HFOSA*(–) *PH2MCONS*(–) *EP1LOWNU*(+)	K7.3-5 K7.3-6
Release Rate (*ESPU239*, g/yr) and Cumulative Release (*ESPU239C*, g) for Dissolved ^{239}Pu				
ESPU239	[10, 10^4, 2×10^4 yr]	[4×10^{-8}, 10^{-2} g/yr]	*EP1LOWPU*(+) *DELPPCO2*(+) *INFIL*(+) *SEEPPRM*(–)	K7.3-7 K7.3-8
ESPU239C	[10, 10^4, 2×10^4 yr]	[10^{-4}, 50 g]	*EP1LOWPU*(+) *DELPPCO2*(+) *INFIL*(+) *PH2MCONS*(–)	K7.3-7 K7.3-8

Table K7.1-2 Summary of Uncertainty and Sensitivity Analysis Results for Radionuclide Movement from the EBS to the UZ Resulting from a Seismically Induced Damaged Area of 10^{-6} (32.6 m^2) at 10 yrs to All CDSP WPs in the Repository (Continued)

Output Variable[a]	Time Interval[b]	Range[c]	Dominant Input Variables[d]	Figures[e]
Release Rate (*ESTC99*, g/yr) and Cumulative Release (*ESTC99C*, g) for Dissolved ^{99}Tc				
ESTC99	[10, 2 × 10^3, 2 × 10^4 yr]	[8, 100 g/yr]	*GOESA*(+) *HLWDRALK*(+) *HLWMASS*(+) *THERMCON*(–) *DSNFMASS*(+) *INFIL*(+)	K7.3-9 K7.3-10
ESTC99C	[10, 2 × 10^3, 2 × 10^4 yr]	[2 × 10^4, 2 × 10^5 g]	*GOESA*(+) *HLWDRALK*(+) *HLWMASS*(+) *DSNFMASS*(+)	K7.3-9 K7.3-10

[a] Dependent variable under consideration.
[b] Time interval [t_1, t_2, t_3], where t_1 is initial or event time, t_2 is time at which variable range (Column c) and dominant input variables (Column d) are determined, and t_3 is the end time for the analysis.
[c] Range of values at time t_2.
[d] Dominant input variables at time t_2 with "+" and "–" indicating positive and negative effects respectively.
[e] Figures presenting detailed analyses.

Table K7.1-3 Summary of Uncertainty and Sensitivity Analysis Results for Radionuclide Movement from the UZS to the SZ Resulting from a Seismically Induced Damaged Area of 10^{-6} (32.6 m^2) at 10 yrs to All CDSP WPs in the Repository

Output Variable[a]	Time Interval[b]	Range[c]	Dominant Input Variables[d]	Figures[e]
Release Rate (*UZIC239*, g/yr) and Cumulative Release (*UZIC239C*, g) for ^{239}Pu Irreversibly Attached to Slow Colloids				
UZIC239	[10, 10^4, 2 × 10^4 yr]	[10^{-13}, 3 × 10^{-10} g/yr]	*EP1LOWPU*(+) *DIAMCOLL*(–) *PH2MCONS*(–)	K7.4-1
UZIC239C	[10, 10^4, 2 × 10^4 yr]	[3 × 10^{-10}, 2 × 10^{-6} g]	*EP1LOWPU*(+) *DIAMCOL*(–) *PH2MCONS*(–)	K7.4-1

Table K7.1-3 Summary of Uncertainty and Sensitivity Analysis Results for Radionuclide Movement from the UZS to the SZ Resulting from a Seismically Induced Damaged Area of 10^{-6} (32.6 m^2) at 10 yrs to All CDSP WPs in the Repository (Continued)

Output Variable[a]	Time Interval[b]	Range[c]	Dominant Input Variables[d]	Figures[e]
Release Rate (*UZIF239*, g/yr) and Cumulative Release (*UZIF239C*, g) for ^{239}Pu Irreversibly Attached to Fast Colloids				
UZIF239	[10, 10^4, 2×10^4 yr]	[2×10^{-16}, 6×10^{-13} g/yr]	*EP1LOWPU*(+) *PH2MCONS*(–) *DIAMCOLL*(–) *GOESA*(+)	K7.4-2
UZIF239C	[10, 10^4, 2×10^4 yr]	[10^{-12}, 3×10^{-9} g]	*EP1LOWPU*(+) *DIAMCOLL*(–) *PH2MCONS*(–)	K7.4-2
Release Rate (*UZNP237*, g/yr) and Cumulative Release (*UZNP237C*, g) for Dissolved ^{237}Np				
UZNP237	[10, 10^4, 2×10^4 yr]	[10^{-7}, 6×10^{-4} g/yr]	*GOESITED*(–) *DELPPCO2*(+) *PH2MCONS*(–)	K7.4-3
UZNP237C	[10, 10^4, 2×10^4 yr]	[4×10^{-4}, 5 g]	*GOESITED*(–) *DELPPC02*(+) *PH2MCONS*(–) *INFIL*(+)	K7.4-3
Release Rate (*UZPU239*, g/yr) and Cumulative Release (*UZPU239C*, g) for Dissolved ^{239}Pu				
UZPU239	[10, 10^4, 2×10^4 yr]	[2×10^{-5}, 4×10^{-3} g/yr]	*EP1LOWPU*(+) *DELPPCO2*(+) *INFIL*(+) *GOESA*(+) *PH2MCONS*(–)	K7.4-4
UZPU239C	[10, 10^4, 2×10^4 yr]	[5×10^{-5}, 20 g]	*EP1LOWPU*(+) *DELPPCO2*(+) *INFIL*(+) *PH2MCONS*(–) *GOESA*(+)	K7.4-4
Release Rate (*UZTC99*, g/yr) and Cumulative Release (*UZTC99C*, g) for Dissolved ^{99}Tc				
UZTC99	[10, 2×10^3, 2×10^4 yr]	[3, 80 g/yr]	*GOESA*(+) *HLWMASS*(+) *THERMCON*(–) *INFIL*(+) *SEEPPRM*(–)	K7.4-5

Table K7.1-3 Summary of Uncertainty and Sensitivity Analysis Results for Radionuclide Movement from the UZS to the SZ Resulting from a Seismically Induced Damaged Area of 10^{-6} (32.6 m^2) at 10 yrs to All CDSP WPs in the Repository (Continued)

Output Variable[a]	Time Interval[b]	Range[c]	Dominant Input Variables[d]	Figures[e]
UZTC99C	[10, 2×10^3, 2×10^4 yr]	[10^4, 10^5 g]	*INFIL(+)* *GOESA*(+) *HLWDRALK*(+) *SEEPPRM*(–) *DSNFMASS*(+)	K7.4-5

[a] Dependent variable under consideration.
[b] Time interval [t_1, t_2, t_3], where t_1 is initial or event time, t_2 is time at which variable range (Column c) and dominant input variables (Column d) are determined, and t_3 is the end time for the analysis.
[c] Range of values at time t_2.
[d] Dominant input variables at time t_2 with "+" and "–" indicating positive and negative effects respectively.
[e] Figures presenting detailed analyses.

Table K7.1-4 Summary of Uncertainty and Sensitivity Analysis Results for Radionuclide Movement in the SZ Across a Subsurface Plane at the Location of the RMEI Resulting from a Seismically Induced Damaged Area of 10^{-6} (32.6 m^2) at 10 yrs to All CDSP WPs in the Repository

Output Variable[a]	Time Interval[b]	Range[c]	Dominant Input Variables[d]	Figures[e]
Release Rate (*SZIC239*, g/yr) and Cumulative Release (*SZIC239C*, g) for ^{239}Pu Irreversibly Attached to Slow Colloids				
SZIC239	[10, 10^4, 2 × 10^4 yr]	[0, 2 × 10^{-10} g/yr]	*SZCOLRAL*(–) *SZGWSPDM*(+) *SZFIPOUO*(–) *GOESA*(+) *PH2MCONS*(–)	K7.5-1
SZIC239C	[10, 10^4, 2 × 10^4 yr]	[0, 10^{-6} g]	*SZCOLRAL*(–) *SZGWSPDM*(+) *SZFIPOUO*(–)	K7.5-1
Release Rate (*SZIF239*, g/yr) and Cumulative Release (*SZIF239C*, g) for ^{239}Pu Irreversibly Attached to Fast Colloids				
SZIF239	[10, 10^4, 2 × 10^4 yr]	[2 × 10^{-16}, 6 × 10^{-13} g/yr]	*EP1LOWPU*(+) *DIAMCOLL*(–) *PH2MCONS*(–)	K7.5-2
SZIF239C	[10, 10^4, 2 × 10^4 yr]	[10^{-12}, 2 × 10^{-9} g]	*DIAMCOLL*(–) *EP1LOWPU*(+)	K7.5-2
Release Rate (*SZNP237*, g/yr) and Cumulative Release (*SZNP237C*, g) for Dissolved ^{237}Np				
SZNP237	[10, 10^4, 2 × 10^4 yr]	[10^{-9}, 2 × 10^{-4} g/yr]	*SZGWSPDM*(+) *GOESITED*(–)	K7.5-3
SZNP237C	[10, 10^4, 2 × 10^4 yr]	[2 × 10^{-4}, 7 g]	*GOESITED*(–) *SZGWSPDM*(+)	K7.5-3
Release Rate (*SZPU239*, g/yr) and Cumulative Release (*SZPU239C*, g) for Dissolved ^{239}Pu				
SZPU239	[10, 10^4, 2 × 10^4 yr]	[0, 3 × 10^{-4} g/yr]	*SZGWSPDM*(+) SZFISPVO(+)	K7.5-4
SZPU239C	[10, 10^4, 2 × 10^4 yr]	[0, 1 g]	*SZGWSPDM*(+) *SZFISPVO*(+)	K7.5-4

Table K7.1-4 Summary of Uncertainty and Sensitivity Analysis Results for Radionuclide Movement in the SZ Across a Subsurface Plane at the Location of the RMEI Resulting from a Seismically Induced Damaged Area of 10^{-6} (32.6 m^2) at 10 yrs to All CDSP WPs in the Repository (Continued)

Output Variable[a]	Time Interval[b]	Range[c]	Dominant Input Variables[d]	Figures[e]
Release Rate (*SZTC99*, g/yr) and Cumulative Release (*SZTC99C*, g) for Dissolved ^{99}Tc				
SZTC99	[10, 2 × 10^3, 2 × 10^4 yr]	[1, 70 g/yr]	*SZGWSPDM*(+) *GOESA*(+) *INFIL*(+)	K7.5-5
SZTC99C	[10, 2 × 10^3, 2 × 10^4 yr]	[?,8 × 10^4 g]	*INFIL*(+) *SZGWSPDM*(+) *SZDIFCVO*(–) *SZFIPOVO*(–)	K7.5-5

[a] Dependent variable under consideration.
[b] Time interval [t_1, t_2, t_3], where t_1 is initial or event time, t_2 is time at which variable range (Column c) and dominant input variables (Column d) are determined, and t_3 is the end time for the analysis.
[c] Range of values at time t_2.
[d] Dominant input variables at time t_2 with "+" and "–" indicating positive and negative effects respectively.
[e] Figures presenting detailed analyses.

Table K7.1-5 Summary of Uncertainty and Sensitivity Analysis Results for Dose to the RMEI from Selected Radionuclides Resulting from a Seismically Induced Damaged Area of 10^{-6} (32.6 m^2) at 10 yrs to All CDSP WPs in the Repository.

Output Variable[a]	Time Interval[b]	Range[c]	Dominant Input Variables[d]	Figures[e]
Dose from ^{239}Pu Irreversibly Attached to Slow Colloids (*DOIC239*, mrem/yr)				
DOIC239	[10, 10^4, 2 × 10^4 yr]	[0, ? mrem/yr]	*SZCOLRAL*(–) *SZGWSPDM*(+) *SZFIPOVO*(–) *SZLODISP*(+) *PH2MCONS*(–)	K7.6-1
Dose from ^{239}Pu Irreversibly Attached to Fast Colloids (*DOIF239*, mrem/yr)				
DOIF239	[10, 10^4, 2 × 10^4 yr]	[0, 4 × 10^{-5} mrem/yr]	*EP1LOWPU*(+) *DIAMCOLL*(–) *SZGWSPDM*(+)	K7.6-2
Dose from Dissolved ^{237}Np (*DONP237*, mrem/yr)				
DONP237	[10, 10^4, 2 × 10^4 yr]	[0, 4 × 10^{-5} mrem/yr]	*SZGWSPDM(+)* *GOESITED*(–) *DSNFMASS*(+)	K7.6-3
Dose from Dissolved ^{239}Pu (*DOPU239*, mrem/yr)				
DOPU239	[10, 10^4, 2 × 10^4 yr]	[0, 0.02 mrem/yr]]	*SZGWSPDM*(+) *SZFISPVO*(+)	K7.6-4
Dose from Dissolved ^{99}Tc (*DOTC99*, mrem/yr)				
DOTC99	[10, 10^4, 2 × 10^4 yr]	[0, 6 mrem/yr]	*MICTC99*(+) *SZGWSPDM*(+) *GOESA*(+) *INFIL*(+)	K7.6-5

[a] Dependent variable under consideration.
[b] Time interval [t_1, t_2, t_3], where t_1 is initial or event time, t_2 is time at which variable range (Column c) and dominant input variables (Column d) are determined, and t_3 is the end time for the analysis.
[c] Range of values at time t_2.
[d] Dominant input variables at time t_2 with "+" and "–" indicating positive and negative effects respectively.
[e] Figures presenting detailed analyses.

Table K7.1-6 Summary of Uncertainty and Sensitivity Analysis Results for Expected Dose to the RMEI (*EXPD05*, mrem/yr) Resulting from Seismic Events

Output Variable[a]	Time Interval[b]	Range[c]	Dominant Input Variables[d]	Figures[e]
Expected Dose for Seismic Ground Motion Events (*EXPDOS*, mrem/yr)				
EXPDOS	[0, 10^4, 2×10^4 yr]	[8×10^{-7}, 3 mrem/yr]	*SCCTHRP*(–)	K7.7.1-1 K7.7.1-2
EXPDOS	[0, 5×10^5, 10^6 yr]	[10^{-3}, 9 mrem/yr]	*WDGCA22*(–) *SCCTHRP*(–)	K7.7.2-1 K7.7.2-2
Expected Dose for Seismic Fault Displacement Events (*EXPDOS*, mrem/yr)				
EXPDOS	[0, 10^4, 2×10^4 yr]	[5×10^{-5}, 0.04 mrem/yr]	*MICTC99*(+) *SZGWSPDM*(+) *DTDRHUNC*(+) *INFIL*(+) *SZFISPVO*(+)	K7.8.1-1 K7.8.1-2
EXPDOS	[10, 5×10^5, 10^6 yr]	[10^{-4}, 0.3 mrem/yr]	*INFIL*(+) *SZGWSPDM*(+) *EP1LOWPU*(+) *WPFLUX*(+) *GOESITED*(–)	K7.8.2-1 K7.8.2-2

[a] Dependent variable under consideration.
[b] Time interval [t_1, t_2, t_3], where t_1 is initial or event time, t_2 is time at which variable range (Column c) and dominant input variables (Column d) are determined, and t_3 is the end time for the analysis.
[c] Range of values at time t_2.
[d] Dominant input variables at time t_2 with "+" and "–" indicating positive and negative effects respectively.
[e] Figures presenting detailed analyses.

Table K9-1. Summary of Selected Sensitivity Analysis Results

Scenario Class	TSPA-LA Model Output (time of maximum mean value)	Key Uncertain Inputs[a]
Total System	Total expected dose 0 to 10,000 years (10,000 years)	Residual stress threshold for SCC (SCCTHRP) Frequency of occurrence of igneous events (IGRATE) Scale factor in ground water specific discharge (SZGWSPDM)
	Total expected dose 10,000 to 1,000,000 years (230,000 years)	Frequency of occurrence of igneous events (IGRATE) Residual stress threshold for SCC (SCCTHRP) General corrosion rate (Alloy 22) temperature dependence (WDGCA22) Scale factor in ground water specific discharge (SZGWSPDM)
Nominal	Expected dose resulting from corrosion processes (720,000 years)	General corrosion rate (Alloy 22) temperature dependence (WDGCA22) Deviation from median yield strength range for outer lid (WDZOLID)
Early Failure Waste Package	Expected dose resulting from early failure of waste packages over 20,000 years (12,000 years)	Probability of early failure per waste package (PROBWPEF) Pointer variable for infiltration scenario (INFIL) Selector for host-rock thermal conductivity scenario (THERMCON)
Early Failure Drip Shield	Expected dose resulting from early failure of drip shields over 20,000 years (2,000 years)	Probability of early failure per drip shield (PROBDSEF) Uncertainty factor accounting for small-scale heterogeneity in fracture permeability (SEEPUNC) Flowing interval porosity in volcanic units (SZFIPOVO)
Igneous Intrusive	Expected dose resulting from igneous intrusion over 20,000 years (20,000 years)	Frequency of occurrence of igneous events (IGRATE) Scale factor in ground water specific discharge (SZGWSPDM)
	Expected dose resulting from igneous intrusion over 1,000,000 years (1,000,000 years)	Frequency of occurrence of igneous events (IGRATE) Scale factor in ground water specific discharge (SZGWSPDM) Pointer variable for infiltration scenario (INFIL)
Igneous Eruptive	Expected dose resulting from volcanic eruption over 20,000 years (20,000 years)	Frequency of occurrence of volcanic eruptions (IGERATE) Pointer variable for long-term inhalation dose conversation factors for exposure to volcanic ash (INHLTPV) Diffusivity of radionuclides in divides (DDIVIDE)
	Expected dose resulting from volcanic eruption over 1,000,000 years (1,000,000 years)	Frequency of occurrence of volcanic eruptions (IGERATE) Depth of soil within which radionuclides affect the biosphere (BTILLAGE)

Table K9-1. Summary of Selected Sensitivity Analysis Results (Continued)

Scenario Class	TSPA-LA Model Output	Key Uncertain Inputs[a]
Seismic Ground Motion	Expected dose resulting from seismic ground motion over 20,000 years (20,000 years)	Residual stress threshold for SCC (SCCTHRP)
	Expected dose resulting from combination of seismic ground motion and corrosion processes over 1,000,000 years (230,000 years)	Residual stress threshold (SCCTHRP) General corrosion rate (Alloy 22) temperature dependence (WDGCA22)
Seismic Fault Displacement	Expected dose resulting from fault displacement over 20,000 years (20,000 years)	Groundwater biosphere dose conversion factor for ^{99}Tc (MICTC99) Scale factor in ground water specific discharge (SZGWSPDM)
	Expected dose resulting from fault displacement over 1,000,000 years (1,000,000 years)	Scale factor in ground water specific discharge (SZGWSPDM) Pointer variable for infiltration scenario (INFIL)

a. Name (in parentheses) is the variable name used in the sensitivity analyses (see Table K3-1).

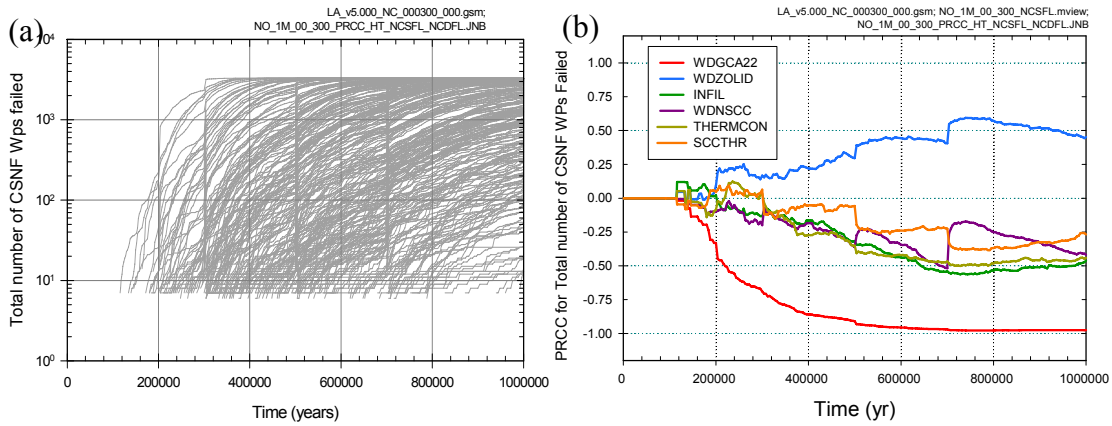

(c)

	NCSFL: 600K yr			NCSFL: 800K yr			NCSFL: 1M yr		
Step[a]	**Variable**[b]	**R^2** [c]	**SRRC**[d]	**Variable**	**R^2**	**SRRC**	**Variable**	**R^2**	**SRRC**
1	WDGCA22	0.86	-0.96	WDGCA22	0.90	-0.98	WDGCA22	0.91	-0.98
2	WDZOLID	0.88	0.13	WDZOLID	0.92	0.14	WDZOLID	0.92	0.10
3	INFIL	0.90	-0.15	INFIL	0.94	-0.13	INFIL	0.93	-0.12
4	THERMCON	0.91	-0.13	THERMCON	0.95	-0.11	THERMCON	0.94	-0.10
5	WDNSCC	0.92	-0.09	SCCTHR	0.95	-0.08	WDNSCC	0.95	-0.09
6	SCCTHR	0.93	-0.08	WDGCUA22	0.96	0.08	WDGCUA22	0.96	0.09
7	WDGCUA22	0.93	0.06	WDNSCC	0.96	-0.05	SCCTHR	0.96	-0.05
8	SEEPPRMN	0.93	0.06	PH2DHLNS	0.96	-0.03			

a: Steps in stepwise rank regression analysis
b: Variables listed in order of selection in stepwise regression
c: Cumulative R^2 value with entry of each variable into regression model
d: Standardized rank regression coefficients (SRRCs) in final regression model

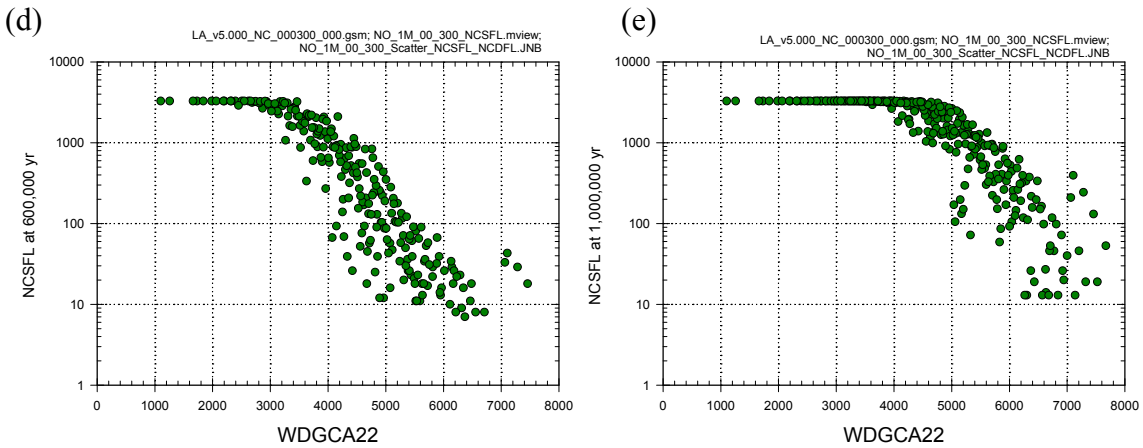

Source: Output DTNs: MO0709TSPAREGS.000 [DIRS 182976]; and MO0709TSPAPLOT.000 [DIRS 183010].

Figure K2-1. Illustration of uncertainty and sensitivity analysis results for time-dependent number of failed CSNF WPs in percolation bin 3 under nominal conditions: (a) *NCSFL* for all (i.e., 300) sample elements, (b) PRCCs for *NCSFL*, (c) stepwise rank regressions for *NCSFL* at 600,000, 800,000 and 1,000,000 years, and (d, e) scatterplots for (*WDGA22*, *NCSFL*) at 600,000 and 1,000,000 years.

(a)

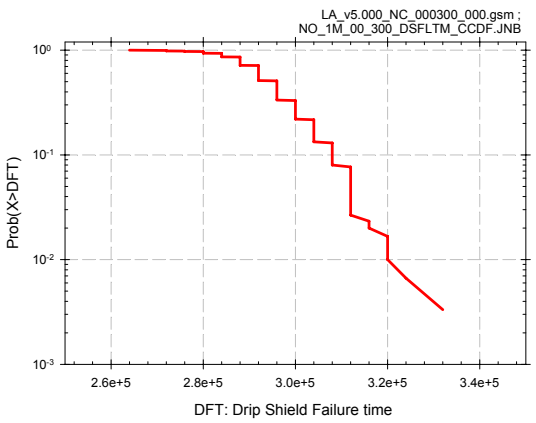

(b)

	DSFLTM		
Step[a]	**Variable[b]**	**R^{2c}**	**SRRC[d]**
1	WDDSAGGC	0.64	-0.82
2	WDDSBEGC	0.93	-0.54

a: Steps in stepwise rank regression analysis

b: Variables listed in order of selection in stepwise regression

c: Cumulative R^2 value with entry of each variable into regression model

d: Standardized rank regression coefficients (SRRCs) in final regression model

(c)

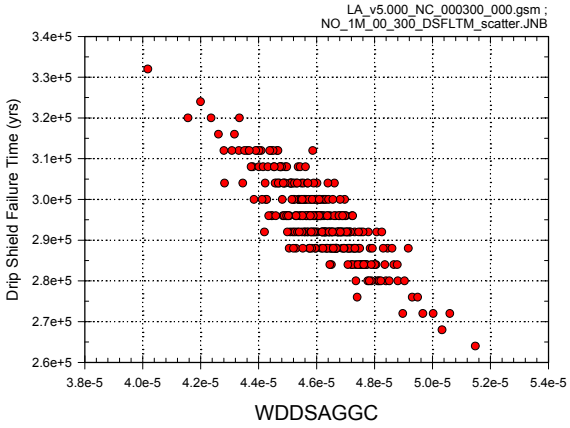

(d)

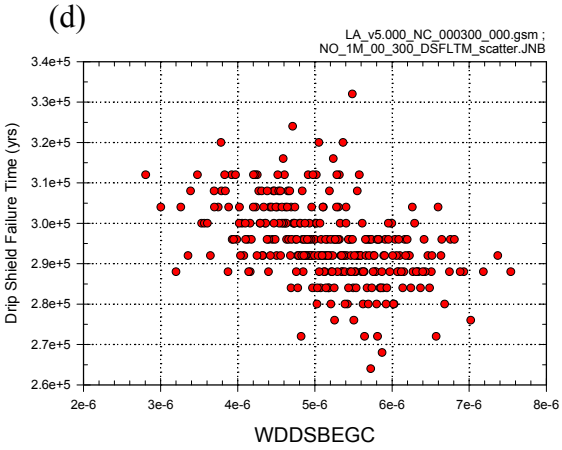

(e)

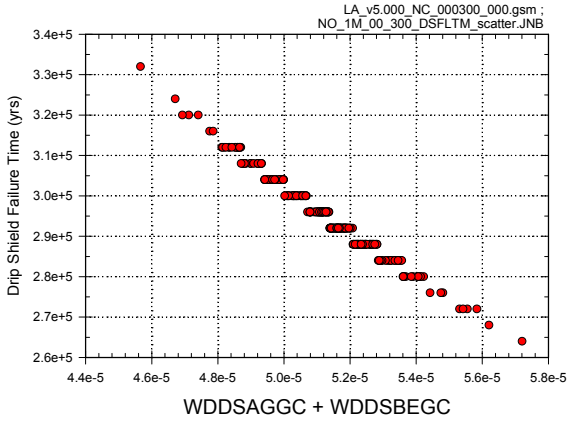

Source: Output DTNs: MO0709TSPAREGS.000 [DIRS 182976]; and MO0709TSPAPLOT.000 [DIRS 183010].

Figure K4.2-1. Uncertainty and sensitivity analysis results for DS failure time (*DSFLTM*, yr) under nominal conditions: (a) CCDF for *DSFLTM*, (b) Stepwise rank regression for *DSFLTM*, and (c,d,e) Selected scatterplots for *DSFLTM*.

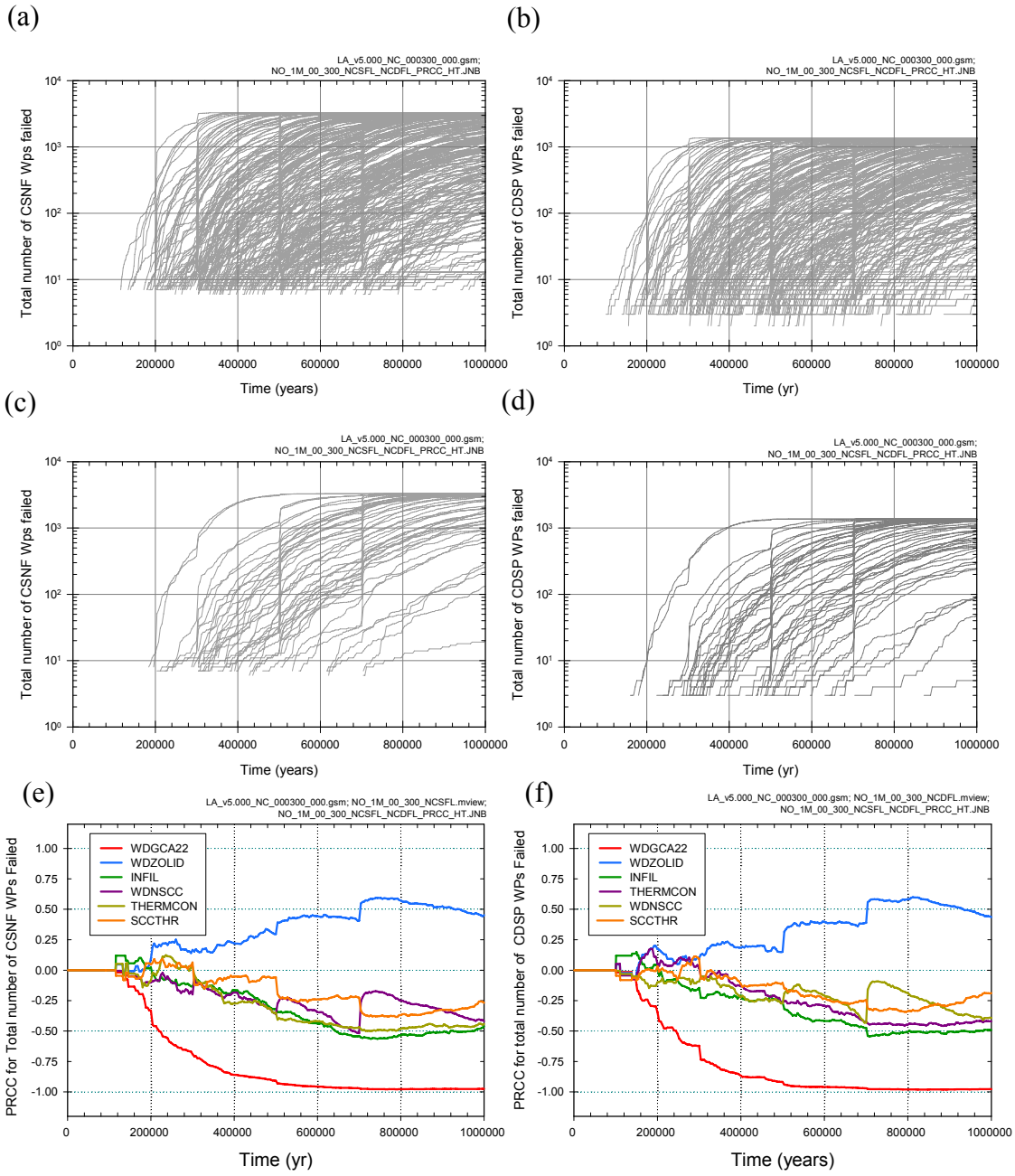

Source: Output DTNs: MO0709TSPAREGS.000 [DIRS 182976]; and MO0709TSPAPLOT.000 [DIRS 183010].

Figure K4.2-2. Time-dependent numbers of failed CSNF WPs (*NCSFL*) and failed CDSP WPs (*NCDFL*) in percolation bin 3 under nominal conditions: (a, b) *NCSFL* and *NCDFL* for all (i.e., 300) sample elements, (c, d) *NCSFL* and *NCDFL* for first 50 sample elements, and (e, f) PRCCs for *NCSFL* and *NCDFL*

(a)

	NCSFL: 600K yr			NCSFL: 800K yr			NCSFL: 1M yr		
Step[a]	**Variable[b]**	**R^{2c}**	**SRRC[d]**	**Variable**	**R^2**	**SRRC**	**Variable**	**R^2**	**SRRC**
1	WDGCA22	0.86	-0.96	WDGCA22	0.90	-0.98	WDGCA22	0.91	-0.98
2	WDZOLID	0.88	0.13	WDZOLID	0.92	0.14	WDZOLID	0.92	0.10
3	INFIL	0.90	-0.15	INFIL	0.94	-0.13	INFIL	0.93	-0.12
4	THERMCON	0.91	-0.13	THERMCON	0.95	-0.11	THERMCON	0.94	-0.10
5	WDNSCC	0.92	-0.09	SCCTHR	0.95	-0.08	WDNSCC	0.95	-0.09
6	SCCTHR	0.93	-0.08	WDGCUA22	0.96	0.08	WDGCUA22	0.96	0.09
7	WDGCUA22	0.93	0.06	WDNSCC	0.96	-0.05	SCCTHR	0.96	-0.05
8	SEEPPRMN	0.93	0.06	PH2DHLNS	0.96	-0.03			

a: Steps in stepwise rank regression analysis
b: Variables listed in order of selection in stepwise regression
c: Cumulative R^2 value with entry of each variable into regression model
d: Standardized rank regression coefficients (SRRCs) in final regression model

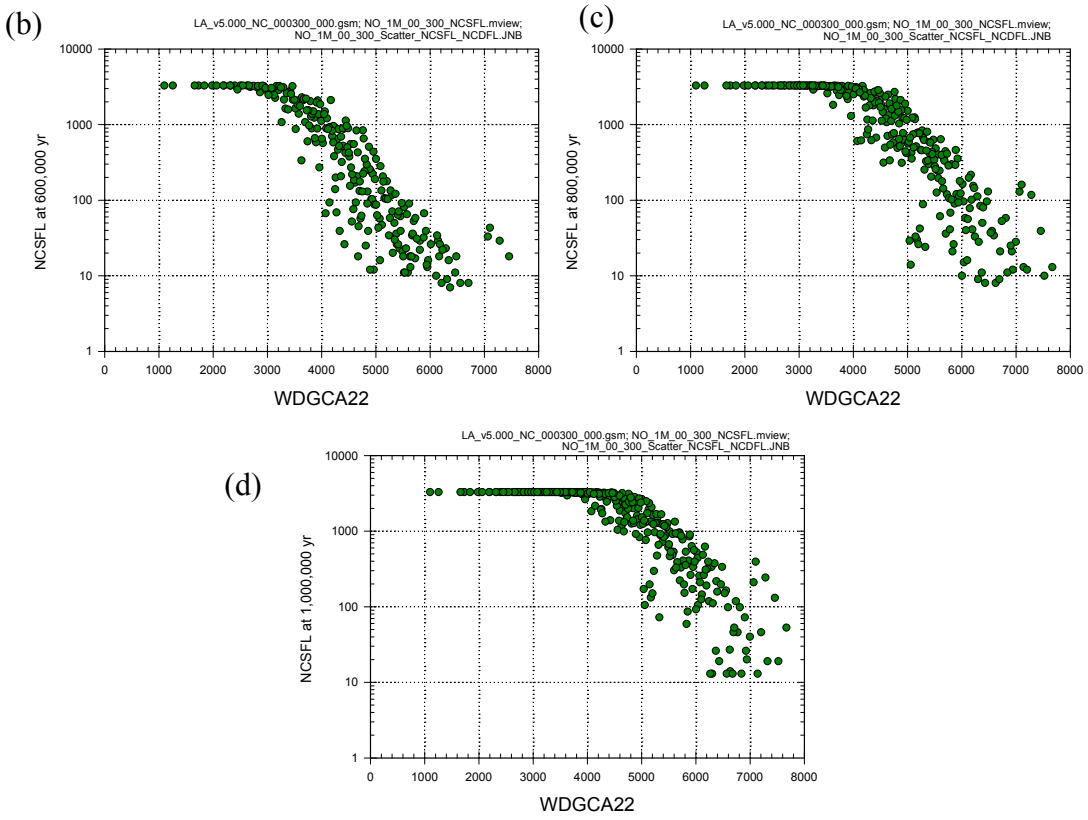

Source: Output DTNs: MO0709TSPAREGS.000 [DIRS 182976]; and MO0709TSPAPLOT.000 [DIRS 183010].

Figure K4.2-3. Stepwise rank regression analyses and selected scatterplots for number of failed CSNF WPs (*NCSFL*) in percolation bin 3 under nominal conditions: (a) Regressions for *NCSFL* at 6×10^5, 8×10^5 and 1×10^6 years, and (b, c, d) Scatterplots for *NCSFL* at 6×10^5, 8×10^5 and 1×10^6 years

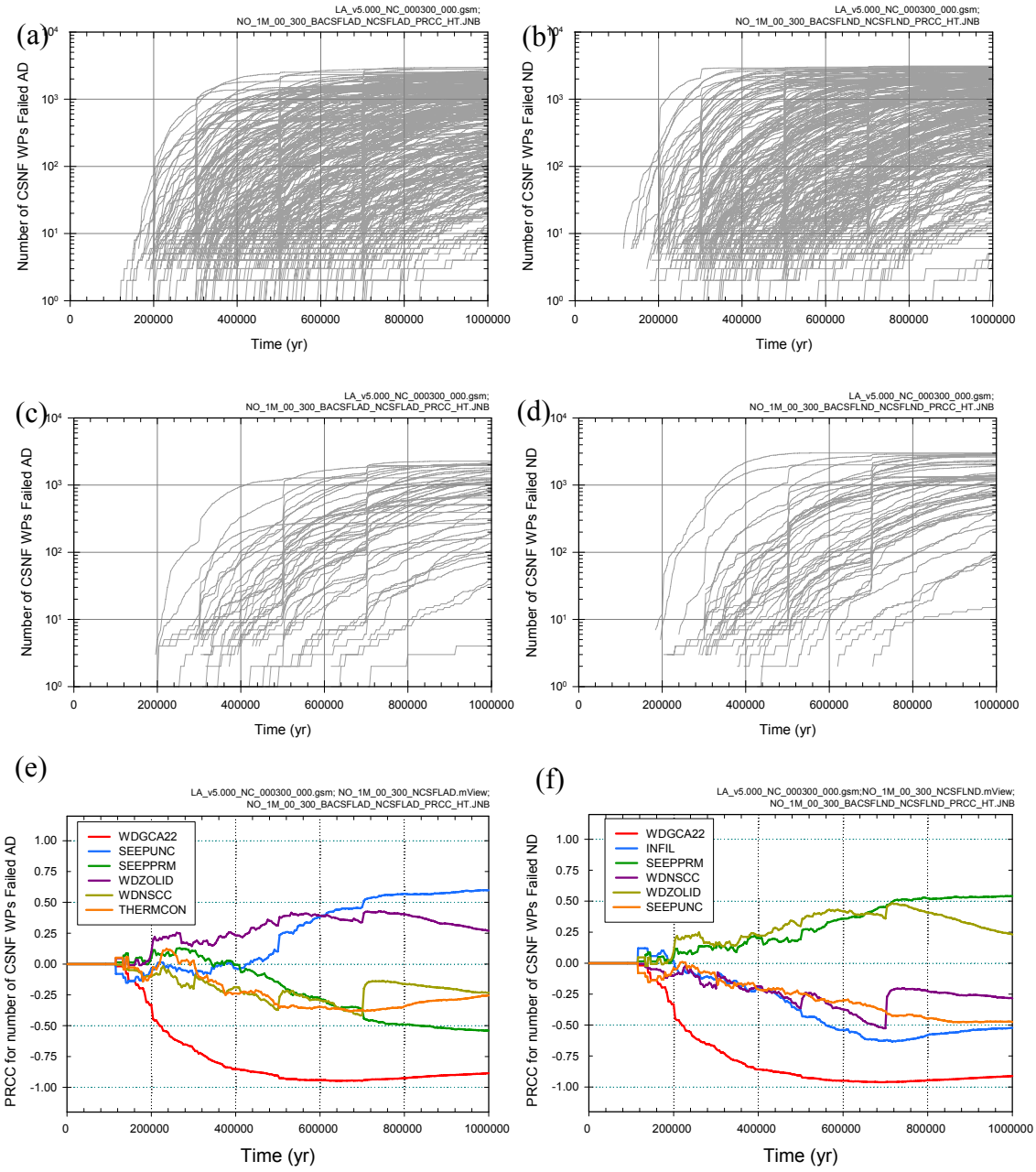

Source: Output DTNs: MO0709TSPAREGS.000 [DIRS 182976]; and MO0709TSPAPLOT.000 [DIRS 183010].

Figure K4.2-4. Time-dependent numbers of failed CSNF WPs experiencing dripping conditions (*NCSFLAD*) and nondripping conditions (*NCSFLND*) in percolation bin 3 under nominal conditions: (a, b) *NCSFLAD* and *NCSFLND* for all (i.e., 300) sample elements, (c, d) *NCSFLAD* and *NCSFLND* for first 50 sample elements, and (e, f) PRCCs for *NCSFLAD* and *NCSFLND*.

(a)

	NCSFLAD: 600K yr			NCSFLAD: 800K yr			NCSFLAD: 1M yr		
Step[a]	**Variable[b]**	**R^{2c}**	**SRRC[d]**	**Variable**	**R^2**	**SRRC**	**Variable**	**R^2**	**SRRC**
1	WDGCA22	0.82	-0.93	WDGCA22	0.73	-0.87	WDGCA22	0.62	-0.81
2	SEEPUNC	0.84	0.15	SEEPUNC	0.79	0.25	SEEPUNC	0.71	0.31
3	WDZOLID	0.86	0.13	SEEPPRM	0.82	-0.18	SEEPPRM	0.78	-0.26
4	THERMCON	0.87	-0.13	WDZOLID	0.85	0.15	ALPHAL	0.79	-0.15
5	SEEPPRM	0.88	-0.09	ALPHAL	0.86	-0.10	WDZOLID	0.81	0.10
6	SCCTHR	0.89	-0.08	THERMCON	0.87	-0.11	THERMCON	0.81	-0.08
7	INFIL	0.89	-0.09	SCCTHR	0.87	-0.08	WDNSCC	0.82	-0.07
8	WDNSCC	0.90	-0.07	WDGCUA22	0.88	0.07	GP1NO3	0.82	0.07
9	WDGCUA22	0.90	0.06						
10	ALPHAL	0.91	-0.06						

(b)

	NCSFLND: 600K yr			NCSFLND: 800K yr			NCSFLND: 1M yr		
Step[a]	**Variable[b]**	**R^{2c}**	**SRRC[d]**	**Variable**	**R^2**	**SRRC**	**Variable**	**R^2**	**SRRC**
1	WDGCA22	0.81	-0.94	WDGCA22	0.78	-0.92	WDGCA22	0.70	-0.87
2	INFIL	0.85	-0.21	INFIL	0.83	-0.24	INFIL	0.76	-0.25
3	WDZOLID	0.87	0.13	WDZOLID	0.85	0.14	SEEPPRM	0.80	0.23
4	THERMCON	0.89	-0.14	SEEPPRM	0.88	0.18	SEEPUNC	0.83	-0.18
5	WDNSCC	0.90	-0.11	SEEPUNC	0.89	-0.13	WDZOLID	0.85	0.11
6	SEEPPRM	0.90	0.11	THERMCON	0.90	-0.11	WDNSCC	0.86	-0.11
7	SEEPPRMN	0.91	0.07	SCCTHR	0.91	-0.07	THERMCON	0.87	-0.10
8	SEEPUNC	0.91	-0.07	WDGCUA22	0.91	0.08	WDGCUA22	0.88	0.08
9	SCCTHR	0.92	-0.07	ALPHAL	0.92	0.06	ALPHAL	0.88	0.07
10	WDGCUA22	0.92	0.07	WDNSCC	0.92	-0.06	SEEPPRMN	0.88	0.06
11				SEEPPRMN	0.92	0.06	KDSNCOL	0.89	0.05

a: Steps in stepwise rank regression analysis

b: Variables listed in order of selection in stepwise regression

c: Cumulative R^2 value with entry of each variable into regression model

d: Standardized rank regression coefficients (SRRCs) in final regression model

Source: Output DTNs: MO0709TSPAREGS.000 [DIRS 182976]; and MO0709TSPAPLOT.000 [DIRS 183010].

Figure K4.2-5. Stepwise rank regression analyses and selected scatterplots for numbers of failed CSNF WPs experiencing dripping conditions (*NCSFLAD*) and nondripping conditions (*NCSFLND*) in percolation bin 3 under nominal conditions: (a, b) Regressions for *NCSFLAD* and *NCSFLND* at 6×10^5, 8×10^5 and 1×10^6 years, and (c, d, e, f) Scatterplots for *NCSFLAD* and *NCSFLND* at 8×10^5 years, and (g, h) Scatterplots comparing *NCSFLAD* and *NCSFLND* at 6×10^5 and 8×10^5 years.

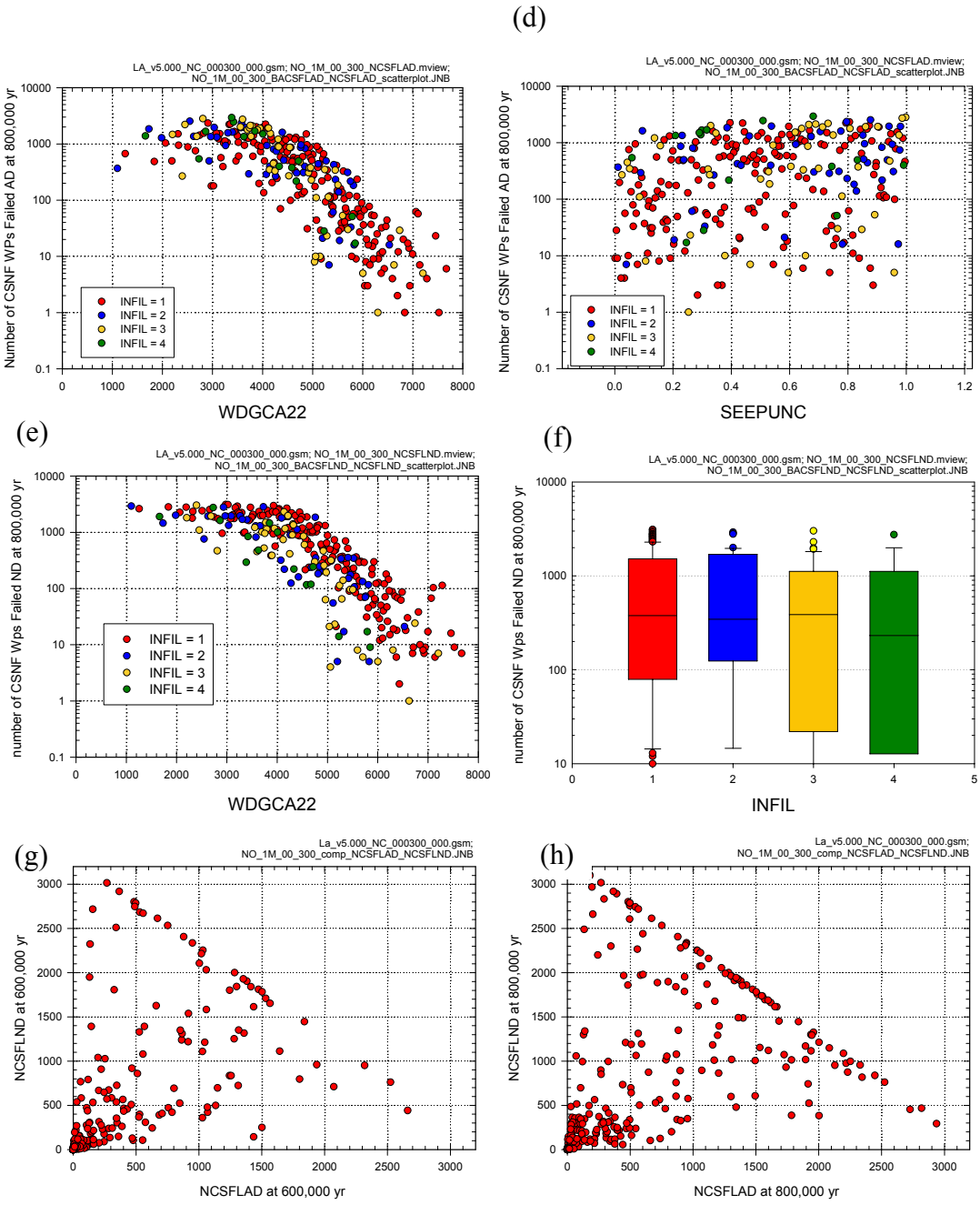

Source: Output DTNs: MO0709TSPAREGS.000 [DIRS 182976]; and MO0709TSPAPLOT.000 [DIRS 183010].

Note In (f), the box extends from 0.25 to 0.75 quantile; lower and upper bar and whisker extend to 0.1 and 0.9 quantile, respectively; dots represent values outside 0.1 to 0.9 quantile range; median indicated by light horizontal line.

Figure K4.2-5. Stepwise rank regression analyses and selected scatterplots for numbers of failed CSNF WPs experiencing dripping conditions (*NCSFLAD*) and nondripping conditions (*NCSFLND*) in percolation bin 3 under nominal conditions: (a, b) Regressions for *NCSFLAD* and *NCSFLND* at 6×10^5, 8×10^5 and 1×10^6 years, and (c, d, e, f) Scatterplots for *NCSFLAD* and *NCSFLND* at 8×10^5 years, and (g, h) Scatterplots comparing *NCSFLAD* and *NCSFLND* at 6×10^5 and 8×10^5 years (continued).

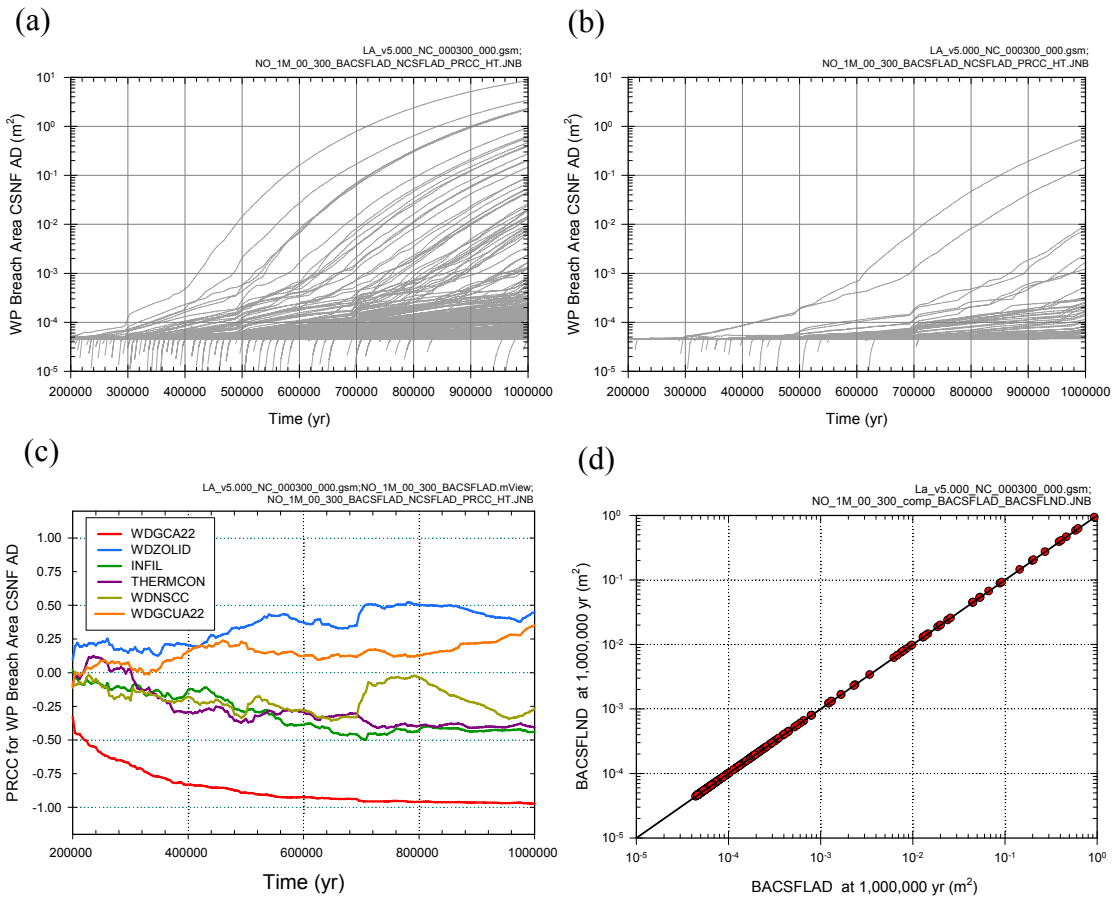

Source: Output DTNs: MO0709TSPAREGS.000 [DIRS 182976]; and MO0709TSPAPLOT.000 [DIRS 183010].

Figure K4.2-6. Time-dependent average breached area on failed CSNF WPs experiencing dripping conditions (*BACSFLAD*) and nondripping conditions (*BACSFLND*) in percolation bin 3 under nominal conditions: (a) *BACSFLAD* for all (i.e., 300) sample elements, (b) *BACSFLAD* for first 50 sample elements, (c) PRCCs for *BACSFLAD*, and (d) Scatterplot comparing *BACSFLAD* and *BACSFLND* at 1×10^6 years.

(a)

	BACSFLAD: 600K yr			BACSFLAD: 800K yr			BACSFLAD: 1M yr		
Step[a]	**Variable[b]**	**R^{2c}**	**SRRC[d]**	**Variable**	**R^2**	**SRRC**	**Variable**	**R^2**	**SRRC**
1	WDGCA22	0.81	-0.93	WDGCA22	0.86	-0.96	WDGCA22	0.91	-0.97
2	WDZOLID	0.83	0.14	WDZOLID	0.89	0.16	WDZOLID	0.92	0.10
3	INFIL	0.85	-0.15	INFIL	0.91	-0.14	INFIL	0.93	-0.12
4	THERMCON	0.87	-0.11	THERMCON	0.93	-0.13	THERMCON	0.94	-0.10
5	SCCTHR	0.87	-0.08	SCCTHR	0.93	-0.08	WDGCUA22	0.95	0.09
6	WDNSCC	0.88	-0.08	WDGCUA22	0.93	0.06	SCCTHR	0.95	-0.08
7							WDNSCC	0.96	-0.05

a: Steps in stepwise rank regression analysis

b: Variables listed in order of selection in stepwise regression

c: Cumulative R^2 value with entry of each variable into regression model

d: Standardized rank regression coefficients (SRRCs) in final regression model

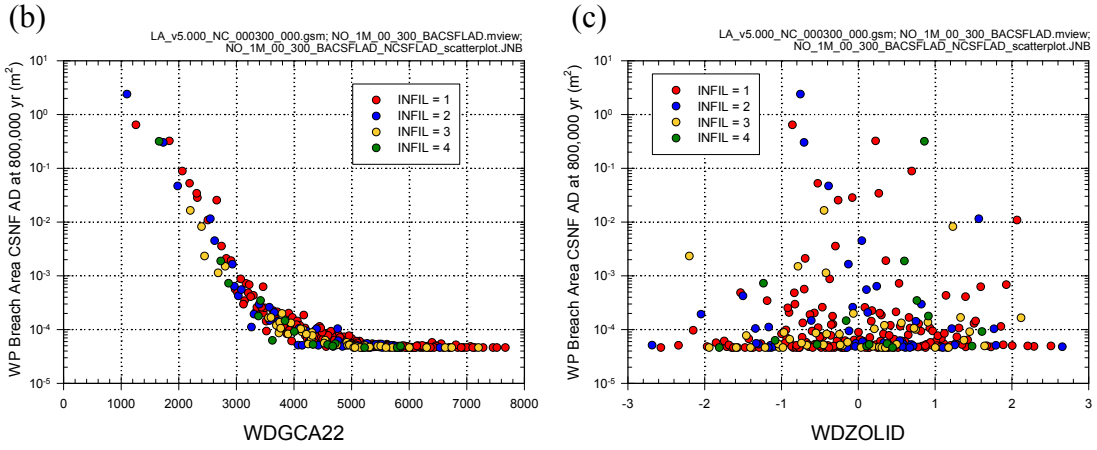

Source: Output DTNs: MO0709TSPAREGS.000 [DIRS 182976]; and MO0709TSPAPLOT.000 [DIRS 183010].

Figure K4.2-7. Stepwise rank regression analyses and selected scatterplots for average breached area on failed CSNF WPs experiencing dripping conditions (*BACSFLAD*) in percolation bin 3 under nominal conditions: (a) Regressions for *BACSFLAD* at 6×10^5, 8×10^5 and 1×10^6 years, and (b, c) Scatterplots for *BACSFLAD* and *NCSFLND* at 8×10^5 years.

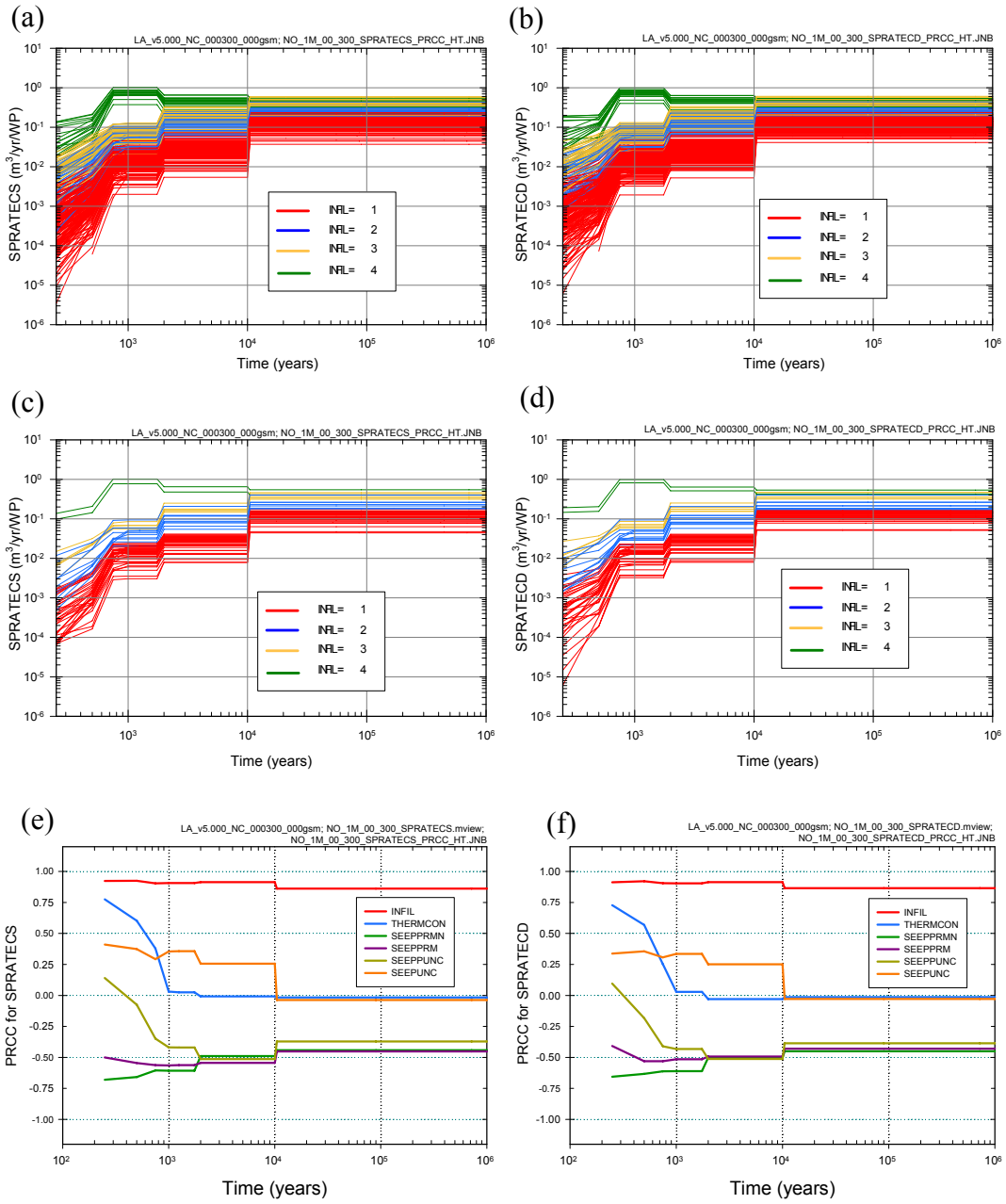

Source: Output DTNs: MO0709TSPAREGS.000 [DIRS 182976]; and MO0709TSPAPLOT.000 [DIRS 183010].

Figure K4.3-1. Time-dependent seepage rates (m^3/yr/WP) into the repository above CSNF WPs (*SPRATECS*) and CDSP WPs (*SPRATECD*) in percolation bin 3 under nominal conditions: (a, b) *SPRATECS* and *SPRATECD* for all (i.e., 300) sample elements, (c, d) *SPRATECS* and *SPRATECD* for first 50 sample elements, and (e, f) PRCCs for *SPRATECS* and *SPRATECD*.

(a)

	SPRATECS: 1K yr			SPRATECS: 50K yr			SPRATECS: 100K yr		
Step[a]	**Variable[b]**	**R^{2c}**	**SRRC[d]**	**Variable**	**R^2**	**SRRC**	**Variable**	**R^2**	**SRRC**
1	INFIL	0.67	0.83	INFIL	0.73	0.86	INFIL	0.68	0.85
2	SEEPPRMN	0.76	-0.28	ALPHAL	0.78	-0.23	ALPHAL	0.73	-0.23
3	ALPHAL	0.82	-0.26	SEEPPRM	0.83	-0.24	SEEPPRMN	0.77	-0.23
4	SEEPPRM	0.85	-0.19	SEEPPRMN	0.87	-0.21	SEEPPRM	0.81	-0.21
5	SEEPUNC	0.87	0.15	SEEPUNC	0.88	0.10	DIFPATHL	0.82	-0.07
6	INRFRCTC	0.88	0.06	DIFPATHL	0.89	-0.05			
7	CORRATSS	0.88	-0.05	INRFRCTC	0.89	0.05			

a: Steps in stepwise rank regression analysis
b: Variables listed in order of selection in stepwise regression
c: Cumulative R^2 value with entry of each variable into regression model
d: Standardized rank regression coefficients (SRRCs) in final regression model

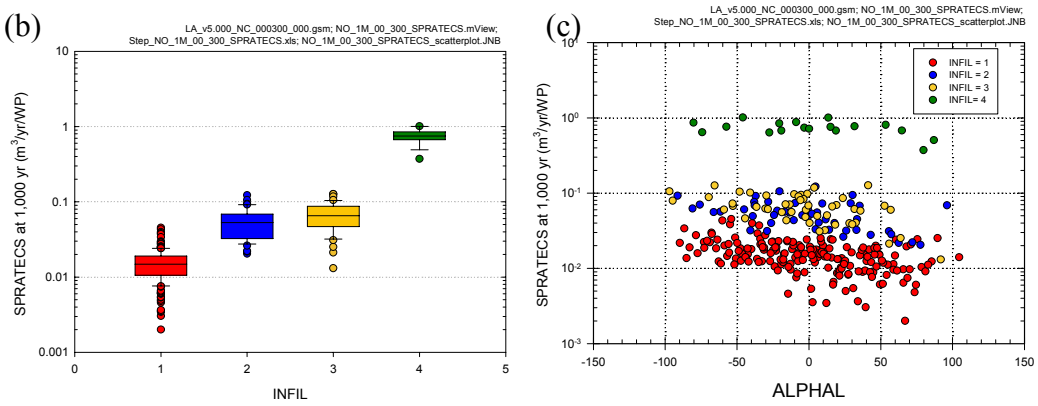

(d)

SEEPPRMN SEEPPRM

Source: Output DTNs: MO0709TSPAREGS.000 [DIRS 182976]; and MO0709TSPAPLOT.000 [DIRS 183010].

Note: In (b), the box extends from 0.25 to 0.75 quantile; lower and upper bar and whisker extend to 0.1 and 0.9 quantile, respectively; dots represent values outside 0.1 to 0.9 quantile range; median indicated by light horizontal line.

Figure K4.3-2. Stepwise rank regression analyses and selected scatterplots for seepage rate (m^3/yr/WP) into the repository above CSNF WPs (*SPRATECS*) in percolation bin 3 under nominal conditions: (a) Regressions for *SPRATECS* at 1000, 5000 and 100,000 years, and (b, c, d, e) Scatterplots for *SPRATECS* at 1000 years.

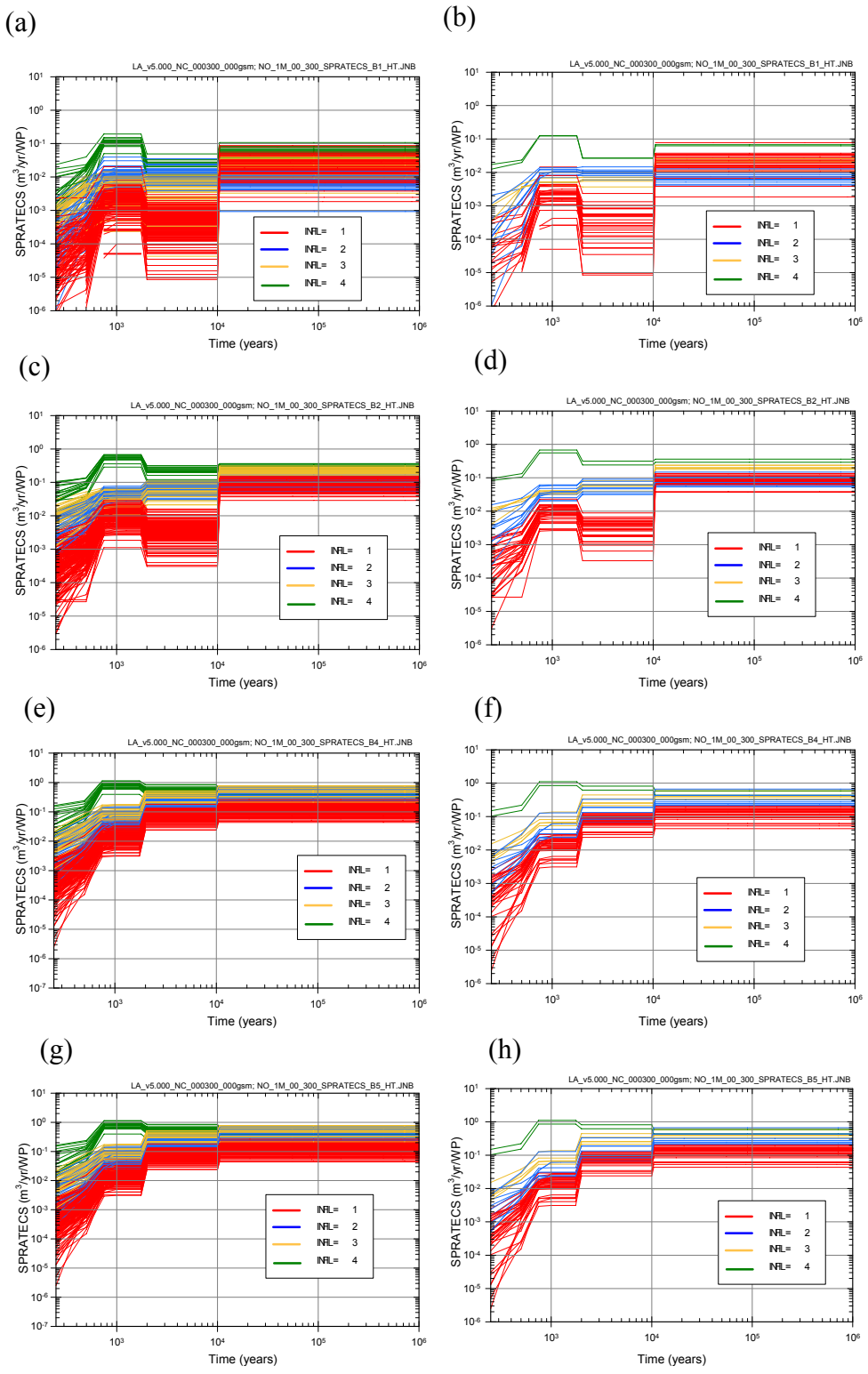

Source: Output DTN MO0709TSPAREGS.000: [DIRS 182976].

Figure K4.3-3. Time-dependent seepage rates (m^3/yr/WP) into the repository above CSNF WPs (*SPRATECS*) in percolation bins 1, 2, 4 and 5 under nominal conditions: (a, c, e, g) *SPRATECS* for all (i.e., 300) sample elements, and (b, d, f, h) *SPRATECS* for first 50 sample elements

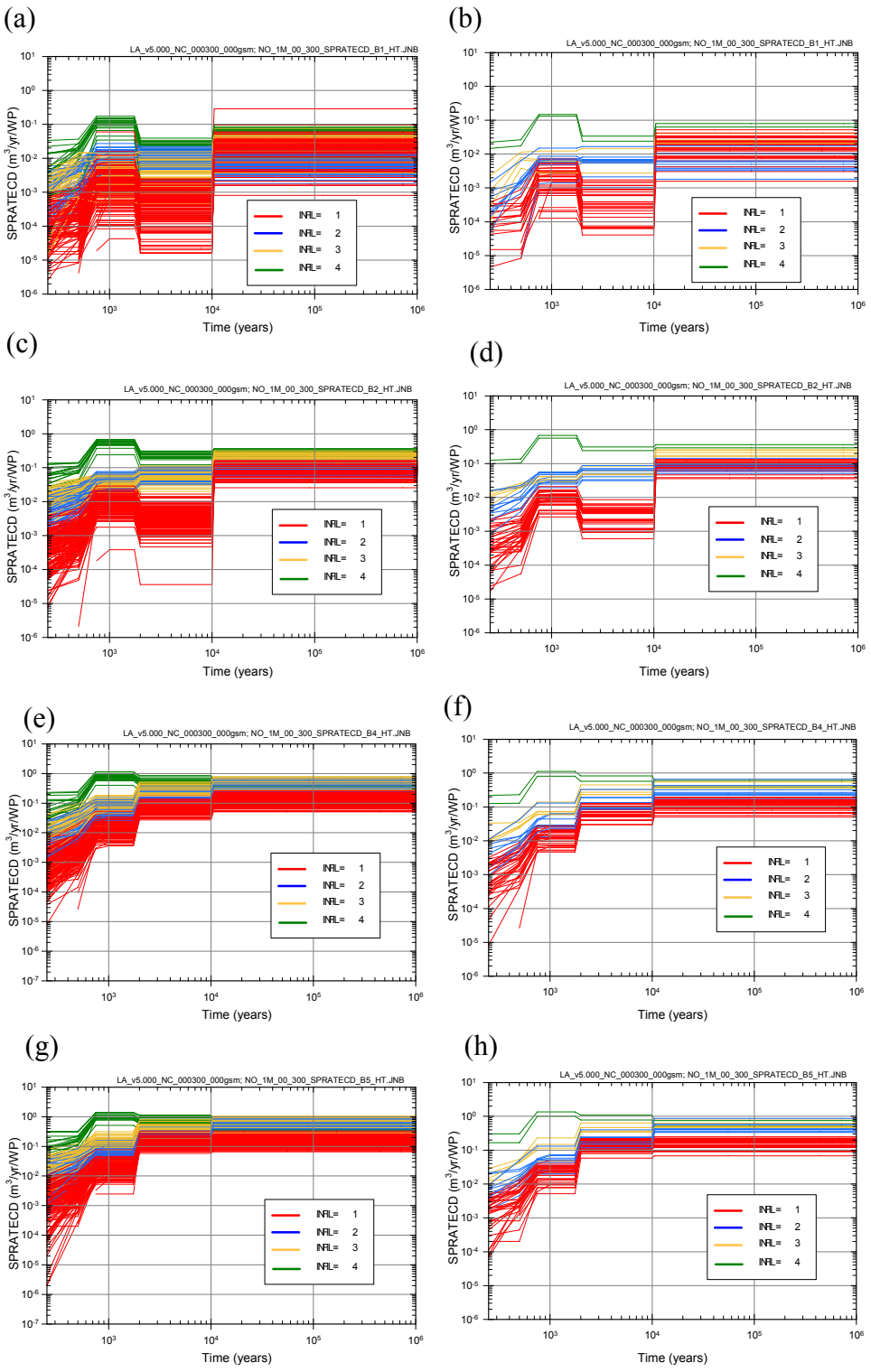

Source: Output DTN: MO0709TSPAREGS.000 [DIRS 182976].

Figure K4.3-4. Time-dependent seepage rates (m^3/yr/WP) into the repository above CDSP WPs (*SPRATECD*) in percolation bins 1, 2, 4 and 5 under nominal conditions: (a, c, e, g) *SPRATECD* for all (i.e., 300) sample elements, and (b, d, f, h) *SPRATECD* for first 50 sample elements

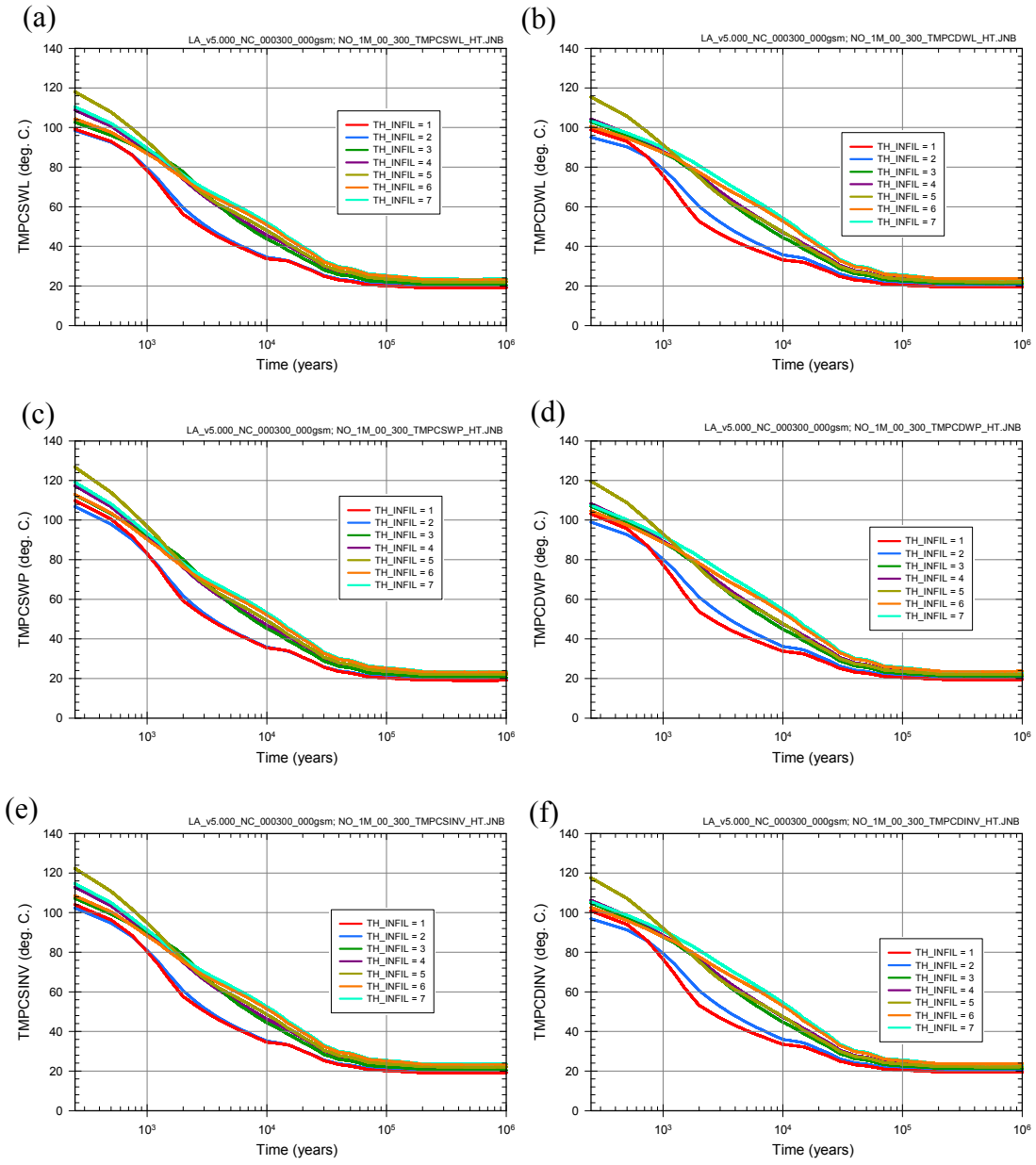

Source: Output DTN: MO0709TSPAREGS.000 [DIRS 182976].

Figure K4.3-5. Time-dependent temperatures in percolation bin 3 under nominal conditions for CSNF WPs at the drift wall (*TMPCSWL*), on the WP (*TMPCSWP*) and in the invert beneath the WP (*TMPCSINV*) and similarly for CDSP WPs at the drift wall (*TMPCDWL*), on the WP (*TMPCDWP*) and in the invert beneath the WP (*TMPCDINV*): (a, c, e) *TMPCSWL*, *TMPCSWP* and *TMPCSINV*, and (b, d, f) *TMPCDWL*, *TMPCDWP* and *TMPCDINV*

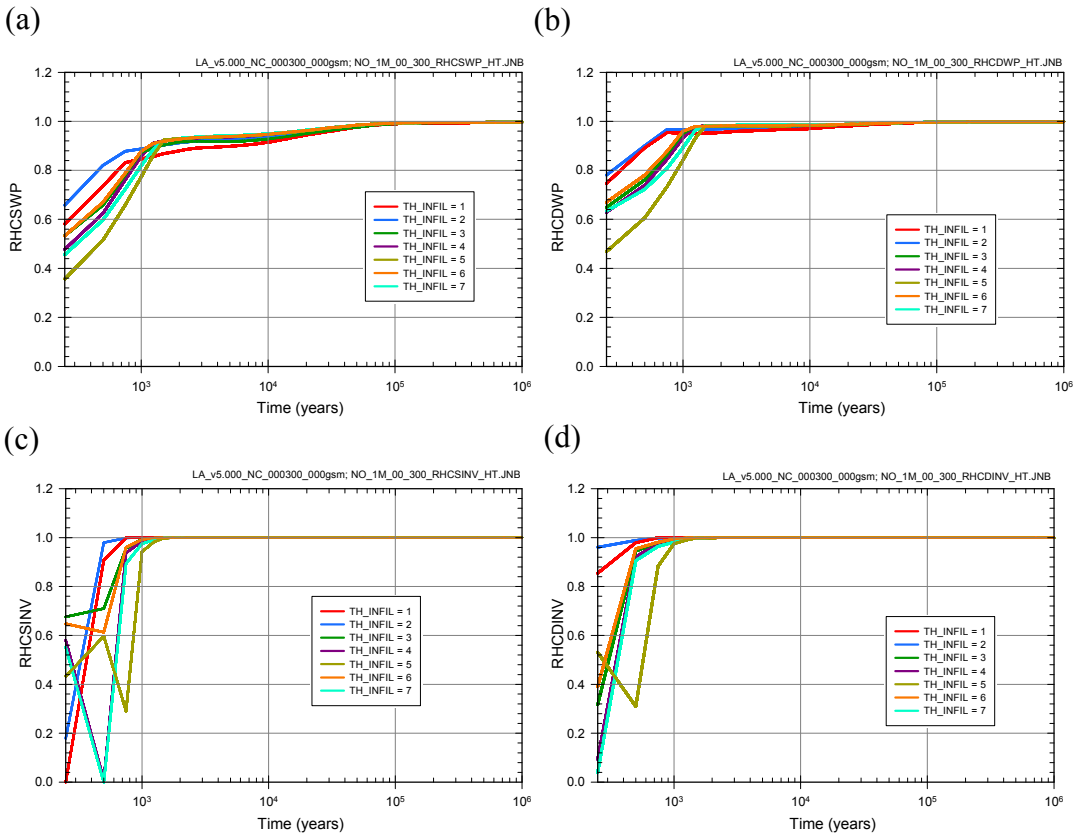

Source: Output DTN: MO0709TSPAREGS.000 [DIRS 182976].

Figure K4.3-6. Time-dependent relative humidities in percolation bin 3 under nominal conditions for CSNF WPs on the WP (*RHCSWP*) and in the invert beneath the WP (*RHCSINV*) and similarly for CDSP WPs on the WP (*RHCDWP*) and in the invert beneath the WP (*RHCDINV*): (a, c) *RHCSWP* and *RHCSINV*, and (b, d) *RHCDWP* and *RHCDINV*

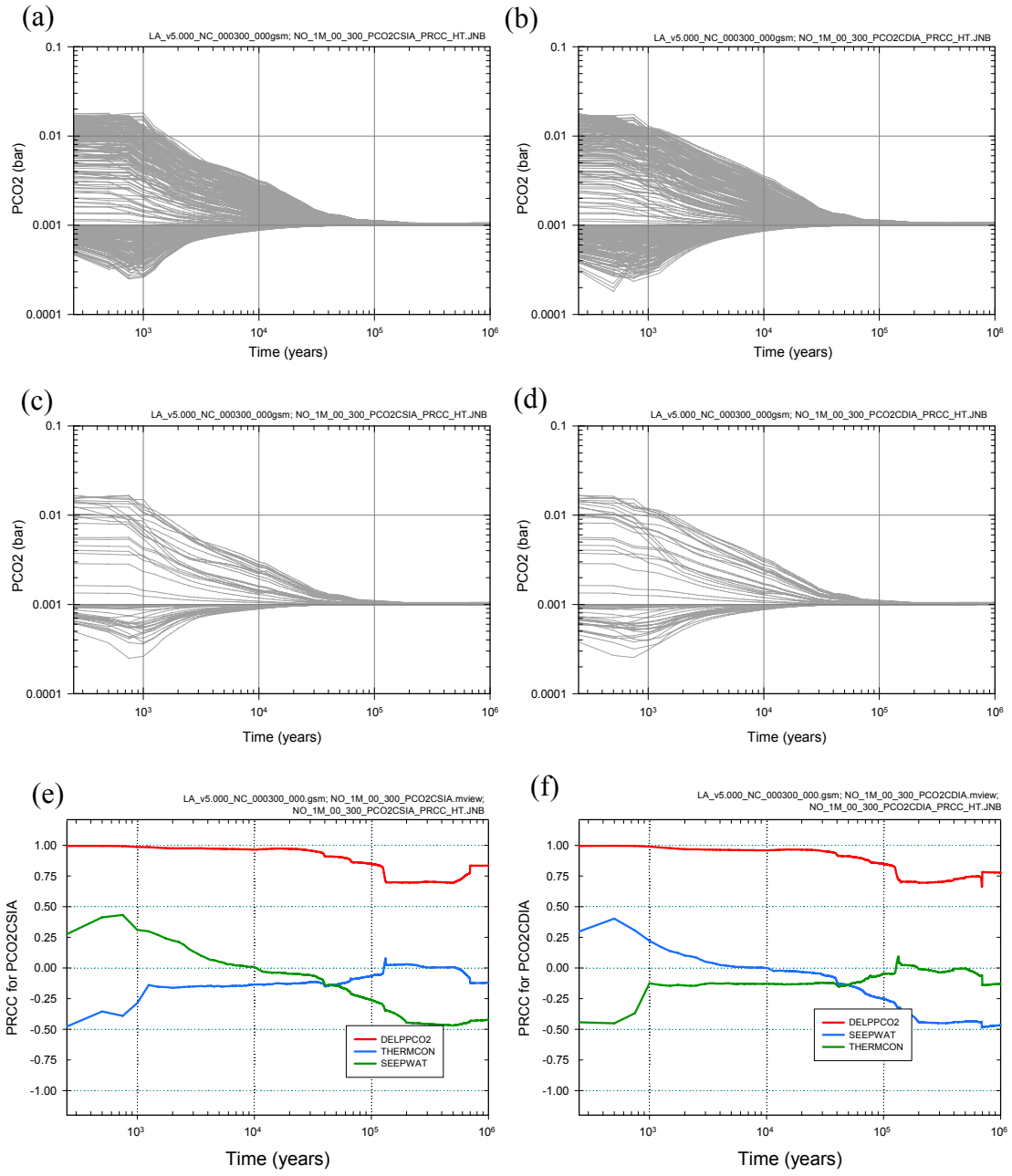

Source: Output DTNs: MO0709TSPAREGS.000 [DIRS 182976]; and MO0709TSPAPLOT.000 [DIRS 183010].

Figure K4.3-7. Time-dependent partial pressures for CO_2 (bars) in the invert for dripping conditions for CSNF WPs (*PCO2CSIA*) and CDSP WPs (*PCO2CDIA*) in percolation bin 3 under nominal conditions: (a, b) *PCO2CSIA* and *PCO2CDIA* for all (i.e., 300) sample elements, (c, d) *PCO2CSIA* and *PCO2CDIA* for first 50 sample elements, and (e, f) PRCCs for *PCO2CSIA* and *PCO2CDIA*

(a)

	PCO2CSIA: 1K yr			PCO2CSIA: 5K yr			PCO2CSIA: 10K yr		
Step[a]	**Variable[b]**	**R^{2c}**	**SRRC[d]**	**Variable**	**R^2**	**SRRC**	**Variable**	**R^2**	**SRRC**
1	DELPPCO2	0.97	0.99	DELPPCO2	0.94	0.97	DELPPCO2	0.92	0.96
2	SEEPWAT	0.97	0.05	WPFLUX	0.94	-0.06	WPFLUX	0.93	-0.06
3	THERMCON	0.98	-0.05	WDDSBEGC	0.94	0.05	WDDSBEGC	0.93	0.05
4				EP1LOWAM	0.94	0.04			

a: Steps in stepwise rank regression analysis
b: Variables listed in order of selection in stepwise regression
c: Cumulative R^2 value with entry of each variable into regression model
d: Standardized rank regression coefficients (SRRCs) in final regression model

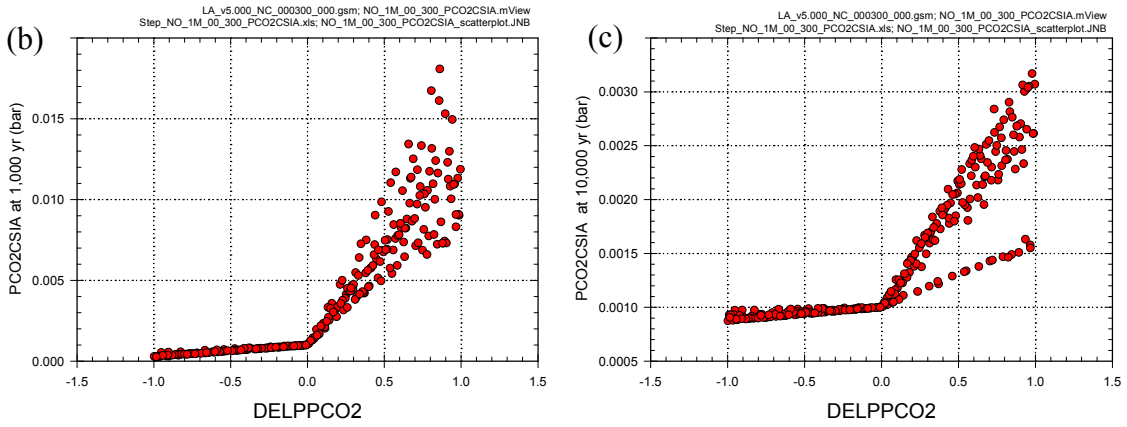

Source: Output DTNs: MO0709TSPAREGS.000 [DIRS 182976]; and MO0709TSPAPLOT.000 [DIRS 183010].

Figure K4.3-8. Stepwise rank regression analyses and selected scatterplots for CO_2 partial pressure (bars) in the invert under dripping conditions for CSNF WPs (*PCO2CSIA*) in percolation bin 3 under nominal conditions: (a) Regressions for *PCO2CSIA* at 1000, 5000 and 10,000 years, and (b, c) Scatterplots for *PCO2CSIA* at 1000 and 10,000 years.

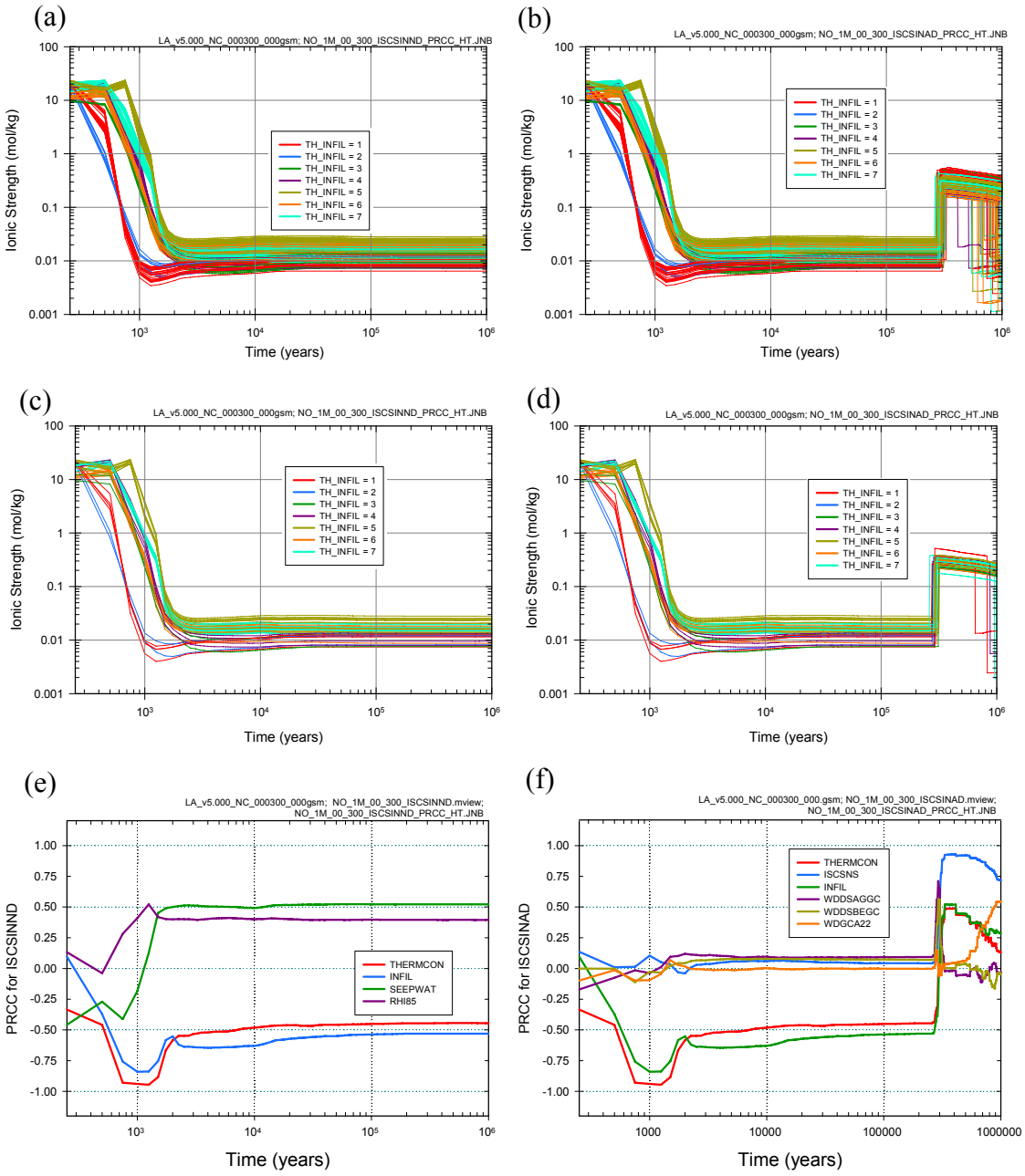

Source: Output DTNs: MO0709TSPAREGS.000 [DIRS 182976]; and MO0709TSPAPLOT.000 [DIRS 183010].

Figure K4.3-9. Time-dependent ionic strength (mol/kg) in the invert for CSNF WPs experiencing nondripping conditions (*ISCSINND*) and dripping conditions (*ISCSINAD*) in percolation bin 3 under nominal conditions: (a, b) *ISCSINND* and *ISCSINAD* for all (i.e., 300) sample elements, (c, d) *ISCSINND* and *ISCSINAD* for first 50 sample elements, and (e, f) PRCCs for *ISCSINND* and *ISCSINAD*.

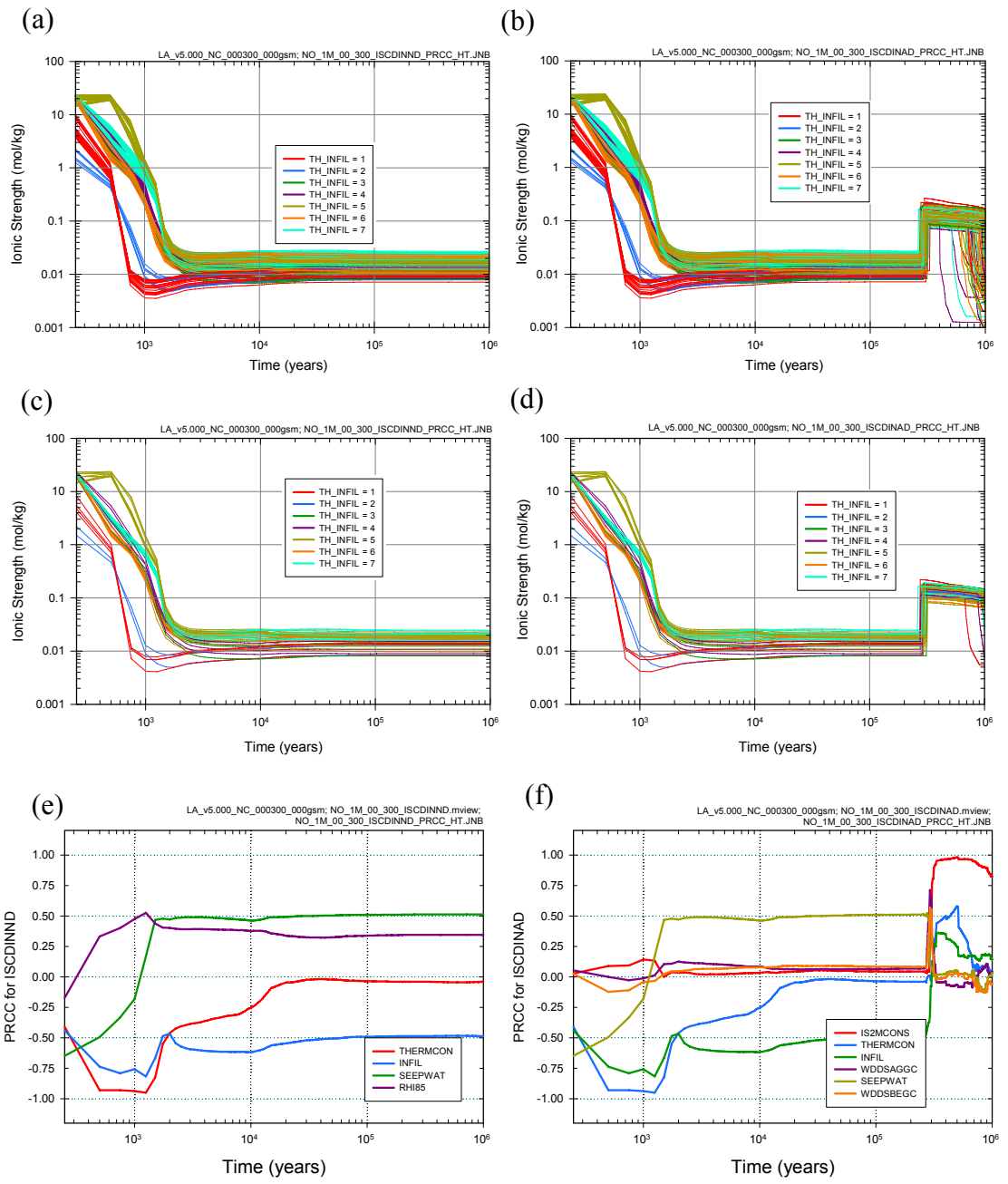

Source: Output DTNs: MO0709TSPAREGS.000 [DIRS 182976]; and MO0709TSPAPLOT.000 [DIRS 183010].

Figure K4.3-10. Time-dependent ionic strength (mol/kg) in the invert for CDSP WPs experiencing nondripping conditions (*ISCDINND*) and dripping conditions (*ISCDINAD*) in percolation bin 3 under nominal conditions: (a, b) *ISCDINND* and *ISCDINAD* for all (i.e., 300) sample elements, (c, d) *ISCDINND* and *ISCDINAD* for first 50 sample elements, and (e, f) PRCCs for *ISCDINND* and *ISCDINAD*.

(a)

	ISCSINAD: 1K yr			ISCSINAD: 50K yr			ISCSINAD: 500K yr		
Step[a]	**Variable[b]**	**R^{2c}**	**SRRC[d]**	**Variable**	**R^2**	**SRRC**	**Variable**	**R^2**	**SRRC**
1	THERMCON	0.65	-0.84	INFIL	0.21	-0.46	ISCSNS	0.80	0.90
2	INFIL	0.90	-0.49	THERMCON	0.40	-0.42	INFIL	0.85	0.23
3	RHI85	0.92	0.14	SEEPWAT	0.53	0.38	THERMCON	0.88	0.16
4	SEEPWAT	0.92	-0.06	RHI85	0.60	0.27	RUBMAXL	0.88	-0.05
5	DELPPCO2	0.92	0.05						
6	KDSNSMEC	0.92	0.04						

a: Steps in stepwise rank regression analysis
b: Variables listed in order of selection in stepwise regression
c: Cumulative R^2 value with entry of each variable into regression model
d: Standardized rank regression coefficients (SRRCs) in final regression model

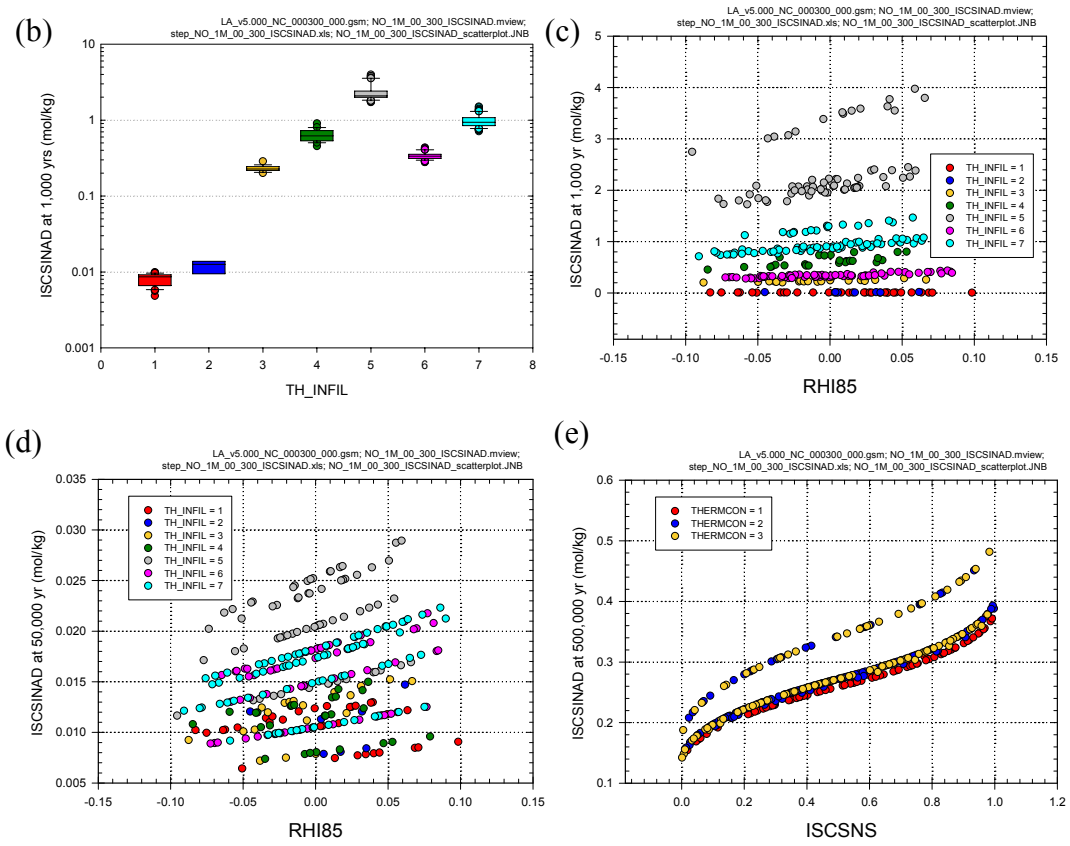

Source: Output DTNs: MO0709TSPAREGS.000 [DIRS 182976]; and MO0709TSPAPLOT.000 [DIRS 183010].

Note: In (b), the box extends from 0.25 to 0.75 quantile; lower and upper bar and whisker extend to 0.1 and 0.9 quantile, respectively; dots represent values outside 0.1 to 0.9 quantile range; median indicated by light horizontal line.

Figure K4.3-11. Stepwise rank regression analyses and selected scatterplots for ionic strength (mol/kg) in the invert for CSNF WPs experiencing dripping conditions (*ISCSINAD*) in percolation bin 3 under nominal conditions: (a) Regressions for *ISCSINAD* at 1000, 50,000 and 500,000 years, and (b, c, d) Scatterplots for *ISCSINAD* at 1000, 50,000 and 500,000 years.

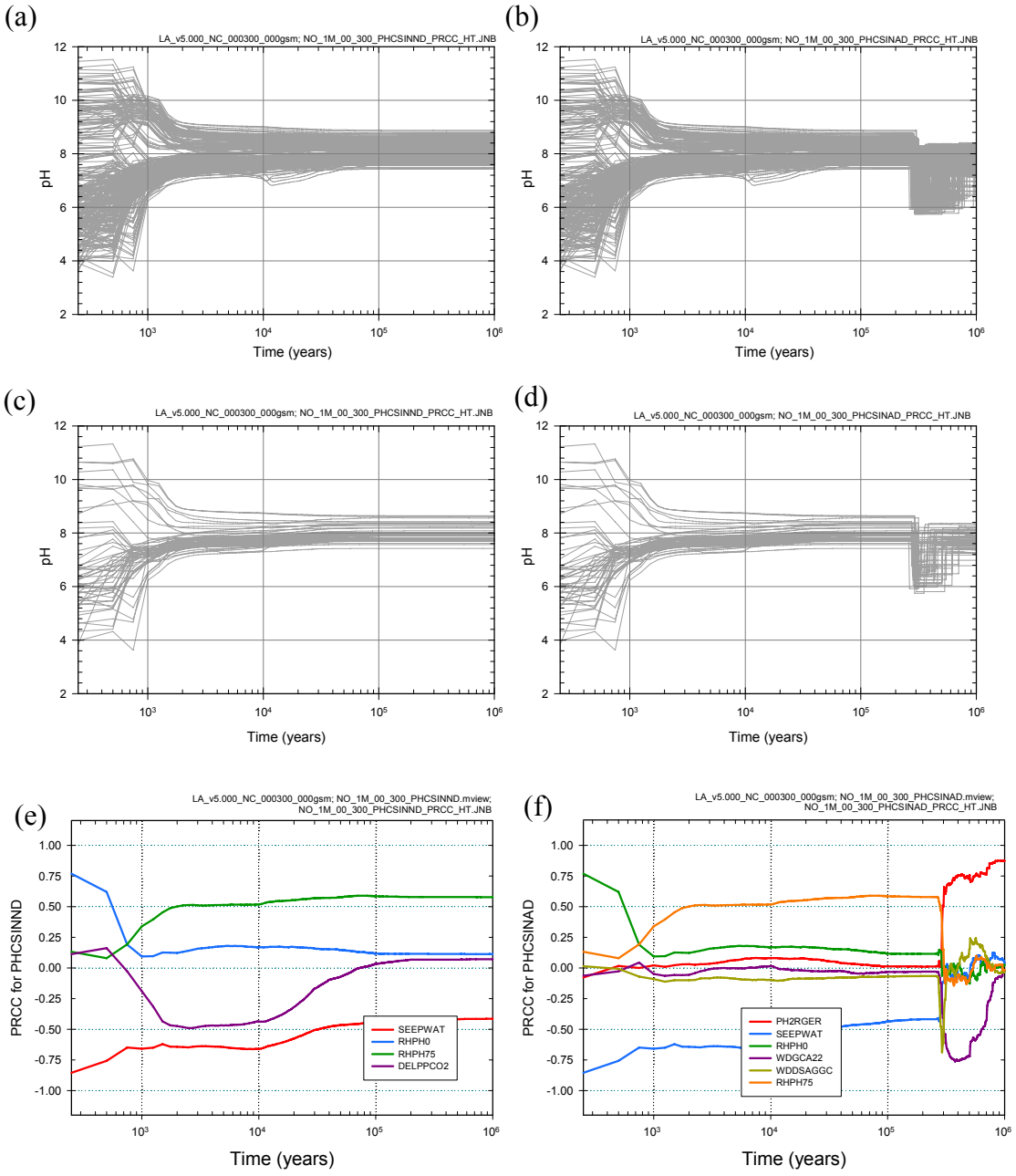

Source: Output DTNs: MO0709TSPAREGS.000 [DIRS 182976]; and MO0709TSPAPLOT.000 [DIRS 183010].

Figure K4.3-12. Time-dependent pH in the invert for CSNF WPs experiencing nondripping conditions (*PHCSINND*) and dripping conditions (*PHCSINAD*) in percolation bin 3 under nominal conditions: (a, b) *PHCSINND* and *PHCSINAD* for all (i.e., 300) sample elements, (c, d) *PHCSINND* and *PHCSINAD* for first 50 sample elements, and (e, f) PRCCs for *PHCSINND* and *PHCSINAD*.

(a)

	PHCSINND: 1K yr			PHCSINND: 50K yr			PHCSINND: 500K yr		
Step[a]	**Variable[b]**	**R^{2c}**	**SRRC[d]**	**Variable**	**R^2**	**SRRC**	**Variable**	**R^2**	**SRRC**
1	SEEPWAT	0.39	-0.61	RHPH75	0.27	0.51	RHPH75	0.28	0.51
2	RHPH75	0.44	0.21	SEEPWAT	0.42	-0.40	SEEPWAT	0.40	-0.36
3	DELPPCO2	0.46	-0.16	RHPH65	0.43	-0.13	RHPH65	0.41	-0.12
4	THERMCON	0.47	0.11	CPUCOLWF	0.45	-0.12			

(b)

	PHCSINAD: 1K yr			PHCSINAD: 50K yr			PHCSINAD: 500K yr		
Step[a]	**Variable[b]**	**R^{2c}**	**SRRC[d]**	**Variable**	**R^2**	**SRRC**	**Variable**	**R^2**	**SRRC**
1	SEEPWAT	0.39	-0.61	RHPH75	0.27	0.51	PH2RGER	0.29	0.58
2	RHPH75	0.44	0.21	SEEPWAT	0.42	-0.40	WDGCA22	0.60	-0.59
3	DELPPCO2	0.46	-0.16	RHPH65	0.43	-0.13	THERMCON	0.63	-0.18
4	THERMCON	0.47	0.11	CPUCOLWF	0.45	-0.12	WDZOLID	0.65	0.16
5							INFIL	0.67	-0.13
6							WDNSCC	0.68	-0.11
7							INRFRCI	0.69	0.09
8							WDGCUA22	0.70	0.08

a: Steps in stepwise rank regression analysis
b: Variables listed in order of selection in stepwise regression
c: Cumulative R^2 value with entry of each variable into regression model
d: Standardized rank regression coefficients (SRRCs) in final regression model

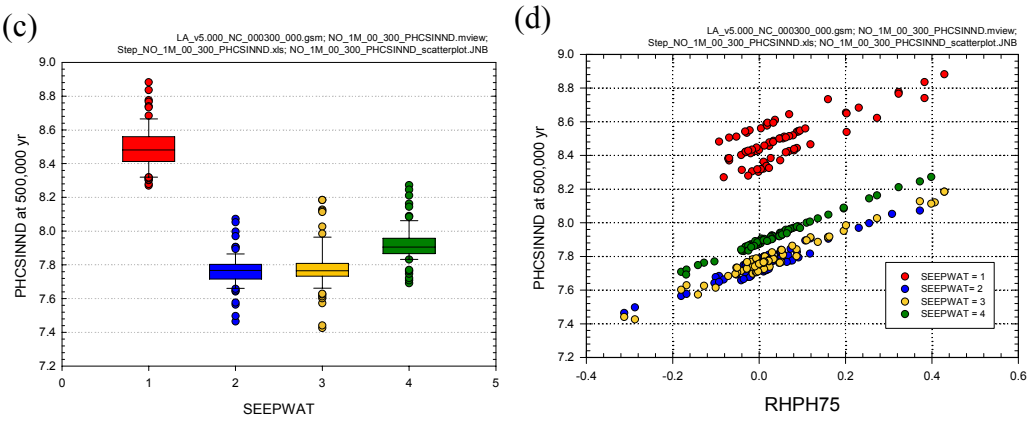

Source: Output DTNs: MO0709TSPAREGS.000 [DIRS 182976]; and MO0709TSPAPLOT.000 [DIRS 183010].

NOTE: In (c, e, g), the box extends from 0.25 to 0.75 quantile; lower and upper bar and whisker extend to 0.1 and 0.9 quantile, respectively; dots represent values outside 0.1 to 0.9 quantile range; median indicated by light horizontal line.

Figure K4.3-13. Stepwise rank regression analyses and selected scatterplots for pH in the invert for CSNF WPs experiencing nondripping conditions (*PHCSINND*) and dripping conditions (*PHCSINAD*) in percolation bin 3 under nominal conditions: (a, b) Regressions for *PHCSINND* and *PHCSINAD* at 1000, 50,000 and 500,000 years, and (c-j) Scatterplots for *PHCSINND* and *PHCSINAD* at 1000, 50,000 and 500,000 years.

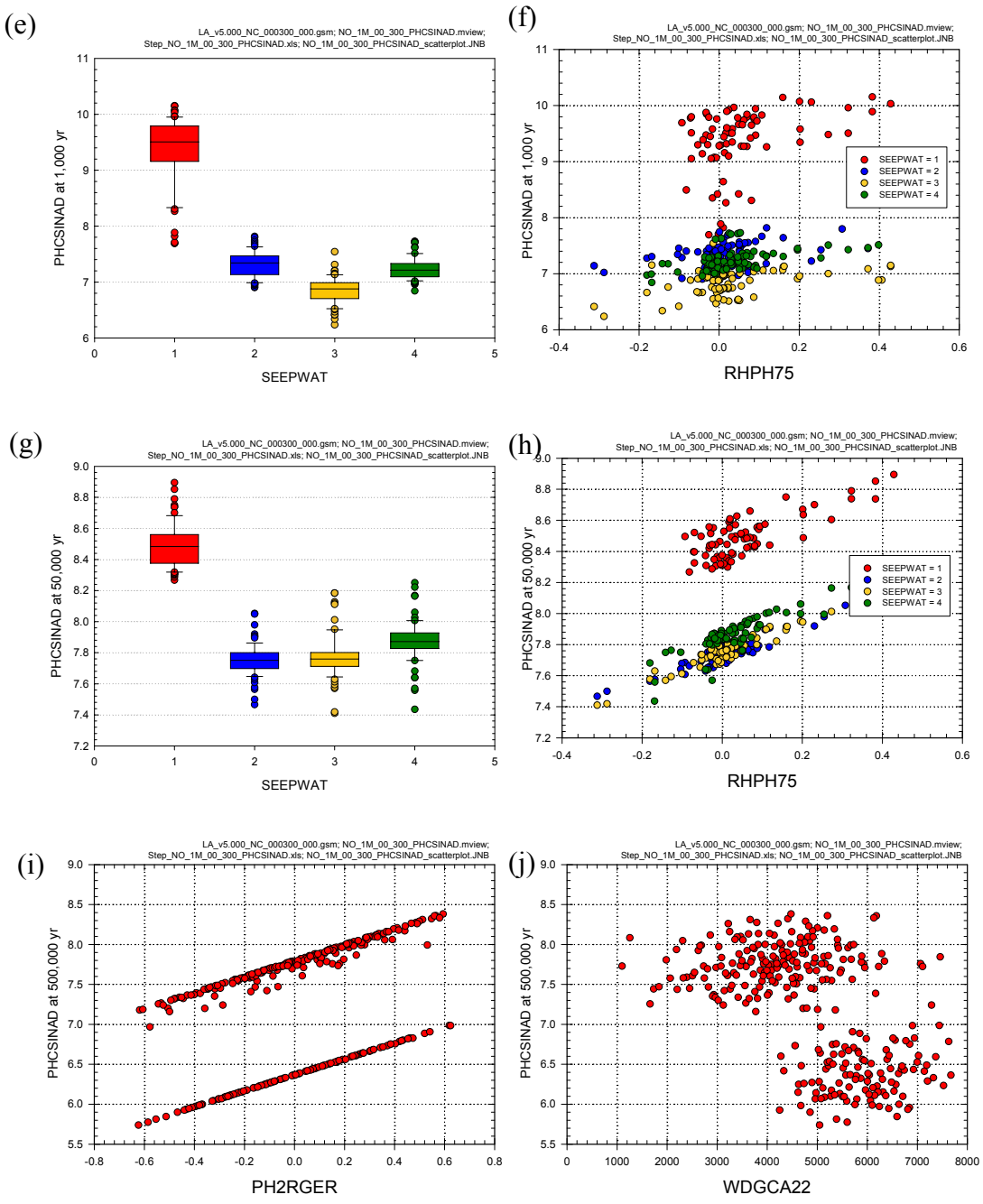

Source: Output DTNs: MO0709TSPAREGS.000 [DIRS 182976]; and MO0709TSPAPLOT.000 [DIRS 183010].

NOTE: In (c, e, g), the box extends from 0.25 to 0.75 quantile; lower and upper bar and whisker extend to 0.1 and 0.9 quantile, respectively; dots represent values outside 0.1 to 0.9 quantile range; median indicated by light horizontal line.

Figure K4.3-13. Stepwise rank regression analyses and selected scatterplots for pH in the invert for CSNF WPs experiencing nondripping conditions (*PHCSINND*) and dripping conditions (*PHCSINAD*) in percolation bin 3 under nominal conditions: (a, b) Regressions for *PHCSINND* and *PHCSINAD* at 1000, 50,000 and 500,000 years, and (c-j) Scatterplots for *PHCSINND* and *PHCSINAD* at 1000, 50,000 and 500,000 years (Continued).

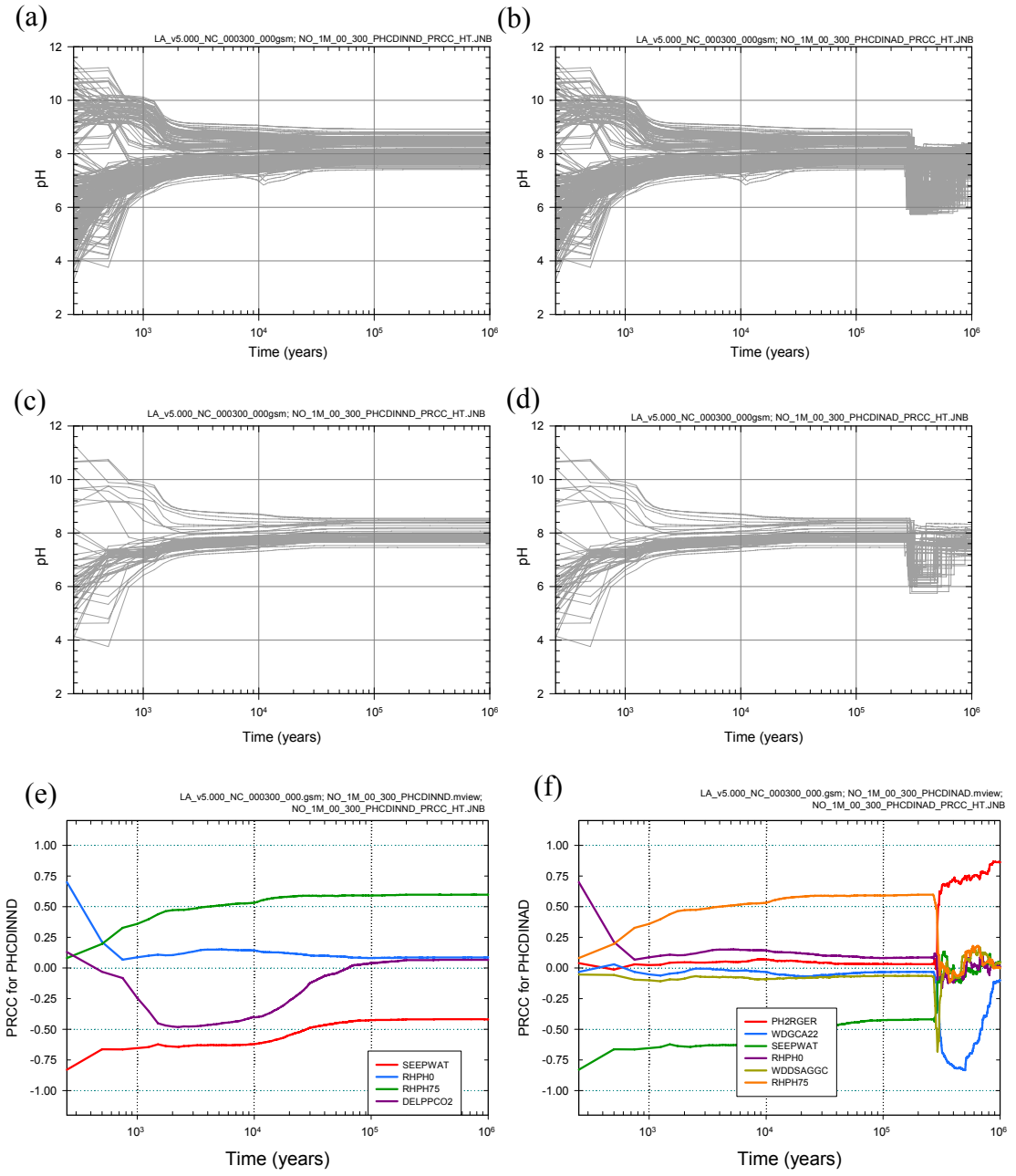

Source: Output DTNs: MO0709TSPAREGS.000 [DIRS 182976]; and MO0709TSPAPLOT.000 [DIRS 183010].

Figure K4.3-14. Time-dependent pH in the invert for CDSP WPs experiencing nondripping conditions (*PHCDINND*) and dripping conditions (*PHCDINAD*) in percolation bin 3 under nominal conditions: (a, b) *PHCDINND* and *PHCDINAD* for all (i.e., 300) sample elements, (c, d) *PHCDINND* and *PHCDINAD* for first 50 sample elements, and (e, f) PRCCS for *PHCDINND* and *PHCDINAD*.

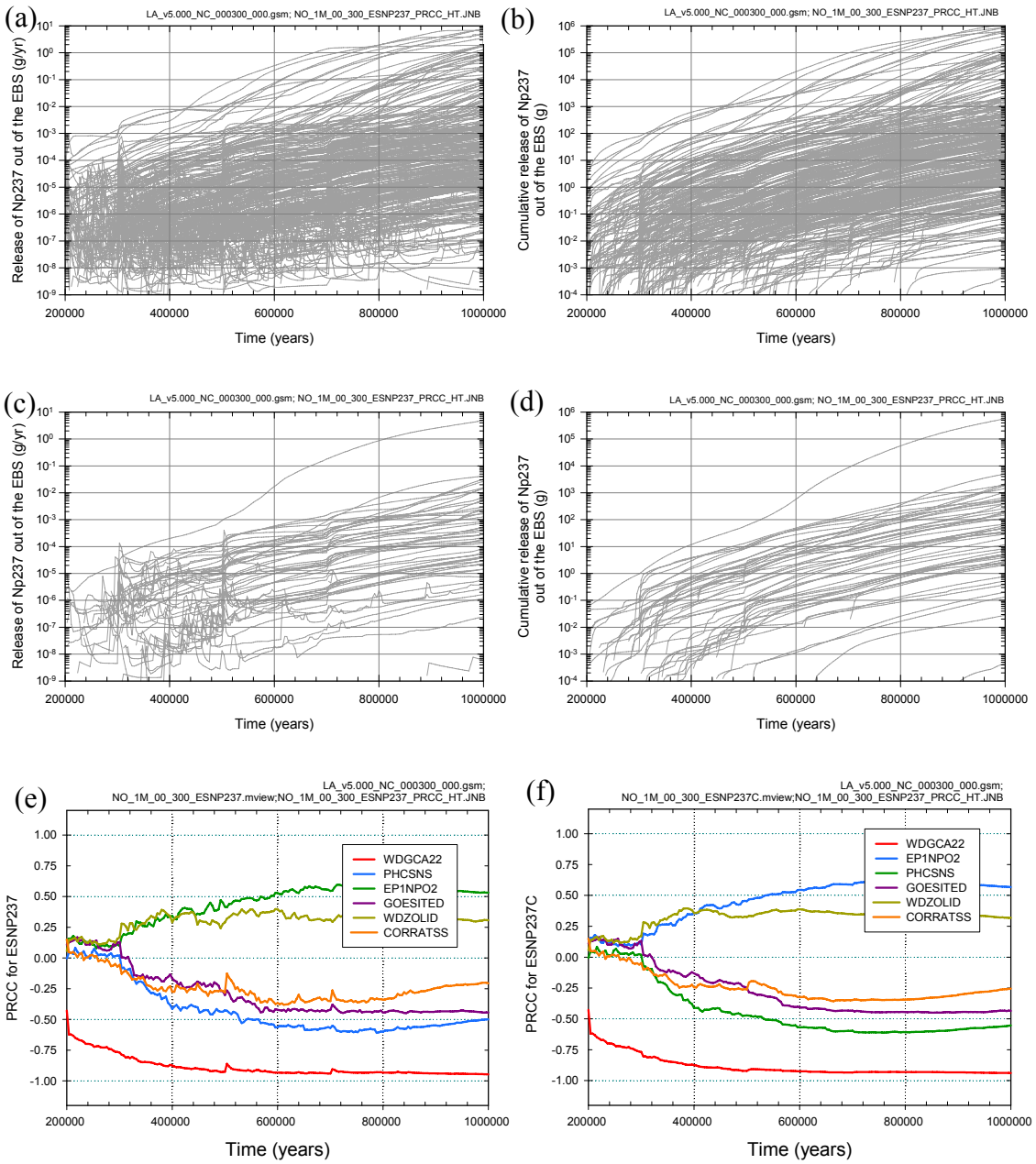

Source: Output DTNs: MO0709TSPAREGS.000 [DIRS 182976]; and MO0709TSPAPLOT.000 [DIRS 183010].

Figure K4.4-1. Time-dependent release rates (*ESNP237*, g/yr) and cumulative (i.e., integrated) releases (*ESNP237C*, g) for movement of dissolved ^{237}Np from the EBS to the UZ under nominal conditions: (a, b) *ESNP237* and *ESNP237C* for all (i.e., 300) sample elements, (c, d) *ESNP237* and *ESNP237C* for first 50 sample elements, and (e, f) PRCCs for *ESNP237* and *ESNP237C*.

(a)

	ESNP237: 400K yr			ESNP237: 600K yr			ESNP237: 800K yr		
Step[a]	Variable[b]	R^{2c}	SRRC[d]	Variable	R^2	SRRC	Variable	R^2	SRRC
1	WDGCA22	0.71	-0.83	WDGCA22	0.74	-0.83	WDGCA22	0.74	-0.83
2	PHCSNS	0.74	-0.16	PHCSNS	0.78	-0.21	EP1NPO2	0.79	0.21
3	WDZOLID	0.76	0.14	EP1NPO2	0.82	0.18	PHCSNS	0.82	-0.21
4	EP1NPO2	0.78	0.13	WDZOLID	0.84	0.12	WDZOLID	0.84	0.11
5	WDNSCC	0.79	-0.11	CORRATSS	0.85	-0.11	EP1LOWNU	0.85	0.09
6	THERMCON	0.80	-0.12	GOESITED	0.86	-0.11	GOESITED	0.87	-0.12
7	SCCTHR	0.81	-0.10	INFIL	0.87	-0.10	CORRATSS	0.87	-0.09
8	INFIL	0.82	-0.09	THERMCON	0.88	-0.10	INFIL	0.88	-0.10
9	WDGCUA22	0.82	0.07	EP1LOWNU	0.89	0.07	SCCTHR	0.89	-0.10
10	CORRATSS	0.83	-0.07	WDNSCC	0.89	-0.08	HFOSA	0.90	-0.09
11				HFOSA	0.90	-0.07	HFOSITED	0.90	-0.07
12				SCCTHR	0.90	-0.08	THERMCON	0.91	-0.07
13				WDGCUA22	0.91	0.07	GOERELAB	0.91	0.08
14				CR2O3SA	0.91	0.06	WDGCUA22	0.91	0.07
15				GOERELAB	0.91	0.05	WDNSCC	0.92	-0.06
16				HFOSITED	0.92	-0.05	DTDRHUNC	0.92	0.05

(b)

	ESNP237C: 400K yr			ESNP237C: 600K yr			ESNP237C: 800K yr		
Step[a]	Variable[b]	R^{2c}	SRRC[d]	Variable	R^2	SRRC	Variable	R^2	SRRC
1	WDGCA22	0.70	-0.82	WDGCA22	0.73	-0.82	WDGCA22	0.74	-0.82
2	PHCSNS	0.74	-0.16	PHCSNS	0.78	-0.22	PHCSNS	0.79	-0.22
3	WDZOLID	0.77	0.16	EP1NPO2	0.82	0.20	EP1NPO2	0.83	0.22
4	EP1NPO2	0.78	0.14	WDZOLID	0.84	0.12	WDZOLID	0.84	0.10
5	THERMCON	0.80	-0.12	CORRATSS	0.85	-0.10	GOESITED	0.86	-0.12
6	WDNSCC	0.81	-0.10	INFIL	0.86	-0.11	CORRATSS	0.87	-0.10
7	INFIL	0.82	-0.10	THERMCON	0.87	-0.10	EP1LOWNU	0.88	0.08
8	SCCTHR	0.83	-0.10	GOESITED	0.88	-0.10	INFIL	0.89	-0.10
9	WDGCUA22	0.83	0.07	WDNSCC	0.89	-0.07	SCCTHR	0.89	-0.10
10				SCCTHR	0.89	-0.08	HFOSA	0.90	-0.08
11				WDGCUA22	0.90	0.06	THERMCON	0.90	-0.07
12				HFOSA	0.90	-0.06	WDGCUA22	0.91	0.07
13				EP1LOWNU	0.90	0.06	WDNSCC	0.91	-0.07
14							GOERELAB	0.92	0.07
15							HFOSITED	0.92	-0.06
16							DTDRHUNC	0.92	0.05

a: Steps in stepwise rank regression analysis
b: Variables listed in order of selection in stepwise regression
c: Cumulative R^2 value with entry of each variable into regression model
d: Standardized rank regression coefficients (SRRCs) in final regression model

Source: Output DTNs: MO0709TSPAREGS.000 [DIRS 182976]; and MO0709TSPAPLOT.000 [DIRS 183010].

Figure K4.4-2. Stepwise rank regression analyses and selected scatterplots for release rates (*ESNP237*, g/yr) and cumulative (i.e., integrated) releases (*ESNP237C*, g) for movement of dissolved ^{237}Np from the EBS to the UZ under nominal conditions: (a, b) Regressions for *ESNP237* and *ESNP237C* at 400,000, 600,000 and 800,000 years, and (c-h) Scatterplots for *ESNP237* and *ESNP237C* at 800,000 years.

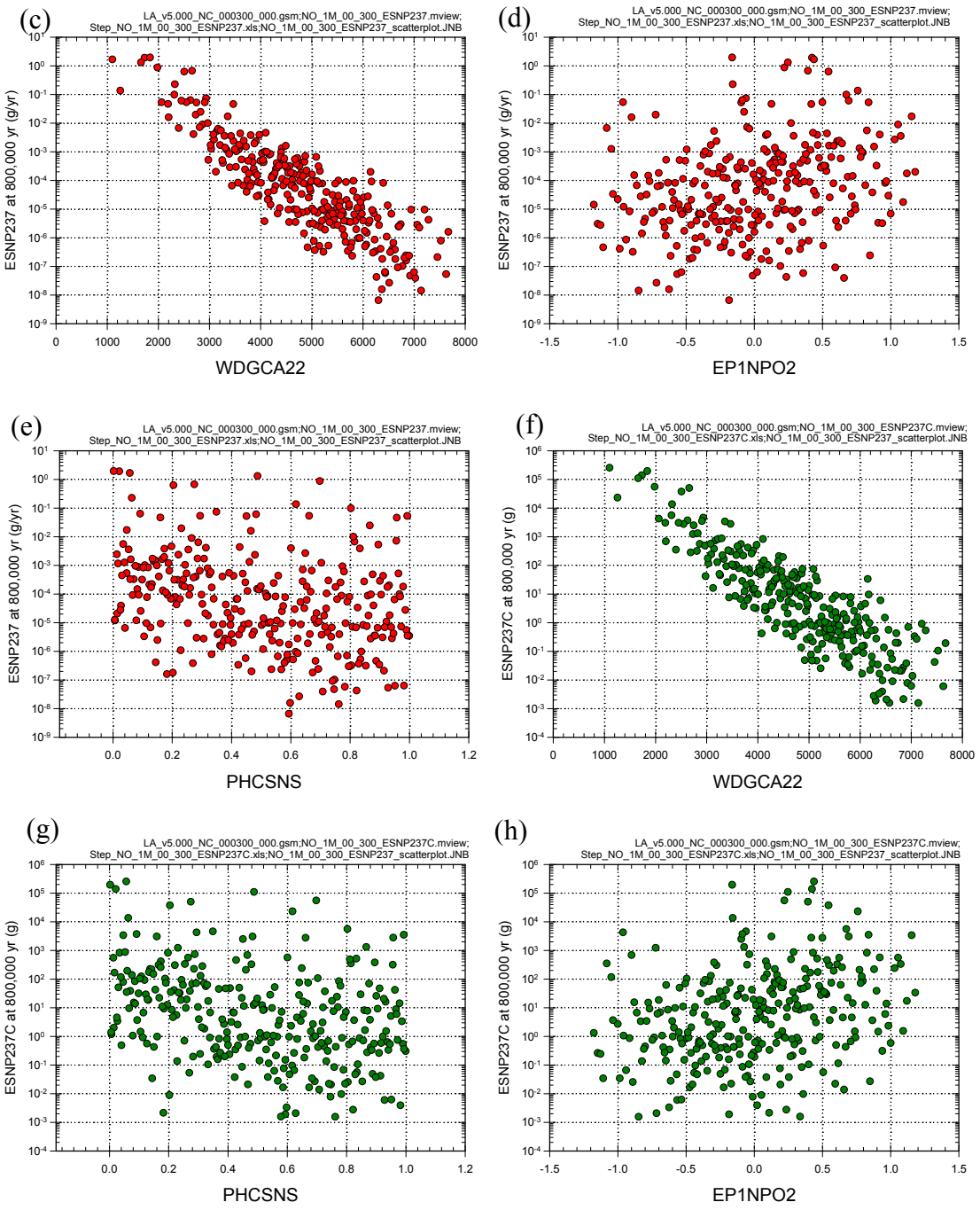

Source: Output DTNs: MO0709TSPAREGS.000 [DIRS 182976]; and MO0709TSPAPLOT.000 [DIRS 183010].

Figure K4.4-2. Stepwise rank regression analyses and selected scatterplots for release rates (*ESNP237*, g/yr) and cumulative (i.e., integrated) releases (*ESNP237C*, g) for movement of dissolved ^{237}Np from the EBS to the UZ under nominal conditions: (a, b) Regressions for *ESNP237* and *ESNP237C* at 400,000, 600,000 and 800,000 years, and (c-h) Scatterplots for *ESNP237* and *ESNP237C* at 800,000 Years (continued).

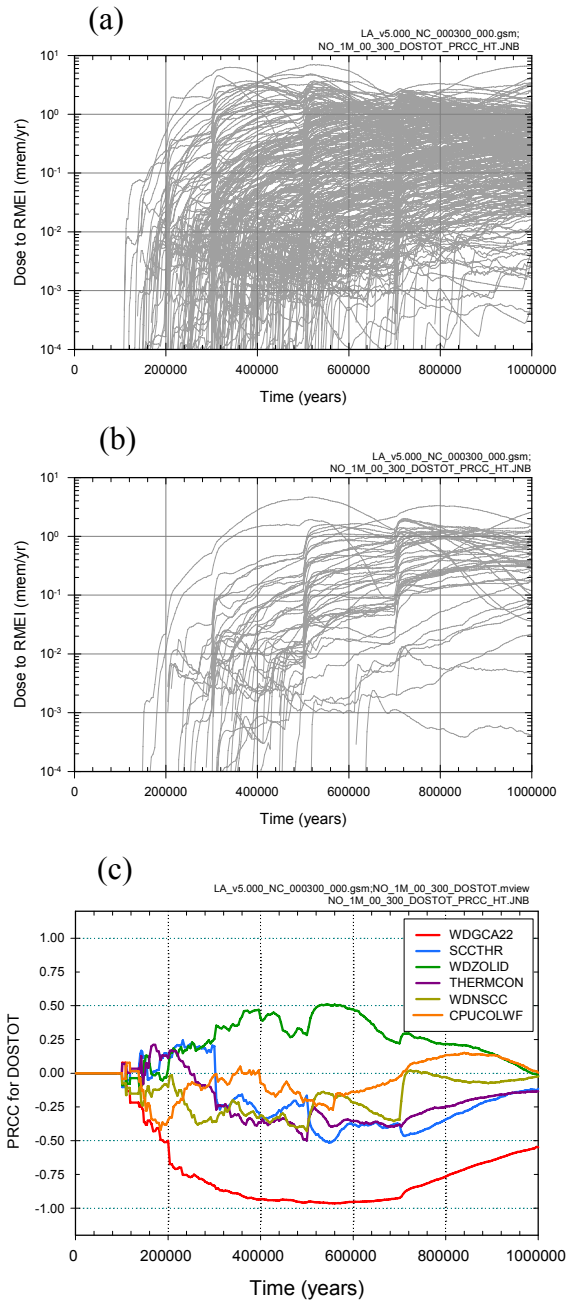

Source: Output DTNs: MO0709TSPAREGS.000 [DIRS 182976]; and MO0709TSPAPLOT.000 [DIRS 183010].

Figure K4.5-1. Dose to RMEI (*DOSTOT*, mrem/yr) for all radioactive species under nominal conditions: (a) *DOSTOT* for all (i.e., 300) sample elements, (b) *DOSTOT* for first 50 sample elements, and (c) PRCCs for *DOSTOT*.

(a)

	DOSTOT: 400K yr			DOSTOT: 600K yr			DOSTOT: 800K yr		
Step[a]	**Variable[b]**	**R^{2c}**	**SRRC[d]**	**Variable**	**R^2**	**SRRC**	**Variable**	**R^2**	**SRRC**
1	WDGCA22	0.77	-0.90	WDGCA22	0.84	-0.94	WDGCA22	0.60	-0.77
2	WDZOLID	0.80	0.16	WDZOLID	0.87	0.14	WDZOLID	0.62	0.16
3	WDNSCC	0.82	-0.12	THERMCON	0.88	-0.10	MICI129	0.63	0.11
4	THERMCON	0.83	-0.12	INFIL	0.89	-0.11	SZWBNDAL	0.65	-0.11
5	INFIL	0.84	-0.10	SCCTHR	0.90	-0.09	SCCTHR	0.65	-0.10
6	SCCTHR	0.85	-0.08	CORRATSS	0.90	-0.07			
7	WDGCUA22	0.85	0.07	WDNSCC	0.91	-0.08			
8	UZRCOL	0.86	-0.07	WDGCUA22	0.91	0.08			
9	CORRATSS	0.86	-0.06	MICTC99	0.92	0.07			
10				DTDRHUNC	0.92	0.05			
11				CSNFMASS	0.92	0.05			

a: Steps in stepwise rank regression analysis
b: Variables listed in order of selection in stepwise regression
c: Cumulative R^2 value with entry of each variable into regression model
d: Standardized rank regression coefficients (SRRCs) in final regression model

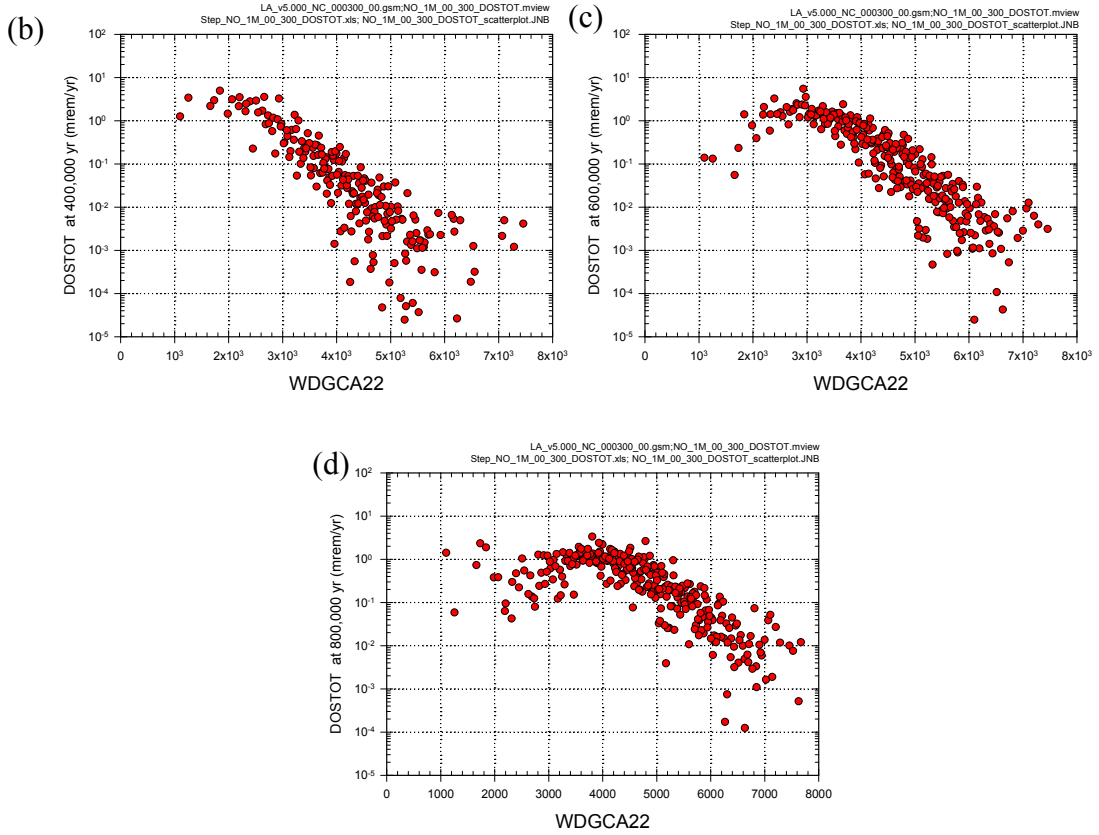

Source: Output DTNs: MO0709TSPAREGS.000 [DIRS 182976]; and MO0709TSPAPLOT.000 [DIRS 183010].

Figure K4.5-2. Stepwise rank regression analyses and selected scatterplots for dose to RMEI (*DOSTOT*, mrem/yr) for all radioactive species under nominal conditions: (a) Regressions for *DOSTOT* at 400,000, 600,000 and 800,000 years, and (b,c,d) Scatterplots for *DOSTOT* at 400,000, 600,000 and 800,000 years.

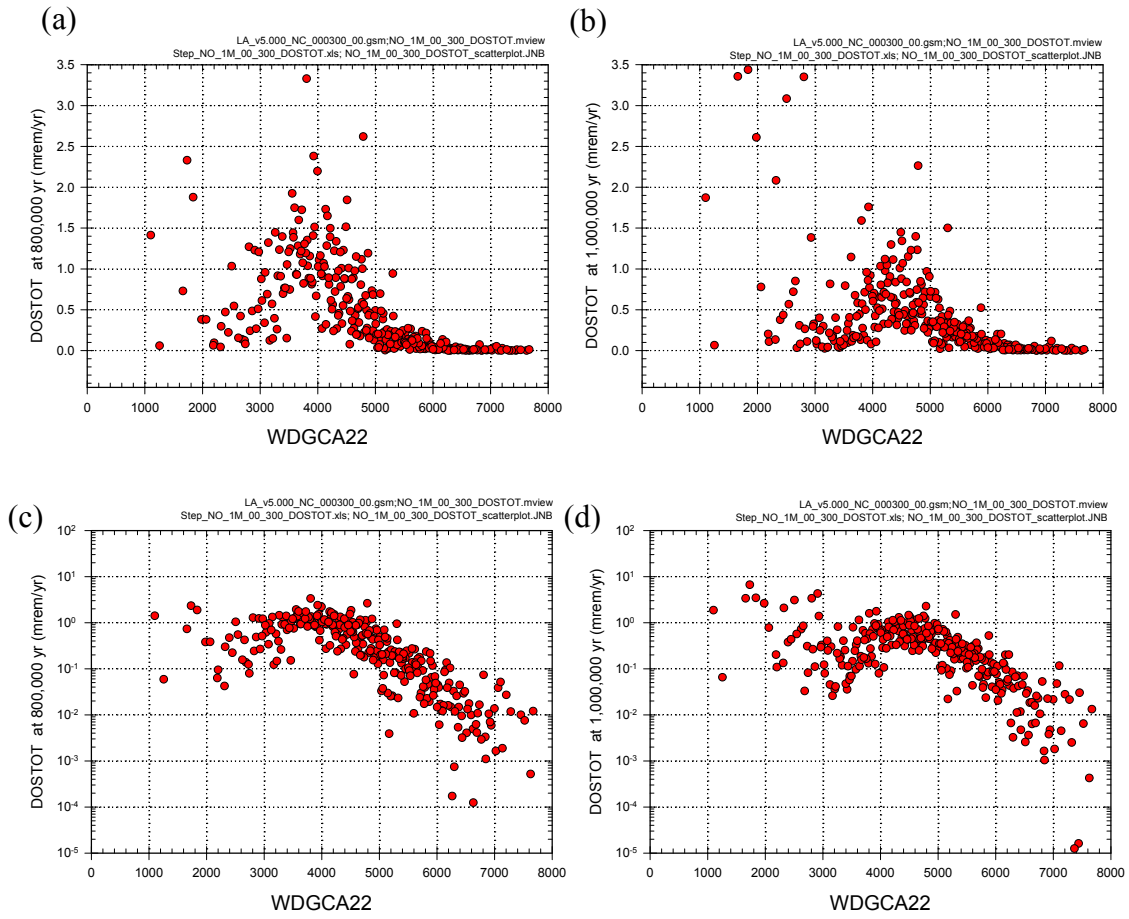

Source: Output DTNs: MO0709TSPAREGS.000 [DIRS 182976]; and MO0709TSPAPLOT.000 [DIRS 183010].

Figure K4.5-3. Selected scatterplots for dose to RMEI (*DOSTOT*, mrem/yr) for all radioactive species under nominal conditions at 800,000 and 1,000,000 years.

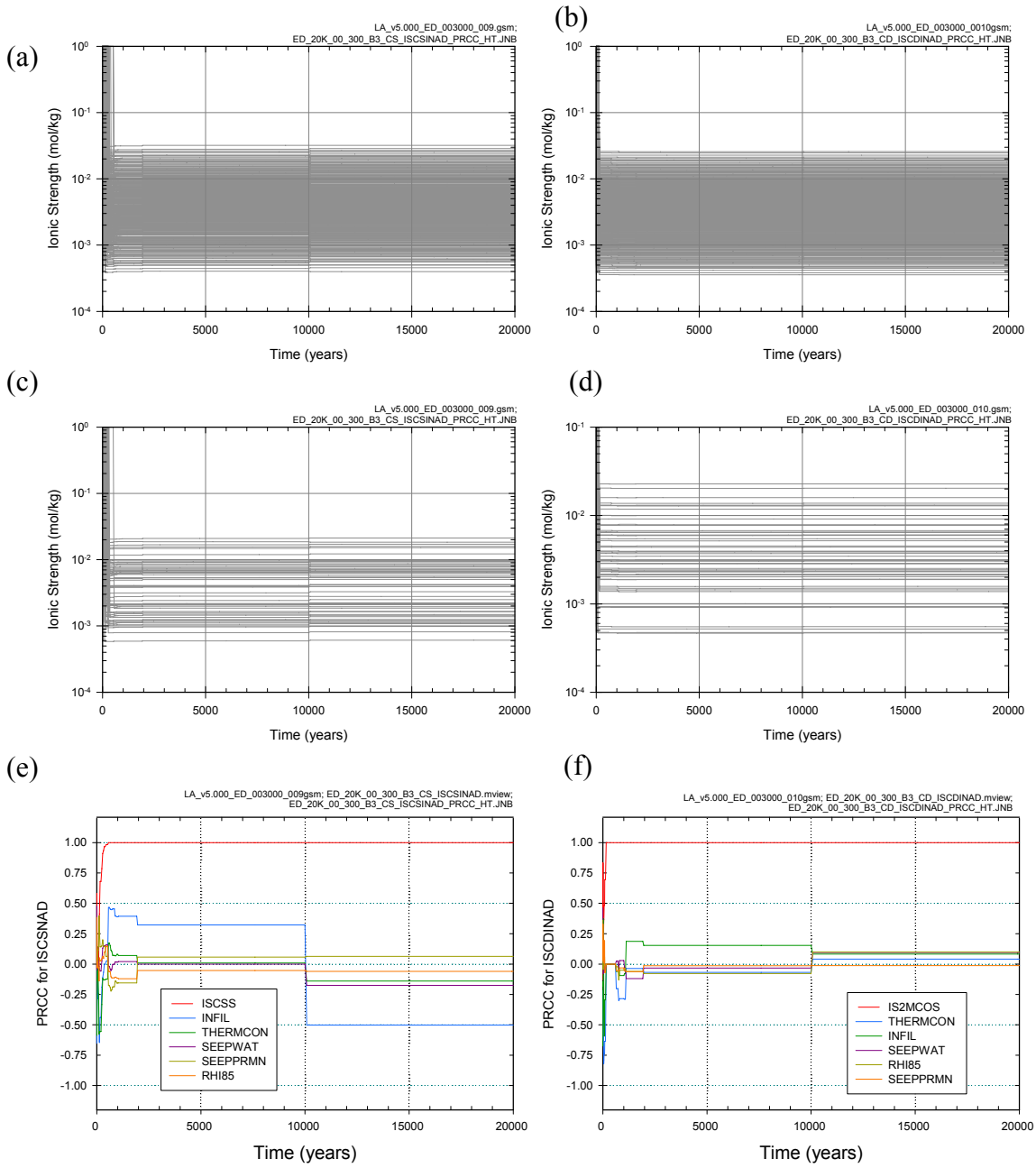

Source: Output DTNs: MO0709TSPASENS.000 [DIRS 183982]; and MO0709TSPAPLOT.000 [DIRS 183010].

Figure K5.2-1 Time-dependent ionic strength (mol/kg) in the invert for CSNF WPs (*ISCSINAD*) and CDSP WPs (*ISCDINAD*) experiencing an early drip shield failure under dripping conditions in percolation bin 3: (a, b) *ISCSINAD* and *ISCDINAD* for all (i.e., 300) sample elements, (c, d) *ISCSINAD* and *ISCDINAD* for first 50 sample elements, and (e, f) PRCCs for *ISCSINAD* and *ISCDINAD*

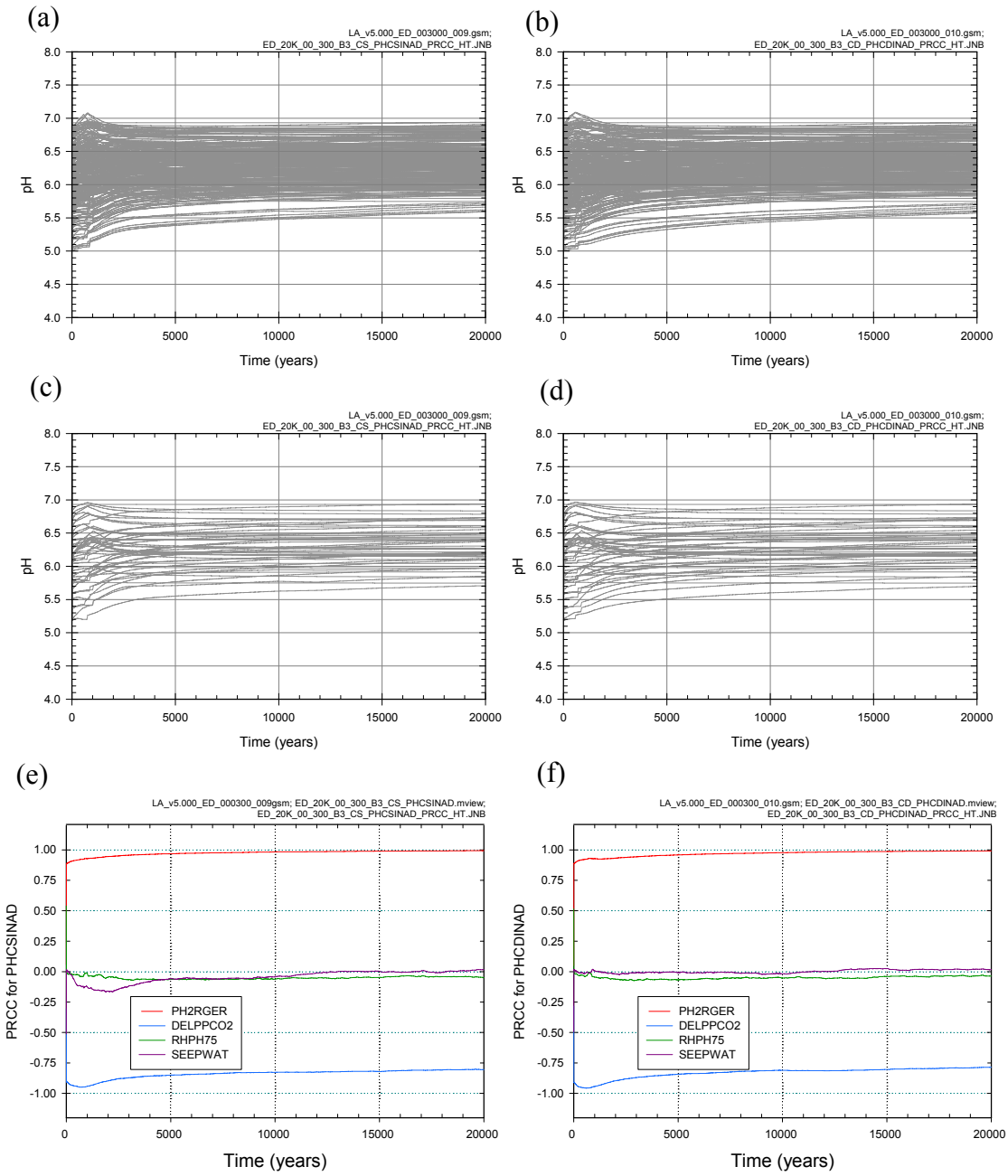

Source: Output DTNs: MO0709TSPAREGS.000 [DIRS 182976]; and MO0709TSPAPLOT.000 [DIRS 183010].

Figure K5.2-2 Time-dependent pH in the invert for CSNF WPs (*PHCSINAD*) and CDSP WPs (*PHCDINAD*) experiencing an early DS failure under dripping conditions in percolation bin 3: (a, b) *PHCSINAD* and *PHCDINAD* for all (i.e., 300) sample elements, (c, d) *PHCSINAD* and *PHCDINAD* for first 50 sample elements, and (e, f) PRCCs for *PHCSINAD* and *PHCDINAD*

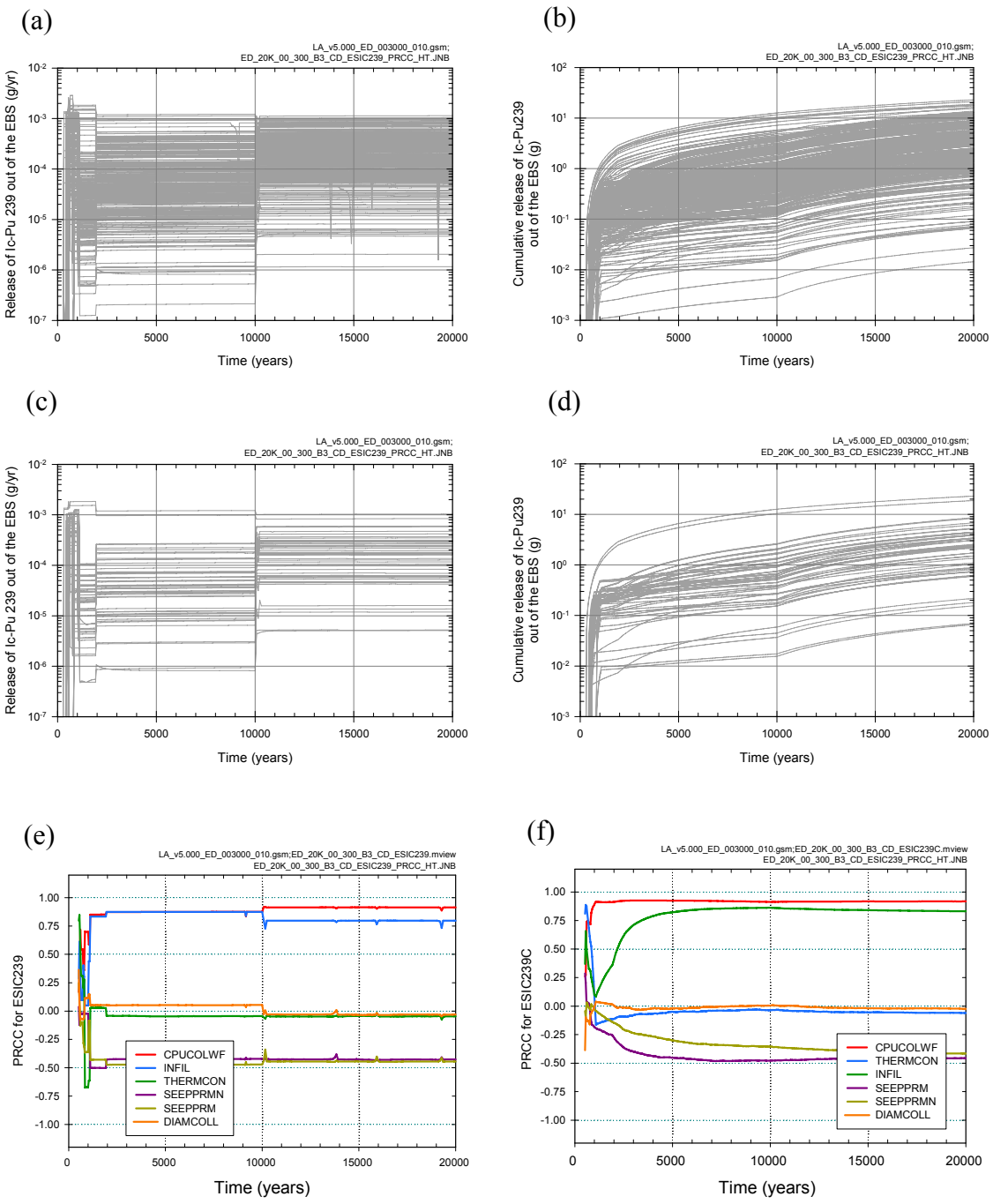

Source: Output DTNs: MO0709TSPAREGS.000 [DIRS 182976]; and MO0709TSPAPLOT.000 [DIRS 183010].

Figure K5.3.1-1. Time-dependent release rates (*ESIC239*, g/yr) and cumulative (i.e., integrated) releases (*ESIC239C*, g) over 20,000 years for the movement of ^{239}Pu irreversibly attached to glass/waste form colloids from the EBS to the UZ resulting from a single early DS failure above a CDSP WP in percolation bin 3 under dripping conditions: (a, b) *ESIC239* and *ESIC239C* for all (i.e., 300) sample elements, (c, d) *ESIC239* and *ESIC239C* for first 50 sample elements, and (e, f) PRCCs for *ESIC239* and *ESIC239C*.

(a)

	ESIC239: 3000 yr			ESIC239: 5000 yr			ESIC239: 10,000 yr		
Step[a]	**Variable[b]**	**R^{2c}**	**SRRC[d]**	**Variable**	**R^2**	**SRRC**	**Variable**	**R^2**	**SRRC**
1	INFIL	0.51	0.68	INFIL	0.51	0.67	INFIL	0.51	0.67
2	CPUCOLWF	0.83	0.58	CPUCOLWF	0.83	0.58	CPUCOLWF	0.83	0.58
3	SEEPPRM	0.86	-0.18	SEEPPRM	0.86	-0.18	SEEPPRM	0.86	-0.18
4	SEEPPRMN	0.88	-0.15	SEEPPRMN	0.88	-0.15	SEEPPRMN	0.88	-0.15
5	ALPHAL	0.90	-0.13	ALPHAL	0.90	-0.13	ALPHAL	0.90	-0.13
6	SEEPUNC	0.90	0.07	SEEPUNC	0.90	0.07	SEEPUNC	0.90	0.07
7	PHCSS	0.90	-0.05	PHCSS	0.90	-0.05	PHCSS	0.90	-0.05

(b)

	ESIC239C: 3000 yr			ESIC239C: 5000 yr			ESIC239C: 10,000 yr		
Step[a]	**Variable[b]**	**R^{2c}**	**SRRC[c]**	**Variable**	**R^2**	**SRRC**	**Variable**	**R^2**	**SRRC**
1	CPUCOLWF	0.68	0.79	CPUCOLWF	0.60	0.74	CPUCOLWF	0.52	0.69
2	INFIL	0.84	0.41	INFIL	0.86	0.52	INFIL	0.86	0.58
3	SEEPPRM	0.85	-0.12	SEEPPRM	0.87	-0.13	SEEPPRM	0.88	-0.15
4	SEEPPRMN	0.86	-0.09	SEEPPRMN	0.88	-0.09	SEEPPRMN	0.89	-0.10
5	ALPHAL	0.87	-0.07	ALPHAL	0.89	-0.08	ALPHAL	0.90	-0.10
6				KDPASMEC	0.89	0.06	SEEPUNC	0.90	0.06
7				CSNFMASS	0.90	0.05	KDPASMEC	0.91	0.05
8				KDAMCOL	0.90	-0.06	CSNFMASS	0.91	0.05
9				GOESA	0.90	-0.06	KDAMCOL	0.91	-0.06
10							RHMUNO20	0.91	-0.05

a: Steps in stepwise rank regression analysis
b: Variables listed in order of selection in stepwise regression
c: Cumulative R^2 value with entry of each variable into regression model
d: Standardized rank regression coefficients (SRRCs) in final regression model

Source: Output DTNs: MO0709TSPAREGS.000 [DIRS 182976]; and MO0709TSPAPLOT.000 [DIRS 183010].

NOTE: In (c, g), the box extends from 0.25 to 0.75 quantile; lower and upper bar and whisker extend to 0.1 and 0.9 quantile, respectively; dots represent values outside 0.1 to 0.9 quantile range; median indicated by light horizontal line.

Figure K5.3.1-2. Stepwise rank regression analyses and selected scatterplots for time-dependent release rates (*ESIC239*, g/yr) and cumulative (i.e., integrated) releases (*ESIC239C*, g) for the movement of ^{239}Pu irreversibly attached to glass/waste form colloids from the EBS to the UZ resulting from a single early DS failure above a CDSP WP in percolation bin 3 under dripping conditions : (a, b) Regressions for *ESIC239* and *ESIC239C* at 3000, 5000 and 10,000 years, and (c-h) Scatterplots for *ESIC239* and *ESIC239C* at 10,000 years.

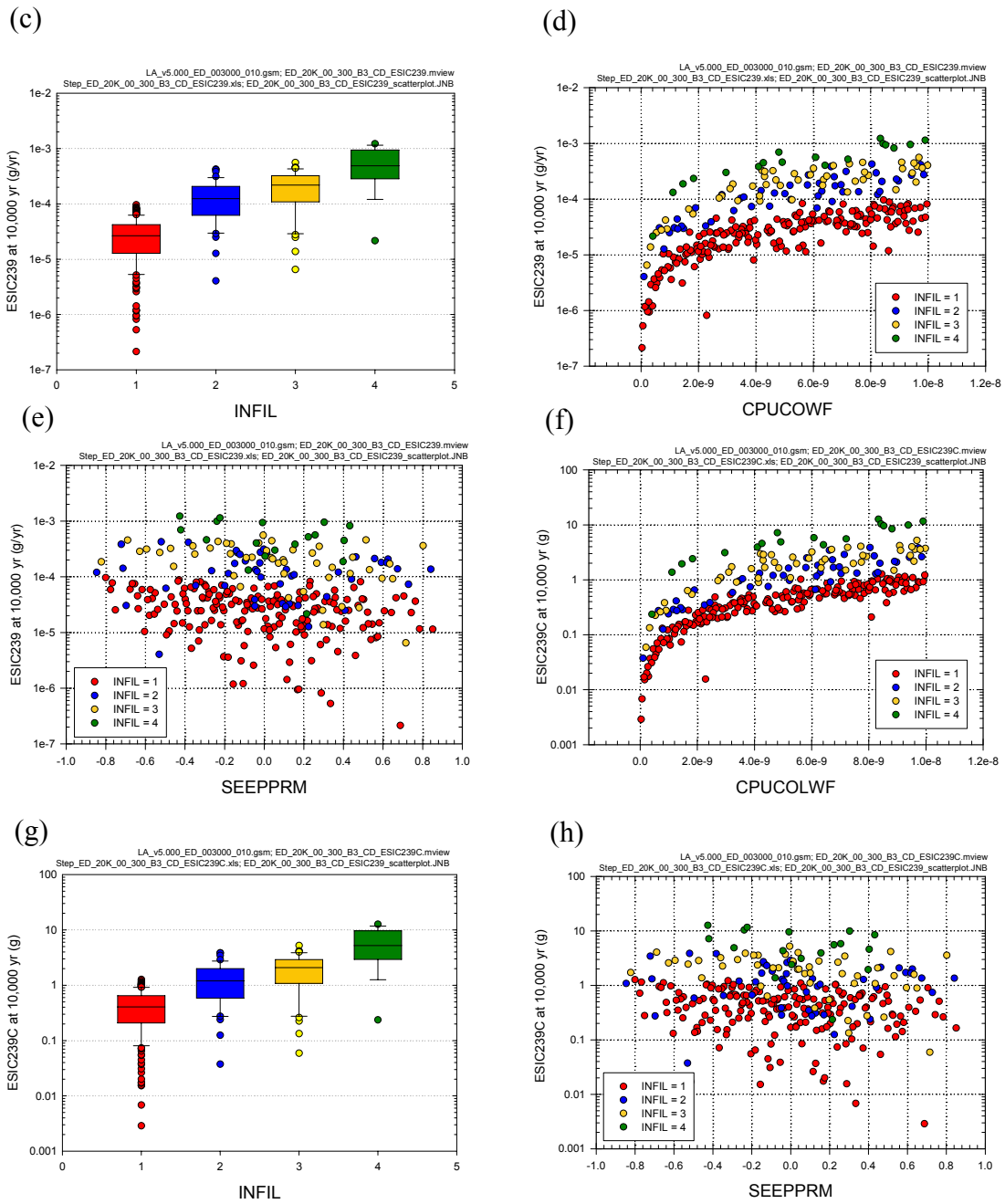

Source: Output DTNs: MO0709TSPAREGS.000 [DIRS 182976]; and MO0709TSPAPLOT.000 [DIRS 183010].

NOTE: In (c, g), the box extends from 0.25 to 0.75 quantile; lower and upper bar and whisker extend to 0.1 and 0.9 quantile, respectively; dots represent values outside 0.1 to 0.9 quantile range; median indicated by light horizontal line.

Figure K5.3.1-2. Stepwise rank regression analyses and selected scatterplots for time-dependent release rates (*ESIC239*, g/yr) and cumulative (i.e., integrated) releases (*ESIC239C*, g) for the movement of ^{239}Pu irreversibly attached to glass/waste form colloids from the EBS to the UZ resulting from a single early DS failure above a CDSP WP in percolation bin 3 under dripping conditions : (a, b) Regressions for *ESIC239* and *ESIC239C* at 3000, 5000 and 10,000 years, and (c-h) Scatterplots for *ESIC239* and *ESIC239C* at 10,000 years (continued).

Figure Removed. See discussion in Section K5.3.1.

Figure K5.3.1-3. Time-dependent release rates (*ESIF239*, g/yr) and cumulative (i.e., integrated) releases (*ESIF239C*, g) over 20,000 years for the movement of ^{239}Pu irreversibly attached to ferrous colloids from the EBS to the UZ resulting from a single early DS failure above a CDSP WP in percolation bin 3 under dripping conditions: (a, b) *ESIF239* and *ESIF239C* for all (i.e., 300) sample elements, (c, d) *ESIF239* and *ESIF239C* for first 50 sample elements, and (e, f) PRCCs for *ESIF239* and *ESIF239C*.

Figure Removed. See discussion in Section K5.3.1.

Figure K5.3.1-4. Stepwise rank regression analyses and selected scatterplots for time-dependent release rates (*ESIF239*, g/yr) and cumulative (i.e., integrated) releases (*ESIF239C*, g) for the movement of ^{239}Pu irreversibly attached to ferrous colloids from the EBS to the UZ resulting from a single early DS failure above a CDSP WP in percolation bin 3 under dripping conditions : (a, b) Regressions for *ESIF239* and *ESIF239C* at 3000, 5000 and 10,000 years, and (c-h) Scatterplots for *ESIF239* and *ESIF239C* at 10,000 years.

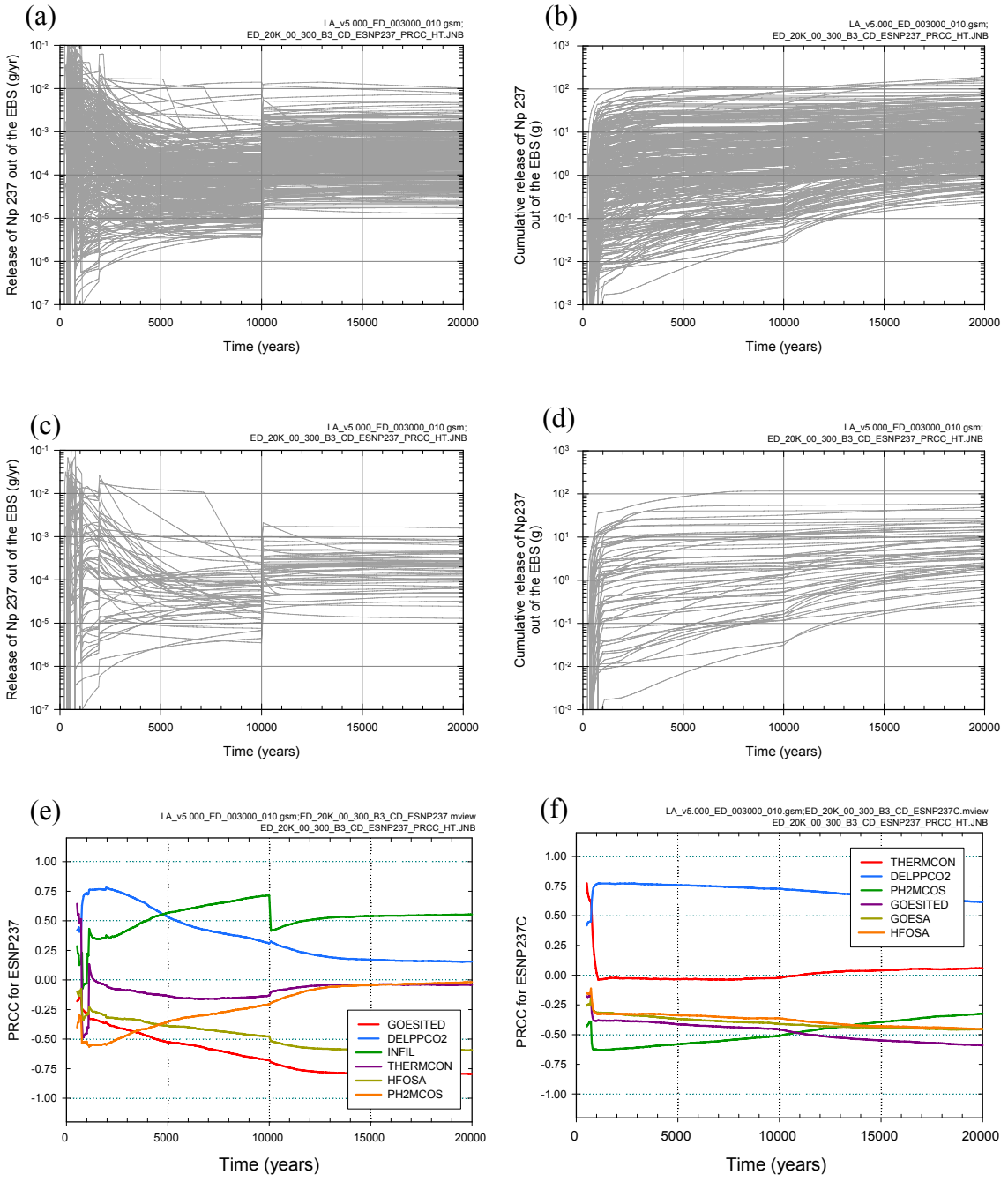

Source: Output DTNs: MO0709TSPAREGS.000 [DIRS 182976]; and MO0709TSPAPLOT.000 [DIRS 183010].

Figure K5.3.1-5. Time-dependent release rates (*ESNP237*, g/yr) and cumulative (i.e., integrated) releases (*ESNP2379C*, g) over 20,000 years for the movement of dissolved ^{237}Np from the EBS to the UZ resulting from a single early DS failure above a CDSP WP in percolation bin 3 under dripping conditions: (a, b) *ESNP237* and *ESNP237C* for all (i.e., 300) sample elements, (c, d) *ESNP237* and *ESNP237C* for first 50 sample elements, and (e, f) PRCCs for *ESNP237* and *ESNP237C*.

(a)

	ESNP237: 3000 yr			ESNP237: 5000 yr			ESNP237: 10,000 yr		
Step[a]	Variable[b]	R^{2c}	SRRC[d]	Variable	R^2	SRRC	Variable	R^2	SRRC
1	DELPPCO2	0.27	0.56	INFIL	0.18	0.45	INFIL	0.29	0.55
2	INFIL	0.37	0.29	DELPPCO2	0.29	0.35	GOESITED	0.43	-0.41
3	PH2MCOS	0.46	-0.32	GOESITED	0.37	-0.30	DSNFMASS	0.48	0.19
4	KDAMSMEC	0.50	0.17	PH2MCOS	0.41	-0.20	HFOSA	0.53	-0.31
5	GOESITED	0.54	-0.21	EP1LOWNU	0.44	0.18	EP1LOWNU	0.57	0.21
6	EP1LOWAM	0.57	0.19	HFOSA	0.47	-0.23	DELPPCO2	0.60	0.16
7	COLGW	0.60	0.16	IS2MCOS	0.51	0.18	IS2MCOS	0.63	0.15
8	HFOSA	0.61	-0.16	KDAMSMEC	0.54	0.15	GOESA	0.65	-0.15
9	IS2MCOS	0.63	0.14	DSNFMASS	0.57	0.13	ALPHAL	0.67	-0.14
10	GOESA	0.65	-0.14	SEEPPRMN	0.59	-0.15	GOERELAB	0.69	0.15
11	DSNFMASS	0.66	0.12	GOESA	0.60	-0.16	SEEPPRMN	0.70	-0.12
12	EP1LOWNU	0.67	0.10	EP1LOWAM	0.62	0.12	KDAMSMEC	0.72	0.11
13	SCHOBOLT	0.69	0.10	GOERELAB	0.63	0.12	HFOSITED	0.72	-0.09
14	WDCRCDEN	0.69	0.09	SCHOBOLT	0.65	0.11	PH2DHLS	0.73	-0.08
15	GOERELAB	0.70	0.09	WDNSCC	0.66	0.09			

(b)

	ESNP237C: 3000 yr			ESNP237C: 5000 yr			ESNP237C: 10,000 yr		
Step[a]	Variable[b]	R^{2c}	SRRC[c]	Variable	R^2	SRRC	Variable	R^2	SRRC
1	DELPPCO2	0.33	0.60	DELPPCO2	0.31	0.58	DELPPCO2	0.27	0.54
2	PH2MCOS	0.50	-0.41	PH2MCOS	0.47	-0.39	PH2MCOS	0.39	-0.35
3	EP1LOWAM	0.56	0.21	EP1LOWAM	0.52	0.20	INFIL	0.46	0.25
4	COLGW	0.61	0.23	COLGW	0.58	0.21	GOESITED	0.51	-0.24
5	KDAMSMEC	0.64	0.16	GOESITED	0.61	-0.20	KDAMSMEC	0.54	0.17
6	GOESITED	0.66	-0.18	KDAMSMEC	0.64	0.16	COLGW	0.58	0.20
7	GOESA	0.68	-0.13	INFIL	0.66	0.17	EP1LOWAM	0.61	0.19
8	INFIL	0.69	0.12	GOESA	0.67	-0.15	GOESA	0.63	-0.18
9	HFOSA	0.70	-0.11	DSNFMASS	0.69	0.13	DSNFMASS	0.65	0.15
10	EP1NPO2	0.71	0.11	WDCRCDEN	0.70	0.12	HFOSA	0.67	-0.16
11	WDCRCDEN	0.72	0.12	HFOSA	0.71	-0.12	WDCRCDEN	0.68	0.12
12	DSNFMASS	0.73	0.11	EP1NPO2	0.72	0.10	IS2MCOS	0.69	0.10
13				IS2MCOS	0.72	0.09	RHPH75	0.70	-0.09
14				GP2NO3	0.73	-0.09	GP2NO3	0.71	-0.09
15				RHPH75	0.74	-0.08	HFOSITED	0.71	-0.10
16							EP1NPO2	0.72	0.11

a: Steps in stepwise rank regression analysis
b: Variables listed in order of selection in stepwise regression
c: Cumulative R^2 value with entry of each variable into regression model
d: Standardized rank regression coefficients (SRRCs) in final regression model

Source: Output DTNs: MO0709TSPASENS.000 [DIRS 183982]; and MO0709TSPAPLOT.000 [DIRS 183010].

Figure K5.3.1-6. Stepwise rank regression analyses and selected scatterplots for time-dependent release rates (*ESNP237*, g/yr) and cumulative (i.e., integrated) releases (*ESNP237C*, g) for the movement of dissolved 237Np from the EBS to the UZ resulting from a single early DS failure above a CDSP WP in percolation bin 3 under dripping conditions: (a, b) Regressions for *ESNP237* and *ESNP237C* at 3000, 5000 and 10,000 years, and (c-h) Scatterplots for *ESNP237* and *ESNP237C* at 10,000 years.

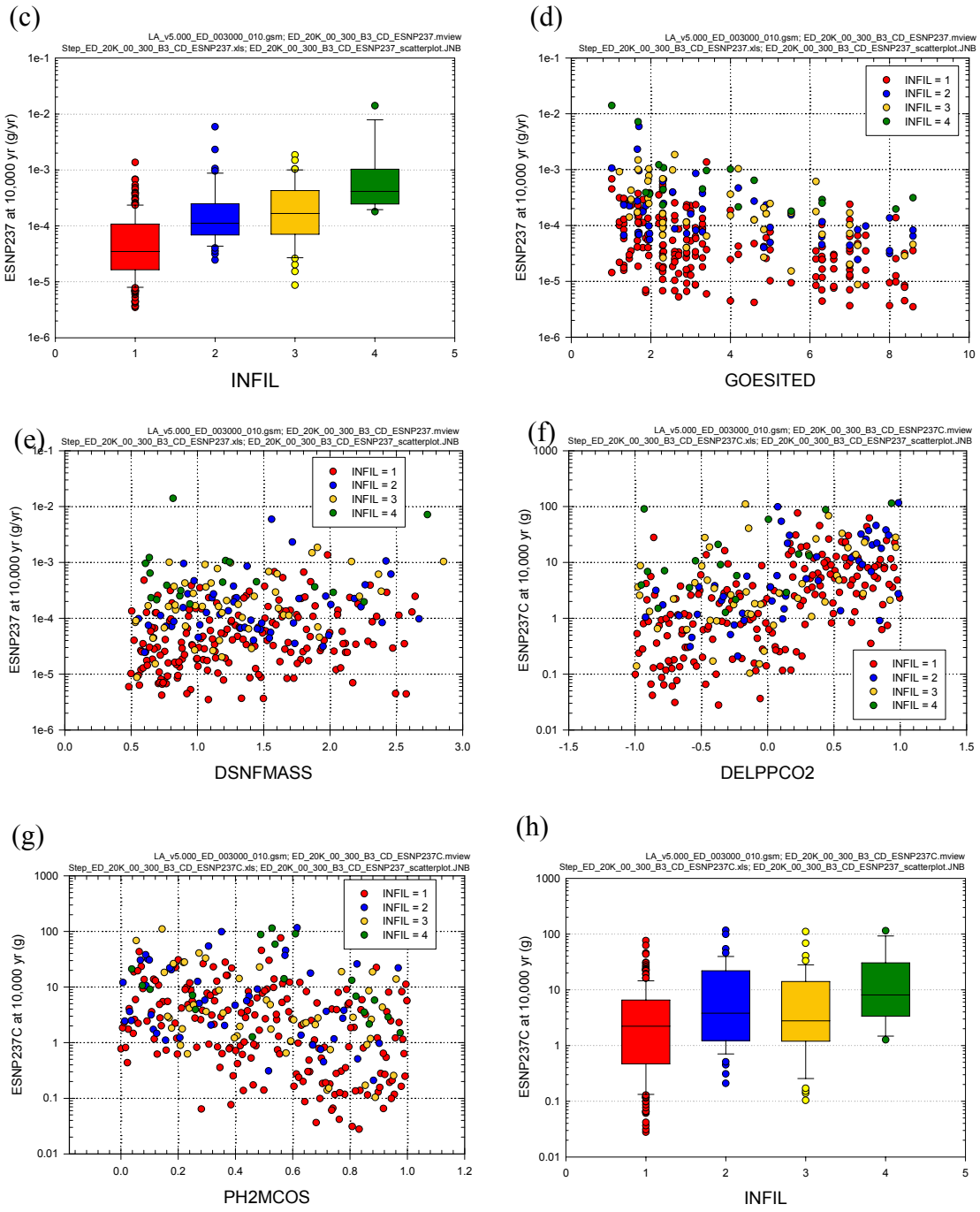

Source: Output DTNs: MO0709TSPASENS.000 [DIRS 183982]; and MO0709TSPAPLOT.000 [DIRS 183010].

NOTE: In (c, h), the box extends from 0.25 to 0.75 quantile; lower and upper bar and whisker extend to 0.1 and 0.9 quantile, respectively; dots represent values outside 0.1 to 0.9 quantile range; median indicated by light horizontal line.

Figure K5.3.1-6. Stepwise rank regression analyses and selected scatterplots for time-dependent release rates (*ESNP237*, g/yr) and cumulative (i.e., integrated) releases (*ESNP237C*, g) for the movement of dissolved 237Np from the EBS to the UZ resulting from a single early DS failure above a CDSP WP in percolation bin 3 under dripping conditions: (a, b) Regressions for *ESNP237* and *ESNP237C* at 3000, 5000 and 10,000 years, and (c-h) Scatterplots for *ESNP237* and *ESNP237C* at 10,000 years (continued).

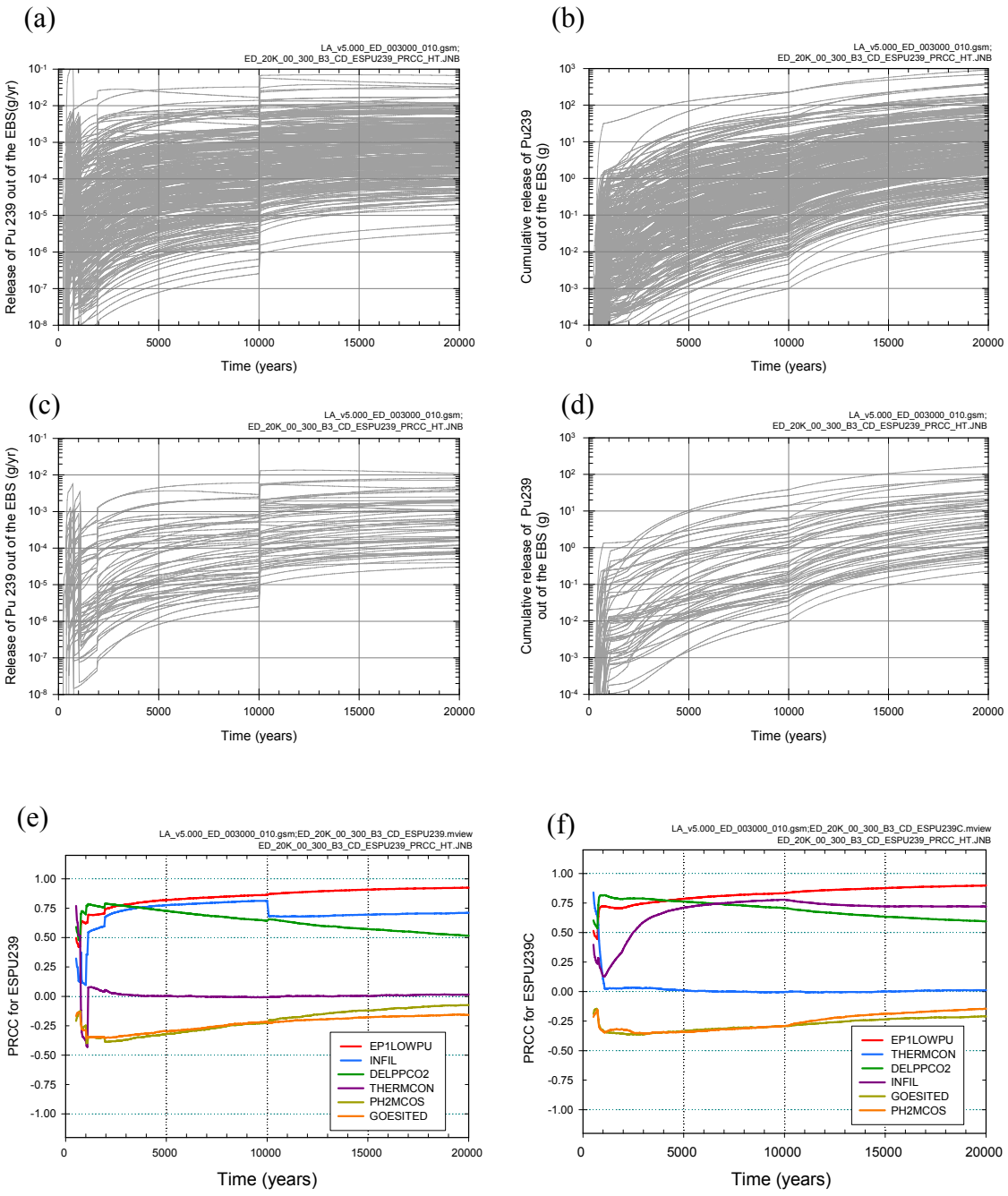

Source: Output DTNs: MO0709TSPAREGS.000 [DIRS 182976]; and MO0709TSPAPLOT.000 [DIRS 183010].

Figure K5.3.1-7. Time-dependent release rates (*ESPU239*, g/yr) and cumulative (i.e., integrated) releases (*ESPU239C*, g) over 20,000 years for the movement of dissolved ^{239}Pu from the EBS to the UZ resulting from a single early DS failure above a CDSP WP in percolation bin 3 under dripping conditions: (a, b) *ESPU239* and *ESPU239C* for all (i.e., 300) sample elements, (c, d) *ESPU239* and *ESPU239C* for first 50 sample elements, and (e, f) PRCCs for *ESPU239* and *ESPU239C*.

(a)

	ESPU239: 3000 yr			ESPU239: 5000 yr			ESPU239: 10,000 yr		
Step[a]	Variable[b]	R^{2c}	SRRC[d]	Variable	R^2	SRRC	Variable	R^2	SRRC
1	EP1LOWPU	0.25	0.51	EP1LOWPU	0.30	0.56	EP1LOWPU	0.38	0.63
2	DELPPCO2	0.48	0.51	INFIL	0.55	0.54	INFIL	0.68	0.56
3	INFIL	0.71	0.50	DELPPCO2	0.73	0.43	DELPPCO2	0.78	0.31
4	PH2MCOS	0.74	-0.16	GOESITED	0.75	-0.14	SEEPPRM	0.79	-0.12
5	GOESITED	0.76	-0.16	PH2MCOS	0.77	-0.13	SEEPPRMN	0.80	-0.08
6	GOESA	0.77	-0.10	SEEPPRM	0.78	-0.10	GOESITED	0.81	-0.10
7	SEEPPRM	0.77	-0.09	GOESA	0.79	-0.09	ALPHAL	0.82	-0.08
8	GP2NO3	0.78	-0.09	EBSDIFCF	0.79	0.12	EBSDIFCF	0.82	0.08
9	RHPH75	0.79	-0.09	GP2NO3	0.80	-0.09	PH2MCOS	0.83	-0.08
10	EBSDIFCF	0.79	0.11	RHPH75	0.81	-0.09	GP2NO3	0.84	-0.09
11	CPUCOLCS	0.80	-0.08	CPUCOLCS	0.81	-0.07	RHPH75	0.84	-0.08
12	HFOSA	0.81	-0.10	ALPHAL	0.82	-0.08	GOESA	0.85	-0.07
13	IS2MCOS	0.81	0.08	HFOSA	0.82	-0.08	DIFPATHL	0.85	-0.06
14	ALPHAL	0.82	-0.08	IS2MCOS	0.83	0.07			
15	EP1LOWNU	0.82	0.07	EP1LOWNU	0.83	0.07			

(b)

	ESPU239C: 3000 yr			ESPU239C: 5000 yr			ESPU239C: 10,000 yr		
Step[a]	Variable[b]	R^{2c}	SRRC[d]	Variable	R^2	SRRC	Variable	R^2	SRRC
1	DELPPCO2	0.28	0.59	EP1LOWPU	0.26	0.53	EP1LOWPU	0.33	0.58
2	EP1LOWPU	0.55	0.50	DELPPCO2	0.50	0.52	INFIL	0.58	0.53
3	INFIL	0.67	0.35	INFIL	0.71	0.47	DELPPCO2	0.74	0.40
4	PH2MCOS	0.71	-0.17	PH2MCOS	0.73	-0.15	GOESITED	0.76	-0.13
5	GOESITED	0.73	-0.18	GOESITED	0.75	-0.16	PH2MCOS	0.78	-0.12
6	GOESA	0.74	-0.11	GOESA	0.76	-0.10	SEEPPRM	0.79	-0.10
7	GP2NO3	0.75	-0.11	GP2NO3	0.77	-0.10	GOESA	0.79	-0.08
8	RHPH75	0.76	-0.09	RHPH75	0.78	-0.10	RHPH75	0.80	-0.10
9	HFOSA	0.77	-0.09	EBSDIFCF	0.79	0.11	GP2NO3	0.81	-0.09
10				HFOSA	0.79	-0.10	EBSDIFCF	0.81	0.11
11				IS2MCOS	0.80	0.08	ALPHAL	0.82	-0.08
12				CPUCOLCS	0.80	-0.07	HFOSA	0.82	-0.09
13				SEEPPRM	0.81	-0.08	EP1LOWNU	0.83	0.08
14				EP1LOWNU	0.81	0.08	IS2MCOS	0.84	0.08
15				ALPHAL	0.82	-0.07			

a: Steps in stepwise rank regression analysis
b: Variables listed in order of selection in stepwise regression
c: Cumulative R^2 value with entry of each variable into regression model
d: Standardized rank regression coefficients (SRRCs) in final regression model

Source: Output DTNs: MO0709TSPASENS.000 [DIRS 183982]; and MO0709TSPAPLOT.000 [DIRS 183010].

Figure K5.3.1-8. Stepwise rank regression analyses and selected scatterplots for time-dependent release rates (*ESPU239*, g/yr) and cumulative (i.e., integrated) releases (*ESPU239*, g) for the movement of dissolved ^{239}Pu from the EBS to the UZ resulting from a single early DS failure above a CDSP WP in percolation bin 3 under dripping conditions: (a, b) Regressions for *ESPU239* and *ESPU239C* at 3000, 5000 and 10,000 years, and (c-h) Scatterplots for *ESPU239* and *ESPU239C* at 10,000 years.

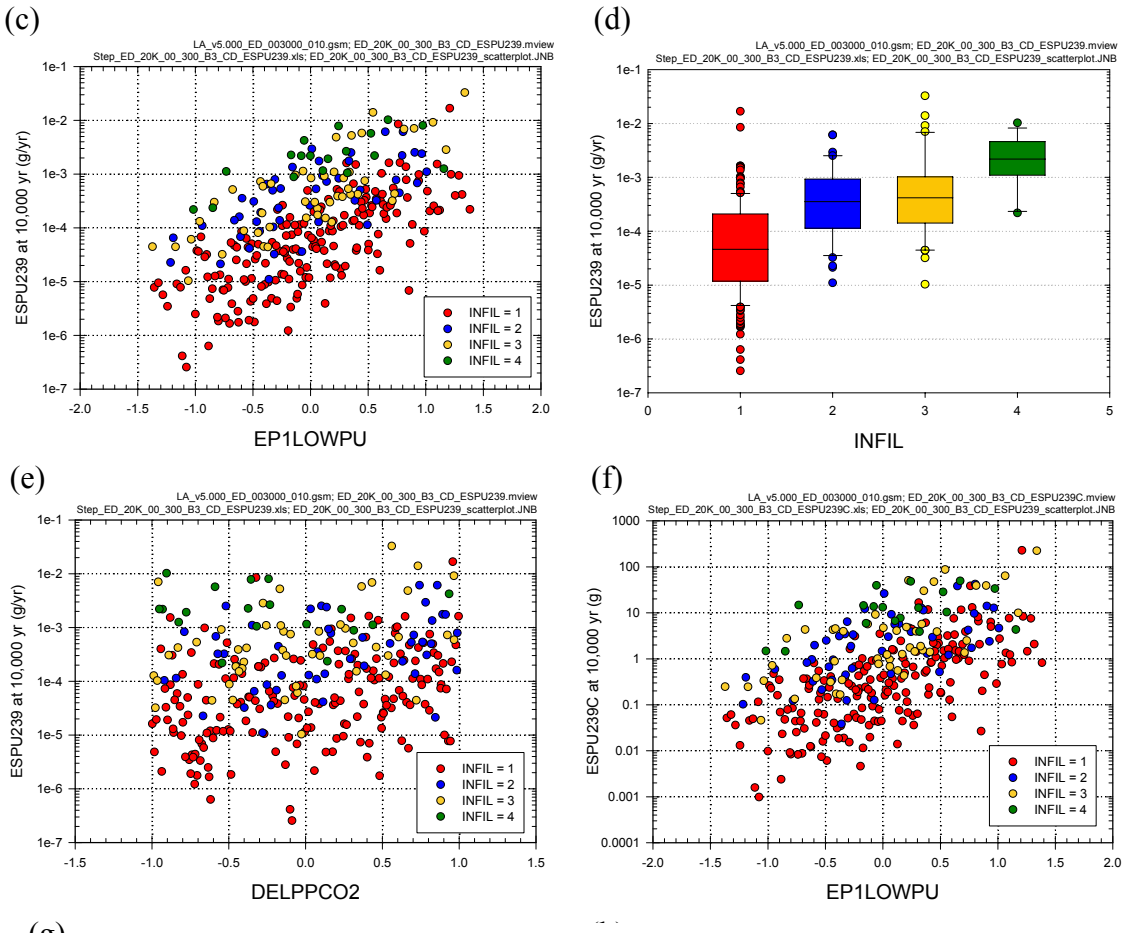

Source: Output DTNs: MO0709TSPASENS.000 [DIRS 183982]; and MO0709TSPAPLOT.000 [DIRS 183010].

NOTE: In (d, g), the box extends from 0.25 to 0.75 quantile; lower and upper bar and whisker extend to 0.1 and 0.9 quantile, respectively; dots represent values outside 0.1 to 0.9 quantile range; median indicated by light horizontal line.

Figure K5.3.1-8. Stepwise rank regression analyses and selected scatterplots for time-dependent release rates (*ESPU239*, g/yr) and cumulative (i.e., integrated) releases (*ESPU239*, g) for the movement of dissolved ^{239}Pu from the EBS to the UZ resulting from a single early DS failure above a CDSP WP in percolation bin 3 under dripping conditions: (a, b) Regressions for *ESPU239* and *ESPU239C* at 3000, 5000 and 10,000 years, and (c-h) Scatterplots for *ESPU239* and *ESPU239C* at 10,000 years (continued).

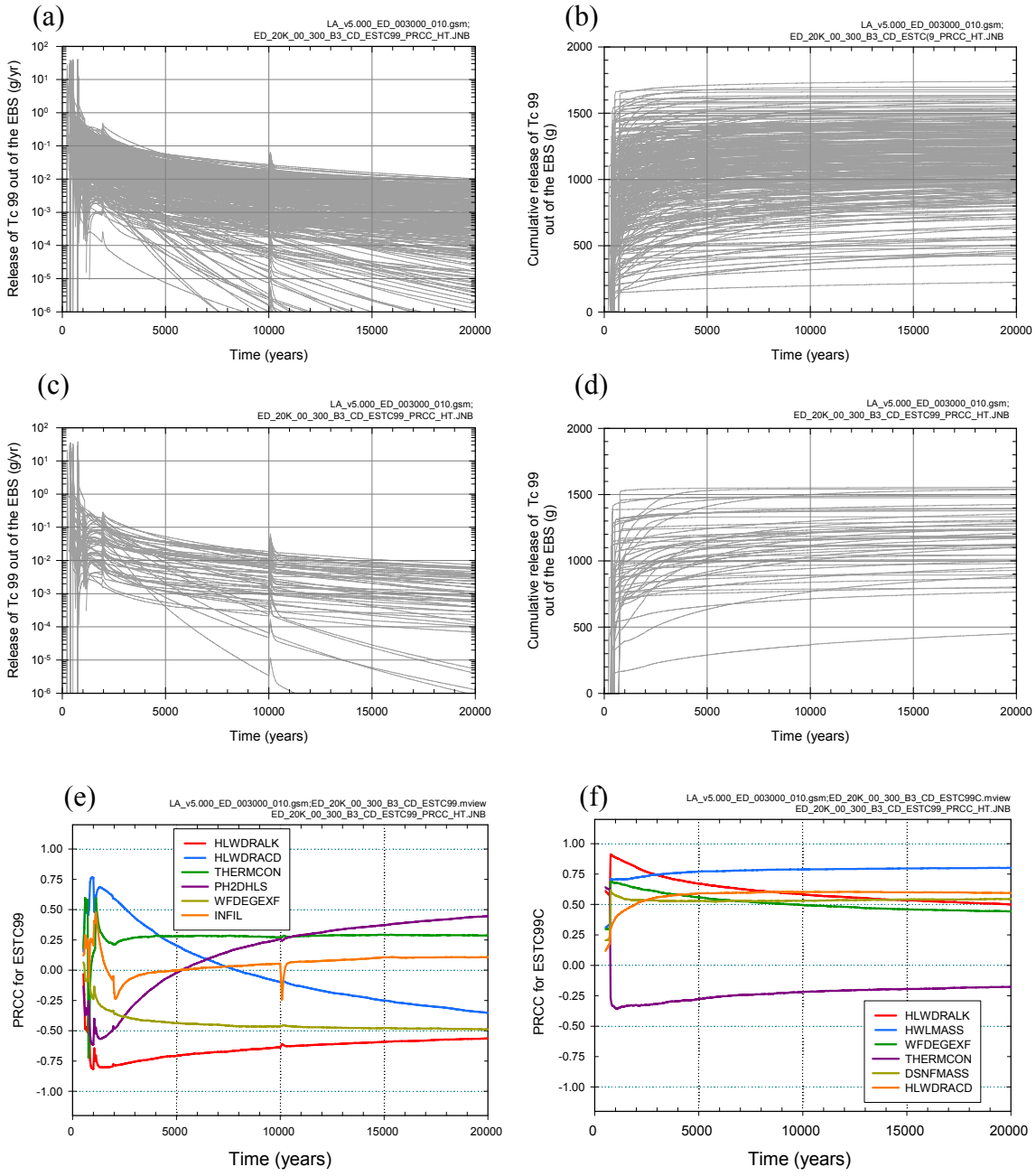

Source: Output DTNs: MO0709TSPASENS.000 [DIRS 183982]; and MO0709TSPAPLOT.000 [DIRS 183010].

Figure K5.3.1-9. Time-dependent release rates (*ESTC99*, g/yr) and cumulative (i.e., integrated) releases (*ESTC99C*, g) over 20,000 years for the movement of dissolved ^{99}Tc from the EBS to the UZ resulting from a single early DS failure above a CDSP WP in percolation bin 3 under dripping conditions: (a, b) *ESTC99* and *ESTC99C* for all (i.e., 300) sample elements, (c, d) *ESTC99* and *ESTC99C* for first 50 sample elements, and (e, f) PRCCs for *ESTC99* and *ESTC99C*.

(a)

	ESTC99: 3000 yr			ESTC99: 5000 yr			ESTC99: 10,000 yr		
Step[a]	**Variable[b]**	**Rc^2**	**SRRC[c]**	**Variable**	**R^2**	**SRRC**	**Variable**	**R^2**	**SRRC**
1	HLWDRALK	0.47	-0.70	HLWDRALK	0.44	-0.67	HLWDRALK	0.34	-0.59
2	WFDEGEXF	0.54	-0.28	WFDEGEXF	0.54	-0.32	WFDEGEXF	0.47	-0.35
3	HLWDRACD	0.59	0.24	THERMCON	0.56	0.15	THERMCON	0.50	0.16
4	PH2DHLS	0.61	-0.16	SEEPPRMN	0.58	0.12	PH2DHLS	0.53	0.15
5	THERMCON	0.63	0.14	RHMU20	0.59	-0.10	HLWDRACD	0.54	-0.10
6	SEEPPRMN	0.65	0.12				SEEPPRMN	0.55	0.10
7	GP4NO3	0.66	-0.10				GP4NO3	0.56	-0.10

(b)

	ESTC99C: 3000 yr			ESTC99C: 5000 yr			ESTC99C: 10,000 yr		
Step[a]	**Variable[b]**	**R^{2c}**	**SRRC[d]**	**Variable**	**R^2**	**SRRC**	**Variable**	**R^2**	**SRRC**
1	HLWDRALK	0.26	0.49	HLWMASS	0.29	0.54	HLWMASS	0.34	0.59
2	HLWMASS	0.49	0.49	HLWDRALK	0.46	0.41	HLWDRACD	0.46	0.34
3	WFDEGEXF	0.60	0.32	WFDEGEXF	0.56	0.29	DSNFMASS	0.57	0.33
4	HLWDRACD	0.68	0.28	HLWDRACD	0.66	0.32	HLWDRALK	0.66	0.33
5	DSNFMASS	0.76	0.30	DSNFMASS	0.74	0.30	WFDEGEXF	0.73	0.26
6	PH2DHLS	0.80	-0.21	PH2DHLS	0.79	-0.23	PH2DHLS	0.79	-0.25
7	THERMCON	0.82	-0.13	THERMCON	0.80	-0.12	THERMCON	0.80	-0.09
8	DELPPCO2	0.82	0.07	CSRINDPO	0.81	0.08	CSRINDPO	0.80	0.08
9	IPCNDMVF	0.83	0.07	IPCNDMVF	0.81	0.07	IPCNDMVF	0.81	0.08
10	CSRINDPO	0.83	0.07	DELPPCO2	0.82	0.07	CORRATSS	0.81	-0.08

a: Steps in stepwise rank regression analysis
b: Variables listed in order of selection in stepwise regression
c: Cumulative R^2 value with entry of each variable into regression model
d: Standardized rank regression coefficients (SRRCs) in final regression model

Source: Output DTNs: MO0709TSPASENS.000 [DIRS 183982]; and MO0709TSPAPLOT.000 [DIRS 183010].

Figure K5.3.1-10. Stepwise rank regression analyses and selected scatterplots for time-dependent release rates (*ESTC99*, g/yr) and cumulative (i.e., integrated) releases (*ESTC99*, g) for the movement of dissolved ^{99}Tc from the EBS to the UZ resulting from a single early DS failure above a CDSP WP in percolation bin 3 under dripping conditions: (a, b) Regressions for *ESTC99* and *ESTC99C* at 3000, 5000 and 10,000 years, and (c-h) Scatterplots for *ESTC99* and *ESTC99C* at 10,000 years.

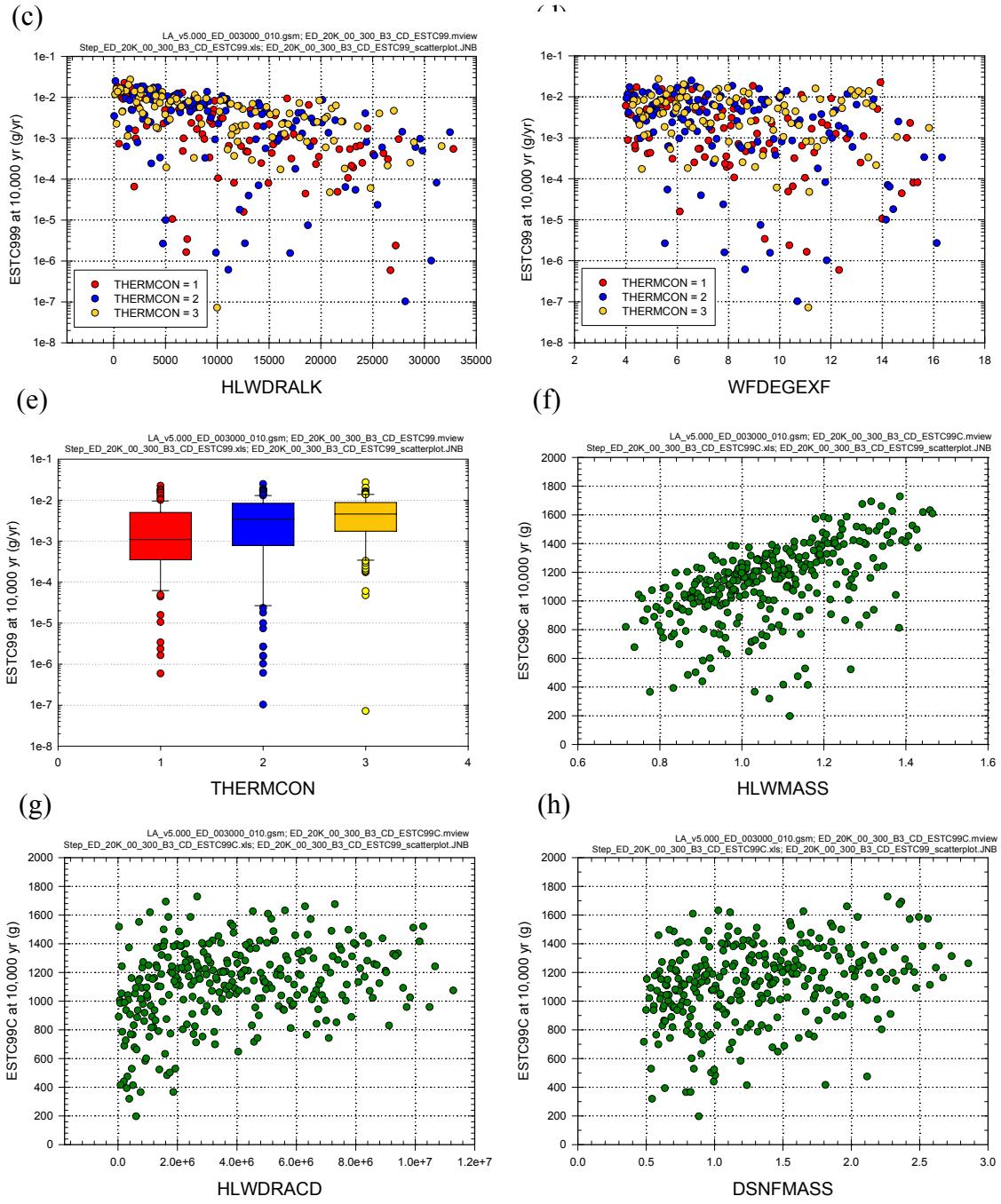

Source: Output DTNs: MO0709TSPASENS.000 [DIRS 183982]; and MO0709TSPAPLOT.000 [DIRS 183010].

NOTE: In (e), the box extends from 0.25 to 0.75 quantile; lower and upper bar and whisker extend to 0.1 and 0.9 quantile, respectively; dots represent values outside 0.1 to 0.9 quantile range; median indicated by light horizontal line.

Figure K5.3.1-10. Stepwise rank regression analyses and selected scatterplots for time-dependent release rates (*ESTC99*, g/yr) and cumulative (i.e., integrated) releases (*ESTC99*, g) for the movement of dissolved ^{99}Tc from the EBS to the UZ resulting from a single early DS failure above a CDSP WP in percolation bin 3 under dripping conditions: (a, b) Regressions for *ESTC99* and *ESTC99C* at 3000, 5000 and 10,000 years, and (c-h) Scatterplots for *ESTC99* and *ESTC99C* at 10,000 years. (Continued)

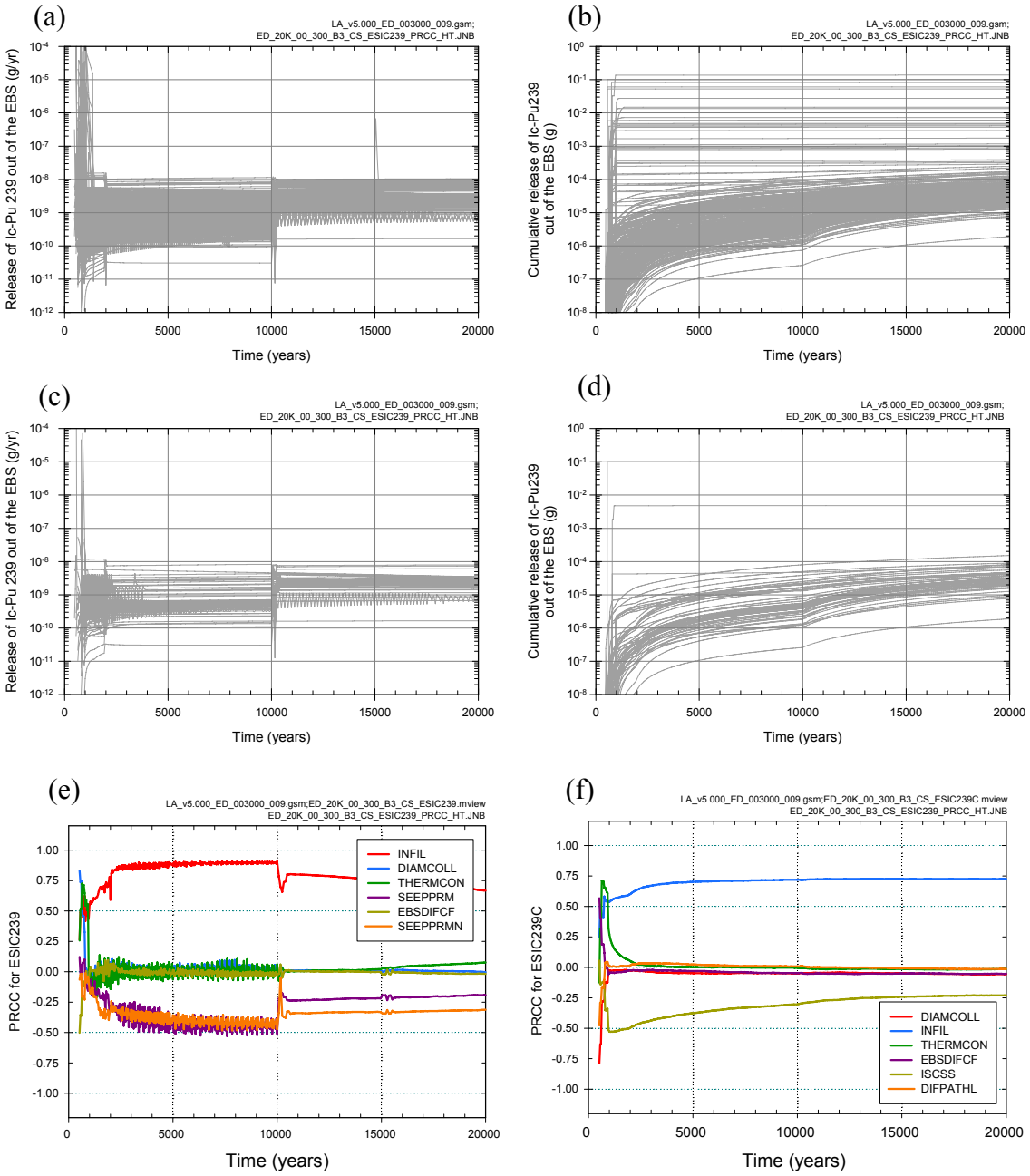

Source: Output DTNs: MO0709TSPASENS.000 [DIRS 183982]; and MO0709TSPAPLOT.000 [DIRS 183010].

Figure K5.3.2-1. Time-dependent release rates (*ESIC239*, g/yr) and cumulative (i.e., integrated) releases (*ESIC239C*, g) over 20,000 years for the movement of ^{239}Pu irreversibly attached to glass/waste form colloids from the EBS to the UZ resulting from a single early DS failure above a CSNF WP in percolation bin 3 under dripping conditions: (a, b) *ESIC239* and *ESIC239C* for all (i.e., 300) sample elements, (c, d) *ESIC239* and *ESIC239C* for first 50 sample elements, and (e, f) PRCCs for *ESIC239* and *ESIC239C*.

Figure Removed. See discussion in Section K5.3.2.

Figure K5.3.2-2. Time-dependent release rates (*ESIF239*, g/yr) and cumulative (i.e., integrated) releases (*ESIF239C*, g) over 20,000 years for the movement of ^{239}Pu irreversibly attached to ferrous colloids from the EBS to the UZ resulting from a single early DS failure above a CSNF WP in percolation bin 3 under dripping conditions: (a, b) *ESIF239* and *ESIF239C* for all (i.e., 300) sample elements, (c, d) *ESIF239* and *ESIF239C* for first 50 sample elements, and (e, f) PRCCs for *ESIF239* and *ESIF239C*.

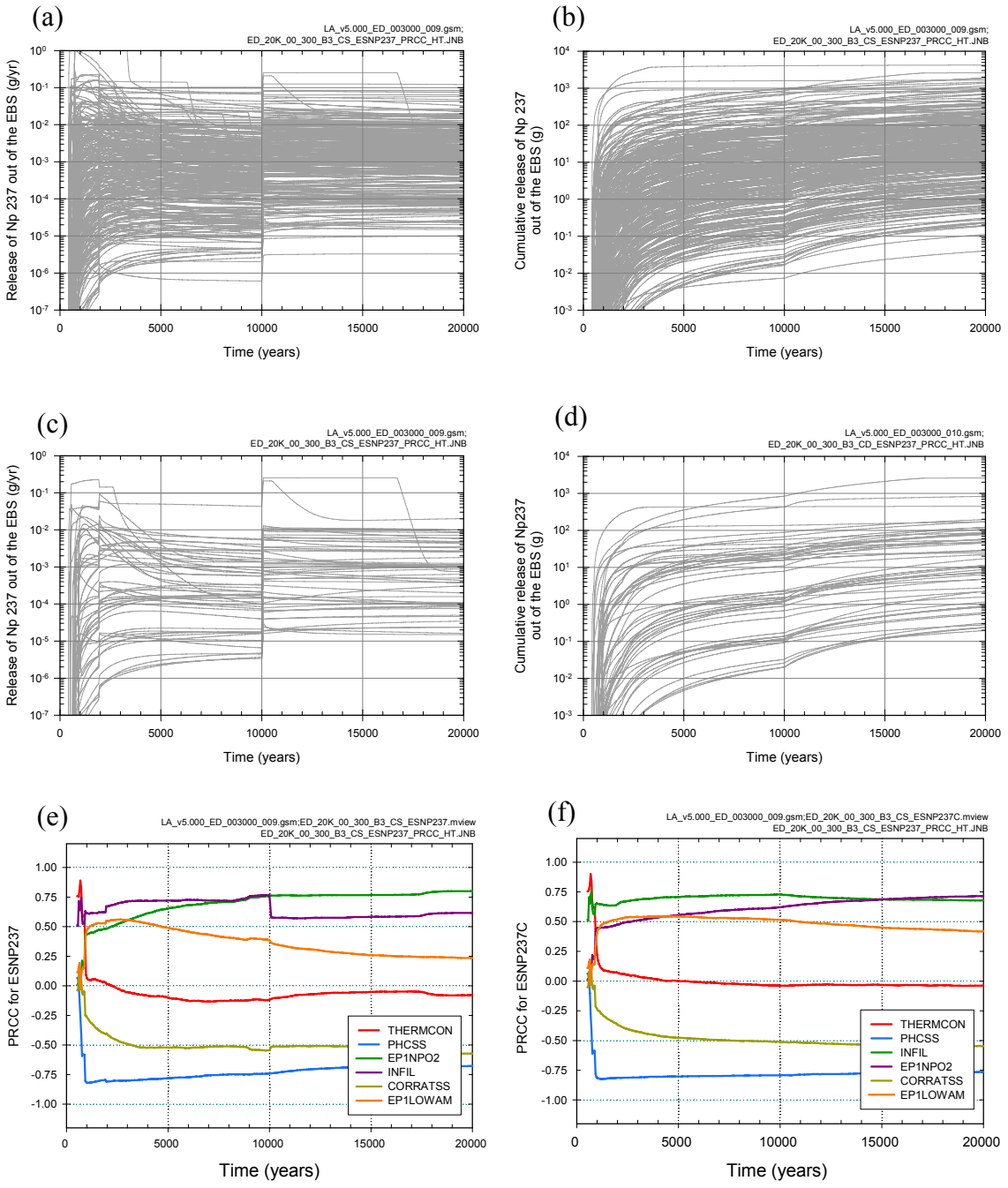

Source: Output DTNs: MO0709TSPASENS.000 [DIRS 183982]; and MO0709TSPAPLOT.000 [DIRS 183010].

Figure K5.3.2-3. Time-dependent release rates (*ESNP237*, g/yr) and cumulative (i.e., integrated) releases (*ESNP237C*, g) over 20,000 years for the movement of dissolved ^{237}Np from the EBS to the UZ resulting from a single early DS failure above a CNSF WP in percolation bin 3 under dripping conditions: (a, b) *ESNP237* and *ESNP237C* for all (i.e., 300) sample elements, (c, d) *ESNP237* and *ESNP237C* for first 50 sample elements, and (e, f) PRCCs for *ESNP237* and *ESNP237C*.

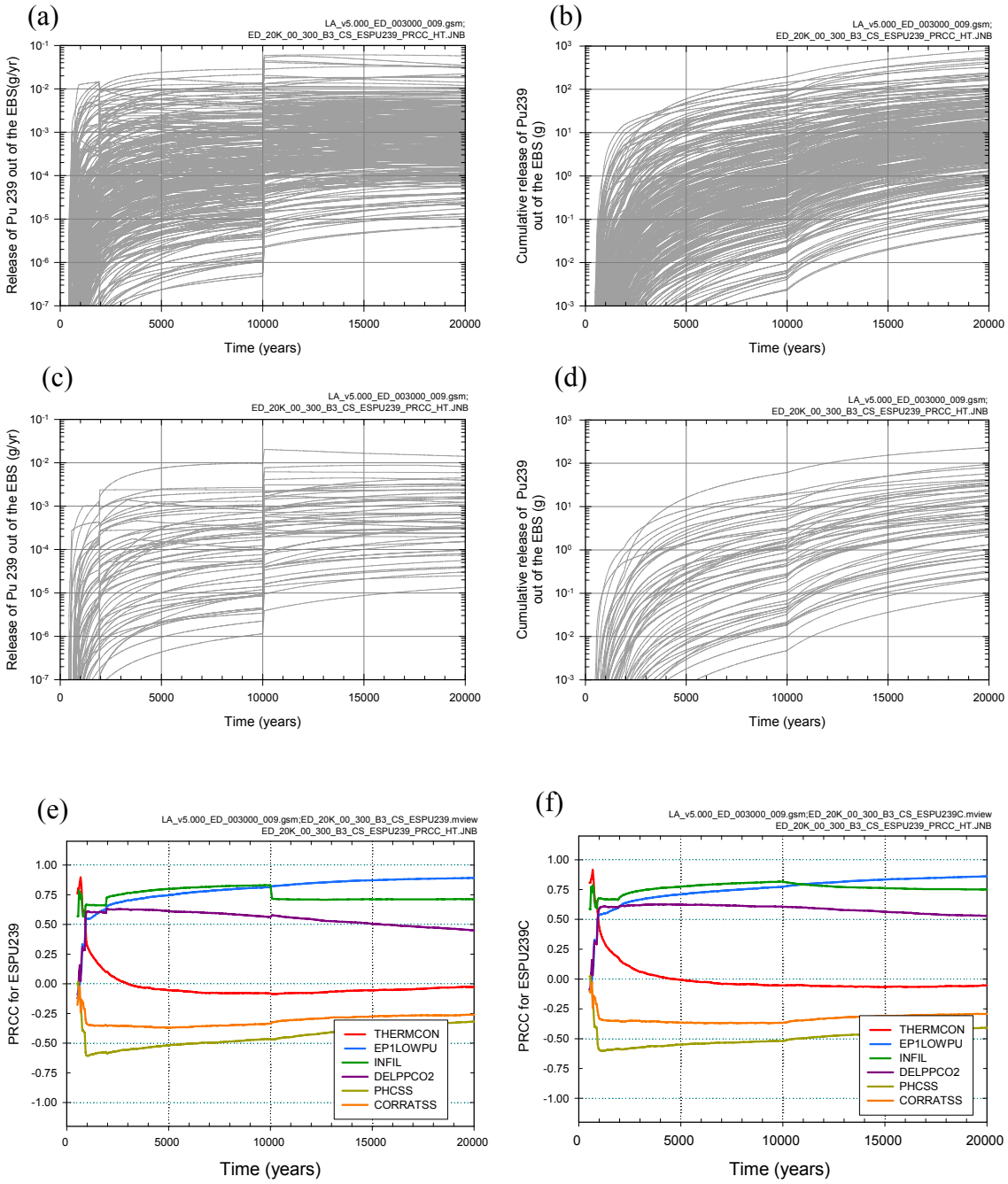

Source: Output DTNs: MO0709TSPASENS.000 [DIRS 183982]; and MO0709TSPAPLOT.000 [DIRS 183010].

Figure K5.3.2-4. Time-dependent release rates (*ESPU239*, g/yr) and cumulative (i.e., integrated) releases (*ESPU239C*, g) over 20,000 years for the movement of dissolved ^{239}Pu from the EBS to the UZ resulting from a single early DS failure above a CNSF WP in percolation bin 3 under dripping conditions: (a, b) *ESPU239* and *ESPU239C* for all (i.e., 300) sample elements, (c, d) *ESPU239* and *ESPU239C* for first 50 sample elements, and (e, f) PRCCs for *ESPU239* and *ESPU239C*.

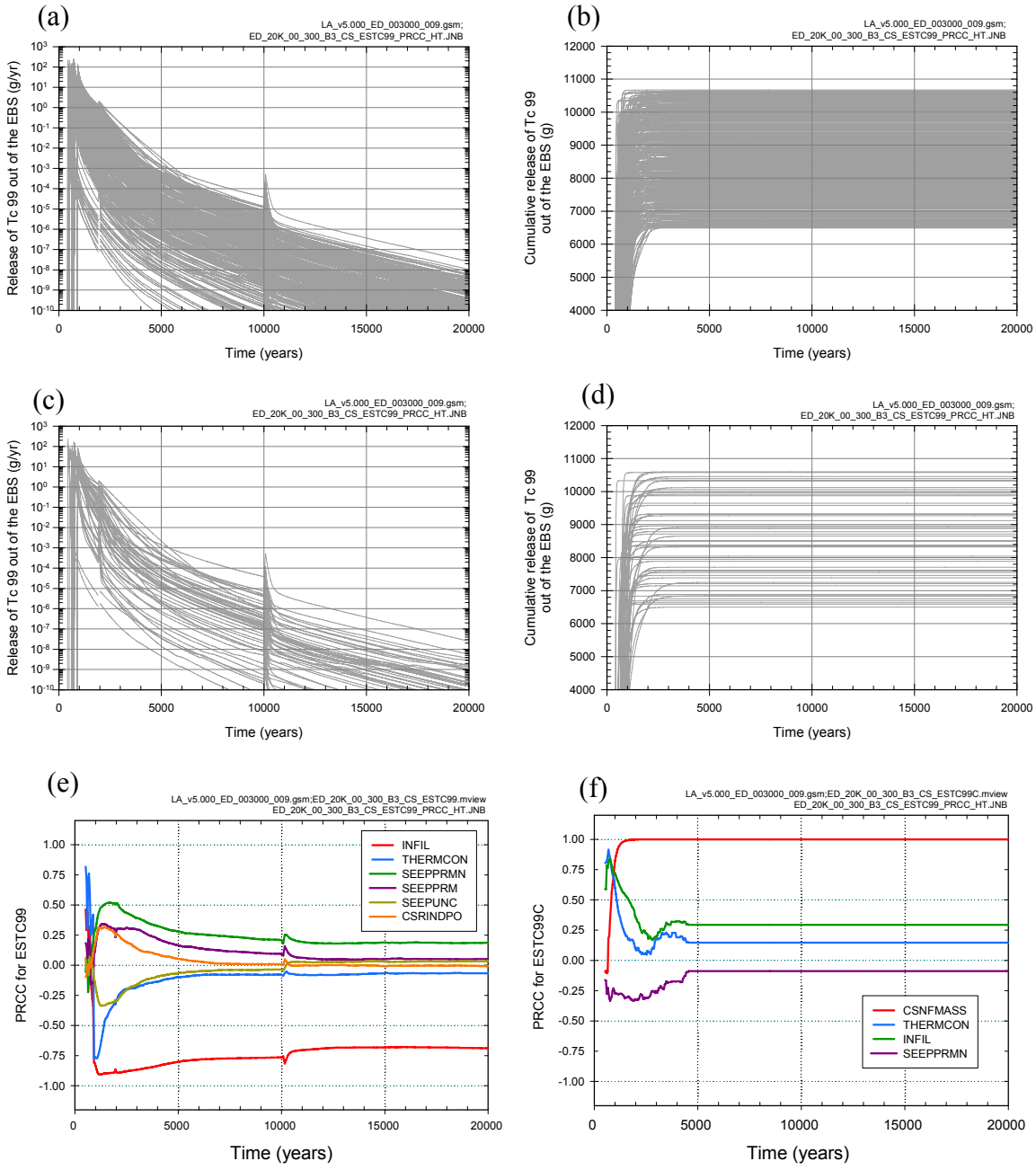

Source: Output DTNs: MO0709TSPASENS.000 [DIRS 183982]; and MO0709TSPAPLOT.000 [DIRS 183010].

Figure K5.3.2-5. Time-dependent release rates (*ESTC99*, g/yr) and cumulative (i.e., integrated) releases (*ESTC99C*, g) over 20,000 years for the movement of dissolved ^{99}Tc from the EBS to the UZ resulting from a single early DS failure above a CNSF WP in percolation bin 3 under dripping conditions: (a, b) *ESTC99* and *ESTC99C* for all (i.e., 300) sample elements, (c, d) *ESTC99* and *ESTC99C* for first 50 sample elements, and (e, f) PRCCs for *ESTC99* and *ESTC99C*.

Figure Removed. See discussion in Section K5.3.3.

Figure K5.3.3-1. Time-dependent release rates (*ESIC239*, g/yr) and cumulative (i.e., integrated) releases (*ESIC239C*, g) over 20,000 years for the movement of ^{239}Pu irreversibly attached to glass/waste form colloids from the EBS to the UZ resulting from the early failure of a CDSP WP in percolation bin 3 under dripping conditions: (a, b) *ESIC239* and *ESIC239C* for all (i.e., 300) sample elements, (c, d) *ESIC239* and *ESIC239C* for first 50 sample elements, and (e, f) PRCCs for *ESIC239* and *ESIC239C*.

Figure Removed. See Discussion in Section K5.3.3.

Figure K5.3.3-2. Time-dependent release rates (*ESIF239*, g/yr) and cumulative (i.e., integrated) releases (*ESIF239C*, g) over 20,000 years for the movement of ^{239}Pu irreversibly attached to ferrous colloids from the EBS to the UZ resulting from the early failure of a CDSP WP in percolation bin 3 under dripping conditions: (a, b) *ESIF239* and *ESIF239C* for all (i.e., 300) sample elements, (c, d) *ESIF239* and *ESIF239C* for first 50 sample elements, and (e, f) PRCCs for *ESIF239* and *ESIF239C*.

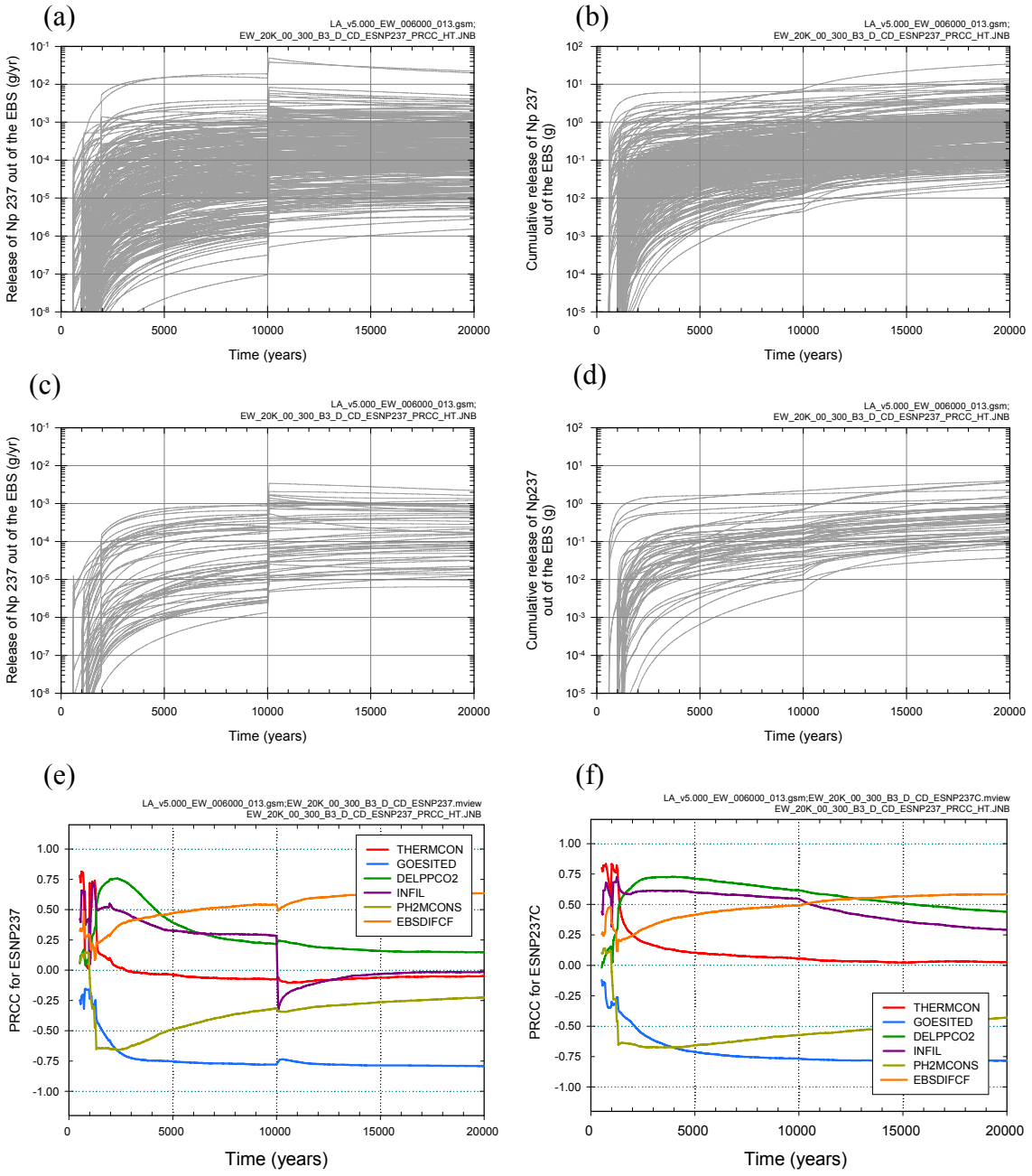

Source: Output DTNs: MO0709TSPASENS.000 [DIRS 183982]; and MO0709TSPAPLOT.000 [DIRS 183010].

Figure K5.3.3-3. Time-dependent release rates (*ESNP237*, g/yr) and cumulative (i.e., integrated) releases (*ESNP237C*, g) over 20,000 years for the movement of dissolved ^{237}Np from the EBS to the UZ resulting from the early failure of a CDSP WP in percolation bin 3 under dripping conditions: (a, b) *ESNP237* and *ESNP237C* for all (i.e., 300) sample elements, (c, d) *ESNP237* and *ESNP237C* for first 50 sample elements, and (e, f) PRCCs for *ESNP237* and *ESNP237C*.

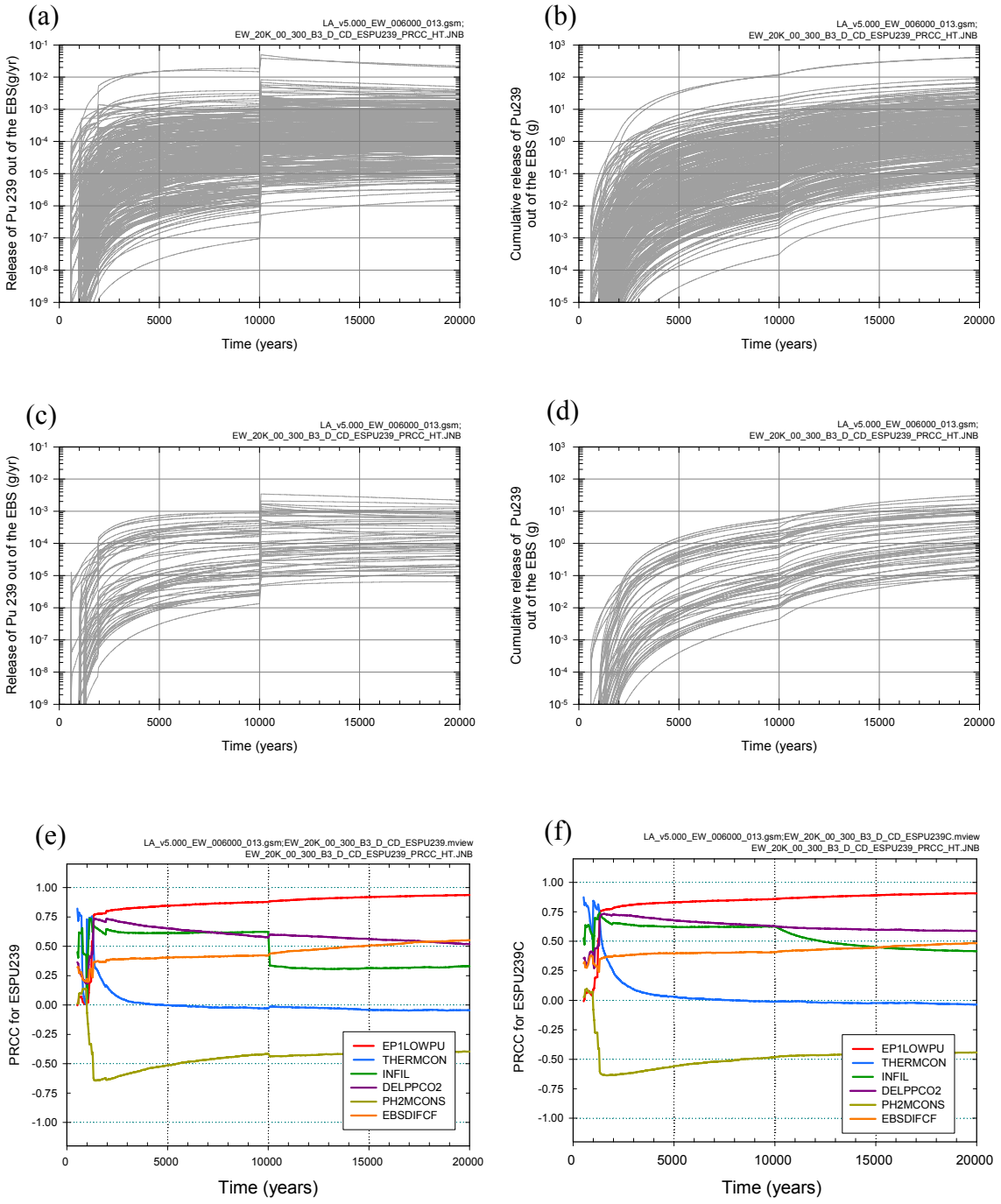

Source: Output DTNs: MO0709TSPASENS.000 [DIRS 183982]; and MO0709TSPAPLOT.000 [DIRS 183010].

Figure K5.3.3-4. Time-dependent release rates (*ESPU239*, g/yr) and cumulative (i.e., integrated) releases (*ESPU239C*, g) over 20,000 years for the movement of dissolved ^{239}Pu from the EBS to the UZ resulting from the early failure of a CDSP WP in percolation bin 3 under dripping conditions: (a, b) *ESPU239* and *ESPU239C* for all (i.e., 300) sample elements, (c, d) *ESPU239* and *ESPU239C* for first 50 sample elements, and (e, f) PRCCs for *ESPU239* and *ESPU239C*.

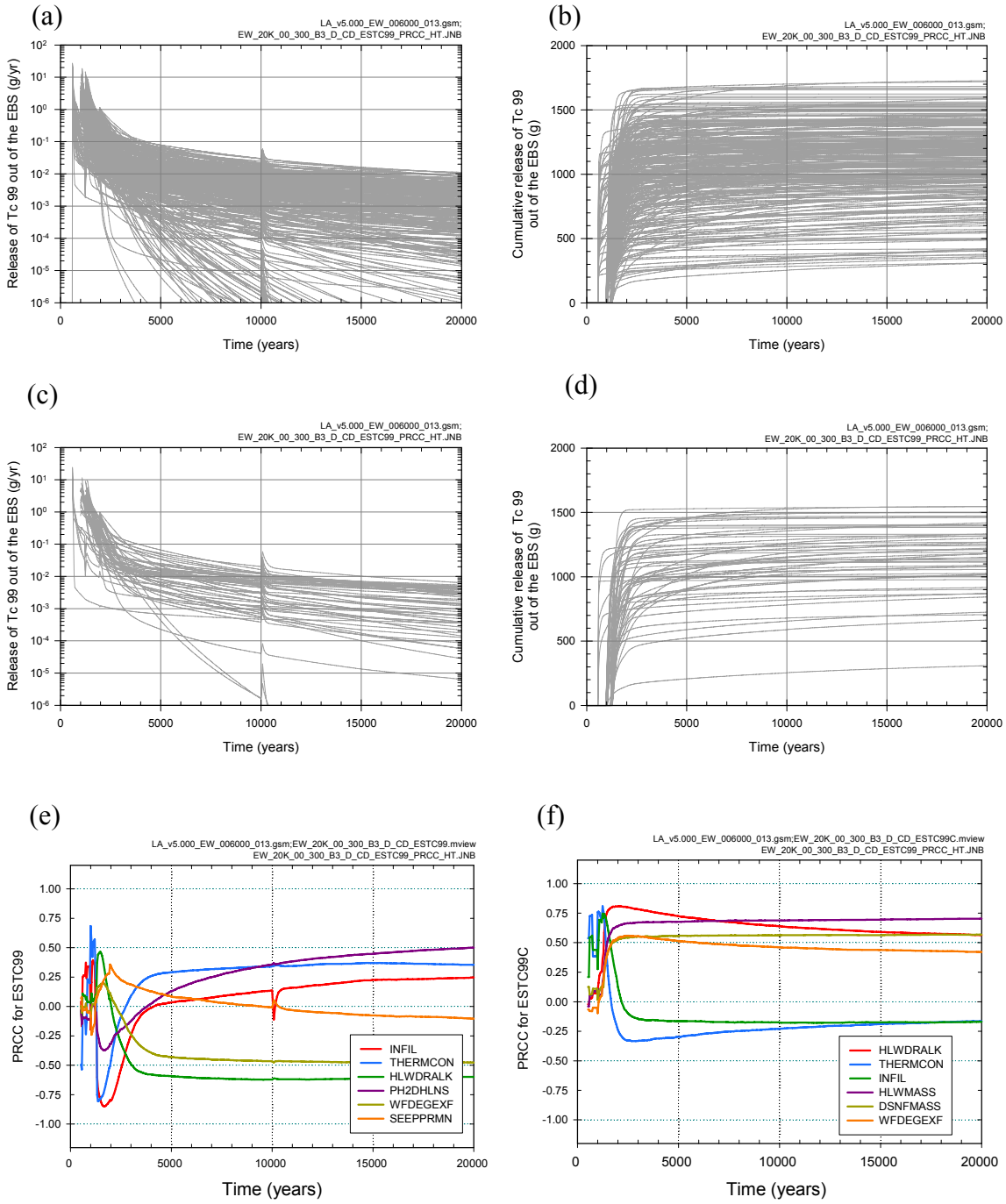

Source: Output DTNs: MO0709TSPASENS.000 [DIRS 183982]; and MO0709TSPAPLOT.000 [DIRS 183010].

Figure K5.3.3-5. Time-dependent release rates (*ESTC99*, g/yr) and cumulative (i.e., integrated) releases (*ESTC99C*, g) over 20,000 years for the movement of dissolved ^{99}Tc from the EBS to the UZ resulting from the early failure of a CDSP WP in percolation bin 3 under dripping conditions: (a, b) *ESTC99* and *ESTC99C* for all (i.e., 300) sample elements, (c, d) *ESTC99* and *ESTC99C* for first 50 sample elements, and (e, f) PRCCs for *ESTC99* and *ESTC99C*.

Figure Removed. See discussion in Section K5.3.5.

Figure K5.3.5-1. Time-dependent release rates (*ESIC239*, g/yr) and cumulative (i.e., integrated) releases (*ESIC239C*, g) over 20,000 years for the movement of ^{239}Pu irreversibly attached to glass/waste form colloids from the EBS to the UZ resulting from the early failure of a CSNF WP in percolation bin 3 under dripping conditions: (a, b) *ESIC239* and *ESIC239C* for all (i.e., 300) sample elements, (c, d) *ESIC239* and *ESIC239C* for first 50 sample elements, and (e, f) PRCCs for *ESIC239* and *ESIC239C*.

Figure Removed. See discussion in Section K5.3.5.

Figure K5.3.5-2. Time-dependent release rates (*ESIF239*, g/yr) and cumulative (i.e., integrated) releases (*ESIF239C*, g) over 20,000 years for the movement of ^{239}Pu irreversibly attached to ferrous colloids from the EBS to the UZ resulting from the early failure of a CSNF WP in percolation bin 3 under dripping conditions: (a, b) *ESIF239* and *ESIF239C* for all (i.e., 300) sample elements, (c, d) *ESIF239* and *ESIF239C* for first 50 sample elements, and (e, f) PRCCs for *ESIF239* and *ESIF239C*.

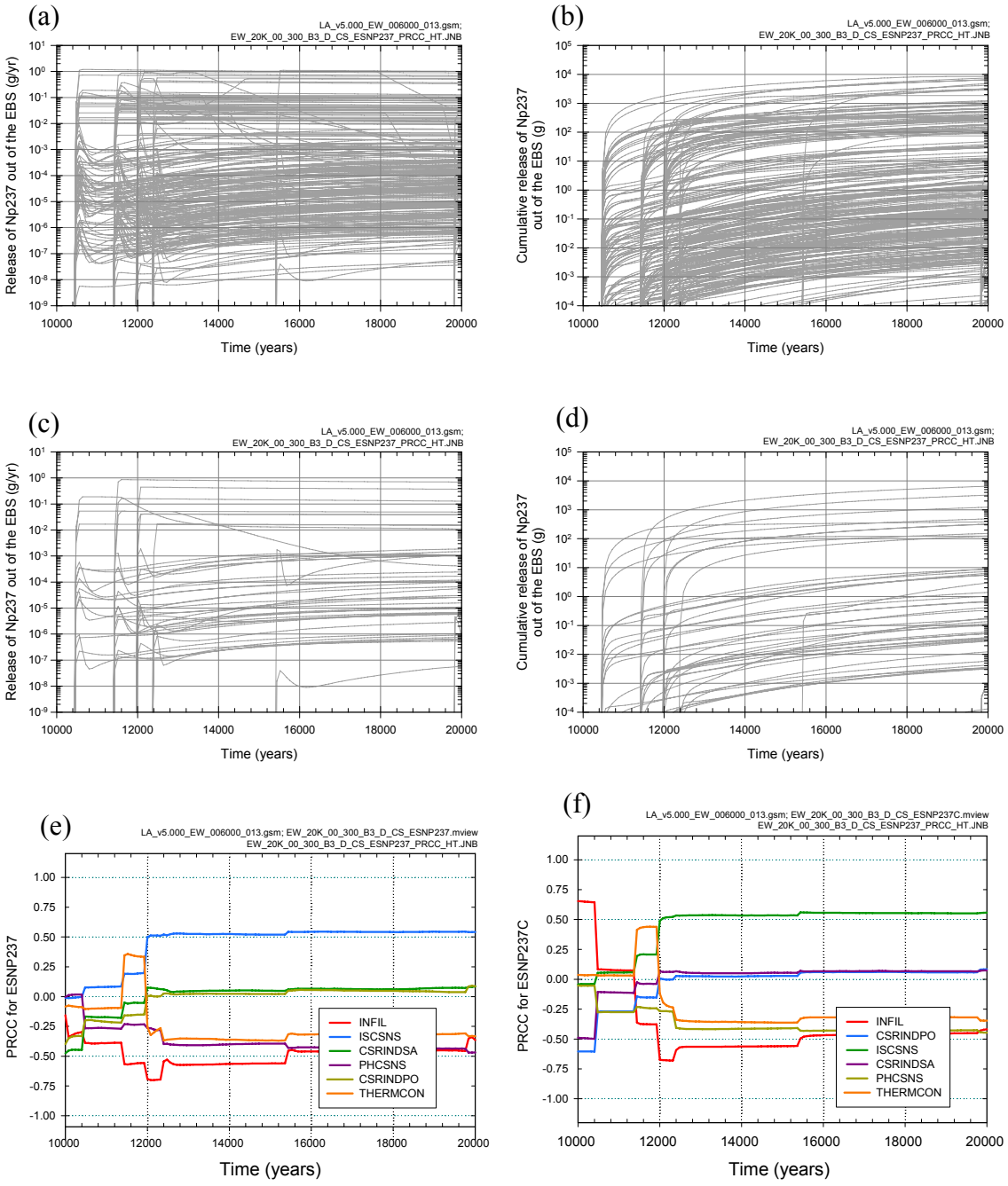

Source: Output DTNs: MO0709TSPASENS.000 [DIRS 183982]; and MO0709TSPAPLOT.000 [DIRS 183010].

Figure K5.3.5-3. Time-dependent release rates (*ESNP237*, g/yr) and cumulative (i.e., integrated) releases (*ESNP237C*, g) over 20,000 years for the movement of dissolved ^{237}Np from the EBS to the UZ resulting from the early failure of a CSNF WP in percolation bin 3 under dripping conditions: (a, b) *ESNP237* and *ESNP237C* for all (i.e., 300) sample elements, (c, d) *ESNP237* and *ESNP237C* for first 50 sample elements, and (e, f) PRCCs for *ESNP237* and *ESNP237C*.

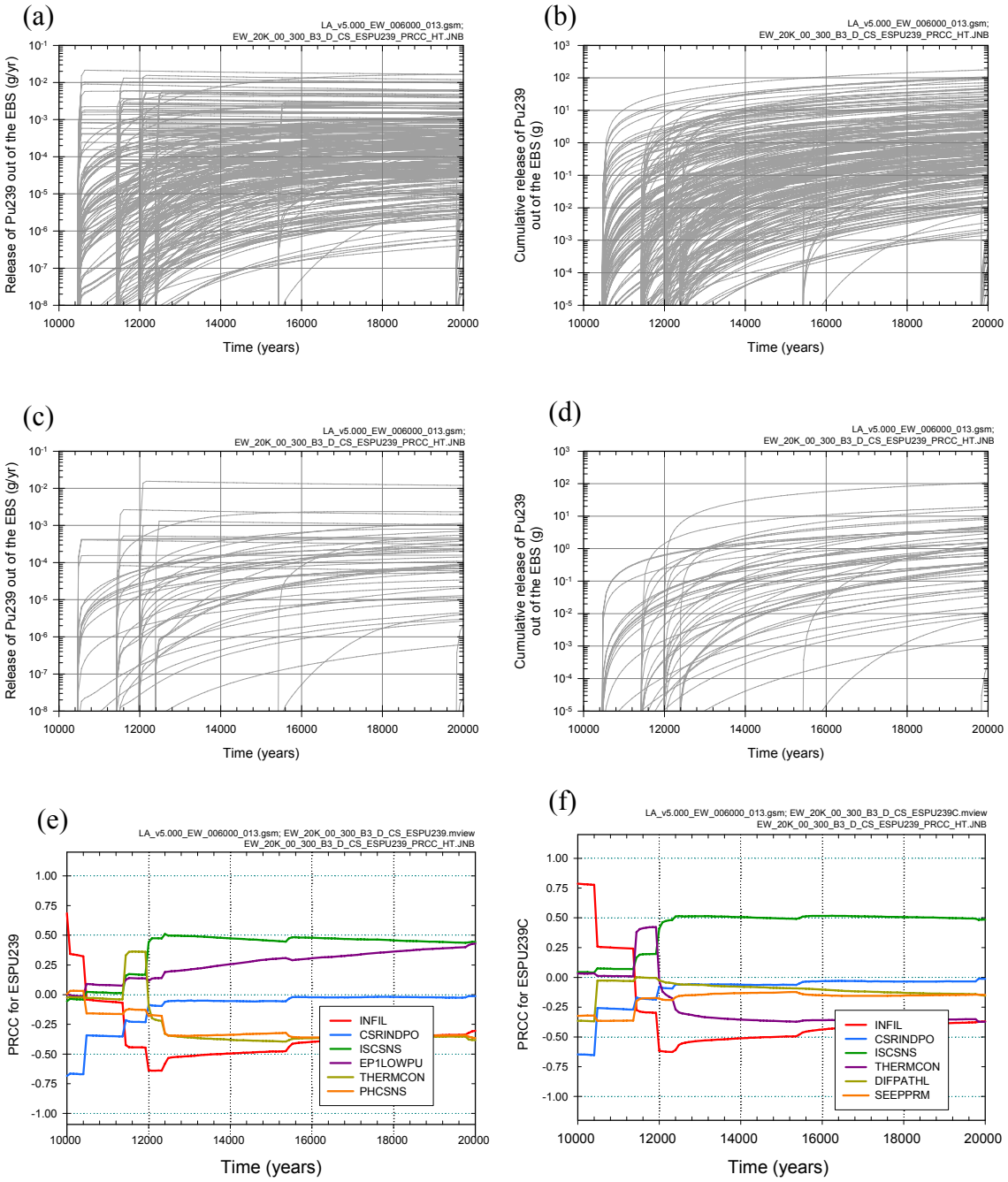

Source: Output DTNs: MO0709TSPASENS.000 [DIRS 183982]; and MO0709TSPAPLOT.000 [DIRS 183010].

Figure K5.3.5-4. Time-dependent release rates (*ESPU239*, g/yr) and cumulative (i.e., integrated) releases (*ESPU239C*, g) over 20,000 years for the movement of dissolved ^{239}Pu from the EBS to the UZ resulting from the early failure of a CSNF WP in percolation bin 3 under dripping conditions: (a, b) *ESPU239* and *ESPU239C* for all (i.e., 300) sample elements, (c, d) *ESPU239* and *ESPU239C* for first 50 sample elements, and (e, f) PRCCs for *ESPU239* and *ESPU239C*.

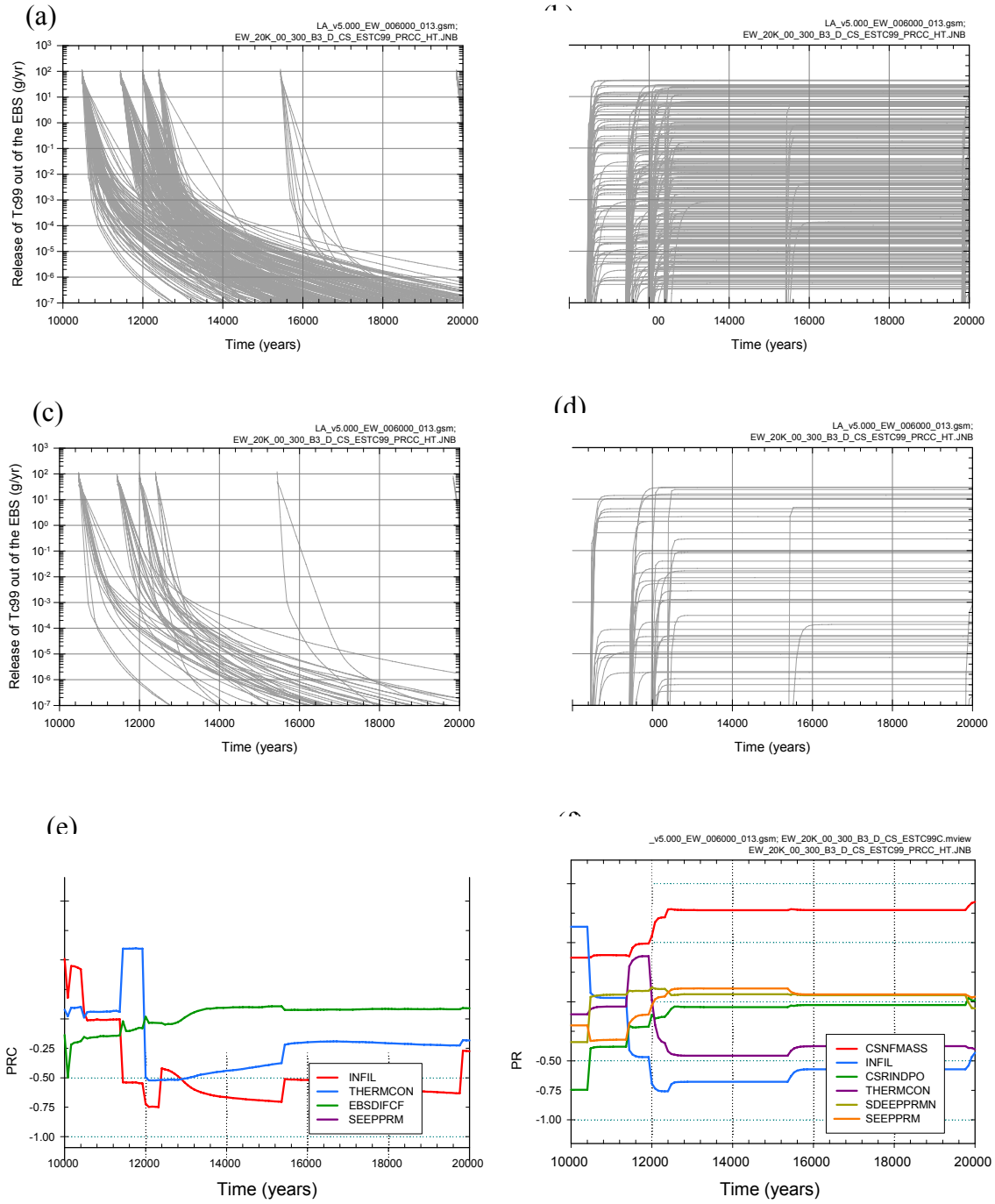

Source: Output DTNs: MO0709TSPASENS.000 [DIRS 183982]; and MO0709TSPAPLOT.000 [DIRS 183010].

Figure K5.3.5-5. Time-dependent release rates (*ESTC99*, g/yr) and cumulative (i.e., integrated) releases (*ESTC99C*, g) over 20,000 years for the movement of dissolved ^{99}Tc from the EBS to the UZ resulting from the early failure of a CSNF WP in percolation bin 3 under dripping conditions: (a, b) *ESTC99* and *ESTC99C* for all (i.e., 300) sample elements, (c, d) *ESTC99* and *ESTC99C* for first 50 sample elements, and (e, f) PRCCs for *ESTC99* and *ESTC99C*.

INTENTIONALLY LEFT BLANK